ACTA PHYSICA

ACADEMIAE SCIENTIARUM HUNGARICAE

TOMUS XXXI FASCICULI 1—3

AKADÉMIAI KIADÓ, BUDAPEST
1972

ACTA PHYS. HUNG. APAHAQ 31 (1—3) 1—276 (1972)

ACTA PHYSICA

A MAGYAR TUDOMÁNYOS AKADÉMIA FIZIKAI KÖZLEMÉNYEI

SZERKESZTŐSÉG ÉS KIADÓHIVATAL: BUDAPEST V., ALKOTMÁNY UTCA 21.

Az *Acta Physica* német, angol, francia és orosz nyelven közöl értekezéseket a fizika tárgyköréből.

Az *Acta Physica* változó terjedelmű füzetekben jelenik meg: több füzet alkot egy kötetet.

A közlésre szánt kéziratok a következő címre küldendők:

Acta Physica, Budapest 502, P. O. B. 24.

Ugyanerre a címre küldendő minden szerkesztőségi és kiadóhivatali levelezés.

Megrendelhető a belföld számára az Akadémiai Kiadónál (Budapest V., Alkotmány utca 21. Bankszámla 05-915-111-46), a külföld számára pedig a „Kultúra" Könyv- és Hírlap Külkereskedelmi Vállalatnál (Budapest I., Fő utca 32. Bankszámla 43-790-057-181 sz.), vagy annak külföldi képviseleteinél és bizományosainál.

Die *Acta Physica* veröffentlichen Abhandlungen aus dem Bereich der Physik in deutscher, englischer, französischer und russischer Sprache.

Die *Acta Physica* erscheinen in Heften wechselnden Umfanges. Mehrere Hefte bilden einen Band.

Die zur Veröffentlichung bestimmten Manuskripte sind an folgende Adresse zu richten:

Acta Physica, Budapest 502, P. O. B. 24.

An die gleiche Anschrift ist auch jede für die Redaktion und den Verlag bestimmte Korrespondenz zu senden. Abonnementspreis pro Band: $ 16.00.

Bestellbar bei dem Buch- und Zeitungs-Aussenhandels-Unternehmen »Kultúra« (Budapest I., Fő u. 32. Bankkonto Nr. 43-790-057-181) oder bei seinen Auslandsvertretungen und Kommissionären.

ACTA PHYSICA

ACADEMIAE SCIENTIARUM HUNGARICAE

TOMUS XXXI

AKADÉMIAI KIADÓ, BUDAPEST
1972

ACTA PHYS. HUNG.

INDEX

TOMUS 31

PROCEEDINGS

of the

2nd SYMPOSIUM ON HADRON SPECTROSCOPY

Balatonfüred, Hungary
6—11 September, 1970

The Symposium on Hadron Spectroscopy was organized by the Hungarian Physical Society under the sponsorship of the European Physical Society and the Hungarian Academy of Sciences. The member institutions of the Vienna—Bratislava—Budapest triangular collaboration shared the organization of the Symposium.

Members of the Organizing Committee:

Prof. H. PIETSCHMANN (Vienna University)

Prof. M. PETRAS (Komenský University, Bratislava)

Prof. G. MARX (Chairman, Roland Eötvös University, Budapest)

Dr. J. KUTI (Secretary, Roland Eötvös University, Budapest)

The final manuscript was submitted for publication to Acta Phys. Hung. on 10th May 1971

Printed in Hungary

A kiadásért felel az Akadémiai Kiadó igazgatója — Műszaki szerkesztő: Várhelyi Tamás

A kézirat nyomdába érkezett: 19.. VII. 24. — Terjedelem: 24 (A/5) ív, 65 ábra

72.72325 Akadémiai Nyomda, Budapest — Felelős vezető: Bernát György

INDEX

Acta Physica Academiae Scientiarum Hungaricae, Tomus 31 (1–3), pp. 5–19 (1972)

THEORETICAL IMPLICATIONS OF RECENT ELECTRON–POSITRON COLLIDING BEAM EXPERIMENTS*

By

J. J. SAKURAI

DEPARTMENT OF PHYSICS, UNIVERSITY OF CALIFORNIA, LOS ANGELES. CALIFORNIA, USA

The theoretical consequences of recent electron – positron colliding beam experiments are summarized from the point of view of tests of pure quantum electrodynamics, the study of the vector mesons ϱ, ω, φ and the frontier region beyond the ϱ, ω and φ.

I. Introduction

Contrary to an earlier announcement of this summer symposium, I am not going to talk on "Vector Mesons—a Decade of Progress". It is clearly impossible to cover the past ten years of vector meson physics in just forty-five minutes. In preparing my present talk on colliding beam physics, however, I have found that it is also impossible to cover this fascinating subject in forty-five minutes. In fact, next week at Frascati, an entire conference, lasting four days, will be devoted to electron–positron colliding beams. In any case I will try to do my best [1].

At the present moment there are three electron-positron colliding beam facilities in operation [2]:

(i) Novosibirsk (VEPP II), $\sqrt{s}|_{\max} = 1.5$ GeV

(ii) Orsay (ACO), $\sqrt{s}|_{\max} = 1.04$ GeV

(iii) Frascati (Adone), $\sqrt{s}|_{\max} = 2.4$ GeV (3 GeV later)

What do we, theoreticians, hope to learn from a series of beautiful experiments performed at these places? There are essentially three areas of investigations which are of immediate theoretical interest:

(i) Tests of pure quantum electrodynamics.
(ii) Study of the known vector mesons, ϱ, ω and φ.
(iii) Exploration of the frontier region beyond ϱ, ω and φ.

I will treat these three topics in the order given here.

* Supported by the National Science Foundation.

II. Pure quantum electrodynamics

Historically, the very idea of colliding beams was first conceived by a Princeton—Stanford group (O'NEIL, RICHTER, PANOFSKY, etc.) to test the validity of quantum electrodynamics in Møller scattering. When we use electron–positron rather than electron–electron colliding beams, we can examine the photon propagator not only for large space-like values of q^2 but also for large time-like values of q^2; in addition, we can explore the high-momentum-transfer behavior of the electron propagator through annihilation into photons.

Fig. 1 represents the Feynman diagram for Bhabha scattering. The predicted differential cross section is

$$\frac{d\sigma}{d\Omega} = \frac{\alpha^2}{2s}\left(\frac{1+\cos^4(\theta/2)}{\sin^4(\theta/2)} - \frac{2\cos^2(\theta/2)}{\sin^2(\theta/2)} + \frac{1+\cos^2\theta}{2}\right). \tag{1}$$

The first (last) term is due to photon exchange in the t-(s-) channel, as represented in Fig. 1a [1b], while the middle term arises from interference of the two diagrams. It is important to note that at fixed *angles* (not fixed t), the cross section is predicted to go down as $1/s$. When the sign of the electric charge of the leptons is not determined, Bhabha scattering at wide angles,

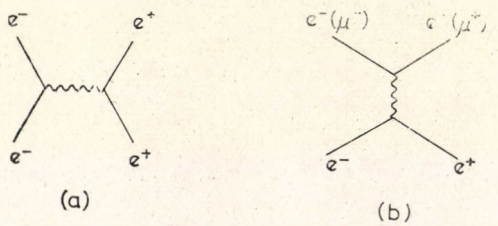

Fig. 1. Diagrams for Bhabha scattering (muon pair production)

say $\theta \approx \pi/2$, can be seen to be more sensitive to possible modifications of the photon propagator in the t channel, i.e. the first term of Eq. (1) is more important.

Wide-angle Bhabha scattering up to $\sqrt{s} = 2.4$ GeV has recently been studied by three different groups at Frascati [3] (the "π–μ Group", the "Boson Group" and the "Bologna—CERN Group"). The data of the "π–μ Group" covering $53° < \theta < 127°$ is shown in Fig. 2. Notice that this is an absolute cross section measurement; the luminosity of Adone was determined simultaneously by the same group through study of small-angle Bhabha scattering ($3.5° < \theta < 6°$) where no breakdown of quantum electrodynamics is expected because of the small values of q^2 involved. If the photon propagator were modified according to the prescription

$$\frac{1}{q^2} \to \frac{1}{q^2} - \frac{1}{q^2+\Lambda^2} \tag{2}$$

we would expect a fractional deviation from the predicted cross section given by

$$\frac{\Delta\sigma}{\sigma_{\text{theoretical}}} \approx -\frac{2q^2}{\Lambda^2} \tag{3}$$

provided $\Lambda^2 \gg q^2$. As seen from Fig. 2, the data points are consistent with $\Lambda = \infty$ (no breakdown of quantum electrodynamics). The experimental results of the three groups at Frascati can be summarized by saying that

$$\Lambda > 3 \text{ GeV} \quad (95\% \text{ confidence}). \tag{4}$$

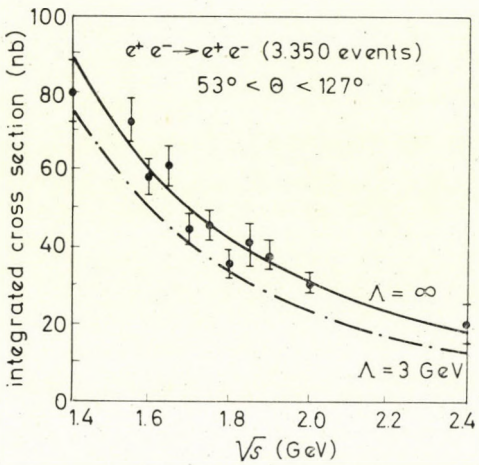

Fig. 2. The integrated cross section for wide-angle Bhabha scattering measured by the "π–μ Group". The Figure includes a few "post-Kiev" points (M. CONVERSI, private communication)

Let us now consider

$$e^+ + e^- \to \mu^+ + \mu^-. \tag{5}$$

This time, only Fig. 1b contributes; so the experiment explores the photon propagator in the time-like region. The predicted cross section is

$$\frac{d\sigma}{d\Omega} = \frac{\alpha^2}{4s}(1 + \cos^2\theta) + O(m_\mu^2/s). \tag{6}$$

Muon pair production has been studied at Frascati up to $s = 4$ GeV^2 by the "π–μ Group" and the "Bologna–CERN Group[3]", and the limit of Λ obtained is again in the neighborhood of 3 GeV. A similar limit has also been established at Novosibirsk [4] where the maximum value of s explored is about 1.7 GeV^2.

In addition to Bhabha scattering and muon pair production, the angular dependence of two-photon annihilation has been studied at Frascati by comparing the photon intensity at $\theta \approx 30°$. Here the electron propagator is involved, and, as pointed out by KROLL [5], it may be more appropriate to parameterize the data using

$$\frac{\Delta\sigma}{\sigma_{\text{theoretical}}} \approx -\frac{2q^4}{\Lambda^4} \tag{7}$$

in place of (3). This is because the Ward identity requires that any modification in the electron propagator must be accompanied by a simultaneous change in the vertex function. The Frascati data of the "$\gamma\gamma$ Group[3]" indicates $\Lambda > 2.1$ GeV for the electron propagator.

To summarize this section of my talk, the limit on Λ obtained by these colliding beam experiments is now approaching that deduced from low-energy precision tests of quantum electrodynamics [6] [e.g. $(g-2)$ of the muon]. A "ghost" of the type discussed by LEE and WICK [7] appears to be rather elusive.

III. ϱ, ω, and φ regions

Let us now turn to electron–positron annihilations into hadrons. As is well known, the process

$$e^+ + e^- \to \pi^+ + \pi^- \tag{8}$$

to order α^2 in the cross section measures the electromagnetic form factor of the charged pion in the time-like region:

$$\sigma(e^+e^- \to \pi^+\pi^-) = (\pi\alpha^2\beta_\pi^3/3s)|F_\pi(s)|^2, \tag{9}$$

where β_π is the velocity of one of the pions in units of c. This annihilation reaction in the ϱ meson region was first studied in pioneering experiments performed at Novosibirsk [8] and Orsay [9].

Can theoreticians guess the form of $F_\pi(s)$? Near the ϱ meson, it is almost a truism to say that the ϱ dominates. A more relevant question is: Does the resonance form of $F_\pi(s)$ near $s = m_\varrho^2$ extrapolate smoothly (in the sense of vector-meson dominance) to low s regions where $F_\pi(s)$ is required to be unity at $s = 0$? One may first try

$$F_\pi(s) = \frac{m_\varrho^2}{m_\varrho^2 - s - im_\varrho \Gamma_\varrho} \tag{10}$$

which is a finite-width version of the simple ϱ dominance expression $m_p^2/(m_p^2 - s)$. This is not quite satisfactory because (i) it does not have the correct

threshold behavior appropriate for a p-wave pion pair, and (ii) it does not become purely real for $s < 4m_\pi^2$. Our task is to construct $F_\pi(s)$ with the right phase (i.e. the phase of $F_\pi(s)$ identical with the phase of the pion–pion scattering amplitude in $T = 1, J = 1^-$ and purely real below the two-pion threshold), the right threshold behavior, the right normalization at $s = 0$, and the right analytic behavior (a branch cut starting at $s = 4m_\pi^2$); at the same time we want $F_\pi(s)$ to exhibit a simple resonance form when the p-wave pion–pion scattering phase shift goes through $\pi/2$ at the ϱ mass, e.g. $F_\pi(s)$ going like the partial wave amplitude

$$(\sqrt{s}/k^3)\, e^{i\delta_{11}} \sin\delta_{11} = \frac{1}{(k^3/\sqrt{s})(-i+\cot\delta_{11})}, \qquad k = \frac{1}{2}(s-4m_\pi^2)^{1/2}. \tag{11}$$

The problem of finding $F_\pi(s)$ with the desired properties listed above has been discussed extensively in the literature starting with the historical paper of FRAZER and FULCO [10]. One of the simplest approaches is to write

$$F_\pi(s) = \frac{D(o)}{D(s)} \tag{12}$$

with

$$D(s) = -i(k^3/\sqrt{s}) + (k^3/\sqrt{s})\ \cot\delta_{11}. \tag{13}$$

As a reasonable expression for the pion–pion phase shift, one may use a relativistic effective-range formula of the kind discussed by CHEW and MANDELSTAM [11]

$$(k^3/\sqrt{s})\ \cot\delta_{11} = k^2 h(s) + a + bk^2. \tag{14}$$

The function $h(s)$, given by

$$h(s) = \frac{2}{\pi}\frac{k}{\sqrt{s}} \ln\left(\frac{\sqrt{s}+2k}{2m_\pi}\right) \tag{15}$$

is needed if $D(s)$ is to be an analytic function except for the right-hand cut starting at $s = 4m_\pi^2$; it is understood that between $s = 0$ and $s = 4m_\pi^2$, we make the following replacement

$$\ln\left(\frac{\sqrt{s}+2k}{2m_\pi}\right) \to i\cot^{-1}\left(\frac{s}{4m_\pi^2-s}\right)^{1/2}, \qquad k \to i\left(m_\pi^2 - \frac{s}{4}\right)^{1/2}. \tag{16}$$

The parameters a and b in (14) are to be determined from the mass and width of the ϱ meson. We can then rewrite Eq. (12) in the vicinity of the ϱ resonance as follows [12]:

$$F_\pi(s)|_{\text{near } s=m_\varrho^2} = \frac{m_\varrho^2[1+d(\Gamma_\varrho/m_\varrho)]}{m_\varrho^2 - s - im_\varrho \Gamma_\varrho (k/k_\varrho)^3 (m_\varrho/\sqrt{s})}, \tag{17}$$

where d is a complicated function of the ϱ mass and is numerically equal to 0.48. Comparing Eq. (17) with Eq. (10), we can regard $[1 + d(\Gamma_\varrho/m_\varrho)]^2$ as a correction factor due to the finite width of the ϱ meson; numerically it is about 1.14.

In Fig. 3 we present the modulus squared of the pion form factor measured at Novosibirsk and Orsay [13]. In each case the full curve is a covariant Breit–Wigner fit where the height (i.e. the absolute normalization) as well as the ϱ mass and ϱ width is left as a free parameter while the dotted curve is a two-parameter fit based on Eq. (17) [14]. The fact that the two curves for the

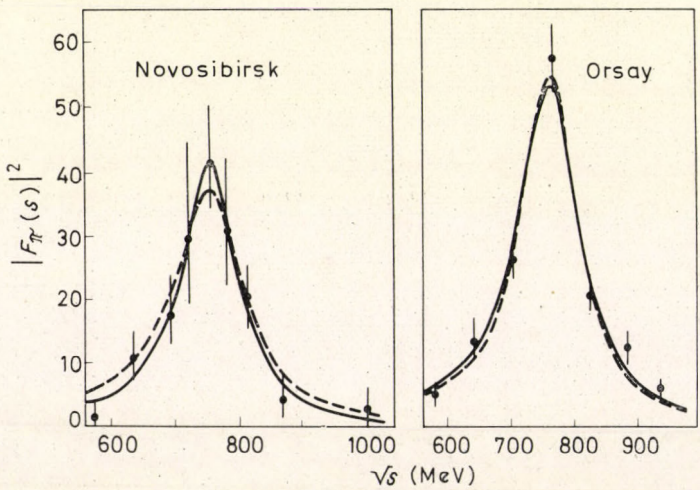

Fig. 3. The pion form factor measured at Novosibirsk and Orsay. In each case the dotted curve is a two-parameter fit based on Eq. (17); the solid curve is a three-parameter fit based on the covariant Breit–Wigner formula, $|F_\pi(s)|^2 = cm_\varrho^4/[(s-m_\varrho^2)^2 + m_\varrho^2 \Gamma_\varrho^2]$ where c as well as m_ϱ and Γ_ϱ is adjustable

Orsay data are practically indistinguishable supports the basic idea of vector-meson dominance that, given the mass and width of the ϱ, the height is no longer a free parameter but is determined by the normalization condition at $s = 0$. One, however, worries more about the discrepancy between Orsay and Novosibirsk apparent in Fig. 3.

Let us now look at the other vector mesons, ω and φ. Quite generally,

we have, at the resonance peak ($s = m_V^2$) of the vector meson V,

$$\sigma_{\text{resonance peak}} = \left(\frac{12\pi}{m_V^2}\right) \frac{\Gamma(V \to e^+ e^-)}{\Gamma_{\text{tot}}} . \tag{18}$$

Sometimes the partial decay width for $V \to e^+e^-$ is expressed in terms of the coupling constant $f_V^2/4\pi$ as follows

$$\Gamma(V \to e^+e^-) = \frac{1}{3}[\alpha^2/(f_V^2/4\pi)]\, m_V + O(m_e^4/m_V^4) , \tag{19}$$

where our normalization convention is such that we insert em_V^2/f_V at a $\gamma - V$ junction.

Comparison of the leptonic decay rates of the various vector mesons is of interest because we can test our current theoretical ideas about broken SU(3), ω—φ mixing, the spectral function (Weinberg) sum rules, etc. The simplest prediction along this line is that of the vector nonet scheme [15] (incorporated into SU(6) and the quark model)

$$\frac{1}{f_\varrho^2} : \frac{1}{f_\omega^2} : \frac{1}{f_\varphi^2} = 9 : 1 : 2 \tag{20}$$

in the limit the vector mesons are all degenerate. A more sophisticated prediction which takes into account symmetry breaking is based on the spectral-function sum rule of WEINBERG [16]

$$\int \frac{\varrho^{(33)}(m^2)}{m^2}\, dm^2 = \int \frac{\varrho^{(88)}(m^2)}{m^2}\, dm^2 , \tag{21a}$$

$$\int \frac{\varrho^{(08)}(m^2)}{m^2}\, dm^2 = 0 , \tag{21b}$$

where $\varrho^{(\alpha\beta)}$ stands for the weight function that appears in the spectral representation of currents with unitary spin indices α and β. These sum rules can be derived from the unmodified Gell–Mann commutation relations for the vector currents (time–time and time–space) with c-number Schwinger terms. They essentially state that the Schwinger terms satisfy exact SU(3) even if SU(3) itself is an approximate symmetry. As is well known, $\varrho^{(33)}$ and $\varrho^{(88)}$ are directly measurable in electron–positron collisions

$$\begin{aligned} \varrho^{(33)}(m^2) &= (s^2/16\pi^3\alpha^2)\sigma_{\text{tot}}(e^+e^- \to T = 1 \text{ hadronic system})|_{s=m^2} \\ \varrho^{(88)}(m^2) &= (3s^2/16\pi^3\alpha^2)\sigma_{\text{tot}}(e^+e^- \to T = 0 \text{ hadronic system})|_{s=m^2} . \end{aligned} \tag{22}$$

If we now make the *additional* hypothesis that (21a) can be well saturated by ϱ, ω and φ, we obtain, in the narrow width approximation [17],

$$\frac{1}{3} m_\varrho \Gamma(\varrho \to e^+e^-) = m_\omega \Gamma(\omega \to e^+e^-) + m_\varphi \Gamma(\varphi \to e^+e^-). \tag{23}$$

Similarly, if we saturate (21b) with ω and φ, we can prove that ω–φ mixing must be of the "current-mixing" type [18] (in the terminology of KROLL, LEE and ZUMINO [19]).

In order to predict how the ω and φ contributions make up the right-hand side of Eq. (23), let us now look at the inverse propagator matrix for the currents. In the pole approximation we have

$$\Delta^{-1} = Aq^2 + B. \tag{24}$$

The crucial observation to be made here is that, as a consequence of the Weinberg sum rules, there can be no symmetry breaking in the B term; this follows because the elements of the Δ matrix at $q^2 = 0$ are just $\int [\varrho^{(\alpha\beta)}(m^2)/m^2]\, dm^2$ which, according to Eq. (21) and its generalizations, satisfy exact SU(3). If we now make the usual hypothesis that the A matrix in Eq. (24) satisfies a first-order symmetry breaking formula, we are led to the following *inverse*-squared mass formula

$$3\left(\frac{\sin^2\theta}{m_\omega^2} + \frac{\cos^2\theta}{m_\varphi^2}\right) + \frac{1}{m_\varrho^2} = \frac{4}{m_{K^*}^2} \tag{25}$$

first written down by COLEMAN and SCHNITZER [20]. Coming back to the lepton-pair decay rates, we can show that the "generalized mixing angle" θ that appears in the mass formula (25) also appears in comparison of $\omega \to e^+e^-$ and $\Phi \to e^+e^-$ [21]:

$$\tan^2\theta = \frac{m_\omega \Gamma(\omega \to e^+e^-)}{m_\varphi \Gamma(\varphi \to e^+e^-)}. \tag{26}$$

Let us know look at the experimental data. If we take the Orsay data [22] for ω and φ and deduce θ using Eq. (26), we get

$$\theta = (34 \pm 2)^\circ \tag{27}$$

to be compared with $\theta = 28^\circ$ obtained from the mass formula (25). This might not appear to be too bad. However, if we look at the ratios of $1/f_V^2$, the Orsay data give

$$\frac{1}{f_\varrho^2} : \frac{1}{f_\omega^2} : \frac{1}{f_\varphi^2} = 9 : 1.28 \pm 0.28 : 1.63 \pm 0.20 \tag{28}$$

which should be compared to the predictions of our scheme [18, 23] 9 : 0.65 : : 1.33. Part of the discrepancy arises from the fact that the Weinberg sum rule in the form (23) appears to be violated:

$$\begin{aligned} \text{LHS of (23)} &= (1.78 \pm 0.16)\ \text{MeV}^2, \\ \text{RHS of (23)} &= (2.47 \pm 0.21)\ \text{MeV}^2, \end{aligned} \tag{29}$$

a difference of (0.69 ± 0.25) MeV^2.

If one is willing to make more assumptions, further predictions are possible. Assuming that the isoscalar form factor of the K meson is dominated by the φ and ω mesons, we can derive [19]

$$\sigma(e^+e^- \to K^+K^-)|_{s=m_\varphi^2} = \frac{\pi}{12} \frac{\alpha^2}{(\Gamma_\varphi^{\text{tot}})^2} \cos^4 \theta \left(1 - \left(\frac{4m_K^2}{m_\varphi^2}\right)\right)^{3/2}, \tag{30}$$

where in the current-mixing scheme the angle θ appearing here must be the same as the angle θ appearing in Eq. (26). The generalized mixing angle deduced from the peak cross section for K pair production by the Orsay group turns out to be $(31 \pm 2)^\circ$ in reasonable agreement with the angle determined from the ratio of $\omega \to e^+e^-$ and $\varphi \to e^+e^-$ [cf. Eqs. (26) and (27)] [24].

I have no time to discuss the interesting and controversial subject of ϱ–ω interference. Let me just mention that it is difficult to understand the published data of the Orsay group [25] on the phase of $\omega \to 2\pi$ using reasonable theoretical models [26]. (I personally do not believe in the data.)

IV. Frontier region

The remaining part of my talk is devoted to a first glimpse at the exciting "frontier region" beyond ϱ, ω and φ. None of the experimental results I will mention has been published, but the data were reported and discussed extensively at the Kiev Conference which preceded this symposium. Let me emphasize in the beginning that the experimental data are extremely preliminary; so are the possible theoretical interpretations I am going to present. Theoreticians working in this field simply have not had enough time to digest the very interesting experimental results.

We first consider two-body hadronic events. At Frascati, measurements of the cross section for two-pion annihilation [Eq. (8)] have been extended up to $\sqrt{s} \approx 2$ GeV by different groups [3] (the "π–μ Group" and the "Bologna-CERN Group"). The data are preliminary because (i) the number of events is still small, (ii) K^+K^- pairs have not been separated from $\pi^+\pi^-$ pairs, and (iii) the radiative corrections have not been applied. Within errors the

two groups agree, and the quoted values of $|F_\pi(s)|^2$ are in the neighborhood of 1/3 to 1/2 at $s \approx 3$ GeV^2. Recall that $F_\pi(s)$ would be unity at all s for a hypothetical point-like pion and that $|F_\pi(s)|^2$ is as large as 50 at the ϱ peak. If we take the naive ϱ dominance expression $m_\varrho^2/(m_\varrho^2 - s)$ for the pion form factor, we obtain $|F_\pi(s)|^2 \approx 0.05$ at $s \approx 3$ GeV^2, which is considerably smaller than the measured value.

Even more interesting are "multi-body events" observed at Novosibirsk [27] ($\sqrt{s} = 1.2$–1.4 GeV) and Frascati [3] ($\sqrt{s} = 1.6$–2.0 GeV). By these the experimentalists usually mean events with two or more charged-particle tracks in their counter–spark-chamber complex which, unfortunately, covers only a limited fraction of 4π. If the number of visible tracks is two, coplanar events are excluded, which means that three-body processes like $\pi^+\pi^-\pi^\circ$ and $\pi^+\pi^-\gamma$ are not being considered here. It is generally assumed that the observed tracks are due to charged hadrons ($\pi^\pm$, $K^\pm$) when they do not produce electromagnetic showers (like electrons), nor do they penetrate without interactions thick absorbers (like muons) placed in front of the last stage of the spark-chamber complex.

The most significant feature of the multi-body events is that the cross section is comparable to, or even larger than, the muon pair cross section (cf. [6]). This, in my opinion, is one of the major discoveries in high-energy physics this year. Since the detector covers only a fraction of 4π, the exact value of the total hadronic cross section depends sensitively on the average multiplicity assumed, but a relatively model-independent number can be deduced for the cross section for four charged particles plus possible neutrals. For example, assuming that the six-prong processes have a negligible cross section, the "Boson Group" at Frascati has deduced [3]

$$\begin{aligned} k\,\sigma\,(e^+e^- \to 4 \text{ charged particles} + \text{possible neutrals}) = \\ = (31 \pm 3) \text{ nb } (\sqrt{s} = 1.6\text{–}2.0 \text{ GeV}), \end{aligned} \tag{31}$$

where k is a numerical factor which depends only weakly on the ratio of two-prong events to four-prong events and is estimated to be in the neighborhood of 1 to 1.3. The data are shown in Fig. 4. When the Novosibirsk events are analyzed in the same manner, even a larger cross section is obtained [27], $\sigma \approx (80 \pm 40)$ nb at $\sqrt{s} \approx 1.3$ GeV. To appreciate the magnitude of the observed multi-body cross section, let us recall that at $\sqrt{s} = 1.3$ GeV and 1.8 GeV, the muon pair cross section is 52 nb and 26 nb, respectively. As a function of the energy, the multi-body cross section does not appear to show resonance structure even though a very broad resonance or a series of overlapping resonances cannot be excluded by the available data. [The dip in Fig. 4 at $\sqrt{s} = 1.85$ GeV is not significant because it is not seen in the data of the other two groups ("Bologna–CERN" and "π–μ")].

What are the possible theoretical interpretations? By far the most popular among theoreticians are "point–like" theories which attempt to relate the large hadronic cross section in electron—positron collisions to the large cross section for inelastic—proton scattering measured in the famous SLAC-MIT collaboration. Indeed, as early as 1967 BJORKEN [28] conjectured that the total hadronic cross section in electron – positron collisions might be as large as a point-like cross section, i.e. something like the muon pair cross section. The

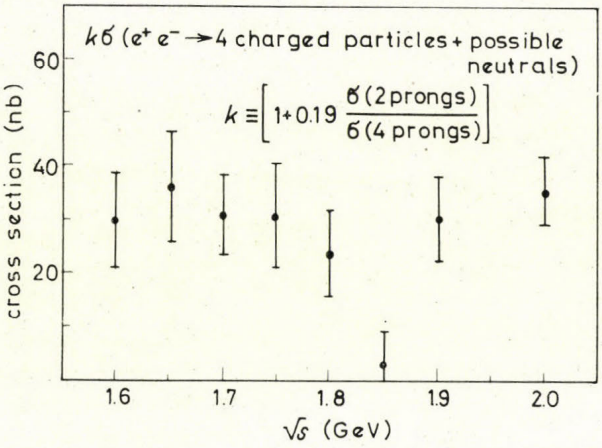

Fig. 4. The total cross section for $e^+ e^- \to 4$ charged particles plus possible neutrals, as measured by the "Boson Group". Note that the numerical factor k is expected to be in the neighborhood of 1 to 1.3

asymptotic energy dependence expected from BJORKEN's argument (based originally on the quadratic divergence of the Schwinger term in the quark density algebra) is of the form $1/s$, which is compatible with the data. This energy dependence can be easily understood on the basis of dimensional considerations; if no "mass" plays an essential role at asymptotic energies, the scale of the cross section which has the dimension of M^{-2} can be set only by $1/s$. In contrast to this $1/s$ dependence, there are asymptotic predictions based on gauge-field algebra or vector-meson dominance which predict a faster fall-off of the hadronic cross section [29]; they appear to be ruled out by the data provided, of course, that the Novosibirsk—Frascati region is already asymptotic.

Before we abandon vector-meson dominance altogether, it is worth examining how large a cross section for multi-pion events is expected from the coupling of the ϱ tail to four-pion states. The only serious calculation along this line is that of KRAMER, URETSKY and WALSH [30] who estimate at Frascati energies

$$\begin{aligned} \sigma(A_2^{\pm}\pi^{\mp}) &\approx 2.0 \text{ nb}, \\ \sigma(A_1^{\pm}\pi^{\mp}) &\approx 3.0 \text{ nb}, \\ \sigma(\omega\pi^{\circ}) &\approx 2.5 \text{ nb}, \\ \sigma(\varrho^{\pm}\varrho^{+}) &\approx 0.3 \text{ nb}. \end{aligned} \tag{32}$$

Notice that the last two final states do not contribute to four-prong events and that only half of the first two final states gives rise to four-prong events. It appears that even if we add them all up, we cannot explain the large cross section observed at Frascati. However, we should keep in mind that the predicted cross section is not entirely negligible.

So far we have tacitly assumed that the observed multi-body events are one-photon processes of the kind represented in Fig. 5(a). One may naturally ask whe ther higher-order electromagnetic processes might compete favorably. In particular let us consider "photon–photon collision" processes represented in Fig. 5(b), which have received much attention in recent weeks. The cross

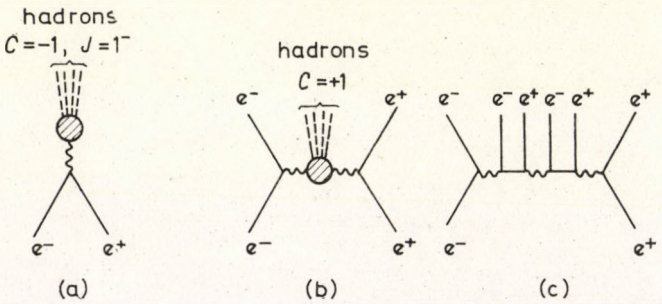

Fig. 5. (a) Conventional one–photon processes; *(b)* "photon–photon collision" processes; *(c)* SERBO mechanism

section for this type of processes is large only when the virtual photons have small q^2 (almost real photons); this means that the electron and positron tend to proceed in the beam direction, hence they necessarily escape the detector placed at large angles. Crude arguments based on counting the powers of α and logarithms suggest

$$\sigma(e^+e^- \to e^+e^- + \text{hadrons}) \sim \left(\frac{\alpha}{\pi}\right)^2 \frac{\alpha^2}{m_\pi^2} \left(\ln\left(\frac{s^2}{m_e^2}\right)\right)^2 \tag{33}$$

up to possible powers of $\ln(s/m_\pi^2)$. More detailed formulas expressing the cross section as an integral over $\sigma(\gamma\gamma \to \text{hadrons})$ have been obtained by BALAKIN, BUDNEV and GINZBURG [31] and by BRODSKY, KINOSHITA and TERAZAWA [32, 33]. It appears from their formulas that this type of mechanisms cannot

give rise to a cross section comparable to the Novosibirsk—Frascati cross section unless (i) the asymptotic cross section for $\gamma\gamma \to$ hadrons is more than an order of magnitude larger than that estimated by factorizable Pomeron couplings or by vector-meson dominance, and/or (ii) the decay width of $\eta(960) \to 2\gamma$ is abnormally large, say > 200 keV (or there are other mesons with very large couplings to 2γ). However, because the cross section is predicted to increase with increasing s, these processes are expected to dominate over one-photon processes at sufficiently high energies.

Even a more radical proposal has been made. It was pointed out by SERBO [34] that the cross section for

$$e^+e^- \to e^+e^- + e^+e^- + e^+e^- \tag{34}$$

represented by Fig. 5(c) is quite large:

$$\sigma(e^+e^- \to e^+e^- + e^+e^- + e^+e^-) =$$
$$= \frac{1}{6}\left(\frac{\alpha}{\pi}\right)^2 \sigma(\gamma\gamma \to e^+e^- + e^+e^-)\left(\ln\left(\frac{s}{m_e^2}\right)\right)^4, \tag{35}$$

where $\sigma(\gamma\gamma \to e^+e^- + e^+e^-)$ is energy-independent at high energies and is given by [35]

$$\sigma(\gamma\gamma \to e^+e^- + e^+e^-) = \frac{\alpha^4}{9\pi m_e^2}\left(\frac{175}{4}\xi(3) - \frac{19}{2}\right) \approx 6\mu\text{b} \tag{36}$$
$$(\xi(3) \approx 1.20).$$

Notice that the scale of the cross section for (34) is determined not by $1/s$ or $1/m^2_{\text{hadron}}$ but by $1/m_e^2 \approx 4(137)^2/m_\pi^2$; in addition, we gain four powers of $\ln(s/m_e^2)$, and at Frascati energies $[\ln(s/m_e^2)]^4 \approx 4(137)^2$. As a result, despite the high powers of α, the cross section is as large as 400 nb at $\sqrt{s} \approx 2$ GeV. When I learned about SERBO's calculation, I started wondering whether low-energy electrons or positrons which do not develop electromagnetic showers might simulate hadrons. Because of the large cross section indicated by Eqs (35) and (36), even if only a small fraction of SERBO-type events get confused with genuine hadronic events, the degree of contamination might be appreciable. I personally doubt that the majority of the multi-body events are of this type, but the experimentalists should be aware of possible backgrounds due to pure QED processes of this kind [36]. [Note added: The possibility that the Frascati (as well as Novosibirsk) groups are seeing SERBO-type processes was extensively discussed in the Informal Meeting on Electron–Positron Colliding Beams, which took place at Frascati a week after this talk was given. Unfortunately there was no unanimity of opinions on the vital question: What percentage of the multi-body events involve electron tracks?]

V. Outlook

In conclusion I would like to mention that the enormous amount of knowledge accumulated in the past few years at Orsay, Novosibirsk and Frascati may well be overshadowed by what we are likely to learn in the next five years. This is because there will be new colliding-beam facilities at Novosibirsk (VEPP III), Cambridge (the CEA By-pass), SLAC (SPEAR) and DESY (DORIS) which will explore higher energy regions with luminosities 20 to 2000 times the present Adone luminosity.

This fascinating field is still in its infancy. I hope I have succeeded in conveying to you some of the enthusiasms and excitements of experimentalists and theoreticians exploring this new frontier of high-energy physics.

REFERENCES

1. Actually I am in a more fortunate position than RICHARD WILSON, who, as a rapporteur at the Kiev Conference, had to cover this interesting subject in fifteen minutes.
2. Throughout the paper $\sqrt{s}$ stands for the total center-of-mass energy of the e^+e^- system. Quite often in the literature, E (the energy per beam) is used. Notice $\sqrt{s} = 2E$.
3. Throughout the paper the various groups working at Frascati (Adone) are referred to in the following manner:
   (i) The "$\pi-\mu$ Group" (or the Conversi-Grilli Group): G. BARBIELLINI et al.; B. BORGIA et al.
   (ii) The "Boson Group" (or the Silvestrini Group): B. BARTOLI et al.
   (iii) The "Bologna–CERN Group" (or the Zichichi Group): V. ALLES-BORELLI et al.
   (iv) The "$\gamma\gamma$ Group" (or the Salvini Group), R. BALDINI-CELIO et al. The Frascati data quoted in our paper are taken from the papers submitted to the Kiev Conference by these four groups.
4. V. E. BALAKIN et al., (contributed paper to the Kiev Conference).
5. N. M. KROLL, Nuovo Cimento, **45A**, 65, 1966.
6. For review see, e.g., S. J. BRODSKY and S. D. DRELL, Ann. Rev. Nucl. Sci., (to be published).
7. T. D. LEE and G. C. WICK, Nucl. Phys., **B9**, 209, 1969.
8. V. L. AUSLANDER et al., Phys. Letters, **25B**, 433, 1967.
9. J. E. AUGUSTIN et al., Phys. Rev. Letters, **20**, 129, 1968; Phys. Letters, **28B**, 508, 1969.
10. W. R. FRAZER and J. R. FULCO, Phys. Rev. Letters, **2**, 365, 1959; Phys. Rev., **117**, 1609, 1960.
11. G. F. CHEW and S. MANDELSTAM, Phys. Rev., **119**, 467, 1960; L. S. BROWN and R. L. GOBLE, Phys. Rev. Letters, **20**, 346, 1968.
12. G. J. GOUNARIS and J. J. SAKURAI, Phys. Rev. Letters, **21**, 244, 1968.
13. The figures are taken from J. HAISSINSKI in the "Proceedings of the Conference on $\pi\pi$ and $K\pi$ Interactions" (May 1969, Argonne National Laboratory) p. 373.
14. Actually a more complete expression, Eq. (11) of [12] has been used in the two-parameter fit.
15. S. OKUBO, Phys. Letters, **5**, 165, 1963.
16. S. WEINBERG, Phys. Rev. Letters, **18**, 507, 1967.
17. T. DAS, V. S. MATHUR and S. OKUBO, Phys. Rev. Letters, **19**, 470, 1967; J. J. SAKURAI, Phys. Rev. Letters, **19**, 803, 1967.
18. R. J. OAKES and J. J. SAKURAI, Phys. Rev. Letters, **19**, 1266, 1967.
19. N. M. KROLL, T. D. LEE and B. ZUMINO, Phys. Rev., **157**, 1376, 1967.
20. S. COLEMAN and H. J. SCHNITZER, Phys. Rev., **134B**, 863, 1964.
21. In the literature, in addition to θ, the angles θ_Y and $\theta_B(=\theta_N)$ also appear frequently. In our scheme (the "current mixing" model) the three angles are related by

$$\tan\theta = (m_\omega/m_\varphi)\ \tan\theta_Y = (m_\varphi/m_\omega)\ \tan\ \theta_B.$$

   See especially KROLL, LEE and ZUMINO [19].

22. J. E. Augustin et al., Phys. Letters, **28B**, 513, 517, 1969; J. C. Bizot et al., Phys. Letters, **32B**, 416, 1970
23. For other theoretical schemes, see H. Sugawara, Phys. Rev. Letters, **21**, 772, 1968; E. Cremmer, Nucl. Phys., **B15**, 131, 1970; I. Kimel, to be published. See also Das, Mathur and Okubo [17].
24. The concept of "current mixing" can be formulated without reference to broken SU(3). This means that the two determinations of θ could agree even if the sum rule (23) were violated. If we use "mass mixing", the θ appearing in Eq. (30) must be compared to θ_V defined by $\tan^2\theta_V = (m_\varphi/m_\omega)$ $[\Gamma(\omega \to e^+e^-)/\Gamma(\varphi \to e^+e^-)]$. Empirically $\theta_V = (41 \pm 3)°$. It therefore appears that the current-mixing is in better agreement with the Orsay data. See also J. J. Sakurai in the "Proceedings of the International Symposium on Electron and Photon Interactions at High Energies" (Liverpool, September 1969) p. 91.
25. J. E. Augustin et al., Nuovo Cimento Letters, **2**, 214, 1969.
26. M. Gourdin, L. Stodolsky and F. M. Renard, Phys. Letters, **30B**, 347, 1969; R. G. Sachs and J. F. Willemsem, Phys. Rev., **D2**, 133, 1970.
27. V. E. Balakin et al. (contributed paper to the Kiev Conference).
28. J. D. Bjorken, Phys. Rev., **148**, 1467, 1967; V. N. Gribov, B. L. Ioffee and I. Ya. Pomeranchuk, Phys. Letters, **24B**, 554, 1967. For more recent "point-like" models, see e.g. S. D. Drell, D. J. Levy and T.-M. Yan, Phys. Rev., **187**, 2159, 1969; N. Cabibbo, G. Parisi and M. Testa, Lett. al Nuovo Cimento, **4**, 35, 1970.
29. J. Dooher, Phys. Rev. Letters, **19**, 600, 1967; J. J. Sakurai in "Quanta, Essays in Theoretical Physics Dedicated to Gregor Wentzel" (edited by P. G. O. Freund, C. J. Goebel and Y. Nambu, University of Chicago Press, Chicago 1970), p. 247.
30. G. Kramer, J. L. Uretsky and T. F. Walsh, Phys. Rev., **D3**, 719, 1971.
31. V. E. Balakin, V. M. Budnev and I. F. Ginzburg, JETP Letters, **11**, 388, 1970 [translated from ZhETF Pis. Red., **11**, 559, 1970] and a more detailed paper contributed to the Kiev Conference.
32. S. J. Brodsky, T. Kinoshita and H. Terazawa, Phys. Rev. Letters, **25**, 972, 1970.
33. "Photon–photon collision" processes have previously been considered by many authors: F. E. Low, Phys. Rev., **120**, 582, 1960; F. Calogero and D. Zeemach, Phys. Rev., **120**, 1860, 1969; N. A. Romero, A. Jaccarini and P. Kessler, C. R. Acad. Sci., Ser. **B296**, 153, 1133, 1969.
34. V. G. Serbo, JETP Letters **12**, 39, 1970 [translated from ZhETF Pis. Red., **12**, 50, 1970].
35. I have been informed by Serbo that Eq. (2) of [34] should be replaced by Eq. (36) of the present paper.
36. The reader may wonder why we do not consider $e^+e^- \to e^+e^- + e^+e^-$ (the process obtained by replacing the hadrons in Fig. 5(b) by an electron-positron pair) which, of course, has an even bigger cross section $\sim(\alpha^4/\pi m_e^2)$ $[\ln(s/m_e^2)]^3$. It can be seen, however, that in this case the two charged tracks emerging from the middle of the photon line must be essentially coplanar; this is because the electron pair is created by almost real photons moving in the beam direction. When the Frascati groups give their multibody cross section, they specifically exclude events with non-coplanarity angles smaller than 20°. On the other hand, $e^+e^- \to e^+e^- + e^+e^-\gamma$ could be confused with $e^+e^- \to \pi^+\pi^-$ + neutrals.

ТЕОРЕТИЧЕСКИЕ ИСТОЛКОВАНИЯ НОВЫХ ЭКСПЕРИМЕНТОВ ПО СТОЛКНОВЕНИЮ ЭЛЕКТРОННОГО И ПОЗИТРОННОГО ПУЧКОВ

Й. Й. САКУРАИ

Резюме

Подытожены теоретические следствия новых экспериментов по столкновению электронного и позитронного пучков с точки зрения прверки чистой квантовой-электродинамики, а также изучения векторных мезонов ϱ, ω, φ, и граничной области выше ϱ, ω и φ.

Acta Physica Academiae Scientiarum Hungaricae, Tomus 31 (1—3), pp. 21—31 (1972)

LIGHT CONE EXPANSIONS AND APPLICATIONS

By

R. A. BRANDT*

DEPARTMENT OF PHYSICS, NEW YORK UNIVERSITY, NEW YORK, USA

Different implications of general light cone expansions of the current products are reviewed.

In this lecture I shall describe some attempts [1–6] made by myself and others in the past two years to increase the domain of applicability of quantum field theory in particle physics. The introduction of current algebra some years ago led to a revival of field theoretic configuration space techniques, but the observable consequences of the equal-time commutation relations of current algebra (with PCAC) are limited to low energy theorems and indirect information obtained from knowledge of amplitudes in the unphysical BJORKEN limit. We shall see here how knowledge of the behaviour of current products near the light cone $x^2 = 0$, rather than just at equal time $x_0 = 0$, leads to a description of a much richer class of physical phenomena.

The relevance of the light cone (LC) to these processes was pointed out in [1], and further studied in [2] and [3]. These investigations involved essentially only the LC behaviour of matrix elements of the current products. In the last year, PREPARATA and myself have derived operator expressions which describe this LC behaviour [6]. Most of this lecture will be concerned with the properties and applications of these operator expansions.

We begin by showing what physical quantities and in what region of momentum space the LC is relevant.

Let us first consider the weak or electromagnetic scattering of a lepton of a hadronic system α to produce an arbitrary final hadronic state. Calling q the momentum transferred to the lepton and ϱ the total momentum of the system α, the total cross-section of interest has the form

$$\frac{d^2\sigma^r}{dq^2\,dv} \propto \int d^4k\theta(k_0)\,\delta(k^2-q^2)\,\delta(k\cdot p-v)\int d^4x e^{-ik\cdot x} \times {}_{\text{in}}\!<\alpha\,|J_\mu(x)\,J_\nu(0)|\,\alpha>_{\text{in}} \varepsilon_r^\mu\,\varepsilon_r^\nu. \tag{1}$$

Here $v = q\cdot\varrho$ is the initial energy variable, r is the polarization of the leptons and J_μ is the hadronic current to which the leptons couple. The matrix element

* A. P. Sloan Foundation Fellow.

in (1) is connected and spin averaged. Changing the orders of integration in (1) gives:

$$\frac{d^2\sigma^r}{dq^2\,d\nu} \propto \int d^4x \Delta_p(x,p,\nu,q^3) \underset{\text{in}}{<} \alpha\,|J_\mu(x)\,J_\nu(0)|\,\alpha \underset{\text{in}}{>} \varepsilon^\mu_r \varepsilon^\nu_r. \tag{2}$$

where we have defined

$$\Delta_+(x,p,\nu,q^2) = \int d^4k e^{-ik\cdot x}\theta(k_0)\,\delta(k^2-q^2)\,\delta(k\cdot p-\nu). \tag{3}$$

The form (2) is very useful for our configuration space purposes. The integral (3) can be simply evaluated in the frame $\varrho = (1,\vec{0}) \equiv \varphi$ (we take $\varrho^2 = 1$) to give

$$\Delta_+(x,\varphi,\nu,q^2) = \frac{\pi}{ir}[e^{i(\nu^2+q^2)^{1/2}r} - h.c.]\,e^{-i\nu t}, \tag{4}$$

where we have written $r = |\mathbf{x}|$, $t = x_0$. We refer to the BJORKEN [7] scaling limit as the A limit

$$\nu \to \infty, \quad q^2 \to \infty, \quad \omega \equiv \frac{q^2}{2\nu} \text{ fixed}, \tag{5}$$

and obtain

$$\Delta_+(x,\varphi,\nu,q^2) \xrightarrow[A]{} \frac{\pi}{ir}[e^{i\nu(r-t)+i\omega r} - e^{-i\nu(r+t)-i\omega r}]. \tag{6}$$

Only the regions $r = \pm t$ in the (first/second) term are important and so we can deduce the covariant result

$$\Delta_+(x,p,\nu,q^2) \xrightarrow[A]{} \frac{\pi}{i\tau}\sin\left(\frac{\nu x^2}{2\tau}+\omega\tau\right) \tag{7}$$

in terms of the "transverse" variable

$$\tau^2 \equiv (p\cdot x)^2 - x^2. \tag{8}$$

It follows from (7) that, in the A limit, $\Delta_+(x,p,\nu,q^2)$ is highly oscillating outside of the region

$$\frac{x^2}{3\tau} \lesssim \frac{1}{\nu}, \quad \tau \lesssim \frac{1}{\omega} \text{ or } \quad x^2 \lesssim \frac{3}{q^2}$$

and, therefore, has effective support on the LC $x^2 \sim 0$. Referring back to (2), we see that the A limit of the cross-section can be obtained simply from the

behaviour of $\langle\alpha| J_\mu(x)J_\nu(0) | \beta\rangle$ on the LC. This is precisely the behaviour we have studied in the previous sections.

For reactions in which a hadronic system produces a lepton pair and an arbitrary final hadronic state, the analysis becomes more complicated because of kinematic restrictions on the k space integration region in the analogue of (1). In the frame $p = (\sqrt{s}, \mathbf{0})$, the physical k space region will have the form $\{| \mathbf{k} | < \varkappa(q^2, s)\}$ for some functions $\varkappa(q^2, s)$. Proceeding as above, it can be shown that the relevant configuration space region is given by

$$|x^2 - \varkappa^{-2}| \lesssim \frac{1}{q^2} . \tag{9}$$

So, for large q^2 and $\varkappa$, the LC is again the dominant region. The extra condition that $\varkappa(q^2, s)$ be large can be satisfied in many cases of interest.

Another important use of the LC is to determine the behaviour of amplitudes for large values of a single mass variable. We illustrate this by consideration of a scalar vertex function

$$A(q^2, k^2) = \int d^4x e^{-iq\cdot x} \langle 0 | T[A(x), B(0)] | p\rangle. \tag{10}$$

Here $A(x)$ and $B(x)$ are scalar currents and $| p >$ is a state of one scalar particle of momentum $p = q - k$ and mass $p^2 = m^2$. We can write (10) as

$$A(q^2, k^2) = \frac{1}{4\pi} (\nu^2 - m^2 p^2)^{-1/2} \int d^4 x \Delta_1(x, p, \nu, q^2) \langle 0 | T[A(x), B(0)]| p\rangle, \tag{11}$$

where $\nu = q \cdot p = 1/2(q^2 + k^2 - m^2)$. Thus, the behaviour of $A(q^2, k^2)$ [11] for $q^2 \to \infty$ and fixed $q^2/2\nu$, i.e., for fixed q^2/k^2, is determined by the LC behaviour of $A(x)B(0)$. A special case of this limit is the old BJORKEN [8] limit $q^2/k^2 \to \to 0$, in which case only the equal time behaviour of $A(x)B(0)$ is relevant. Another special case is the limit $q^2 \to \infty$ with k^2 fixed so that $q^2/2\nu \to 1$. This limit is important because it determines the number of subtractions needed in fixed k^2 dispersion relations.

Having established the relevance of the LC, we turn to a description of what happens there.

The behaviour of products $A(x)B(0)$ of (renormalized) local field operators at short distances $x^\mu \to 0$ has, in recent years, been understood in renormalized perturbation theory [9–11] and in soluble field theoretic models. One obtains operator expansions of the form

$$A(x)\, B(0) \xrightarrow[x\to 0]{} \sum_{i=0}^{N} F_i(x)\, O_i(0)\,, \tag{12}$$

where $O_1, \ldots, O_N$ is a finite set of local field operators and $F_i(x)$ are functions with singularities $(1/x)^{d_i - d_A - d_B}$ (apart from logs), where the d's are the dimensions of the fields [12]. The momentum space limit corresponding to (12) is, however, unphysical and so, although there are applications, the usefulness of expansions like (12) is somewhat limited. Of much greater physical interest is the behaviour of products like $A(x)B(0)$ near the light cone (LC) $x^2 \to 0$.

It can be shown that operator product expansions near the LC exist and have the form

$$A(x)\,B(0) \xrightarrow[x^2 \to 0]{} \sum_{i=0}^{M} \sum_{n=0}^{\infty} F_{in}(x)\, x^{\alpha_1} \ldots x^{\alpha_n}\, O^{(n)}_{i\alpha,\ldots\alpha_n}(0)\,, \tag{13}$$

where $\{O^{(n)}_{i\,\alpha_1 \ldots \alpha_n}\}$ is an infinite set of local field operators satisfying

$$\dim O^{(n)}_{i\alpha,\ldots\alpha_n} = d_i + n$$

and $F_{in}(x) \sim F_i(x)$ for $x^2 \to 0$. Thus, rather than a finite number of fields as occurs in the short distance case (12), an infinite number of fields occur in the LC expansion (13). Each term

$$T_{in}(x) \equiv x^{\alpha_1} \ldots x^{\alpha_n}\, O^{(n)}_{i\alpha,\ldots\alpha_n}(0)$$

has the same dimension d_i and carries the same LC singularity $\sim F_i(x) \sim$ $\sim x^{d_A + d_B - d_i}$. The short distance behaviour of $T_{in}(x)$ is, however, $x^{d_A + d_B + d_i + n}$ and hence it only contributes a short distance singularity if $n \leq d_i - d_A - d_B$.

We shall not go into the derivation of expansions like (13), but will exhibit a specific example in φ^4 theory. For notational simplicity, we shall here ignore all logarithmic factors even though they actually occur in perturbation theory. We want to discuss the renormalized scalar current operator $j(x) \equiv$ $\equiv :\varphi(x)\,\varphi(x):$. Here and elsewhere we use the colon notation $:A(0)B(0):$ to denote a generalized Wick product of renormalized fields obtained from the ordinary product $A(x)B(0)$ by first subtracting off the singular expansion (12) (or a trivial modification of it) and then taking the limit $x^\mu \to 0$. The resulting quantity can be shown to be a finite local field operator having the same quantum numbers as the free field ordinary Wick product $:A(0)B(0):$ [9–11]. The relevant dimensions in the theory under consideration are $\dim I = 0$, $\dim \varphi =$ $= 1$, $\dim \partial_\alpha \varphi = 2$, $\dim :\varphi\varphi: = 2$, etc. Here I is the unit operator — the trivial local field.

$$j(x)\,j(0) \xrightarrow[x \to 0]{} c_1 \left(\frac{1}{x^2}\right)^2 I + c_2 \left(\frac{1}{x^2}\right) J(0) + c_3 \left(\frac{1}{x^2}\right) x^\alpha :\varphi\, \partial_\alpha \varphi:(0)\,. \tag{14}$$

Here and elsewhere x^2 means $x^2 - i\varepsilon x_0$.

Note that, for $x \to 0$, $(1/x^2)$ is a power more singular than $(1/x^2)x^\alpha$. Near the LC, however, each function has the same singularity and, in fact, an infinite number of terms with this singularity occurs in the LC expansion. The result is

$$J(x)J(0) \xrightarrow[x^2 \to 0]{} c_1 \left(\frac{1}{x^2}\right)^2 I + \frac{1}{x^2} \sum_{n=0}^{\infty} x^{\alpha_1} \ldots x^{\alpha_n} O^{(n)}_{\alpha_1 \ldots \alpha_n}(0). \tag{15}$$

where dim $O^{(n)} = n + 2$. Thus, each term in the sum has dimension two, and carries a LC singularity $1/x^2$. For consistency with (14), we must have

$$O^{(0)} = c_2 j' \quad \text{and} \quad O^{(1)}_{\alpha_1} = c_3 : \varphi \partial_{\alpha_1} \varphi : .$$

The other terms in (15) do not contribute to the short distance limit (14).

We can now calculate the LC behaviour of, for example, the expectation value of $j(x)j(0)$ in the one-particle state of momentum p. We can write

$$\langle p | O^{(n)}_{\alpha_1 \ldots \alpha_n}(0) | p \rangle = a_n p_{\alpha_1} \ldots p_{\alpha_n} + b_n g_{\alpha_1 \alpha_2} p_{\alpha_3} \ldots p_{\alpha_n} + \ldots, \tag{16}$$

where the omitted terms each involve at least one $g_{\alpha\beta}$. Only the first term in (16) therefore contributes to the leading LC singularity of (15). Thus, defining

$$p(\lambda) = \sum_{n=0}^{\infty} a_n \lambda^n, \tag{17}$$

we obtain

$$\langle p | J(x) J(0) | p \rangle_c \xrightarrow[x_2 \to 0]{} \frac{1}{x^2} f(x \cdot p) \tag{18}$$

as the leading LC singularity of the connected matrix element.

Expansions of the form (13) exist and describe the LC behaviour of the product of any local field operators im each order of renormalized perturbation theory and, more generally, in any theory in which expansions of the form (12) exist for all local field products at short distances. They might therefore be abstracted from these models and assumed to be true in the real world. The usefulness of such expansions stems from the fact that they describe the configuration space limit corresponding to the physical momentum space limit in which a very massive current interacts with hadronic systems in a high-energy inelastic collision. Knowledge of the LC expansion for the relevant current product determines the behaviour of the appropriate inelastic cross-sections in the specified limits. The relevance of the LC behaviour of the proton–proton *matrix element* of the product of electromagnetic currents to deep inelastic electron–proton scattering has already been noted [1–3]. The advantages provided by the *operator* expansions are, however, numerous. For example,

they predict (by dimensional analysis) the *strength* of the LC singularity and thereby provide a means of measuring the dimensions of interacting fields; they determine, by their form, properties of inelastic form factors in *several* variables, and they provide relations between form factors describing *different* experiments corresponding to different matrix elements of the current products. Several such applications of LC operator expansions will be described below. The main conclusion we reach is the following: the present experimental results are in good agreement with the canonical singularity structure of renormalizable field theories — they provide no evidence for unrenormalizable theories and/or non-canonical dimensionality.

Expansions similar to (15) are valid for any products in any renormalizable field theory. As an example which will be applied below, we display the result for conserved vector currents:

$$\begin{aligned} J_\mu(x)J_\nu(0) \xrightarrow[x^2\to 0]{} & (\partial_\mu\partial_\nu - g_{\mu\nu}\Box)x^{-2}\sum_n x^{\alpha_1}\dots x^{\alpha_n}R_{0\alpha_1\dots\alpha_n}(0) + \\ & + i\varepsilon_{\mu\nu\alpha\beta}\partial^\alpha x^{-2}\sum_n x^{\alpha_1\cdots}x^{\alpha_n}R^\beta_{\alpha_1\dots\alpha_n}(0) + \\ & + [g_{\mu\nu}\partial_\alpha\partial_\beta - g_{\alpha\nu}\partial_\beta\partial_\mu - g_{\alpha\mu}\partial_\beta\partial_\nu + g_{\alpha\mu}g_{\beta\nu}\Box]\times \\ & \times(\log -x^2)\sum_n x^{\alpha_1}\dots x^{\alpha_n}R^{\alpha\Delta}_{\alpha_1\dots\alpha_n}(0). \end{aligned} \tag{19}$$

Here the $(\log x^2)$ term does not violate our neglect of logs since the log goes away after it is differentiated.

As we have already mentioned, an immediate consequence of our derivations is that operator product expansions near the LC will be valid in any theory in which operator product expansions at short distances are valid. In addition to the renormalizable perturbation theories, this class of theories includes all known exactly soluble field theoretic models. More generally, or rather more phenomenologically, if, as seems to be indicated, short distance expansions are valid in the real world, then so are LC expansions.

Because of a phenomenon which occurs in the Thirring model, we are forced at this point to be more precise about the notion of dimensionality which we have been using. One says that a local field $\chi(x)$ has dimension d if there exists a one-parameter group $U(s)$ of unitary transformations such that

$$V(s)\chi(x)V^{-1}(s) = s^d\chi(sx). \tag{20}$$

Examples are the free massless scalar field with $d = 1$ and free spinor field with $d = 3/2$. We shall refer to this notion of dimension as "dynamical" dimension. For the usual fields in free field theories, dynamical dimension coincides with naive dimension. We shall say a field has canonical dimension if

it has a dynamical dimension equal to that of the corresponding free field. In a theory in which all local fields have dimensions and short distance expansions, such as (12), are valid, application of (20) to (12) implies that the $F_i(x)$ behave as stated like $(1/x)^{d_i - d_A - B}$, with no logarithmic factor. This is what happens in free field theories.

In any finite order of a renormalizable perturbation theory, because of the *occurrence* of logarithmic factors, the renormalized fields do not have well-defined dynamical dimensions. Nevertheless, the short distance behaviour of any Whightman function is, apart from logarithmic factors, the same as it would be if the fields did have canonical dynamical dimensions. Put differently, the short distance behaviour is determined, apart from logs, by the naïve dimensions of the fields. In particular, the nature of short distance expansions, and, by our analysis, of LC expansions are so determined. We shall describe this situation by saying that the fields have effective canonical dimensions.

In any theory with effective canonical dimensionality and with short distance expansions, LC expansions very similar to those given above will exist. Included in such theories are free field models, renormalizable perturbation theories in any finite order, and most of the known exactly soluble models. In theories with effective non-canonical dynamical dimensionality and with short distance expansions, our derivations show that LC expansions will also exist. In these theories, the singular functions will, of course, be somewhat different from those encountered above. The Thirring model is the only one we know of that exhibits non-canonical dynamical dimensionality [13].

A final point we should mention concerns the nature of the sum (if it exists) of the perturbative expansions of the renormalizable field theories. It is possible, and has been suggested, that the logarithmic factors occurring in each order sum up to a power, and so change the dynamical dimensions of the fields. This is what happens in the Thirring model. We suspect that this Thirring model phenomenon arises because of the zero mass particle present and will not occur in realistic models with no massless particles. There is no evidence that the logs of renormalizable perturbation theories add up to a power [14]. In the following we shall point out the existence of empirical indications of the validity of effective canonical dimensionality.

Our purpose now is to use the expansion (19) to study the process $e + p \to e +$ anything. The relevance of the LC behaviour of the matrix element $\langle p | [J_\mu(x), J_\nu(0)] | p \rangle$ to the A limit in this reaction has been known for some time [1–3]. Our use of the *operator* expansion will, however, enable us to deduce a number of new results from the observed scaling behaviour. We follow the notation of [3], where more details and references can be found. We shall first work with the result (19) of ignoring logarithmic factors and afterwards discuss the effect of these logs and of their possible role in changing the singularity structure.

The total cross-section (1) of interest can be written

$$\frac{d^2\sigma}{dq^2\,d\nu} = \frac{\pi\alpha^2}{E^2|q|^2\sin^2(\theta/2)}\left[W_2(q^2,\nu)\cos^2\frac{\theta}{2} + 2W_1(q^2,\nu)\sin^2\frac{\theta}{2}\right], \tag{21}$$

where E is the initial electron energy and θ the scattering angle, and we have set the proton mass equal to unity: $p^2 = 1$. The structure functions are defined by

$$\frac{1}{2\pi}\int d^4x e^{iq\cdot x}\langle p|[J_\mu(x), J_\nu(0)]|p\rangle = (p_\mu - \varrho q_\mu)(p_\nu - \varrho q_\nu)W_2(q^2,\nu) - \\ - \left(q_{\mu\nu} - \frac{q_\mu q_\nu}{q^2}\right)W_1(q^2,\nu), \tag{22}$$

where $\varrho \equiv -\nu/q^2 = (2\omega)^{-1}$, and the A limits are

$$\lim_A \nu W_2(q^2,\nu) = F_2(\varrho), \tag{23}$$

$$\lim_A W_1(q^2,\nu) = F_1(\varrho). \tag{24}$$

The transverse and longitudinal structure functions are

$$F_T = F_1, \quad F_L = \varrho F_2 - F_1. \tag{25}$$

Experimentally [15], Eq. (23) is well satisfied in a non-trivial way [$F_2(\varrho) \sim$ $\sim$ const. for $\varrho \geqq 2$] and F_L/F_T is small, as suggested by the gluon model [16].

It is convenient to introduce new structure functions by writing

$$\frac{1}{2\pi}\int d^4x e^{iq\cdot x}\langle p|[J_\mu(x), J_\nu(0)]|p\rangle = [q^2 p_\mu p_\nu - \nu(p_\mu q_\nu + q_\mu p_\nu) + \\ + \nu^2 g_{\mu\nu}]V_2(q^2,\nu) - (q^2 g_{\mu\nu} - q_\mu q_\nu)V_1(q^2,\nu). \tag{26}$$

Eqs. (22)–(26) imply

$$\lim_A (-\nu^2)V_2(q^2,\nu) = \varrho F_2(\varrho), \tag{27}$$

$$\lim_A \nu V_1(q^2,\nu) = \varrho\, F_L(\varrho). \tag{28}$$

In configuration space Eq. (26) reads:

$$\frac{1}{2\pi}\langle p|[J_\mu(x), J_\nu(0)]|p\rangle = -[\Box q_\mu p_\nu - (p\cdot\partial)(p_\mu\partial_\nu + p_\nu\partial_\mu) + \\ + (p\cdot\partial)^2 g_{\mu\nu}]\hat{V}_2(x^2, x\cdot p) - (\partial_\mu\partial_\nu - \Box g_{\mu\nu})\hat{V}_1(x^2, x\cdot p), \tag{29}$$

in terms of the Fourier transforms

$$V_i(q^2, \nu) = \int d^4x e^{iq\cdot x} \hat{V}_i(x^2, x\cdot p). \tag{30}$$

The A limit of the V_i's is given by the LC behaviour of the $\hat{V}_i$'s and these can be determined from (19). We define as in (4)–(7) the matrix elements

$$\langle p|\sum_n x^{\alpha_1}\ldots x^{\alpha_n} R_{0\alpha_1\ldots\alpha_n}(0)|p\rangle = f_0(x\cdot p)+O(x^2), \tag{31}$$

$$\langle p|\sum_n x^{\alpha_1}\ldots x^{\alpha_n} R^{\alpha\beta}_{2\alpha_1\ldots\alpha_n}(0)|p\rangle = g^{\alpha\beta}f(x\cdot p)+p^\alpha p^\beta p_2(x\cdot p)+O(x^2). \tag{32}$$

Comparison with Eq. (29), using

$$\mathrm{Im}\,(x^2 - i\varepsilon x_0)^i = \pi\varepsilon(x_0)\delta(x^2),\ \mathrm{Im}\log(-x^2 + i\varepsilon x_0) = \pi\varepsilon(x_0)\theta(x^2), \tag{33}$$

gives the results

$$\hat{V}_2(x^2, x\cdot p) \xrightarrow[x^2\to 0]{} -\varepsilon(x_0)\theta(x^2)f_2(x\cdot p), \tag{34}$$

$$\hat{V}_1(x^2, x\cdot p) \xrightarrow[x^2\to 0]{} -\varepsilon(x_0)\delta(x^2)f_0(x\cdot p). \tag{35}$$

These are precisely the LC behaviours shown in [3] to be equivalent to the scaling laws (27) and (28) or (23) and (24). Indeed, direct substitution of (34) and (35) into (30) gives the results (27) and (28) with

$$\varrho F_2(\varrho) = -2\pi\int d\lambda\, e^{-i\lambda/2\varrho}\lambda f_2(\lambda), \tag{36}$$

$$\varrho F_L(\varrho) = -\frac{\pi i}{2}\int d\lambda\, e^{-i\lambda/2\varrho} f_0(\lambda). \tag{37}$$

We have thus derived the validity of the scaling laws (27) and (28) in the large class of theories in which (26) holds. Strictly speaking, because these theories really give extra logrithmic factors, we can only deduce that (27) and (28) are valid apart from powers of $\log q^2$. Indeed, it is a known fact that in low orders these theories give scaling apart from logs. This is satisfactory, since the presence of such logarithmic factors could easily escape experimental detection at present. One might think that this result is trivial because we have built in scaling via the mass independence of (26). The point is, however, that, because of the possibility of non-canonical dimensions, mass independence is not equivalent to scaling. We can thus reach the strong conclusion that the observed scaling behaviour is consistent with canonical dimensionality, but not with many types of non-canonical dimensionality. If a single operator

with a non-vanishing proton–proton matrix element in (26) had a dimension significantly less than its canonical one, then the scaling limits (27) and/or (28) would be divergent by the corresponding power of q^2. If we further believe in the relevance of a perturbative model, then we can conclude that the logarithmic factors in the model do not add up to significantly change the singularity structure. It is therefore an interesting and non-trivial fact that *non-trivial scaling is equivalent to the presence of the LC singularity structure required by canonical dimensionality.*

We have thus seen how the existence of operator product expansions like (19) enables one to correlate experimental results with the nature of possible field theoretic models for the hadrons. In addition to providing evidence for essentially canonical dimensionality, the observed scaling strongly suggests the relevance of renormalizable field theories. Non-renormalizable models, made finite, say, by the introduction of infitely many subtraction constants, possess much worse LC singularities. A further major advantage of our formalism is that, unlike the matrix element statements like (34) and (35), it enables one to compare and relate different processes since these processes simply involve different matrix elements of the same operators.

Before leaving electroproduction, we wish to comment on what happens if $F_L = 0$. It is clear from the above analysis that, neglecting the unlikely possibility that the proton–proton matrix element of each $R_{0\alpha_1 \dots \alpha_n}$ in (19) vanishes, $F_L = O$ means that the leading allowed singularity $1/x^2$ in the first piece of (19) is not present. Assuming canonical dimensionality, this means that the $(1/x^2)$ must be replaced by $(\log x^2)$. This comes from both the non-leading contributions of the given operators satisfying dim $R_{\alpha_1 \dots \alpha_n} = n + 2$ and from the leading contributions of additional operators satisfying dim $R_{\alpha_1 \dots \alpha_n} = n + 4$. Calling the matrix element of the sum of these operators still $f_0(x \cdot p)$ as in (31), (32) becomes replaced by

$$\hat{V}_1(x^2, x \cdot p) \xrightarrow[x^2 \to 0]{} -\varepsilon(x_0)\theta(x^2)\,[f_0(x \cdot p) + 2f(x \cdot p)]. \tag{38}$$

To conclude, we shall briefly mention some further applications of the formalism we have developed. Detailed treatments of these applications have been given elsewhere [4, 5].

An especially interesting application [5] is to study the recent measurement [17] of the cross-section $d\sigma/dq^2$ for the reaction proton + proton $\to$ μ pair + anything. Here the double-proton matrix element $\langle pp' | J_\mu(x) J_\nu(0) | pp' \rangle$ is involved and the relevant region is given by (9) with $\varkappa^2 = [(s + q^2 - 4m^2)/|4s] - q^2$ even though $s = (p + p')^2 \to \infty$ in the scaling limit. Most of the experimental points correspond to the LC $x^2 \sim 0$ and so the expansion (19) can be used. The matrix element of $R = \Sigma x^{\alpha_1} \dots x^{\alpha_n} R_{0\alpha_1 \dots \alpha_n}$ etc., is now more complicated, but Regge theory provides an enormous simplification in

that it implies that, for example $\langle pp' \,|R|\, pp' \rangle \underset{s\to\infty}{\rightrightarrows} s^{\varrho}[h(p \cdot x) + h(p' \cdot x)]$ [5]. Further use of Regge theory for the dimensionless structure functions above the value $\varrho \sim 2$ suggested by SLAC enables us to express the cross-sections in terms of a two-parameter function which can be fit very nicely to the data which fall ~ 5 orders of magnitude for $2 \leqq q^2 \leqq 6$ GeV^2.

Another class of applications involves the determination of the asymptotic behaviour of vertex functions when a mass becomes large, as described above [4]. Knowledge of this asymptotic behaviour, plus the information, learned from the electroproduction and μ pair results, that asymptotia sets in at $q^2 \sim 2$ GeV^2, enables us to write the analogue of finite energy sum rules in the mass variable and thus approximately calculate both the "infinite" mass contributions and the continuum contributions. These contributions give corrections to the result of simply saturating the mass dispersion relation with a low lying meson. In this way we can understand, for example, pion pole dominance of matrix elements of the divergence of the axial vector current and we can estimate corrections to vector meson dominance which are in good agreement with experiment. Consider, for example, the $\pi \to 2\gamma$ off-shell amplitude. The asymptotic behaviour in the photon-mass variable is determined from the second piece of Eq. (19). This information enables us to obtain an experimentally correct determination of the rate and also to relate the amplitude to, say, the electroproduction ones via Eq. (19).

REFERENCES

1. R. A. Brandt, Phys. Rev. Letters, **22,** 1149, 1969.
2. R. A. Brandt, Phys. Rev. Letters, **23,** 1260, 1969.
3. R. A. Brandt, Phys. Rev. D., **1,** 2808, 1970.
4. R. A. Brandt and G. Preparata, Brookhaven Preprint, 1970.
5. G. Altarelli, R. A. Brandt and G. Preparata, Rockefeller Preprint.
6. R. A. Brandt and G. Preparata, CERN Preprint TH. 1208, 1970.
7. J. D. Bjorken, Phys. Rev., **179,** 1547, 1969.
8. J. D. Bjorken, Phys. Rev., **148,** 1469, 1966.
9. K. Wilson, unpublished.
10. R. A. Brandt, Ann. Phys. (N. Y.) **44,** 221, 1967.
11. W. Zimmermann, Comm. Math. Phys., **6,** 161, 1967.
12. This dimensional concept is discussed in [9–11] and below.
13. This property of the Thirring model was discovered by K. Wilson, SLAC–PUB–734 (1970).
14. The most recent and elegant account can be found in K. Symanzik, DESY 70–20, 1970.
15. M. Breidenbach et al., Phys. Rev. Letters, **23,** 935, 1969.
16. C. Callan and D. J. Gross, Phys. Rev. Letters, **22,** 156, 1969.
17. J. H. Christenson, G. S. Hicks, L. M. Lederman, P. J. Limon, B. G. Pope and E. Zavattini, to be published.

РАЗЛОЖЕНИЕ В БЛИЗИ СВЕТОВОГО КОНУСА И ЕГО ПРИМЕНЕНИЯ

Р. А. БРАНДТ

Резюме

Приведён обзор различных применений общего разложения близи светового конуса для произведений токов.

Acta Physica Academiae Scientiarum Hungaricae, Tomus 31 (1—3), pp. 33—49 (1972)

RECENT DEVELOPMENTS IN INELASTIC ELECTRON–NUCLEON SCATTERING*

By

F. J. GILMAN

STANFORD LINEAR ACCELERATOR CENTER, STANFORD UNIVERSITY
STANFORD, CALIFORNIA 94305, USA

Inelastic electron—nucleon scattering is discussed. The theoretical ideas are compared with recent experimental data on proton and deuteron target. Particular attention is payed to the duality aspect of the data.

High energy inelastic electron–nucleon scattering probes the instantaneous charge distribution of the nucleon and provides a method for investigating possible substructure. In the year that has passed since the International Symposium on Electron and Photon Interactions at High Energies at Liverpool, a number of important developments have taken place in both the experimental and theoretical aspects of inelastic electron–nucleon scattering [1]. The Kiev conference has, in particular, seen the discussion of a large amount of new data from SLAC, including data on both electron–proton and electron–neutron inelastic scattering [2]. I propose to discuss here these developments, with particular attention to some theoretical consequences of the recent experimental data and to recent work on duality and resonance behavior. A discussion of other aspects of inelastic lepton—hadron scattering and related processes can be found in the proceedings of the Liverpool Symposium and the more recent Naples meeting [3].

The process of inelastic electron–nucleon scattering is shown in Fig. 1 where an electron (with energy E) is incident on a nucleon (of four-momentum

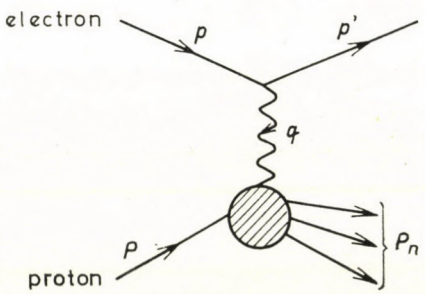

Fig. 1. Kinematics of inelastic electron–nucleon scattering

* Work supported by the U. S. Atomic Energy Commission.

P) and scatters (with resulting final energy E') by an angle θ due to the exchange of a single photon (of four-momentum q). If we do not observe the hadronic final state, as is the case in most of the experiments done until very recently, then the double differential cross section can be written as

$$\frac{d^2\sigma}{d\Omega' dE'} = \frac{4\alpha^2 E'^2}{q^4}\left[2W_1(\nu, q^2)\sin^2\frac{\theta}{2} + W_2(\nu, q^2)\cos^2\frac{\theta}{2}\right], \tag{1}$$

where the structure functions W_1 and W_2 depend on the two (Lorentz scalar) variables $\nu = -q \cdot P/M_N$ and q^2, which can be written in terms of laboratory quantities as (neglecting the lepton mass)

$$\begin{aligned} \nu &= E - E', \\ q^2 &= 4EE' \sin^2\frac{\theta}{2}. \end{aligned} \tag{2}$$

If we know ν and q^2 (from measuring the incident and scattered electron) then the invariant mass W of the final hadrons is fixed by

$$s = W^2 = 2M_N\nu + M_N^2 - q^2. \tag{3}$$

The structure functions W_1 and W_2 that appear in Eq. (1) arise from the quantity

$$\begin{aligned} W_{\mu\nu} &\equiv \frac{1}{4\pi\alpha}\sum_n \langle P|J_\mu^{(em)}(0)|n\rangle\langle n|J_\nu^{(em)}(0)|P\rangle (2\pi)^3\,\delta^{(4)}(p_n - P - q) \equiv \\ &\equiv W_1(\nu, q^2)[\delta_{\mu\nu} - q_\mu q_\nu/q^2] + W_2(\nu, q^2)[(P_\mu - P\cdot q q_\nu/q^2)(P_\mu - P\cdot q q_\nu^{/q^2})]/M_N^2, \end{aligned} \tag{4}$$

which is just $(1/4\pi^2\alpha)$ times the imaginary part of the Feynman amplitude for forward Compton scattering of photons of mass$^2 = -q^2$. Since the optical theorem relates the imaginary part of the forward elastic amplitude to the total cross section, it is no surprise that one can also define [4] total virtual photon–nucleon cross sections for transversely and longitudinally polarized photons, σ_T and σ_S, which are related to W_1 and W_2 and can be used instead of them to describe the results of inelastic electron–nucleon experiments. The relation of W_1 and W_2 to σ_T and σ_S is

$$\begin{aligned} W_1 &= \frac{K}{4\pi^2\alpha}\sigma_T, \\ W_2 &= \frac{K}{4\pi^2\alpha}\frac{q^2}{q^2+\nu^2}(\sigma_T + \sigma_S). \end{aligned} \tag{5}$$

where $K = \nu - q^2/2M_N = (W^2 - M_N^2)/(2M_N)$. Kinematic constraints force σ_S to vanish at $q^2 = 0$, while σ_T at $q^2 = 0$ is just the total photoabsorption cross section for real photons.

Although the kinematics certainly are straightforward and contain no surprises, the experiments on inelastic electron–nucleon scattering have yielded one surprise after another. First was its large size. This size may be simply summarized as being roughly point-like: When the cross section at fixed q^2 is integrated over ν one obtains a result which is the same order of magnitude as the Mott cross section for scattering from a point proton.

The same measurements which showed the point-like size of the scattering also showed a second phenomenon, the scaling behavior proposed by BJORKEN [5]. "Scaling" is the statement that as ν and $q^2 \to \infty$, νW_2 and W_1 become non-trivial functions of the dimensionless ratio $\omega = 2M_N\nu/q^2$ only, rather than functions of both ν and q^2 as would be the case *a priori*. We may look for the scaling behaviour in the data where ν and q^2 are finite by studying the behavior of νW_2 and W_1 at any fixed value of ω as we vary q^2 (and therefore ν) and see if they tend to (non-zero) limiting values as q^2 becomes large. An example of this for νW_2 at $\omega = 4$ is shown in Fig. 2, where νW_2 is seen to have

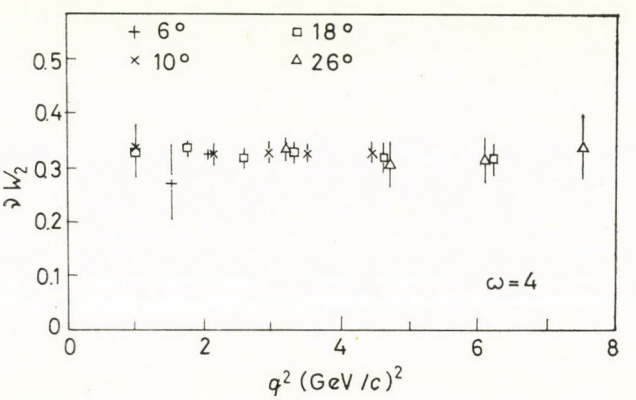

Fig. 2. Values of νW_2 at fixed $\omega = 4$ and various values of q^2

the same value over almost a decade of values of q^2. It is worth emphasizing here that since scaling is a statement of behavior as ν and $q^2 \to \infty$, any other dimensionless variable, ω', such that $\omega' \to \omega$ as ν and $q^2 \to \infty$ is, in principle, just as suitable as ω for studying the scaling behavior of the data. Another variable could in fact lead to the scaling behavior sooner in the sense that νW_2 and W_1 could become independent of q^2 (and hence equal to their $q^2 \to \infty$ limit) for smaller values of q^2 if they are studied as functions of q^2 at fixed ω' rather than ω. This in fact appears to be the case for inelastic electron–proton

scattering where the variable [2, 6]

$$\omega' = 1 + s/q^2 = \omega + M_N^2/q^2 \tag{6}$$

results, particularly for $1 < \omega < 4$, in a more rapid approach to the scaling behavior. This can be seen in Figs. 3 and 4 where we have νW_2 plotted versus ω and ω' for various values of q^2 (all corresponding to $W > 2$ GeV so that we stay away from the prominent N* resonances), and it is clear that νW_2 is more independent of q^2 for smaller values of q^2 when plotted versus ω'. In particular, we can see from Fig. 3, that νW_2 decreases toward its asymptotic value as q^2 increases for fixed ω in the range $1 < \omega < 4$. Fig. 4 shows that νW_2 scales (i.e. is a function of ω' only) to within the accuracy of the data for ω' in the range $1 < \omega' < 10$ as long as $q^2 \geq 1$ GeV^2 and $W > 2$ GeV. Such a small value of q^2 for the onset of scaling is rather remarkable.

In our discussion of scaling and plots of νW_2 we have used a third experimental finding, namely that $R = \sigma_S/\sigma_T$ is small and does not depend

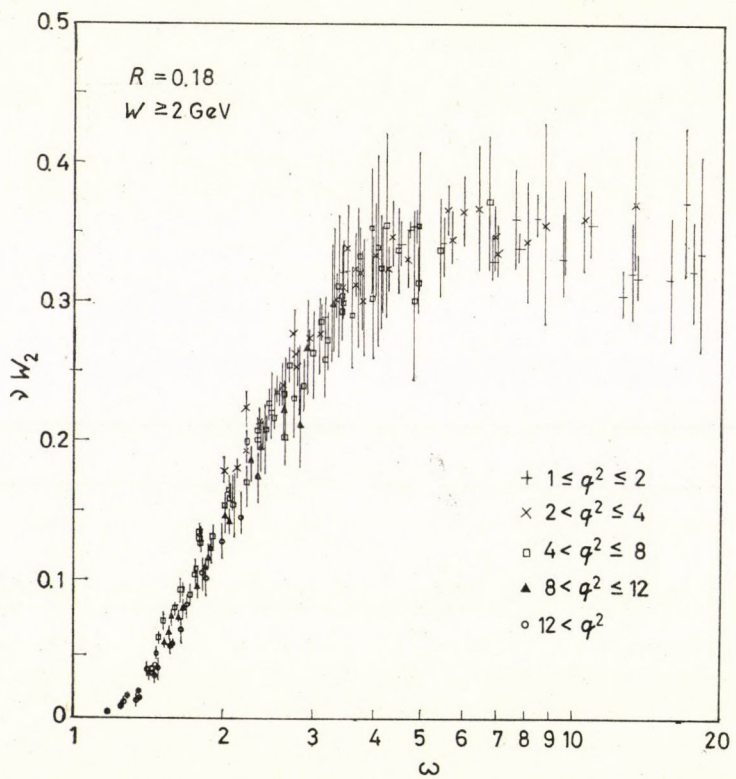

Fig. 3. Values of νW_2 versus $\omega = 2M_N\nu/q^2$ for data with $W > 2$ GeV and various ranges of q^2 (in GeV^2)

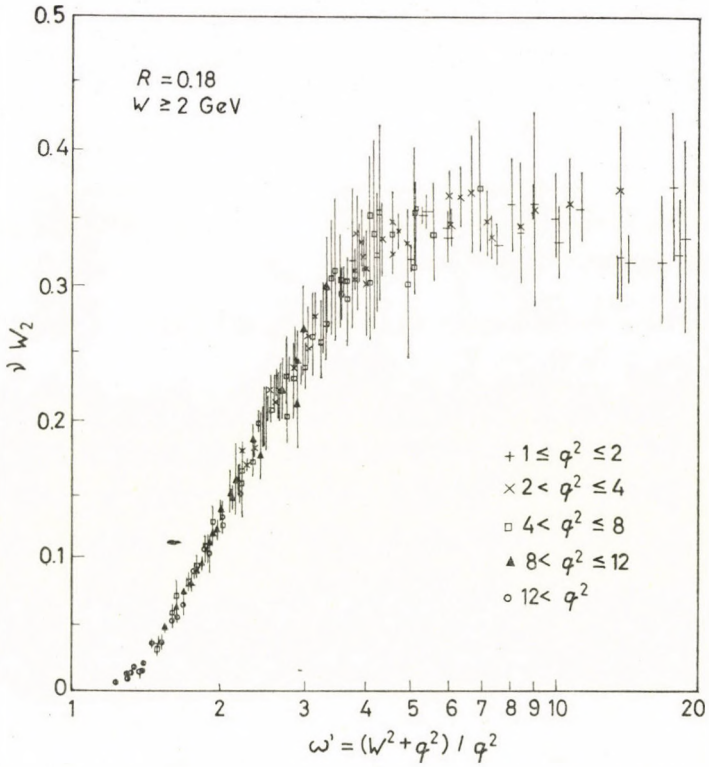

Fig. 4. Values of νW_2 versus $\omega' = 1 + W^2/q^2$ for data with $W > 2$ GeV and various ranges of q^2 (in GeV^2)

strongly on ν, q^2, or ω. The knowledge of R is equivalent to being able to explicitly separate the contributions of W_1 and W_2 to the double differential cross section, Eq. (1). This separation is accomplished by measuring scattering (or interpolating from measurements) at different angles, but the same values of ν and q^2, and has been reported [2] in some detail at Kiev. The value of R obtained by averaging over the 23 interpolated points between ω of 1 and 10 is 0.18 ± 0.05. This is certainly small, and given the possible systematic errors it is possible, although unlikely, that $R = 0$. In any case, it is now possible to plot W_1 and νW_2 at places where the separation has been made and roughly verify the scaling behaviour for *both* W_1 and νW_2. Alternately, one can choose a constant (or some other functional form) for R which is consistent with the data, and plot νW_2 and W_1 for all the data points, as we have done above for νW_2. Such plots are consistent with both νW_2 and W_1 scaling for $1 < \omega' < 10$ (again, as long as $q^2 > 1$ GeV^2 and $W > 2$ GeV).

Some of the most exciting new data concerns the inelastic electron scattering off deuterium, which allows deduction of inelastic electron–neutron cross

sections. Neglecting corrections for internal motion, final state interactions, and Glauber corrections, which should all be small, the neutron cross sections are given by the difference of the deuterium and hydrogen cross sections. Assuming that the ratio of longitudinal to transverse cross sections (or $W_1/\nu W_2$) is the same for the neutron and proton, $\nu W_{2n}/\nu W_{2p} = D/H - 1$. This quantity is shown in Fig. 5 plotted versus ω [7]. Clearly $\nu W_{2n}/\nu W_{2p}$ is smaller than unity in the range $1.5 < \omega < 6$, and further $\nu W_{2n}/\nu W_{2p}$ is a function of ω within the accuracy of the data, i.e., the neutron data also appears to scale. If one plots $\nu W_{2p} - \nu W_{2n}$ from this data plus the earlier proton data, then there appears to be a maximum between ω of 3 and 4, at which point $\nu W_{2p} - \nu W_{2n} = 0.1$ and the ratio $\nu W_{2n}/\nu W_{2p} \approx 2/3$.

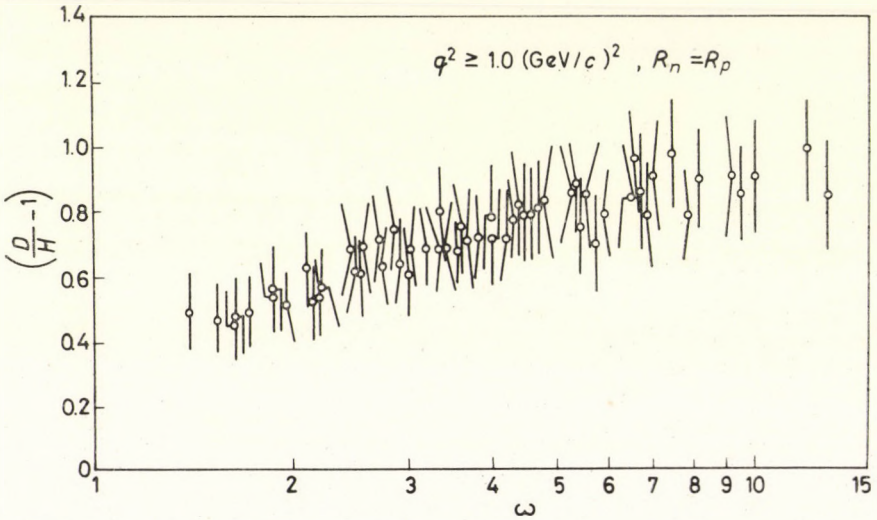

Fig. 5. Values of $(D/H\text{-}1)$ plotted versus ω. All data points have $q^2 \geq 1$ GeV^2. Assuming $R = \sigma_S/\sigma_T$ is the same for neutron and proton and neglecting deuterium corrections (which should be small), the ordinate is $\nu W_{2n}/\nu W_{2p}$

The difference between neutron and proton inelastic scattering is direct evidence for an isospin-dependent and therefore non-diffractive (i.e. not due to Pomeron exchange in the language of Regge theory) component of the virtual photon–nucleon scattering amplitude [8]. Another piece of evidence for such a non-diffractive part lies in the behavior of νW_2 and W_1 for large ω (say $\omega > 10$). Since at large ν and fixed q^2, $\nu W_2 \propto q^2(\sigma_T + \sigma_S)$, one would expect νW_2 to fall with increasing ν at fixed q^2 if there is such a non-diffractive component. Unfortunately, there is no separation of νW_2 and W_1 for $\omega \geq 10$ (nor are there data available with large values of q^2 for $\omega > 10$), and therefore one cannot even say for sure that there is scaling in this region. If we use the same small value of R found for $\omega < 10$, then the data are consistent with

a scaling behavior and νW_2 decreasing for large values of ω. Alternately, one can consider directly the values of σ_T at points (Table III of [2]) where a separation has been made and presented at Kiev. One then finds that σ_T appears to be a maximum between ω of 3 and 4 and at $q^2 = 1.5$ GeV^2 falls at least as much with increasing energy as the total photoabsorption cross section does over the same ν (or W^2) range as at $q^2 = 0$. Thus, with reasonable assumptions it does appear that νW_2 and σ_T do fall with increasing ω, but exactly how much is beyond the ability of present accelerators to establish.

Some of the striking aspects of the data discussed above, particularly the scaling behavior and point-like magnitude of the data, arise naturally in the parton model [9]. In this model one considers the electron–nucleon scattering as taking place in an infinite momentum frame at very large ν and q^2 and the electron is assumed to scatter instantaneously and incoherently off point constituents (partons) of the proton. With these assumptions one finds [9]

$$\nu W_2(\nu, q^2) = \sum_N P(N) \sum_{i=1}^{N} Q_i^2 \, x f_{Ni}(x) = F_2(x = q^2/2m\nu), \tag{7}$$

where $P(N)$ is the probability of N partons, Q_i is their charge and $f_{Ni}(x)$ is their longitudinal momentum distribution in terms of the fraction, $x = 1/\omega$, of the total longitudinal momentum of the nucleon which they carry in the infinite momentum frame. Clearly, since F_2 is a function only of $x = 1/\omega$ in Eq. (7), we have the scaling behavior. The point-like magnitude has been put in through the assumption of point constituents.

Several sum rules follow from Eq. (7). If we assume the same momentum distribution for each of the N partons, then

$$\int_0^1 dx_i \, x_i f_{Ni}(x_i) = 1/N \,, \tag{8}$$

and the sum rule

$$\int_0^1 F_2(x) \, dx = \sum_N P(N) \sum_{i=1}^{N} \frac{Q_i^2}{N} \tag{9}$$

for the mean squared parton charge follows. Partons with $Q_i = \pm 1$ of course yield $\sum_{i=1}^{N} Q_i^2/N = 1$, while for a proton with three quarks as partons, $\sum_i Q_i^2/3 = 1/3$, and a quark-antiquark sea with equal amounts of $p\bar{p}$, $n\bar{n}$, and $\lambda\lambda$ quarks gives $\sum_i Q_i^2/N = 2/9$. Experimentally [2]

$$\begin{aligned} &\int_{0,1}^{1} dx \, F_{2p}(x) \simeq 0.14 \\ &\qquad\qquad (\pm 15\%) \\ &\int_{0,1}^{1} dx \, F_{2n}(x) \simeq 0.10 \end{aligned} \tag{10}$$

from the values of $F_2(\omega)$ constructed with the small angle (6° and 10°) data. The large angle data (with larger values of q^2) and/or using ω' to construct F_2 from the small angle data yield slightly smaller values for $\int_0^1 dx\, F_{2p}(x)$. Since $\int_0^{0.1} dx F_2(x)$, although unmeasured, with any reasonable extrapolation of F_2 to $x = 0$ is less than about 0,03, we see that $\int_0^1 F_{2p}(x)dx$ and $\int_0^1 F_{2n}(x)dx$ are too small to agree with either the simple three-quark or quark-antiquark sea model. One is forced to either disregard the sum rule because an assumption used in its derivation is wrong (e.g., on the same momentum distribution for each parton), or to invoke the presence of neutral partons in addition to the charged ones in order to lower the mean square charge below 2/9. In the first case the sum rule is incorrect, and in the second case it leads to *ad hoc* models with neutral partons to patch up the discrepancy with experiment. Either way the parton model suffers a loss in predictive power.

The assumption on the momentum distribution does not enter the sum rule

$$\int_0^1 \frac{dx}{x} F_2(x) = \sum_N P(N) \sum_{i=1}^N Q_i^2 , \tag{11}$$

which simply follows by integrating Eq. (7) for νW_2 with respect to x and using the normalization condition

$$\int_0^1 dx\, f_{Ni}(x) = 1 . \tag{12}$$

The sum rule (11) was originally proposed by GOTTFRIED [10] in the form

$$\int_0^\infty \frac{d\nu}{\nu} \nu W_2(\nu, q^2) = 1 \tag{13}$$

for the proton (but *not* the neutron) for all q^2 within the context of the quark model [11]. At $q^2 = 0$ this sum rule for the proton is trivially satisfied due to the contribution of the Born term and vanishing (see Eq. (5)) of the continuum. The derivative with respect to q^2 at $q^2 = 0$ of Eq. (13) leads to [10]

$$\int_0^\infty \frac{d\nu}{\nu} \sigma_T(\nu) = 4\pi^2 \alpha \left[\frac{< r^2 >_{1p}}{3} - \frac{(\mu_p)^2}{4M_N^2} \right] \simeq 420\ \mu\text{b} , \tag{14}$$

where $\sigma_T(\nu)$ is the total photon–proton cross section at $q^2 = 0$. If $\sigma_T(\infty)$ is non-zero, the left-hand side of Eq. (14) diverges logarithmically (a similar disease affects Eqs. (11) and (13) if $F_2(0)$ or $\nu W_2(\infty, q^2)$ is not zero). The manner in which Eq. (13) is satisfied at $q^2 = 0$ (by the Born term), however, suggests that if we are to make any sense of Eq. (14), the constant part (due Pomeron exchange in Regge language) of the total cross section (or νW_2) corresponding

to the diffractive part of forward Compton scattering should not be counted in the sum rule. Rather, we should include only the direct channel resonances and non-diffractive part of the amplitude. Unfortunately, it is difficult and, more importantly, ambiguous to separate an amplitude into "resonant" and "non-resonant" or "non-diffractive" and "diffractive" contributions, particularly at low energies. If we proceed boldly and subtract from $\sigma_T(\nu)$ at high energies the quantity $\sigma_T(\infty) \simeq 100\ \mu$b as the constant part of the photon–proton total cross section at high energies [12], then we obtain values [13] ranging from 400 to 550 μb for the integral on the left-hand side of Eq. (14), depending on how we extrapolate the constant part of σ_T at high energies into the low energy region ($W < 2.0$ GeV). Thus, if we interpret Eq. (13) as being a sum rule for the non-diffractive part of the forward Compton amplitude, it appears to be quite possible that the resulting Eq. (14) is satisfied within the rather large ambiguities in defining what is meant by the words "non-diffractive part".

Going to the opposite limit of large q^2 and using the scaling property of νW_2, Eq. (13) goes over to Eq. (11) with the right-hand side equal to 1 in the simple three-quark model [11]. Experimentally, we have that [2]

$$\int_{1/12}^{1} \frac{dx}{x} F_{2p}(x) = 0.58 \quad (\pm 10\%) \tag{15}$$

from the 6° and 10° data. Again, a finite value of $F_2(x)$ at $x = 0$ (i.e. ω or $\nu = \infty$) leads to a logarithmically divergent integral, and if we interpret Eq. (13) as discussed above, we must again somehow extract the non-diffractive part of the amplitude. This is impossible to do without more complete data for the large values of ω. We note, however, that it is possible to obtain the value of 1 given in Eq. (13) for

$$\int_{0}^{1} \frac{dx}{x} F_{2p}(x)$$

with a suitable non-diffractive component of $\nu W_{2p} = F_{2p}$ above $\omega = 12$ (below $x = 1/12$). Then a large part of the observed F_{2p} *both* above and below $\omega = 12$ would have to be non-diffractive in character, something which the present data does not disagree with, but does not necessarily show to be true, either. In summary, it is possible for a suitably interpreted version of Eq. (13) to be true from $q^2 = 0$ to ∞, but it is difficult to give an unambiguous definition of the part of νW_{2p} which is to be included in the sum rule.

The question of extracting a particular component of the amplitude is avoided if we consider

$$\int_{0}^{1} \frac{dx}{x} [F_{2p}(x) - F_{2n}(x)], \tag{16}$$

because the constant part of $F_2(x)$ as $x \to 0$ or $\omega \to \infty$ presumably cancels between the proton and neutron. In a model where the nucleon is made of three quarks or three quarks plus any number of neutral partons (the same neutral partons or quark—antiquark sea for both) the integral in (16) should equal 1/3. Experimentally [2]

$$\int_1^{12} \frac{d\omega}{\omega} [F_{2p}(\omega) - F_{2n}(\omega)] = \int_{1/12}^{1} \frac{dx}{x} [F_{2p}(x) - F_{2n}(x)] = 0.13 \quad (\pm 40\%). \quad (17)$$

A reasonable form (e.g. const./$\omega^{1/2}$) for $F_{2p} - F_{2n}$ for large ω (small x) could make the integral from 0 to 1 in x (1 to ∞ in ω) equal to 1/3, although it requires pushing the values of $F_{2p} - F_{2n}$ to the upper limits of the error bars in the presently available data [2].

In brief, while the parton model is an easy way to remember certain features of the data, detailed qualitative comparison of the resulting sum rules [9] leads to a fairly complicated picture. If taken seriously, sum rules of the form $\int_0^1 dx F_2(x)$ indicate the need for neutral partons, while those of the form

$$\int_0^1 \frac{dx}{x} F_2(x)$$

in any reasonable quark type parton model [14] indicate the need for a large non-diffractive component to the forward virtual photon–nucleon amplitude both above and below $\omega \simeq 10$. Still, the simplest way to remember the data *qualitatively* is a parton model, in which the nucleon is made of three quarks and a quark-antiquark sea, with possibly some neutral partons [15].

Finally, with regard to sum rules, we note that the BJORKEN inequality [16]

$$\int_0^\infty d\nu [W_{2p}(\nu, q) + W_{2n}(\nu, q^2)] \geq 1/2 \,, \quad (18)$$

which can be rewritten at large q^2 using scaling as

$$\int_1^\infty \frac{d\omega}{\omega} (F_{2p} + F_{2n})(\omega) \geq 1/2, \quad (19)$$

is formally satisfied by the data if the upper limit of integration is taken to be at $\omega = 5$. One previously worried that the BJORKEN inequality would be trivially satisfied due to the constant part of $\nu W_2(\nu, q^2)$ as $\nu \to \infty$ ($F_2(\omega)$ as $\omega \to$ $\to \infty$), which leads to the logarithmic divergence of the integral discussed before. However, since we now know that between $\omega = 1$ and 5 νW_{2p} is rather different than νW_{2n}, we can have some confidence that most of the integrand

in this region of ω is not due to a diffractive part of νW_2 and hence the inequality may well be non-trivially satisfied. Similarly, the ADLER sum rule [17] for inelastic neutrino scattering,

$$\int_1^\infty d\nu \, [W_2^{(\bar{\nu})}(\nu, q_2^2) - W_2^{(\nu)}(\nu, q^2)] = 1 \,, \tag{20}$$

from which the BJORKEN inequality is derived, now can be plausibly argued as being correct, but we shall not know for sure until actual experiments are done with neutrinos and anti-neutrinos.

In our discussion of various sum rules above we have seen the importance to the success of several sum rules in the presence of a large non-diffractive component of the forward Compton amplitude for virtual photons. As noted earlier, direct and unambiguous experimental evidence now exists for at least some non-diffractive, isospin-dependent component from the observation of a difference between electron–proton and electron–neutron inelastic scattering. The apparent decrease in νW_2 or $\sigma_T(\nu, q^2)$ for large ω or ν is also evidence for such a component. Such a non-diffractive component of a forward amplitude and the corresponding decreasing total cross section at high energy is correlated with the presence and behavior of resonances at low energy, at least for purely hadronic processes. This correlation is part of the more general concept of duality, and takes quantitative form in terms of finite energy sum rules [18].

Thus we might guess that the resonances, and in particular those resonances that give rise to prominent bumps in the total cross section, could have a behavior which is correlated with other features of inelastic electron scattering [19]. In particular, we would like to compare the behavior of the resonances to the behavior of νW_2 and W_1 in the scaling limit where ν and $q^2 \to \infty$. In the study of the behavior of the resonances, the variable ω' introduced previously, which results in νW_2 and W_1 exhibiting scaling for smaller values of q^2, has an additional advantage. If νW_2 is considered as a function of ω, the resonances occur at values of $\omega > 1$, with any particular resonance moving toward $\omega = 1$ as q^2 increases. On the other hand, the nucleon pole term in νW_2, corresponding to elastic scattering, always occurs at $\omega = 1$. With respect to $\omega' = 1 + W^2/q^2$, however, the nucleon and all other resonances occur at values of $\omega' > 1$ and move toward 1 as q^2 increases. The nucleon is then not treated in a special way compared to other resonances. As we will shortly see, this also allows one to understand in another way the connection found [20] in the parton model between the behavior of the elastic form factors and of νW_2 as $\omega \to 1$.

The behavior of the resonances in comparison to νW_2 in the scaling limit can be seen [19] in Fig. 6 where we have plotted the data for νW_2 versus ω' (assuming $R = \sigma_S/\sigma_T = 0$). The dashed line, which is the same in all cases, is a

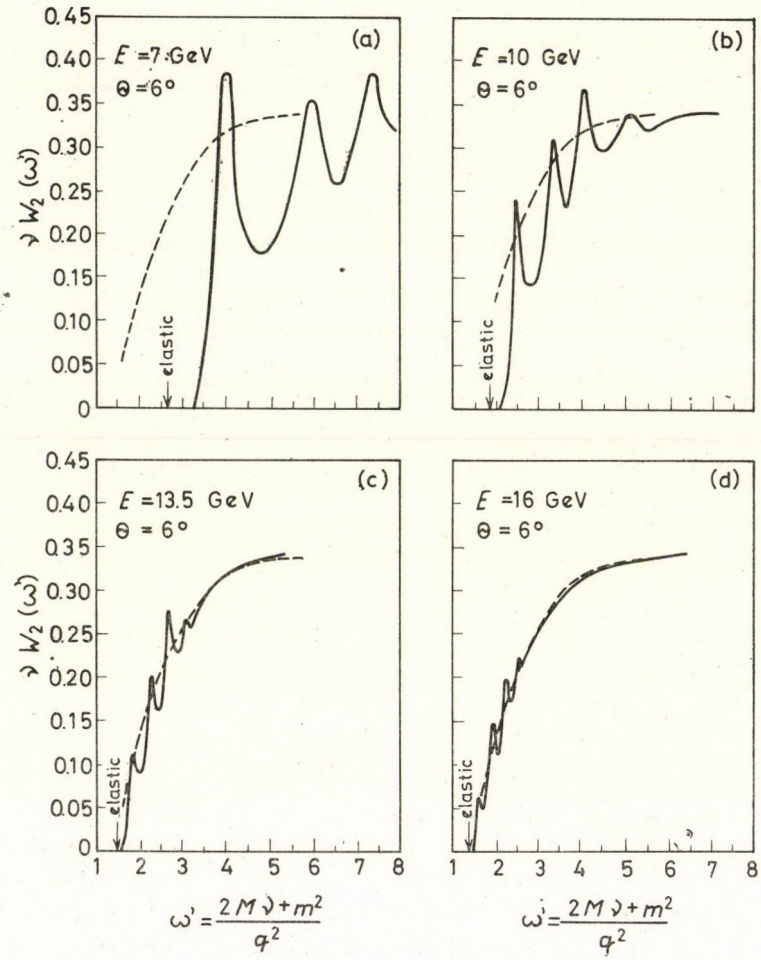

Fig. 6. The function νW_{2p} plotted versus $\omega' = (2M_N\nu + m^2)/q^2$ with $m^2 = M_N$. The solid lines are smooth curves drawn through the $\theta = 6°$ data at various incident energies. The dashed curve, which is the same in all cases, is a smooth curve through large ν and q^2 data. All data are plotted assuming $R = \sigma_S/\sigma_T = 0$. $E = 7$ GeV involves values of q^2 all of which are considered outside the scaling region

smooth curve through the high energy 10° data [21] in the region beyond the prominent resonances ($W > 2.0$ GeV) and with large q^2 ($3 < q^2 < 7$ GeV^2) [22]. We call this dashed line, therefore, the "scaling limit curve" $\nu W_2(\omega')$. The solid lines are smooth curves through the 6° data at various incident energies. As the incident energy E increases, so does q^2 and the resonances and elastic peak move toward $\omega' = 1$.

We note two important things from Fig. 6. First, as similar graphs of the 10° data in the resonance region also show [23], the prominent resonances do not disappear at large q^2 relative to a "background" under them which

has the scaling behavior. Secondly, as q^2 changes, the prominent resonances roughly follow in magnitude the scaling limit curve. Thus, as q^2 changes both the prominent resonances and any "background" have a behavior which is closely correlated with the scaling behavior of νW_2. Note that the ratio of the height of the resonance peak to background and the correlation of the resonance peak height to the scaling limit curve could be seen if we plotted the data with respect to other variables (in particular, ω). However, in addition to not showing the onset of scaling behavior for $W > 2$ GeV at smaller values of q^2, the other plots often require very careful inspection to see these relevant features of the data, while ω' plots allow one to see it at a glance [24].

Thus, at least the prominent resonances do not seem to be a separate entity with a behavior divorced from that of the rest of the data, but instead appear to be an intrinsic part of the scaling behavior. One, of course, cannot determine without a detailed partial wave analysis of the hadronic final state exactly what the many broad, low-spin N^* resonances that we know to exist are doing as a function of q^2. But the behavior of the prominent N^*'s that we can see gives us the clue to what is happening. Using the duality framework [25], we would say that the nucleon and other resonances at low energy build (in the sense of finite energy sum rules) the relevant non-Pomeron exchanges at high energy, which will result in a falling $\sigma_T(q^2, \nu)$ or νW_2 curve and a difference between νW_{2p} and νW_{2n}.

What is unique to studying duality in electroproduction is the experimentally observed scaling behavior. This allows us to consider data at fixed values of ω' but different values of q^2 and W^2, both within and outside the region of prominent resonances. Thus we can compare the *data* where there are prominent narrow resonances directly with *data* for $\nu W_2(\omega')$ for large q^2 and W^2 where nature has accomplished the appropriate averaging of the many broad resonances and the background present there. One can give this comparison quantitative form [26] in terms of finite energy sum rules where we find that $\nu W_2(\omega')$ acts as a smooth averaging function for $\nu W_2(\nu, q^2)$, i.e. the area under $\nu W_2(\nu, q^2)$ should be the same as that under the scaling limit curve $\nu W_2(\omega')$ if we integrate at fixed $q^2 \geq 1$ GeV^2 up to a value of ν or ω' above which the scaling behavior, $\nu W_2(\nu, q^2) = \nu W_2(\omega')$, is true.

In spite of the existence of explicit models [27] of the structure functions as sums of resonances, there has been a point of confusion as to how resonances, which are known to have excitation form factors which fall rapidly with increasing q^2, can be consistent with the "deep inelastic" data which are supposed to be characterized by a slow q^2 variation. The confusion results from the fact that the "deep inelastic" data exhibit (for fixed W, say) more than one q^2 dependence. If $1 + W^2/q^2$ corresponds to an ω' which is larger than ≈ 5, $\nu W_2(\omega')$ varies very slowly and $\sigma_T \propto (1/q^2)\nu W_2 \propto 1/q^2$; but if $1 + W^2/q^2$ corresponds to $\omega' \lesssim 3$, then $\nu W_2(\omega')$ varies rapidly with ω' and hence with q^2

at fixed W. Thus the cross section at, say, $W = 3$ GeV should start falling as $1/q^2$ for small q^2, but when $q^2 \gtrsim 4$ GeV^2, so that we are below the knee of the νW_2 curve, σ_T should fall much faster. We can put this in quantitative form as follows: if $G(q^2)$ is the excitation form factor of the hadronic final state of mass W and

$$G(q^2) \to c(1/q^2)^{n/2} \tag{21}$$

as $q^2 \to \infty$, while νW_2 can be parametrized as

$$\nu W_2(\omega') \to c'(\omega' - 1)^p \tag{22}$$

as $\omega' \to 1$, then we must have

$$n = p + 1. \tag{23}$$

Thus each hadronic final state of mass W, if it is to participate in the scaling behavior, must have an excitation form factor with the same power of fall-off in q^2 as $q^2 \to \infty$, and this power is related to the power with which νW_2 rises at threshold. If we apply this in the low energy region to a given resonance of mass W_R (including the nucleon), we see that all resonances which follow $\nu W_2(\omega')$ in magnitude must have the same power of fall-off in q^2 as $q^2 \to \infty$ (including the elastic with $n \simeq 4$), and again this is related to the behavior of νW_2 at threshold. Eq. (23) for the case of the elastic peak is just the relation of DRELL and YAN [20] first found in the parton model.

The rather local averaging of the resonances by $\nu W_2(\omega')$ seen in Fig. 6 encourages one to go further and make the very strong assumption that at large q^2 the elastic contribution to νW_2 is averaged in the sense of finite energy sum rules by $\nu W_2(\omega')$. Specifically, one assumes that the area under the elastic peak (delta function) in νW_2 is the same as the area under the scaling limit curve $\nu W_2(\omega')$, from $\omega' = 1$ to an ω' corresponding to a hadron mass $W = W_t$ near physical pion threshold. This allows [19] one not only to again establish the connection (23) between the elastic form factor's behavior as $q^2 \to \infty$ and the behavior of νW_2 near $\omega' = 1$, but also allows a quantitative calculation of νW_2 near $\omega' = 1$ from elastic scattering data [28]. Furthermore, the same assumption also predicts from the behavior of the elastic form factors that $R = \sigma_S/\sigma_T \to 0$ as $q^2 \to \infty$ and $\omega' \to 1$, as well as $\nu W_{2n}/\nu W_{2p} \to (\mu_n/\mu_p)^2 = 0.47$ in the same limit. As can be seen from Fig. 5, the 6° and 10° data seem to show that this last prediction is not far from the truth, but only the large-angle deuterium data to be taken soon at SLAC will go to small enough values of ω' to really tell if this is true.

There are many other interesting aspects of inelastic electron–nucleon scattering and related processes which unfortunately cannot be discussed in

this talk, but which are of great importance and will be discussed by others at this Symposium. As already noted, the observation of a difference between electron–proton and electron–neutron inelastic scattering makes it very likely that neutrino and anti-neutrino inelastic scattering are also different. One should also expect non-zero asymmetries in the scattering of polarized electrons or muons on polarized protons, something which will likely be investigated experimentally in the near future. Slightly further afield is the behavior of the cross section for $e^- + e^+ \to$ hadrons. The observation at Frascati of large (i.e. point-like) cross sections is very exciting and again indicates the possible relevance of parton ideas. Such ideas may also be relevant in studying the behavior of muon pair production in hadron–hadron collisions [29].

Altogether, the last few months have seen some real progress in inelastic scattering both experimentally and theoretically. Furthermore, I think that our theoretical progress has not all been of the negative kind, i.e. the elimination of some of the proposed theories and models. We not only have direct experimental evidence for the presence of a substantial non-diffractive, isospin-dependent component of the forward Compton amplitude for virtual photons, but I think we have a much more unified understanding of the relation between the behavior of the elastic form factors and the threshold behavior of νW_2, the behavior of the resonance excitation and the scaling behavior, etc. However, we still do not have a detailed quantitative theory which does more than relate one kind of observed behavior to another. Perhaps this should be no surprise, since such a quantitative theory would probably have to come quite close to being a complete theory of strong interactions and of the composition of hadrons.

REFERENCES

1. For a review of the experimental and theoretical situation as of a year ago, see the invited talks of R. E. TAYLOR and F. J. GILMAN in Proceedings of the Fourth International Symposium on Electron and Photon Interactions at High Energies, Liverpool, 1969.
2. E. D. BLOOM et al., "Recent Results in Inelastic Electron Scattering", SLAC–Pub–796, report presented at the XVth International Conference on High Energy Physics, Kiev, USSR, 1970.
3. See in particular the talk of C. H. LLEWELLYN SMITH, "An Introduction to Highly Inelastic Lepton Scattering and Related Processes", CERN TH–1188, July 1970.
4. L. N. HAND, Phys. Rev., **129**, 1834, 1963. For the connections between the various amplitudes and the kinematics of inelastic scattering, see F. J. GILMAN, Phys. Rev., **167**, 1365, 1968.
5. J. D. BJORKEN, Phys. Rev., **179**, 1547, 1969.
6. More generally, we have $\omega' = (2M_N\nu + m^2)/q^2 = \omega + m^2/q^2$, where m has the dimensions of a mass. Clearly, $\omega' \to \omega$ as $q^2 \to \infty$. We have taken $m = M_N$ in Eq. (6), which, aside from its simplicity, is consistent with the value $m^2 \simeq 0.9$ GeV^2 obtained in a best fit [2] to the data for νW_2.
7. Given the size of the presently quoted errors, one cannot determine if ω or ω' plots are better for $\nu W_{2n}/\nu W_{2p}$.
8. Recall the connection between the imaginary part of the forward Compton amplitude for photons of (mass)$^2 = -q^2$ and the structure functions W_1 and W_2 given in Eq. (4).

When we discuss the "non-diffractive component", in the following we shall always be referring to that part of the forward Compton amplitude which is not due to Pomeron exchange in the language of Regge theory and which leads to a falling part of total cross sections at high energy. It is interesting that the high energy γn and γp total cross sections at $q^2 = 0$ as analyzed in D. O. CALDWELL et al., Phys. Rev. Letters, **25,** 613, 1970, have non-diffractive parts (i.e., the parts falling with energy) which are approximately in the ratio 2/3. This is precisely the ratio expected in the quark model for "deep inelastic" scattering, corresponds to $I = 0$ and $I = 1$ exchanges in Compton scattering with pure F-type coupling at the baryon vertex, and equals $\nu W_{2n}/\nu W_{2p}$ between ω of 3 and 4, where $\nu W_{2p} - \nu W_{2n}$ is a maximum.

9. R. P. FEYNMAN, Phys. Rev. Letters, **23,** 1415, 1969, and unpublished lectures; J. D. BJORKEN and E. A. PASCHOS, Phys. Rev., **185,** 1975, 1969.
10. K. GOTTFRIED, Phys. Rev. Letters, **18,** 1174, 1967.
11. The possible correlation terms vanish in the quark model for the proton, but not for the neutron (see [10]). At large q^2, the correlation terms for both the neutron and proton vanish, and using the scaling behavior of νW_2, Eq. (13) goes over to Eq. (11) with 1 on the right-hand side for the proton and 2/3 for the neutron if we take the quark model for the nucleon to calculate $\sum_i Q_i^2$ in Eq. (11).
12. M. DAMASHEK and F. J. GILMAN, Phys. Rev., D1, 1319, 1970.
13. F. J. GILMAN, unpublished.
14. One is already fairly restricted also by the small measured values of $R = \sigma_S/\sigma_T$, which demand the dominance of spin 1/2 charged partons, and by the deviation of $\nu W_{2n}/\nu W_{2p}$ from unity, which demands different charged partons in the proton and neutron, i.e. the existence of *some* non-diffractive component.
15. Such models have been recently discussed by K. KITANI and H. YOSHII, Tokyo Institute of Technology preprints, July 1970, unpublished.
16. J. D. BJORKEN, Phys. Rev. Letters, **16,** 408, 1966.
17. S. L. ADLER, Phys. Rev., **143,** 1144, 1966.
18. See R. DOLEN, D. HORN, and C. SCHMID, Phys. Rev., **166,** 1768, 1968; H. HARARI, Phys. Rev. Letters, **20,** 1395, 1968; P. FREUND, Phys. Rev. Letters, **21,** 235, 1968; F. J. GILMAN, H. HARARI and Y. ZARMI, Phys. Rev. Letters, **21,** 323, 1968.
19. E. D. BLOOM and F. J. GILMAN, Phys. Rev. Letters, **25,** 1140, 1970.
20. S. D. DRELL and T. M. YAN, Phys. Rev. Letters, **24,** 181, 1970. See also G. WEST, Phys, Rev. Letters, **24,** 1206, 1970.
21. E. D. BLOOM et al., Phys. Rev. Letters, **23,** 930, 1969; M. BREIDENBACH, MIT thesis, 1970. unpublished.
22. The actual data points from both the small and large angle data used in constructing $\nu W_2(\omega')$ can be seen in Fig. 4.
23. See also the prominent resonance peaks in $\sigma_T + \varepsilon\sigma_S$ at $q^2 = 0$, 1, 2 and 4 GeV^2 in Fig. 9 of R. E. TAYLOR, [1].
24. Aside from the scaling behavior which gives an additional reason for preferring ω' rather than ω, the choice between ω' and ω for plotting the data is somewhat similar to the choice between ν and s to extrapolate high energy Regge pole fits into the low energy region. Although an extrapolation using s instead of ν in the forward amplitude for pion-nucleon charge exchange results in a much poorer averaging of the low energy resonances, this does not change the physics, i.e, that the sum of the resonance contributions to the amplitude suitably averaged is equal to the Regge pole amplitude, and the two should not be added to each other. Similarly, here one may get a better or worse local averaging using a different variable, but it does not change the physics of the correlation between the behavior of resonance excitation and the scaling behavior.
25. This application of duality ideas to inelastic electron scattering differs from the previous one of H. HARARI, Phys. Rev. Letters, **22,** 1078, 1969, in the interpretation of the data for resonance electroproduction and the behaviour of νW_2 for large ω, aside from the fact that the proposal of Pomeron-exchange dominance given in the above paper is ruled out by the difference between electron—proton and electron—neutron inelastic scattering.
26. See Eq. (1) and the discussion following it in E. D. BLOOM and F. J. GILMAN [19].
27. See in particular the Veneziano-like model of P. V. LANDSHOFF and J. C. POLKINGHORNE, Nuclear Phys., **B19,** 432, 1970, and the work of G. DOMOKOS and S. KÖVESI-DOMOKOS, Johns Hopkins University preprint, 1970, unpublished.
28. The calculated $\nu W_2(\omega')$ curve for $1 > \omega' > 1.5$, using an appropriate choice of W_t, averages the data in the resonance region of the highest energy (17.7 GeV) 10° data, and appears

to agree also with the scaling limit curve which results from the analysis of the large angle data with $W < 2$ GeV (see [19]). Also see the talk of M. NAUENBERG at this Symposium on finite energy sum rules to construct $\nu W_2(\omega)$.

29. Some of these subjects have been covered in the talks at this Symposium by Drs. KUTI, GÁLFI, KUNSZT, SARTORI and BRANDT.

РАЗВИТИЕ В ОБЛАСТИ ИЗУЧЕНИЯ НЕУПРУГОГО РАССЕЯНИЯ ЭЛЕКТРОНОВ НА НУКЛОНАХ

Ф. ДЖ. ГИЛМАН

Резюме

Рассмотрено неупругое рассеяние электронов на нуклонах. Теоретические выводы сравниваются с новыми экспериментальными данными, полученными на протонной и электронной мишенях. В частности, обращено внимание на аспект двойственности экспериментальных данных.

Acta Physica Academiae Scientiarum Hungaricae, Tomus 31 (1—3), pp. 51—54 (1972)

FINITE ENERGY SUM RULES AND SCALING*

By

M. NAUENBERG

UNIVERSITY OF CALIFORNIA, SANTA CRUZ, USA

A conjectured finite-energy sum rule is evaluated for deep-inelastic electron—proton scattering. The possibility that the sum rule is satisfied locally is also examined.

Finite energy sum rules have been applied successfully to relate the average value of strong interaction resonance cross-sections in a two-particle reaction with its Regge asymptotic high energy behavior [1]. Recently it has been proposed [2–4] that if the scaling limit [5] is valid for inelastic electron–nucleon scattering, an analogous sum rule may hold for the imaginary part $W_2(\nu, q^2)$ of forward virtual photon–nucleon scattering. For large values of q^2 and $\nu = qp/M$, where q and p are the photon and nucleon momenta, the function νW_2 appears experimentally [6] to scale, i.e., it becomes a function of only the ratio of ν and q^2,

$$\nu W_2(\nu, q^2) \to F(\omega), \tag{1}$$

where $\omega = 2M\nu/q^2$. The conjectured finite energy sum rule for large q^2 is

$$\frac{1}{q^2}\int_{q^2/2M}^{\nu_m} d\nu \nu W_2(\nu, q^2) = \frac{1}{2M}\int_1^{2M\nu_m/q^2} d\omega\, F(\omega)\,, \tag{2}$$

where the upper range of integration ν_m may be determined by the condition that for $\nu \lesssim \nu_m$ the scaling behavior, Eq. (1), becomes valid.

In this note we discuss an experimental test of the finite energy sum rule, Eq. (2), and apply it to the available data [6, 7]. Setting $\nu = K + q^2/2M$, where K is the equivalent real photon energy, and K_m a fixed energy above the resonance region, we differentiate both sides of Eq. (2) with respect to q^2. After separating out the contribution from the elastic form factors G_E and G_M, we obtain

$$F(\omega_m) = -\frac{q^4}{K_m}\frac{d}{dq^2}\left[p(q^2) + \frac{1}{q^2}\int_{K_t}^{K_m} dK \nu W_2(\nu, q^2)\right], \tag{3}$$

* Research supported by a grant from the National Science Foundation.

where

$$p(q^2) = \frac{1}{2M} \frac{G_E^2(q^2) + \dfrac{q^2}{4M} G_m^2(q^2)}{1 + \dfrac{q^2}{4M}}$$

and

$$\omega_m = 1 + \frac{2MK_m}{q^2}, \quad K_t = m_\pi \left(1 + \frac{m_\pi}{2M}\right).$$

In this form it is very convenient to test the finite sum rule: we can substitute on the right-hand side of Eq. (3) the measured values of the elastic and inelastic nucleon form factors in the resonance region, and compare the result directly with the observed asymptotic behavior of νW_2. In order to carry out the integral over the resonances for fixed values of q^2, it is necessary to interpolate the observed values of νW_2, which are measured for a discrete set of values $q_j^2 = 4E(E - \nu_i) \sin^2 \theta/2$, where E and θ are the incident energy and scattering angle of the electron. We obtained a good fit to the available resonance data [7] with an inverse cubic polynomial in q^2,

$$\nu W_2 = \frac{K}{\nu} \frac{q^2}{(1+q^2/\nu)} (a_0 + a_1 q^2 + a_2 q^4 + a_3 q^6)^{-1}, \tag{4}$$

where the coefficients a_i are functions of K [8].

The result for $F(\omega_m)$, leaving out the contribution from the elastic form factors and setting $K_m = 1.64$ BeV is shown in Fig. 1, curve *a*. For comparison the directly measured values of νW_2 and 6° and 10° are also shown. All these points lie below curve *a* indicating that the sum rule is not too well satisfied at the observed values of q^2, $1 \lesssim q^2 \lesssim 7$ $(\text{BeV/c})^2$. The elastic form factor contribute an additional 10% to F_m increasing the discrepancy. It is clear that a better agreement would be obtained if curve *a* where shifted somewhat to the right. This can be done by changing the scaling variable ω to $\omega^1 = \omega + m^2/q^2$ in Eq. (2), where $m \simeq 1$ BeV, as was pointed out by BLOOM and GILMAN [3]. These authors also report that for this variable, νW_2 scales better for larger values of q^2, although the relevant data have not been made available yet.

We have also examined the possibility that the sum rule is satisfied locally. We consider the cases when the integral contains only the first pion–nucleon resonance, and the first and second resonances, setting $K_m = 0.50$ and 0.91 BeV, respectively. The result, again leaving out the elastic form factor, is shown in Fig. 1, curves *b* and *c*, which should overlap with curve *c*, if scaling is valid. The elastic form factor contributes an additional 30% to curve *b* and almost 100% to curve *c*, increasing the discrepancy.

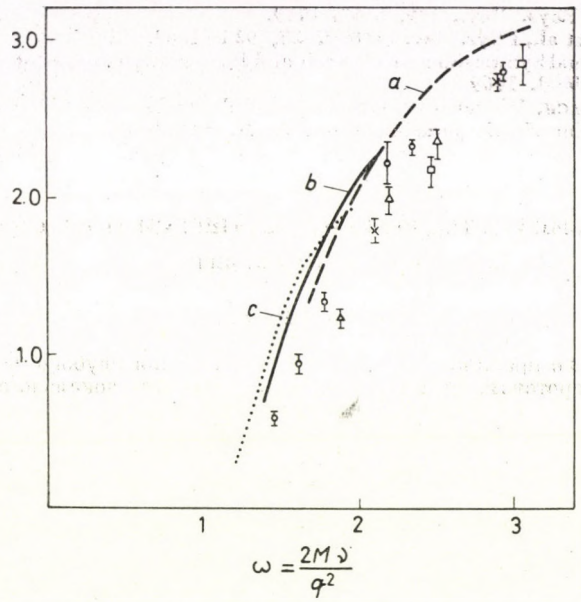

Fig. 1. The three curves shown give the values of $F(\omega)$, Eq. (3), obtained from the resonance data, [7], leaving out the contribution of the elastic from factors. *a* — The dashed curve is obtained by including in the integral, Eq. (3), all the prominent pion–nucleon resonances; $K_m = 1.64$ BeV; *b* — the solid curve includes only the 1236 and 1520 MeV pion–nucleon resonances; $K_m = 0.91$ BeV; *c* — the dotted curve includes only the 1230 resonance; $K_m = 0.5$ BeV. For comparison we have plotted the observed values of νW_2 above the resonance region obtained at 6° and 10° ([6]) assuming $\sigma_L/\sigma_T = 0.2$

In conclusion we note that while the finite energy sum rule is not too well satisfied in the presently observed range $1 \lesssim q^2 \lesssim 7$ (BeV/c)^2, the result is nevertheless encouraging, particularly if we leave out the contribution from the elastic form factors. The different curves shown in Fig. 1 have similar shapes and may converge for larger values of q^2.

I would like to thank Professors C. BOUCHIAT, P. MEYER and J. TRAN THANH VAN for their hospitality at Orsay where this work was carried out, and Dr. G. MENNESSIER for his assistance with the computer program.

REFERENCES

1. R. DOLEN, D. HORN and C. SCHMID, Phys. Rev., **166,** 1768, 1968. For a recent application to forward real photon scattering, see M. DAMASHEK and F. GILMAN, Phys. Rev., **10,** 1819, 1970. A corresponding sum rule for virtual photons has been suggested by HARARI, Phys. Rev. Letters, **22,** 1078, 1969.
2. H. LEUTWYLER and J. STERN, CERN Report TH. 1135, Feb. (1970). We consider in this note only the special case of Eq. (12) with $\xi = 0$.
3. V. GUPTA and RAJASEKARAN, preprint submitted to the XVth International Conference on High Energy Physics, Kiev, 1970.
4. E. BLOOM and F. GILMAN, SLAC–Pub. 779. The finite energy sum rule in this paper corresponds to Eq. (2) with ω substituted by $\omega' = \omega + m^2/q^2$, where m^2 is an adjustable parameter.

5. J. BJORKEN, Phys. Rev., **179,** 1547, 1969.
6. E. D. BLOOM et al., Phys. Rev. Letters, **23,** 930, 1969. R. TAYLOR, Proceedings of the International Symposium on Electron and Photon Interactions at High Energies, Liverpool, England. 1969
7. M. BREIDENBACH, Massachusetts Institute of Technology, Ph. D. Thesis, 1970.
8. For a discussion of this parametization, see M. NAUENBERG, Phys. Rev. Letters, **24,** 625 1970.

ПРАВИЛА СУММ КОНЕЧНЫХ ЭНЕРГИЙ И КАЛИБРОВКА

М. НАУЕНБЕРГ

Резюме

Предложено правило сумм конечных энергий для глубоко неупругого рассеяния электронов на протонах. Рассматривается возможность локального выполнения этого правила сумм.

Acta Physica Academiae Scientiarum Hungaricae, Tomus 31 (1—3), pp. 55—73 (1972)

BROKEN SCALE INVARIANCE IN INELASTIC LEPTON–NUCLEON SCATTERING

By

G. SARTORI

INSTITUTE OF PHYSICS, THE UNIVERSITY, PADOVA, ITALY

Broken scale invariance in inelastic lepton–nucleon scattering is discussed studying current commutators near to light-cone and their equal time limits. Models, based on WILSON's ideas, are proposed here to provide a more general frame than canonical models.

I. Introduction

I shall mainly review some work I have done in collaboration with CICCARIELLO, GATTO and TONIN (Sections IV, V and VI) [1, 2], and some previous related results by other authors (Sections I, II and III), concerning broken scale invariance and its applications to inelastic lepton–hadron scattering.

Finally (Section VII), I shall briefly comment on some relevant very recent experimental results from SLAC [40, 41].

Since the local algebra of currents has been proposed by GELL-MANN, a lot of sum rules have been derived which connect measurable quantities to ETC's between local operators. Particularly interesting are the ETC's involving e.m. or weak currents or their derivatives.

The model-independent parts of such commutators are easy to write down, at least if one believes in some symmetry scheme. More intriguing to compute are the model-dependent parts. To solve the problem, suggestions have been sought in canonical Lagrangian models such as the quark model, the gluon model, field algebra, or others.

Unfortunately, as JOFFE and VAINSTEIN [3], JACKIW and PREPARATA [4] and ADLER and TUNG [5] have shown, equal time commutators calculated by naive canonical manipulations of the field operators generally cannot be used in asymptotic sum rules. In fact, they do not always agree with those computed from Feynman diagrams via $q_0 \to i\infty$ limit.

The source of trouble has to be sought in the singular nature of products of local operators evaluated at the same space-time point. Such singularities can hardly be treated correctly unless one is able to solve exactly the model.

An economical way to bypass the problem, has been suggested by WILSON [6]. According to WILSON the commutator of two local operators, $A(x)$ and $B(0)$, can be expanded, when $x_\mu \to 0$, in the following asymptotic

series:

$$[A(x),\ B(0)] \approx \sum O_n(0)\ C_n(x). \tag{1}$$

In Eq. (1) the equality holds in the weak sense, the $C_n(x)$'s are tempered distributions which contain the whole x_μ-dependence and for locality must vanish outside the light cone; the $O_n(0)$'s form a generally infinite set of independent local operators.

From Eq. (1), by taking the limit $x_0 \to 0$, one formally gets the following expansion for the equal time commutator between $A(x)$ and $B(0)$:

$$[A(\vec{x}, 0), B(0)] = \sum_{k=0} S^{\tau_1 \dots \tau_k}(A, B; 0)\, \partial_{\tau_1} \dots \partial_{\tau_k} \cdot \delta^{(3)}(\vec{x}). \tag{2}$$

$S^{\tau_1 \dots \tau_k}$, the k-order Schwinger term, may also be infinite (in this sense Eq. (2) is a formal development of an equal time commutator): when finite, it is a linear combination of local operators and has physical dimension (in units of length)

$$l_S(k) = l_A + l_B + k + 3, \tag{3}$$

l_A and l_B, which are negative numbers, are the physical dimensions of A and B.

The r.h.s. of Eq. (2) turns out to be certainly a finite sum in theories that do not contain dimensioned parameters, provided the number of operators with dimensions $\geq l_A + l_B + 3$ is finite.

If, moreover, the set of such operators is known, the r.h.s. of Eq. (2) is determined apart from a few numerical constants. Theories that do not contain dimensioned parameters are insensible to a change of the unit of length, that is with respect to a scale transformation or, which is the same, with respect to a dilatation of space and time:

$$x_\mu \to e^\lambda x_\mu; \qquad \lambda \text{ real}$$

II. Scale and conformal invariance

The idea that scale invariance could be a useful concept in theoretical physics is rather old and dates to the works of GURSEY [7], WESS [8], FULTON, ROHRLICH and WITTEN [9], and KASTRUP [10].

KASTRUP [11] and MACK [12] in particular suggested that strong interactions become scale-invariant at short distances, that is at large energies, when all the masses and dimensioned coupling constants of renormalized interactions loose their relative weights.

Such asymptotic scale invariance, however, cannot be considered the consequence of an exact symmetry. In fact, it is easy to prove that in a scale-invariant theory, discrete states with non-vanishing masses are ruled out, cross-sections fall off too rapidly, the lack of dimensioned parameters prevents one

from defining asymptotic states: to mention but a few of the difficulties one meets.

Therefore asymptotic scale invariance must be considered only as a broken symmetry. This amounts to saying that one believes in the existence of a limiting theory, called by WILSON skeleton theory, which obtains when all masses and dimensioned coupling constants vanish.

In such a situation, whenever the theory is renormalizable, one expects only operators of dimensions $\geqslant l_S(k)$, as given in Eq. (3), to contribute to the k-order Schwinger-term; those of dimensions $> l_S(k)$, when finite, occur suitably multiplied by symmetry breaking parameters.

In Lagrangian field theories scale invariance is often accompanied by a larger space-time symmetry, associated to the group of conformal transformations. The conformal group is a 15-parameter non-compact and non-semisimple Lie group, isomorfic to SO(2, 4). It contains as a subgroup the Poincaré group, and is defined as the group of the following non-linear transformations in the Minkowsky space:

$$x'_\mu = a_\mu + \Lambda_\mu{}^\nu x_\nu, \qquad \text{(inhomogeneous Lorentz transformations)}$$

$$x'_\mu = e^\lambda x_\mu;\ \lambda \text{ real}, \qquad \text{(dilatations)}$$

$$x'_\mu = \frac{x_\mu + c_\mu x^2}{1 + 2cx + c^2 x^2}. \qquad \text{(special conformal transformations)}$$

The Lie algebra of the conformal group is specified by the following commutators among the generators of infinitesimal transformations:

$$[M_{\mu\nu}, D] = 0, \tag{4a}$$

$$[P_\mu, D] = iP_\mu, \tag{4b}$$

$$[M_{\mu\nu}, K_\varrho] = i(g_{\varrho\nu} K_\mu - g_{\varrho\mu} K_\nu), \tag{4c}$$

$$[P_\mu, K_\nu] = 2i(g_{\mu\nu} D - M_{\mu\nu}), \tag{4d}$$

$$[K_\mu, K_\iota] = 0, \tag{4e}$$

$$[D, K_\mu] = iK_\mu, \tag{4f}$$

where $M_{\mu\nu}$ and P_μ are the generators of the Poincaré group, D is the dilatation charge and K_μ are the generators of special conformal transformations.

The commutators among the generators of the inhomogeneous Lorentz group are well known and have not been written down.

The field-theoretically admissible representations of the conformal al-

gebra have been discussed in a review paper by MACK and SALAM [13]. They are defined through the following relations:

$$
\begin{aligned}
[\Phi_a(x), P_\mu] &= i\,\partial_\mu \Phi_a(x), \\
[\Phi_a(x), M_{\mu\nu}] &= i\,[(x_\mu \partial_\nu - x_\nu \partial_\mu)\,\delta_a^b (i\,\Sigma_{\mu\nu})_a{}^b]\,\Phi_b(x), \\
[\Phi_a(x), D] &= i\,(-l_a^b + x^\varrho\,\partial_\varrho\,\delta_a^b)\,\Phi_b(x), \\
[\Phi_a(x), K_\mu] &= i\,[-2 l_a^b x_\mu + (2 x_\mu x^\varrho\,\partial_\varrho - x^2\,\partial_\mu)\,\delta_a^b - \\
&\qquad - 2\,i\,x^\varrho (\Sigma_{\mu\varrho})_a{}^b + \varkappa_a{}^b]\,\Phi_b(x),
\end{aligned}
$$

where $\Phi_a(x)$ is a finite or infinite set of local fields, $\Sigma_{\mu\nu}$, l and $\varkappa_\mu$ are finite or infinite matrices, and a sum over repeated indices is understood.

According to the type of the matrices $\Sigma_{\mu\nu}$, l and $\varkappa_\mu$, one gets the following classes of representations:

1. $\varkappa_\mu \equiv 0$. l is real and proportional to a unit matrix if $\Sigma_{\mu\nu}$ form an irreducible representation of the Lie algebra of the homogeneous Lorentz group.

2. $\Sigma_{\mu\nu}$, l and $\varkappa_\mu$ are finite dimensional; $\varkappa_\mu \neq 0$, but nilpotent.

3. $\Sigma_{\mu\nu}$, l and $\varkappa_\mu$ are infinite dimensional.

A local operator $\Phi(x)$ satisfying the above commutation relations will be said to be covariant with respect to conformal transformations. For the 1. class representations, l will be called the scale dimension of the field; it necessarily coincides with the physical dimension of $\Phi(x)$ only if the theory is scale-invariant.

III. Broken conformal invariance in Lagrangian field theories

It is also instructive to see how conformal symmetry comes about in canonical Lagrangian field theories.

This point has been analyzed for instance by WESS [8], MACK and SALAM [13] and GROSS and WESS [14].

In canonical Lagrangian theories of conformal covariant fields a slightly modified form of Nöether's theorem teaches how to construct the generators of the conformal transformations out of the canonical conjugate variables.

One can verify in this way that the divergence of the dilatation current vanishes, as expected, if and only if there are no dimensioned parameters in the theory.

It has also been proved [13, 14] that in a large class of Lagrangian field theories, including among others almost all renormalizable ones, the divergences of the special conformal currents are proportional to the divergence of the dilatation current, so that scale invariance implies invariance with respect to the entire conformal group. When such a situation is realized, one speaks of

minimal breaking of conformal symmetry. A minimal breaking of conformal symmetry in canonical Lagrangian field theories allows for a redefinition, à la Belinfante–Möller, of the energy momentum tensor, as a symmetric tensor, which I shall call $\theta_{\mu\nu}$. In terms of $\theta_{\mu\nu}$ the conformal currents, their divergences and their associated charges assume the following simple form:

$$\theta_{\mu\nu} = \theta_{\nu\mu}\,, \tag{5a}$$

$$M_{\mu\nu\varrho} = x_\nu\,\theta_{\mu\varrho} - x_\varrho\,\theta_{\mu\nu}\,, \tag{5b}$$

$$D_\mu = x^\nu\,\theta_{\mu\nu}\,, \tag{5c}$$

$$K_{\mu\nu} = x_\nu\,D_\mu + x^\varrho\,M_{\mu\nu\varrho}\,, \tag{5d}$$

$$\partial^\mu\,\theta_{\mu\nu} = 0\,, \tag{6a}$$

$$\partial^\mu\,M_{\mu\nu\varrho} = 0\,, \tag{6b}$$

$$\partial^\mu\,D_\mu = \theta^\mu_\mu\,, \tag{6c}$$

$$\partial^\mu\,K_{\mu\nu} = 2x_\nu\,\theta^\mu_\mu\,, \tag{6d}$$

$$P_\mu = \int d^3\,x\theta_{0\mu}(x)\,, \tag{7a}$$

$$M_{\mu\nu} = \int d^3\,x M_{0\mu\nu}(x)\,, \tag{7b}$$

$$D = \int d^3\,x D_0(x)\,, \tag{7c}$$

$$K_\mu = \int d^3\,x K_{0\mu}(x)\,. \tag{7d}$$

If the symmetry is exact, $\theta_{\mu\nu}$ is traceless and carries pure spin 2.

This result is due to CALLAN, COLEMAN and JACKIW [15] who have also proved that the matrix elements of $\theta_{\mu\nu}$ are less singular than the homologous matrix elements of any other permissible energy-momentum tensor, in every order of perturbation theory.

IV. A non-Lagrangian model exhibiting smoothly broken conformal and U(3) ⊗ U(3) symmetries

After the short digression of the preceding sections let me now leave the limits of Lagrangian field theories. I want to retain, however, the following results which will be some of the defining hypotheses of the model worked out by CICCARIELLO, GATTO, TONIN and myself [2].

I shall assume:

i) the existence of a symmetric divergenceless energy momentum tensor, $\theta_{\mu\nu}$.

ii) The possibility of defining the charges

$$P_\mu,\ M_{\mu\nu},\ D \text{ and } K_\mu$$

in terms of $\theta_{\mu\nu}$ as specified in Eqs. (6a, b, c, d) and (7,a b, c, d).

iii) The existence of a symmetry limit in which the energy momentum tensor is traceless and transforms covariantly with respect to the entire conformal group as a first class tensor with scale dimension –4 and spin 2. In this limit the charges P_μ, $M_{\mu\nu}$, D and K_μ form a Lie algebra which is isomorfic to the Lie algebra of the conformal group.

To further specify the model, we have assumed – according to WILSON's philosophy – the existence of the following linearly independent local operators:

a) The traceless part of the energy-momentum tensor.

b) The 18 currents j_μ^α, where $\alpha = (a, A)$, $a = 0, \ldots, 8$ and A specifies the parity.

The associated charges

$$Q^\alpha = \int d^3x j_0^\alpha(x)$$

are the generators of a chiral U(3)⊗U(3).

c) The scalar and pseudoscalar fields w^A which are SU(3)⊗SU(3) singlets but not U(3)⊗U(3) singlets.

d) The scalar and pseudoscalar fields u^a which transform as tensors of a representation $(3,\bar{3})\otimes(\bar{3},3)$ of SU(3) ⊗ SU(3).

The transformation properties of these operators with respect to P, C, and PCT are the usual ones.

The breaking of the U(3) ⊗ U(3) symmetry is specified by assuming that the operator

$$\theta_{00}^{(s)} \equiv \theta_{00}(x) - \varepsilon^\alpha\left(\langle u^\alpha - \langle u^\alpha\rangle_0\right) - \varepsilon^A\left(w^A(x) - \langle w^A\rangle_0\right) \tag{8}$$

is a U(3) ⊗ U(3) singlet.

The symmetry breaking parameters ε^α and ε^A are dimensioned constants.

An immediate consequence of this assumption is $PCAC$ in the form:

$$\partial^\mu j_\mu^\alpha = S^{\alpha BC}\,\varepsilon^B\,w^C + F^{\alpha\beta\gamma}\,\varepsilon^\beta\,u^\gamma, \tag{9}$$

where $S^{\alpha BC}$ and $F^{\alpha\beta\gamma}$ are related to the transformation properties of w^A and u^α with respect to U(3) ⊗ U(3) transformations.

The skeleton theory is obtained in the limit ε^α, $\varepsilon^A \to 0$; it is conformal and U(3) ⊗ U(3)-invariant and the limit of the operators mentioned above transform in it covariantly as tensors of the first class with the following scale dimensions:

$$l_\theta = -4\,; \quad l_j = -3\,; \quad l_w = -\Delta'; \quad l_u = -\Delta\,.$$

Apart from eventual derivatives of such operators or c-numbers, there are no other operators with scale dimensions > -4.

In the true theory the breaking of the conformal symmetry is specified through Eq. (6c):

$$\partial^\mu D_\mu = \theta^\mu_\mu$$

and the assumption that θ^μ_μ is not an independent field. We have proved that in our hypotheses*

$$\theta^\mu_\mu = (4-\Delta)\,\varepsilon^\alpha\,(u^\alpha - \langle u^\alpha\rangle_0) + (4-\Delta')\,\varepsilon^A\,(w^A - \langle w^A\rangle_0)\,. \tag{10}$$

This relation states the partial conservation of the dilatation current. In fact, it can also be derived following the standard procedure used to prove PCAC provided one adds the assumption that the singlet part of $\theta_{\mu\nu}$, $\theta^{(s)}_{00}(x)$ has scale dimension (-4).

In our model this has not been assumed but can be proved to be true.

Let me now justify some of our assumptions and make some additional remarks about their significance.

The use of the group U(3) $\otimes$ U(3) as a broken symmetry group is not new; it had already been considered by GELL-MANN, who also emphasized that the non-conservation of the axial baryon number is required by the high mass of the η' [16]. Δ and Δ' are not generally entire numbers. WILSON has pointed out that the renormalized fields have not necessarily the same dimensions as the unrenormalized ones; in fact, they do not generally satisfy the same canonical commutation relations. This fact, which has been explicitly checked in the Thirring model by WILSON [17] and by LOWENSTEIN [18], can be considered as a renormalization effect of the dilatation charges Δ and Δ'.

The assumptions $\Delta, \Delta' < 4$ express the requirement that the breakings of the internal and of the conformal symmetries occur together and assure that they are due to a superrenormalizable piece of the Hamiltonian.

The condition $\Delta \geq 1$ is an immediate consequence of the semipositivity of the spectral function in the Lehmann representation for $\langle 0 \mid T\{u^\alpha(x)u^\alpha(0)\} \mid 0\rangle$, which requires this object being at least as singular as $1/x^2$ when $x_\mu \to 0$.

An analogous reasoning gives $\Delta' \geq 1$.

The number of local fields with low dimensions, allowed in the model, is the minimum consistent with a symmetry scheme based on a broken U(3) $\otimes$ $\otimes$ U(3).

The existence of the fields w^A (first proposed by GLASHOW [19]) as vehicles of symmetry breaking is required for instance to justify the large mean mass of the ϱ-multiplet and the masses of nucleons, as has been noted by WILSON [6].

* See also [12].

V. Computing equal time commutators

Let me now come to the technical problem of computing the equal time commutators among the local operators of the model.

We have assumed that they are regular in the symmetry limit $\varepsilon^A, \varepsilon^\alpha \to 0$, i.e. that the symmetry is smoothly broken, at least as far as the equal time commutators are concerned, Particularly strong restrictions come from this assumption, if taken in conjunction with the hypothesis of the existence of a limited number of operators with low dimensions. All other conditions to be imposed on the equal time commutators of the model come from the assumed internal and space–time symmetries. Let me discuss this point in greater detail, starting from Eq. (2). The eventual tensor properties of A and B with respect to transformations of some group (whether it is a symmetry group or not) fix the tensor properties of the Schwinger terms with respect to transformations of the same group.

Such tensor properties can be analyzed conveniently in terms of infinitesimal transformations. This in turn amounts to requiring the validity of the Jacobi identity at different times:

$$[Q(t_2), [A(\vec{x}, t_1), B(0)]] = [[Q(t_2), A(\vec{x}, t_1)], B(0)] + [A(\vec{x}, t_1), [Q(t_2), B(0)]], \quad (11)$$

where $Q(t_2)$ is a generator of the group. If the symmetry is exact so that Q does not depend on time, it is sufficient to take the limit $t_1 \to 0$ in Eq. (11) in order to get an equal times Jacobi identity. But if the symmetry is broken and Q does depend on time, in order to get an equal times Jacobi identity it is not sufficient to take in Eq. (11) the two limits $t_2 \to 0$, $t_1 \to 0$, when such limits cannot be interchanged. Thus, in general, one must expect that the equal times Jacobi identity, among two covariant local operators and a non-conserved charge, is violated by terms which are proportional to the breaking parameters.

It may also occur that the equal times Jacobi identity is satisfied in the skeleton theory, where the symmetry is exact, but not in the true theory, because in the latter one or both of the operators A and B loose their exact covariance. In this case too, corrections proportional to the breaking parameters must be expected.

In any case, however, the violating terms are not completely arbitrary, but can be determined apart from a few parameters by a spurion analysis.

So, practically, in our model we must impose the following set of conditions:

A) Conditions which come from the discrete symmetries P, C and PCT are almost obvious and will not be discussed.

B) Poincaré covariance. Considerable technical advantages are obtained by introducing a positive time-like vector n_μ, which acts as a spurion of the Lorentz group, and by substituting to the equal time commutators, the com-

mutators $\delta(nx)$ $[A(x), B(0)]$ calculated on the space-like hyperplane of equation $n \cdot x = 0$. In this way one obtains formal covariance by sight. $S^{\tau_1 \cdots \tau_k}$ $(A, B; 0)$ becomes a function of n_μ and its n_μ-dependence can be easily analyzed through differential methods. The validity of the equal times Jacobi identities involving one generator of the inhomogeneous Lorentz group allows to determine completely the Schwinger terms of the equal time commutator between $A(x)$ and $B(0)$.

These conditions must clearly be satisfied by the ETC's of any acceptable theory, and in our model they turn out to be essential in checking or imposing consistency between our commutators and conservation or partial conservation properties of the local operators involved.

C) D and K_μ covariance must be imposed only within the skeleton theory; in the true theory they are violated by terms proportional to the symmetry breaking parameters. The conditions which come from dilatation covariance have already been discussed.

K_μ covariance gives rise to complicated relations among the Schwinger terms of the equal time commutator between A and B. Their most striking effects can be roughly resumed in the following statement: the local operator $\partial_{\mu_1} \ldots \partial_{\mu_j} C(0)$ $(j = 1, 2, \ldots)$ contributes in the k-order Schwinger term of $[A(x), B(0)]_{\text{e.t.}}$ if $C(0)$ contributes in the $(k + j)$-order Schwinger term of the same commutator [2].

D) Further conditions must be obeyed by the equal time commutators involving the (0μ) components of the energy-momentum tensor. These conditions come from the covariance of the operators of the skeleton theory with respect to transformations of the conformal group and from the particular form that has been postulated for the generators in terms of $\theta_{\mu\nu}$.

Restrictions of this kind concern Schwinger terms up to the second order [2]. Those coming from dilatations and special conformal transformations may be violated by terms proportional to the symmetry breaking parameters.

E) Covariance with respect to U(3) $\otimes$ U(3) transformations implies obviously that all the Schwinger terms in the equal time commutator between A and B can get contributions only from operators which transform according to a representation contained in the Kronecker product of the representations according to which A and B transform. This statement must be taken in a strict sense only within the skeleton theory: in the true theory it must be substituted by the results of a spurion analysis.

In this way, by means of simple group theoretical considerations, we have been able to compute in our model, in terms of a few numerical parameters, all the equal time commutators among the local operators w^A, u^α, j_μ^α and $\theta_{\mu\nu}$ and the equal time commutators between j_μ^α and $\partial_\varrho j_\nu^\beta$. The only exceptions are the equal time commutators involving only space components of the energy-momentum tensor.

We have thus obtained a realization of GELL-MANN's program of extending current algebra to include the energy-momentum tensor.

Some of the commutators we have calculated are reported, in truncated form, in Tables I, II, III and IV. In the following section I shall discuss only some of their most striking aspects and important applications.

Table I

$$[\theta_{00}(\vec{x},0),\ \theta_{00}(0)]_T = -i\partial_0\,\theta_{00}\,\delta^{(3)}(x) + 2i\theta_{0j}\,\partial_j\,\delta^{(3)}(x)$$

$$[\theta_{00}(\vec{x},0),\ \theta_{0l}(0)]_T = -i\partial_0\,\theta_{0l}\,\delta^{(3)}(x) + i(\theta_{jl}\,\partial_j + \theta_{00}\,\partial_l)\,\delta^{(3)}(x)$$

$$[\theta_{00}(\vec{x},0),\ \theta_{kl}(0)]_T = -i\partial_0\,\theta_{kl}\,\delta^{(3)}(x) + i(\theta_{0l}\,\partial_k + \theta_{0k}\,\partial_l)\,\delta^{(3)}(x)$$

$$[\theta_{0k}(\vec{x},0),\ \theta_{0l}(0)]_T = -i\partial_k\,\theta_{0l}\,\delta^{(3)}(x) + i(\theta_{0l}\,\partial_k + \theta_{0k}\,\partial_l)\,\delta^{(3)}(x)$$

$$\begin{aligned}[\theta_{0k}(\vec{x},0),\ \theta_{lm}(0)]_T = {} & -i\partial_k\,\theta_{lm}\,\delta^{(3)}(x) + \\ & + i\left\{\frac{4}{3}\,\delta_{nk}\,\theta_{lm} + \frac{1}{3}\,\delta_{lm}\,\theta_{nk} + \frac{1}{2}\,[\delta_{nl}\,\theta_{km} + \delta_{nm}\,\theta_{kl} - \right. \\ & - \delta_{kl}\,\theta_{nm} - \delta_{km}\,\theta_{nl}] - \frac{1}{9}\,\delta_{nk}\,\delta_{lm}[\theta_{00} - (4-\Delta')^2\,\varepsilon^B\,w^B - \\ & - (4-\Delta)^2\,\varepsilon^\beta\,u^\beta] - p^{n'k',l'm'}_{nk\ ,lm}\,[k_1^{(1)}\,\varepsilon_{n'l'}\,\theta_{k'm'} + \\ & \left. + k_2^{(1)}\,\delta_{n'l'}\,\delta_{k'm'}\,\theta_{jj} - \delta_{n'l'}\,\delta_{k'm'}(k_3^{(1)}\,\varepsilon^\beta\,u^\beta + k_4^{(1)}\,\varepsilon^B\,w^B)]\right\}\partial_n\,\delta^{(3)}(x)\end{aligned}$$

$$p^{n'k',l'm'}_{nk\ ,lm} \equiv \frac{1}{2}\,(p^{n'k'}_{nk}\,p^{l'm'}_{lm} + p^{l'm'}_{nk}\,p^{n'k'}_{lm})$$

$$p^{n'k'}_{nk} \equiv \frac{1}{2}\,(\delta_{nn'}\,\delta_{kk'} + \delta_{nk'}\,\delta_{kn'} - \frac{2}{3}\,\delta_{nk}\,\delta_{n'k'})$$

$k_1^{(1)}, k_2^{(1)}, k_3^{(1)}$ and $k_4^{(1)}$ are real numbers.

In the r.h.s. 's all local operators are evaluated at $x = 0$.

Table II

$$[j_0^\alpha(\vec{x},0),\ \theta_{00}(0)]_T = i\partial^\mu\,j_\mu^\alpha\,\delta^{(3)}(x) + ij_r^\alpha\,\partial_r\,\delta^{(3)}(x)$$

$$[j_0^\alpha(\vec{x},0),\ \theta_{0m}(0)]_T = ij_0^\alpha\,\partial_m\,\delta^{(3)}(x)$$

$$\begin{aligned}[j_0^\alpha(\vec{x},0),\ \theta_{mn}(0)]_T = {} & -i\delta_{mn}\left[\frac{3-\Delta}{3}\,\partial^\mu\,j_\mu^\alpha + \frac{\Delta+\Delta'}{3}\,\varepsilon^B\,S^{\alpha BC}\,w^C\right]\delta^{(3)}(x) + \\ & + i\left[\frac{1}{2}\,j_m^\alpha\,\partial_n + j_n^\alpha\,\partial_m) - 2k_1\,p^{m'n'}_{mn}\,j^\alpha_{m'}\,\partial_{n'}\right]\delta^{(3)}(x)\end{aligned}$$

$$[j_k^\alpha(\vec{x},0),\ \theta_{00}(0)]_T = i[\partial_0\,j_k^\alpha - \partial_k\,j_0^\alpha]\,\delta^{(3)}(x) + ij_0^\alpha\,\partial_k\,\delta^{(3)}(x)$$

$$\begin{aligned}[j_k^\alpha(\vec{x},0),\ \theta_{0m}(0)]_T = {} & i\left[\left(k_1 - \frac{1}{2}\right)\partial_k j_m^\alpha - \frac{2}{3}\,k_1\,\partial_m\,j_k^\alpha + \left(k_1 + \frac{1}{2}\right)\delta_{km}\,\partial_r\,j_r^\alpha\right]\delta^{(3)}(x) + \\ & + i\left[\left(1 + \frac{2}{3}\,k_1\right)j_k^\alpha\,\partial_m + \left(\frac{1}{2} - k_1\right)j_m^\alpha\,\partial_k - \left(\frac{1}{2} + k_1\right)\delta_{mk}\,j_r^\alpha\,\partial_r\right]\delta^{(3)}(x)\end{aligned}$$

$$[j^{\alpha}(\vec{x},0),\theta_{mn}(0)]_T = i\left\{\left(k_1+\frac{1}{2}\right)p_{mn}{}^{ii}\delta_{kr}(\partial_s j_0^{\alpha}-\partial_0 j_s^{\alpha})+\frac{1}{3}\delta_{mn})\pm(\partial_0 j_k^{\alpha})+(\partial_k j_0^{\alpha})\right\}\delta^{(3)}(x)+$$

$$+i\left\{j_0^{\alpha}\left[\frac{1}{2}(\delta_{km}\partial_n+\delta_{kn}\partial_m)+k_1(\delta_{km}\partial_n)+(\delta_{kn}\partial_m-\frac{2}{3}\delta_{mn}\partial_k)\right]\right\}\delta^{(3)}(x)$$

k_1 is a real number,

$$S^{\alpha BC}=3s\sqrt{\frac{2}{3}}\,\delta^{ao}\,\delta^{A\circ\mathcal{R}}(\delta^{B\circ\mathcal{R}}\delta^{C\mathcal{V}}-\delta^{B\mathcal{V}}\delta^{C\circ\mathcal{R}})$$

s is an integer $\neq 0$.

In the r.h.s. 's all local operators are evaluated at $x=0$.
Only truncated commutators are reported.

Table III

$$[j_0^{\bar{\alpha}}(\vec{x},0),j_0^{\bar{\beta}}(0)]_T = iC^{\bar{\alpha}\bar{\beta}\bar{\gamma}}j_0^{\bar{\gamma}}\delta^{(3)}(x)$$

$$[j_0^{\bar{\alpha}}(\vec{x},0),j_k^{\bar{\beta}}(0)]_T = iC^{\bar{\alpha}\bar{\beta}\bar{\gamma}}j_k^{\bar{\gamma}}\delta^{(3)}(x)$$

$$[j_l^{\bar{\alpha}}(\vec{x},0),j_k^{\bar{\beta}}(0)]_T = -i\{b_1 C^{\bar{\alpha}\bar{\beta}\bar{\gamma}}\delta_{kl}j_0^{\bar{\gamma}}+b_2 D^{\bar{\alpha}\bar{\beta}\bar{\gamma}}\varepsilon_{klm}j_m^{\bar{\gamma}}+E^{\bar{\alpha}\bar{\beta}\bar{C}}\varepsilon_{klm}j_m^{(0,C)}\}\delta^{(3)}(x)$$

$$[j_0^{\bar{\alpha}}(\vec{x},0),u^{\beta}(0)]_T = iF^{\bar{\alpha}\beta\gamma}u^{\gamma}\delta^{(3)}(x)$$

$$[j_k^{\bar{\alpha}}(\vec{x},0),u^{\beta}(0)]_T = 0$$

Notations: $\alpha=(a,A)$: $a=0,1,2,\ldots 8$

$A=\mathcal{V}$ (vector or scalar) or $\mathcal{R}$ (axial or pseudoscalar).

$\bar{\alpha}=(\bar{a},A)$: $\bar{a}=1,2,\ldots,8$

Summation over repeated indices is always understood.

$C^{\alpha\beta\gamma}\equiv f^{abc}\psi^{ABC}$; $C^{\bar{\alpha}\bar{\beta}\bar{\gamma}}f^{\bar{a}\bar{b}\bar{c}}\psi^{ABC}$

f^{abc} structure constants of U(3)

$f^{\bar{a}\bar{b}\bar{c}}$ structure constants of SU(3)

$\psi^{ABC}=\begin{cases}0 \text{ if the number of "axial" indices } \mathcal{R} \text{ is odd}\\ 1 \text{ if the number of "axial" indices } \mathcal{R} \text{ is even}\end{cases}$

$D^{\alpha\beta\gamma}\equiv d^{abc}\bar{\psi}^{ABC}$; $D^{\bar{\alpha}\bar{\beta}\bar{\gamma}}=d^{\bar{a}\bar{b}\bar{\gamma}}\bar{\psi}^{ABC}$

d^{abc} are defined according to Gell-Mann's proposal:

$$\{\lambda^a;\lambda^b\}=2d^{abc}\lambda^c$$

$\bar{\psi}^{ABC}=\begin{cases}0 \text{ if the number of "axial" indices } \mathcal{R} \text{ is even}\\ 1 \text{ if the number of "axial" indices } \mathcal{R} \text{ is odd}\end{cases}$

$$E^{\bar{\alpha}\bar{\beta}\bar{c}}\equiv\left(\sqrt{\frac{2}{3}}b_2+b_3\right)\delta^{\bar{\alpha}\bar{\beta}}\delta^{CA}+\left(\sqrt{\frac{2}{3}}b_2+b_4\right)\delta^{\bar{a}\bar{b}}(\delta^{A\mathcal{V}}\delta^{B\circ\mathcal{R}}+\delta^{A\circ\mathcal{R}}\delta^{B\mathcal{V}})\delta^{C\mathcal{V}}.$$

$$F^{\bar{\alpha}\beta\gamma}=f^{\bar{a}bc}\psi^{ABC}\delta^{A\mathcal{V}}+d^{\bar{a}bc}\delta^{A\circ\mathcal{R}}(\delta^{B\circ\mathcal{R}}\delta^{C\mathcal{V}}-\delta^{B\mathcal{V}}\delta^{C\circ\mathcal{R}}).$$

b_1, b_2, b_3, b_4, are real numbers.

Only truncated commutators are reported.

Table IV

$$[j_k^{\bar{\alpha}}(\vec{x}, 0), \partial_0 j_l^{\bar{\beta}}(0)]_T = i \Big\{ \delta^{\bar{\alpha}\bar{\beta}} c_1 \delta_{kl} \theta_{jj} + c_2 \theta_{kl}] +$$

$$+ G^{\{\bar{\alpha}\bar{\beta}\}\gamma\delta} \delta_{kl} \varepsilon^{\gamma} u^{\delta} + G^{\{\bar{\alpha}\bar{\beta}\}CD} \delta_{kl} \varepsilon^{C} w^{D} + \frac{1}{2} C^{\bar{\alpha}\bar{\beta}\bar{\gamma}} [(1 + b_1) \cdot$$

$$\cdot (\partial_k j_l^{\bar{\gamma}} - \partial_l j_k^{\bar{\gamma}}) + \partial_k j_l^{\bar{\gamma}} + \partial_l j_k^{\bar{\gamma}} - b_1 \delta_{kl} \partial^{\mu} j_{\mu}^{\bar{\gamma}}] -$$

$$- \frac{b_2}{2} D^{\bar{\alpha}\bar{\beta}\bar{\gamma}} \varepsilon_{klm} (\partial_0 j_m^{\bar{\gamma}} - \partial_m j_0^{\bar{\gamma}}) - \frac{E^{\bar{\alpha}\bar{\beta}C}}{2} \varepsilon_{klm} (\partial_0 j_m^{(0,C)} - \partial_m j^{(0,C)}) \Big\}$$

$$\delta^{(3)}(x) - i \{ C^{\bar{\alpha}\bar{\beta}\bar{\gamma}} [\delta_{lm} j_k^{\bar{\gamma}} + \delta_{km} j_l^{\bar{\gamma}} + b_1 \delta_{kl} j_m^{\bar{\gamma}}] +$$

$$+ b_2 D^{\bar{\alpha}\bar{\beta}\bar{\gamma}} \varepsilon_{klm} j_0^{\bar{\gamma}} + E^{\bar{\alpha}\bar{\beta}C} \varepsilon_{klm} j_0^{(0,C)} \} \partial_m \delta^{(3)}(x)$$

$$[j_0^{\bar{\alpha}}(\vec{x}, 0), \partial_0 j_k^{\bar{\beta}}(0)]_T = i C^{\bar{\alpha}\bar{\beta}\bar{\gamma}} \partial_0 j_k^{\bar{\gamma}} \delta^{(3)}(x) + i \{ b_1 C^{\bar{\alpha}\bar{\beta}\bar{\gamma}} \delta_{kl} j_0^{\bar{\gamma}} + b_2 D^{\bar{\alpha}\bar{\beta}\bar{\gamma}} \varepsilon_{klm} j_m^{\bar{\gamma}} +$$

$$+ E^{\bar{\alpha}\bar{\beta}C} \varepsilon_{klm} j_m^{(0,C)} \} \partial_l \delta^{(3)}(x)$$

c_1 and c_2 are real numbers.

$G^{\{\bar{\alpha}\bar{\beta}\}\gamma\delta}$ and $G^{\{\bar{\alpha}\bar{\beta}\}CD}$ are sets of real constants.

In the r.h.s. 's all local operators are evaluated at $x = 0$.
Only truncated commutators are reported.

VI. Discussion of the equal time commutators

A) The equal time commutators $[\theta_{\mu\nu}, \theta_{\varrho\sigma}]$ (see Table I), at least for the moment, are interesting only from a theoretical point of view. In connection with them we have rederived as a particular case, SCHWINGER's [23] theorem, and checked previous model-independent results by BOULAWARE and DESER [24].

B) The equal time commutators between the components of a SU(3) current and those of the energy-momentum tensor are reported in Table II. From the first three rows of the Table, one realizes that the U(3) ⊗ U(3) singlet part of $\theta_{\mu\nu}$ is a non-covariant operator which differs from $\theta_{\mu\nu}$ only for the addition of spin 0 fields:

$$\theta_{\mu\nu}^{(s)} = \theta_{\mu\nu} - g_{\mu\nu} [\varepsilon^{\alpha}(u^{\alpha} - \langle u^{\alpha} \rangle_0) + \varepsilon^{A}(w^{A} - \langle w^{A} \rangle_0)] - (-g_{\mu\nu} + g_{\mu 0} g_{\nu 0}) \cdot$$

$$\cdot \left[\frac{\Delta}{3} \varepsilon^{\alpha}(u^{\alpha} - \langle u^{\alpha} \rangle_0) + \frac{\Delta'}{3} \varepsilon^{A}(w^{A} - \langle w^{A} \rangle_0) \right]. \tag{12}$$

As already noted, the most interesting commutators, because of their connection to experimentally measurable quantities, are the commutators among currents and currents derivatives. They determine [25–32]:

a) The divergent part of e.m. self masses and the leading divergences of weak self masses;

b) The asymptotic behaviours of e.m. and weak amplitudes, and a number of electro- and neutrino-production sum rules, some of which I shall mention. To this end I have recalled in Appendix A some standard notations and results relevant to the problem of inelastic lepton scattering from unpolarized targets.

c) For the ETC's $[j_\mu^\alpha j_\nu^\beta]$ which are reported in Table III, we have found an expression which is more general than the one provided by the quark model. In the $P \to \infty$ limit the ETC's between two SU(3) $\otimes$ SU(3) currents determine many sum rules, of which I wish to recall the DASHEN–FUBINI–GELL-MANN sum rule [33–35], the backward BJORKEN asymptotic sum rule [36] and the GROSS and LLEWELLYN–SMITH sum rule [30].

Recently JACKIW et al. [31] and CORNWALL et al. [32] have proved that the integral

$$\int_0^2 \frac{F_l(\omega)}{\omega}\, d\omega\,,$$

provided it converges, is proportional to the q-number first order Schwinger term in the ETC between $j_k^{\text{e.m.}}$ and $j_k^{\text{e.m.}}$. In our model we find no operator Schwinger terms in this ETC, so the integral diverges or vanishes. In the second case the semipositivity of $F_l(\omega)$ implies that the integrand is zero.

D) The equal time commutators $[j_\mu^\alpha, \partial_\varrho j_\nu^\beta]$ are reported in Table IV. Their forward matrix elements determine in the $P \to \infty$ limit the asymptotic sum rules related to electro- and neutrino-production, which are expressed in terms of integrals over the functions $F_i(\omega)$ and $\bar{F}_i(\omega)$ defined in Eqs (A.3) and (A.7). Only terms which do not contain derivatives contribute to the integral over d^3x of these forward matrix elements. Therefore, as is seen from Table IV, only the matrix elements of the energy momentum tensor contribute to the sum rules. The other non-derivative terms are in fact matrix elements of spin 0 fields, and vanish when $P_z \to \infty$. So the asymptotic sum rules for electro- and neutrino-production on nucleons can be expressed in terms of only the two parameters c_1 and c_2, which multiply the components of $\theta_{\mu\nu}$ appearing in the expression of the equal time commutator (see Table IV), and their r.h.s.'s turn out to be proportional to the masses of the targets. MACK [37] has pointed out that this result holds whichever is the target, owing to the universality of the forward matrix elements of the energy-momentum tensor.

The CALLAN–GROSS sum rules [28], when evaluated in our model, give [1, 2]:

$$I_l = \int_0^2 d\omega\omega F_l(\omega) = -2/3\; c_1 \left\{= 2/3\; c_2\right\}^*, \tag{13a}$$

$$I_l = \int_0^2 d\omega\omega F_l(\omega) = 2/3(c_1 + c_2)\; \left\{= 0\right\}^*. \tag{13b}$$

The results marked with a star hold only if the sum rule of JACKIW et al. [31] converges. The same convention will be used in the sequel too. Comparing with the experimental data obtained at SLAC [38] for $F_l(\omega)$ we find:

$$\{-c_1 = 0.54 \pm 0.06\}^* \tag{14}$$

The neutrino production sum rules are similarly determined in terms of the two parameters c_1 and c_2 [1, 2]:

$$\bar{I}_t = \int_0^2 d\omega\omega\{\bar{F}_t^{\nu}(\omega) + \bar{F}_t^{\bar{\nu}}(\omega)\} = -4c_1 \ \{= 2.16 \pm 0.24\},^* \tag{15a}$$

$$\bar{I}_l = \int_0^2 d\omega\omega\{\bar{F}_l^{\nu}(\omega) + \bar{F}_l^{\bar{\nu}}(\omega)\} = -4(c_1 + c_2) \ \{= 0\},^* \tag{15b}$$

$$\bar{I}_3 = \int_0^2 d\omega\omega\{\bar{F}_3^{\nu}(\omega) + \bar{F}_3^{\bar{\nu}}(\omega)\} = 0, \tag{15c}$$

where the label $\nu(\bar{\nu})$ refers to neutrino (anti-neutrino) processes.

Noting that when $P_z \to \infty$, the forward matrix elements of $\theta_{\mu\nu}$ coincide with those of its singlet part $\theta_{\mu\nu}^{(s)}$, defined in Eq. (12), it is possible to calculate the ratio of the total neutrino + antineutrino cross-sections into $S = 1$ and $S = 0$ states [1, 2]:

$$\frac{\sigma_{\text{tot}}(\Delta S = 1)}{\sigma_{\text{tot}}(\Delta S = 0)} = \tan^2\theta, \tag{16}$$

where θ is the Cabibbo angle.

BJORKEN has shown [36] that when E is much greater than M, but not so large as to make the cut offs due to unitarity, or intermediate boson exchange, operative

$$\sigma_{\text{tot}}^{\nu p} + \sigma_{\text{tot}}^{\bar{\nu} p} \to \frac{G^2 ME}{\pi} \frac{i}{4}\left(\dot{J}_{zz} - \frac{4}{3}\dot{J}_{xx} - \frac{2}{3}i\dot{J}_{xy}\right), \tag{17a}$$

$$\sigma_{\text{tot}}^{\nu n} + \sigma_{\text{tot}}^{\bar{\nu} n} \to \frac{G^2 ME}{\pi} \frac{i}{4}\left(\dot{J}_{zz} - \frac{4}{3}\dot{J}_{xx} + \frac{2}{3}i\dot{J}_{xy}\right), \tag{17b}$$

where the definition of Eq. (A.9) has been used. In our model the r.h.s.'s of Eqs. (17a and b) coincide and can be computed in terms of c_1 and c_2. The result is [2]

$$\frac{3c_2 - c_1}{3} \frac{G^2 ME}{\pi} \left\{= (0.7 \pm 0.1) \frac{G^2 ME}{\pi}\right\}^*. \tag{18}$$

If one neglects $S = 1$ transitions, $\sigma^{\nu n} = \sigma^{\bar{\nu} p}$ is obtained as the result of a simple isospin rotation and the experimental result [39]

$$\sigma_{\mathrm{tot}}^{\nu p}+\sigma_{\mathrm{tot}}^{\nu n}=\frac{G^2\,ME}{\pi}(1.02\pm 0.3) \tag{19}$$

can be compared with the starred result of Eq. (18). The agreement is not fantastic, but within the experimental errors. I wish to recall, however, that the assumption of convergence of the integral

$$\int_0^2 d\omega\,\frac{F_l(\omega)}{\omega}$$

is essential to the prediction of Eq. (18).

VII. Additional remarks and conclusion

At the recent Conference of Kiev [40] and at the beginning of this Symposium [41] some new data from SLAC have been reported which seem to be in disagreement with the universality of $J_{\mu\nu}$ (defined in Eq. (A.9)) predicted by our model. In fact, the function $\nu W_2^{\mathrm{neutron}}(\omega, q^2)$ has been found sensibly different from $\nu W_2^{\mathrm{proton}}(\omega, q^2)$. So, before concluding, I think some comments are in order about such a possible discrepancy. Various possibilities exist:

1. One may be so optimistic as to hope that the function $\nu W_2^{\mathrm{neutron}}(\omega, \nu)$ which for large values $(1/16\leq \omega \leq 2)$ of ω has been found $< \nu W_2{}^{\mathrm{proton}}(\omega, \nu)$, at small values of ω becomes so large that the integrals $I_{l(l)}^{\mathrm{neutron}}$ and $I_{l(l)}^{\mathrm{proton}}$ defined in Eqs. (13a, b) coincide.

2. One may prefer to modify the model, for instance, by admitting the existence of a set of 16 operators $\theta_{\mu\nu}^{\alpha}$, which carry spin 2 and dimensions —4, and transform as tensors of a representation (8, 1) + (1, 8) of SU(3) ⊗ SU(3). Such operators can contribute in the equal time commutator $[j_\mu^\alpha, \partial_\varrho j_\nu^\beta]$ and their contributions which depend on three new parameters, are competitive with those of $\theta_{\mu\nu}$.

If the sum rule of JACKIW et al. converges, one of the parameters can be determined; besides, the ratio F/D for the coupling of $\theta_{\mu\nu}^{\alpha}$ to the nucleons can be computed from independent data, so beside c_1 two new parameters enter the asymptotic sum rules for electro- and neutrino-production on protons and neutrons, and the available experimental data are sufficient only to determine them. No testable prediction can be made in this case.

It must also be noted that in this way one gives up one of the most appealing features of the model, consisting in a sort of bootstrap which realizes in the equal time commutators among the (minimum number of) operators which are required to generate and to break the symmetries.

3. In a recent paper [43] NAUENBERG has shown, through a phenomenological fit, that the experimental data for the proton are not yet asymptotic enough as to assure that $\nu W_2^{\text{proton}}(\omega, \nu)$ really scales.

If credit is given to such an interpretation of experiments, the data for the neutron too must be considered only sub-asymptotic, and one need not modify the model to justify them. The situation is illustrated by the following example. Suppose

$$\nu W_2(\omega, \nu) = F_2(\omega) + \left(\frac{M^2}{\nu}\right)^{\eta/2} F_2'(\omega) . \tag{20}$$

If $\eta > 0$ is sufficiently small and $F_2'(\omega)$ depends on isotopic spin, the contribution of the second term in the r.h.s. of Eq. (20) can account for the differences between the neutron and proton data, but cannot be distinguished from the contribution of an exactly scaling term.

In our model such contribution could be explained for instance by simply assuming that the operators $\theta_{\mu\nu}^{\alpha}$ exist, but with dimensions $-(4 + \eta)$, so they would contribute in WILSON's [44] expansion for $[j_\mu^\alpha(x), \partial_\varrho j_\nu^\beta(0)]$, but not at equal times. While waiting for more precise or more asymptotic experiments, this position is perhaps the most appealing one to adopt from our point of view.

In any case, whichever is the interpretation of the experimental data, the philosophy which is behind the model keeps its validity.

To conclude I would stress that models of the kind proposed here, based on WILSON's ideas, appear to provide a more general frame than canonical models, allowing inclusion of limiting cases of the canonical formalism. In this sense, such models are related for instance to the discussion of possible limiting cases of field algebra [45–48], where ambiguous products $j_\mu(x)j_\nu(x)$ of operators, taken at the same point, appear in the equal time commutators. Such ambiguities are here evaded essentially through the assumption of the existence of a small number of low-dimension operators which, after fixing a broken symmetry scheme, for want of something better, have been selected according to a principle of economy.

Appendix

In this Appendix some standard notations and results relevant to the problem of inelastic lepton scattering from unpolarized targets are recalled.

In the laboratory frame E and E' are the energies of the incident and scattered lepton, P_μ is the momentum of the target and M its mass, θ is the scattering angle of the lepton; $q^2 = -4EE' \cdot \sin^2 \theta/2$ and $\nu = q \cdot P = M(E - E')$ are the squared momentum transfer and the energy transfer to the lep-

tons, respectively. The structure functions for electroproduction are defined from

$$\frac{1}{M^2}\left(P_\mu - \frac{(P\cdot q)\,q_\mu}{q^2}\right)\left(P_\nu - \frac{(P\cdot q)\,q_\nu}{q^2}\right) W_2(q^2,\nu) - \left(g_{\mu\nu} - \frac{q_\mu q_\nu}{q^2}\right)\times$$
$$\times\, W_1(q^2,\nu) = \frac{P_0}{M}\int \frac{d^4x}{2\pi}\, e^{iqx}\langle P|[j_\mu^{\text{e.m.}}(x), J_\nu^{\text{e.m.}}(0)]|P\rangle\,. \tag{A.1}$$

The inelastic differential cross section in terms of W_1 and W_2 is

$$\frac{d\sigma}{d\Omega dE'} = \frac{\alpha^2}{4E^2\sin^4\theta/2}\,[W_2(q^2,\nu)\cos^2\theta/2 + 2W_1(q^2;\nu)\sin^2\theta/2]; \tag{A.2}$$

Following BJORKEN [26] I shall also define:

$$\omega = -q^2/\nu$$
$$F_1(\omega) = \lim_{\substack{\nu\to\infty \\ \omega \text{ fixed}}} MW_1(q^2;\nu)\,, \tag{A.3a}$$

$$F_1(\omega) = \lim_{\substack{\nu\to\infty \\ \omega \text{ fixed}}} \nu/M\;\; W_2(q^2;\nu), \tag{A.3b}$$

$$F_t(\omega) = F_1(\omega), \tag{A.4a}$$

$$F_l(\omega) = \frac{F_2(w)}{\omega} - F_1(\omega)\,. \tag{A.4b}$$

The structure functions for neutrino production are defined from

$$\frac{P_0}{M}\int \frac{d^4x}{2\pi}\, e^{iq\cdot x}\langle P|[j_\mu(x), j_\nu^+(0)]|P\rangle = \frac{P_\mu P_\nu}{M^2}\,\overline{W}_2(q^2;\nu) -$$
$$- g_{\mu\nu}\,\overline{W}_1(q^2;\nu) - \frac{i}{2M}\,\varepsilon_{\mu\nu}{}^{\alpha\beta}P_\alpha q_\beta \overline{W}_3(q^2;\nu) + \ldots \tag{A.5}$$

and the cross section is:

$$\frac{\pi}{EE'}\frac{d\sigma}{d\Omega dE'} = \frac{E'}{E}\frac{G^2}{2\pi}\left[\overline{W}_2(q^2;\nu)\cos^2\theta/2 + \right.$$
$$\left. + 2\,\overline{W}_1(q^2;\nu)\sin^2\theta/2 + \frac{E+E'}{M}\quad{}_3(q^2;\nu)\sin^2\theta/2\right]. \tag{A.6}$$

For neutrino-production one defines:

$$\bar{F}_1(\omega) = \lim_{\substack{\nu\to\infty \\ \omega \text{ fixed}}} M\overline{W}_1(q^2;\nu)\,. \tag{A.7a}$$

$$\bar{F}_2(\omega) = \lim_{\substack{\nu\to\infty \\ \omega \text{ fixed}}} \nu/M\,\overline{W}_2(q^2;\nu)\,, \tag{A.7b}$$

$$\bar{F}_3(\omega) = \lim_{\substack{\nu\to\infty \\ \omega \text{ fixed}}} \nu/M\,\overline{W}_3(q^2;\nu)\,, \tag{A.7c}$$

$$J_{\mu\nu} \equiv \lim_{P_z\to\infty} \int d^3x\, \langle P_z|[J_\mu(\vec{x},0), J_\nu^+(0)]|P_z\rangle\,, \tag{A.8}$$

$$\dot{J}_{\mu\nu} = \lim_{P_z\to\infty} \int \frac{d^3x}{P_0} \left\langle P_z \left| \left[\frac{d}{dt} J_\mu(\vec{x},0), J_\nu^+(0)\right]\right| P_z\right\rangle. \tag{A.9}$$

REFERENCES

1. S. Ciccariello, R. Gatto, G. Sartori and M. Tonin, Phys. Letters, **30B,** 546, 1969.
2. S. Ciccariello, R. Gatto, G. Sartori and M. Tonin, Ann. Phys. (N. Y.) **65,** 265, 1971.
3. B. Joffe and A. Vainstein, JEPT Letters, **6,** 341, 1967.
4. R. Jackiw and G. Preparata, Phys. Rev. Letters, **22,** 975, 1969.
5. S. Adler and W. Tung, Phys. Rev. Letters, **22,** 978, 1969.
6. K. G. Wilson, Phys. Rev., **179,** 1499, 1969.
7. F. Gursey, Nuovo Cimento, **3,** 988, 1956; Ann. Phys., **24,** 211, 1963.
8. J. Wess, Nuovo Cimento, **18,** 1086, 1960.
9. T. Fulton, T. Rohrlich and L. Witten, Rev. Mod. Phys., **34,** 442, 1962.
10. H. A. Kastrup, Ann. Physik, **7,** 388, 1962.
11. H. A. Kastrup, Phys. Rev., **142,** 1060, 1962; Nucl. Phys., **58,** 561, 1964; Phys. Rev., **143,** 1041, 1966; **150,** 1189, 1966.
12. G. Mack, Nucl. Phys., **B5,** 499, 1968; Phys. Letters, **26B,** 515, 1968.
13. G. Mack and A. Salam, Ann. Phys., **53,** 174, 1969.
14. D. J. Gross and J. Wess, Phys. Rev., **D2,** 753, 1970.
15. C. G. Callan, S. Coleman and R. Jackiw, Ann. Phys. (N. Y.) **59,** 42, 1970.
16. L. Brown and M. Gell-Mann, Lectures at Hawai Summer School, 1969, Calt 68–244, 1970.
17. K. G. Wilson, Phys. Rev., **D2,** 1473 and 1478, 1970.
18. J. Lowenstein, Comm. Math. Phys., **16,** 265, 1970.
19. S. L. Glashow, in "Hadrons and Their Interactions" ed. A. Zichichi, Academic Press, New York, 1968.
20. M. Tonin, Nuovo Cimento, **47A,** 919, 1967.
21. S. Ciccariello, G. Sartori and M. Tonin, Nuovo Cimento, **63A,** 846, 1969.
22. G. Sartori, Lettere al Nuovo Cimento, IV, 583, 1970.
23. J. Schwinger, Phys. Rev., **130,** 407, 1963.
24. D. G. Boulaware and S. Deser, J. Math. Phys., **8,** 1468, 1967.
25. M. Gell-Mann, Phys. Rev., **125,** 1067, 1962.
26. J. D. Bjorken, Phys. Rev., **179,** 1547, 1969.
27. J. M. Cornwall and R. E. Norton, Phys. Rev., **173,** 1637, 1968; **177,** 2584, 1969.
28. C. G. Callan and D. G. Gross, Phys. Rev. Letters, **22,** 156, 1969.
29. J. D. Bjorken and E. A. Paschos, SLAC PUB 678, 1969.
30. D. J. Gross and C. H. Llewellyn-Smith, Nucl. Phys., **B14,** 337, 1970.
31. R. Jackiw, R. Van Royen and G. B. West, Preprint CTP-MIT 118, 1970.

32. J. M. Cornwall, D. Carrigan and R. E. Norton, Phys. Rev. Letters, **24,** 1141, 1970.
33. S. Fubini, Nuovo Cimento, **43A,** 161, 1966.
34. R. Dashen and M. Gell-Mann, Phys. Rev. Letters, **17,** 340, 1966.
35. S. Adler, Phys. Rev., **143,** 1144, 1967.
36. J. D. Bjorken, Phys. Rev., 1**D,** 1376, 1970.
37. G. Mack, Preprint, University of Miami, 1970.
38. M. Breidenback et al., Phys. Rev. Letters, **23,** 935.
39. I. Buganov et al., Phys. Letters, **29B,** 524, 1969; 30**B,** 364, 1969.
40. R. Taylor, reported at the XVth International Conference on High Energy Physics, Kiev, 1970.
41. F. J. Gilman, these Proceedings, p. 33.
42. K. Sarma and G. Renninger, Phys. Rev. Letters, **20,** 399, 1968.
43. M. Nauenberg, Phys. Rev. Letters, **24,** 625, 1970.
44. Wilson's expansion for $[j_\mu^\alpha(x), j_\nu^\beta(0)]$ has been analyzed by L. Bonora and I. Vendramin, Nuovo Cim., **70,** 441, 1970, and by G. Mack (Preprint, University of Miami, 1970).
45. S. Ciccariello, G. Sartori and M. Tonin, Nuovo Cimento, **55A,** 847, 1968.
46. K. Bardacki, Y. Frishman and M. B. Halpern, Phys. Rev., **170,** 1353, 1968.
47. J. D. Bjorken and R. Brandt, Phys. Rev., **177,** 2331, 1969.
48. R. Gatto, Rivista del Nuovo Cimento, **1,** 514, 1970.

НАРУШЕННАЯ КАЛИБРОВОЧНАЯ ИНВАРИАНТНОСТЬ ПРИ НЕУПРУГОМ РАССЕЯНИИ ЛЕПТОНОВ НА НУКЛОНАХ

Г. САРТОРИ

Резюме

С помощью изучения коммутаторов тока вблизи светового конуса рассматривается нарушенная калибровочная инвариантность при неупругом рассеянии лептонов на нуклонах. Предложены модели, основанные на идеях Вильсона, и обеспечивающие более общее описание, чем канонические модели.

Acta Physica Academiae Scientiarum Hungaricae, Tomus 31 (1—3), pp. 75—84 (1972)

SCALE INVARIANCE, GOLDSTONE BOSONS AND THE f′ TRAJECTORY*

By

Y. FUJII

INSTITUTE OF PHYSICS, COLLEGE OF GENERAL EDUCATION, UNIVERSITY OF TOKYO, TOKYO, JAPAN

We propose that the f′ trajectory at $\alpha_{f'} = 0$ can serve the role of a Goldstone boson for cale invariance and discuss experimental consequences that follow from such an association.

Introduction

One of the most important questions on scale invariance in elementary particle physics is how good this invariance is in the real world. In this connection GELL-MANN [1] emphasized that there are two ways in which scale invariance manifests itself. In one way *(i)* the masses of all the particles will be massless in the limit of scale invariance. The invariance is violated to the extent that the nucleon mass, for example, has a value $\sim$1 GeV. In another way *(ii)*, the particles may be massive even in the limit of scale invariance provided there is a Nambu—Goldstone boson, i.e. a massless scalar meson. A measure of violation of scale invariance would be given by how much massive this Goldstone boson is in the actual world. The arguments on these points will be reviewed briefly in the following.

As an illustration consider the matrix element of the stress-energy-momentum tensor $\theta_{\mu\nu}$ between the states of a spinless particle. Using Lorentz covariance, parity conservation, time-reversal invariance, one can write the most general form given by [1]

$$\langle p'|\theta_{\mu\nu}|p\rangle = \frac{1}{2E}\left[2P_\mu P_\nu F(k^2)+(k^2\delta_{\mu\nu}-k_\mu k_\nu)G(k^2)\right], \tag{1}$$

where p_μ, p'_μ are the momenta of the particle in the initial and final states, and

$$P_\mu = \frac{1}{2}(p_\mu+p'_\mu), \quad k_\mu = p_\mu - p'_\mu .$$

* Enlarged version of the paper by C. B. Chiu, Y. Fujii, and W. W. Wada, Lett. Nuovo Cimento, **1**, 110, 1971.

One can check that the form (1) is consistent with the conservation law $\partial_\mu \theta_{\mu\nu} = 0$. The first form factor $F(k^2)$ is normalized as

$$F(0) = 1. \tag{2}$$

One now uses the fact that $\theta_{\mu\nu}$ is traceless in the limit of scale invariance;

$$\theta_{\mu\mu} = 0. \tag{3}$$

This is derived from the geometrical consideration. The only question is how to modify the usual definition of the "canonical" stress–energy–momentum tensor derived from the field theoretic Lagrangian. See the papers by STRATHDEE and TAKAHASHI [2], and by GELL-MANN [1].

Imposing the condition (3) onto (1) one obtains

$$0 = \langle p'|\theta_{\mu\mu}|p\rangle = \frac{1}{2E}\,[2P^2\,F(k^2) + 3k^2 G(k^2)], \tag{4}$$

which gives a constraint on two form factors $F(k^2)$ and $G(k^2)$. Particularly interesting is their behavior for $k^2 \approx 0$. Noting $P^2 \approx p^2 \approx -m^2$ in this limit one finds two cases: If $G(k^2)$ is finite at $k^2 = 0$, Eq. (4) gives

$$-2m^2 F(0) = 0,$$

which combined with (2) gives

$$m^2 = 0.$$

This corresponds to the case *(i)* mentioned above. On the other hand, one may assume that $G(k^2)$ has a pole at $k^2 = 0$. Eq. (4) is then satisfied by

$$G(k^2) = \frac{2}{3}\,\frac{m^2}{k^2}\,. \tag{5}$$

This pole can be interpreted as the emergence of a massless scalar boson (the Nambu–Goldstone boson) which will be hereafter called the θ_λ meson.

The matrix element (1) is the "form factor" of a coupling of the particle to the graviton, since $\theta_{\mu\nu}$ is a source of the graviton. Eq. (5) will correspond to the fact that the diagram (a) of Fig. 1 contains a part which is dominated by the exchange of the θ_λ as illustrated by the diagram (b). One realizes a close analogy to the pion dominance in the weak coupling of a hadron to the leptons.

In the diagram (b) the constant for the graviton—θ_λ junction is denoted by f_θ (times the gravitational constant) while the coupling of a hadron labeled by i to θ_λ is denoted by $f_{\theta ii}$. The amplitude corresponding to the diagram (b) is then given by

$$G(t) = \frac{f_\theta f_{\theta ii}}{-t}, \tag{6}$$

where $t = -k^2$. Comparing this with (5) one obtains the relation

$$m_i^2 = \frac{3}{2} f_\theta f_{\theta ii}, \tag{7}$$

which is the exact analogue of the Goldberger–Treiman relation.

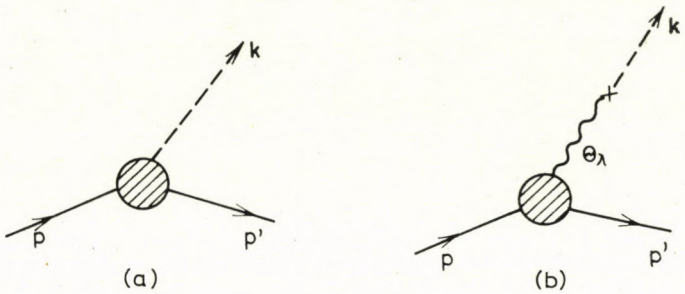

Fig. 1. Diagrams for $\langle p'|\theta_{\mu\nu}|p\rangle$

Now the question is whether there is a scalar meson which is light enough to be considered as an approximate Goldstone boson. The meson should be isoscalar as far as the electromagnetic mass differences are neglected. There are some candidates like ε (750 $\sim$ 900 MeV) or S* (1070 MeV). They are, however, almost as heavy as the nucleon or the ϱ meson, etc. This would mean that there is no preference of the second mechanism (the emergence of the Goldstone boson) over the first one in which finite masses of the ordinary particles are the manifestation of the violation of scale invariance.

It would be here worthwhile to recall that our concept of the particles had been changed drastically in the last decade. We have now the Regge pole theory. What we are going to do in this paper is to try to apply this new concept to the Goldstone boson so that one may consider the real world to be very close to the limit of scale invariance.

Being motivated in this way one can look at the Chew–Frautschi plot to find immediately that there is a trajectory which goes very close to the origin. It is the (exchange degenerate) φ — f′ trajectory. The value of t_θ for which

this trajectory passes through the abscissa, is the order of $\pm m_\pi^2$. One might say that there is some spinless, isoscalar object having the squared mass t_θ. Of course, no such particle has been observed experimentally. One usually appeals to the so-called ghost killing mechanism. The simplest of such is the choosing nonsense mechanism by which the scattering amplitude corresponding to the exchange of this trajectory contains a numerator which behaves like $\sim \alpha(t)$ so that the pole behavior at $\alpha(t) = 0$ is cancelled. We are going to see if this "nonsense point" of the f′ trajectory is identified as the Goldstone boson we are looking for.

Consider scattering of the particle i and the particle j in the t channel. The scattering amplitude will then be given by

$$T(t) \sim \frac{\alpha(t)}{\sin \pi\alpha(t)} . \tag{8}$$

The Feynman amplitude, on the other hand, corresponding to the exchange of a meson θ_λ whose mass is assumed to be exactly zero just for simplicity is given by

$$T(t) \sim \frac{f_{\theta ii} f_{\theta jj}}{t} . \tag{9}$$

Comparing (8) and (9), and accepting the linear trajectory, one realizes that the coupling strength $f_{\theta ii}$ cannot be a constant, but should be proportional to $\sqrt{t}$;

$$f_{\theta ii}(t) = \sqrt{t}\, g_{\theta ii} , \tag{10}$$

where $g_{\theta ii}$ is a constant, or at least finite at $t = 0$. This is, no matter how strange it may appear, an inevitable conclusion from the choosing nonsense mechaitsm and the factorizability of the residue functions. Note also that the Veneziano—Lovelace amplitude gives the same result. Substituting (10) into (6) one obtains

$$G(t) = \frac{f_\theta g_{\theta ii} \sqrt{t}}{-t} .$$

The second term of (4) then vanishes for $t \to 0$ if f_θ is finite at $t = 0$. The only way in which the second term survives so that the nonsense point of the f′ trajectory serves as a Goldstone boson is that f_θ is inversely proportional to $\sqrt{t}$;

$$f_\theta(t) = \frac{1}{\sqrt{t}} F_\theta , \tag{11}$$

where F_θ is a constant, or at least finite at $t = 0$. One may argue at this point if a singular form (11) may cause any serious difficulty. Before answering this question, we discuss what the particle picture of our θ_λ will look like.

The behavior as given by Eq. (10) is supposed to be true for every hadron, so that the pole t^{-1} is always cancelled in any amplitude of the hadron interactions. This means that the θ_λ can never be observed as a particle as long as one is looking at the strong interactions of hadrons. The same would be true also for the interactions of hadrons and photons if the photons are absorbed or emitted always through vector mesons. The situation is not clear for the weak interaction. It is rather likely that the pole t^{-1} appears in the amplitudes involving gravitons. The θ_λ is then a real particle which may decay into a number of gravitons or be produced through the graviton-hadron collision, for example. In the following we discuss other questions which will arise from our approach.

I. Graviton—θ_λ mixing

Practically one does not have to worry about the singular behavior (11), since in the lowest order terms in the extremely small gravitational coupling constant the factor $1/\sqrt{t}$ is so designed as to be cancelled by another factor $\sqrt{t}$ in (10). In principle, however, one can investigate the effect of the higher order terms. We are particularly interested in the infinite sum of the diagrams like those in Fig. 2. This mixing problem between the θ_λ and graviton can be

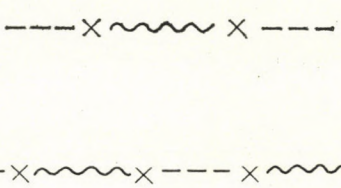

Fig. 2. Examples of diagrams due to the mixing between the graviton and the θ_λ

solved basically. At this moment, however, we can report only the results of an exercise — the mixing problem between a massless vector meson and a scalar meson, θ_λ. The mixing interaction is given by $k_\mu \varepsilon_\mu f_\theta(t)$, where ε_μ is the polarization vector and $f_\theta(t)$ will have the form (11). After solving the Dyson equation in the matrix form, one obtains the results summarized as follows:

(i) The vector meson remains massless after the mixing is turned on.

(ii) The squared mass t_θ is changed to $\tilde{t}_\theta$ by the amount which is second order in the gravitational coupling constant.

(iii) The fields V_μ and φ are related to the diagonalized fields $\tilde{V}_\mu$ and $\tilde{\varphi}$ as follows:

$$V_\mu = b_{11}\tilde{V}_\mu + b_{12}\partial_\mu\tilde{\varphi},$$
$$= b_{21}\partial_\mu\tilde{V}_\mu + b_{22}\tilde{\varphi}.$$

The constants are determined as

$$b_{11} = 1, \quad b_{12} \propto f_\theta(\tilde{t}_\theta),$$
$$b_{21} = 0, \quad b_{22} = 1.$$

The result of b_{12} shows that an infinity can be avoided if

$$\tilde{t}_\theta \neq 0.$$

These qualitative results are expected to remain the same if one replaces the vector meson by the graviton. The analogue of the first point *(i)* will say that main features of Einstein's gravitation theory remain unaltered. It is clear, however, that the second order tensor field which describes the graviton is no longer traceless. If the spinless part corresponding to this trace turns out to be massless, the resulting modification of Einstein's theory may be somewhat similar to DICKE's theory [3].

II. SU_3 transformation property of θ_λ

It is well-known that φ and f′ are very close to the "ideal" mixing of SU_3 so that they transform like $\bar{\lambda}\lambda$ in terms of quarks. It is natural to expect that our θ_λ also transforms in this way. If one appeals to the simple-minded quark counting model, one immediately obtains

$$g_{\theta\pi\pi} = 0\,,$$
$$\frac{g_{\theta\eta_8\eta_8}}{g_{\theta K\bar{K}}} = \frac{4}{3}\,, \tag{12}$$

where η_8 represents the purely octet η meson. Combining (12) with (7), one gets the mass relations

$$m_\pi^2 = 0\,, \qquad \frac{m_{\eta 8}^2}{m_K^2} = \frac{4}{3}\,,$$

which are consistent with GMO mass formula. If one applies the same procedure to the nonet vector and tensor mesons, one obtains the familiar equal spacing law, but with

$$m_\varrho^2 = 0, \quad m_{A_2}^2 = 0\,,$$

since the ϱ as well as the A_2 do not contain the strange quarks. One realizes that we need something else to give the masses of these lowest levels. It is not yet clear which of the mechanisms *(i)* and *(ii)* is responsible for these

masses. (See, however, the following Section IV). Focusing our attention to the SU_3 breaking part at present, we modify the previous formula (7) to the form

$$\delta m_i^2 = \frac{3}{2} F_\theta g_{\theta ii}, \tag{13}$$

where we have replaced f_θ and $f_{\theta ii}$ by F_θ and $g_{\theta ii}$, respectively, by using (10) and (11).

Similar calculations can also be carried out for the fermions. Corresponding to (13) one obtains the result,

$$\delta m_i = 3 F_\theta g_{\theta ii}. \tag{14}$$

Again the θ_λ gives no contribution to the nonstrange baryons like N or Δ. Contrary to the squared mass formula (13) for the mesons, one obtains the linear mass formula (14) for the baryons. Again using the simple quark counting for the estimate of the coupling constants, one obtains the equal spacing law for the baryon masses (neglecting the mass difference between Λ and Σ). For the later use, we quote one of the results

$$\frac{g_{\theta K\bar{K}}}{g_{\theta\Sigma\bar{\Sigma}}} = \frac{2m_K^2}{m_\Sigma - m_N}, \tag{15}$$

which is easily obtained from (13) and (14).

III. Broken chiral symmetry

According to our scheme, we find that the Hamiltonian ($= -\theta_{44}$) contains a part which is dominated by the θ_λ. This part clearly transforms like $\bar{\lambda}\lambda$. On the other hand, GMOR Hamiltonian

$$H' = u_0 + cu_8,$$

which violates chiral $SU_3 \times SU_3$ has the similar SU_3 transformation property. In fact, the constant c was found to be very close to $-\sqrt{2}$. In the approximation in which the pion mass is neglected, c is exactly equal to $-\sqrt{2}$ so that the whole H' transforms like $\bar{\lambda}\lambda$. One may speculate that the part of the Hamiltonian which is dominated by θ_λ is identical with the GMOR Hamiltonian. If this is really the case, the $SU_3 \times SU_3$ violating Hamiltonian is almost invariant under scale transformation, contrary to GELL-MANN's conjecture that GMOR Hamiltonian also violates scale invariance [1].

IV. Exotic nature of the θ_S

As was emphasized in Section II, we need something which lifts up the SU_3 multiplets other than pseudoscalar octet. The violation of scale invariance associated with this might be of the type *(i)* without the Goldstone boson. It seems still worthwhile to explore the possibility that there is another Goldstone boson, which will be called θ_S. We expect that there is another unitary singlet trajectory which is almost degenerate with the f′ trajectory. This trajectory will couple to the hadrons other than pairs of octet pseudoscalar mesons. This suggests that the new trajectory is exotic in a sense that it does not allow simple quark counting.

We also noticed that the GMOR Hamiltonian is the part dominated by the θ_λ. On the other hand, we know that there must be the part of the Hamiltonian which violates chiral $U_3 \times U_3$ but conserves $SU_3 \times SU_3$ [4]. The term having this property must also be exotic in a sense that it cannot be represented by the form $\bar{q}q$. It seems therefore natural to speculate that this is the part which is dominated by the θ_S.

In this connection it is also interesting to note that ARNOLD [5] proposed recently that there is an exotic, and Pomeron-like trajectory which has the unit intercept and the "normal" slope. Our θ_S may belong to a daughter of ARNOLD's trajectory.

V. An experimental test

If we make a full use of the simple-minded quark counting, we can predict results which can be tested in ordinary high energy physics. Noting that the f (1250) contains only non-strange quarks, one obtains, for example,

$$\frac{g_{\mathrm{f}\mathrm{K}\bar{\mathrm{K}}}}{g_{\mathrm{f}\Sigma\bar{\Sigma}}} = \frac{1}{2}\,\frac{g_{\mathrm{f}'\mathrm{K}\bar{\mathrm{K}}}}{g_{\mathrm{f}'\Sigma\bar{\Sigma}}},$$

where the factor 2 in the denominator of the right-hand side comes from the fact that the Σ^+, for example, contains two proton quarks, while it contains only one lamda quark. By assuming some smoothness condition along the trajectory, the right-hand side can be replaced by (1/2) $(g_{\theta\mathrm{K}\bar{\mathrm{K}}}/g_{\theta\Sigma\bar{\Sigma}})$, for which one can use Eq. (15). Further using the SU_3 argument, one arrives at the relation

$$\frac{g_{\mathrm{f}\pi^+\pi^-}}{g_{\mathrm{f}\mathrm{p}\bar{\mathrm{p}}}} = \frac{4}{3}\,\frac{m_{\mathrm{K}}^2}{m_\Sigma - m_{\mathrm{N}}}.$$

In order to test this new relation, we consider the ratio

$$R_\pi = \frac{\sigma_T(\pi\mathrm{N})_{\mathrm{f}}}{\sigma_T(\mathrm{N}\mathrm{N})_{\mathrm{f}}}, \tag{16}$$

where $\sigma_T(\pi N)$, for example, is the part of the πN total cross section dominated by the exchange of the f. One may be able to extract such a part from the high energy πN total cross section by subtracting the asymptotic cross section.

With the aid of the optical theorem, the ratio (16) is put into the form

$$R_\pi = \frac{1}{2m_N} \frac{ImF(\pi N)_f}{ImF(NN)_f},$$

where $F(\pi N)_f$, which is the πN forward scattering amplitude dominated by the exchanged f, is proportional to $g_{f\pi\pi} g_{fNN}$, while $F(NN)_f$ is proportional to $(g_{fNN})^2$. One finally obtains

$$R_\pi = \frac{1}{2m_N} \frac{g_{f\pi^+\pi^-}}{g_{f\bar{p}p}} = \frac{2}{3} \frac{m_K^2}{m_N(m_\Sigma - m_N)} \cong 0.69 . \tag{17}$$

In the same way one obtains

$$R_K = \frac{\sigma_T(KN)_f}{\sigma_T(NN)_f} = \frac{1}{2} R_\pi \cong 0.35 . \tag{18}$$

The experimental data are shown in Table I. Since the asymptotic values for πN and NN cross sections have large uncertainties, we have used two sets of numbers [6–8]. Although it seems premature to draw any definite conclusion, the agreement is at least encouraging.

Table I

Experimental data (from 6 to 20 GeV/c) for R_π and R_K

	Case 1	Case 2
R_π	0.39–0.45	0.84–1.10
R_K	0.19–0.22	0.28–0.40

REFERENCES

1. M. Gell-Mann, Lectures delivered at the Summer School of Theoretical Particle Physics, University of Hawaii, Honolulu, Hawaii, 1969.
2. J. Stratdhee and Y. Takahashi, Nucl. Phys., **8,** 113, 1958. See also Y. Takahashi, Phys. Rev., **D3,** 622, 1971.
3. See, for example, H. Y. Chiu and W. F. Hoffmann, "Gravity and Relativity", W. A. Benjamin, Inc., New York, 1964, p. 143.
4. Y. Fujii, Phys. Rev., **D2,** 896, 1970.
5. R. C. Arnold, Phys. Rev., **D3,** 2250, 1971.
6. W. Rarita, R. Riddell, C. B. Chiu and R. J. N. Phillips, Phys. Rev., **165,** 1615, 1968.
7. G. H. Trilling, Phys. Rev. Letters, **24,** 177, 1970.

8. The asymptotic cross sections, σ_∞, used are (See [6] and [7])
$\sigma(\mathrm{KN})_\infty = 17.0$ mb,
$\sigma(\pi\mathrm{N})_\infty = 20.5$ mb and $\sigma(\mathrm{NN})_\infty = 34.8$ mb for Case 1,
$\sigma(\pi\mathrm{N})_\infty = 18.1$ mb and $\sigma(\mathrm{NN})_\infty = 38.9$ mb for Case 2.

КАЛИБРОВОЧНАЯ ИНВАРИАНТНОСТЬ, БОЗОНЫ ГОЛЬДСТОУНА, И ТРАЕКТОРИЯ f′

Я. ФУДЗИЙ

Резюме

Предложена идея, согласно которой для сохранения калибровочной инвариантности траектория f′ при $\alpha_{f'} = 0$ может играть роль бозона Гольдстоуна. Дискутируются экспериментальные следствия, вытекающие из такой ассоциации.

Acta Physica Academiae Scientiarum Hungaricae, Tomus 31 (1—3), pp. 85—98 (1972)

DEEP-INELASTIC SCATTERING OF POLARIZED ELECTRON BEAM FROM POLARIZED NUCLEON TARGET

By

L. GÁLFI, P. GNÄDIG, J. KUTI, F. NIEDERMAYER and A. PATKÓS

INSTITUTE FOR THEORETICAL PHYSICS, ROLAND EÖTVÖS UNIVERSITY, BUDAPEST

Spin-dependent effects in deep-inelastic electron—proton scattering are discussed.

Introduction

In this report we hope to convince you that spin-dependent effects in deep-inelastic electron–proton scattering are interesting and should yield new information on many questions arisen in the intensive analysis of the spin-averaged SLAC-MIT data [1]. These data shed light on the behaviour of two famous structure functions $W_1(q^2, \nu)$ and $W_2(q^2, \nu)$ vehemently discussed during the last two years [2].

Our group at the Eötvös University started a program last July to investigate the spin-dependent effects measurable by using polarized electron beam scattered on polarized nucleon target. The motivation for this program was that "theoretical explanations" of the SLAC-MIT data on $W_1(q^2, \nu)$ and $W_2(q^2, \nu)$ differed widely. One possibility to test these ideas is to turn to polarization effects.

It turns out from our analysis [3] that the spin-dependent structure functions, which we denote here by $d(q^2, \nu)$ and $g(q^2, \nu)$ should be more selective than the present spin-averaged data.

To our knowledge, there has been only little effort in the literature to shed more light on spin-dependent effects in deep-inelastic electron–proton scattering. Some time ago (1966) BJORKEN wrote down a sum rule for the corresponding cross sections [4] and dismissed it as "worthless". This negative conclusion has been reconsidered in a recent SLAC preprint [5]. Beyond this, we have found only a few attempts to clarify the polarizability contribution of the spin-dependent functions to the hyperfine splitting in the hydrogen atom [6]. Hyperfine splitting is interesting in itself, and we have investigated this problem in the light of the present theoretical situation [3].

I. Kinematics of the scattering process

The scattering amplitude is shown in Fig. 1. Here (p, α) denotes the four-momentum and polarization vector of the proton; (k_1, β) and (k_2, β') are similar notations for the electron beam before and after the emission of a virtual photon of four-momentum q. P_n stands for the hadrons produced in the collision.

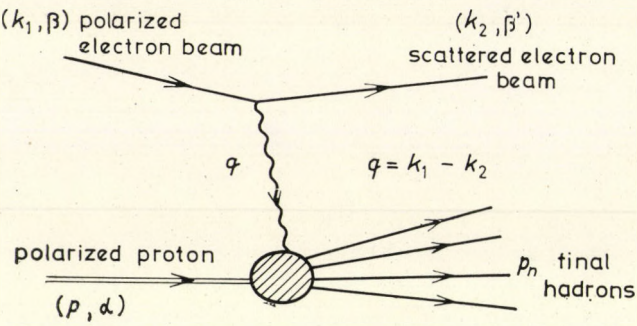

Fig. 1. Inelastic scattering of polarized electron beam from polarized proton target

We sum over final hadrons and the polarization of the scattered electron beam. The differential cross section with proton polarization α and electron polarization β is*:

$$d\sigma_{\alpha\beta} = \frac{1}{4} e^4 q^{-4} [(k_1 \cdot p)^2 - m^2 M^2]^{-1/2} \cdot L^{\beta}_{\mu\nu} \cdot W^{\nu\mu}_{\alpha} \cdot \frac{d^3 k_2}{(2\pi)^3 2E'} . \tag{1}$$

The leptonic part is given by

$$L^{\beta}_{\mu\nu} = \sum_{\beta'} \overline{W}_{\beta'}(k_2)\, \gamma_\mu W_{\beta}(k_1) \cdot \overline{W}_{\beta}(k_1)\, \gamma_\nu W_{\beta'}(k_2) . \tag{2}$$

The hadron amplitude is split into symmetric and antisymmetric parts in the (μ, ν) indices:

$$W^{\alpha}_{\mu\nu}(p, q) = \int d^4 x e^{iqx} \langle p \cdot \alpha | [J_\mu(x), J_\nu(0)] | p, \alpha \rangle = W^{S}_{\mu\nu}(p, q) + i W^{A}_{\mu\nu}(p, q) . \tag{3}$$

From (PT) invariance we read off

$$\begin{aligned} W^{S}_{\mu\nu}(p, q) &= \frac{1}{2} \sum_{\alpha} \int d^4 x e^{iqx} \langle p, \alpha | [J_\mu(x), J_\nu(0)] | p, \alpha \rangle , \\ i W^{A}_{\mu\nu}(p, q) &= \frac{1}{2} \int d^4 x e^{iqx} \{ \langle p, \alpha | [J_\mu(x), J_\nu(0)] | p, \alpha \rangle - (\alpha \rightarrow -\alpha) \} . \end{aligned} \tag{4}$$

* Normalization of states $< p', r \mid p, s > = 2p_0(2\pi)^3 \delta(p' - p)\delta_{rs}$, spinor normalization: $\overline{W} \cdot W = 2m$, $p^2 = M^2$ and $\nu = p \cdot q$.

The definition of the four real structure functions is:

$$W^s_{\mu\nu}(p,q) = \left(\frac{q_\mu q_\nu}{q^2} - g_{\mu\nu}\right) 4\pi M \cdot W_1(q^2,\nu) + \frac{1}{M^2}\left(p_\mu - \frac{pq}{q^2}q_\mu\right)\times$$
$$\times \left(p_\nu - \frac{pq}{q^2}q_\nu\right) 4\pi M \cdot W_2(q^2,\nu)\,, \tag{5}$$

$$W^A_{\mu\nu}(p\cdot q) = \epsilon_{\mu\nu\varrho\sigma}\, q^\varrho\, \alpha^\sigma\, d(q^2,\nu) + (\alpha q)\,\epsilon_{\mu\nu\varrho\sigma}\, q^\varrho\, p^\sigma g(q^2,\nu)\,. \tag{9}$$

Similar splitting can be performed on the leptonic piece of the amplitude:

$$L^\beta_{\mu\nu} = L^s_{\mu\nu} + iL^A_{\mu\nu}\,,\quad L^A_{\mu\nu} = 2m\,\epsilon_{\mu\nu\varrho\sigma}\cdot q^\varrho\,\beta^\sigma\,. \tag{7}$$

In order to analyze spin-dependent effects, we turn to the antisymmetric combination:

$$\frac{d^2\sigma^{\uparrow\uparrow}}{d\Omega dE'} - \frac{d^2\sigma^{\uparrow\downarrow}}{d\Omega dE'} = \alpha^2\,\frac{E'}{\pi\cdot M\cdot E}\,\frac{1}{q^2}\cdot$$
$$\cdot\left\{(E+E'\cos\theta)\,d(q^2,\nu) + (E-E'\cos\theta)\,(E+E')\,Mg(q^2,\nu)\right\}. \tag{8}$$

Here E and E' are, respectively, the initial and final electron energies, as viewed in the laboratory frame, and θ is the electron scattering angle. $d\sigma^{\uparrow\uparrow}$ is the cross section when the spins of electron and proton are parallel and along the direction of motion of the incident electron; $d\sigma^{\uparrow\downarrow}$ is the cross section for antiparallel spins. The electron mass is neglected in Eq. (8).

II. Light-cone behaviour and scaling laws

It is widely recognized [7] that deep-inelastic electron scattering measures the light-cone behaviour of the commutator functions of two electromagnetic currents sandwiched between identical proton states. We go to coordinate-space by Fourier transformation:

$$X^A_{\mu\nu}(p,x) = (2\pi)^{-4}\int d^4q e^{-iqx}\, W^A_{\mu\nu}(p,q)\,,$$
$$iX^A_{\mu\nu}(p,x) = \frac{1}{2}\left\{\langle p,\alpha|[J_\mu(x),J_\nu(0)]|p,\alpha\rangle - (\alpha\to -\alpha)\right\}. \tag{9}$$

Similarly, the Fourier transforms of the structure functions:

$$A_d(p,x) = (2\pi)^{-4}\int d^4q e^{-iqx} d(q^2,\nu),$$
$$A_g(p,x) = (2\pi)^{-4}\int d^4q e^{-iqx}\, g(q^2,\nu).$$

In terms of these amplitudes we write:

$$X^A_{\mu\nu}(p,x) = i\epsilon_{\mu\nu\varrho\sigma}\,\partial^\varrho\,\alpha^\sigma\,A_d(p,x) - (\alpha\cdot\partial)\,\epsilon_{\mu\nu\varrho\sigma}\,\partial^\varrho\,p^\sigma\,A_g(p,x)\,. \tag{10}$$

$A_d(p,x)$ and $A_g(p,x)$ are invariant functions of two independent Lorentz scalars; x^2 and $M^{-2}(px)^2$ or x^2 and $-x^2 + M^{-2}(px)^2$ can be choosen for convenience.

We have proved that $A_d(p,x)$ and $A_g(p,x)$ vanish outside the light-cone and they have correct support properties in momentum space to apply the Jost—Lehmann representation to them. In the proton rest frame:

$$\begin{aligned} A_d(p,x) &= i\int_0^\infty d\lambda^2 \Delta(x,\lambda^2)\,\varphi_d(x_0,\lambda^2)\,,\\ \Delta(x,\lambda^2) &= \frac{1}{2\pi}\epsilon(x_0)\left\{\delta(x^2) - \theta(x^2)\,\frac{\lambda^2}{2}\,\frac{J_1(\sqrt{\lambda^2 - x^2})}{\sqrt{\lambda^2\cdot x^2}}\right\}. \end{aligned} \tag{11}$$

Provided the integral

$$a_d\,(M^{-2}(px)^2) = \int_0^\infty d\lambda^2\cdot\varphi_d(M^{-2}(px)^2,\lambda^2)$$

converges, we can write $A_d(p,x)$ in the form

$$A_d\,(p,x) = \frac{i}{2\pi}\,\epsilon(x_0)\,\delta(x^2)\,a_d(x_0) + R_d(p,x)\,, \tag{12}$$

where $R_d\,(p,x)$ is less singular than $1/x^2$ on the light-cone. The Fourier transformed form of Eq. (12) yields the asymptotic behaviour in the deep-inelastic limit when $\omega = -2\nu/q^2$ is fixed and $\nu\to\infty$:

$$\begin{aligned} d(q^2,\nu) &\sim \frac{1}{\nu}\,\alpha(\xi), \quad \xi = \frac{M}{\omega}\,,\\ a_d\,(x_0) &= -\frac{1}{2\pi M}\int_{-M}^{M} d\xi\; e^{i\xi x_0}\,\alpha(\xi)\,. \end{aligned} \tag{13}$$

$\alpha(\xi)$ has to vanish for $|\,\xi\,| > M$.

$R_d(p,x)$ cancels the leading δ-singularity in the forbidden region in momentum space where $d(q^2,\nu)$ is forced to vanish because of support conditions.

It may happen that the leading δ-singularity of $A_d\,(p,x)$ is missing in special dynamical models. In that case $\int d\lambda^2\cdot\varphi_d(x_0,\lambda^2) = 0$ is satisfied identically. Apart from more singular cases, the integral

$$b_d(M^{-2}(px)^2) = -\frac{1}{4}\int_0^\infty d\lambda^2 \cdot \lambda^2 \cdot \varphi_d(M^{-2}(px)^2) \tag{14}$$

converges and we write

$$A_d(p,x) = \frac{i}{2\pi}\,\epsilon(x_0)\,\theta(x^2)\,b_d(M^{-2}(px)^2) + S_d(p,x)\,, \tag{15}$$

where $S_d(p, x)$ vanishes on the light-cone in the limit $x^2 \to 0$. Again, Fourier representation shows that the scaling limit is determined by the leading light-cone singularity in Eq. (15):

$$\begin{aligned} d(q^2,\nu) &\to \frac{\gamma(\xi)}{2\nu^2}\,, \\ b_d(x_0) &= -\frac{1}{M^2}\int_0^M d\xi\,\frac{\sin \xi x_0}{x_0}\,\gamma(\xi)\,, \end{aligned} \tag{16}$$

where $\gamma(\xi)$ is restricted to $|\xi| \leq M$.

The observed scaling behaviour of $W_1(q^2, \nu)$ and $W_2(q^2, \nu)$ puts stringent restrictions on the "scaling" of $d(q^2, \nu)$ and $g(q^2, \nu)$. The general constraints have been derived from $W^\alpha_{\mu\nu}(p, q) \cdot a^\mu \cdot a^{\nu *} \geq 0$, which is valid for any complex four-vector a^μ. With properly choosen a_μ's we find four inequalities:

$$\begin{aligned} &V_1(q^2,\nu) + M^2 \cdot V_2(q^2,\nu) \geq 0, \\ &q^2 V_1(q^2,\nu) + \nu^2 \cdot V_2(q^2,\nu) \geq 0, \\ &d^2(q^2,\nu) \leq (V_1(q^2,\nu) + M^2 \cdot V_2(q^2,\nu))\,(q^2 \cdot V_1(q^2,\nu) + \nu^2 \cdot V_2(q^2,\nu)), \\ &g^2(q^2,\nu) \leq M^{-2}(q^2 \cdot V_1 + \nu^2 \cdot V_2) \cdot V_1^2\,(\nu/M\sqrt{V_1 + M^2 V_2} - \\ &\qquad - \sqrt{q^2 V_1 + \nu^2 V_2})^{-2}. \end{aligned} \tag{17}$$

Here we have introduced two local functions instead of $W_1(q^2, \nu)$ and $W_2(q^2, \nu)$:

$$\begin{aligned} W^s_{\mu\nu}(p,q) = &[q_\mu q_\nu - q^2 g_{\mu\nu}] \cdot V_1(q^2,\nu) + \\ &+ [(p_\mu q_\nu + p_\nu q_\mu)(pq) - p_\mu p_\nu \cdot q^2 - (pq)^2 \cdot g_{\mu\nu}]\,V_2(q^2,\nu). \end{aligned} \tag{18}$$

We put into (17) the observed behaviour of $W_1(q^2, \nu)$ and $W_2(q^2, \nu)$. We find *in scaling limit* the very interesting upper bounds on $d(q^2, \nu)$ and $g(q^2, \nu)$:

$$d(q^2,\nu) \leq \frac{1}{\nu^{1/2}} \cdot \text{scaling function, if } F_l(\xi) \neq 0,$$

$$d(q^2, \nu) \leq \frac{1}{\nu} \cdot (\text{scaling function}) \qquad \text{if } F_l(\xi) = 0,$$

$$g(q^2, \nu) \leq \frac{1}{\nu^{3/2}} \cdot (\text{scaling function}) \qquad \text{if } F_l(\xi) \neq 0, \tag{19}$$

$$g(q^2, \nu) \leq \frac{1}{\nu^2} \cdot (\text{scaling function}) \qquad \text{if } F_l(\xi) = 0.$$

Here $V_1(q^2, \nu) \to 1/2\nu \; F_l(\xi) \cdot \xi^{-1}$ and $F_l(\xi) = 0$ is allowed by the present data. The restriction (19) on $d(q^2, \nu)$ is consistent with a leading $\in (x_0)\delta(x^2)$ singularity in $A_d(p, x)$. However, derivatives of $\delta(x^2)$ are forbidden by the bound in *any local representation* for $A_d(p, x)$.

The $\delta(x^2)$-singularity in $A_g(p, x)$ is ruled out by (19). The corresponding "smooth" scaling behaviour follows from the form, analogous to (15):

$$A_g(p, x) = \frac{i}{2\pi} \in (x_0) \cdot \theta(x^2) \cdot b_g(M^2(px)^2) + S_g(p, x), \tag{20}$$

$$g(q^2, \nu) \to \frac{\beta(\xi)}{2\nu^2},$$

$$b_g(x_0) = -\frac{1}{M^2} \int_0^M d\xi \, \frac{\sin \xi x_0}{x_0} \beta(\xi). \tag{21}$$

From this analysis, we expect the scaling law for $\nu \cdot d(q^2, \nu)$ or $\nu^2 \cdot d(q^2, \nu)$ depending on more detailed dynamics, and for $\nu^2 \cdot g(q^2, \nu)$. Fractional powers of ν could appear in the scaling laws, but this would imply less regular "theories" which we do not want to discuss here.

The missing $\delta(x^2)$-singularity in $g(q^2, \nu)$ is not a real surprise, because we have used the experimental input for $V_1(q^2, \nu)$ and $V_2(q^2, \nu)$. The $\delta(x^2)$-singularity is missing in $V_2(q^2, \nu)$ and the four structure functions are coupled through the inequalities in (19).

The next step is to calculate the equal-time commutators. It is easy to see from Eqs. (9), (12), (15) and (20) that

$$X^A_{ik}(p, x_0 = 0, \mathbf{x}) = a_d(0)\delta^{(3)}(\mathbf{x}) \cdot \in_{ikl} \cdot \alpha^l \tag{22}$$

Only the $\delta(x^2)$-singularity of $Ad(p, x)$ contributes to the equal-time commutator of the space-space components. No gradient terms appear in (22). In quark algebra [4, 5] we have

$$[J_i(0, \mathbf{x}), J_k(0)] = -2i \in_{ikl} \cdot J^l_5(0) \cdot \delta^{(3)}(\mathbf{x}) + \text{gradient terms.} \tag{23}$$

The commutator algebra in (23) sandwiched between identical proton states, is

$$X_{ik}^{A}(p, x_0 = 0, \mathbf{x}) = 4M \cdot Z\delta^{(3)}(\mathbf{x}) \cdot \epsilon_{ikl} \cdot \alpha^l + \text{gradient terms} \qquad (24)$$

$$\langle p, \alpha \mid J_5^{\mu}(0) \mid p, \alpha \rangle = -2MZ \cdot \alpha^{\mu}.$$

In our analysis Z is given in terms of a measurable integral:

$$Z = -\frac{1}{4\pi M^2} \int_0^M d\xi \alpha(\xi) \ . \qquad (25)$$

From isospin algebra:

$$Z = \begin{cases} \bar{Z} + \dfrac{1}{6}\left|\dfrac{G_A}{G_V}\right| & \text{quark algebra; proton target;} \\ \bar{Z} - \dfrac{1}{6}\left|\dfrac{G_A}{G_V}\right| & \text{quark algebra; neutron target.} \end{cases}$$

Here $\left|\dfrac{G_A}{G_V}\right| \approx 1.2$ is the ratio of β-decay coupling constants and $\bar{Z}$ is a model-dependent isoscalar contribution. Depending upon the sign of $\bar{Z}$, the magnitude of Z must be greater than 0.2 for either proton or neutron target [5]. In field algebra the antisymmetric piece of the equal-time commutator should vanish identically.

III. J-plane analysis

The forward virtual Compton amplitude is defined by

$$M_{\mu\nu}^{\alpha}(p, q) = i \int d^4 x e^{iqx} \langle p, \alpha | T(J_{\mu}(x), J_{\nu}(0)) | p, \alpha \rangle + \text{polynomial}.$$

The scattering process, described by the S-matrix element $\epsilon_{\mu}^{*}(q^2) M_{\alpha}^{\mu\nu}(p, q) \epsilon_{\nu}(q^2)$ is shown in Fig. 2. $\epsilon_{\mu}(q^2)$ is the polarization vector of the virtual photon. We define the symmetric and antisymmetric pieces:

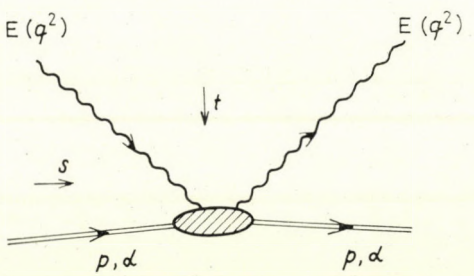

Fig. 2. Virtual Compton scattering on polarized proton

$$M^S_{\mu\nu}(p,q) = \frac{1}{2}[M^{\alpha}_{\mu\nu}(p,q) + M^{-\alpha}_{\mu\nu}(p,q)],$$

$$M^A_{\mu\nu}(p,q) = \frac{1}{2}[M^{\alpha}_{\mu\nu}(p,q) - M^{-\alpha}_{\mu\nu}(p,q)].$$

The imaginary parts are

$$\text{Im}\, M^S_{\mu\nu}(p,q) = W^S_{\mu\nu}(p,q),$$
$$\text{Im}\,(-iM^A_{\mu\nu}(p,q)) = W^A_{\mu\nu}(p,q).$$

The covariant expansion of the antisymmetric amplitude is

$$M^A_{\mu\nu}(p,q) = i\epsilon_{\mu\nu\varrho\sigma}\, q^{\varrho}\, \alpha^{\sigma} \cdot D(q^2,\nu) + i(\alpha q)\, \epsilon_{\mu\nu\varrho\sigma}\, q^{\varrho}\, p^{\sigma}\, G(q^2,\nu). \tag{26}$$

The imaginary parts of the scalar amplitudes are the spin-dependent structure functions:

$$\text{Im}\, D(q^2,\nu) = d(q^2,\nu),\ \text{Im}\, G(q^2,\nu) = g(q^2,\nu).$$

$D(q^2,\nu)$ is even in ν, $G(q^2,\nu)$ is odd in ν. It is convenient to perform the Regge–Sommerfeld–Watson transformation on two linear combinations* given by

$$H_1(q^2,\nu) = \frac{M^2}{2}[D(q^2,\nu) + (pq)\, G(q^2,\nu)],$$

$$H_2(q^2,\nu) = -\frac{M^4}{2(pq)}\, G(q^2,\nu).$$

There are twelve independent S-channel helicity amplitudes but eight of them vanish in the forward direction. Crossing gives us $H_1(q^2,\nu)$ and $H_2(q^2,\nu)$ in terms of the t-channel helicity amplitudes:

$$H_1(q^2,\nu) = \frac{M^4}{4(\nu^2 - q^2 M^2)}\left[\frac{\nu}{M}\left(F^S_{1-\frac{1}{2};1-\frac{1}{2}}(q^2,\nu) - F^S_{1\frac{1}{2};1\frac{1}{2}}(q^2,\nu)\right) + \sqrt{2q^2}\, F^S_{1\frac{1}{2};0-\frac{1}{2}}(q^2,\nu)\right],$$

$$H_2(q^2,\nu) = -\frac{M^4}{4(\nu^2 - q^2 M^2)}\left[\frac{M}{\nu}\left(F^S_{1-\frac{1}{2};1-\frac{1}{2}}(q^2,\nu) - F^S_{1\frac{1}{2};1\frac{1}{2}}(q^2,\nu)\right) + \frac{\sqrt{2q^2}}{q^2}\, F_{1\frac{1}{2};0-\frac{1}{2}}(q^2,\nu)\right]. \tag{27}$$

* In the first paper of [3] the imaginary parts of $H_1(q^2,\nu)$ and $H_2(q^2,\nu)$ are used as $W_3(q^2,\nu)$ and $W_4(q^2,\nu)$ (up to a constant factor).

Eight conspiracy equations are derived for the eight vanishing S-channel amplitudes expressed in terms of the t-channel ones. After R–S–W transformation on the t-channel helicity amplitudes we get poles + cuts + background:

$$H_1(q^2, \nu) = \sum_i \beta_i^-(q^2) \cdot \nu^{\alpha_i^-(0)-1} + \sum_k q^2 \beta_k^+(q^2) \cdot \frac{\alpha_k^+(0)-1}{\alpha_k^+(0)} \cdot \nu^{\alpha_k^+(0)-2} + \\ + \text{cuts} + \text{background} \tag{28}$$

The signs $\pm$ refer to signature. The leading Pomeranchuk trajectory is decoupled from $H_1(q^2, \nu)$ and $H_2(q^2, \nu)$. This can be demonstrated by turning to the conspiracy equations. The leading singularity, which satisfies the conspiracy equations and theorems on the spin-dependence of high-energy amplitudes [8], is the negative parity piece of the Pomeranchuk cut:

$$\begin{aligned} d(q^2, \nu) &= \beta_p(q^2) \frac{\nu^{\alpha_p(0)}}{\ln \nu} + \text{lower terms}, \\ g(q^2, \nu) &= -\beta_p(q^2) \frac{\nu^{\alpha_p(0)-1}}{\ln \nu} + \text{lower terms}. \end{aligned} \tag{29}$$

There is an attempt to describe the leading scaling behaviour by the leading term in the R–S–W expansion [9]. This idea tries to identify the leading light-cone singularity with the leading J-plane object.

The scaling functions $\alpha(\xi)$ and $\beta(\xi)$ are singular at $\xi = 0$ in that case, and the residue function $\beta_p(q^2)$ has definite q^2-asymptotics to give rise to the desired scaling behaviour of $d(q^2, \nu)$ and $g(q^2, \nu)$. Integrals involving $\alpha(\xi)$ and $\beta(\xi)$ remain meaningful even with $\alpha(\xi)$ and $\beta(\xi)$ singular at $\xi = 0$, since $A_d(p, x)$ and $A_g(p, x)$ are tempered distributions, so that every operation has to be treated in distribution-theoretic sense. In this picture we find the scaling law:

$$\begin{aligned} d(q^2, \nu) &\sim \frac{1}{2\nu} \alpha(\xi), \\ g(q^2, \nu) &\sim -\frac{1}{2\nu^2} \alpha(\xi). \end{aligned} \tag{30}$$

First, one takes the scaling of $\nu^2 g(q^2, \nu)$ for granted, then the behaviour of $d(q^2, \nu)$ follows from (29). The common $\beta_p(q^2)$ in (29) gives rise to the very interesting point that $d(q^2, \nu)$ and $g(q^2, \nu)$ are *not independent* in scaling limit.

This result is independent of the location of the leading J-plane singularity in the deep-inelastic limit if such an object can be singled out at all. The

character of the J-plane singularity appears in the behaviour of $\alpha(\xi)$ near to $\xi = 0$. (30) follows from the R–S–W representation and the identification mentioned above.

IV. Spin-dependent effects in the parton model

We have calculated the structure functions $d(q^2, \nu)$ and $g(q^2, \nu)$ in a simple field-theoretic model [10] which indicates point-like parton interpretation in the spin-dependent case, too. The calculation is tedious and lengthy. The results are transparent and provocative because they do not contain any free parameters.

We have found scale invariance for $\nu \cdot d(q^2, \nu)$ and $\nu^2 \cdot g(q^2, \nu)$ with explicit scaling functions in the deep inelastic region at large values of ω [3].

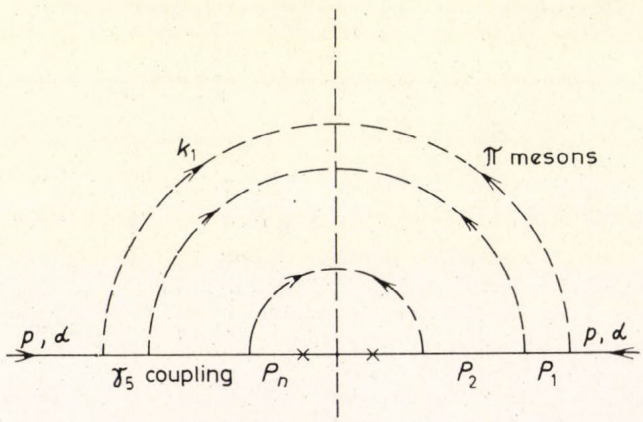

Fig. 3. The current scatters on the proton. Scattering on pions does not give rise to spin-dependent effects

We summarize here only the essential points in the calculation. The technique is the same as applied by DRELL et al. to the spin-averaged amplitudes. We "undress" the current operator and go into the interaction picture with the U-matrix

$$U(t) = \left(e^{-i\int_{-\infty}^{t} dt' H_I(t')}\right)_+ .$$

The free or "undressed" current is related to the fully interacting current by $J_\mu(x) = U^{-1}(t)_{j\mu}(x)U(t)$ where $j_\mu(x)$ has the same form in terms of in-fields as does $J_\mu(x)$ in terms of interacting Heisenberg fields.

One proves for the spin-dependent amplitude in scaling limit:

$$\lim W^{\alpha}_{\mu\nu}(p,q) = \int d^4x e^{iqx} [\langle UP_\alpha | j_\mu(x) j\nu(0) | UP_\alpha \rangle]_{p\to\infty} \quad q^2 \cdot \nu \to \infty \quad \omega > 1 \qquad |UP_\alpha\rangle \equiv U(0)|P,\alpha\rangle. \tag{31}$$

Equation (31) suggests parton-interpretation [10, 11] which may be more general than simple models, manifested in $H_I(t)$. Detailed analysis in the pseudoscalar theory shows that one gets the main contribution to the spin-dependent structure functions from the ladder diagrams (Fig. 3).

We give some explicit formulae to indicate the main points of the calculation. The contribution of π° mesons with n rungs is

$$|Up_\alpha\rangle = \text{const.} \int \frac{d^3p_n}{\sqrt{2E_n}} \cdot \prod_{i=1}^{n} \frac{d^3k_i}{\sqrt{2\omega_i}} \delta^{(3)}(\vec{p} - \vec{p}_n - \vec{k}_1 - \ldots - \vec{k}_n) \times \tag{32}$$

$$\sum_\beta \frac{\bar{u}(p_n,\beta)\gamma_5(M+\hat{p}_{n-1\,n-1})\gamma_5 \ldots \gamma_5(M+\hat{p}_1)\gamma_5 u(p,\alpha)}{(2E_1)\ldots(2E_{n-1})(E_p - E_1 - \omega_1)\ldots(E_p - E_n - \omega_1 - \ldots - \omega_n} |p_n\beta; k_1 k_2 \ldots k_n\rangle,$$

$$W^{\alpha}_{\mu\nu}(p,q) = \text{const.} \int \prod_{i=1}^{n} \frac{d^3k_i}{2\omega_i} \delta(q^2 + 2p_n q) \times \tag{33}$$

$$\times \frac{T_r\left\{(M+\hat{p})\frac{1+\gamma_5\hat{\alpha}}{2}\gamma_5 \ldots (M+\hat{p}_n)\gamma_\mu(M+\hat{p}_n+\hat{q})\gamma_\nu(M+\hat{p}_n)\gamma_5\ldots\gamma_5(M+\hat{p})\gamma_5\right\}}{(2E_1)^2\ldots(2E_n)^2(E_p-E_1-\omega_1)^2\ldots(E_p-E_n-\omega_1-\ldots-\omega_n)^2}.$$

To include the contribution of charged pions is only simple algebra. The antisymmetric piece of Eq. (33) permits the calculation of $d(q^2, \nu)$ and $g(q^2, \nu)$ in the pseudoscalar theory:

$$iW^{A}_{\mu\nu}(p,q) = \text{const.} \int \prod_{i=1}^{n} \frac{d^3k_i}{2\omega_i} \delta(q^2 + 2q_n q)$$

$$\frac{Tr\{(M+\hat{p})\hat{\alpha}(M+\hat{p}_1)\gamma_5\ldots\gamma_\mu(M+\hat{p}_n+\hat{q})\gamma_\nu\ldots}{(2E_1)^2\ldots(2E_n)^2(E_p-E_1-\omega_1)^2\ldots} \tag{34}$$

$$\frac{\gamma_5(M+\hat{p}_1)\gamma_5\}}{(E_p-E_1-\omega_1-\ldots-\omega_n)^2}.$$

One starts from Eq. (34) to work out the practical details. For the calculations we refer to [3]. It turns out that the scaling laws (for proton or neutron):

$$d(q^2,\nu) \sim \frac{1}{2\nu}\alpha(\xi), \qquad g(q^2,\nu) \sim \frac{1}{2\nu^2}\beta(\xi) \tag{35}$$

are general consequences of the special transverse momentum cut-off [10] in a large class of models. We have tried this in the pseudoscalar model and in other models where the pions were replaced by vector mesons [3]. At large ω we have found the scaling function, both for proton and neutron, without free parameters. This makes it possible to estimate the polarization effects in different parton models.

The physical interpretation is simple and transparent. The current is scattered on point-like constituents, $d(q^2, \nu)$ and $g(q^2, \nu)$ measure the spin-distribution of the partons inside the physical nucleon:

$$W^{\alpha}_{\mu\nu}(p, q) = \sum_N P(N) \int_0^1 dx\, f_N(x)\, W^{\beta(p_n,\alpha,p)}_{\mu\nu}(p_n, q)\,, \tag{36}$$

where $p_n = xp$. $P(N)$ is the probability that we find N partons inside the proton, $f_N(x)$ is the probability that the "proton—parton" has a four-momentum xp. The polarization $\beta(P_n, \alpha, p)$ of this parton depends on the polarization of the physical proton.

The current scatters on the spin one-half charged constituents described by $W^{\beta}_{\mu\nu}(p_n, q)$. The results one deduces from these models can be generalized to parton models without concrete field-theoretic background [12]. In our Letter [3] we have chosen a simple quark model to study spin-dependent effects. In the light of the field-theoretic analysis we have now more general results.

We emphasize again that the scaling law in (35) seems to be rather common property of different dynamical models based on point-like constituents. The scaling functions can be calculated explicitly and we find sizeable polarization effects in the deep-inelastic region.

V. Conclusion

Spin-dependent effects in the deep-inelastic region should be analyzed by measuring the asymmetry

$$A = \frac{d\sigma_{\alpha\beta} - d\sigma_{-\alpha\beta}}{d\sigma_{\alpha\beta} + d\sigma_{-\alpha\beta}}\,. \tag{37}$$

Incident polarized electron or muon beams should be focused onto a polarized target. Scattered electrons or muons at fixed angles are momentum-analyzed and identified using magnetic spectrometers. The theoretical estimations [3, 5] predict raw asymmetries which may well be within the range of electron scattering experiments in the future.

Table I

Predictions and correlations of the different theoretical descriptions

Scaling behaviour	Constitution of the proton	Light-cone singularity Constitution of the electric current	Leading light-cone singularity leading J-plane object
$d(q^2,\nu) \sim \frac{1}{2\nu}\alpha(\xi)$ $g(q^2,\nu) \sim \frac{1}{2\nu^2}\beta(\xi)$	parton-like point constituent with nonzero spin $\alpha(\xi) \neq -\alpha(\xi)$ $Z = -\frac{1}{4\pi M}\int_0^M d\xi\alpha(\xi)$	$A_d(p,x) \sim \epsilon(x_0)\,\delta(x^2)$ $A_g(p,x) \sim \epsilon(x_0)\,\theta(x^2)$ non-vanishing equaltime space-space commutator is possible constituents with non-zero spin are expected	condition of identification: $\alpha(\xi) = -\beta(\xi)$
$d(q^2,\nu) \sim \frac{1}{2\nu^2}\gamma(\xi)$ $g(q^2,\nu) \sim \frac{1}{2\nu^2}\beta(\xi)$	not parton-like	$A_d(p,x) \sim \epsilon(x_0)\,\theta(x^2)$ $A_g(p,x) \sim \epsilon(x_0)\,\theta(x^2)$ equal-time commutator vanishes no restriction on the spin-constitution	identification impossible
$g(q^2,\nu) \sim \frac{1}{2\nu^\epsilon}\beta(\xi)$ $\frac{3}{2} \leqq \epsilon < 2$	not parton-like	$\sigma_s(q^2,\nu) = 0 \nrightarrow$ half-integer spin constituents are present $A_g(p,x) \sim \epsilon(x_0)\,\theta(x^2)\,b(x_0)$ $b(x_0)$ singular	condition of identification: $d(q^2,\nu) \sim \frac{1}{2\nu^{1+\epsilon}}\alpha(\xi)$ $\alpha(\xi) = -\beta(\xi)$

Longitudinally polarized muon beams have been formed from the decay of pions in flight at the major accelerator sites. The Serpukhov accelerator and the Batavia accelerator will give rise to more intense and higher-energy pion beams; this should make muon experiments of this kind feasible. It may also be possible to produce a high-energy polarized electron beam at SLAC.

Another attempt in thinking about the feasibility of the spin-dependent measurement is to use the unpolarized SLAC beam and to try to measure the polarization of the *scattered* electron beam.

We are aware of the experimental difficulties. The motivation for our analyzis is that experimental data on $d(q^2, \nu)$ and $g(q^2, \nu)$ could help a lot in testing different ideas stimulated by the SLAC–MIT experiment.

We have investigated the consistency of Finite-Energy Sum Rules with ideas presented here and the contribution of $d(q^2, \nu)$ and $g(q^2, \nu)$ to the hyperfine splitting of the hydrogen ground-state in different theoretical models [3].

In conclusion, the predictions of the different theoretical considerations are summarized in Table I.

REFERENCES

1. For a review of experimental data see R. E. TAYLOR, SLAC–PUB–677.
2. For a review on recent theoretical ideas, see F. J. GILMAN, SLAC–PUB–674.
3. L. GÁLFI, J. KUTI and A. PATKÓS, Physics Letters **31B**, 465, 1970; detailed investigation will be published in a forthcoming paper.
4. J. D. BJORKEN, Phys. Rev. **148**, 1467, 1966.
5. J. D. BJORKEN, SLAC–PUB–670.
6. C. K. IDDINGS, Phys. Rev. **138B**, 446, 1965; S. D. DRELL and J. D. SULLIVAN, Phys. Rev. **154**, 1477, 1967; V. L. CHERNIAK, B. V. STRUMINSKI and G. M. ZINOVJEV Dubna preprint, E2–4718.
7. R. A. BRANDT, Rockefeller University preprint 1969; L. S. BROWN, Lectures given at the Boulder Summer Institute for Theoretical Physics, 1969; R. J. JACKIW, R. VAN ROYEN and G. B. WEST, Massachusetts Institute of Technology, Preprint 1970; H. LEUTWYLER and J. STERN, TH. 1138-CERN, preprint 1970.
8. A. H. MUELLER and T. L. TRUEMAN, I. II, Phys. Rev. **160**, 1296, 1967 and 1306, 1967.
9. H. HARARI, Phys. Rev. Letters **22**, 1078, 1969; H. D. I. ABARBANEL, M. L. GOLDBERGER and S. B. TREIMAN, Phys. Rev. Letters, **22**, 500, 1969.
10. S. D. DRELL, D. I. LEVY and TUNG-MOW-YAN, SLAC–PUB–685.
11. R. P. FEYNMAN, Cal. Tech., preprint.
12. J. D. BJORKEN and E. A. PASCHOS, SLAC–PUB–572.

ГЛУБОКО НЕУПРУГОЕ РАССЕЯНИЕ ПОЛЯРИЗОВАННОГО ПУЧКА ЭЛЕКТРОНОВ НА ПОЛЯРИЗОВАННОЙ НУКЛОННОЙ МИШЕНИ

Л. ГАЛФИ, П. ГНЭДИГ, Й. КУТИ, Ф. НИДЕРМАЙЕР и А. ПАТКОШ

Резюме

Рассмотрены эффекты, зависящие от спина при рассеянии электронов на протонах.

Acta Physica Academiae Scientiarum Hungaricae, Tomus 31 (1—3), pp. 99—108 (1972)

SCATTERING OF LIGHT BY LIGHT USING ELECTRON-POSITRON COLLIDING BEAMS

By

Z. KUNSZT, R. M. MURADYAN and V. M. TER ANTONYAN

JOINT INSTITUTE FOR NUCLEAR RESEARCH, DUBNA, USSR

We discuss the process $e^- + e^+ \to \gamma +$ hadrons. Using automodelity, vector-meson dominance and the parton model, we give an estimate of the deep-inelastic cross section, showing that it might be comparable to the cross section of the deep-inelastic reaction $e^- + e^+ \to H +$ anything H being a singled-out hadron. Some of the one-meson contributions are calculated in the quark model.

I. Introduction

As electron–positron and electron–electron storage rings will be considerably developed in the next few years, further new interesting experiments will be feasible if the energies and luminosities anticipated are achieved [1]. First of all the reactions of higher order in electromagnetic interactions are interesting. By storage ring machines the following reactions may be studied:

$$e^- + e^+ \to \text{hadrons} \tag{1}$$

$$e^- + e^+ \to \text{hadrons} + \gamma \tag{2}$$

$$e^- + e^+ \to \text{hadrons} + \mu^- + \mu^+ \tag{3}$$

$$e^- + e^\mp \to \text{hadrons} + e^- + e^\mp \tag{4}$$

The corresponding Feynman diagrams and the expected order of the cross sections are given in Fig. 1. Process (2) is of third order in the electromagnetic coupling constant and its cross section most likely does not decrease faster than the cross section for process (1).

The significance of process (2), which can be considered as generalized Bhabha and Möller scattering, is based on the increase of the cross section near forward direction with increasing energy. As a consequence, the additional factors α and α^2 in the cross sections for process (2) and (1) will be compensated at higher energies as first shown by LOW ten years ago [2]. Each process above gives information for the C-even hadronic states, and their cross sections are connected with the fundamental process of photon–photon scattering.

The present practical importance of Reaction (4) has been realized at Orsay [3], Novosibirsk [4] and SLAC [5]. It represents a powerful method especially for the study of photon–photon scattering. The cross section is given as follows [5]:

$$\sigma^H(s) \sim \alpha^2 \left(\ln \frac{E}{m_e}\right)^2 \int_{S_{th}}^{4E^2} \frac{ds}{s} f\left(\sqrt{\frac{s}{4E^2}}\right) \sigma_{\gamma\gamma}^H(s)\,, \tag{5}$$

where $\sigma_{\gamma\gamma}^H(s)$ is the cross section for the reaction $\gamma\gamma \to$ hadrons, s is the c.m. energy squared, and $f(x)$ is a known function

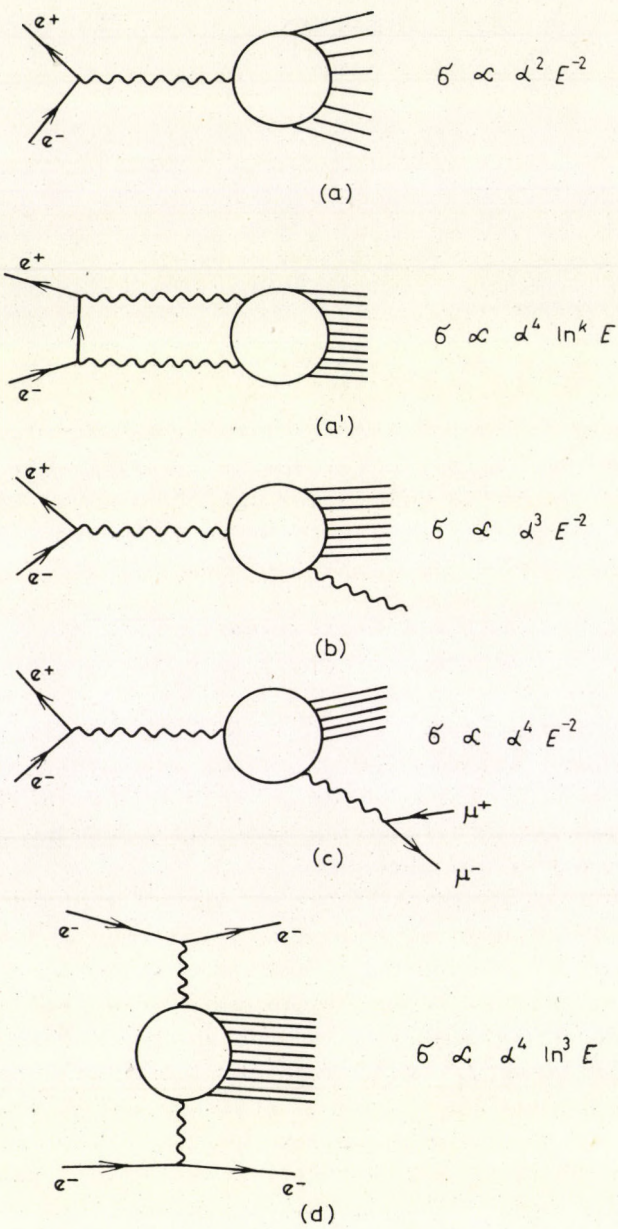

Fig. 1

$$f(x) = (2 + x^2)^2 \log \frac{1}{x} - (1 - x^2)\ (3 + x^2).$$

(As to the resonant scattering of light by light see [6]).

We discuss only Reaction (2), in the deep-inelastic region. Its importance in the investigation of hadron systems with even charge parity conjugation has been studied by CREUTZ and EINHORN [7]. In particular, they thoroughly investigated the $\gamma\pi^-\pi^+$ final state.

In Section II the kinematics is presented and we discuss how to minimize the background. In Section III, using vector-meson dominance (VDM) and the parton model, we give a rough estimate of the deep-inelastic cross section. Finally, in Section IV we briefly review the one-meson contributions.

II. Kinematics

In the one-photon exchange approximation there are two types of amplitudes, as shown in Fig. 2.

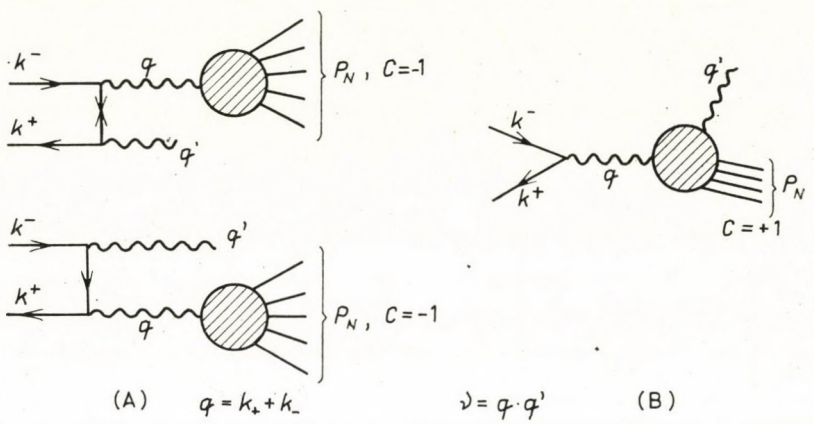

Fig. 2. Feynman diagrams which represent Reaction 2

For experiments which treat the charges symmetrically the interference term between these two types of diagrams vanishes by charge conjugation invariance

$$d\sigma = d\sigma^- + d\sigma^+ \propto |A|^2 + |B|^2. \tag{6}$$

The magnitude of A up to order e^3 can be exactly calculated using Q.E.D. and the knowledge of the cross section for Reaction (3). Therefore, we can measure the magnitude of B in a "charge symmetric" experiment.

The contributions of the C-odd amplitudes to the spin average cross sections with respect to the variable ν and Ω (solid angle of the final photon) are:

$$\frac{d\sigma^{(-)}}{d\Omega\, d\nu} = \frac{8\nu\alpha^3}{q^2} \frac{(1 - a^2/\nu)^2 + \cos^2\Theta}{\sin^2\Theta} \varrho(q^2 - 2\nu), \tag{7}$$

where ϱ is defined as follows:

$$\varrho_{\mu\nu}(\tilde{q}) = \sum_N (2\pi)^4 \delta(q-q'-P_N) \langle 0|J_\mu(0)|P_N\rangle \langle P_N|J_\nu(0)|0\rangle = \\ = (-\tilde{q}^2 g_{\mu\nu} + \tilde{q}_\mu \tilde{q}_\nu)\, \varrho(\tilde{q}^2)\,, \tag{8}$$

where $\tilde{q} = q - q'$, $\tilde{q}^2 = q^2 - 2\nu$.

$J_\mu(x)$ is the electromagnetic current of hadrons. Using knowledge of $\varrho(\tilde{q}^2)$ from Reaction (3), this contribution can be removed. The C-even spin average cross section has the form

$$\frac{d\sigma^{(+)}}{d\nu\, d\Omega} = \frac{2\alpha^3 \nu}{q^6}\left[\overline{W}_1^\gamma(q^2,\nu) + \frac{1}{2}\sin^2\Theta\, \overline{W}_2^\gamma(q^2,\nu)\right], \tag{9}$$

where the inelastic form-factors $\overline{W}_i^\gamma$ are defined as

$$\overline{W}_{\mu\nu}^\gamma = \sum_N (2\pi)^4 \delta(q-q^1-p_N) \int d^4x\, d^4y\, e^{-iq(x-y)}\, \Gamma^N_{\mu\nu}(x,y)\,, \tag{10}$$

where

$$\Gamma^N_{\mu\nu}(x,y) \equiv \langle N|\, T(J_\mu(x)\, J_\varrho(0)\,|0\rangle \langle N|\, T(J_\nu(y)\, J^\varrho(0)\,|0\rangle$$

and

$$\overline{W}_{\mu\nu}^\gamma = \left(-g_{\mu\nu} + \frac{q_\mu q_\nu}{q^2}\right) \overline{W}^\gamma,(q^2,\nu) + \frac{1}{\nu}\left(q_\mu - \frac{q^2}{\nu} q'_\mu\right)\left(q_\nu - \frac{q^2}{\nu} q'_\nu\right) \overline{W}_2^\gamma(q^2,\nu). \tag{11}$$

A more detailed kinematical analysis including spin-dependent effects is presented in [8].

Performing such experiments one encounters the question of distinguishing the internal bremsstrahlung process, represented by diagram B in Fig. 2, from the large background of external bremsstrahlung and photons coming from π° decays. Because of the known features of the external bremsstrahlung photons, the photons radiated by the hadron blob have to be observed at large angles with respect to the direction of the beam and the momenta of the other charged particles involved. To reduce the background one has to know something about the production mechanism of hadrons. (As to the background, see the analysis of the inelastic Compton scattering given in [9].)

BJORKEN and BRODSKY have pointed out [10] that there are two possible extremes. On the one hand, the jet picture, where the distribution of the transverse momenta of secondaries relative to a particular axis is given by an exponential law. Therefore, energetic photons measured at large angles with respect to the jet axis should mainly be due to internal bremsstrahlung (see Fig. 3(a)). On the other hand, the statistical model predicts a distribution of

secondaries which falls off with energy exponentially. According to this model, the mean value of the energy of pions should be $\langle E_\pi \rangle \sim 400$ MeV. If the production of hadrons exhibits such a "statistical" behaviour, very energetic photons transversal to the beam directions should be observed (see Fig. 3(b)).

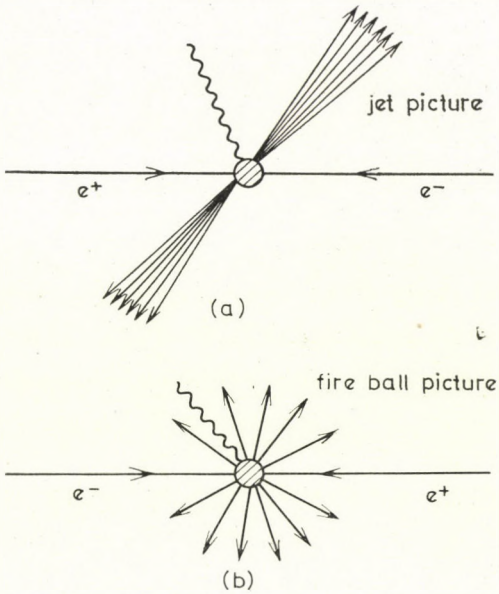

Fig. 3. Graphical schemes for the two possible extremes of the production mechanism of hadrons

Hopefully, measurements of Reaction (1) will provide us with the necessary information to set up an experiment where photons produced by internal bremsstrahlung can be distinguished from the large background.

III. Estimate for the deep-inelastic cross section

To give a rough estimate for the energy-dependence and the magnitude of the cross section, we use automodelity, VMD and the parton model.

The approximate automodelity or scale invariance principle was formulated for lepton—hadron processes at high energies and large momentum transfers [11].

This principle gives the asymptotic form of the structure functions $\overline{W}_i^\gamma(q^2, \nu)$ which are homogeneous functions of corresponding dimensions under the scale transformation

$$q \to \lambda q, \quad q' \to \lambda q'. \tag{12}$$

From Eq. (9) it is clear that the functions $\overline{W}_i^\gamma$ are dimensionless. From the automodelity principle it follows that

$$\overline{W}_i^\gamma(\lambda^2 q^2, \lambda^2 \nu) = \overline{W}_i^\gamma r(q^2, \nu) \qquad i = 1, 2$$

These requirements can be satisfied by putting

$$\overline{W}_i^{\gamma}(q^2, \nu) = \bar{F}_i^{\gamma}\left(\frac{q^2}{2\nu}\right) \qquad i = 1, 2 \tag{13}$$

at high beam and photon energies.

The vector-meson dominance model can be used for the processes with real photons. It might, however, not be used for virtual photons in the far-off time-like region. We use VMD only for the real photon as shown in Fig. 4.

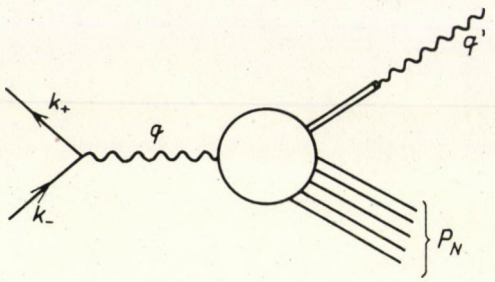

Fig. 4. Vector meson dominance for the real photon

The model connects the C-even part of the cross section for Reaction (2) with the cross section for the reaction

$$e^- + e^+ \to V + \text{hadrons}, \tag{14}$$

V being a singled-out vector meson (cf. [12] and [13]). The second rank tensor of Eq. (10) can be rewritten as

$$\overline{W}_{\mu\nu}^{\gamma} = \sum_N (2\pi)^4 \delta(q - q' - P_N)\left(\frac{1}{2\gamma\nu}\right)^2 \langle 0|J_\mu(0)|P_N, V(q')\rangle \times \\ \times \langle P_N, V(q')|J_\nu(0)|\rangle + \text{interference terms}. \tag{15}$$

Neglecting the interference term, we obtain

$$\overline{W}_1^{\gamma} = \sum \frac{3m_v\,\pi}{\gamma_v^2}\,\overline{W}_1^{v}, \tag{16a}$$

$$\overline{W}_2^{\gamma} = \sum \frac{3\pi}{\gamma_v^2}\,\frac{\nu}{m_v}\,\overline{W}_2^{v}\cdot\left(\frac{\nu}{q^2}\right), \tag{16b}$$

where $\overline{W}_1^{v}$ and $\overline{W}_2^{v}$ are the structure functions for the process of Eq. (14). They are connected with the structure functions of electroproduction on vector

mesons by the substitution law:

$$\overline{W}^{v}_{\mu\nu}(q, q') = W^{v}_{\mu\nu}(q, -q'). \tag{17}$$

The cross section for electroproduction on vector meson has the usual form:

$$\frac{d\sigma}{dE'\,d\Omega} = \frac{\alpha^2}{4E^2 \sin^4 \Theta/2} \left(W^{v}_2(q^2, \nu) \cos^2 \Omega/2 + 2\,\overline{W}^{v}_1 \sin^2 \Theta/2\right). \tag{18}$$

Integrating over the photon solid angle in Eq. (9), and introducing the new variable

$$\omega = \frac{2\nu}{q^2}\,, \tag{19}$$

we can rewrite the cross section given in Eq. (9) as follows:

$$\frac{d\sigma}{d\omega} = \frac{2\pi\alpha^3\,\omega}{q^2}\left[\overline{W}^{\gamma}_1 + \frac{1}{3}\,\overline{W}^{\gamma}_2\right].$$

Using the relations given in Eqs. (16), we obtain:

$$\frac{d\sigma}{d\omega} = \frac{2\pi\alpha^3\,\omega}{q^2} \sum_{v} \left(\frac{3m_v\,\pi}{\gamma_v^2}\,\overline{W}^{v}_1 + \frac{\pi}{2\gamma_v^2}\,\omega\,\frac{\nu}{m_v}\,\overline{W}^{v}_2\right).$$

In the limit $-q^2 \to \infty$, $\nu \to \infty$ and when ω is fixed, the BJORKEN scale invariance behaviour for $\overline{W}_i$ is assumed [14] to be:

$$\begin{aligned} &\lim_{\substack{q^2,\,\nu\to\infty \\ \omega\ \text{fixed}}} \frac{\nu}{m_v}\,\overline{W}^{v}_2 = \bar{F}^{v}_2(\omega)\,, \\ &\lim_{\substack{q^2,\,\nu\to\infty \\ \omega\ \text{fixed}}} m_v\,\overline{W}^{v}_1 = \bar{F}^{v}_1(\omega)\,. \end{aligned} \tag{20}$$

Obviously, the structure functions $\overline{W}^{\gamma}_i$ exhibit the same automodel behaviour:

$$\lim_{\substack{q^2,\,\nu\to\infty \\ \omega\ \text{fixed}}} \begin{cases} \overline{W}^{\gamma}_1 \approx \sum\limits_{v} \dfrac{3\pi}{\gamma_v^2}\,\bar{F}^{v}_1(\omega)\,. \\ \overline{W}^{\gamma}_2 \approx \sum\limits_{v} \dfrac{3\pi}{2\gamma_v^2}\,\omega \bar{F}^{v}_2(\omega)\,. \end{cases} \tag{21}$$

Therefore, the deep-inelastic cross section for Reaction (2) reads as follows:

$$\frac{d\sigma^{(+)}}{d\omega} = \frac{6\pi^2\,\alpha^3\,\omega}{q^2} \sum \frac{1}{\gamma_v^2}\left(\bar{F}^{v}_1(\omega) + \frac{\omega}{6}\,\bar{F}^{v}_2(\omega)\right). \tag{22}$$

We assume that the asymptotic form factors $\bar{F}_1^v(\omega)$ and $\bar{F}_2^v(\omega)$ can be obtained by analytic continuation of the form factors of deep-inelastic electroproduction $F_1^v(\omega)$ and $F_2^v(\omega)$. This assumption has been proposed by several authors [12, 13]. It is worth noticing that such a property can be shown in a simple field theoretic model. In Veneziano-type models, however, the asymptotic form factor $\bar{F}_2(\omega)$ diverges [15].

Supposing that such an analytic continuation is possible, we find (see Eq. 17):

$$F_1^v(\omega) = \bar{F}_1^v(\omega), \tag{23a}$$

$$F_2^v(\omega) = -\bar{F}_2^v(\omega). \tag{23b}$$

For annihilation and electroproduction the physical region has a common boundary, therefore, we can estimate the magnitude of the cross section, Eq. (22), near $\omega \sim 1$ using the knowledge of the asymptotic form factors of electroproduction. The parton model of BJORKEN and PASCHOS [9] should be useful in estimating the order of magnitude of $F_{1,2}^v(\omega)$. For spin 1/2 partons we have:

$$F_1^v(\omega) = \frac{1}{2}\,\omega F_2^v(\omega). \tag{24}$$

Therefore, the cross section (Eq. (22)) can be written as

$$\frac{d\sigma^+}{d\omega} = \frac{2\pi^2\alpha^3}{q^2}\,\omega^2 \sum_v \frac{1}{\gamma_v^2} F_2^v(\omega), \quad \text{near } \omega \sim 1. \tag{25}$$

Since the parton–antiparton cloud gives the main contributions, the magnitude of $F_2^v(\omega)$ is of the same order as for electroproduction on protons. The behaviour of $F_2^v(\omega)$ near $\omega \sim 1$, however, is different from $F_2^{\text{proton}}(\omega)$. In such parton models (the parton spin is 1/2) we have at $\omega = 1$ the following threshold theorems [12]:

for fermions

$$F_2(\omega) = C_n(\omega - 1)^{2n+1} + \ldots \qquad n = 0, 1, 2, \ldots, \tag{26a}$$

and for bosons:

$$F_2(\omega) = C_n'(\omega - 1)^{2n} + \ldots \qquad n = 0, 1, 2. \tag{26b}$$

Therefore, assuming smooth behaviour near $\omega \sim 1$ and that $C_0 \neq 0$, we find that $\bar{F}_2(\omega)$ is larger for bosons than for fermions (see Fig. 5).

The most important contribution comes from the ϱ meson, Using the experimental values of the factors γ_v [1], we obtain:

$$\frac{d\sigma^\gamma}{d\omega} = \frac{d\sigma^v}{d\omega} \geqslant 0.1. \tag{27}$$

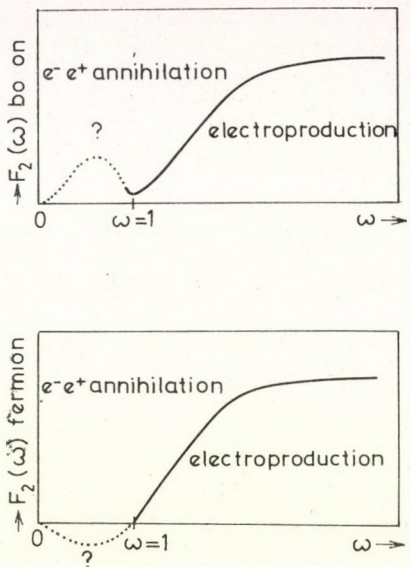

Fig. 5. Asymptotic structure functions for electroproductions and their possible continuations to the region of annihilation

Integrating the cross section (Eq. (25)) over the region $\omega = 0.77$–0.99, at the virtual photon mass square $q^2 \approx 50$ GeV^2 we find

$$\Delta\sigma \sim 10^{-35} - 10^{-36} \text{ cm}^2.$$

Therefore, despite the additional factor α in the cross section for Reaction (2), we expect that it will be comparable with the cross section of the deep-inelastic reaction $e^+ + e^- \rightarrow H +$ anything, H being a singled-out hadron [12].

REFERENCES

1. J. Haissinki, in Proceedings of the 1969-CERN School of Physics, Leysin, Preprint CERN 69—29, 1969.
2. F. Low, Phys. Rev., **120,** 582, 1960.
3. N. Arteaga Romero, A. Jaccarini and P. Kessler, Preprint, College de France, PAM, 7002, 1970.
4. N. Budniev et al., contribution to the XVth International Conference on High Energy Physics, Kiev, 1970.
5. S. Brodsky, P. Kinoshita and R. Terazawa, contribution to the XVth International Conference on High Energy Physics, Kiev, 1970.
6. Z. Kunszt, R. M. Muradyan and V. M. Ter-Antonyan, to be published.
7. M. J. Creutz, M. B. Einhorn, Phys. Rev. Letters, **24,** 341, 1970 and Preprint SLAC–PUB–700, 1970.
8. Z. Kunszt, R. M. Muradyan and V. M. Ter-Antonyan, Preprint, Dubna, 1970.
9. J. D. Bjorken and E. A. Paschos, Phys. Rev., **185,** 1975, 1969.
10. J. D. Bjorken and S. F. Brodsky, Preprint SLAC–PUB–662, 1969.
11. V. A. Matveev, R. M. Muradyan, and A. H. Tavkhelidze, in Proceedings of the International Seminar on Vector Mesons and Electromagnetic Interactions, Dubna 2-4816, 1969; Dubna preprint E2-4968, 1970.

12. S. D. Drell, D. Levy, T. M. Yan, preprint, SLAC–PUB–556, 1969.
13. J. Pestieau, and P. Roy, Phys. Letters, **30B**, 483, 1969.
14. J. D. Bjorken, Phys. Rev., **179**, 1547, 1969.
15. P. V. Landshoff and J. C. Polkinghorne, Preprint DAMPT, **70**/5 Cambridge, 1970.
16. L. D. Soloviev, Phys. Letters, **16**, 345, 1965.
17. R. Van Royen, V. F. Weisskopf, Nuovo Cimento, **50**, 617, 1967.

РАССЕЯНИЕ СВЕТА НА СВЕТЕ, ИСПОЛЬЗУЯ СТАЛКИВАЮЩИЕСЯ ЭЛЕКТРОННЫЙ И ПОЗИТРОННЫЙ ПУЧКИ

З. КУНСТ, Р. М. МУРАДЯН и В. М. ТЕР-АНТОНЯН

Резюме

Рассмотрены процессы $e^- + e^+ \to \gamma +$ адроны. Пользуясь аппроксимацией с помощью векторных мезонов, партонной моделью, и автомодельностью, сделана оценка для глубоко неупругого сечения, которая показывает, что оно сравнимо с сечением глубоко неупругой реакции $e^- + e^+ \to H +$ что- то, где H-есть выбранный адрон. Некоторые из одномезонных вкладов вычислены по модели кварков.

Acta Physica Academiae Scientiarum Hungaricae, Tomus 31 (1—3), pp. 109—122 (1972)

POSSIBLE BOOTSTRAP ORIGIN OF MATHEMATICAL QUARKS*

By

R. H. CAPPS**

DEPARTMENT OF NUCLEAR PHYSICS, WEIZMANN INSTITUTE OF SCIENCE, REHOVOT, ISRAEL

A set of self-consistency conditions based on very simple assumptions is derived. The conditions imply that hadrons have a surprising number of quark-model properties.

I. Introduction

My talk concerns the question, "Why does the quark model work?" But before I attempt to answer this question, I shall ask another, namely, "Why don't physicists worry about this question more than they do?" After all, the quark model is surprisingly successful. Five or six years ago, when this success was first becoming apparent, most physicists who were impressed with the quark model believed that the reason behind it was simply that quarks existed, and would be discovered. This was a reasonable hope. However, after years of unsuccessful quark searches, most of us do not believe in physical quarks any more. So why do we not worry more about the model's success? My own opinion is that we have become too familiar with the model by now, and some of us are so infatuated with learning the various rules and diagrams involving quarks that we forget that the reason why these rules work is still a mystery. In short, some physicists today think that the quark model works because it has always worked. As this is not really a satisfactory reason, I will propose another; that self-consistency conditions of the bootstrap type force hadrons to behave as quark composites.

Before discussing some self-consistency conditions, I will list and comment briefly on what I consider the three main successes of the quark model.

1) A simple rule for exotic states.

2) $SU(6)_W$ symmetry.

3) A simple matrix rule for meson–hadron–hadron coupling ratios.

You all know what exotic means: internal quantum numbers for which no known strongly coupled particles or resonances exist. The fact that there are exotic quantum numbers is not surprising. In any conceivable universe in which some particles possess nonzero values of an additive internal quantum number, the number of internal quantum states corresponding to particles is

* Supported in part by the U.S. Atomic Energy Commission.

** On leave from Purdue University, Lafayette, Indiana, U.S.A.

either finite or infinite. It is certainly not surprising if it is finite, and if it is, the nonresonating quantum states can be called exotic. Furthermore, some states made of two nonexotic particles will be exotic in such a universe. Thus, the quark model is successful not because exotics exist, but because the prescription for exoticity is simple in the model. The prescription is that only quark-antiquark and three-quark states are not exotic.

In order to discuss the second and third successes of the above list, I will first consider what the meson—quark—quark interaction should be in the quark model. Actually, if hadrons were composites of heavy quarks, bound very relativistically, it would not be easy to explain hadrons with realistic physical interactions. However, most physicists today do not try to think of physical quarks when they discuss quark models; rather they think of rules that can be expressed simply in terms of quarks. The term "mathematical quark" is used sometimes to mean that the quarks are not supposed to be real physical particles. My main aim here is to find why the mathematical quark is such a useful concept.

The following is a simple rule for the interaction of meson with mathematical quarks. The quantum numbers a of a meson M_a may be expressed in terms of a square matrix A_{ij}, where this matrix is the coefficient in an expansion of the quantum numbers in quark–antiquark states. Symbolically,

$$a \sim \Sigma_{ij} A_{ij} \bar{Q}_i Q_j. \tag{1}$$

The bar denotes an antiquark. The interaction constant for the process $b \to M_a + d$, where b and d are quarks, is simply λA_{db}, where λ is a constant of proportionality. One can represent this rule with the diagram of Fig. 1(a);

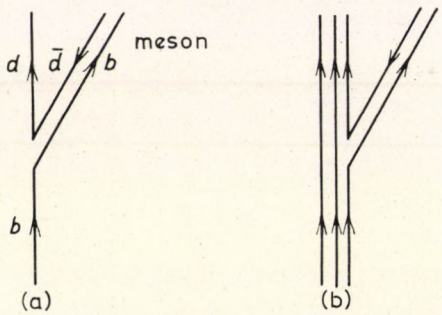

Fig.

this diagram means that the interaction constant is proportional to the coefficient of the $Q_d Q_b$ term in the expansion of the meson wave function.

If the hadrons are considered to be composed of quarks, a simple rule for meson–hadron–hadron interactions is to assume that this interaction is the

sum of the interaction of the meson with all the constituent quarks. This is represented in Fig. 1(b) for the interaction of mesons with baryons (assumed composed of three quarks).

This rule automatically implies SU(n) symmetry, where n is the number of the quark states. If we include the quark spin-component quantum numbers, SU(6) is the group. Because of the charge-conjugation of the meson, one can show that the group must be applied in the $SU(6)_W$ manner; I do not have time to explain this here [1]. The point is that the quark model leads to $SU(6)_W$ naturally, so the success of this symmetry is a success of the quark model.

We next consider the question: does the simple interaction rule given above imply more than $SU(6)_W$ symmetry? Since the mesons correspond both to the singlet and regular representations of the group [i.e. to the representation **1** + **35** of SU(6)], the above construction relates the interactions of the **1** and **35** meson states, and thus does imply more than the symmetry. This extra interaction prediction works fairly well, so I have listed it above as the third success of the quark model.

We must be a little careful about applying this interaction rule. Taken at face value it says that the interactions of the **35** and **1** mesons are proportional to matrix elements of the group generators and identity matrix. Such a rule would say that the meson interactions do not connect different representations, such as the 56 and 70-fold representations of SU(6). Since the observed even- and odd-parity baryon Regge trajectories correspond to these two representations, this rule would imply that such odd-parity states as the Λ^* (1520) and Σ^* (1660) would not decay strongly into meson-baryon states, in contradiction to experiment. Quark model enthusiasts are not troubled with this problem, because they point out that the odd-parity baryons correspond to three-quark states with some orbital angular momentum, and it is easy to write things down so that the meson-56–70- interaction exists. Thus, the physical existence of this interaction is neither a success nor failure of the quark model; I mention it here only because it is something any correct theory must predict.

I will give a short derivation of a set of consistency equations in Section II of this paper, and study the implications for MMM (meson—meson—meson) interactions and MBB (meson—baryon—baryon) interactions in Sections III(A) and III(B), respectively.

II. The consistency conditions

Some of the consistency equations that I will write are algebraically the same as equations derived from two to seven years ago. Among the people who have contributed to the development of the bootstrap equations are

CUTKOSKY [2], POLKINGHORNE [3], CHIU and FINKELSTEIN [4], and myself]5, 6]. The starting points for the derivations have been different; for example, a simple potential model was used in [2] and [3], and N/D dispersion relations were used in [5]. Somewhat later, in [6], superconvergence relations were used to derive similar equations. The recent development of the duality principle has led to great progress in this field, by allowing derivations of consistency conditions that are more plausible than the early derivations, and also lead to a more complete set of conditions. I will give a duality argument here.

I will consider both MM and MB scattering in the s-channel, at an intermediate energy, near the backward (small u) direction. It is assumed that t-channel Regge exchange may be neglected in this region. The duality principle may be written [7]:

$$\langle \operatorname{Im} T_{ui}^{\text{Regge}} \rangle = \langle \operatorname{Im} T_{si}^{\text{res}} \rangle . \tag{2}$$

Here i denotes the internal quantum numbers of the amplitude; i.e., i might represent $\pi^+ p$ scattering in the s channel, in which case it would correspond to $\pi^- p$ scattering in the u channel. The symbol T_{ui}^{Regge} denotes the amplitude for the exchange of u-channel Regge trajectories, T_{si}^{res} is the contribution of resonances to the s-channel amplitude, and $< >$ denotes some sort of semi-local average over energy. I assume that the external particles belong to a set of degenerate mesons and a set of degenerate baryons. If the amplitude i is exotic in the s channel, this condition implies that the trajectories of opposite signatures must be exchange degenerate, and that the residues are numerically equal. From now on I will simply assume the exchange degeneracy of the trajectories, and concentrate on the implications of the condition for the residues.

I now want to digress a little to show how a simple type of diagram, based on the duality principle of Eq. (2), makes plausible the fact that the quark model might lead to solutions of the consistency conditions. These are the "duality diagrams" of ROSNER and HARARI, and they have increased the popularity of consistency conditions based on duality [7, 8]. I will illustrate this with the baryon-exchange contributions to MB scattering. If the MBB interactions follow the rules of Fig. 1, then the left-hand side of Eq. (2) corresponds to the baryon-exchange diagram of Fig. 2(a), while the right-hand side of Eq. (2) corresponds to the baryon-resonance diagram of Fig. 2(b). However, it is clear that if one twists the lines a little, Figs 2(a) and 2(b) are identical, so it is not surprising that the quark model leads to a solution of the conditions. This argument is quite useful as a pedagogical device, but it does not serve the purpose of my talk, for two reasons. First, the argument is unclear in several aspects, among them the role played by the parities of the particles. Second, the quark construction is assumed at the beginning. I am interested in showing not just that a quark model satisfies the conditions, but also that models not

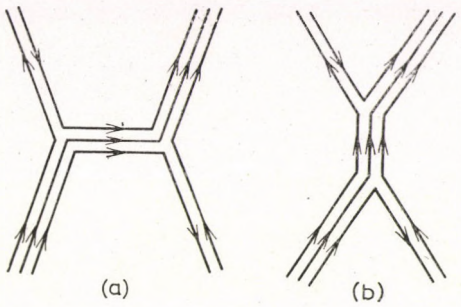

Fig. 2

interpretable in terms of quarks do not satisfy them. Therefore, I must write the consistency equations for the residues in an algebraic form.

The residue condition that follows from Eq. (2) is,

$$\alpha_i(X_{ui}^{(+)} - X_{ui}^{(-)}) = Z_{si}^{(+)} - Z_{si}^{(-)}, \tag{3}$$

where α_i is a kinematic factor, $X_{ui}^{(\pm)}$ is the sum of the residues at small u of the trajectories of signature $(\pm)$, and the $Z^{(\pm)}$ are the contributions of resonances of parities $(\pm)$ to the right-hand side of Eq. (2). The minus sign in front of $Z^{(-)}$ is appropriate, because the contributions to backward elastic scattering of resonances of opposite parities are opposite. The resonances lie on s-channel Regge trajectories, so that the Z_{si} are proportional to the residues of these trajectories. We define constants $\beta_i^{(\pm)}$ by the equation:

$$Z_{si}^{(\pm)} = \alpha_i \beta_i^{(\pm)} X_{si}^{(\pm)}, \tag{4}$$

where $X_{si}^{(\pm)}$ are the residues at small s of the s-channel trajectories. The constants $\alpha_i \beta_i^{(\pm)}$ involve phase space factors and also the variation of the residues between the Regge and resonances regions. Substitution of Eq. (4) into Eq. (3) yields

$$X_{ui}^{(+)} - X_{ui}^{(-)} = \beta_i^{(+)} X_{si}^{(+)} - \beta_i^{(-)} X_{si}^{(-)}. \tag{5}$$

It is important to realize that no assumption has been made between Eqs. (3) and (5), as the constants $\beta_i^{(\pm)}$ are defined by the requirement that Eq. (4) is true.

I now make the assumption that the $\beta_i^{(\pm)}$ are independent of the internal index i. This implies that the residues of the various trajectories are proportional as functions of energy. Basically, this assumption means that the degenerate mesons are dynamically similar, and the degenerate baryons are dynamically similar, i.e., these degeneracies are not accidental. A fuller discussion of the assumption is given in a recent paper [9].

It is now easy to find restrictions on the values of $\beta_i^{(\pm)}$. Application of Eq. (5) to a process exotic in the s channel implies $X_{ui}^{(+)} = X_{ui}^{(-)}$. Application to the crossed process (obtained by reversing the roles of the s and u channels) then implies that $\beta^{(+)} = \beta^{(-)}$. We then consider two possibilities; $X_{ui}^{(+)} - X_{ui}^{(-)}$ either is zero for all i, or is non-zero for at least one i. In the first case, the following consistency condition is automatically valid:

$$X_{ui}^{(+)} - X_{ui}^{(-)} = \pm (X_{si}^{(+)} - X_{si}^{(-)}), \tag{6}$$

although the $\pm$ sign on the right is superfluous in such a case. If $X_{ui}^{(+)} - X_{ui}^{(-)} \neq 0$ for some i, application of Eq. (5) to the amplitude for this i and to the crossed amplitude, together with the condition $\beta^{(+)} = \beta^{(-)}$, implies $\beta^{(+)2} = 1$, or Eq. (6). This equation is the condition that the $X_{si}^{(+)} - X_{si}^{(-)}$ are components of an eigenvector of the s–u crossing matrix, with eigenvalue ± 1. Thus, the condition is a generalization of that of CHEW's reciprocal bootstrap model [10]. In our case, the sign of the eigenvalue depends on whether or not the residue changes sign between the resonance and Regge regions.

Our basic bootstrap equations are Eq. (6) and the corresponding equations that may be obtained for the s–t and u–t pairs of channels, together with the requirements that the set of lowest states on the mesonic and baryonic Regge trajectories should correspond to the sets of external mesons and baryons.

III. Implications of the conditions

(A) MMM interactions

I label the external particles in the s and u channels according to the scheme,

$$\begin{aligned} s: &\quad a + b \to c + d, \\ u: &\quad c + b \to a + d. \end{aligned} \tag{7}$$

We consider first the cases for which a and c are mesons of the same parity, and b and d are either both baryons of the same parity or both mesons of the same parity. We use the labels to refer to both internal quantum numbers and the z-components of the particle spins. We consider only backward scattering, for which the spin-components behave as internal quantum numbers under crossing. The set of mesons must include all the antiparticles, and so must be a self-conjugate set. A complete set of self-conjugate states exists in a self-conjugate set, for convenience, we take all meson states to be self-conjugate.

We consider first the case of MM scattering, where all external mesons are of the same parity. We define the coupling constant of the u-channel trajec-

tory r of even signature (whose physical particles are of even parity) with the final state $a + d$ to be d_{adr} and the corresponding coupling of the trajectory s of odd signature to be f_{ads}. The quantities $X_{ui}^{(\pm)}$ are then given by

$$X_{ui}^{(+)} = \Sigma_r d_{adr} d_{cbr}^*, \quad X_{ui}^{(-)} = \Sigma_s f_{ads} f_{cbs}^*. \tag{8}$$

I have defined the X to be the residues at the small u appropriate for backward s-channel scattering. However, it is more convenient to evaluate the residues at the u of the lowest states on the trajectories, so that the d and f are ordinary meson–meson–meson coupling constants. Thus, the trajectories are labeled by their lowest states. This continuation in u actually introduces a proportionality constant into each of the equations of Eq. (8). However, my assumption concerning the proportionality of the residues of amplitudes of different i allows me to divide out one of the constants, and I choose the relative f/d normalization so that the other cancels also.

The self-conjugate property of the mesons a and c implies that the d_{ijk} and f_{ijk} are Hermitean in the final two indices. From this and Eq. (8), one may write the consistency condition of Eq. (6) in the form,

$$\Sigma_r d_{adr} d_{crb} - \Sigma_s f_{ads} f_{csb} \mp a \rightleftharpoons c = 0, \tag{9}$$

where $a \rightleftharpoons c$ denotes the preceding terms with a and c reversed. The physical states on one of the sets of trajectories have the same parity as the external particles. Our bootstrap hypothesis requires that the set of lowest states on this set of trajectories corresponds to the set of external mesons, and that we later must consider amplitudes with all possible external parity combinations. For MM scattering, we need not consider s–t and u–t channel consistency conditions, as we can permute indices so that every meson exchange is an s–u channel exchange.

I will describe the solution to this type of MMM consistency condition only briefly, as it has been worked out a few years ago. More details are given in [6].

We have taken all the meson states to be self-conjugate. Because of the Bose principle, the d's and f's refer to interactions of even and odd orbital parity, respectively. Since reversing the first two indices corresponds to reversing the directions of the two particles coupled to a trajectory particle, the d and f are symmetric and antisymmetric, respectively, in the first two indices. This, together with the Hermiticity in the last two indices, implies that the d are real and completely symmetric, and the f are imaginary and completely antisymmetric.

One can show that if the lower signs in Eqs. (6) and (9) are taken, there is no nontrivial solution. So we take the upper signs from here on out. This means that the eingenvalue of $X^{(+)}$—$X^{(-)}$ under $s \rightleftharpoons u$ crossing is $(+1)$. A

rather trivial solution exists, with only one state interacting with itself with one symmetric interaction constant; we consider this too trivial. If all f's vanish, it can be shown that one can always choose an appropriate basis so that any solution becomes a direct sum of these disconnected one-state solutions. Hence, a non-triviality requirement implies that the f's do not all vanish.

If one sums Eq. (9) over all permutations of the external particles, a, b, c and d, including a minus sign for odd permutations, the d terms all are cancelled because of the symmetry property $d_{ijk} = d_{jik}$. The resulting equation can be written in the form

$$\Sigma_s (f_{ads} f_{csb} + f_{acs} f_{bsd} + f_{abs} f_{dsc}) = 0 . \tag{10}$$

This is the Jacobi identity for the f's. Together with the antisymmetry property, it implies that the f's must be proportional to the structure constants of a Lie group. A set of particles, all of whose interactions are of the f type, is the set of odd-parity mesons, so our bootstrap equation implies that the odd-parity mesons which interact with each other must correspond to the regular representation of a Lie group. The first use of this type of argument was by CUTKOSKY, who used a potential model involving only vector mesons [2].

We have not yet extracted all the information from Eq. (9), so we continue the argument of [6]. If the d's and f's are regarded as matrices in the space of the last two indices, and the upper sign in Eq. (9) is taken, this equation may be written in terms of matrix commutators, i.e.,

$$[d_a, d_c] - [f_a, f_c] = 0. \tag{11}$$

Since the f commutator exists, so must the d commutator, and so particles of both parities must exist. We may then consider the scattering amplitudes for which three of the external particles are of odd parity and one is of even parity. Our conclusions concerning the symmetry of the d's and f's remain valid if we use them to apply to all MMM interactions, the d and f applying when the product of the three intrinsic parities is even and odd, respectively. Our three odd-one even process leads then to a consistency equation in which each term is bilinear in the d and f. If we follow the procedure used in deriving Eqs. (9) and (11), this new equation in matrix form is,

$$[d_a, f_c] - [f_a, d_c] = 0. \tag{12}$$

This last equation is symmetric in the interchange $a \rightleftharpoons c$, corresponding to the choice of the lower sign in the crossing equation, Eq. (6). It is appropriate to choose this different sign when dealing with an amplitude for which the product of the intrinsic parities changes from the initial to the final state.

These amplitudes are odd in the momentum k_s, which is odd under crossing for collinear amplitudes (i.e., $k_s = -k_u$). Since the coupling constants are defined with this kinematic factor removed, an extra minus sign is introduced into the crossing equations for the coupling constants.

By taking a rather complicated permutation sum of the states a, b, c, and d, one can derive from this equation the matrix equation

$$[d_a, f_b] = -\Sigma_r f_{abr}(d_r)\,. \tag{13}$$

Since the f_{abr} are proportional to structure constants, this equation implies) that d_a transforms either as a singlet under group transformations (if all f_{aij} vanish), or as a regular representation (if some f_{aij} do not vanish). Furthermore, it can be shown that the ratio between these two types of interactions is fixed. This requirement cannot be met with all simple Lie groups. For example, the only simple second rank group that gives a solution is SU(3); the other two (C_2 and G_2) do not, because they do not possess a completely symmetric interaction involving the regular representation only. It may be (though I have not proved it) that only SU(n) gives solutions, in which case the consistency conditions have implied another of the properties of the quark model.

The meson states of both parities must correspond to the singlet and regular representations (though the odd-parity singlet does not interact with pairs of odd-parity mesons). The quantum numbers of each parity set may be written in terms of the quark–antiquark construction of Eq. (1). It has been shown in [6] that the solution to the consistency equations is written simply in terms of these matrices, i.e.;

$$d_{abr} = C\ \mathrm{Tr}\ [(AB + BA)\ R], \tag{14a}$$

$$f_{abr} = C\ \mathrm{Tr}\ [(AB - BA)\ R], \tag{14b}$$

where C is a proportionality constant and Tr denotes the trace. In these equations, the indices are those of the quark—antiquark construction; there is an even-parity and odd-parity meson state for each pair of values of the indices. The d and f apply when the products of intrinsic parities are even and odd, respectively. This solution is a solution to the consistency equations obtained with all possible parity combinations for the external particles. The matrices for the singlet mesons are multiples of the identity matrix. The f constants involving singlets are zero, while Eq. (14a) defines the d constants for both singlet and regular-representation mesons. We conclude that our consistency equations do imply that mesons possess some properties of quark-antiquark composites.

I want to comment further on one feature of these solutions. Recall that by taking a simple permutation sum of Eq. (9), with the upper sign, I

obtained a simple equation involving only the f constants. One cannot obtain a simple equation involving the d constants alone. Therefore, it appears that odd-parity mesons are the more fundamental, and it is not surprising that these are the lightest observed states on the exchange-degenerate meson trajectories. Physically, the lowest states on the even-parity trajectories are one unit of angular momentum higher than the lowest states on the corresponding odd-parity trajectories. I must emphasize again that the quantum numbers involved in the equations do not include total angular momentum, but are the internal quantum numbers and spin component along the direction of the collinear interactions.

(*B*) *MBB interactions*

I will simply assume that states of baryonic number greater than one should not exist. (I do not know whether or not simple solutions to the self-consistency equations exist that involve states of greater baryon numbers.) With this assumption, baryon—baryon scattering is simple, because all states are exotic. This implies that for every $BB \to BB$ amplitude the contribution of exchange-degenerate mesonic trajectories of opposite signatures must cancel. We already found that the quantum numbers of the meson sets of opposite parity must be the same; now we find that the couplings to each baryon pair are the same for a pair of exchange-degenerate trajectories.

This simplifies the treatment of meson—baryon scattering. We need consider only amplitudes for which the parities of the external mesons are the same; the only important parities in the MB problem are those of the baryons. I will use the capital letters D and F to denote the MBB interactions; D applying when the two baryons have the same parity, F applying when the two baryons have opposite parity.

Again, I use the labels of Eq. (7) to describe the scattering in the s and u channels, with a and c self-conjugate mesons, and b and d baryons. The s–u channel consistency equations then follow from the same arguments as before. If b and d have the same parity, the condition may be obtained by replacing the f and d by F and D in Eq. (11). If b and d have opposite parity, one can make the same replacements in Eq. (12). The two resulting equations may be combined into one equation, if we regard the D_i and F_i as matrices corresponding to the meson i in a space which is the direct sum of the baryon states of even and odd parities. This combination equation is

$$[D_c - F_c,\ D_a + F_a] = 0. \tag{15}$$

We recall again that in the space of even and odd-parity baryon states, the D are non-zero only in the diagonal corners that connect states of the same parity, and the F are non-zero only in the off-diagonal corners.

In the case of meson—baryon scattering, the s–t and u–t channel consistency conditions are different in nature from the s–u conditions, and so must be considered also. In these conditions, the t-channel residues involve mesonic trajectories, and are bilinear in an MBB coupling constant and an MMM constant. Because of the symmetry of the MMM constants [the d's and f's of Sec. III(A)] it is convenient to take the sum and difference of the s–t and u–t equations. One does this by writing the s–t equation, reversing the a and c labels, and adding and subtracting. The resulting two equations are,

$$(s\text{–}t)+(u\text{–}t)$$

$$\{D_c+F_c, D_a+F_a\}_+ = K\,\Sigma_m\, d_{acm}(D_m+F_m), \tag{16}$$

$$(s\text{–}t)-(u\text{–}t)$$

$$[D_c+F_c, D_a+F_a] \;= K'\Sigma_m f_{acm}(D_m+F_m), \tag{17}$$

where K and K' are constants and the d and f are the MMM interaction constants of Eqs. (14b).

These three equations, Eqs. (15), (16) and (17), are the consistency equations for the MBB interactions. The derivation and discussion of these equations that I give here are contained in a paper soon to be published [11]. The MMM interaction constants f_{acm} of Eq. (17) are proportional to the structure constants of the group, if all indices refer to regular representation states, and $f_{acm} = 0$ if one or more indices refer to singlet states. Thus Eq. (17) implies that the $D + F$ are a representation of the Lie algebra. If the meson index i refers to a regular-representation state, $(D + F)_i$ represents the generator associated with i; if i is a singlet state, the matrix $(D + F)_i$ commutes with all the generator matrices, and thus is diagonal in every irreducible subspace of the baryon space.

The anticommutator relation, Eq. (16), is new, and to the best of my knowledge, was first discussed in [11]. It is well-known that the anticommutators of matrices representing the generators can be written as a linear combination of the generator matrices and identity matrix *only* in the fundamental representation; for this representation these matrices form a complete set. Thus Eq. (16) implies that the $D + F$ behave like operators in *quark space*, i.e., in the space of the fundamental representation. It is easy to establish that Eq. (16) is satisfied in the quark representation. In fact, for SU(3), Eq. (16) is a standard equation for anticommutators given, for example, by GASIOROWICZ [12]. In GASIOROWICZ, the right-hand side contains a d_{acm} term and a $\delta_{ac}\, I$ term, where I is the identity matrix [12]. Our d is defined for singlet as well as regular representation states, and our d_{acm} term contains the $\delta_{ac}\, I$ term of [12] implicitly.

On the other hand, the baryons cannot correspond simply to quarks of one

parity. If baryons of only one parity existed, the F would vanish, and Eqs. (15) and (17) would be contradictory. Thus the conditions imply that the baryons cannot be simple quarks, but must have many quark-model properties.

I have found two types of solutions to the three equations [11]. In the first, the quantum numbers and interactions of the sets of baryons of both parities are the same. The simplest example is the case where the baryons of each parity correspond to the fundamental representation. In this type of solution, each of the two terms of the commutator of Eq. (15) vanishes for every a and c. This implies that for MB scattering, each quantity $X_{ui}^{(+)} - X_{uj}^{(-)}$ vanishes, so there is no eigenvector of the s–u crossing matrix. In a bootstrap sense, the baryons are bootstrapped entirely by meson exchange, so we can say there is no static limit. This type of solution does not correspond to reality, as the quanta of the baryons of odd and even parities are not the same.

In the second type of solution, the two terms of the commutator of Eq. (15) do not each vanish for all a and c. In the simplest example that I have found, the baryons are all simple N-quark composites, where $N \geq 2$. Since the choice $N = 2$ would correspond to integral-spin baryons, I will consider the three-quark case, and call the quarks α, β and γ. The interaction $D + F$ is in the space of only one quark, which I will call the α quark. In symbols,

$$D_a + F_a = \varkappa A^{\alpha}, \tag{18}$$

where

$$\langle \alpha'\beta'\gamma' \,|A^{\alpha}|\, \alpha\beta\gamma \rangle = A_{\alpha'\alpha}\, \delta_{\beta'\beta}\, \delta_{\gamma'\gamma}.$$

Here $A_{\alpha'\alpha}$ is the matrix element associated with the meson state a by Eq. (1), and $\varkappa$ is a constant of proportionality. This interaction will satisfy Eqs. (16) and (17). The s–u condition, Eq. (15), will be satisfied also if $(D_c - F_c)$ is equal to $\varkappa C^{\beta}$, since the α and β quarks are independent.

These interactions will satisfy all the conditions provided that they are consistent with our definitions of D and F in the space of baryons of both parities. It must be possible to assign each irreducible representation in the baryon space a definite parity in such a way that the D connect only states of the same parity and the F connect only states of the opposite parity. This is easy to do with our choice of interactions, as the D and F matrices are given simply by

$$D_a = \frac{1}{2}\varkappa(A^{\alpha} + A^{\beta})$$

$$F_a = \frac{1}{2}\varkappa(A^{\alpha} - A^{\beta}).$$

Clearly, if the baryon states of opposite symmetry under exchange of the α and β quarks are assigned opposite parity, everything will be all right.

If the group is (SU(6), the three-quark representations that are symmetric under the interchange of the first two quarks are the representations **56** and **70,** while those antisymmetric under this interchange are the **20** and another **70.** Thus, the corresponding solution involves the multiplets $\mathbf{56}^+$, $\mathbf{70}^+$, $\mathbf{70}^-$ and $\mathbf{20}^-$, where the superscript is the parity. In this solution, one can show that the $\mathbf{56}^+$ and $\mathbf{70}^-$ are coupled strongly together, and relatively weakly to the $\mathbf{70}^+$ and $\mathbf{20}^-$. Since the observed baryon spectrum seems to correspond to even parity trajectories of the **56** representation and odd-parity trajectories of the **70** representation, this solution may be valid approximately.

IV. Conclusion

At present we do not know how well the self-consistency conditions are met experimentally. The predicted results do not correspond exactly with experiment. On the other hand, we have made several assumptions that are unnecessary for the deriving of conditions, but were made only for simplicity, and we know these assumptions are not true exactly. An example is the assumption that meson states of the same parity (that are the lowest states on their Regge trajectories) are degenerate. It would be interesting to see if realistic modifications of some of our simple assumptions lead to predicted hadron spectra and hadron—hadron—hadron interaction ratios that agree even better with experiment. I hope that the next few years illuminate this question.

I can summarize my main result in two sentences. A set of self-consistency conditions based on very simple assumptions requires that the hadrons of any solution have a surprising number of quark-model properties. If these conditions are approximately valid physically, this might be the reason that the quark model works so well, even though quarks themselves do not exist.

REFERENCES

1. A lucid discussion of $SU(6)_w$ symmetry is given by H. J. LIPKIN and S. MESHKOV, Phys. Rev., **143,** 1269, 1966.
2. R. E. CUTKOSKY, Phys. Rev., **131,** 1888, 1963.
3. J. C. POLKINGHORNE, Ann. Phys. (N. Y.), **34,** 153, 1965.
4. C. B. CHIU and J. FINKELSTEIN, Phys. Letters, **27B,** 510, 1968.
5. R. H. CAPPS, Phys. Rev. Letters, **10,** 312, 1963.
6. R. H. CAPPS, Phys. Rev., **171,** 1591, 1968.
7. A lucid discussion of the duality principle is given by HAIM HARARI, Phys. Rev. Letters, **22,** 562, 1969. This paper contains references to earlier discussions of duality.
8. J. L. ROSNER, Phys. Rev. Letters, **22,** 689, 1969.
9. R. H. CAPPS, "Baryon Crossing Condition from Duality", (to be published in Phys. Rev. D.)
10. G. F. CHEW, Phys. Rev. Letters, **9,** 233, 1962.
11. R. H. CAPPS, "Induction of Quark-Like Structure of Baryons", (to be published in Phys. Rev. D.).
12. STEPHEN GASIOROWICZ "Elementary Particle Physics" John Wiley and Sons, New York. 1966, Eq. (17.18).

ВОЗМОЖНОСТЬ БУТСТРАПНОГО ПРОИСХОЖДЕНИЯ МАТЕМАТИЧЕСКИХ КВАРКОВ

Р. Х. КЭППС

Резюме

Установлен ряд условий самосогласованности основанных на очень простых предположениях. Эти условия влекут за собой то, что адроны обладают удивительно большим числом свойств модели кварков.

Acta Physica Academiae Scientiarum Hungaricae, Tomus 31 (1—3), pp. 123—128 (1972)

A PARTON APPROACH TO DUAL MODELS

By

P. OLESEN*

CERN, GENEVA, SWITZERLAND

The problem of correspondence of very high order unrenormalized Feynman diagrams to the dual model is discussed. The very high order Feynman diagrams are investigated using a statistical formalism recently developed.

The parton picture was applied originally to inelastic hadron—hadron scattering where it turned out to be quite useful. About a year ago NIELSEN [1] proposed a picture for dual models which in some respects is rather similar to the parton picture. In NIELSEN's view dual models are considered as the limit of very high order unrenormalised Feynman diagrams. NIELSEN also found [1] an electric analogue for dual models which expresses the N-point Veneziano amplitude in terms of the heat generation in a conducting disc of uniform resistivity. Again this result looks rather analogous to Feynman diagrams, where one can think of the Feynman parameters as the resistances of the propagators, and the virtual momenta as the currents passing through the propagators. Of course, there is also the difference that in Feynman diagrams the resistances are variables of integrations which run from 0 to ∞, whereas in the electric analogue for dual models the resistance is a constant proportional to the universal slope of the Regge trajectories. Feynman diagrams also have complicated cuts which are absent in the simple N-point function.

Nevertheless, it is an interesting problem to try to find out in which sense do very high order Feynman diagrams correspond to dual models. SAKITA and VIRASORO [2] and NIELSEN and OLESEN [3] have tried to make the connection more quantitative. The motivation for this kind of work has not only been to obtain a nice physical picture of dual models, but also to try to find a good starting point for introducing fermions in dual models. The idea is, of course, that since everybody knows how to introduce spin in Feynman diagrams, it should not be impossible to apply the parton picture with spinning partons. However, this idea is only good enough, if first of all we know how to treat the scalar case.

Apart from the potential possibilities connected with the spin problem, the parton view has other nice features. If we consider the complicated diagram

* On leave of absence from the Niels Bohr Institute, Copenhagen, Denmark.

in Fig. 1 as representing in some sense a dual N-point function, it is clear that the picture is dual — there is no sense in adding the s- and t-channel singularities in the case of a four-point function. In some sense the picture in Fig. 1 represents a generalization of the quark picture. Instead of quark lines we draw a "world-sheet" filled with partons, and we can stretch the sheet in various ways so as to illustrate the formation of poles in various channels (in much the same way as in the quark picture).

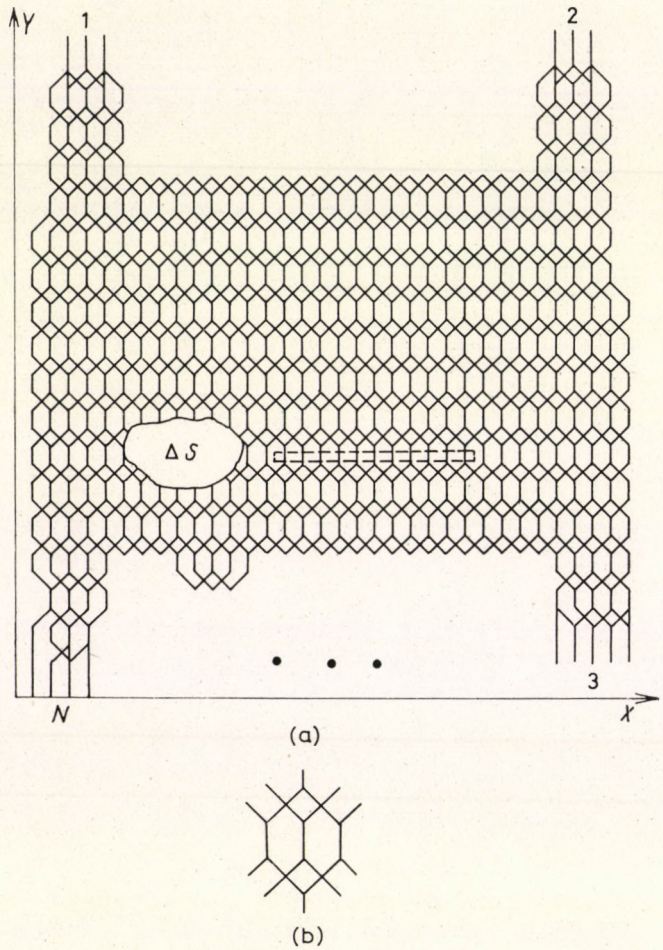

Fig. 1

Now let us turn to the quantitative connection between Feynman diagrams and dual models. I shall briefly outline the main problems, and as far as a possible solution to these problems is concerned, I shall use a statistical formalism for treating very high order Feynman diagrams recently developed [4].

As our starting point, we take the following exact formula for the Feynman amplitude:

$$F_n(p_i\, p_k, m^2) = \int_0^\infty \frac{\prod_{i=1}^{n} d\,\alpha_i}{\Delta_n(\alpha)^2}\, e^{\sum_{i=1}^{n} \alpha_i k_i(\alpha)^2}\, e^{-m^2 \sum_{i=1}^{n} \alpha_i}\,. \tag{1}$$

Here p_i are the external momenta, α_i are the Feynman parameters, and m is the parton mass. The momenta $k_i(\alpha)$ satisfy Kirchoff's equations, i.e. momentum conservation at each vertex and

$$\sum_{\text{loop}} \alpha_i\, k_i(\alpha) = 0, \tag{2}$$

where the sum goes over any loop (with suitable sign conventions for the momenta). The formula (1) is valid in a kinematical region without dynamical singularities, and in the following we shall restrict our considerations to such a region.

The advantage of using Eq. (1) is that the total heat generation $\Sigma \alpha_i k_i(\alpha)^2$ appears in an exponentiated form, just as in dual models. However, the resistances α_i are integration variables. Therefore, the first problem consists in arguing that there exist effective mean values of the α_i, $\bar{\alpha}_i$ say. If so, we could take the exponent outside the integral and we would have something that looks very much like a dual amplitude.

The concept of a mean value is only meaningful in a statistical framework. Therefore, in [4] we have considered very high order Feynman diagrams from the point of view of statistics. It is rather natural to consider Eq. (1) as a mean value of the exponentiated heat generation with respect to the normalized distribution function

$$d_n(\alpha) = e^{-m^2 \sum_{i=1}^{n} \alpha_i} / \Delta_n(\alpha)^2 F_n(0, m^2)\,. \tag{3}$$

Of course, we then define mean resistances by

$$\bar{\alpha}_i = \int \prod_{j=1}^{n} d\,\alpha_j\, d_n(\alpha)\, \alpha_j\,, \tag{4}$$

and similarly we can define higher momenta $\overline{\alpha_i\, \alpha_j}$, etc. These quantities have very nice properties. One can, e.g., show that the average mean resistance $\bar{\alpha}$ approaches a constant for $n \to \infty$,

$$\frac{1}{n} \sum_{i=1}^{n} \bar{\alpha}_i = \bar{\alpha} = \frac{1}{m^2} \left(1 - \frac{2k}{n}\right), \tag{5}$$

where k is the number of loop momenta to be integrated, and n is the number of propagators. The higher moments $\overline{\alpha_i \alpha_k}$, etc., also satisfy nice sum rules. When you put everything together (see [4]), it turns out that you can show the following rather nice result:

Let $G(x)$ be a function such that

$$0 \leq |\, G''(x)| \leq M, \qquad x = \sum_{i=1}^{n} \alpha_i \Phi_i, \qquad \Phi_i = 0\left(\frac{1}{n}\right), \tag{6}$$

then

$$\begin{aligned} F_\eta(\Phi) &= \int_0^{\infty} \frac{\prod_{i=1}^{n} d\alpha_i}{\Delta_n(\alpha)^2}\, G\left(\sum_{i=1}^{n} \alpha_i \Phi_i\right) e^{-m^2 \sum_{i=1}^{n} \alpha_i} \\ &\xrightarrow[n\to\infty]{} G\left(\sum_{i=1}^{n} \bar{\alpha}_i \Phi_i\right) F_n(0) \xrightarrow[n\to\infty]{} G\left(\bar{\alpha} \sum_{i=1}^{n} \Phi_i\right) F_n(0). \end{aligned} \tag{7}$$

Thus, the statistical distribution (3) is such that for $n \to \infty$ it preserves the functional form of G,

$$\overline{G\left(\sum_{i=1}^{n} \alpha_i \Phi_i\right)} \;\to\; G\left(\bar{\alpha} \sum_{i=1}^{n} \Phi_i\right), \tag{8}$$

provided the conditions (6) are satisfied. Now, in particular the function $G(x) = e^x$ satisfies (6) provided $\Phi_i \leq 0$ and hence

$$\begin{aligned} &\int_0^{\infty} \frac{\prod_{i=1}^{n} d\alpha_i}{\Delta_n(\alpha)^2}\, e^{\sum_{i=1}^{n} \alpha_i \Phi_i} e^{-m^2 \sum_{i=1}^{n} \alpha_i} \\ &\xrightarrow[n\to\infty]{} e^{\sum_{i=1}^{n} \bar{\alpha}_i \Phi_i} \int_0^{\infty} \frac{\prod_{i=1}^{n} d\alpha_i}{\Delta_n(\alpha)^2}\, e^{-m^2 \sum_{i=1}^{n} \alpha_i}. \end{aligned} \tag{9}$$

Notice that the integral on the left-hand side of (9) would be the same as the Feynman amplitude if the Φ's were replaced by $k_i(\alpha)^2$. Therefore, the statistical formalism has brought us part of the way to show that the exponentiated heat in F_n could be brought outside the integral. We are not yet finished, of course, since the k_i in (1) depend on the α's. However, it is clear that we only have a chance of applying (9) if k_i^2 is of order $1/n$. What does this mean?

Let us return to Fig. 1. The external hadrons are composed of a large number of partons. We can obviously divide the hadron momenta (p_{H} say) in various ways among the constituent partons. Now we have to be very careful, because if we give a few partons a relatively high momentum (whereas

the rest of the external partons are "soft") then they are not likely to be exchanged already at a few GeV. This is because the hard partons are likely to retain their movements inside the hadrons practically unaffected by the scattering process going on if the energies of the external hadrons are large compared with the parton mass. Self-consistency requires m to be of the order a few hundered MeV, and hence at a few GeV hard parton exchanges are not very important. Therefore, since we want a dynamical picture which is valid uniformly at all energies, as a first approximation we should only consider exchange of soft partons. Now, if the number of propagators is n, it follows from the geometry of Fig. 1 that an external hadron contains $\approx \sqrt{n}$ partons. To make them soft, each parton should carry a momentum of order $p_{\mathrm{H}}/\sqrt{n}$. By Kirchhoff's laws the virtual partons carry then also momenta of order $p_{\mathrm{H}}/\sqrt{n}$. Thus

$$k_i(\alpha)^2 \approx 0\,(p_{\mathrm{H}^2}/n). \tag{10}$$

By means of the statistical formalism one can now argue that the average mean resistance $\bar{\alpha}$ in Eq. (5) is a good statistical description of the most important region of integration when the k's are as small as given by (10). Therefore, the approximation

$$F_n(p_i\,p_k, m^2) \approx \int_0^\infty \frac{\prod_{i=1}^{n} d\alpha_i}{\Delta_n(\alpha)^2}\, e^{i\sum_{i=1}^{n}\alpha_i\, k_i(\bar{\alpha})^2}\, e^{-m^2\sum_{i=1}^{n}\alpha_i} \tag{11}$$

should be good when $n \to \infty$ (for a more detailed discussion of Eq. (11), see [4]). Actually, one can show that Eq. (11) is an upper limit when $n \to \infty$ for the Feynman amplitude (1), and since the k's are anyhow small, this makes us rather confident that Eq. (11) is a good approximation. Using (9) it then follows that

$$F_n(p_i\,p_k, m^2) \to e^{\bar{\alpha}\sum_{i=1}^{n} k_i(\bar{\alpha})^2}\, F_n(0, m^2), \quad n \to \infty\,. \tag{12}$$

The result (12) is based on the physical assumption of soft partons, and on the approximation (11). If one is not content with (11) one can expand $k_i(\alpha)^2$ in a power series. This leads to quite complicated problems, since the derivatives of k_i^2 are oscillating in sign. Since (11) can be justified statistically [4] for large n, we shall not go into these problems.

Having obtained the Gaussian form (12) of the Feynman amplitude, we now face the next problem, namely to treat a net resistors (with a common resistance $\bar{\alpha}$) in the limit when the number of resistors go to infinity. This is a well known problem to electrical engineers, and the solution consists in replacing the network by a continuous distribution of resistance. Thus we replace

the complicated Feynman net by a conducting sheet of uniform resistance (proportional to $\bar{\alpha}$). We refer to this approximation as the continuous approximation. The conducting sheet remembers its origin through the resistance $\bar{\alpha}$, which via Eq. (5) depends on the underlying field theory through the ratio k/n (which depends on which field theory you consider). The rest then consists in solving a potential theory problem, with Neumann boundary conditions. Summing over all graphs of very high order one gets the answer [1–4]

$$\int \prod_{i=j}^{N} dz_i \prod_{i \neq j} |z_i - z_j|^{-\alpha' p_i p_j}, \tag{13}$$

where p_i are the external hadron momenta. Eq. (13) is the N-point amplitude. Although its derivation from Eq. (12) is valid only in a region without dynamical singularities, we can use Eq. (13) to continue into a region with singularities. This is one of the merits of the continuous approximation.

Let me finish with the remark that from Eqs. (5), (12) and (13) one can calculate the Regge slope α' in terms of k/n and the parton mass m. It turns out that α' vanishes in a Φ^4 model, thus this model is useless for the purpose of constructing dual models. Only if you include Φ^3 vertices in the complicated Feynman net do you get a non-trivial answer. For the net in Fig. 1 one finds

$$\alpha' = \sqrt{3}/10\pi m^2 \tag{14}$$

corresponding to a parton mass $m = 230$ MeV. Note that Fig. 1 has Φ^3 as well as Φ^4 vertices. The latter are introduced in order to make the energy spectrum nice.

REFERENCES

1. H. B. Nielsen, NORDITA preprint, 1969.
2. B. Sakita and M. A. Virasoro, Phys. Rev. Letters, **24**, 1146, 1970.
3. H. B. Nielsen and P. Olesen, Phys. Letters, **32B**, 203, 1970.
4. P. Olesen, Nuclear Phys., **B29**, 77, 1971.

ПАРТОННЫЙ ПОДХОД К ДУАЛЬНЫМ МОДЕЛЯМ

П. ОЛЕСЕН

Резюме

Рассмотрена проблема соответствия неперенормированных диаграмм Фейнмана очень высокого порядка с дулальной моделью. Диаграммы Фейнмана очень высокого порядка изучены при помощи недавно разработанного статистического формализма.

Acta Physica Academiae Scientiarum Hungaricae, Tomus 31 (1—3), pp. 129—137 (1972)

SPIN AND UNITARY SPIN IN THE DUAL RESONANCE MODEL

By

I. MONTVAY

INSTITUTE FOR THEORETICAL PHYSICS, ROLAND EÖTVÖS UNIVERSITY, BUDAPEST

The recent developments in constructing dual amplitudes with spins and unitary symmetry are briefly reviewed.

I. Introduction

A considerable amount of work in the Veneziano theory has been done in the model with neutral, scalar Reggeons only. In this model there is a single family of trajectories, the ground state being a neutral, scalar particle. As a consequence, the intercept of the leading trajectory is negative. One may ask how much this simple model reflects the real world. The mere fact that physicists consider such models expresses their strong belief that the physical world is not the only one possible mathematically. One can fulfil the axioms *including unitarity* without ϱ-mesons. Nevertheless ϱ-mesons do exist, thus one must once abandon the spinless world. In fact, a great deal of work has been done in the last two years in the direction of physical Reggeons with positive intercepts.

It is interesting to note that the two classical examples (the $\pi\pi\pi\omega$ and $\pi\pi\pi\pi$ amplitudes) both involve spin and unitary spin. In spite of this, the systematic inclusion of positive intercept trajectories and especially fermion trajectories represents a lot of nontrivial problems. After the success of the 4π amplitude it is tempting to try the many-pion amplitudes. The isospin structure of them was given quickly by PATON and CHAN [1]. The integral representation of the invariant amplitude in the case of 4π is [2]:

$$\int_0^1 dv\, v^{-1-\alpha(s)}(1-v)^{-1-\alpha(t)}\left\{-1-\alpha(s)-\alpha(t)\right\},$$

where

$$s=(p_1+p_2)^2; \qquad t=(p_2+p_3)^2;$$

$$p_1+p_2+p_3+p_4=0; \qquad \alpha(s)=\alpha_\varrho(s)-1=a_\varrho-1+\alpha s.$$

Therefore, the invariant for the N-pion amplitude can be of the general form

$$\int d\varphi_N(v,p)\,P(v_{ij};s_{ij}).$$

Here p is a polynomial in the channel invariants

$$s_{i,j} = (p_{i+1}+p_{i+2}+\ldots+p_j)^2\,; \quad 0 \leq i < j \leq N-1\,; \quad p_1+p_2+\ldots+p_N = 0$$

and in the corresponding channel integration variables

$$v_{0,i} = v_i\,(i = 1,\ldots,N-1)\,; \qquad v_{i,j} = \frac{(1-v_{i+1}\,v_{i+2}\ldots v_{j-1})\,(1-v_i\ldots v_j)}{(1-v_{i+1}\ldots v_j)\,(1-v_i\ldots v_{j-1})}$$

$$v_1 = v_{N-1} = 0\,; \qquad (2 \leq i+1 < j \leq N-1).$$

The integral without the polynomial P is the spinless N-point amplitude:

$$\int d\varphi_N(v,p) = \int \frac{dv_2\,dv_3\ldots dv_{N-2}}{(1-v_2v_3)\,(1-v_3v_4)\ldots(1-v_{N-3}\,v_{N-2})} \prod_{(i,j)} v_{i,j}^{-1-\alpha(s_{i,j})} =$$

$$= \int \prod_{i=2}^{N-2} dv_i\, v_i^{-1-\alpha(s_{0,i})}\,(1-v_i)^{a-1} \prod_{2\leq i\leq j\leq N-2} (1-v_i\,v_{i+1}\ldots v_j)^{-2\alpha p_i p_{j+1}}.$$

Explicit expressions for the many-pion amplitude were given by OLIVE and ZAKRZEWSKY [3] and by RITTENBERG and RUBINSTEIN [4]. These amplitudes are, however, not completely satisfactory as they do not factorize along the daughter trajectories.

The many-pion amplitudes are still simple in the sense that external spins are not present in them. In the general case the amplitude has spin indices. Instead of an invariant one has to construct functions of the particles' momenta showing the appropriate covariance property. In principle it would be possible to deal with helicity amplitudes familiar in the Regge theory, or with several invariant amplitudes multiplying the independent covariants. A more direct and simple way is, however, to consider the M-functions ("spinor amplitudes") which are the S-matrix elements between spinor states. The M-functions are free from kinetical singularities and have simple covariance, crossing and factorization properties.

The factorization is a severe restriction and at the same time a very powerful tool in every zero-width resonance model. It says that the residuum of a pole corresponding to a given intermediate state must factorize into the product of the appropriate lower point functions. If we have, for instance, the 6π amplitude, then by factorization we can get $A_1\pi\pi\pi$, $A_2\pi\pi\pi$, $\varrho\varrho\pi\pi$, etc. By subsequent factorizations the whole amplitude can be traced back to the vertices. Therefore, the only physical content of a dual resonance model is the spectrum of particles and the trilinear couplings among them. A constructive way of building up the amplitudes is thus to specify the spectrum of particles (which can be external as well as intermediate states) and to fix their couplings. Then by calculating the residua and summing up the poles, one has

the amplitude of an arbitrary process. It can be seen that the procedure is very similar to the van Hove model of Reggeization. The difference is that a simultaneous description of the crossed channels is also aimed both at low and high energies. There are several papers which start from this standpoint or more precisely from its advanced variant, the Reggeized supermultiplet [5]. The spectrum of these models is, however, too much unphysical as the internal states span SU(6, 6) representations.

The SU(6,6) symmetry which is a relativistic version of SU(6) points toward quarks. In fact, already the PATON—CHAN unitary symmetry factors for the N-point functions are easily interpreted in terms of the Rosner–Harari duality diagrams strongly reminiscent of quarks. Therefore, it is perfectly reasonable to try to extend the PATON—CHAN SU(3) factors to SU(6) in order to get a description of the external spins on the same footing as external unitary spin. Indeed, this was done by MANDELSTAM, BARDAKCI and HALPERN [6] (MBH). In the MBH model the M-functions for the hadron are projected out by factorization from the "scattering amplitudes" UB of quarks. Here B is the scalar Veneziano amplitude and U a spin and unitary spin factor, being a product of quark wave functions. The main failure of this model is also the unphysical degeneracy of intermediate states: there are 144 ground state mesons and 1728 ground state baryons (instead of 36 and 56, respectively). In spite of its unphysical features the MBH model is one of the greatest achievments of the last years, as a consequence of its fascinating simplicity and its factorization at all the daughter levels.

The unphysical degeneracy of the leading trajectory in SU(6, 6) theories is on the same footing as the long standing problem of the parity doubling of fermion Regge trajectories. It was demonstrated recently on an explicit example in the van Hove model by CARLITZ and KISLINGER [7] that there is a theoretical possibility to avoid the parity doubling by means of standing j-plane cuts. Such standing cuts were introduced in the Veneziano model by several authors to avoid the degeneracy of internal states [8–10]. In the SU(6,6) models (or the Sl(6, C) model [11]) the CARLITZ—KISLINGER cuts appear both in fermion and meson channels. This makes the high-energy predictions at high momentum transfer problematic.

An essentially different method of constructing Veneziano type amplitudes for general processes was proposed in a work of DOMOKOS, KÖVESI-DOMOKOS and SCHÖNBERG [12]. It is based on a general Fourier—Mellin integral representation which gives in pole approximation the Veneziano amplitude. In this proposal the internal Sl(2, C) group of Möbius transformations of the KOBA—NIELSEN integrand [13] for the spinless amplitude is combined in a nontrivial way with the Lorentz group transforming the external spins. The interesting possibility in this approach is that it gives a framework for going beyond the pole approximation.

The main drawback of all the above models is very easy to summarize: it is the lack of factorization. Even the factorization of the spinless amplitude holds only in a limited sense. Strictly speaking, factorization with ghost states cannot be regarded as factorization. Another uncertainty is due to the possible inclusion of satellite terms which do not contribute in one or more channels to the leading trajectory. An interesting question is whether it would be possible to make out of two bad things a good one, that is, to use the satellite ambiguity for ghost killing.

II. Ghost killing with satellites

The possibility of adding satellite terms to the generalized Veneziano amplitudes seems to leave a considerable freedom in the construction of dual resonance models. This arbitrariness is presumably weakened by factorization. Nevertheless, at the first sight it seems that every level density and every coupling strength can be fitted with a suitable choice of satellite terms.

Let us illustrate this in the simple case of scalar $N = 4$ point functions. The integral representation of a typical satellite term is

$$[V(m, M; n, N) = \int_0^1 dv\, v^{-1-\alpha(s)}(1-v)^{-1-\alpha(t)} v^m (1-v)^n (\alpha s)^N (\alpha t)^M \qquad (1)$$
$$\alpha(s) = a + \alpha s\,.$$

This term gives contributions in the points $s_i = (i-a/\alpha)$; $\alpha(s) = M + i - m$, $M + i - m - 1, \ldots, 0$ $(i = m,\ m+1,\ m+2, \ldots)$ on the s-channel Chew—Frautschi plot, and in $t_j = (j - a/\alpha)$; $\alpha(t) = N + j - n$, $N + j - n - 1, \ldots, 0$ $(j \geq n)$ on the t-channel Chew—Frautschi plot. Let us suppose for the moment that we know the "good" residua, corresponding to the physical level density and physical couplings. Then in the representation

$$B(s,t) = \sum_{n=0}^{\infty} \sum_{\nu=0}^{n} \frac{S_{n\nu}\, t^\nu}{n - \alpha(s)} = \sum_{m=0}^{\infty} \sum_{\mu=0}^{m} \frac{T_{m\mu}\, S^\mu}{m - \alpha(t)} \qquad (2)$$

the coefficients $S_{n\nu}$ and $T_{m\mu}$ are known. The good residua can be built in an amplitude of Veneziano type if one adds satellite terms in the following order:

$$\begin{aligned} B(s,t) = {} & \sigma_{00}\ V(0,0;1,0) + \tau_{00}\ V(1,0;0,0) + \sigma_{11}\ V(1,1;2,0) + \\ & + \sigma_{10}\ V(1,0;2,0) + \tau_{11}\ V(2,0;1,1) + \tau_{10}\ V(2,0;1,0) + \\ & + \sigma_{22}\ V(2,2;3,0) + \sigma_{21}\ V(2,1;3,0) + \sigma_{20}\ V(2,0;3,0) + \\ & + \tau_{22}\ V(3,0;2,2) + \tau_{21}\ V(3,0;2,1) + \tau_{20}\ V(3,0,2,0) + \ldots \end{aligned} \qquad (3)$$

The coefficients $\sigma_{00}, \tau_{00}, \sigma_{11} \ldots$ are chosen successively to fit $S_{00}, T_{00}, S_{11}, \ldots$ (For a similar construction see [14].) It is clear that the physical residua (without ghosts) can be fitted by this procedure on any finite number (k) of the lowest levels. The convergence as $k \to \infty$ depends, however, on the explicit form of the prescribed residua.

A different procedure for (partial) ghost killing was proposed in [15], where the ghosts were "killed" everywhere on a finite number $(k+1)$ of highest daughter trajectories. The amplitude is given there in the form

$$\begin{gathered} A(s,t) = A_s(s,t) + A_t(s,t) \\ A_s(s,t) = \int_0^1 dv\, v^{-1-\alpha(s)} (1-v)^{+k-\alpha(t)} \left(K_0(x) + vK_1(x) + \ldots + v^k K_k(x)\right) \\ x = \alpha(t)\,; \quad A_t : (s \leftrightarrow t)\,. \end{gathered} \tag{4}$$

For definiteness let us choose the "good" residua to be

$$\bar{R}_n(\alpha(t)) = (-1)^n \frac{[\alpha(t)+a]^n}{n!}\,. \tag{5}$$

Then the functions $K_i(x)$ are given explicitly [15] by

$$K_i(x) = e^{-2x} \sum_{i_1+2i_2+\ldots+li_l=i} \frac{1^{-i_1} \ldots l^{-i_l}}{i_1! \ldots i_l!} \left(k-a-\frac{x}{2}\right)^{i_1} \left(k-\frac{2x}{3}\right)^{i_2} \ldots \left(k-\frac{lx}{l+1}\right)^{i}. \tag{6}$$

Writing the amplitude $A(s,\ t)$ as a sum of s-channel poles

$$A(s,t) = \sum_{n=0}^{\infty} \frac{R_n(\alpha(t))}{n-\alpha(s)}\,, \tag{7}$$

it follows from the construction that the residua $R_n(\alpha(t))$ conicide with $_n(\alpha(t))$ for $n = 0,\ 1, \ldots,\ k$.

In $A(s,\ t)$ the leading trajectories of the two channels are separated, the piece A_s, for instance, contributes in the t-channel only to the $(k+1)$-th and lower daughters, but it gives entirely the highest $(k+1)$ trajectories in the s-channel. Therefore, questions concerning duality may arise. Duality can be formulated requiring the fulfilment of the finite energy sum rule

$$\sum_{n=0}^{N} R_n(\alpha(t)) = N^{\alpha(t)+1} \frac{r(\alpha(t))}{\Gamma(a(t)+2)} + 0(N^{\alpha(t)})\,; (N \to \infty) \tag{8}$$

($r(\alpha(t))$ being the residuum of the leading Regge-pole exchanged in the t-channel). This fixes the asymptotic behaviour of the residua in the following way:

$$R_N(\alpha(t)) = N^{\alpha(t)} \frac{r(\alpha(t))}{\Gamma(\alpha(t)+1)} + 0(N^{\alpha(t)-1})\,. \tag{9}$$

The amplitude $A(s, t)$ satisfies Eqs. (8) and (9) as it is meromorphic and Regge-behaved in s. But looking at Eq. (5) one sees at once that Eq. (9) can be valid only for $N \geqslant k$. This implies that a distinction can be made between the resonances occurring in $A(s, t)$: the resonances on the highest $k + 1$ trajectories are *physical* (they have physical couplings), but those on the lower daughters are *supplementary*, they are partly ghosts and they are responsible for the Regge behaviour in the direct channel. (One has to remark that a similar situation is to be expected in every dual model, as the asymptotic behaviour (Eq. (9)) can only be produced by the far-out daughters.)

III. Higher symmetries in dual models

In this Section we give a short and simple derivation of dual models with relativistic SU(6) symmetry in the case of meson four-point functions. The starting point is the PATON—CHAN unitary symmetry factor

$$\delta_{A_1}^{B_2}\,\delta_{A_2}^{B_3}\,\delta_{A_3}^{B_4}\,\delta_{A_4}^{B_1}. \tag{10}$$

Here A_i, B_i denote the SU(3) nonet indices of the i-th meson. An immediate generalization to relativistic SU(6) would be

$$\delta_{\alpha_1}^{\beta_2}\,\delta_{\alpha_2}^{\beta_3}\,\delta_{\alpha_3}^{\beta_4}\,\delta_{\alpha_4}^{\beta_1}, \tag{11}$$

where $\alpha_i = A_i\,a_i$, $\beta_i = B_i\,b_i$ and a_i, b_i denote the Lorentz spinor indices of the i-th meson. Eq. (11) is, however, incorrect as parity conservation requires

$$M(p_1\,p_2\,p_3\,p_4)_{a_1\,a_2\,a_3\,a_4}^{b_1\,b_2\,b_3\,b_4} = \eta\,M(p_{1s}\,p_{2s}\,p_{3s}\,p_{4s})_{\dot a_1\dot a_2\dot a_3\dot a_4}^{\dot b_1\dot b_2\dot b_3\dot b_4} =$$

$$= \eta \left(\frac{\hat p_1}{m}\right)_{b_1 b_1'} \left(\frac{\hat p_2}{m}\right)_{b_2 b_2'} \left(\frac{\hat p_3}{m}\right)_{b_3 b_3'} \left(\frac{\hat p_4}{m}\right)_{b_4 b_4'} M(p_{1s}\,p_{2s}\,p_{3s}\,p_{4s})_{a_j'}^{b_i'} \left(\frac{\check p_1}{m}\right)_{a_1' a_1} \left(\frac{\check p_2}{m}\right)_{a_2' a_2} \times \tag{12}$$

$$\times \left(\frac{\check p_3}{m}\right)_{a_3' a_3} \left(\frac{\check p_4}{m}\right)_{a_4' a_4};\; p_s = (p_0, -\underset{\sim}{p}),\; \hat p = p^\mu \sigma_\mu,\; \check p = p_s^\mu \sigma_\mu.$$

Here M is the four-meson M-function, $\eta = +1$ is the product of the parities and m is the meson mass. Otherwise we used the notations of [9]. The most simple change of Eq. (11) consistent with parity conservation is the following:

$$\delta_{\alpha_1}^{\beta_2} = \delta_{A_1}^{B_2}\,\delta_{a_1}^{b_2} \to [\delta - (p_2\,p_1)]_{\alpha_1}^{\beta_2} = \delta_{A_1}^{B_2}\left[\delta_{b_2 a_1} - \left(\frac{\hat p_2 \check p_1}{m^2}\right)_{b_2 a_1}\right]. \tag{13}$$

Therefore, a possible four-meson amplitude is:

$$M(p_1\,p_2\,p_3\,p_4)_{\alpha_1\alpha_2\alpha_3\alpha_4}^{\beta_1\beta_2\beta_3\beta_4} = \int dv\, v^{-1-\alpha(s)}(1-v)^{-1-\alpha(t)}\,[\delta - (p_2\,p_1)]_{\alpha_1}^{\beta_2} \cdot$$
$$\cdot\,[\delta - (p_3\,p_2)]_{\alpha_2}^{\beta_3}\,[\delta - (p_4\,p_3)]_{\alpha_3}^{\beta_4}\,[\delta - (p_1\,p_4)]_{\alpha_4}^{\beta_1}. \tag{14}$$

Here $\alpha(s)$ denotes the (negative intercept) trajectory of the 0^- particles in the 36-plet. This amplitude is identical to the MBH amplitude for 4 mesons. Applying the same method to meson—baryon scattering one arrives at the Sl(6, C) symmetric amplitude of [9] which coincides with the SU(6, 6) amplitude if the 4 coupling constants are properly choosen. Let us now investigate the factorization properties of the spin-dependent part of the above amplitude, say in the s-channel $[s = (p_1 + p_2)^2]$. The first and third factors belong entirely to the initial and final states, respectively. The other two factors can be written as follows:

$$[\delta-(p_3\,p_2)]^{\beta_3}_{\alpha_2} = \frac{1}{2}[\delta-(p_3\,p_{12})]^{\beta_3}_{\varrho_{12}}[\delta+(p_{12}\,p_2)]^{\varrho_{12}}_{\alpha_2} + \\ + \frac{1}{2}[\delta+(p_3\,p_{12})]^{\beta_3}_{\varrho_{12}}[\delta-(p_{12}\,p_2)]^{\varrho_{12}}_{\alpha_2};\; p_{ik} = p_i + p_k,\; p_{ik}^2 = m^2. \tag{15}$$

The two terms on the right-hand side are already factorized, thus multiplying by the other two terms coming from the last factor in Eq. (14), one has four 36-plets as intermediate states. It can be shown that there are two 36^--plets and two 36^+-plets, one of each having imaginary couplings ("ghosts").

The superfluous intermediate states can be easily eliminated at the ground state pole by the method of [16], which consists of multiplying the unwanted pieces of the covariants by the integration variable of the channel:

$$M = \int_0^1 dv\, v^{-1-\alpha(s)}(1-v)^{-1-\alpha(t)}\left\{\frac{1}{2}[\delta-(p_4\,p_{23})]^{\beta_4}_{\varrho_{23}}[\delta+(p_{23}\,p_3)]^{\varrho_{23}}_{\alpha_3}+\right. \\ \left.+\frac{1-v}{2}[\delta+(p_4\,p_{23})]^{\beta_4}_{\varrho_{23}}[\delta-(p_{23}\,p_3)]^{\varrho_{23}}_{\alpha_3}\right\}\left\{\frac{1}{2}[\delta-(p_3\,p_{12})]^{\beta_3}_{\varrho_{12}}\right. \\ [\delta+(p_{12}\;p_2)]^{\varrho_{12}}_{\alpha_2}\;+\frac{v}{2}[\delta+(p_3\,p_{12})]^{\beta_3}_{\varrho_{12}}[\delta-(p_{12}\,p_2)]^{\varrho_{12}}_{\alpha_2}\Big\}\Big\{\frac{1}{2} \\ [\delta-(p_2\,p_{41})]^{\beta_2}_{\varrho_{41}}[\delta+(p_{41}\,p_1)]^{\varrho_{41}}_{\alpha_1}+\frac{1-v}{2}[\delta+(p_2\,p_{41})]^{\beta_2}_{\varrho_{12}} \\ \left.[\delta-(p_{41}\,p_1)]^{\varrho_{12}}_{\alpha_1}\right\}\left\{\frac{1}{2}[\delta-(p_1\,p_{34}))^{\beta_1}_{\varrho_{34}}[\delta+(p_{34}\,p_4)]^{\varrho_{34}}_{\alpha_4}+\right. \\ \left.+\frac{v}{2}[\delta+(p_1\,p_{34})]^{\beta_1}_{\varrho_{34}}[\delta-(p_{34}\,p_4)]^{\varrho_{34}}_{\alpha_4}\right\}. \tag{16}$$

In this amplitude the ground state is a pure (and physical) 36^--plet. The excited states, however, are still degenerate. The degeneracy everywhere can be removed by multiplying by some functions $f(v)$ and $f(1-v)$ instead of v and $(1-v)$, respectively if

$$f(0) = 0\,,\quad \frac{d^n f(0,1)}{dv^n} = 0 \qquad (n = 1, 2, \ldots)\,. \tag{17}$$

Such an amplitude was constructed in [17], where it was shown that in doing so the amplitude gets pieces with exponential behaviour. This shows that the scalar Veneziano spectrum multiplied by pure SU(6) couplings is no more dual in the sense of satisfying finite energy sum rules.

Another possibility of modifying Eq. (16) is to remove the degeneracy on the first $(k+1)$ trajectories by the method of [15]. The resulting amplitude is the following [9]:

$$
\begin{aligned}
M_s = & \int_0^1 dv\, v^{-1-\alpha(s)}(1-v)^{-1-\alpha(t)}[\delta-(p_2 p_1)]_{\alpha_1}^{\beta_2}[\delta-(p_4 p_3)]_{\alpha_3}^{\beta_4}\times \\
& \times(1-v)^{k+1}(-a)^{B_0}\int_0^1 d\tau\, \tau^{-a-1}(-\log\tau)^{B_0-1}\, e^{\alpha(t)v(\tau-1)}\left[R_0^{(k)}(v\,\alpha(t),\tau)+\right. \\
& +\ldots+v^k R_k^{(k)}(v\alpha(t),\tau)\Big]\Bigg\{[\delta-(p_3 p_2)]_{\alpha_2}^{\beta_3}[\delta-(p_1 p_4)]_{\alpha_4}^{\beta_1}-\frac{\sqrt{a\log\tau}}{\Gamma\left(B_0+\frac{1}{2}\right)}\times \\
& \times\left[(p_3 p_{12})-(p_{12} p_2)\right]_{\alpha_2}^{\beta_3}[\delta-(p_1 p_4)]_{\alpha_4}^{\beta_1}+[\delta-(p_3 p_2)]_{\alpha_2}^{\beta_3}[(p_1 p_{34})-(p_{31} p_4)]_{\alpha_4}^{\beta_1}]+ \\
& +\frac{a\log\tau}{\Gamma(B_0+1)}[(p_3 p_{12})-(p_{12} p_2)]_{\alpha_2}^{\beta_3}[(p_1 p_{34})-(p_{34} p_4)]_{\alpha_4}^{\beta_1}\Bigg\};\ M=M_s+M_t,
\end{aligned}
\tag{18}
$$

where

B_0 = free parameter, $a=\alpha(0)$; $p_1+p_2+p_3+p_4=0$;

$$
\begin{aligned}
R_l^{(k)}(x,\tau) = & \sum_{i_1+\ldots+li_l=i}\frac{1^{-i_1}\ldots l^{-i_l}}{i_1!\ldots i_l!}\left[\tau\left(1+\frac{x\tau}{2}\right)+k-\frac{x}{2}\right]^{i_1} \\
& \ldots\left[\tau^l\left(1+\frac{lx\tau}{l+1}\right)+k-\frac{lx}{l+1}\right]^{i_l}.
\end{aligned}
\tag{19}
$$

The piece M_t can be obtained from M_s interchanging the roles of the s- and t-channels.

In summary, the factorization properties of the dual amplitudes of spinning particles offer a lot of questions to be studied in the future. The application of the dual model to most of the physical processes becomes possible presumably only after knowing the answers to these questions.

REFERENCES

1. J. E. Paton and Chan Hong Mo, Nucl. Phys., **B10,** 516, 1969.
2. C. Lovelace, Phys. Letters, **28B,** 264, 1968.
3. D. Olive and W. J. Zakrzewski, Nucl. Phys., **B21,** 303, 1970.
4. V. Rittenberg and H. R. Rubinstein, Phys. Rev. Letters, **25,** 191, 1970; J. D. Dorren, V. Rittenberg and H. R. Rubinstein, Nucl. Phys., **B20,** 663, 1970.

5. R. Delbourgo and P. Rotelli, Phys. Letters, **30B,** 192, 1969. and Nuovo Cimento, **69,** 412, 1970.
6. S. Mandelstam, Phys. Rev., **184,** 1621, 1969; **D1,** 1734, 1970; **D1,** 1745, 1970; K. Bardacki and M. B. Halpern, Phys. Rev., **183,** 1456, 1969.
7. R. Carlitz and M. Kislinger, Phys. Rev. Letters, **24,** 186, 1970.
8. K. Bardakci and M. B. Halpern, Phys. Rev. Letters, **24,** 428, 1970.
9. I. Montvay, ITP-Budapest Reports, No. 277, 278, 280, 1970.
10. L. P. Lebrun, Lett. Nuovo Cimento, **3,** 819, 1970. G. Venturi, Lett. Nuovo Cimento, **3,** 753, 1970 and Cambridge preprint, DAMPT 70/28.
11. I. Montvay, ITP Budapest report, 273, 1970.
12. G. Domokos, S. Kövesi-Domokos and E. Schönberg, Phys. Rev., **D2,** 1026, 1970.
13. Z. Koba and H. B. Nielsen, Nucl. Phys., **B10,** 633, 1969.
14. R. E. Kreps and M. S. Milgram, Phys. Rev., **D1,** 2271, 1970.
15. I. Montvay, ITP Budapest report, 278, 1970.
16. I. Montvay, Phys. Letters, **30B,** 653, 1969.
M. B. Green and R. L. Heimann, Phys. Letters, **30B,** 642, 1969.
17. R. Carlitz, S. Ellis, P. G. O. Freund and S. Matsuda, GALTECH preprint, CALT 68—260.

СПИН И УНИТАРНЫЙ СПИН В ДУАЛЬНОЙ РЕЗОНАНСНОЙ МОДЕЛИ

И. МОНТВАИ

Резюме

Приведён краткий обзор последних достижений в области построения дуальных амплитуд с унитарной симметрией и спинами.

Acta Physica Academiae Scientiarum Hungaricae, Tomus 31 (1—3), pp. 139—146 (1972)

ON THE OFF-MASS-SHELL CONTINUATION OF THE VENEZIANO MODEL

By

F. CSIKOR*

JOINT INSTITUTE FOR NUCLEAR RESEARCH, DUBNA, USSR

The problem of incorporation of currents into the Veneziano model is studied. The case of axial vector current is treated in detail on the example of the off-shell $\pi\pi \to \pi\pi$, $A_\mu\pi \to \pi\pi$ and $A_\mu\pi \to A_\mu\pi$ processes.

Introduction

Recently some interest has been devoted to the incorporation of currents into the Veneziano model. The case of vector currents has been extensively studied by BROWER and WEIS and others [1] in the framework of the generalized Veneziano model. At the present stage of development of this theory it is not yet possible to study axial currents in this framework. Therefore, as we want to study axial currents, we shall confine ourselves to four-point functions only. Thus our treatment will be more physical in the sense that the particles (external and leading trajectory particles) will have their physical masses.

As a particularly simple example we shall study the scattering amplitudes of the $A_\mu\pi \to A_\mu\pi$, $A_\mu\pi \to \pi\pi$, $\pi\pi \to \pi\pi$ processes. The reasons for choosing these processes are:

a) The related on-shell processes have very simple Veneziano amplitudes as only a single trajectory contributes and the problems of external particle spin can also be solved (at least to leading trajectory level) in this case.

b) These processes form a relatively closed subsystem in the bootstrap scheme of all processes.

c) Using the soft pion method, one may extract information on the pion electromagnetic form factor.

We first list some fundamental properties of our model which we believe mean an improvement compared with numerous other attempts. In a Veneziano model with linear trajectories and daughters it is natural to assume that the axial vector current is saturated not only by the π and A_1 mesons, therefore we take into account the higher mass π and A_1 mesons (Fig. 1), too. Furthermore, we have carefully carried out the off-shell continuation in the momentum of one final π in the $A_\mu\pi \to \pi\pi$, $\pi\pi \to \pi\pi$ amplitudes and also in the

* On leave of absence from Roland Eötvös University, Budapest.

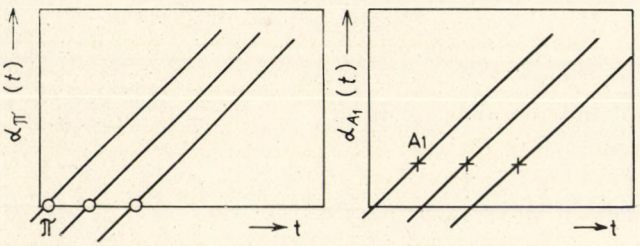

Fig. 1

momentum of one of the initial pions in the $\pi\pi \to \pi\pi$ amplitude. This is necessary, if one wants to compare the Veneziano model with current algebra and divergence algebra (e.g., it is essential in the determination of the pion form factor, too.)

Finally, we have to realize that at present we may hope to construct a model which is satisfactory on the leading trajectory level only. One reason for this is that it is the case for the $A_1\pi \to A_1\pi$ amplitude (which is related to the $A_\mu\pi \to A_\mu\pi$ amplitude); another reason will be mentioned below.

Preliminaries

The definitions of our amplitudes are the following:

$$\begin{aligned} T_{\mu\nu}\begin{pmatrix} iljn \\ qpq'k \end{pmatrix} &= \int d^4x e^{-ipx} \langle \pi q' j | T\big(A^l_\mu(x)\, A^n_\nu(0)\big) | \pi q i \rangle , \\ T_\mu \begin{pmatrix} iljn \\ qpq'k \end{pmatrix} &= i \int d^4x e^{-i'px} \langle \pi q' j | T\big(A^l_\mu(x)\, \partial \cdot A^n(0)\big) | \pi q i \rangle , \\ T \begin{pmatrix} iljn \\ qpq'k \end{pmatrix} &= \int d^4x e^{-ipx} \langle \pi q' j | T\big(\partial \cdot A^l(x)\, \partial \cdot A^n(0)\big) | \pi q i \rangle , \end{aligned} \tag{1}$$

where A_μ is the axial vector current, i, l, j, n are isospin indices, q, p, q', k are momenta.

The amplitudes are connected by the PCAC equations:

$$T_{\mu\nu} k^\nu = T_\mu + i(\delta_{il}\delta_{jn} - \delta_{in}\delta_{lj})(q+q')_\mu \frac{F_\pi(t)}{2(2\pi)^3} , \tag{2}$$

$$T_\mu p^\mu = T + i\, \Sigma^{iln}(t) , \tag{3}$$

where $F_\pi(t)$ is the pion electromagnetic form factor and $\Sigma^{iln}(t)$ is the σ-term:

$$\Sigma^{iln}(t) = -\, i \int d^4x \delta(x_0)\, e^{-ipx} \langle \pi q' j | [A^l_0(x), \partial \cdot A^n(0)] | \pi q i \rangle . \tag{3'}$$

The residues of $T_{\mu\nu}$ at the appropriate values of p^2 and k^2 are proportional to the $A_1^*(\pi^*)\pi \to A_1^{**}(\pi^{**})\pi$ amplitudes, where the stars denote the higher

mass A_1 (or π) particles. Similarly T_μ is connected to the $A_1^*(\pi^*)\pi \to \pi^{**}\pi$ and T to the $\pi^*\pi \to \pi^{**}\pi$ amplitudes.

In constructing the model, we shall proceed in the order $T \to T_\mu \to T_{\mu\nu}$. The number of independent invariant functions (using all the crossing and isospin constraints) is 2 for the amplitude T, 6 for T_μ and 20 for $T_{\mu\nu}$. Thus, for the sake of brevity, we shall deal here only with the $I_s = 2$ amplitudes and shall not write down all the formulas. We refer the reader for details and complete formulas to the original papers.

The amplitude T

The first task is to construct the $\pi^*\pi \to \pi^{**}\pi$ amplitude. This is given by the same expression as the $\pi\pi \to \pi\pi$ amplitude. E.g., the $I_s = 2$ amplitude is, as it is well known:

$$f_\varrho f_\varrho' B(t, u)\big(1 - \alpha(t) - \alpha(u)\big), \tag{4}$$

where

$$B(t, u) = \frac{\Gamma\big(1-\alpha(t)\big)\,\Gamma\big(1-\alpha(u)\big)}{\Gamma(2-\alpha(t)-\alpha(u))}\,; \quad \alpha(t) = \frac{1}{2} + b(t - m_\pi^2)$$

and b is the universal trajectory slope. As LOVELACE [2] pointed out, this expression is a good candidate for the off-shell amplitude, as it satisfies the Adler condition. Later on SUURA [3], OSBORN [4] and CSIKOR [5] pointed out the necessity of including the higher mass pion poles. So the off-shell amplitude is obtained by the replacements:

$$f_\varrho \to f(p^2),\ f_\varrho' \to f(k^2)$$

where

$$f(p^2) = \Gamma\left(\frac{1}{2} - \alpha(p^2)\right)\bar{f}(p^2)$$

and $\bar{f}(p^2)$ has no poles at all. The argument of the Γ function is $-\alpha_\pi(p^2)$, which yields the expected pole structure.

As pointed out by CSIKOR [5] and ELLIS and OSBORN [6], the daughter structure of this amplitude is far from being realistic. In fact, an infinite number of satellite terms are needed to correct this. So we content ourselves by saying that the above amplitude is correct only to the leading trajectory level.

The above ideas can be extended to other processes, such as $K\pi$ and KK scattering [4, 7]. This off-shell Veneziano model is in reasonable agreement with the chiral symmetry breaking model of GELL-MANN, OAKES and RENNER.*

* In the literature there has been some debate about this statement. We want to emphasize that all the diseases can be cured by taking into account explicit momentum dependence of the type described above and satellites. We refer to the recent paper by YONEYA et al. [8], which illustrates this point.

The amplitude T_μ

A number of attempts have been made to construct the amplitude T_μ already in the early times of Veneziano theory [9]. However, all these attempts keep the final state pions on the mass-shell (and take into account only the lowest π and A_1 poles). An amplitude which is off the mass-shell in both p_μ and k_μ has been given in [10]. This amplitude is by no means satisfactory as it contains an unphysical pole at $p^2 = 0$. A model which avoids this difficulty has been given in [11] and we shall now explain the main ideas of this work.

Before starting with the construction, it is convenient to state two simple theorems.

a) If a concrete model for T, T_μ satisfies the PCAC Eq. (3) (for all momenta p_μ, k_μ), exhibits the correct pole structure and satisfies the crossing conditions, then the expression of T_μ taken at $k_\mu = 0$ will be automatically transversal.

b) If in addition to the conditions of theorem a), the amplitude T satisfies the Adler–Weissberger condition, then $F_\pi(t)$, as determined from T_μ in the soft pion limit, has the correct normalization.

So in the construction we have to concentrate only on the conditions of these theorems.* We assume that T_μ is a sum of three terms:

$$T_\mu = T_\mu^{(1x0)} + T_\mu^{(0x0)} + t_\mu, \tag{5}$$

where $T_\mu^{(1x0)}$ contributes only to the on-shell amplitudes $A_1^* \pi \to \pi^{**}\pi$, $T_\mu^{(0x0)}$ contributes only to the on-shell amplitudes $\pi^*\pi \to \pi^{**}\pi$, and t_μ does not contribute to the amplitudes on the mass-shell. t_μ ensures that the PCAC Eq. (3) is fulfilled.

The $A_1^*\pi \to \pi^{**}\pi$ scattering amplitude is given by the well known GOEBEL, BLACKMON, WALI expression [13], e.g. the $I_s = 2$ amplitude is:

$$\begin{aligned} f'_\varrho[\mu(k_\mu(2\alpha(u) - \alpha(t) - 1) - (q + q')\mu(1 - \alpha(t))) \\ -2\mu'\,(k_\mu + (q + q')_\mu)]\, B\,(t,\ u), \end{aligned} \tag{6}$$

μ', μ correspond to the s and d wave-coupling constants of $A_1^* \to \varrho\pi$ decay, μ', μ are free parameters.

$T_\mu^{(1x0)}$ is obtained from the expression (6) by the following replacements:

$$\begin{aligned} f_\varrho &\to f(k^2), \\ \mu \cdot l_\mu &\to \left(g_{\mu\lambda}\,\mu(p^2) - p_\mu p_\lambda \frac{\mu(p^2) - \mu(0)}{p^2}\right) \cdot l^\lambda, \\ \mu' \cdot l_\mu &\to \left(g_{\mu\lambda}\,\mu'(p^2) - p_\mu p_\lambda \frac{\mu'(p^2) - \mu'(0)}{p^2}\right) \cdot l^\lambda, \end{aligned} \tag{7}$$

* These theorems underline the importance of a careful continuation in the momentum k_μ. In fact, in s. [3, 12] this continuation was not carried out carefully, which led to difficulties in the determination of the pion form factor, namely at the kinematics $k_\mu = 0$ T_μ turned out to have a longitudinal component, too.

where l_μ is an arbitrary momentum. The function $f(k^2)$ is the same as before, and

$$\mu(p^2) = \Gamma\left(\frac{3}{2} - \alpha(p^2)\right) \bar{\mu}(p^2)$$

with $\bar{\mu}(p^2)$ a nonsingular function $\left(\frac{3}{2} - \alpha(p^2) = -\alpha_{A_1}(p^2)\right)$.

Similarly, $T_\mu^{(0x0)}$ is obtained from the $\pi^*\pi \to \pi^{**}\pi$ amplitude given in Eq. (5) by the following replacements:

$$f_\varrho \to \frac{f(p^2) - f(0)}{p^2} p_\mu, \qquad f'_\varrho \to f(k^2). \tag{8}$$

The above construction ensures that on the mass-shell $T_\mu^{(1x0)}$ and $T_\mu^{(0x0)}$ contribute only to the relevant amplitudes. Moreover $p^\mu (T_\mu^{(1x0)} + T_\mu^{(0x0)}) - T - i\,\Sigma^{in}(t)$ has no singularity in the variable p^2, so we have a chance that t_μ (which is determined from the PCAC Eq. (3)) is also nonsingular in p^2.

The determination of t_μ is a little tricky.* For details we refer to [11]; here we note only that non-Veneziano type terms necessarily occur. To see this let us write down the PCAC equation (T_i denote the invariant functions of T_μ):

$$T_1 \cdot p^2 + T_2 \frac{s+u-2m_\pi^2}{2} + T_3 \frac{s-u}{2} = T(s, t, u, p^2, k^2) - T(m_\pi^2, t, m_\pi^2, 0, t). \tag{9}$$

The last term is the σ term, which has clearly non-Veneziano form, and generates a non-Veneziano type term in t_μ, too. These non-Veneziano type terms exhibit fixed power behaviour for large s.

Using the soft pion method one gets the following expression for the pion electromagnetic form factor:

$$\begin{aligned} F_\pi(t) = \text{const.} \Big\{ & \big(\mu(t) - \mu(0)\big)\big(1 - \alpha(t)\big) + 2\big(\mu'(t) - \mu'(0)\big) - \\ & - 4t\big(\eta(t) - \bar{\eta}(t, 0)\big) + b\bar{f}(0)\,\Gamma\left(\frac{1}{2} - \alpha(0)\right) + \\ & + f(0)\,\Gamma\left(\frac{3}{2} - \alpha(0)\right) b\left(\psi\left(\frac{1}{2}\right) - \psi\left(\frac{3}{2} - \alpha(t)\right)\right)\Big\} \cdot B(m_\pi^2, t), \end{aligned} \tag{10}$$

* Our main guide is that we have to avoid unphysical poles.

where $\psi(x) = \Gamma'(x)/\Gamma(x)$ is the logarithmic derivative of the Γ function, $\bar{\eta}(t)$, $\eta(t, 0)$ are unknown, nonsingular functions (which come from the nonuniqueness of t_μ). The pole structure of this expression is as expected. The lesson to be drawn from this complicated expression is, that without additional assumptions one cannot make any definite prediction for $F_\pi(t)$.

The $T_{\mu\nu}$ amplitude

The $T_{\mu\nu}$ amplitude can be constructed from the relevant on-shell amplitudes using very similar ideas. Of course, the calculations are rather lengthy (we have 20 independent invariant functions). So we point out here only the special difficulties. For details we refer to [14].

The first difficult point is the on-shell $A_1\pi \to A_1\pi$ amplitude. The new features are of course connected with the non-zero spin of the external particles. Furthermore, we have now non-trivial factorization conditions, as illustrated in

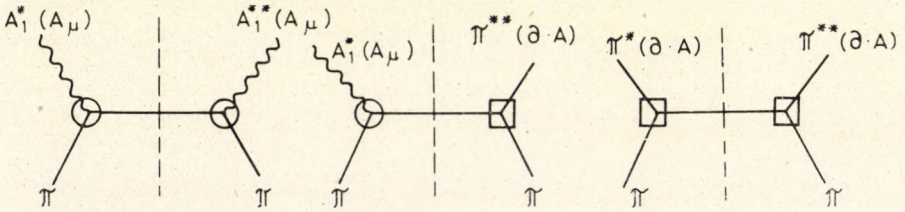

Fig. 2

Fig. 2. All these questions are treated in detail in [15] and [16]. We have essentially accepted the solution of LASLEY and CARRUTHERS with some modifications.* As a result we have got a *unique* three-parameter (+ free coupling constants) solution.

This solution can be extended with some effort to the $A_1^*\pi \to A_1^{**}\pi$ amplitudes. As one of the invariant functions vanishes if A_1^* and A_1^{**} is the same particle, the extension for $A_1^* \neq A_1^{**}$ yields nontrivial information.

As in the case of T_μ, $T_{\mu\nu}$ will be built up as a sum of several terms:

$$T_{\mu\nu} = T_{\mu\nu}^{(1x1)} + T_{\mu\nu}^{(1x0)} + T_{\mu\nu}^{(0x1)} + T_{\mu\nu}^{(0x0)} + t_{\mu\nu}.$$

The meaning of the various terms should be clear from the discussion of the T_μ amplitude. Only the construction of $T_{\mu\nu}^{(1x1)}$ gives rise to new difficulties, as not all parameters appear in product form in the on-shell amplitudes (e.g.

* First the Adler condition is imposed incorrectly in [15]; secondly, we have removed one of the conditions of [15], which means a restriction on the signature of a daughter trajectory; third we have kept $m^2 \neq 0$ throughout the calculation. Details of this as well as comments on WHIPPMAN's paper are given in [17].

the coupling constants of the $A_1^* A_1^{**} \varrho$ vertex do not). Clearly some additional assumptions are needed here which, of course, increase the arbitrariness of the procedure.

We want to note that the factorization condition (illustrated in Fig. 2) is not satisfied automatically for our amplitude. So we have to impose this, which severely restricts the arbitrariness of $t_{\mu\nu}$.

A final remark concerns the FUBINI—DASHEN—GELL-MANN sum rule [18]. Our amplitude does not satisfy this sum rule automatically. If we impose it, we get severe restrictions for the pion electromagnetic form factor $F_\pi(t)$. Among others, this restriction fixes the ratio of the two coupling constants of $A_1 \to \varrho\pi$ decay, namely (using the notation of [19]) we get $|G_T/G_L| = = 0.90—1.1$. The experimental number is [20] 0.65 ± 0.25. While this is quite appealing, for large t the restricted $F_\pi(t)$ behaves only as $|t|^{-1/2} \log b|t|$. So we prefer to say that our amplitude does not satisfy the FDGM sum rule.

Concluding remarks

The procedure for the construction of current amplitudes outlined above is clearly applicable to other processes, too. The main difficulty is that until now we have no really reliable on-shell amplitudes for the physically most interesting cases [21], e.g. for the case of a proton target. An interesting attempt in this direction has been made by KONETSCHNY and MAJEROTTO [22], although the on-shell amplitudes and also the continuation are very crude yet. Clearly, a real progress in the construction of on-shell amplitudes would induce a progress in the construction of current amplitudes, too.*

REFERENCES

1. R. C. BROWER and J. H. WEIS, Phys. Rev., **188**, 2486, 2495, 1969. and to be published; H. SUGAWARA, Tokyo Univ. of Education, preprint; I. OHBA, Progr. Theor. Phys., **42**, 432, 1969; M. BANDER, Nucl. Phys., **B13**, 587, 1969; D. Z. FREEDMAN, Phys. Rev., **1D**, 1133, 1970, and others.
2. C. LOVELACE, Phys. Letters, **28B**, 264, 1968.
3. H. SUURA, Phys. Rev. Letters, **23**, 551, 1969.
4. H. OSBORN, Nuclear Phys., **B17**, 141, 1970.
5. F. CSIKOR, JINR preprint E2-4865, Dubna, 1969.
6. J. ELLIS and H. OSBORN, Phys. Letters, **31B**, 580, 1970.
7. F. CSIKOR, Phys. Letters, **31B**, 141, 1970.
8. T. YONEYA, A. KANAZAWA and M. HARUYAMA, Lett. Nuovo Cimento **4**, 459, 1970.
9. H. J. SCHNITZER, Phys. Rev. Letters, **22**, 1154, 1969. R. ARNOWITT, P. NATH, Y. SRIVASTATA and M. H. FRIEDMAN, Phys. Rev. Letters, **22**, 1158, 1969; S. P. DE ALWIS, D. A. NUTHBROWN, P. BROOKER and J. M. KOSTERLITZ, Phys. Letters, **29B**, 362, 1969; J. L. ROSNER and H. SUURA, Phys. Rev., **187**, 1905, 1969; Y. OYANAGI, Nucl. Phys., **14B**, 375, 1969.
10. R. ARNOWITT, M. H. FRIEDMAN and P. NATH, Phys. Rev., **1D**, 1813, 1970.

* A more refined continuation along the lines explained here is under investigation (private communication by W. KONETSCHNY).

11. F. Csikor, JINR preprint E4-4959 Dubna 1970 and Yadern. Fiz. (Soviet J. Nuclear Phys.) **12,** 1039, 1970.
12. P. H. Frampton, Phys. Rev., **1D,** 3141, 1970.
13. C. J. Goebel, M. L. Blackmon and K. C. Wali, Phys. Rev., **182,** 1487, 1969.
14. F. Csikor, ITP Budapest Rep. No. 284, 1970 and Yadern. Fiz. (Soviet J. Nuclear Phys.) **14,** 232, 1971.
15a. P. Carruthers and F. Cooper, Phys. Rev., **1D,** 1223, 1970.
b. E. Lasley and P. Carruthers, Phys. Rev., **2D,** 1724, 1970.
16. M. L. Whipmann, Phys. Rev., **1D,** 701, 1970.
17. F. Csikor, Phys. Rev. **3D,** 3237, 1971.
18. S. Fubini, Nuovo Cimento, **43,** 1, 1966; R. Dashen and M. Gell-Mann in "Proc. of the Third Coral Gables Conf. on Symmetry Principles at High Energy" ed. B. Kursunoglu, A. Perlmutter, and I. Sakmar, W. H. Freeman and Co., San Francisco, 1966.
19. F. J. Gilman and H. Harari, Phys. Rev., **165,** 1803, 1968.
20. J. Ballam et al., Phys. Rev., **1D,** 94, 1970.
21. For a review, see I. Montvay: these Proceedings, p. 129.
22. W. Konetschny and W. Majerotto, Nuovo Cimento, **1A,** 188, 1971.

О ПРОДОЛЖЕНИИ МОДЕЛИ ВЕНЕЗИАНО ВНЕ МАССОВОЙ ПОВЕРХНОСТИ

Ф. ЧИКОР

Резюме

Изучена проблема включения токов в модель Венезиано. Детально рассматривается случай аксиального векторного тока на примере процессов вне массовой поверхности $\pi\pi \to \pi\pi$, $A_\mu\pi \to \pi\pi$, и $A_\mu\pi \to A_\mu\pi$.

Acta Physica Academiae Scientiarum Hungaricae, Tomus 31 (1—3), pp. 147—151 (1972)

SOME REMARKS ON "ENERGY-DEPENDENT" REPRESENTATIONS

By

K. SZEGŐ and K. TÓTH
CENTRAL RESEARCH INSTITUTE FOR PHYSICS, BUDAPEST

After explaining the meaning of energy dependent representation, we sketch how it can be obtained for the case of the SL(2, C) group. Some physical applications are also treated.

Some time ago we examined the problem how one can expand a general two-particle—two-particle scattering amplitude in terms of Lorentz group representations at any s and t values [1]. To do this, first one has to define the scattering amplitude as a function on the group in question. As we noticed in [1], a possible and in some sense desirable way is the following:

$$f_{\lambda_1\lambda_2\lambda_3\lambda_4}(s,t) = \langle p_1 s_1\lambda_1, p_2 s_2\lambda_2 |T| p_3 s_3\lambda_3, p_4 s_4\lambda_4\rangle = \\ = \langle \tilde{P} = \tilde{p}_1+\tilde{p}_2, \tilde{p}_1-\tilde{p}_2, s_1\lambda_1 s_2\lambda_2 |\Lambda T| \tilde{P}_1'\tilde{p}_3-\tilde{p}_4, s_3\lambda_3 s_4\lambda_4\rangle = f_H(\Lambda) \tag{1}$$

where

$$\tilde{P} = \left(\frac{m_1+m_2}{2\sqrt{m_1 m_2}}\sqrt{s-(m_1-m_2)^2},\ 0,\ 0,\ \frac{m_1-m_2}{2\sqrt{m_1 m_2}}\sqrt{s-(m_1+m_2)^2}\right) = \\ \text{if } s \geqslant (m_1+m_2)^2$$

$$= \left(\frac{m_1+m_1}{2\sqrt{m_1 m_2}}\sqrt{(m_1+m_2)-s},\ 0,\ 0,\ \frac{m_1-m_2}{2\sqrt{m_1 m_2}}\sqrt{(m_1-m_2)^2-s}\right) \\ \text{if } s \leqslant (m_1-m_2)^2.$$

Λ is a Lorentz transformation acting on two-particle states, its detailed form together with $\tilde{p}_1$—$\tilde{p}_2$, $\tilde{p}_3$—$\tilde{p}_4$ can be found in [1], $\tilde{P}' = \tilde{P}(1 \leftrightarrow 3,\ 2 \leftrightarrow 4)$. If we now perform the expansion using the ordinary $|j_0\sigma jm\rangle$ basis* of the Lorentz group, we get

$$f_H(\Lambda) = \sum \mathfrak{D}^{j_0\sigma}_{jmj'm'}(\Lambda) T_H(s, j_0\sigma\ldots). \tag{2}$$

For continuous variables, like σ, integration is meant in Eq. (2). The expansion coefficients, i.e. the T functions in Eq. (2) are quite complicated due to $\langle \tilde{P} \ldots . / j_0\sigma jm \ldots . \rangle$ type coefficients in it. The main problem with the

* In the $|j_0\sigma jm\rangle$ basis, j_0 and σ characterize an irreducible representations. To label the vectors of a representation space one chooses a subgroup of the Lorentz group; generally it is the rotation group. The $|jm\rangle$ states are representations of the rotation group. For further details, see, e.g. [3].

latter is that the little group of $\tilde{P}$ is different from that chosen to label vectors in irreducible Lorentz representation spaces. To simplify the expansion we have to make the two groups identical. Since the little group is given, this is what we want to introduce as "basis labelling" group. This problem, together with finding the representation matrix elements, was solved in [2].

As the first step, let us write $\tilde{P}$ in the following way:

$$\tilde{P} = f(s)\left(\frac{1+v}{2},\ 0,\ 0,\ \frac{1-v}{2}\right), \tag{3}$$

then $\tilde{P}^2 = s = f^2(s)\, v$. Comparing Eq. (3) with Eq. (2):

$$f(s) = [(m_1 + m_2)\sqrt{s-(m_1-m_2)^2} + (m_1 - m_2)\sqrt{s-(m_1+m_2)}\,]^2/2\sqrt{m_1 m_2} \qquad \text{if } s \geqslant (m_1 + m_2)^2 \tag{4}$$

and a similar expression below the pseudothreshold, hence

$$v = s/f^2(s) \tag{5}$$

is a nice function of s.

Let M_i and N_i be the generators of the Lorentz group commuting as

$$[M_i,\ M_j] = i\varepsilon_{ijk}M_k,\ [M_i,\ N_j] = i\varepsilon_{ijk}N_k,\ [N_i,\ N_j] = -i\varepsilon_{ijk}M_k.$$

Here M_i generates the rotations, N_i the boosts. It is not hard to find out that the little group of P is generated by

$$S_1 = \frac{1+v}{2}M_2 + \frac{1-v}{2}N_1, \quad S_2 = -\frac{1+v}{2}M_1 + \frac{1-v}{2}N_2$$
$$S_3 = M_3 \tag{6}$$

commuting as

$$[S_1,\ S_2] = ivS_3,\ [S_1,\ S_3] = -iS_2,\ [S_2,\ S_3] = iS_1. \tag{7}$$

The Casimir operator of this subgroup, what we call sometimes interpolating group, IG, is $S_1^2 + S_2^2 + vS_3^2$. The structure of this interpolating group and the corresponding algebra as well as its basis depend on the parameter v which is proportional to s. One can check that in the $s > 0$ region it is isomorphic to SU(2), at $s = 0$ to E(2), in the $s < 0$ region to SU(1, 1) — if the masses are unequal. As s and, together with it, v vary, this group interpolates between them smoothly.

However, if the masses are equal, $v = s/|s|$, hence going to $s = 0$ from above, we always have SU(2), and coming from below always SU(1, 1). Now,

since at $s = 0$ both SU(2) and SU(1, 1) are little groups, their minimal extension is a little group too, which is SL(2, C). This fact is well-known, but it is amusing to recover it in this way.

If we choose the interpolating group as basis labelling group, then the basis of the Lorentz group will also depend on s, as well as its representations; and in this sense we shall work with energy-dependent representations.

The need for energy dependent representations appears not only in this case. Examination of the dynamical symmetries of a charged spinless harmonic oscillator in a constant magnetic field presents a similar problem [4]. Such representations are also useful when treating the H-atom problem [5].

In the following, we shall briefly sketch how one can find the explicit basis functions. The details can be found in [2]. We start with the basic formula for SL(2, C) representation [6]:

$$U_g \Phi(z) = (\beta z+\delta)^{J_0+\sigma-1} \overline{(\beta z+\delta)}^{-J_0+\sigma-1} \Phi\left(\frac{\alpha z+\gamma}{\beta z+\delta}\right), \tag{8}$$

where $\Phi(z)$ are infinitely differentiable functions of one complex variable,

$$g = \begin{pmatrix} \alpha & \beta \\ \gamma & \delta \end{pmatrix} \in \mathrm{SL}(2, \mathrm{C}),\ \alpha\delta - \beta\gamma = 1.$$

Relation (8) does not specify the functions $\Phi(z)$. To do this, we can set additional equations.

First of all we derive from Eq. (8) the form of the generators as differential operators acting on $\Phi(z)$. If we form out of them the operators $M_i N_i$ and $M^2 - N^2$, we get simple numbers, so the function space of Φ is irreducible.

To define basis functions we form the S_i operators and set

$$(S_1^2 + S_2^2 + vS_3^2)\,\Phi = vj(j+1)\,\Phi,\ S_3\Phi = m\Phi. \tag{9}$$

If we require that Φ should be one valued and regular at $z = 0$, we obtain Φ uniquely. From Eq. (9) we can learn that the Φ functions serve not only as basis functions for SL(2, C) representations, but at the same time they are representation functions of the interpolating group.

From our basic relation it is not hard to see that if we restrict ourselves to the SU(1, 1) subgroup of the Lorentz group, the z plane breaks up to two disjoint regions since

$$\begin{aligned} &|z'| > 1 \text{ if } |z| > 1 \text{ and } |z'| < 1 \text{ if } |z| < 1, \\ &z' = \frac{\alpha z+\bar{\beta}}{\beta z+\bar{\alpha}} \quad \begin{pmatrix} \alpha & \bar{\beta} \\ \beta & \bar{\alpha} \end{pmatrix} \in \mathrm{SU(1,1)} \subset \mathrm{SL(2,C)}. \end{aligned} \tag{10}$$

This means that the SU(1, 1) type basis will appear with multiplicity two.

We do not think it is necessary to give here the detailed form of the Φ functions, as they are rather complicated. The inquirer can found it in [2]. But we emphasize again that though the structure of the algebra changes radically with v, the Φ functions change smoothly, without the appearing of any type of singularities.

One may ask whether our representation is unitary or not. This depends on whether one can or one cannot introduce a scalar product into the space of the functions. It turns out that it is possible only for special j_0 and σ values; for the others, the positive definiteness condition cannot be maintained; hence we have to work with some generalization of the scalar product what is called invariant bilinear functional [6]. Using this, we were able to calculate the normalization of the basis, the finite group representation matrix elements and overlap functions between different bases [2].

Finishing our discussion we make some remarks about the application of this formalism for generalized partial wave analysis.

If in the expansion of the scattering amplitude we use energy dependent representations instead of $|j_0\sigma jm>$ basis, the T functions of Eq. (2) will be simple reduced matrix elements, which, because of the Wigner—Eckart theorem depend only on the Casimirians. As the scattering amplitude is expanded in terms of Lorentz representations, one tends to write Lorentz Casimirians into T. However, the scattering amplitude has a larger symmetry group, the Poincaré one, and our group is its subgroup. Hence the reduced matrix elements depend only on Poincaré Casimirians, e.g. on s and W^2.

Since T does not depend on j_0 and σ, we can perform the summation on it in Eq. (2); in this way we get an expansion of the scattering amplitude in terms of the interpolating group. This result seems to be trivial, but the whole procedure is not useless.

We can conclude that the generalization of the ordinary partial wave analysis is not singular at $s = 0$, whereas in the unequal case the old fashioned one is; consequently, the introduction of Toller or Lorentz poles is not the only theoretical way-out. Secondly, as the reduced matrix elements do not depend on the SL(2, C) Casimirians in general, the introduction of Lorentz poles is a bit artificial. However, as generally at $s = 0$ a large number of Regge poles contribute with almost equal weight, the SL(2, C) expansion can be useful to handle them since it can correlate them, at least in some sense. The detailed description of these and further results will be published elsewhere [1b, 7].

REFERENCES

1. K. SZEGŐ and K. TÓTH, Nuovo Cimento **66A**, 371, 1970.
K. TÓTH, Nuovo Cimento, **66A**, 323, 1970.
2. K. SZEGŐ and K. TÓTH, Journal of Math. Phys. **12**, 846, 1971, **12**, 853, 1971.

3. M. A. NAIMARK, "Linear Representations of the Lorentz Group" Pergamon Press, London, 1964.
4. J. KATRIEL and G. ADAM, Phys. Rev. Letters, **23**, 1310, 1970.
5. G. GYÖRGYI, to be published.
6. I. M. GELFAND, M. I. GRAEV and N. YA. VILENKIN, "Generalized Functions", Vol. 5. Academic Press, New York, 1966.
7. K. SZEGŐ and K. TÓTH, to be published in Phys. Rev., D, 1972.

НЕКОТОРЫЕ ЗАМЕЧАНИЯ ОТНОСИТЕЛЬНО ПРЕДСТАВЛЕНИЙ ЗАВИСЯЩИХ ОТ ЭНЕРГИИ

К. СЕГЁ и К. ТОТ

Резюме

После объяснения понятия «представление зависящее от энергии» рассматривается, как оно может быть получено для случая групп SL (2, C). Описываются некоторые физические применения.

Acta Physica Academiae Scientiarum Hungaricae, Tomus 31 (1—3), pp. 153—163 (1972)

LEPTONIC AND SEMI-LEPTONIC WEAK INTERACTIONS*

By

H. PIETSCHMANN

INSTITUTE FOR THEORETICAL PHYSICS, THE UNIVERSITY, VIENNA, AUSTRIA

New results on leptonic and semi-leptonic weak processes are reviewed. Recent references on this subject are accumulated.

1. Introduction

Weak Interactions has become such a vast field that it is clearly impossible to review all of it in mere 45 minutes. Hence this talk is restricted by its title to leptonic and semi-leptonic weak interactions. Within this more confined part of the field, we still put accents: we shall emphasize the hadronic matrix elements of the weak currents, for this is a symposium on hadron spectroscopy after all.

Naturally, new results reported at the Kiev conference will form the most important ingredients to this talk. For all those, who wish to elaborate on a particular aspect of leptonic and semi-leptonic weak interactions, we accumulate references at the end to papers which appeared during this year. Working backwards into older references is then a matter of routine even for the less experienced worker.

The reason why we chose leptonic and semi-leptonic weak interactions as the topic of this review is very simple: for this part of weak interaction there exists a very fine model which covers such a wide variety of different physical phenomena that it may even be called a theory! Of course, everybody knows that higher order weak interactions are as yet completely un-understood and therefore forbid the strict use of the word "theory". In the last Section, we elaborate on various trials to cope with this difficult challenge, thereby just proving that nothing is really known as yet. However, the Sections in between will hopefully show that one can get an overwhelming amount of fun out of the play with lowest order alone, showing that despite the incomplete framework, a lot of good physics can be done with the present model.

* Supported by "Fonds zur Förderung der wissenschaftlichen Forschung".

2. The theoretical model

Leptonic and semi-leptonic weak interactions can be described by the following effective S-operator within the $V—A$-theory

$$(S-I)_{\text{eff}} = \frac{-iG}{\sqrt{2}} \int d^4x d^4y \frac{1}{2} \{J_\lambda^+(x)\, K^{\lambda\sigma}(x-y)\, l_\sigma(y) + \text{h.c.}\} + O(G^2), \quad (1)$$

where there are essentially two competing models for $K^{\lambda\sigma}(x)$, the current-current model (C.C.) and the intermediate vector boson model (I.V.B.). In these models, $K^{\lambda\sigma}(x)$ takes the forms

$$K^{\lambda\sigma}(x) = g^{\lambda\sigma}\, \delta^{(4)}(x) \qquad \text{(C. C.)}, \quad (2a)$$

$$K^{\lambda\sigma}(x) = \frac{g^2\sqrt{2}}{G}\, \Delta_F^{\lambda\sigma}(x, m_W^2) \quad \text{(I. V. B.)}. \quad (2b)$$

Of course, in the I.V.B. case, the effective S-operator (1) does not describe production processes of W-bosons. So far, they have not been observed anyway.

The leptonic current is given by

$$l_\lambda(x) = \sum_l \bar{\psi}_l(x)\, \gamma_\lambda(1+\gamma_5)\, \psi_{\nu_l}(x) \qquad l = e, \mu \quad (3)$$

and the total weak current consists of 3 parts

$$J_\lambda(x) = l_\lambda(x) + \cos\theta j_\lambda^\pi(x) + \sin\theta j_\lambda^K(x), \quad (4)$$

where j_λ^π and j_λ^K have the transformation properties of pions and kaons, i.e. $\Delta I = 1, \Delta Y = 0$ and $\Delta I = 1/2, \Delta Y = \Delta Q$, respectively. The fact that the total weak current contains the Cabibbo angle θ has nothing to do with SU_3 symmetry. At this early stage, it is just the expression of the fact, that the three parts of the weak current are governed by only two independent coupling constants. SU_3 symmetry will be introduced in Section 5.

3. Muon decay

The only experiment which tests the S-operator (1) without the disturbing effects of strong interactions is the decay of the muon. For a sample with polarization P, the spectrum of electron with energy E and momentum q can be parameterized in the following general way:

$$N(E, \Omega) = \frac{G^2}{24\pi^4} m_\mu^2 qE \left\{3 - 3x + \frac{2}{3}\varrho(4x-3) + 6\eta\varepsilon\left(\frac{1}{x} - 1\right) - P\frac{q}{E}\cos\theta\xi\left[1 - x + 2\delta\left(\frac{4}{3}x - 1\right)\right]\right\} + O(\varepsilon^2), \quad (5)$$

where θ is the angle between muon polarization and direction of electron momentum and

$$\begin{aligned} \varepsilon &= m_e/m_\mu, \\ x &= 2E/m_\mu, \\ 2\varepsilon &\leq x \leq 1. \end{aligned} \tag{6}$$

The predicted values from the S-operator (1) as well as the best experimental results are collected in Table I.

Table I

The parameters of muon decay

Parameter	$V-A$ prediction		Experiment [1]
Michèl	ϱ	3/4	0.7518 ± 0.0026
Shape	δ	3/4	0.7540 ± 0.0085
Asymmetry	ξ	-1	-0.973 ± 0.014
Eta	η	0	-0.12 ± 0.21
Helicity of e^-	h^-	-1	-1.0 ± 0.13

It is remarkable, that in spite of the impressive accuracy of the data, other invariants (scalar, pseudoscalar, tensor) in the S-operator (1) are not excluded with great precision. In fact, we have [1]

$$\begin{aligned} G_S &< 0.33\ G, \\ G_P &< 0.33\ G, \\ G_T &< 0.28\ G \end{aligned}$$

If the coefficient of the axial vector is left open to be determined from experiments, one obtains [1]

$$0.76\ G < G_A < 1.20\ G.$$

The phase angle obtained between the vector and axial vector is:

$$\sphericalangle\,(V, A) = (180 \pm 15)^\circ.$$

4. Tests of the structure of the S-operator

One of the important consequences of the S-operator (1) is the absence of neutral lepton currents. Of course, those currents can occur via combined weak-electromagnetic interactions. Therefore, the best test is that for neutral

neutrino currents since neutrinos do not participate in electromagnetic interactions. The present best value is [3]

$$\Gamma(K^+ \to \pi^+ \nu\bar{\nu})/\Gamma(K^+) < 1.2 \cdot 10^{-6}.$$

This particular process forms also the crucial test for the theory of semi-weak *CP*-violation of MARSHAK et al.[5] which definitely predicts a rate of order g^3, i.e. about 10^{-7}.

Another well studied neutral lepton current process is $K_L^0 \to \mu^+\mu^-$. Its branching ratio is now limited by $8{,}2 \cdot 10^{-9}$ with 90% confidence level [6]. This means an upper limit for the cut-off in the second order weak matrix element of 29 GeV in the I.V.B. model and of 15 GeV in the C.C. model.

The *S*-operator (1) predicts the occurrence of so-called "diagonal processes" with about the same strength as μ-decay. The present upper limit for $e\bar{\nu}_e$-scattering is [7]

$$\sigma_{e\bar{\nu}} < 4\sigma_{VA}.$$

The Leningrad group reported at the Kiev conference a measurement of the circular polarization of photons from capture of thermal neutrons in the process $n + p \to d + \gamma$ in agreement with theoretical predictions.

In actual laboratory experiments it is very hard to determine the mass of the neutretto. Its upper limit is still rather high, namely 1,6 MeV. Pontecorvo reported in Kiev a rather indirect cosmological argument which limits the neutretto mass to

$$m_{\nu_\mu} < 200 \text{ eV}.$$

The argument relies on statistical equilibrium in the early state of the universe after the big bang and on the energy distribution between radiation and matter at this time. Our knowledge on the age of the universe also enters the argument.

Rather intense studies in various places are devoted to double beta decay. This enormously interesting field has been opened with the first definite detection in 1968 by KIRSTEN et al. [10]. In Kiev, FIORINI [13] reported on a new experiment on ^{76}Ge carried out in the Mont Blanc tunnel. Preliminary results yield

$$\tau_{1/2} > 1.5 \cdot 10^{21} \text{ ys}$$

for the neutrino-less decay into $^{76}\text{Se} + 2e^-$. The experiment is being continued.

5. Baryonic matrix element of the weak current

As a consequence of Lorentz invariance, the most general matrix element of the weak current between spin 1/2 baryon states of momenta p' and p can be

expressed through six functions of one variable (form factors) in the following way [14]:

$$\langle p' \,|J_\lambda(0)|\, p \rangle = N_B\ \bar{u}(p')\,\{F_1(q^2)\gamma_\lambda + F_2(q^2)i\sigma_{\lambda\nu}\,q^\nu + F_3(q^2)q_\lambda +$$

$$+ [G_1(q^2)\gamma_\lambda + G_2(q^2)q_\lambda + G_3(q^2)i\sigma_{\lambda\nu}q^\nu]\gamma_5\}\ u(p), \tag{7}$$

where q is the momentum transfer

$$q = p' - p \tag{8}$$

and N_B is some unimportant normalization factor.

A further restriction on the number of form factors is possible if the concept of G parity is invoked. The vector current operator is even under G-parity transformations, whereas the axial vector is odd. Therefore, if no additional pieces are added to the S-operator (1), the vector and axial vector matrix elements should show the same behaviour under G transformations since the latter are good symmetry operations with respect to strong interactions. This excludes the so-called "second class currents", terms with $F_3(q^2)$ and $G_3(q^2)$.

Another constraint is the conserved vector current (C.V.C.) hypothesis. It consists of two separate parts:

(i) the weak vector current is conserved

(ii) the weak vector current is the rotated isovector part of the electro magnetic current.

The first part requires that for transitions within an isomultiplet $F_3(q^2)$ vanishes identically. For transitions between different isomultiplet it requires $F_1(0) = 0$.

The freedom in the baryonic matrix elements of the weak current is most severely reduced by the Cabibbo theory. Within the framework of this theory, all form factors F_1 and G_1 at vanishing momentum transfer can be expressed through two constants, G_1^f and G_1^d

$$F_1(0)_{AB} = c_f^{AB}\,, \tag{9a}$$

$$G_1(0)_{AB} = c_f^{AB}\,G_1^f + c_d^{AB}\,G_1^d\,, \tag{9b}$$

where c_f and c_d are Clebsch–Gordan coefficients for f-type and d-type currents of SU_3. They are listed in Table II. It is seen from this that in the case of neutron decay one has for example

$$(G_1/F_1)^1_{np} = G^f + G_1^d\,. \tag{10}$$

Table II

Clebsch-Gordan coefficients of the Cabibbo theory

Matrix element	c_f	c_d
(n, p)	1	1
(Σ, Λ)	0	$\sqrt{2/3}$
(Λ, p)	$-\sqrt{3/2}$	$-1/\sqrt{6}$
(Σ^-, n)	-1	1
(Ξ^-, Λ)	$\sqrt{3/2}$	$-1/\sqrt{6}$

Let us now confront this refined model with experience. Firstly, there is a fit to the coupling constants for $\Delta Y = 0$ transitions (including nuclear β-decays) by PAUL [15]. (Note that this fit does not yet include new results reported at the Kiev conference). Intrinsic scalar and tensor currents are ruled out with comforting accuracy:

$$G_S/G = -0.001 \pm 0.006$$
$$G_T/G = -0.0004 \pm 0.0003.$$

The ratio G_1/F_1 for neutron decay becomes a bit unpleasantly high:

$$(G_1(0)/F_1(0))_{np} = 1.262 \pm 0.008.$$

This rather high value is corroborated by a result reported in Kiev by EROZOLIMSKY [16]:

$$(G_1(0)/F_1(0))_{np} = 1.27 \pm 0.025.$$

This result was obtained from a measurement of the angular correlation in β-decay.

In principle, all parameters of the Cabibbo theory can be determined from $\Delta Y = 0$ transitions only, so that $|\Delta Y| = 1$ transitions are then completely specified. To this end, one had to use (Σ, Λ) decays. In practice, it is much better to use a least squares adjustment of all measurements to the three parameters θ, G_1^f and G_1^d. Such a fit has been reported in Kiev by the Heidelberg group [17]. The old value of 1.23 for $(G_1/F_1)_{np}$ has been used in this fit, however. The result is

$$\theta = 0.242 \pm 0.004,$$
$$G_1^f = 0.460 \pm 0.015,$$
$$G_1^d = 0.771 \pm 0.016.$$

If one allows for different Cabibbo angles θ_V and θ_A in the vector and axial vector matrix elements, the results remain unchanged. The two angles agree within one standard deviation.

From these values, the axial vector to vector ratio for Λ decay is predicted to be

$$(G_1/F_1)_{\Lambda p} = G_1^f + \frac{1}{3} G_1^d = 0.72 \,.$$

Three measurements have been reported in Kiev:

[18]: $\left| 0.66 \begin{matrix} + 0.14 \\ - 0.11 \end{matrix} \right|$

[19]: 0.65 ± 0.09

ANL: $0.35 \begin{matrix} + 0.27 \\ - 0.14 \end{matrix}$.

The last measurement is based on 110 events only and is a preliminary result. The second class pseudotensor form factor in Λ-decay is consistent with zero [19]

$$(G_3(0)/F_1(0)_{\Lambda p} = -0.1 \pm 0.6,$$

and the (normalized) weak magnetism form factor is consistent with unity [19]:

$$\left(F_2(0)/F_1(0)\right)_{\Lambda p} = 1.1 \pm 0.6.$$

For Σ^--decay, the Cabibbo theory predicts

$$(G_1(0)/F_1(0)_{\Sigma^- n} = G_1^f - G_1^d = -0.31.$$

On the basis of 607 events, the Heidelberg group gets the opposite sign [17]:

$$0.20 \pm 28.$$

Nevertheless, the disagreement is only two standard deviations.

6. Mesonic matrix element of the weak current

The matrix element of the weak current between pseudoscalar meson states of momenta k' and k can be expressed through 2 form factors

$$\langle k' \,|J_\lambda(0)|\, k \rangle = N_M\{(k' + k)_\lambda f_+(q^2) + q_\lambda, f_-(q^2)\} \,, \qquad (11)$$

where N_M is again an unimportant normalization factor and q is again the momentum transfer, $k'—k$. The form factors are conventionally parameterized in the following way:

$$f_{\pm}(q^2) = f_{\pm}(0)\left\{1 + \lambda_{\pm}\frac{q^2}{\mu^2} + \ldots\right\}, \tag{12}$$

where μ is the pion mass. The ratio of the form factors is called ξ

$$f_-(q^2)/f_+(q^2) \equiv \xi(q^2). \tag{13}$$

The important example for such a matrix element is, of course, K_{l3} decay, i.e. $K^+ \to \pi^0 l^+ \nu_l$ and equivalent modes for other charge states. We shall restrict to charged kaons here. Let us summarize the unfortunate situation by simply saying that it is still — after so many years — in a state of confusion. The naive K^* dominance model requests $\lambda_+ = 0{,}03$. For some time, the world average for this parameter settled at the close enough value of 0.029 ± 0.008. In Kiev, new results were reported by the SLAC–Berkeley collaboration [28]:

$$K_{e3}: \qquad \lambda_+ = 0.07 \pm 0.03,$$
$$K_{\mu 3}: \qquad \lambda_+ = 0.09 \pm 0.02.$$

The same experiment yielded the following "allowed domain" for λ_- and $\xi(0)$:

$$-0.30 < \lambda_- < 0.10,$$
$$-2.5 < \xi(0) < -0.12,$$

whereas the ANL, Yale collaboration who investigated the polarization of μ' s from $K_{\mu 3}$ decay obtained

$$\xi = -0.86 \pm 0.08.$$

This situation is rather unfortunate, because there is considerable interest in these parameters from current algebra. The old MATHUR–OKUBO–PANDIT–CALLAN–TREIMAN relation has been revived and extended to points nearer or inside the physical region (see [41–43]). These relations all require small negative values for ξ.

Some authors also study the influence of the much discussed $\varkappa$-meson on K_{l3} parameters. Typically, a mass of 1000–1100 MeV is required [30, 48] to obtain agreement with the experiments. In this connection it is interesting to comment on some predictions derived from the Veneziano model [44–47].

These predictions can also be born out from current algebra calculations provided the $\varkappa$ mass is fixed at the K* mass; in other words, the $\varkappa$ must be assumed to be a K*-daughter.

7. Models for higher orders

In recent months more and more effort has been concentrated once again on setting up a theory of weak interactions in which higher orders can be calculated consistently. There are now essentially 6 different approaches:

a) The LEE–WICK ghost [49].

b) The GELL-MANN, GOLDBERGER, KROLL, LOW model [50]. This model is in contradiction with the experiment on $e\bar{\nu}$ scattering, because this matrix element still diverges in higher orders.

c) KUMMER–SEGRÉ type models [51]. A number of variations and consequences of this model have been reported in Kiev. Here, the intermediate bosons are scalar and a number of heavy leptons are predicted. The price one pays for the renormalizability of the theory is that universality and conserved vector currents cannot be incorporated in a natural and obvious way.

d) Another field theoretic model has been set up by EFIMOV and SELTSER [54]. These authors change the neutrino field essentially in the following way.

$$\psi_\nu(x) \to \int d^4y\, K(x-y)\, \psi_\nu(y). \tag{14}$$

Hence they can manufacture a neutrino propagator which damps higher orders to yield a finite number of infinite renormalization constants. The price is, of course, loss of uniformity among leptons.

e) Rather interesting seems to be the attempt by FIVEL and MITTER [56] to use the methods of non-polynomial Lagrangians in weak interactions. This investigation leaves enough room for further developments in different directions.

f) Finally, let me mention the attempt of the Vienna group [57, 58] to investigate the S-operator (1) with an unspecified and completely general structure tensor $K^{\lambda\sigma}(x)$.

REFERENCES

Muon decay:

1. S. E. DERENZO, R. H. HILDEBRAND and C. VOSSLER, Phys. Letters, **28B**, 401, 1968.
2. L. MATTESON and G. PERESSUTTI, Letters Nuovo Cimento, **3**, 57, 1970.

Neutral lepton currents:

3. J. H. KLEMS, R. H. HILDEBRAND and R. STIENING, Phys. Rev. Letters, **24**, 1086, 1970.
4. R. S. WILLEY, Phys. Rev., **D1**, 2182, 1970.
5. S. OKUBO, C. RYAN and R. E. MARSHAK, Nuovo Cimento **34**, 753, 759, 1964; R. E. MARSHAK, Report presented at the XVth International Conference on High Energy Physics, Kiev, 1970.

6. A. R. Clark, T. Elioff, R. C. Field, H. J. Frisch, R. P. Johnson, L. T. Kerth and W. A. Wenzel, Report presented at the XVth International Conference on High Energy Physics, Kiev, 1970.

Diagonal processes:

7. F. Reines and H. S. Gurr, Phys. Rev. Letters, **24,** 1448, 1970.
8. D. C. Cundy, G. Myatt, F. A. Nezrick, J. B. M. Pattison, D. H. Perkins, C. A. Ramm, W. Venus and H. W. Wachsmuth, Phys. Letters, **31B,** 478, 1970.
9. D. Yu. Bardin, S. M. Bilenky and B. Pontecorvo, Phys. Letters, **32B,** 121, 1970.

Double β-decay:

10. T. Kirsten, D. A. Schaeffer, E. Norton and R. W. Stoenner, Phys. Rev. Letters, **20,** 1300, 1968.
11. H. Primakoff, Springer Tracts Mod. Phys., **53,** 1970.
12. H. Primakoff and D. H. Sharp, Phys. Rev. Letters, **23,** 501, 1969.
13. E. Fiorini, A. Pullia, G. Bertolini, F. Cappellani and G. Restelli, Letters Nuovo Cimento, **3,** 149, 1970.

Baryon decays:

14. H. Pietschmann, Acta Phys. Austr., Suppl. **5,** 88, 1968.
15. H. Paul, Nucl. Phys,, A **154,** 160, 1970.
16. B. G. Erozolimsky, L. N. Bondarenko, Yu. A. Mostovoy and B. A. Obinjakov, Report presented at the XVth International Conference on High Energy Physics, Kiev, 1970.
17. H. Ebenhöh, R. Eisele, H. Filthuth, W. Föhlisch, V. Hepp, E. Leitner, W. Presser, H. Schneider, T. Thuow and G. Zech, Report presented at the XVth International Conference on High Energy Physics, Kiev, 1970.
18. M. Baggett, N. Baggett, F. Eisele, H. Filthuth, H. Rehse, V. Hepp, R. Howard, E. Leitner and G. Zech, Report presented at the XVth International Conference on High Energy Physics, Kiev, 1970.
19. K. H. Althoff, R. M. Brown, D. Freytag, K. S. Heard, J. Heintze, R. Mundhenke, H. Rieseberg, V. Soergel, H. Stelzer and A. Wagner, Report presented at the XVth International Conference on High Energy Physics, Kiev, 1970.
20. D. H. Wilkinson, Phys. Letters, **31B,** 447, 1970.
21. D. A. Dicus and R. E. Norton, Phys. Rev., **D1,** 1360, 1970.
22. N. Cabibbo and L. Maiani, Phys. Rev., **D1,** 707, 1970.
23. T. Pradhan and M. Pattnaik, Phys. Rev., **D1,** 200, 1970.
24. J. Dittrich and F. Janouch, Prague preprint UJV2432-F.
25. G. Rajasekaran and K. V. L. Sarma, Nucl. Phys., **B18,** 568, 1970.
26. U. E. Schröder, Nucl. Phys., **B15,** 125, 1970.
27. A. Frenkel, these Proceedings, p. 165.

Meson decays:

28. Drickey et al., Report presented at the XVth International Conference on High Energy Physics, Kiev, 1970.
29. D. R. Botterill, R. M. Brown, A. B. Clegg, I. F. Corbett, G. Culligan, J. Mcl. Emmerson, R. C. Field, J. Garvey, P. B. Jones, N. Middlemas, D. Newton, T. W. Quirk, G. L. Salmon, P. H. Steinberg and W. S. C. Williams, Phys. Letters, **31B,** 325, 1970.
30. Fayyazuddin, Riazuddin, Phys. Rev., **D1,** 317, 361, 1970.
31. K. Kang, Phys. Rev. Letters, **25,** 414, 1970.
32. S. Oneda, H. Umezawa and S. Matsuda, Phys. Rev. Letters, **25,** 71, 1970.
33. S. P. de Alvis, Phys. Rev., **D1,** 2131, 1970.
34. S. N. Biswas, R. Dutt, P. Nanda and L. K. Pandit, Phys. Rev., **D1,** 1445, 1970.
35. T. Becherrawy, Phys. Rev., **D1,** 1452, 1970.
36. E. S. Ginsberg, Phys. Rev., **D1,** 229, 1970.
37. C. Ryan, Phys. Rev., **D1,** 299, 1970.
38. D. Haidt, D. Rein, R. Rodenberg and P. Zerwas, Nuovo Cimento, **67A,** 113, 1970.
39. T. Kaneko, Progr. Theor. Phys., **43,** 856, 1970.
40. G. Murtaza and Harun-ar-Rashid, Z. Physik, **230,** 65, 1970.
41. R. Dashen and M. Weinstein, Phys. Rev. Letters, **22,** 1337, 1969.
42. V. S. Mathur and S. Okubo, Rochester preprint UR-875-305.
43. G. Denardo, Letters Nuovo Cimento, **3,** 319, 1970.
44. Y. Hara, Phys. Rev., **D1,** 874, 1970.

45. F. Hussein and M. S. K. Razmi, Letters Nuovo Cimento, **3**, 339, 1970.
46. F. C. P. Chan, M. Y. Chan and H. Chen, Letters Nuovo Cimento, **3**, 203, 1970.
47. H. Kurokawa, Progr. Theor. Phys., **43**, 1406, 1970.
48. N. F. Nasrallah and K. Schilcher, Beirut preprint.

Models for higher orders:

49. T. D. Lee and G. C. Wick, Nucl. Phys., **B9**, 209, 1969; Nucl. Phys., **B10**, 1, 1969.
50. M. Gell-Mann, M. Goldberger, N. Kroll and F. Low, Phys. Rev., **179**, 1518, 1969.
51. W. Kummer and G. Segrè, Nucl. Phys., **64**, 585, 1965.
52. S. H. Patil and J. S. Vaishya, Nucl. Phys., **B19**, 338, 1970.
53. E. A. Lord, Nuovo Cimento, **68A**, 184, 1970.
54. G. V. Efimov and Sh. Z. Seltser, Dubna preprint submitted to Ann. Phys. (N. Y.).
55. D. Yu. Bardin, S. M. Bilenky and B. Pontecorvo, Phys. Letters, **32B**, 121, 1970.
56. D. I. Fivel and P. K. Mitter, Maryland preprint 70—029.
57. H. Pietschmann, Springer Tracts Mod. Phys., **52**, 193, 1970; Acta Phys. Austr., Suppl., **7**, 1970.
58. H. Pietschmann and H. Stremnitzer, Nucl. Phys., **B**, **22**, 493, 1970.
59. A. Bailin and D. Bailin, Nucl. Phys., **B17**, 317, 1970.

W-Production:

60. R. W. Brown, A. K. Mann and J. Smith, Phys. Rev. Letters, **25**, 257, 1970.
61. F. A. Berends and G. B. West, Phys. Rev., **D1**, 122, 1970.

Radiative decays:

62. R. J. Macek, A. K. Mann, W. K. McFarlane and J. B. Roberts, Phys. Rev., **D1**, 1249, 1970.
63. S. Iwao, Progr. Theor. Phys., **43**, 144, 1970.
64. M. G. Smoes, Nucl. Phys., **B20**, 237, 1970.
65. W. Kummer and M. Schweda, Nuovo Cimento, **67A**, 305, 1970.
66. W. Konetschny and W. Kummer, Nuovo Cimento, **65A**, 715, 1970.

Neutrino induced reactions:

67. T. L. Jenkins, F. E. Kinard and F. Reines, Phys. Rev., **185**, 1599, 1969.
68. O. Nachtmann, Nucl. Phys., **B18**, 112, 1970.
69. T. Iwata, T. Takemura and T. Kobayashi, Progr. Theor. Phys., **43**, 552, 1970.

Miscellaneous:

70. C. Cronström and M. Noga (Bootstrap and Cabibbo theory) Nucl. Phys., **B17**, 477, 1970.
71. J. Hosek (Model of leptons), Prag preprint UJV 2435-F.

ЛЕПТОННЫЕ И ПОЛУЛЕПТОННЫЕ СЛАБЫЕ ВЗАИМОДЕЙСТВИЯ

Х. ПИТЧМАН

Резюме

Приведён обзор новых результатов в области изучения лептонных и полулептонных процессов. Собраны новые работы по данной теме.

Acta Physica Academiae Scientiarum Hungaricae, Tomus 31 (1—3), pp. 165—171 (1972)

REMARKS ON "A NEW FIT OF THE PARAMETERS FOR CABIBBO'S THEORY"

By

A. FRENKEL and P. HASENFRATZ

CENTRAL RESEARCH INSTITUTE FOR PHYSICS, BUDAPEST

Some of the theoretical uncertainties inherent in the theory of weak interactions and their possible influence on the fitted value of the Cabibbo angle are discussed. Special attention is given to the problem of the q^2-dependence of the form factors.

At present an intensive experimental study of the semileptonic decays of the baryon octet is in progress in several laboratories. At the XVth International Conference on High Energy Physics the results of "A New Fit of the Parameters for Cabibbo's Theory" has been presented [1]. The value of the Cabibbo angle in the case of a one-angle fit $\theta = \theta_V = \theta_A$ turned out to be

$$\theta = 0.242 \pm 0.004, \tag{1}$$

i.e. the relative statistical error is smaller than 2%. The mean value depends, however, on many approximations which are introduced in order to arrive at working formulas with a reasonable number of free parameters. In the present paper we would like to make some remarks concerning these approximations.

One of the sources of the theoretical uncertainty is the q^2-dependence of the six form factors $f_i^{B\to B'}(q^2)$, entering the hadronic part of the matrix element of the $B \to B'lv$ decay:

$$\begin{aligned}\langle B'|j^\alpha(0)|B\rangle = \bar{u}_{B'}(p')\Bigg\{ & f_1^{B\to B'}(q^2)\gamma^\alpha + i f_2^{B\to B'}(q^2)\sigma^{\alpha\beta}\frac{q_\beta}{\frac{1}{2}(M+M')} + \\ & + f_3^{B\to B'}(q^2)\frac{q^\alpha}{\frac{1}{2}(M+M')} + f_4^{B\to B'}(q^2)\gamma^\alpha\gamma_5 + \\ & + i f_5^{B\to B'}(q^2)\sigma^{\alpha\beta}\gamma_5\frac{q_\beta}{\frac{1}{2}(M+M')} + f_6^{B\to B'}(q^2)\gamma_5\frac{q^\alpha}{\frac{1}{2}(M+M')}\Bigg\} u_B(p).\end{aligned} \tag{2}$$

The well known notations used in Eq. (2) are the same as in [2] and [3].

Both experimental and theoretical information on the general behaviour of the form factors indicate that they are slowly varying functions of q^2. In

the neighbourhood of the point $q^2 = 0$ this smoothness condition may be expressed by saying that, to a good approximation, one may write the form factors in the form

$$f(q^2) = f(0)\left[1 + \lambda \frac{q^2}{M_p^2}\right] \qquad \text{if } f(0) \neq 0, \quad (3)$$

$$= \lambda \frac{q^2}{M_p}, \qquad \text{if } f(0) = 0. \quad (4)$$

with slopes λ of the order of magnitude 1. E.g., for the electromagnetic form factors f_1^n and f_1^p of the proton and neutron, the experimental results obtained at Stanford support this hypothesis:*

$$f_1^p(q^2) = f_1^p(0)\left[1 + 2.05 \frac{q^2}{M_p^2}\right], \quad (5)$$

$$f_1^n(q^2) = 1.05 \frac{q^2}{M_p^2}. \quad (6)$$

The physical region of q^2 in the hyperon decays $B \to B'lv$ extends from m_l^2 to $(M—M')^2 \approx (150\ \text{MeV})^2$. The contribution of the q^2-dependence of the form factor may be represented on the average by

$$\left\langle \lambda \frac{q^2}{M_p^2} \right\rangle \approx \lambda \left(\frac{75\ \text{MeV}}{940\ \text{MeV}}\right)^2 \approx 0.006\,\lambda. \quad (7)$$

Although an accumulation of the contributions coming from different form factors is not excluded, their influence on the fitted value of the Cabibbo angle is probably smaller than the relative statistical error in Eq. (1). This means that from a purely pragmatic point of view it is of no importance at present whether the q^2-dependence of the form factors is neglected or not. However, from a theoretical point of view the question of the q^2-dependence is of outmost importance, and this is why we think that it is worthy to discuss some problematic features of the method of the calculation of the slopes, adopted in [1]. This method has been described in [2] and [3]. The vector form factor $f_1^{B\to B'}(q^2)$ is written in the form

$$f_1^{B\to B'}(q^2) = f_1^{B\to B'}(0)\left[1 + \lambda_1^{B\to B'} \frac{q^2}{M_p^2}\right]. \quad (8)$$

The values at $q^2 = 0$ are then connected with the electromagnetic form factors of the nucleons given in Eqs. (5) and (6) through the SU(3) symmetry:

$$f_1^{B\to B'}(0) = c_p^{B\to B'} f_1^p(0) + c_n^{B\to B'} f_1^n(0). \quad (9)$$

* See the Note added in proof.

In Eq. (9) $c_{p,n}^{B\leftarrow B'}$ are SU(3) Clebsch–Gordan coefficients multiplied by cos θ for $\Delta S = 0$, and by sin θ for $\Delta S = 1$ decays. On the other hand, all the slopes $\lambda_1^{B\to B'}$ are taken to be equal to each other and are equated to the physical slope of the form factor $f_1^{n\to p}(q^2)$, calculated from the slopes of $f_1^p(q^2)$ and $f_1^n(q^2)$:

$$\lambda_1^{B\to B'} = \lambda_1^{n\to p} = \lambda_1^p - \lambda_1^n = 2.05—1.05 = 1.00. \tag{10}$$

The only possible theoretical motivation known to us for taking all the slopes equal is the application of the vector meson octet dominance model in its pure form. In this model the isoscalar and isovector form factors are equal to each other and have the simple form

$$f^s(q^2) = f^v(q^2) = \frac{m_8^2}{m_8^2 - q^2}, \tag{11}$$

where m_8 is the SU(3) symmetric mass of the vector meson octet. The various $f_1^{B\to B'}(q^2)$ form factors are then expressed through f^s and f^v:

$$f^{B\to B'}(q^2) = c_s^{B\to B'} f^s(q^2) + c_v^{B\to B'} f^v(q^2) = (c_s^{B\to B'} + c_v^{B\to B'}) \left(1 + \frac{M_p^2}{m_8^2} \frac{q^2}{M_p^2}\right), \tag{12}$$

i.e. a common slope

$$\lambda^{B\to B'} = \frac{M_p^2}{m_8^2} \tag{13}$$

emerges. However, in this model we have

$$f_1^p(q^2) = \frac{1}{2}\left(f^s(q^2) + f^v(q^2)\right) = 1 + \frac{M_p^2}{m_8^2} \frac{q^2}{M_p^2}, \tag{14}$$

$$f_1^n(q^2) = \frac{1}{2}\left(f^s(q^2) - f^v(q^2)\right) = 0, \tag{15}$$

a result which is in contradiction to the experimental formulas (5) and (6), the the value of M_p^2/m_8^2 being 1.2, if we take $m_8 = 1/2(m_\varrho + m_{K^*})$, and 1.5 if we take $m_8 = m_\varrho \approx m_\omega$. Thus the theoretical model which motivates relation (10) is incompatible with the experimental data used in this relation.

While pointing out this weakness of the method adopted by the Heidelberg group, we are not able to propose a procedure which would be surely more reliable. Just to illustrate the strong dependence of the slopes on the method of calculation, we describe below another way of handling the slopes. Let us denote in the exact SU(3) limit the form factors by $\tilde{f}_1^{B\to B'}(\tilde{q}^2)$. They are then related to the form factors $\tilde{f}^p(\tilde{q}^2)$, $\tilde{f}^n(\tilde{q}^2)$ through the SU(3) relations given in

Table I. Now we write each form factor in the form

$$\tilde{f}_1(\tilde{q}^2) = \tilde{f}_1(0)\left[1+\lambda_1 \frac{\tilde{q}^2}{M_8^2}\right] = \qquad \text{if } \tilde{f}_1(0) \neq 0, \quad (16)$$

$$= \tilde{\lambda}_1 \frac{\tilde{q}^2}{M_8^2}, \qquad \text{if } \tilde{f}_1(0) = 0, \quad (17)$$

$$\tilde{q}^2 = (p_{M_8} - p'_{M_8})^2, \quad (18)$$

Table I

SU (3) relations between the form factors

Decay $B \to B'$	$\tilde{f}_1^{B\to B'}$
$n \to p$	$\cos\theta\,[\tilde{f}_1^p(\tilde{q}^2) - \tilde{f}_1^n(\tilde{q}^2)]$
$\Sigma^+ \to \Lambda$	$\sqrt{\frac{3}{2}}\cos\theta\,\tilde{f}_1^n(\tilde{q}^2)$
$\Sigma^- \to \Lambda$	$-\sqrt{\frac{3}{2}}\cos\theta\,\tilde{f}_1^n(\tilde{q}^2)$
$\Lambda \to p$	$\sqrt{\frac{3}{2}}\sin\theta\,\tilde{f}_1^p(\tilde{q}^2)$
$\Sigma^- \to n$	$\sin\theta\,[\tilde{f}_1^p(\tilde{q}^2) + 2\tilde{f}_1^n(\tilde{q}^2)]$
$\Xi^- \to \Lambda$	$\sqrt{\frac{3}{2}}\sin\theta\,[\tilde{f}_1^p(\tilde{q}^2) + \tilde{f}_1^n(\tilde{q}^2)]$
$\Xi^- \to \Sigma^\circ$	$\sqrt{\frac{1}{2}}\sin\theta\,[\tilde{f}_1^p(\tilde{q}^2) - \tilde{f}_1^n(\tilde{q}^2)]$

where M_8 stands for the SU(3) symmetric mass of the baryon octet. Let us then assume that the SU(3) symmetry breaking may be described by changing only the masses, i.e. that we have

$$\begin{aligned} &\tilde{f}_1(0) \to f_1(0) = \tilde{f}_1(0), \\ &\tilde{\lambda}_1 \to \lambda'_1 = \tilde{\lambda}_1 \\ &M_8 \to 1/2(M + M'), \\ &\tilde{q}^2 \to q^2 = (p_{M'} - p'_{M'})^2, \end{aligned} \quad (19)$$

where the quantities without the tilde stand for the physical values. The slopes λ'_1 are related to the slopes λ_1 used in Eq. (8) by the formula:

$$\lambda'_1 \frac{M_p^2}{\frac{1}{4}\left(M+M'\right)^2} = \lambda_1. \quad (20)$$

The result of this calculation is presented in Table II. We see that now the slopes are far from being equal to each other.

Table II

The slopes $\lambda_1^{B\to B'}$

Decay $B\to B'$	$\lambda_1^{B\to B'}$
$n \to p$	1.0
$\Sigma^+ \to \Lambda$	0.83
$\Sigma^- \to \Lambda$	—0.82
$\Lambda \to p$	1.7
$\Sigma^- \to n$	3.2
$\Xi^- \to \Lambda$	1.8
$\Xi^- \to \Sigma^\circ$	0.56

We do not think that the introduction of the SU(3) breaking through the masses only is a correct procedure. As pointed out to us by RENNER, this method surely fails in the meson decays. Moreover, both methods discussed above extrapolate the experimental formulas (5) and (6), valid in the region $q^2 \leq 0$, to the domain $m_l^2 \leq q^2 \leq (M - M')^2$.

All what has been said about the vector form factors $f_1^{B\to B'}(q^2)$ can be repeated for the weak magnetism form factors $f_2^{B\to B'}(q^2)$. In the evaluation of the slopes of the other four form factors many new difficulties arise, both theoretical and experimental. But as we have told earlier, the considerable theoretical uncertainties in the slopes do not seem to influence the value of the Cabibbo angle very strongly. There are, however, other sources of possible theoretical errors, which may be more important. One of them is connected with the fact that the Wigner–Eckart theorem which gives Eq. (9) may be violated also at the point $q^2 = 0$, because the physical baryon states do not form an exact SU(3) multiplet. Moreover, the hypothesis that in the octet current

$$J^\alpha = c_v V^\alpha_{1-i2} + c_A A^\alpha_{1-i2} + d_v V^\alpha_{4-i5} + d_A A^\alpha_{4-i5}, \tag{21}$$

we have

$$c_V = c_A = \cos\theta \quad d_V = d_A = \sin\theta \tag{22}$$

comes from the well-known universality hypothesis of Gell-Mann. It is possible however that Eq. (21) holds but Eq. (22) does not hold. The expected uncertainties from these sources are of the order of 20%, and indeed such discrepancies have been found between the values of the Cabibbo angle obtained from meson

decays, baryon decays and nuclear β decays. Thus we think that the level of precision of the existing theory is about 20%, and that such an error may be inherent in the fitted mean values of the Cabibbo angles, among others also in the mean value given in Eq. (1).

Note added in proof. While this paper [4] was in press, one of us (A.F.) had the opportunity to meet Dr. I. BENDER, who kindly pointed out that in our paper we worked with a wrong value $\lambda_1^n = 1.05$ of the neutron slope. This error comes from the fact that we took over a misprinted formula (V,1b) of [2]. The correct formula reads

$$\left(\frac{dG_E^n}{dq^2}\right)_{q^2=0} = -(0{,}563 \pm 0{,}001)\, M_p^{-2},$$

and it leads to $\lambda_1^n = -0.085$. Using this small value of the neutron slope, it is easily seen from our Table I, that the breaking procedure defined in Eq. (19) gives small $\lambda_1' = \lambda_1^n$ slopes for the $\Sigma^{\pm} \to \Lambda$ decays and slopes λ_1' which are practically equal to the proton slope $\lambda_1^p = 2.05$ for the other decays. If we now express these slopes λ_1' through the slopes λ_1 defined in Eq. (20) we arrive at the result (in the same order as in Table II)

$$\lambda_1^{B\to B'} = 2{,}1 - 0{,}067 - 0{,}066\ 1{,}7\ 1{,}4\ 1{,}1 \text{ and } 1{,}2.$$

Thus we have for example,

$$f_1^{\Sigma^-\to n}(q^2) = \sin\theta\left[1 + 1{,}4\,\frac{q^2}{M_p^2}\right], \text{ etc.}$$

We still see an appreciable variation in the values of our "non-zero" slopes. Unfortunately, as has been reemphazised recently by M. ROOS [5], the available experimental data are far from being sensitive to SU (3) breaking effects even at $q^2 = 0$. Still less are they sensitive to the breaking in the slopes.

*

The authors are indebted to Prof. H. PIETSCHMANN and Dr. H. STREMNITZER for valuable discussions. One of the authors (A. F.) is indebted to Professors B. RENNER and H. SCHNEIDER for interesting discussions and comments.

REFERENCES

1. H. EBENHÖH, F. EISELE, H. FILTHUTH, W. FÖHLISCH, V. HEPP, E. LEITNER, W. PRESSER, H. SCHNEIDER, T. THOUW and G. ZECH, "A New Fit of the Parameters for Cabibbo's Theory" Preprint of the Institut für Hochenergiephysik der Universität Heidelberg, August 20, 1970.
2. I. BENDER, V. LINKE and H. J. ROTHE, Z. Physik, **212**, 190, 1968.
3. F. EISELE, R. ENGELMANN, H. FILTHUTH, W. FÖHLISCH, V. HEPP, E. LEITNER, W. PRESSER, H. SCHNEIDER and G. ZECH, Z. Physik, **225**, 383, 1969.
4. A. FRENKEL and P. HASENFRATZ, Preprint KFKI—70—23—HEP.
5. M. ROOS, Preprint TH—1349—CERN.

ПРИМЕЧАНИЯ К ОДНОМУ НОВОМУ СПОСОБУ ОПРЕДЕЛЕНИЯ ПАРАМЕТРА КАБИББО

А. ФРЕНКЕЛЬ и П. ГАЗЕНФРАТЦ

Резюме

Рассмотрены некоторые неопределенности, имеющиеся в теории слабых взаимодействий, и их возможное влияние на значение угла Кабиббо. Особое внимание уделяется проблеме q^2-зависимости форм-фактора.

Acta Physica Academiae Scientiarum Hungaricae, Tomus 31 (1—3), pp. 173—191 (1972)

REGULARIZATION OF QUANTUM ELECTRODYNAMICS THROUGH NON-POLYNOMIAL LAGRANGIANS

By

P. BUDINI

INTERNATIONAL CENTRE FOR THEORETICAL PHYSICS, TRIESTE, ITALY

and

G. CALUCCI

INSTITUTE OF THEORETICAL PHYSICS, THE UNIVERSITY, TRIESTE, ITALY

A model for regularizing quantum electrodynamics through a non-polynominal Lagrangian describing the interaction of the electron field with an auxiliary field is given. A gauge invariant Lagrangian density is obtained. This kind of regularization avoids the difficulties connected with indefinite metric. Renormalization of quantum electrodynamics is performed for irreducible diagrams. In the hypothesis that this kind of regularization is the physical basis for the elimination of divergences in quantum electrodynamics, the physical implications are discussed. In particular, the limits of validity of quantum electrodynamics are discussed in terms of the coupling constant between the electron and the regularizing field. It is found that the present limits of validity of quantum electrodynamics imply for this coupling constant an upper limit larger than the weak coupling constant. The possibility of regularization through weak interactions is discussed. In this model, for every reasonable coupling constant, the electromagnetic self-mass of the electron is only a fraction of the total mass.

Introduction

Quantum electrodynamics, after renormalization, constitutes the only example of self-consistent relativistic quantum theory where every physical process can be quantitatively foreseen in principle to any given order of approximation of physical interest. But, despite the success of renormalization, the mere existence of infinities remains something difficult to accept and, because of the divergence of renormalization constants, precludes the understanding of the fundamental constants like charges and masses.

All attempts to obtain a physical regularization of quantum electrodynamics by taking into account the influence of the electromagnetic properties of strongly and weakly interacting particles in quantum electrodynamics were condemned to frustration.

Leaving aside the purely mathematical regularization, obtained by "cutting off" the divergent integrals, which has no pretence of physical interpretation, the most commonly used regularization procedures requested not only the introduction in the theory of new highly massive fields, but also imposed their interaction with the electron and photon fields to be non-physical, i.e. with imaginary charges.

Recent papers [1] on the non-polynomial realization of chiral interaction Lagrangian and on convergence properties [2, 3] of these Lagrangians, when

inserted in a properly defined S matrix theory, have induced us to study a regularization of quantum electrodynamics which might have a better chance than the previous ones of physical interpretation.

We will still need a new field interacting with photons and electrons, but the mechanism of removal of divergences will not be obtained by subtraction, i.e. by postulating an imaginary coupling constant, but by postulating for this field a non-polynomial mode of interaction.

A simplified model will be presented in Paragraph 2, and it will be shown in Paragraph 3 that divergences are removed while all known well-established results of quantum electrodynamics are obtained. For real processes the regularizing field will give corrections to be compared with the form factors of the usual "cut off" techniques, and the limits of validity of quantum electrodynamics will be discussed in Paragraph 5 in terms of the coupling constant of the new field with the electron—photon fields.

At the end of the paper the possible physical interpretations of this interaction will be discussed.

1. The model

We start from the Lagrangian density:

$$\mathscr{L} = \mathscr{L}^0_\gamma + \mathscr{L}^0_\psi + e\,\mathscr{L}^e_\psi + \mathscr{L}^0_\varphi + f\,\mathscr{L}^\varphi_\psi + ef\,\mathscr{L}^{\varphi e}_\psi, \tag{1}$$

where

$$\mathscr{L}^0_\psi = -:\bar{\psi}(\hat{\partial} + m)\,\psi:; \quad \mathscr{L}^0_\gamma = -\frac{1}{2}:\partial_\mu A_\nu\,\partial^\mu A^\nu:,$$

$$\mathscr{L}^e_\psi = -ie:\bar{\psi}\,\hat{A}\,\psi:$$

are the standard electrodynamics Lagrangians, $\mathscr{L}^0_\varphi$ is the free Lagrangian for a scalar (or pseudoscalar) field φ and $\mathscr{L}^\varphi_\psi$ its interaction Lagrangian with the Dirac electron field ψ.

We will assume $\mathscr{L}^q_\psi$ to be a non-polynomial function of φ and of such a form as to imply, by postulating a minimal electromagnetic interaction, the existence of $\mathscr{L}^\varphi_\psi$, i.e. an interaction of the fields φ, ψ and the electromagnetic field.

Our final aim is to obtain, by summing $\mathscr{L}^e_\psi$ with the non-polynomial $\mathscr{L}^{e\varphi}_\psi$ a non-polynomial Lagrangian density

$$L_e = \mathscr{L}^e_\psi + f\,\mathscr{L}^{\varphi e}_\psi \tag{2}$$

of such a form as to regularize quantum electrodynamics for processes with no real φ quantum in the final and initial states.

It is easy to see that a simple choice for $f\mathscr{L}_{\psi}^{\varphi e}$ is then:

$$f\mathscr{L}_{\psi}^{\varphi e} = if\frac{\bar{\psi}\hat{A}\psi}{1+f\varphi^r}\varphi^r . \tag{3}$$

We will take for r the value 2, and Eq. (2) gives:

$$L_e = \frac{-i\bar{\psi}\hat{A}\psi}{1+f\varphi^2} . \tag{4}$$

Eq. (3) with $r = 2$ implies two possible simple forms for $\mathscr{L}_{\psi}^{\varphi}$:

$$\mathscr{L}_{\psi}^{\varphi} = -\frac{1}{2}\frac{\bar{\psi}\gamma_\mu \overleftrightarrow{\partial}_\mu \psi}{1+f\varphi^2}\cdot\varphi^2 \tag{5a}$$

if the field φ is electrically neutral, and also

$$\mathscr{L}_{\psi}^{\varphi} = \frac{1}{2}\frac{\bar{\psi}\gamma_\mu\psi\varphi^*\overleftrightarrow{\partial}_\mu\varphi}{1+f\varphi^2} \tag{5b}$$

if the φ field is charged* (in this case $\varphi^*\varphi$ is meant for φ^2).

With these choices the $\mathscr{L}$ will be de visu gauge invariant.

Finally, the gauge invariant interaction Lagrangian we obtain is:

$$L_I = L_e + f\mathscr{L}_{\psi}^{\varphi}, \tag{6}$$

where L_e is, in the language of SALAM and STRATHDEE [2, 3], supernormal, and will give rise to regularization while $\mathscr{L}_{\psi}^{\varphi}$, given by Eq. (5a) or (5b) is normal (renormalizable) and represents the interaction of the electron field with the regularizing field φ. For $f \to 0$ the fields ψ and φ become disconnected and L_e reduces to the standard interaction Lagrangian of quantum electrodynamics $\mathscr{L}_{\psi}^{e}$ as it should. We will see that in any case, owing to the known experimental limits of validity of quantum electrodynamics, f has to be very small.

The general term of the perturbation expansion of the S matrix constructed from this model will have the form:

$$S_n = \langle F| \int dx_1 \ldots \int dx_n\, T\big((eL_e + f\mathscr{L}_{\psi}^{\varphi})\ldots(eL_e + f\mathscr{L}_{\psi}^{\varphi})_n\big)|\, I\rangle \tag{7}$$

in such a way that for a given power of the electric charge we have a power series expansion in f coming both from the denominators in L_e, summable with

* In this case a Lagrangian density describing the electromagnetic interaction of the φ field has to be added to Eq. (1).

the EFIMOV–FRADKIN–SALAM method, and from the $\mathscr{L}_\varphi^\varphi$ Lagrangian densities. The contributions from the latter terms have two, in a way opposite, features: in general, they are small because of the factor f^m, $m \geq 2$; but they give rise to divergent integrals because $\mathscr{L}_\varphi^\varphi$ is renormalizable but not supernormal, and one should eliminate these divergences by renormalizing the $\mathscr{L}_\varphi^\varphi$ interaction.

For the moment we shall leave them out. The price to pay is that the regularization for some processes is not gauge invariant (to the order f^2) and one has to introduce a photon mass renormalization (finite) to obtain gauge invariant f-independent radiative connections.

It will be shown in Paragraph 4 that if the $\mathscr{L}_\varphi^\varphi$ terms are taken into account, one can obtain to a given power in e a regularized expansion of the S-matrix which can be made gauge invariant up to an arbitrary power of f.

2. Regularization of the primitive divergent matrix elements

In the following we shall assume the initial and final states to be vacuum states for the field. The interaction Lagrangian will be L_e, given by Eq. (4), and the summation of the series expansion in f implied in L_e will be performed with the EFIMOV–FRADKIN method adopting the SALAM [3] convention for the integration in the Symanzik region.

We will start with the

A) Electron self-energy

To lowest order the matrix element is [4]:

$$\Sigma(p) = \frac{ie^2}{(2\pi)^4} \iint \gamma_\mu \frac{i(\hat{p} - \hat{k}) - m}{(p-k)^2 + m^2} \gamma^\mu \frac{1}{(k-q)^2} F(q^2)\, d^4 q d^4 k \tag{8}$$

corresponding to the graph of Fig. 1, where

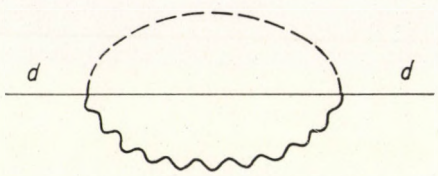

Fig. 1. Self-energy diagram: ——— electron; WWW photon; — — — propagator Eq. (10)

$$F(q) = \delta(q) + \int_{\alpha - i\infty}^{\alpha + i\infty} K(s)(q^2)^{s-2}\, ds\,, \quad 0 < \alpha < 1\,,$$
$$K(s) = \frac{i}{(2\pi)^5} \frac{\pi s/2}{\sin \pi s/2} (-f^2)^{s/2}\, \Gamma(2-s)(4\pi)^{2-2s} \tag{9}$$

represents the Fourier transform of the expectation value:

$$\left\langle T\left(\frac{1}{1+f\varphi^2(x)}\,\frac{1}{1+f\varphi^2(y)}\right)\right\rangle_0 \tag{10}$$

computed according to the method mentioned above.

We refer to the paper of SALAM and STRATHDEE [3] for all problems related to the definition and computation of the propagators (10) and for the discussion of the limits of validity and ambiguities.

It is to be pointed out that for computational reasons the φ field has been taken of zero mass.

It is important to note that for the regularization of quantum electrodynamics, which is our first aim, the computation of $\Sigma(p)$ for p spacelike and its analytic extension of all p-vectors is a valid procedure. We will see later that the known ambiguities of Eq. (9) do not affect the observable radiative corrections but only the values of the renormalization constants.

The integration in d^4q can be performed with the result (see Appendix):

$$\int \frac{F(q)}{(k-q)^2}\,d^4q = \frac{1}{k^2} + \int_{\alpha-i\infty}^{\alpha+i\infty} \Xi(s)(k^2)^{s-1}\,ds = \tilde{D}(k), \tag{11}$$

where $0 < \alpha < 1$ and:

$$\Xi(s) = \frac{i}{4}\,\frac{1}{\sin \pi s/2}\,\Gamma(1-s)(-f^2)^{s/2}(4\pi)^{-2s}.$$

The first term when inserted in Eq. (8) would give back the standard, divergent matrix element. If we now go with the integration in s from the right to the left of the imaginary axis, we have to add the contribution of the pole of the integrand at $s = 0$. This contribution exactly cancels the term $1/k^2$. This cancellation gives rise to the regularization of $\Sigma/(p)$, which in fact becomes:

$$\Sigma(p) = \frac{ie^2}{(2\pi)^4}\int d^4k \int_{\alpha-i\infty}^{\alpha+i\infty} \Xi(s)\,\frac{-2i(\hat{p}-\hat{k})-4m}{(p-k)^2+m^2}\,(k^2)^{s-1}\,ds, \tag{12}$$

where now $-1 < \alpha < 0$.

It is convenient to write:

$$\Sigma(p) = X(p^2)\,i\hat{p} + Y(p^2)\,m \tag{13}$$

so that $4mY = Tr\Sigma$ and $4p^2 X = iTr\hat{p}\,\Sigma$.

The expressions X and Y are convergent for $\alpha < 0$ as can be seen by sight by counting the exponent of k^2.

In Eq. (12) regularization might be considered attained by a modification of the photon propagator $1/k^2$ which is substituted by Eq. (11); in this way, problems with gauge invariance do not arise, provided we modify all the photon propagators in the same way.

The integration of the euclidean space k can be performed exactly (see Appendix) with the result:

$$X(p^2) = \frac{2e^2}{(2\pi)^4} \int_{\alpha-i\infty}^{\alpha+i\infty} \Xi(s) \left[y_1(s, p^2) + y_2(s, p^2) \right] ds, \tag{14'}$$

$$Y(p^2) = \frac{4e^2}{(2\pi^4)} \int_{\alpha-i\infty}^{\alpha+i\infty} \Xi(s)\, y_1(s, p^2)\, ds, \tag{14''}$$

with

$$y_v(s, p^2) = -\frac{1+(v-1)s}{v}\, m^{2s} \frac{\pi^3}{\sin \pi s} F(1-s, -s; v+1; -p^2/m^2).$$

Both Eqs. (14') and (14'') are the convergent integrals for f-finite. Since s has a negative real part, they both diverge for $f \to 0$.

In order to separate from Eqs. (14') and (14'') an f-independent part, it is now convenient to shift the integration again to the right of the imaginary axis. The result is* (see Appendix):

$$Y(p^2) = -\frac{e^2}{(2\pi)^2} \left\{ \gamma + \frac{1}{2} \frac{p^2}{m^2} F(1, 1; 3; -p^2/m^2) + \ln (fm^2/16\pi^2) + i\varphi/2 \right\} + \\ + \frac{4e^2}{(2\pi)^4} \int_{\alpha-i\infty}^{\alpha+i\infty} \Xi(s)\, y_1(s, p^2)\, ds, \tag{15}$$

$$X(p^2) = \frac{1}{2} Y(p^2) + \frac{e^2}{(4\pi)^2} \left\{ 1 + \gamma + \frac{1}{3} \frac{p^2}{m^2} F(1, 1; 4; -p^2/m^2) + \ln(fm^2/16\pi^2) + \right. \\ \left. + i\varphi/2 \right\} - \frac{2e^2}{(2\pi)^4} \int_{\alpha-i\infty}^{\alpha+i\infty} \Xi(s)\, y_2(s, p^2)\, ds. \qquad 0 < \alpha < 1 \tag{16}$$

The logarithmic terms diverge for $f \to 0$ and represent the main part of the mass renormalization constant δm. The f-independent, finite terms will give rise to observable radiative corrections. The term with the integral is convergent and contains a constant factor f^α with $\alpha > 0$. It will then go to 0 with $f \to 0$. It obviously represents the correction to the radiative corrections due to the regularizing field.

* γ is the Euler Mascheroni constant.

One can easily perform the renormalization by subtraction, with the result*:

$$\Sigma_{ren}(p) = i\hat{p}\,X(p^2)+mY(p^2)-m[Y(-m^2)-X(-m^2)]- \\ -(i\hat{p}+m)\{X(-m^2)+2m^2[\dot{Y}(-m^2)-\dot{X}(-m^2)]\}. \tag{17}$$

Here the only f-dependent terms are the integral in s which vanish for $f \to 0$. For $f \neq 0$ they represent the effect of regularization on radiative corrections. The derivative functions multiplying $(i\hat{p} + m)$ contain, as they should, a new (infrared) divergent term for $p^2 \to -m^2$ which is connected with the vanishing photon mass (see Appendix B).

The electron selfmass of electromagnetic origin is given, apart from terms going to zero with f^2, by:

$$\delta m = m\frac{3e^2}{(4\pi)^2}\left[-\gamma-\ln(fm^2/16\pi^2)+\frac{1}{2}-i\varphi/2\right]. \tag{18}$$

The imaginary part comes from the necessity of substituting, in the calculations, $-f^2$ with $e^{i\varphi}f^2$. We have then to take the limit $\varphi \to \pm\,\pi$, and in principle any real average of the limit is acceptable. In Eq. (18) this amounts substituting $i\varphi/2$ with $b\pi$, b being any real constant.

B) The vertex part

In the spirit of considering the present model mainly as a regularization procedure, the simplest recipe for regularizing the vertex part is by defining it in such a way that the Ward identity is satisfied:

$$\frac{\partial\,\Sigma(p)}{\partial\,p_\mu} = i\gamma_\mu L + i\,\Lambda_\mu^{ren}(p,p), \tag{19}$$

where $\Lambda_\mu^{ren}(p, p')$ is the finite vertex part giving rise to vertex radiative corrections. The regularized irreducible vertex implied by Eq. (19) is given by:

$$\Lambda_\mu(p',p) = \frac{ie^2}{(2\pi)^4}\iint \gamma_\nu S_c(p'-k)\,\gamma_\mu S_c(p-k)\,\gamma^\nu D_c(k-q)\,F(q)\,d^4q\,d^4k \tag{20}$$

corresponding to the graph (a) in Fig. 2. In this case, L is given by the coefficient in curly braces of $(i\hat{p} + m)$ in Eq. (17). Taking the model more rigorously as a Lagrangian field theory, one would obtain for the irreducible vertex (in x

* The dot means derivation with respect to p^2.

space) [3]:

$$\Lambda_\mu(x_1, x_2, x_3) = \sum_{n_1 n_2 n_3} (f^2)^{n_1+n_2+n_3} \frac{(n_1+n_2)!}{n_3!} \frac{(n_2+n_3)!}{n_1!} \frac{(n_3+n_1)!}{n_2!} \times \tag{21}$$

$$\times \Delta^{n3}(x_1-x_2)\, \Delta^{n1}(x_2-x_3)\, \Delta^{n2}(x_3-x_1)\, \gamma_\nu S_c(x^3-x_1)\, \gamma_\mu S_c(x_1-x_2)\, \gamma^\nu D_c(x_1-x_3)$$

corresponding to the graph (b) in Fig. 2.

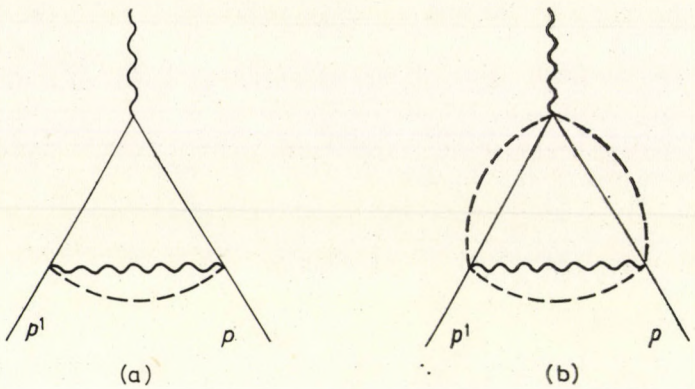

Fig. 2. Vertex diagram

Clearly, the vertex is still regularized and the observable $\Lambda^{ren}(p', p)$ obtained from Eq. (21) will be the same as the one obtained from Eq. (20), while the f-dependent terms corresponding to the corrections to the purely electromagnetic terms $\Lambda^{ren}(p', p)$ due to regularization will be changed. But for small f these terms will in any case be very small, and will not give rise to observable effects.* So that, except for particular purposes, Eq. (20) is to be preferred for its simplicity. The renormalization of Eq. (20) proceeds immediately from the of $\Sigma(p)$ already given.

C) Vacuum polarization

To second order the vacuum polarization is given [1] by:

$$\Pi_{\mu\nu}(k) = \frac{ie^2}{(2\pi)^4} T_r \iint \gamma_\mu \frac{i(\hat{p}-\hat{k})-m}{(p-k)^2+m^2} \gamma_\nu \frac{i(\hat{p}-\hat{q})-m}{(p-q)^2+m^2} F(q^2)\, d^4q\, d^4p\,, \tag{22}$$

where $F(q)$ is given by Eq. (9).

The tensor $\Pi_\mu(k)$ can be split in two parts as usual

$$\Pi_{\mu\nu}(k) = g_{\mu\nu} M(k_2) + [k_\mu k_\nu - k^2 g_{\mu\nu}] N(k^2), \tag{23}$$

* One could obtain Eq. (21), and even a more general form compatible with the Ward identity applied to the self-energy part, if one used the Lagrangian $L_1 = L_e + f\mathcal{L}^{\varphi}_{1}$ in a gauge-invariant way.

where the first term is there because we lost gauge invariance in the process of regularization so that a mass term for the photon is produced. (Fig. 3).

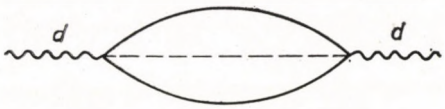

Fig. 3. Vacuum polarization

Owing to the presence of spin 1/2 and mass in both virtual particles, the actual calculations become more involved than in the electron self-energy; in particular, it is much more difficult to produce the final result as a simple integral over the auxiliary variable s.

We can in any case give the following expressions for M and N:

$$M(k^2) = \frac{ie^2}{(2\pi)^4} 4\pi \int \frac{p^3 dp}{p^2+k^2+m^2} \left[\left(2p^2 A(p^2)+4m^2 B(p^2)\right) J_0(k,p) - \right.$$
$$\left. - 2kpA(p^2) J_1(k_1 p)\right], \tag{24}$$

$$N(k^2) = \frac{ie^2}{(2\pi)^4} \frac{32}{3k^2} \int \frac{p^3 dp}{p^2+k^2+m^2} \left[p^2 A(p^2) J_0(k,p) + \right.$$
$$\left. + 3kpA(p^2) J_1(k,p) - 4p^2 A(p^2) J_2(k,p)\right], \tag{25}$$

where

$$J_0 = \frac{\pi}{x^2}\left(1-\sqrt{1-x^2}\right),$$

$$J_1 = \frac{\pi}{x^3}\left(1-\frac{1}{2}x^2-\sqrt{1-x^2}\right), \qquad \text{with} \qquad x = \frac{2kp}{p^2+k^2+m^2},$$

$$J_2 = \frac{\pi}{x^4}\left(1-\frac{1}{2}x^2-\sqrt{1-x^2}\right),$$

and (26)

$$B(p^2) = \int_{\alpha-i\infty}^{\alpha+i\infty} K(s)\, b_1(s,p^2)\, ds\,, \tag{26}$$

$$A(p^2) = \int_{\alpha-i\infty}^{\alpha+i\infty} K(s)\left[b_1(s,p^2)-b_2(s,p^2)\right] ds\,, \tag{27}$$

$$b_v(s,p^2) = y_v(s-1,p^2). \tag{28}$$

Let us consider first the gauge invariant part of $\pi_{\mu\nu}$.

Studying the asymptotic behaviour of J_i when $p^2 \to \infty$ $(x \to 0)$

$$J_0 \sim \frac{\pi}{2}\left(1+\frac{x^2}{4}\right), \qquad J_1 \sim \frac{\pi}{8}x, \quad J_2 = \frac{\pi}{8}\left(1+\frac{x^2}{2}\right) \tag{29}$$

we see that we can perform the integration in p, for $-1 < |\operatorname{Re} s| < 0$ in expression $N(k^2)$.

We are thus in the same situation as for the electron self-energy; we could now, if we had the explicit expression of the integrand, shift the contour of integration in s to right of the origin.

In this case the integration in p is more involved, nevertheless the separation of the f-dependent renormalization term from the f-independent radiative correction can be shown.

We remember the necessity of renormalization that in this case amounts, roughly speaking, to subtracting $N(0)$ from $N(k^2)$:

$$N(k^2)-N(0)=\frac{ie^2}{(2\pi)^4}\frac{32\pi}{3}\int p^3\,dp\left\{\frac{1}{p^2+k^2+m^2}\cdot\frac{1}{k^2}[p^2J_0(k,p)+\right. \tag{30}$$

$$\left.+3kpJ_1(k,p)-4p^2J_2(k,p)]+\frac{1}{p^2+m^2}\left[\frac{\pi}{2}\frac{p^4}{(p^2+m^2)^2}-\frac{3\pi}{4}\frac{p^2}{(p^2+m^2)}\right]\right\}A(p^2)\,.$$

Now we note that the first term in the expansion for $p^2\to\infty$ of the first square bracket is just the second square bracket with a minus sign, which is due to the fact that the expansion of J_i for $k^2\to 0$ is the same as for $p^2\to\infty$; therefore, the term in curly braces goes, effectively, like $1/p^4$.

Going back to the integral representation of A, Eq. (27), we see that (inverting the order of integrations) it is possible to shift the contour to $0<\alpha<1$ keeping still the integral on convergent. So doing we have to take into account the contribution of the pole at $s=0$ which is independent of f and amounts to:

$$\frac{ie^2}{(2\pi)^4}\frac{32\pi}{3}\int p^3\,dp\left\{\frac{1}{p^2+k^2+m^2}\,\frac{1}{k^2}[\,p^2J_0(k,p)+3kpJ_1(k,p)-4p^2J_2(k,p)]+\right.$$

$$\left.+\frac{1}{p^2+m^2}\left[\frac{\pi}{2}\frac{p^4}{(p^2+m^2)^2}-\frac{3\pi}{4}\frac{p^2}{p^2+m^2}\right]\right\}\frac{1}{p^2+m^2} \tag{31}$$

and represents the radiative corrections.

For the renormalization term $N(0)$ the shift cannot be done without losing the convergence in p; when $\operatorname{Res}<0$, it contains a coefficient f raised to a negative power, and diverges when $f\to 0$.

As far as the M term is concerned, we see that the integration in p, $-1<\operatorname{Res}<0$, is diverging. This term should not show up if the full gauge invariant Lagrangian L_{I} is used. In case we wish to regularize M in this non-gauge invariant formulation, the simplest thing to do is to change the regularizing term in the Lagrangian L_e to the form:

$$L_e'=-i\frac{\bar\psi\hat A\psi}{(1+f^{1/2}\varphi)^2}\,. \tag{32}$$

This produces a slightly different $K(s)$:

$$K'(s) = \frac{i}{(2\pi)^5} \cdot \frac{\pi s}{\sin \pi s} (-f)^s (s+1)^2 \Gamma(2-s) (4\pi)^{2-2s},$$

which, however, cause the disappearance of the pole at $s = -1$ in A and B. Thus the contour in s can be shifted between -2 and -1, where the integration in p converges. As we can verify in a model where the integration can be actually done, i.e. when one of the mass of the electron is put to zero, the integration yields a pole at $s = -1$; the residuum of this pole, which is a term in $1/f$, independent of the external momenta, is just the quadratically divergent mass renormalization of the photon which we expect to find in non gauge invariant electrodynamics.

It is easily seen that the other results are very slightly affected by this change of the Lagrangian, which is quite unimportant for what refers to electron self-energy.

We have discussed the regularization of primitive divergent graphs. The regularization and renormalization of higher order processes will proceed from these in the usual way.

3. Gauge invariance

It is obvious that if one constructs the S matrix expansion with the full gauge invariant L_I given by Eq. (6), no problems with gauge invariance will arise; for example, the non-gauge invariant term M in Eq. (23) will not appear; nevertheless, this procedure is cumbersone even for the simplest physical processes.

We will now show through an example that from the full S matrix expansion a manageable gauge invariant subseries can be extracted which will in turn justify the choice of L_e given by Eq. (4) as a regularizing interaction Lagrangian density for small values of f.

Since we wish to discuss gauge invariance together with regularization, we shall first study the most significant case of vacuum polarization to second order. The general matrix term contributing will be:

$$S_n = \langle F \mid \int dx T((eL e + f\mathscr{L}^{\varphi}_{\psi}) \ldots (eL e + f\mathscr{L}^{\varphi}_{\psi}) (f\mathscr{L}^{\varphi}_{\psi}) \ldots (f\mathscr{L}^{\varphi}_{\psi})) \mid I \rangle, \quad (33)$$

where any number of $f\mathscr{L}^{\varphi}_{\varphi}$ can be added.

Let us now split again

$$L_n = -i\bar{\psi}\hat{A}\psi + if\varphi^2 \frac{\bar{\psi}\hat{A}\psi}{1+f\varphi^2} = \mathscr{L}^{e}_{\psi} + f\mathscr{L}^{\varphi e}_{\psi}, \quad (34)$$

and take $\mathscr{L}^{\varphi}_{\varphi}$ given by Eq. (5), and make the convention that while the EFIMOV–SALAM summation is made for the denominators $1 + f\varphi^2$ in the contraction, we take into consideration all terms of Eq. (33) which are proportional to $e^2 f^n$ with $n \leq 2$. That is:

$$S_2 = e^2 \langle F| \int dx T(\mathscr{L}^{e}_{\varphi} \mathscr{L}^{e}_{\varphi} + f^2 \mathscr{L}^{\varphi e}_{\varphi} \mathscr{L}^{\varphi e}_{\varphi} + f^2 \mathscr{L}^{e}_{\varphi} \mathscr{L}^{\varphi}_{\varphi} \mathscr{L}^{\varphi e}_{\varphi} + + f^2 \mathscr{L}^{\varphi}_{\varphi} \mathscr{L}^{\varphi}_{\varphi} \mathscr{L}^{\varphi e}_{\varphi} \mathscr{L}^{\varphi e}_{\varphi}) |I\rangle . \tag{35}$$

This will give a gauge invariant vacuum polarization matrix element of the form:

$$\Pi = e^2 [\Pi_0 + f^2(\Pi_1 + \Pi_2 + \Pi_3 + \Pi_4)] \tag{36}$$

corresponding to the graphs in Fig. 4 where the dotted line represents the propagator Eq. (9), without the δ term. It is clear that $\Pi_0 + f^2\Pi_1$ is identical with the regularized non gauge invariant vacuum polarization of the last paragraph; Π_2 is also regularized; Π_3 and Π_4 instead are divergent.

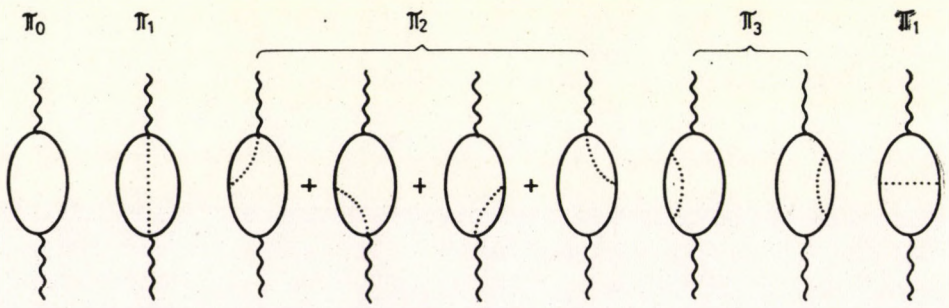

Fig. 4. Gauge-invariant vacuum polarization. The dotted line represents the Green function (9) without the δ term

The divergences of π_3 and π_4 which are due to the interaction of the electron with the φ field are to be removed by renormalization. These divergences are not any more to be considered divergences of pure electrodynamics.

Once the renormalization has been done, one can continue the procedure of regularization introducing two other factors $(L^{\varphi e}_{\varphi} + \mathscr{L}^{\varphi}_{\varphi})$. In this way the previous graphs become convergent and we introduce other ones, requiring renormalization, which have an f^4 in front. The procedure can be continued producing terms with higher and higher powers of f. If we stop the procedure at a certain order f^{2n}, we have a set renormalizable and regularized graphs, for which gauge invariance holds up to terms in f^{2n+2}.

4. Physical interpretation

In quantum electrodynamics regularization with indefinite metric is usually regarded as a device to introduce mathematical rigour in the renormalization procedures of subtraction of divergent integrals. Consequently, physical consequences are only deduced in the limit of infinite regularizing masses.

If, as in our model, regularization might have a physically plausible origin, then one is tempted to analyse which are its implications on the observables of the corresponding theory.

The first obvious consideration is that if the photon propagator is modified as implied by Eq. (11), then also real processes where it appears as a factor in the matrix amplitude should be correspondingly modified. The simplest example is Möller scattering which is represented by the graph in Fig. 5.*

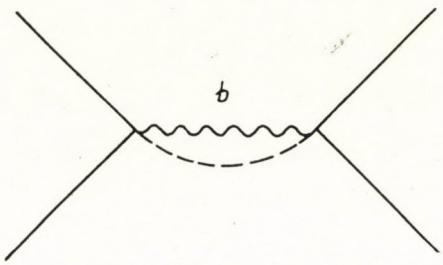

Fig. 5. Möller scattering

The modification of the amplitude amounts to substitute the photon propagator $1/k^2$ with Eq. (11). For high spacelike values the propagator behaves like $-2(4\pi)^4/f^2k^6$.

In a study of the limits of validity of quantum electrodynamics in which the photon propagator was multiplied with the factor $\Lambda^2/(k^2 + \Lambda^2)$, the experimental data on electron–electron scattering (FARLEY [5]) give a lower limit for Λ:

$$\Lambda_{\min} > 4M\,, \tag{37}$$

where M is the nucleon mass.**

The corresponding upper limit for f is:

$$f < \frac{(4\pi)^2}{\sqrt{2}\Lambda^2} \approx \frac{7}{M^2}\,. \tag{38}$$

* For other processes like electron–positron annihilation one should modify the electron propagator and vertices with both Lagrangian L_e and L_φ in order to preserve gauge invariance.

** Since the behaviour is k^{-6} the modified propagator is assumed to have the form $\Lambda^4/k^2(\Lambda^2 + k^2)^2$.

If we insert this value of f in the electron self-mass implied by the model given by Eq. (18), we obtain an upper limit for the electromagnetic mass:

$$\frac{\delta_m}{m} > 3 \cdot 10^{-2} . \tag{39}$$

In Fig. 6 we have plotted $\delta m/m$ as a function of $f M^2$. It is seen that if f is equal to the weak coupling constant

$$f \cong \frac{1{,}01}{\sqrt{2}} 10^{-2} M^{-2}$$

we still obtain a $\delta m/m \sim 5.5 \cdot 10^{-2}$.

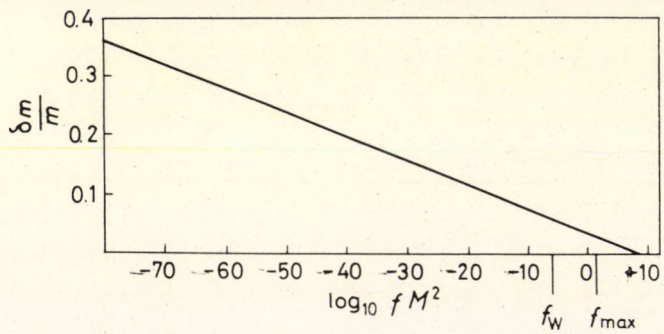

Fig. 6. Electromagnetic self-energy as a function of the coupling constant. $f_{\max}$ corresponds to the present limit of validity of electrodynamics; f_W is the Fermi coupling constant

The present lower limit of f coming from the experimental test on quantum electrodynamics is then compatible with f being of the order of the weak coupling constant.

One is tempted then to search for a possible weak interaction capable of giving rise to a physical regularization of quantum electrodynamics.

One of the simplest possibilities would be an electron—pion interaction of the type:*

$$-\frac{G}{\sqrt{2}} \bar{\psi} \gamma_\mu (1+\gamma_5) \psi J^{(3)\mu}, \tag{40}$$

which is the $\Delta Q = 0$ counterpart of the one responsible for the $\pi^+ \to \pi^0 + + e + \nu$ decay, with $J_\mu^{(3)}$ representing the isospin current density in non-

* An even conceptually simpler possibility would be to take for φ a spinor field and identify it with the electron itself. But in this case difficulties of computational and statistical character are encountered.

polynomial form; in our model it should have the form:

$$J_{\mu}^{(3)} = \frac{\varphi^* \partial_\mu \varphi - (\partial_\mu \varphi^*)\varphi}{1 + \frac{G}{\sqrt{2}} \boldsymbol{\varphi} \cdot \boldsymbol{\varphi}} . \tag{41}$$

It is easy to see that if (40) exists, it would be difficult to observe, because it is competitive with the electron—pion interaction through photon and ϱ, ω, φ. Further, the corresponding non-conservation of parity would only be quadratic in the weak coupling constant in purely electrodynamical processes. The electromagnetic correction due to the emission and absorption of photons from the charged φ field would also be difficult to observe, because they are ruled by the Lagrangian $ef\mathscr{L}_{\varphi}^{\varphi e}$.

From Fig. 6 it is seen that in order to get $\delta m/m \simeq 1$, that is to have a wholly electromagnetic origin of the electron mass, one would need $f \sim 10^{-250}\,\mathrm{M}^{-2}$, that is an interaction much weaker than every known one.

The conclusion is that if the described model corresponds to physical reality, as a consequence, the electromagnetic electron mass is at the most only a fraction of the total.

5. Conclusion

It has been shown, through a particular example, that in principle the non-linear nature of polynomial Lagrangians is adequate to furnish a mathematical tool for regularizing quantum electrodynamics. The ambiguities connected with non-polynomial field theory do not seem to affect at all the observable radiative correction, only the renormalization constants; and these ambiguities are certainly not more disturbing than the ones connected with indefinite metric in the commonly used regularization procedures, while the computation apparatus allows a clear insight in the regularization mechanism and in the renormalization procedures.

One is then brought to think that this might be the basis for a physical elimination of divergences in quantum electrodynamics.

The basic physical hypothesis is the existence of an interaction Lagrangian density which could be of the type $J\mu\, J^{\mu}$ where the first current is the electron one and the second a non-polynomial one. Since the present experimental upper limit for the coupling constant for the regularizing field with the electron is certainly larger then the coupling constant of the weak interactions, then this interaction could be a candidate for the regularizing field. In the moment one accepts the hypothesis of a physical basis for the regularization, the renormalization constants acquire a physical meaning. The underlying interaction gives the cut for purely electromagnetic effects. In particular, if the interaction

were the weak one, the electromagnetic self-mass of the electron would only be a fraction of the total, but even if the regularizing field had a much lower coupling with the electron, a purely electromagnetic origin of the electron mass seems unlikely.

While this work was on the way of being completed, we learned of a research based on an idea of A. SALAM who proposes gravitational field as a regulator for renormalizable theories. We take pleasure in thanking A. SALAM and his co-workers for communicating us their results before publication, and for interesting discussions.

Appendix

A) — Here some integrals occurring in the calculations are considered, and it is shown how they reduce to a definite type of the double integral.

Let us consider the integrals coming from Eqs. (12), (14). They are:

$$y_1(s, p^2) = 4\pi \iint \frac{1}{p^2+q^2+m^2-2pq\cos\alpha} (q^2)^{s-1} q^3 \, dq \sin^2\alpha \, d\alpha ,$$

$$y_2(s, p^2) = 4\pi \iint \frac{pq\cos\alpha}{p^2+q^2+m^2-2pq\cos\alpha} (q^2)^{s-1} q^3 \, dq \sin^2\alpha \, d\alpha$$

with the substitution $q^2 = p^2x$, $p^2 + m^2 = p^2\nu$ they become:

$$\begin{aligned} y_1(s,p^2) &= 2\pi p^{2s} \, I_0(s, \nu), \\ y_2(s,p^2) &= 2\pi p^{2s} \, I_1(s, \nu). \end{aligned} \tag{A.1}$$

The integral found in Eq. (11) is of the same type y_1 with $m = 0$, i.e. $\nu = 1$. So we have essentially to calculate the integrals

$$I_m(\varrho, \nu) = \int_0^\infty dx \int_0^\pi \sin^2\alpha \, d\alpha \, \frac{x^{\varrho+m/2}}{x+\nu} \frac{(\cos\alpha)^m}{1-\dfrac{2\sqrt{x}}{x+\nu}\cos\alpha} \tag{A.2}$$

for $m = 1,2$ and we start considering them for $\nu > 1$.

In this situation we can expand the integrand in power and integrate term by term

$$I_m(\varrho, \nu) = \Sigma_n 2^n \int_0^\infty x^{\varrho+m/2+n/2}(x+\nu)^{-1-n} \, dx \int_0^\pi [(\cos\alpha)^{m+n} - (\cos\alpha)^{m+n+2}] \, d\alpha, \tag{A.3}$$

where the sum is constrained by the condition $m + n =$ even [6]. Now simply

expanding the binomial factor, we recognize the form of an hypergeometric series and we obtain:

$$I_m(\varrho, \nu) = \Sigma_n 2^n \nu^{\varrho+m/2-n/2} (-)^{n+1} \frac{\pi}{\sin \pi \left(\varrho + \frac{m+n}{2}\right)} \binom{\varrho+(m+n)/2}{n} \pi \frac{(m+n-1)!!}{(m+n+2)!!},$$

$$I_0(\varrho, \nu) = -\frac{1}{2} \nu^{\varrho} \frac{\pi^2}{\sin \pi\varrho} F(\varrho+1, -\varrho; 2; 1/\nu) =$$

$$= -\frac{1}{2} (\nu-1)^{\varrho} \frac{\pi^2}{\sin \pi\varrho} F(1-\varrho, -\varrho; 2; 1/(1-\nu)), \tag{A.4}$$

$$I_1(\varrho, \nu) = -\frac{1}{4} (\varrho+1) \nu^{\varrho} \frac{\pi^2}{\sin \pi\varrho} F(\varrho+2, -\varrho; 3; 1/\nu) =$$

$$= -\frac{1}{4} (\varrho+1)(\nu-1)^{\varrho} \frac{\pi^2}{\sin \pi\varrho} F(1-\varrho, -\varrho; 3; 1/(1-\nu)).$$

Another formula which we shall use in an expansion of the hypergeometric function with respect to parameters, needed in Eqs. (15) and (16), is the following:

$$F(1-\varrho, -\varrho; l; z) \sim 1 - \frac{\varrho}{l} z F(1, 1; \varrho+1; z) \tag{A.5}$$

$$\text{for } \varrho \to 0$$

This can easily be obtained from the series representation.

B) — Infrared divergence. In order to compute Eq. (17), we need $\dot{X}(p^2)$ and $\dot{Y}(p^2)$. We have:

$$\dot{Y}(p^2) = -\frac{e^2}{(2\pi)^2} \left\{ \frac{1}{2m^2} \left[F(1, 1; 3; -p^2/m^2) - \frac{1}{3} \frac{p^2}{m^2} F(2, 2; 4; -p^2/m^2) \right] \right\} +$$

$$+ \frac{4e^2}{(2\pi)^4} \int \Xi(s) \dot{y}_1(s, p^2) \, ds,$$

$$\dot{X}(p^2) = -\frac{e^2}{(2\pi)^2} \left\{ \frac{1}{3m^2} \left[F(1, 1; 4; -p^2/m^2) - \frac{1}{4} \frac{p^2}{m^2} F(2, 2; 5; -p^2/m^2) \right] \right\} +$$

$$+ \frac{4e^2}{(2\pi)^4} \int \Xi(s) \dot{y}_2(s, p^2) \, ds + \frac{1}{2} \dot{Y}(p^2).$$

Since

$$F(2,2; 4; z) = -\frac{6}{z^3} [2z + (2-z) \ln (1-z)],$$

we see that a term in $\dot{Y}$ (and therefore also in $\dot{X}$) diverges logarithmically when $p^2 \to -m^2$, independently of the value of f. This is the usual infrared divergence and can be eliminated in the usual way in real processes [4].

C) — We wish here to give explicitly the integration of expression (11) and discuss then a bit further the scattering process.

The integration is made by summing all the polar contributions on the positive real axis, with the result:

$$\widetilde{D}(k^2) = \frac{1}{k^2} + \frac{f}{(4\pi)^2} e^{i\varphi/2}\left[-\frac{\pi}{2}\cos x - \sin x \ln x + a(x)\right], \tag{C.1}$$

where

$$x = \xi\, e^{i\varphi/2} = \frac{f}{(4\pi)^2} k^2 e^{i\varphi/2},$$

and

$$a(x) = \Sigma_n \frac{(-)^n x^{2n+1}}{(2n+1)!} \psi(2n+2).$$

$a(x)$ is an entire, odd function of x, real for x real, which can be expressed in terms of the exponential integral.

As previously done, we have also here to take the mean in the limit $\varphi \to \pm\pi$, obtaining

$$\widetilde{D}(k^2) = \frac{1}{k^2} + \frac{f}{(4\pi)^2}\left\{\sinh\xi\,(\gamma + \ln\xi) + \frac{1}{2}[e^{-\xi} E_{in}(-\xi) - e^{\xi} E_{in}(\xi)] + \pi b e^{-\xi}\right\}$$

$$E_{in}(\xi) = \int_0^{\xi} (1 - e^{-t})\, dt/t. \tag{C.2}$$

Using now the asymptotic expansion of the exponential integral we can see the behaviour of $\widetilde{D}(k^2)$ in some limiting cases:

For $k^2 \to +\infty$ (spacelike)

$$\widetilde{D}(k^2) \sim -2\frac{(4\pi)^2}{f^2}\frac{1}{k^6}$$

as previously seen.

For $k^2 \to -\infty$ (timelike)

$$\widetilde{D}(k^2) \sim \frac{f}{(4\pi)^2}\{b e^{-\xi} + i\pi \sinh(-\xi)\}$$

showing therefore a positive imaginary part which grows exponentially, and a real part, also exponentially growing, but with undetermined coefficient. It is reasonable to foresee that in case of non-zero mass φ field the imaginary part will arise only after a finite threshold.

Finally, when $k^2 \to 0$, we have:

$$\tilde{D}(k^2) \sim \frac{1}{k^2} + \pi b \frac{f}{(4\pi)^2} .$$

REFERENCES

1. F. GÜRSEY, Nuovo Cimento, **16,** 230, 1960; S. WEINBERG, Phys. Rev. Letters, **18,** 188, 1967 J. SCHWINGER, Phys. Letters, **24B,** 473, 1967; F. GÜRSEY and N. CHANG, Phys. Rev., **164,** 1752, 1967; S. WEINBERG, Phys. Rev., **166,** 1568, 1968.
2. S. OKUBO, Progr. Theor. Phys., **11,** 80, 1954; G. V. EFIMOV, Sov. Phys. JEPT, **17,** 1417, 1963; G. V. EFIMOV, Nuovo Cimento, **32,** 1046, 1964; G. V. EFIMOV, Nucl. Phys., **74,** 657, 1965; E. S. FRADKIN, Nucl. Phys., **49,** 624, 1963; B. W. LEE and B. ZUMINO, CERN Preprint, TH 1053; 1969; M. K. VOLKOV, Ann. Phys. (NY), **49,** 202, 1968; R. DELBOURGO, Lettere al Nuovo Cimento **2,** 354, 1969; A. SALAM and J. STRATHDEE, ICTP Preprint, IC/69/17.
3. A. SALAM and J. STRATHDEE, ICTP Preprint, IC/69/120.
4. J. M. JAUCH and F. ROHRLICH, The Theory of Photons and Electrons, Addison Wesley Pub. Co., Reading, Mass., USA, 1955.
5. F. J. M. FARLEY, Rivista del Nuovo Cimento Vol. I, 59 1969.
6. I. S. GRADSHTEYN and I. M. RYZHIK, Tables of Integrals, Series and Products, Academic Press, New York and London, 1965.

РЕГУЛЯРИЗАЦИЯ КВАНТОВОЙ ЭЛЕКТРОДИНАМИКИ С ПОМОЩЬЮ НЕПОЛИНОМИАЛЬНЫХ ЛАГРАНЖИАНОВ

П. БУДИНИ и Г. КАЛУЧЧИ

Резюме

Предложена модель для регуляризации квантовой электродинамики с помощью неполиномиальных лагранжианов, описывающих взаимодействие электронного поля с вспомогательным полем. Получена лагранжева плотность, удовлетворяющая условию калибровочной инвариантности. При регуляризации такого рода избегаются трудности, связанные с неопределенностью метрики. Выполнена перенормировка квантовой электродинамики для несократимых диаграмм. Предполагая, что такого рода регуляризация является физической основой для устранения расходимостей в квантовой электродинамике, обсуждаются вытекающие из неё физические следствия. В частности, исследованы границы применимости квантовой электродинамики в терминах коэффициента связи между электроном и регуляризующим полем. Установлено, что эти границы применимости квантовой электродинамики включают в себя для упомянутого коэффициента связи такой верхний предел, который больше, чем коэффициент слабой связи. Обсуждается возможность регуляризации через слабые взаимодействия. В этой модели собственная электромагнитная масса электрона при любых разумных значениях коэффициента связи составляет только часть полной массы.

Acta Physica Academiae Scientiarum Hungaricae, Tomus 31 (1—3), pp. 193—213 (1972,

SYMMETRY OF LEPTONS

By

S. NAKAMURA*

MAX PLANCK INSTITUTE FOR PHYSICS AND ASTROPHYSICS, MUNICH, GFR

and

S. SATO

DEPARTMENT OF PHYSICS, RIKKYO UNIVERSITY, TOKYO, JAPAN

By assuming that (ν_e, e^-) and (μ^+, ν_μ) belong to the spinor representations $\vartheta_{1/2,\,0}$ and $\vartheta_{0,\,1/2}$ of the rotation group of SU(2)×SU(2), the selection rules for isospin τ and hypercharge spin ζ are formulated for the pure leptonic processes. As a result, self-current processes such as

$$\nu_e(\tilde{\nu}_e) + e^- \to \nu_e(\tilde{\nu}_e) + e^-$$

belong to the allowed transition, while μ — e exchange processes such as

$$\mu^\pm \to e^\pm + \nu_e(\tilde{\nu}_e) + \nu_\mu(\tilde{\nu}_\mu)$$

belong to the forbidden transition.

Leptonic bosons are introduced which are responsible for the mediation of the pure leptonic processes, and their masses and coupling constants are inferred:

$$M_L \cong 130 \text{ BeV} \sim 200 \text{ BeV},$$

$$\frac{G_L^2}{4\pi} \cong 1 \cdot 10^{-1},$$

$$\frac{F_L^2}{4\pi} \cong 1 \cdot 10^{-3}.$$

1. Classification of lepton multiplets

We are still far from the ultimate understanding of the questions: What are leptons? And how do they interact with each other on the one hand and with hadrons on the other? More specifically one may ask:

I) Why do leptons exist in addition to baryons?

II) Why do the muon μ and mu-neutrino ν_μ appear as the brothers of the electron e and the el-neutrino ν_e?

III) Why are the masses of ν_e and ν_μ both vanishingly small?

When a scheme of baryon–lepton symmetry was introduced by SAKATA [1] and TAKETANI [2], emphasis was laid on a unified understanding of leptons and baryons. According to their authors, any scheme for baryons which cannot also provide a reasonable scheme for leptons should be rejected. For instance,

* On leave of absence from the University of Tokyo and Nihon University, Tokyo, Japan.

the SU(3) scheme was successful in classifying eight or nine hadrons, but seems to be unsatisfactory for the classification of the four types of leptons [3]. In fact, the inevitability of the existence of two kinds of the subgroup SU(2) (muon family and electron family) is not proved by the SU(3) scheme [4].

In previous articles, the present authors [5–6] have classified leptons and baryons on the basis of the composite particle model and $SU(2) \times SU(2)$ symmetry. First we decomposed the wave functions of leptons and baryons into two parts: one, which we call the "L" part for leptons and the "F" part for baryons, describes the motion in the Minkowski space and has the lepton number $n(L)$ (L part) or the baryon number $n(F)$ (F part). The other, which we now call the "ladon part", describes the behaviour in the charge space.

To describe the "ladon" part, we introduced two kinds of fundamental spinors t and s (together with their antiparticles t^* and s^*); t is the wave function for isospin τ whose version was first introduced by HEISENBERG [8]:

$$t = \begin{pmatrix} \alpha \\ \beta \end{pmatrix}, \tag{1.1}$$

$$\begin{aligned} \tau_3 \alpha &= +\frac{1}{2}\alpha, \\ \tau_3 \beta &= -\frac{1}{2}\beta, \end{aligned} \tag{1.2}$$

where τ_3 is the third component of the isospin vector $\vec{\tau}$. On the other hand, s is the wave function for hypercharge spin $\vec{\zeta}$.

$$s = \begin{pmatrix} \xi \\ \eta \end{pmatrix}, \tag{1.3}$$

$$\begin{aligned} \zeta_3 \xi &= +\frac{1}{2}\xi, \\ \zeta_3 \eta &= -\frac{1}{2}\eta. \end{aligned} \tag{1.4}$$

The third component ζ_3 of the hypercharge spin vector $\vec{\zeta}$ is defined by the GELL-MANN–NISHIJIMA–NAKANO formula [7]:

$$Q = \tau_3 + \zeta_3, \tag{1.5}$$

$$\zeta_3 = \frac{Y}{2}. \tag{1.6}$$

(Y is hypercharge)

As is well known, two independent spins τ and ζ can be accommodated in a sheme of the four-dimensional rotation group, and we have the relation:

$$\tau_1 = \frac{1}{2}(T_{23}+T_{01}), \qquad 1, 2, 3, \text{ cyclic.}$$

$$\zeta_1 = \frac{1}{2}(T_{23}-T_{01}), \tag{1.7}$$

where $T_{\mu\nu}$, $(\mu, \nu = 1, 2, 3, 0)$ are generators of rotations in the $\mu\nu$ plane. Under reflection in this charge space of $SU(2)\times SU(2)$,

$$\tau_i \to \zeta_i, \qquad \zeta_i \to \tau_i, \qquad i = 1, 2, 3 \tag{1.8}$$

and

$$t \to s, \quad s \to t. \tag{1.9}$$

In other words, t and s belong to an irreducible representation in the four-dimensional space including reflections, and correspond to $\vartheta_{1/2,0}$ and $\vartheta_{0,1/2}$, which transform into each other under reflections. Let us assume that the "ladon part" of $\begin{pmatrix}\nu_e\\ e^-\end{pmatrix}$ is described by $t = \begin{pmatrix}\alpha\\ \beta\end{pmatrix}$ and that of $\begin{pmatrix}\mu^+\\ \nu_\mu\end{pmatrix}$ by $s = \begin{pmatrix}\xi\\ \eta\end{pmatrix}$. We define the charge of leptons by the following relation:

$$Q = \tau_3 + \zeta_3 + h, \tag{1.10}$$

where

$$h = +1/2 \text{ for the muon family,}$$
$$= -1/2 \text{ for the electron family.}$$

The quantum numbers of leptons thus introduced are given in Table I.

For the interactions involving leptons, we require

$$\Delta h = 0, \tag{1.11}$$

which unifies the separate conservation laws of muon number and of electron number. If we put

$$h = 0, \text{ for baryons,} \tag{1.12}$$

the relation (1.10) includes the GELL-MANN–NISHIJIMA–NAKANO formula (1.5) for hadrons. Moreover, for the "L" part we require the conservation law of lepton number

$$\Delta n(L) = 0, \tag{1.13}$$

where

	L	L^*
$n(L)$	$+1$	-1.

Table I

Quantum numbers of leptons and leptonic bosons

	Representation	τ_3	ζ_3	h	Q	l
μ^+	$\vartheta_{0,\,1/2}$	0	+1/2	+1/2	+1	+1
ν_μ		0	−1/2	+1/2	0	+1
ν_e	$\vartheta_{1/2,\,0}$	+1/2	0	−1/2	0	+1
e^-		−1/2	0	−1/2	−1	+1
U^+	$\vartheta_{1,\,0}$	+1	0	0	+1	0
U^0		0	0	0	0	0
U^-		−1	0	0	−1	0
V^+	$\vartheta_{0,\,1}$	0	+1	0	+1	0
V^0		0	0	0	0	0
V^-		0	−1	0	−1	0
W^0	$\vartheta_{0,\,0}$	0	0	0	0	0

l: lepton number, Q: charge
h: helicity (muon number and electron number)

We used here the KONOPINSKI—UHLENBECK—KAWAKAMI scheme [23] where $\mu^+(\mu^-)$ and e^- (e^+) are particles (antiparticles).

We have tacitly assumed that ν_e and ν_μ can be described by the four-component Dirac spinors for making multiplets in SU(2)×SU(2) in combination with e^- and μ^+, respectively. Preliminarily experimental upper limits of $m\nu_e$ and $m\nu_\mu$ are given as follows:

$$m\nu_e < 60 \text{ eV}, \ (90\% \text{ confidence}),$$

(K. E. BERGKVIST, Top. Conf. Weak Interactions, CERN, 1969; L. M. LANGER and R. J. D. MOFFAT, Phys. Rev., **88**, 689, 1952, H. DANIEL, Rev. Mod. Phys., **40**, 659, 1968.

$$m\nu_\mu < 700 \text{ KeV}, \ (90\% \text{ confidence}).$$

G. BACKENSTOSS, S. CHARALMBUS, H. DANIEL, H. KOCH, CH. V. D. MALSBURG, G. POVEL, H. SCHMITT, and L. TASCHER).
(The present authors are indebted to Professor H. DANIEL for this information before publication.)

The values of $m\nu_e$ and $m\nu_\mu$ as well as the selection rules have an important bearing on the cosmological effects [24] of the reactions involving ν_e and ν_μ.

Many of the recent measurements on the energy spectra of β-rays in the allowed transitions and in the forbidden transitions show the non-vanishing Fierz term (b) besides the linear term (a) which is given by the weak magnetism:

$$C(w) = a\,w + b/w,$$

(C/W) is a correction factor for the shape of β-rays in addition to the regular terms).

If we believe in the non-vanishing value of b, we need not necessarily abandon the two-component character for ν_e. (D. BERÉNYI, Acta Physica Hungarica, **22**, 25, 1967; see also H. DANIEL, Rev. Modern Phys., **40**, 659, 1968.)

In this way, we realize that the existence of two kinds of leptons, the muon family and the electron family, is indispensable in order to give the irreducible representation of the $SU(2) \times SU(2)$ including the reflections, and that these two families will transform into each other by the reflections in the charge space. This seems to be one of the most attractive features of the $SU(2) \times SU(2)$ scheme, which affords us a more natural classification of leptons than does the SU(3) scheme.

With regard to the possible interactions of leptons, we have two clues: the mass spectra of leptons and the weak interactions of leptons. Before entering these analyses, let us first consider the selection rules for the leptonic processes in terms of the quantum numbers and the composite particle model introduced above.

2. Selection rules of the leptonic processes

To date we know of leptonic processes of the following three kinds:

I) leptonic processes of hadrons,
II) weak processes among leptons,
III) electromagnetic processes of leptons.

In the universal theory of the current—current model of weak interactions, the hadron currents in the non-leptonic weak interactions, the hadron currents and the lepton currents in the leptonic interactions of hadrons, and the lepton currents in the pure leptonic weak interactions have been dealt with on an equal footing, by considering the analogy with electromagnetic currents. Also, their interactions are meant to couple with the same coupling constants, after allowance has been made for the weak angles θ. We have, however, taken the different view-point that these four currents mentioned above should be treated separately because their behaviours with regard to the selection rules are quite diverse. For instance, we suggested that the leptonic processes of hadrons are mediated by strong mesons, such as ϱ, A_1; K*, K_c, by assuming weak interactions of the strong mesons with the lepton currents, *but the pure leptonic processes should be mediated in terms of the "leptonic bosons"* which are entirely different from the strong mesons.

In the present model we see that the leptonic boson should have the structure:

$$(L^* \cdot L) \times (\text{ladon part}).$$

The ladon part is made up of any of the t^*t, s^*s, t^*s and s^*t combinations, while the strong mesons are made up of

$$(F^* \cdot F) \times (\text{ladon part}).$$

In other words, the structures in the "ladon" part may not be the same; they differ from each other in their Minkowski parts, (L^*L) for the leptonic boson and (F^*F) for the strong meson. As a result, we have good reason to suppose that the interactions of the strong mesons with the lepton currents and the interactions of leptonic bosons with the hadron currents can *never* be ascribed to the strong interaction category. However, we may introduce the interactions of the leptonic bosons with the lepton currents in the category of the strong interactions, by choosing suitable selection rules (see Fig. 1) in the charge space.

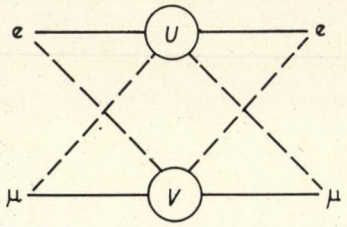

Fig. 1. Selection rules ——— allowed transition $\Delta\tau = 0$, $\Delta\zeta = 0$. G_L; - - - - - forbidden transition $\Delta\tau_3 = \pm 1$, $\Delta\zeta_3 = \mp 1$, F_L

It must be noted that the selection rules for the forbidden transitions as well as those for the allowed transitions differ from each other only in terms of the quantum numbers, τ and ζ, but both obey the conservation of the muon number and lepton number, which is denoted by the selection rule:

$$\Delta h = 0, \quad h = -1/2 : (\nu_e, e^-), \quad h = +1/2 : (\mu^+, \nu_\mu).$$

The possible existence of strong interactions among leptons has been conjectured in view of the large mass difference between muon and electron, the possible deviations of the magnetic moments of the muon and the electron from the QED [9] values, and the anomalies of the high energy muons in cosmic rays [10].

Now let us formulate the selection rules in the charge space for the leptonic processes. For the strong interactions among leptons we may introduce charge independence and hypercharge independence by taking an analogy with the strong interactions among hadrons

$$\Delta\tau = 0, \tag{2.1}$$

$$\Delta\zeta = 0. \tag{2.2}$$

Among pure leptonic processes, we can easily classify the allowed and forbidden transitions by considering the conservation laws of τ, ζ and h.

Allowed transitions:

$$
\begin{array}{lccccccl}
 & e^- + \nu_e(\tilde{\nu}_e) & & \to e & + \nu_e(\tilde{\nu}_e) & & & \\
\tau_3 & -\frac{1}{2} & +\frac{1}{2} & \left(-\frac{1}{2}\right) & -\frac{1}{2} & +\frac{1}{2} & \left(-\frac{1}{2}\right), & \Delta\tau_3 = 0, \\
\zeta_3 & 0 & 0 & (0) & 0 & 0 & (0), & \Delta\zeta_3 = 0, \\
h & +\frac{1}{2} & +\frac{1}{2} & \left(-\frac{1}{2}\right) & +\frac{1}{2} & +\frac{1}{2} & \left(-\frac{1}{2}\right), & \Delta h = 0,
\end{array}
\tag{2.3}
$$

$$
\begin{array}{lccccccl}
 & \mu^- + \nu_\mu(\tilde{\nu}_\mu) & & \to \mu^- & + \nu_\mu(\tilde{\nu}_\mu) & & & \\
\tau_3 & 0 & 0 & (0) & 0 & 0 & (0), & \Delta\tau_3 = 0, \\
\zeta_3 & -\frac{1}{2} & -\frac{1}{2} & \left(+\frac{1}{2}\right) & -\frac{1}{2} & -\frac{1}{2} & \left(+\frac{1}{2}\right), & \Delta\zeta_3 = 0, \\
h & -\frac{1}{2} & +\frac{1}{2} & \left(-\frac{1}{2}\right) & -\frac{1}{2} & +\frac{1}{2} & \left(+\frac{1}{2}\right), & \Delta h = 0,
\end{array}
\tag{2.4}
$$

$$e^- + \nu_\mu(\tilde{\nu}_\mu) \to e^- + \nu_\mu(\tilde{\nu}_\mu), \tag{2.3'}$$

$$\mu^- + \nu_e(\tilde{\nu}_e) \to \mu^- + \nu_e(\tilde{\nu}_e). \tag{2.4'}$$

Also (2.3′) and (2.4′) which are derived from the neutral currents obey the allowed selection rules. Forbidden transitions:

$$
\begin{array}{lcccccl}
 & \mu^+ \to \nu_\mu & & + e^+ & + \nu_e, & & \\
\tau_3 & 0 & 0 & +\frac{1}{2} & +\frac{1}{2}, & & \Delta\tau_3 = +1, \\
\zeta_3 & +\frac{1}{2} & -\frac{1}{2} & 0 & 0, & & \Delta\zeta_3 = -1, \\
h & +\frac{1}{2} & +\frac{1}{2} & +\frac{1}{2} & -\frac{1}{2}, & & \Delta h = 0.
\end{array}
\tag{2.5}
$$

It is obvious that the charge exchange processes from muon to electron and vice versa belong to the forbidden transitions. The selection rules for the forbidden transition are inferred as follows:

$$\Delta\tau_3 = \pm 1, \tag{2.6}$$

$$\Delta\zeta_3 = \pm 1, \tag{2.6}$$

$$\Delta h = 0, \tag{2.7}$$

while with regard to the allowed transitions we can show the conservation law of τ_3, ζ_3 and h.

$$\Delta\tau_3 = 0,$$
$$\Delta\zeta_3 = 0, \tag{2.8}$$
$$\Delta h = 0. \tag{2.7}$$

We are not sure whether the law of charge independence (2.1) and that of hypercharge independence (2.2) hold or not, as far as these transitions are concerned. With (2.7) we can exclude the neutrino-flip process.

The allowed transitions mentioned here are related to the neutral current processes or the self current processes. However, no concrete evidence has been presented to require the suppression of these processes in the framework of the pure leptonic processes. The suppression of the neutral currents is required in the leptonic weak processes of hadrons such as $\nu_\mu + \mathrm{p} \to \nu_\mu + \mathrm{p}$, $\mathrm{K} \to \pi + + \mathrm{e}^+ + \mathrm{e}^-$ and $\mathrm{K} \to \pi + \nu + \tilde{\nu}$.

3. Leptonic bosons

Let us introduce the leptonic bosons which couple with the lepton currents by the Yukawa type interactions. We may use the leptonic bosons of the following types in the charge space of SU(2)×SU(2):

$$\vartheta_{1,0} : U(U^+, U^0, U^-),$$
$$\vartheta_{0,1} : V(V^+, V^0, V^-).$$

We assume between the leptonic bosons (U, V) and the lepton currents Yukawa type interactions, which obey the allowed selection rules (2.1)–(2.2):

$$H_G = G_U(\overline{\nu_\mathrm{e}\,\mathrm{e}^-})\, O_\lambda^e \begin{pmatrix} U^0 & \sqrt{2}\,U^+ \\ \sqrt{2}\,U^- & -U^0 \end{pmatrix} \begin{pmatrix} \nu_\mathrm{e} \\ \mathrm{e}^- \end{pmatrix} + \\ + G_V(\overline{\mu^+\nu_\mu})\, O_\lambda^\mu \begin{pmatrix} V^0 & \sqrt{2}\,V^+ \\ \sqrt{2}\,V^- & -V^0 \end{pmatrix} \begin{pmatrix} \mu^+ \\ \nu_\mu \end{pmatrix} + \mathrm{h.c.} \tag{3.1}$$

Here G_U and G_V are the coupling constants of the allowed transitions. If we put

$$G_U = G_V \equiv G_L, \tag{3.2}$$

we can prove the invariance of the Hamiltonian H_G under the reflections in the τ — ζ charge space of SU(2)×SU(2) which leads to μ—e symmetry. O_λ^U and O_λ^V represent the Dirac operators in the Minkowski space. Since we take the KONOPINSKI–MAHMOUD–KAWAKAMI scheme, we have to assume

$$O_\lambda^U = \gamma_\lambda(1+\gamma_5),$$
$$O_\lambda^V = \gamma_\lambda(1-\gamma_5). \tag{3.3}$$

Strictly speaking, the assumption (3.4) breaks the reflection invariance in the $\tau - \zeta$ space.

(In the present discussion we omitted the leptonic bosons $\vartheta_{1/2,\ 1/2}$ and $\vartheta_{0,0}$ for the sake of simplicity. The boson $\vartheta_{0,0}$ which we call W^0 is useful for (2.3′) and (2.4′). see (3.9).)

The interactions between the leptonic bosons (U and V) and the lepton currents in the forbidden transitions obeying the selection rules (2.6) may be formulated as follows:

$$H_F = F_V(\overline{\nu_e e^-})\, O_\lambda^e \begin{pmatrix} V_\lambda^0 & \sqrt{2}\ V_\lambda^+ \\ \sqrt{2}\, V_\lambda^- & -V_\lambda^0 \end{pmatrix} \begin{pmatrix} \nu_e \\ e^- \end{pmatrix} + \\ + F_U(\overline{\mu^+ \nu_\mu})\, O_\lambda^\mu \begin{pmatrix} U_\lambda^0 & \sqrt{2}\ U_\lambda^+ \\ \sqrt{2}\, U_\lambda^- & -U_\lambda^0 \end{pmatrix} \begin{pmatrix} \mu^+ \\ \nu_\mu \end{pmatrix} + \text{h.c.} \tag{3.4}$$

Again we put

$$F_U = F_V \equiv F_L \tag{3.5}$$

for the sake of the μ—e symmetry.

For μ — e decay, we can make use of the allowed transitions (3.1) for one vertex, and of the forbidden transition (3.4) for the other vertex:

$$\mu^+ \to \nu_\mu + U^+, \qquad F_U$$
$$U^+ \to \tilde{e}^+ + \nu_e, \qquad G_U \tag{3.6}$$

$$\mu^+ \to \nu_\mu + V^+, \qquad G_V$$
$$V^+ \to \tilde{e}^+ + \nu_e, \qquad F_V \tag{3.7}$$

For $e^- + \nu_e(\tilde{\nu}_e) \to e^- + \nu_e(\tilde{\nu}_e)$, we can make use of the allowed transitions for both vertices:

$$e^- \to e^- + U^0, \qquad G_U$$
$$U^0 + \nu_e(\tilde{\nu}_e) \to \nu_e(\tilde{\nu}_e), \qquad G_U \tag{3.8}$$

$$e^- \to e^- + W^0, \qquad G_W$$
$$W^0 + \nu_\mu(\tilde{\nu}_\mu) \to \nu_\mu(\tilde{\nu}_\mu) \qquad G_W \tag{3.9}$$

From (3.6)–(3.7) we obtain the rate of μ — e decay which can be compared with experiment. Thus we have:

$$\frac{G_L F_L}{M_L^2} = \frac{g_\beta}{\sqrt{2}}, \tag{3.10}$$

where $M_L(M_P)$ is the mass of the leptonic boson (proton), and g_β is the Fermi coupling constant for the β-decay of the neutron.

$$g_\beta = \frac{1.0 \cdot 10^{-5}}{M_p^2} \,. \tag{3.11}$$

GELL-MANN, GOLDBERGER, KROLL and LOW [11] have proposed possible deviations from the universal theory of the leptonic weak interactions in order to solve the divergence difficulties inherent in the leptonic weak processes at small distances. They proposed that the diagonal processes such as (2.3)–(2.4) might be described by a coupling constant larger than that for the non-diagonal process such as (2.5). A number of developments [12] followed which afford the tests of their proposal. Experimentally, the tests would be quite difficult in the case of the antineutrino $\tilde{\nu}_e$ produced as a reactor fission product, be-

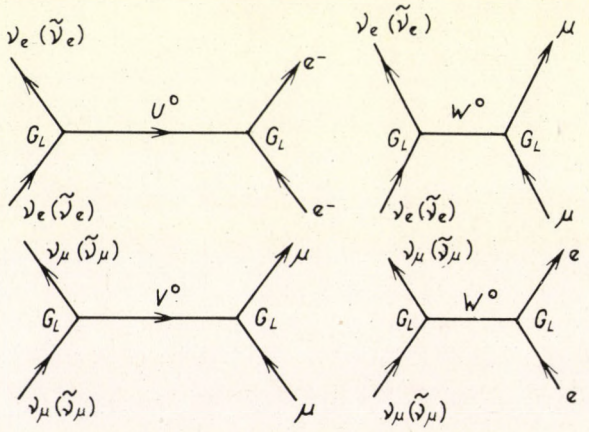

Fig. 2. The neutral current processes

cause contamination by γ-quanta might be considerable. The preliminary result [13] reported favours the prediction; the enhancement in the diagonal process $\tilde{\nu}_e + e^- \to \tilde{\nu}_e + e^-$ compared to that in the non-diagonal processes amounted to as much as a factor of 10 in the effective Fermi coupling constants, G_{ND} and g_β:

$$G_D \approx 10\, G_{ND} = 10\, g_\beta^* . \tag{3.12}$$

This result seems also to agree with our prediction that the process $\tilde{\nu}_e + + e^- \to \tilde{\nu}_e + e^-$ is described by the coupling constant G_L^2, while the process

* The latest report by REINES gives the ratio by a suppressed factor of $<4g_\beta$, XVth International Conference on High Energy Physics, Kiev, 1970, see [13].

$\mu \to e + \nu_e + \nu_\mu$ is described by the coupling constant $G_L F_L$. If we put

$$G_L = 10\ F_L, \tag{3.13}$$

we are able to account for the data reported by REINES et al.

In order to evaluate the magnitude of the coupling constant G_L, let us assume the following relation:

$$G_L^2 : g_s^2 \cong m_0 : M_0\,, \tag{3.14}$$

where $m_0(M_0)$ are the bare mass of leptons (baryons). g_s denotes the coupling constant of the strong interactions of baryons. For the sake of comparison, we take

$$\frac{g_s^2}{4\pi} \cong \frac{g_{\varrho\,\mathrm{NN}}^2}{4\pi} \approx 2\,, \tag{3.15}$$

because we assume that the spin of the leptonic bosons now considered is 1. Further, by assuming

$$\begin{aligned} m_0 &\cong \quad 50\ \mathrm{MeV}, \\ M_0 &\cong 1{,}000\ \mathrm{MeV}, \end{aligned} \tag{3.16}$$

we obtain from the relation (3.14):

$$\frac{G_L^2}{4\pi} \cong 10^{-1}. \tag{3.17}$$

By comparing with relation (3.13) we now have:

$$\frac{F_L^2}{4\pi} \cong 10^{-3}. \tag{3.18}$$

By inserting (3.17) and (3.18) into (3.11) we obtain

$$M_L \cong 130\ \mathrm{BeV}. \tag{3.19}$$

In recent astronomical developments [14], the effects of the various kinds of neutrino reactions have been studied. However, we cannot admit their conclusions as evidence in the present discussion, because the astronomical investigations depend essentially on the models used.

4. Discussion

We have come to the conclusion that leptonic bosons have the meso-strong interactions given by (3.18). This conclusion is apparently in contradiction to the current opinion that leptons have no strong interaction other than the electromagnetic one.

We share partly the current opinion that the interactions between leptons and hadrons should be described by the weak interaction. But we find that no experiment has confirmed the rejection of strong interactions among pure leptonic processes. The point-like structure of lepton currents can be understood by the assumption that leptonic bosons have the large mass given by (3.24).

Along this line of thought, we assume that leptonic bosons interact weakly with the baryon currents,

$$\frac{f_L^2}{4\pi} \lesssim 10^{-13} \tag{4.1}$$

by taking an analogy with the weak interactions between strong mesons and the lepton currents:

$$\frac{f_\pi^2}{4\pi} \simeq 10^{-15}/m_\pi^2\,, \qquad (\pi^\pm \to l^\pm + \nu_e)\,, \tag{4.2}$$

$$\frac{f_\varrho^2}{4\pi} \simeq 10^{-13}\,, \qquad (\varrho^\pm \to l^\pm + \nu_e)\,. \tag{4.3}$$

We do not share the current opinion that the weak boson interacts with the fermion current universally and with the semi-weak coupling constants

$$\frac{f_W^2}{4\pi} \simeq 10^{-7}\,, \tag{4.4}$$

since there is no experimental evidence in favour of such an assumption.

We now have to check the results of the present scheme with experiment.

Since we assume that either the interaction between the strong mesons and the lepton currents, or that between leptonic mesons and the baryon currents are weak, the processes relating hadrons and leptons would not be essentially modified. For instance, the leptonic decays of π, K, ϱ . . . receive no big contribution from the leptonic boson channels in view of the weak coupling given by (4.1) [21].

One of the interesting effects of the present scheme will be found in the

production of leptonic bosons by neutrino impact on protons [21]. In the current version of the weak boson, we expect the following reaction:

$$\begin{array}{l} \nu_\mu + \mathrm{p} \to W^+ + \mu^- + \mathrm{p} \xrightarrow{\text{Coulomb}} \mu^- + \mathrm{p} \\ \qquad\qquad\quad \dashrightarrow \mu^+ + \tilde{\nu}_\mu \\ \qquad\qquad\quad \dashrightarrow \mathrm{e}^+ + \nu_\mathrm{e} \end{array} \tag{4.5}$$

In this case the branching ratio of $W^+ \to \mu^- + \tilde{\nu}_\mu$ to $W^+ \to \mathrm{e}^+ + \nu_\mathrm{e}$ will be governed by the μ — e symmetry. But in the leptonic boson channel, we expect:

$$\begin{array}{l} \nu_\mu + \mathrm{p} \xrightarrow{G_L} V^+ + \mu^- + \mathrm{p} \xrightarrow{\text{Coulomb}} \mu^- + \mathrm{p} \\ \qquad\qquad\quad \dashrightarrow \mu^+ + \tilde{\nu}_\mu, (G_L) \\ \qquad\qquad\quad \dashrightarrow \tilde{\mathrm{e}}^+ + \nu_\mathrm{e}, (F_L) \end{array} \tag{4.6}$$

$$\begin{array}{l} \nu_\mu + \mathrm{p} \xrightarrow{F_L} U^+ + \mu^- + \mathrm{p} \xrightarrow{\text{Coulomb}} \mu^+ + \mathrm{p} \\ \qquad\qquad\quad \dashrightarrow \mu^+ + \tilde{\nu}_\mu, (F_U) \\ \qquad\qquad\quad \dashrightarrow \mathrm{e}^+ + \nu_\mathrm{e}, (G_U). \end{array} \tag{4.7}$$

As a result, we are led to expect the violation of the μ — e symmetry, in one case:

$$\frac{\Gamma(\mathrm{e})}{\Gamma(\mu)} = \left(\frac{F_L}{G_L}\right)^2 k \tag{4.8}$$

and in the other case:

$$\frac{\Gamma(\mathrm{e})}{\Gamma(\mu)} = \left(\frac{G_L}{F_L}\right)^2 k, \tag{4.9}$$

where k, the phase factor ratio, is given by:

$$\begin{aligned} k &= \frac{(1-\Theta_\mathrm{e}^2)^2\,(1+\Theta_\mathrm{e}^2)}{(1+\Theta_\mathrm{e}^2)^2\,(1+\Theta_\mu^2)}\,, \\ \Theta_\mathrm{e} &= \frac{m_\mathrm{e}}{M_L}\,, \qquad \Theta_\mu = \frac{m_\mu}{M_L}\,. \end{aligned} \tag{4.10}$$

The production cross section itself would not be modified drastically, because in the threshold region it is determined essentially by the factor

$$\left(\frac{G_L}{M_L}\right)^2 \quad \text{or} \quad \left(\frac{F_L}{M_L}\right). \tag{4.11}$$

and in the higher energy region, the unknown form factor for the leptonic boson vertex should work to suppress the rapid increase of the cross section.

Actually, it may be the case that both of the leptonic bosons, U and V, exist and contribute to the μ — e decay. We would then expect the simultaneous occurrence of the two processes, (4.6) in F_L and (4.7) in G_L, which again proves the μ — e asymmetry.

In that case, from the considerations leading to (3.19) we have

$$M_U = M_V \cong 200 \text{ BeV}. \tag{3.19a}$$

We have introduced the neutral leptonic bosons, U^0 and V^0, in addition to the charged bosons, $U^{\pm}$ and $V^{\pm}$, thereby enabling us to establish the strong interactions among leptons, symmetric in the charge space of SU(2)×SU(2). If we take the values of mass and coupling constant according to (3.18) and (3.19) for the leptonic bosons, we are led to expect the production of U^0 and V^0 in high-energy leptonic reactions in the cosmic rays, together with their subsequent decays into lepton pairs and also into γ-rays.

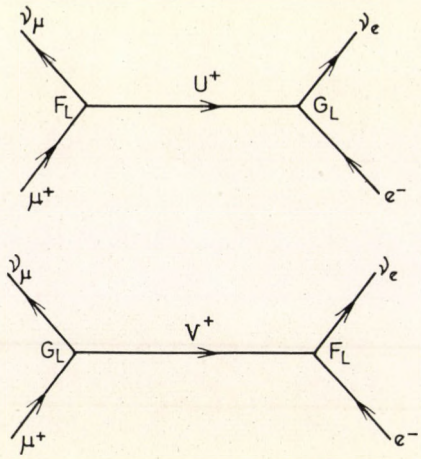

Fig. 3. μ—e decay through the leptonic bosons

$$\frac{U : \vartheta_{1,0}, \quad V : \vartheta_{0,1}, \quad W : \vartheta_{0,0}}{(\nu_e, e^-) : \vartheta_{1/2,0}, \quad (\mu^+, \nu_\mu) : \vartheta_{0,1/2}}$$

It is interesting to note that in terms of the U^0 and V^0 channels the breakdown of the μ — e symmetry is expected in the high-energy inelastic reactions of muon and electron by proton, while in terms of the W^0 channel, the breakdown of the μ — e symmetry is not expected. This will be easily seen by compar-

ing the following reactions with each other:

$$\begin{aligned}
&\mu^- + \mathrm{p} \xrightarrow{G_L} \mu^- + \mathrm{p} + V^0 \\
&\qquad\qquad\qquad\qquad \begin{cases} \xrightarrow{G_L} \mu^+ + \mu^- \\ \xrightarrow[G_L]{} \mathrm{e}^+ + \mathrm{e}^- \end{cases} \\
&\mu^- + \mathrm{p} \xrightarrow{F_L} \mu^- + \mathrm{p} + U^0 \\
&\qquad\qquad\qquad\qquad \begin{cases} \xrightarrow{G_L} \mathrm{e}^+ + \mathrm{e}^- \\ \xrightarrow[F_L]{} \mu^+ + \mu^- \end{cases} \\
&\mathrm{e}^- + \mathrm{p} \xrightarrow{G_L} \mathrm{e}^- + \mathrm{p} + U^0 \\
&\qquad\qquad\qquad\qquad \begin{cases} \xrightarrow{G_L} \mathrm{e}^+ + \mathrm{e}^- \\ \xrightarrow{F_L} \mu^+ + \mu^-, \end{cases} \\
&\mathrm{e}^- + \mathrm{p} \xrightarrow{F_L} \mathrm{e}^- + \mathrm{p} + V^0 \\
&\qquad\qquad\qquad\qquad \begin{cases} \xrightarrow{G_L} \mu^+ + \mu^- \\ \xrightarrow{F_L} \mathrm{e}^+ + \mathrm{e}^-. \end{cases}
\end{aligned} \tag{4.12}$$

As a result, we are led to predict the dominant processes:

$$\begin{aligned}
&\mu^- + \mathrm{p} \to \mu^- + \mathrm{p} + \mu^+ + \mu^-, \\
&\mathrm{e}^- + \mathrm{p} \to \mathrm{e}^- + \mathrm{p} + \mathrm{e}^+ + \mathrm{e}^-,
\end{aligned} \tag{4.13}$$

and the suppressed processes:

$$\begin{aligned}
&\mu^- + \mathrm{p} \to \mu^- + \mathrm{p} + \mathrm{e}^+ + \mathrm{e}^-, \\
&\mathrm{e}^- + \mathrm{p} \to \mathrm{e}^- + \mathrm{p} + \mu^+ + \mu^-.
\end{aligned} \tag{4.14}$$

In cosmic rays hard showers consisting of hard muons, including no electrons, have been reported. Although a plausible explanation has been given to account for the mechanism of hard muon showers, the present scheme leading to the μ — e asymmetry may also afford a way of explanation.

We also expect contributions from the neutral leptonic boson channels to the collision processes of leptons:

$$\begin{aligned}
&\mathrm{e}^- + \mathrm{e}^- \to \mathrm{e}^- + \mathrm{e}^-,\ \mu^\pm + \mu^\pm \to \mu^\pm + \mu^\pm, \\
&\mu^+ + \mathrm{e}^- \to \mu^+ + \mathrm{e}^-.
\end{aligned} \tag{4.15}$$

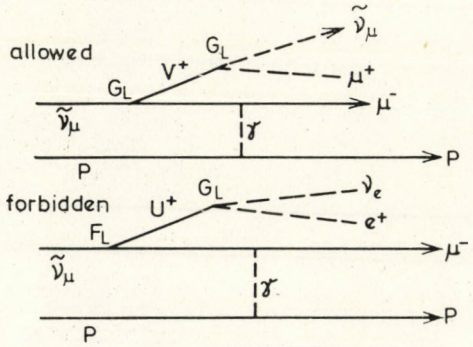

Fig. 4.(a) The predicted inelastic neutrino processes ($\tilde{\nu}_\mu$ comes from $\pi^+ \to \mu^+ + \tilde{\nu}_\mu$ in the KONOPINSKI–UHLENBECK scheme)

dominant processes:

$$\tilde{\nu}_\mu + \mathrm{p} \to \mu^- + \mathrm{p} + V^+ \to \mu^- + \mathrm{p} + \mu^+ + \tilde{\nu}_\mu,$$
$$\nu_\mu + \mathrm{p} \to \mu^+ + \mathrm{p} + V^- \to \mu^+ + \mathrm{p} + \mu^- + \nu_\mu,$$

suppressed processes (by a factor of $(F_L/G_L)^2 \sim 1/100$):

$$\tilde{\nu}_\mu + \mathrm{p} \to \mu^- + \mathrm{p} + U^+ \to \mu^- + \mathrm{p} + \mathrm{e}^+ + \nu_\mathrm{e},$$
$$\nu_\mu + \mathrm{p} \to \mu^+ + \mathrm{p} + V^- \to \mu^+ + \mathrm{p} + \mathrm{e}^- + \tilde{\nu}_\mathrm{e}.$$

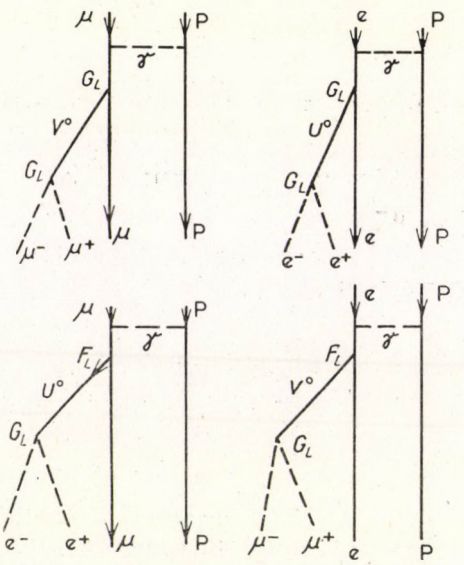

Fig. 4.(b). The predicted inelastic muon (electron) processes

dominant processes: $\mu + \mathrm{p} \to \mu + \mathrm{p} + V^0 \to \mu + \mathrm{p} + \mu^- + \mu^+,$
$\mathrm{e} + \mathrm{p} \to \mathrm{e} + \mathrm{p} + U^0 \to \mathrm{e} + \mathrm{p} + \mathrm{e}^- + \mathrm{e}^+,$

suppressed processes (by a factor of $(F_L/G_L)^2 \sim 10^{-2}$?):

$$\mu + \mathrm{p} \to \mu + \mathrm{p} + U^0 \to \mu + \mathrm{p} + \mathrm{e}^- + \mathrm{e}^+,$$
$$\mathrm{e} + \mathrm{p} \to \mathrm{e} + \mathrm{p} + V^0 \to \mathrm{e} + \mathrm{p} + \mu^- + \mu^+.$$

It is expected that the cross sections of the processes mediated by leptonic boson interactions would exceed those mediated by electromagnetic interactions by a factor of $G_L^2/e^2 \simeq 30$, when the mass of the leptonic bosons can be taken negligible compared with the four-momentum transfer in these processes.

Further, we are led to predict the following resonance reactions for the collisions of pairs of leptons:

$$\begin{aligned} e^+ + e^- &\to U^0 \to e^+ + e^-, \\ \mu^+ + \mu^- &\to V^0 \to \mu^+ + \mu^-. \end{aligned} \tag{4.16}$$

All these leptonic processes need more than 1000 BeV (in the laboratory system) for the energy of the incident leptons, and their direct observation would not be easy except in cosmic rays, where the anomalous events of muon components and photon components have been reported, such as the deviation of the sec Θ-dependence, although not confirmed [19—21].

In contrast to ordinary weak bosons, we assumed (meso)-strong interactions only between leptons and the leptonic bosons. As a result, we are led to expect shorter life-times for leptonic bosons than for ordinary weak bosons. We have

$$\frac{1}{\tau_L} \cong \frac{G_L^2}{4\pi} \frac{M_L c^2}{\pi} .$$

By inserting $M_L \sim 100$ BeV, $G_L^2/4\pi \sim 2 \cdot 10^{-1}$ we obtain

$$\tau_L \cong 3 \cdot 10^{-26} \text{ sec.} \tag{4.17}$$

The decay schemes may be any of the following modes:

$$\begin{aligned} &U^{\pm} \to e^{\pm} + \nu_e(\tilde{\nu}_e), \quad V^{\pm} \to \mu^{\pm} + \tilde{\nu}_\mu(\nu_\mu), \\ &U^0 \to e^+ + e^-, \ \nu_e + \tilde{\nu}_e, \quad V^0 \to \mu^+ + \mu^-, \ \nu_\mu + \tilde{\nu}_\mu . \end{aligned} \tag{4.18}$$

If the coupling constants for the interactions of leptonic bosons are as large as $G_L^2/4\pi \sim 10^{-1}$, significant contributions to the magnetic moments of the muon and electron would be expected. According to recent experiments, the deviation of these magnetic moments from the Q.E.D. values is [15, 16]:

$$\delta\mu_m \leq 5 \cdot 10^{-7}, \tag{4.19}$$

$$\delta\mu_e \leq 2 \cdot 10^{-9}. \tag{4.20}$$

From the leptonic boson channel, the contributions to the magnetic moments

can be determined [15–18]:

$$|\delta\mu_m| \cong \frac{G_L^2}{4\pi}\,\frac{1}{2\pi}\left(\frac{m_\mu}{M_L}\right)^2 \cong 2\cdot 10^{-8}, \tag{4.21}$$

$$|\delta\mu_e| \cong \frac{G_L^2}{4\pi}\,\frac{1}{2\pi}\left(\frac{m_e}{M_L}\right)^2 \cong 5\cdot 10^{-13}. \tag{4.22}$$

It is obvious that the values given by (4.21) and (4.22) do not interfere with the experimental upper limits (4.19) and (4.20). More elaborate investigations, both theoretical and experimental, are desirable to find trace of the leptonic bosons. The current version on leptons, i.e. that leptons have no strong interaction among each other and that the form factor for the pure leptonic vertex is of point-like nature, may be valid only within the scope of the present stage of the experimental techniques. If the available energy increases by an order of magnitude, or if the precision of the present observation becomes more elaborate by an order of magnitude, the unexpected version will be opened.

One of the authors (S. N.) wishes to thank Professor W. HEISENBERG for kind discussions about this work. He has greatly benefited from the warmest hospitality shown to him by Professor W. HEISENBERG and Professor H. P. DÜRR. In the course of valuable discussions the authors have obtained very much useful information from Professor H. DANIEL on beta-rays and the muon physics, from Dr. N. SCHMITZ, Dr. I. DERADO. Dr. K. BUCHNER and Dr. P. SCHLAMP on the high energy experiments, and from Professor S. HAYAKAWA, Professor T. KITAMURA, and Dr. WADA on cosmic rays. The authors are also grateful to Dr. A. BREGMAN for his careful work in reading the manuscript.

Appendix

In the text, we have introduced the symmetric interactions and the symmetry breaking interactions between leptonic bosons and leptons. The former is taken to be rotational invariant in the four-dimensional charge space of $SU(2)\times SU(2)$.

The latter is assumed to be axial symmetric in the same space. In view of the experimental evidence we are forced to assume that the coupling constants for all of these leptonic interactions (symmetric and symmetry breaking) are in the category of meso-strong interactions.

We shall now formulate *i)* the interactions between the hadron currents and the leptonic bosons and *ii)* those between the lepton currents and the strong mesons. We are led, by comparison with the observations, to conclude that these interactions are of the weak category with the coupling constant $f^2/4\pi \sim 10^{-13} \sim 10^{-15}$. We assumed that the weak interactions of hadrons in the non-leptonic modes are symmetric in the three-dimensional charge space of O(3):

$$\Delta\varkappa = 0. \tag{A.1}$$

Here

$$\vec{\varkappa} = \vec{\tau} + \vec{\zeta}. \tag{A.2}$$

plays the role of a generator. This assumption led to the $\Delta I = 1/2$ rule. On the other hand, we know that neutral currents are to be suppressed in the case of the leptonic weak interactions of hadrons. This forces us to assume that the interaction Hamiltonian is *axial symmetric* in the three-dimensional charge space of $\varkappa$:

$$\Delta\varkappa \neq 0, \quad \Delta\varkappa_{\pm} = 0, \qquad \varkappa_{\pm} = (\varkappa_1 \pm i\varkappa_2)/2, \tag{A.3}$$

where

$$\varkappa_1 = \begin{pmatrix} 0 & 0 & 0 \\ 0 & 0 & -i \\ 0 & i & 0 \end{pmatrix}, \quad \varkappa_2 = \begin{pmatrix} 0 & 0 & i \\ 0 & 0 & 0 \\ -i & 0 & 0 \end{pmatrix}, \quad \varkappa_3 = \begin{pmatrix} 0 & -i & 0 \\ i & 0 & 0 \\ 0 & 0 & 0 \end{pmatrix}. \tag{A.4}$$

For instance, we formulate the weak interactions of pions and kaons with leptons which obey the selection rule (A.3):

$$\begin{aligned} H_S^W = {} & f_\pi^e (\bar{\nu}_e O_\lambda^e e^- \cdot \partial_\lambda \pi^+ + \bar{e}^- O_\lambda^e \nu_e \cdot \partial_\lambda \pi^-) + \\ & + f_\pi^M (\bar{\mu}^+ O_\lambda^\mu \nu_\mu \cdot \partial_\lambda \pi^+ + \nu_\mu O_\lambda^\mu \mu^+ \cdot \partial_\lambda \pi^-) + \\ & + f_\varkappa^e (\bar{\nu}_e O_\lambda^e e^- \cdot \partial_\lambda K^+ + \bar{e}^- O_\lambda^e \nu_\mu \cdot \partial_\lambda K^-) + \\ & + f_\varkappa^\mu (\bar{\mu}^+ O_\lambda^\mu \nu_\mu \cdot \partial_\lambda K^+ + \bar{\nu}_\mu O_\lambda^\mu \mu^+ \cdot \partial_\lambda K^-) + \text{h.c.} \end{aligned} \tag{A.5}$$

where

$$O_\lambda^e = \gamma_\lambda(1+\gamma_5), \quad O_\lambda^\mu = \gamma_\lambda(1-\gamma_5).$$

And, in accordance with the empirical facts of the μ — e symmetry, we put

$$f_\pi^e = f_\pi^\mu, \tag{A.6}$$

$$f_K^e = f_K^\mu. \tag{A.7}$$

In the three-dimensional charge space of $\varkappa$, hadron multiplets are reorganized into triplets and singlets:

$$\begin{aligned} K &: \frac{-K^- + K^+}{\sqrt{2}}, \quad \frac{-K^- - +K}{i\sqrt{2}}, \quad \frac{\bar{K}^0 - \bar{K}^0}{\sqrt{2}}, \\ k_0 &: \frac{\bar{K}^0 + K^0}{\sqrt{2}} \\ \pi &: \frac{\pi^- + \pi^+}{\sqrt{2}} \quad \frac{\pi^- - \pi^+}{i\sqrt{2}}, \pi^0, \quad \eta : i\eta \end{aligned} \tag{A.8}$$

$$R: \frac{\Xi^- - p}{\sqrt{2}}, \quad \frac{\Xi^- - p}{i\sqrt{2}}, \quad \frac{\Xi^0 - N}{\sqrt{2}},$$
$$R_0: i\frac{\Xi^0 + N}{\sqrt{2}}, \tag{A.9}$$
$$\Sigma: \frac{\Sigma^- + \Sigma^+}{\sqrt{2}}, \quad \frac{\Sigma^- - \Sigma^+}{i\sqrt{2}}, \quad \Sigma^0 \ \Lambda: i\Lambda.$$

It is interesting to note that the forbidden selection rule (2.6) can be derived from the conservation law of a $\vec{\varkappa}$ vector, which is just applied to the weak hadronic interactions in the non-leptonic mode: (A.1) and (A.2). When we operate $\varkappa_i$ on the lepton multiplets, t and s, we have to use the two-dimensional representation:

$$\varkappa_1 = \begin{pmatrix} 0 & 1 \\ 1 & 0 \end{pmatrix}, \quad \varkappa_2 = \begin{pmatrix} 0 & -i \\ i & 0 \end{pmatrix}, \quad \varkappa_3 = \begin{pmatrix} 1 & 0 \\ 0 & -1 \end{pmatrix} \tag{A.10}$$

instead of the three-dimensional representation (A.4). We thus introduce a 0(3) space in which $\varkappa_i$ plays the role of generator of rotation. In this $\varkappa$ space. both spinors, t and s, correspond to $\vartheta_{1/2}$, and the leptonic bosons, U and V, to ϑ_1; as a result, the interaction Hamiltonian of the forbidden transition (3.4) is formulated:

$$H = F_u t^* \varkappa_i t \varphi_i + F_v S^* \varkappa_i S \varphi_i. \tag{A.11}$$

Here φ_i represents the wave function for U_i or V_i in the $\varkappa$ space. As far as μ-e decay is concerned, one kind of φ_i in a universal interaction with the selection rule (A.1) would be enough. In this case, the neutral current process and the charged current process should be related by the $\varkappa$-charge independence, which will be a matter of further experimental studies.

REFERENCES

1. S. SAKATA, Prog. Theor. Phys., **16**, 686, 1956.
2. M. TAKETANI and Y. KATAYAMA, Prog. Theor. Phys., **24**, 661, 1960.
3. A. GAMBA, R. E. MARSHAK and S. OKUBO, Proc. Nat. Acad. Sci., **45**, 881, 1959.
4. Z. MAKI, Y. OHNUKI and S. SAKATA, Proc. International Conference on Elementary Particles, Kyoto, 1965, p. 109.
5. S. NAKAMURA and S. SATO, Prog. Theor. Phys., **36**, 159, 1966; S. NAKAMURA and S. SATO, Prog. Theor. Phys., **40**, 379, 1968.
6. S. NAKAMURA and S. SATO, Suppl. Progr. Theor. Phys., **48**, 1, 1971.
7. M. GELL-MANN, Phys. Rev., **92**, 833, 1953; T. NAKANO and K. NISHIJIMA, Prog. Theor. Phys., **10**, 581, 1953; K. NISHIJIMA, Prog. Theor. Phys., **13**, 285, 1955.
8. W. HEISENBERG, Zeitschr. f. Physik, **77**, 1, 1932; **78**, 156, 1932.
9. J. SCHWINGER, Ann. of Phys., **2**, 407, 1957; I. KOBZAREV and L. B. OKUN, JETP **14**, 508, 1962; M. TAKETANI and M. SAWAMURA, Prog. Theor. Phys., **27**, 287, 1962; F. J. M. FARLEY, Proc. Roy. Soc., **285**, 248, 1965; Y. NÉEMAN, Phys. Rev., **134**, B1355, 1964; R. D.

YENNIE, Proc. 1967 Electron-Photon Int. Symposium, Stanford, p. 32; S. NAKAMURA, H. MATSUMOTO, N. NAKAZAWA and H. UGAI, Prog. Theor. Phys. Ext., 422, 1968.
10. R. SUGANO, Prog. Theor. Phys., **28,** 659, 1962; T. KITAMURA and R. SUGANO, Prog. Theor. Phys., **36,** 1014, 1966; M. M. NEITO, Phys. Rev. Letters, **21,** 488, 1968.
11. M. GELL-MANN, M. L. GOLDBERGER, N. M. KROLL and F. E. LOW, Phys. Rev., **179,** 1518, 1969.
12. M. LEVY, Preprint, 1970; D. YU. BARDIN, S. M. BILENKY and B. PONTECORVO, Phys. Letters, **32B,** 68, 1970; T. KINOSHITA, J. PESTIEAU, P. ROY and H. TEREZAWA, Preprint, 1970.
13. F. REINES, H. GURR, T. JENKINS and J. MUNSEE, Proc. Int. Sem. on Neutrino Physics, Moscow, 1968; F. REINES, preprint, 1970; Phys. Rev. Letters, **24,** 1448, 1970, C. H. ALBRIGHT, Phys. Rev. **D1,** 1330, 1970; H. J. STEINER, Phys. Rev. Letters, **24,** 746, 1970.
14. R. B. STOTHERS, Phys. Rev. Letters, **24,** 538, 1970; M. A. RUDERMAN, Topical Conf. on Weak Interactions, 1969, CERN; C. HAYASHI, R. HOSI and D. SUGIMOTO, Prog. Theor. Phys. Suppl., **22,** 1, 1962; B. PONTECORVO, Z. H. Eksp. i. Teor. Fiz., **36,** 1615, 1959; H. Y. CHIU, Ann. Rev. Nucl. Sci., **16,** 591, 1966.
15. F. J. M. FARLEY, Rivista del Nuovo Cimento, Ser. 1. Vol. 1. 59, 1969.
16. J. BAILEY, W. BARTL, G. VON BOCHMANN, R. C. A. BROWN, F. J. M. FARLEY, H. JÖSTLEIN, E. PICASSO and R. W. WILLIAMS, Phys. Letters, **28B,** 287, 1968.
17. E. PICASSO, Preprint, 1970.
18. J. C. WESLEY and A. RICH, Phys. Rev. Letters, **24,** 1320, 1970.
19. S. HIGASHI, T. KITAMURA, Y. MISHIMA, S. MIYAMOTO, Y. WATASE, and H. SHIBATA, Nuovo Cimento, **38,** 107, 1965; H. E. BERGESON, J. W. KEUFFEL, M. O. LARSON, E. R. MARTIN and G. W. MASON, Phys. Rev. Letters, **19,** 1487, 1967; T. MATANO et al. Canadian Journ. of Phys., **46,** 369, 1968; Int. Conf. Cosmic Rays, Budapest, 1969.
20. J. D. BJORKEN, S. PAKVAKA, W. SIMONS and S. F. TUAN, Phys. Rev., **184,** 1345, 1969; S. HAYAKAWA and K. KIKUCHI, Prog. Theor. Phys., **41,** 570, 1969.
21. H. E. BERGESON et. al., Phys. Rev. Letters, **21,** 1089, 1968; J. W. KEUFFEL et al., Proc. 11th Int. Conf. on Cosmic Rays, IV, 183, 1969.
22. T. D. LEE and C. N. YANG, Phys. Rev. Letters, **4,** 307, 1960; T. D. LEE and C. N. YANG, Phys. Rev., **119,** 1410, 1960; Y. YAMAGUCHI, Prog. Theor. Phys., **23,** 1117, 1960; experimentally no evidence has been found for the weak bosons.
23. E. J. KONOPINSKI and E. UHLENBECK, Phys. Rev., **92,** 1045, 1953; I. KAWAKAMI, Prog. Theor. Phys., **19,** 459, 1958; M. KONUMA, Nucl. Phys., **5,** 504, 1958.

СИММЕТРИЯ ЛЕПТОНОВ

С. НАКАМУРА и С. САТО

Резюме

Сформулированы правила отбора для изоспина и гиперзарядового спина ζ для чисто лептонных процессов при предположении, что (μ^+, ν_μ) и (ν_e, e^-) принадлежат к спинорным представлениям $\vartheta_{1/2,0}$ и $\vartheta_{0,1/2}$ групп вращения $SU(2) \times SU(2)$. Из них следует, что в то время как процессы обмена μ-е, такие как

$$\nu_e(\tilde{\nu}_e) + e^- \to \nu_e(\tilde{\nu}_e) + e^-$$

принадлежат к запрещенным переходам, процессы с μ-е собственным током, такие как

$$\mu^\pm \to e^\pm + \nu_e(\tilde{\nu}_e) + \nu_\mu(\tilde{\nu}_\mu)$$

принадлежат к разрешенным переходам.

Введены лептонные бозоны, благодаря которым происходит передача чисто лептонных процессов, определены их массы и коэффициенты связи.

$$M_L \cong 130 \text{ BeV} \sim 200 \text{ BeV},$$

$$\frac{G_l^2}{4\pi} \cong 1 \cdot 10^{-1},$$

$$\frac{F_l^2}{4\pi} \cong 1 \cdot 10^{-3}.$$

Acta Physica Academiae Scientiarum Hungaricae, Tomus 31 (1–3), pp. 215–239 (1972)

OMEGA-RHO INTERFERENCE IN STRONG INTERACTIONS

By

M. Roos*

CERN, GENEVA, SWITZERLAND

Phenomenological formalism for ω—ϱ mixing is given and its effect on strong interaction is discussed in many reactions.

1. Introduction

It was first pointed out by GLASHOW [1] in 1961 that ϱ–ω mixing due to electromagnetism could be important, because of the nearness in mass of the ϱ and ω mesons. Since then many theoretical papers [2–6] have treated the problem, most thoroughly in recent times [3–6].

The phenomenological evaluation of ϱ–ω interference effects is essentially the same whether concerned with photoproduction, colliding electron beams, or strong production. In this talk I shall restrict myself to a few brief remarks of particular concern to strong interactions. Most of my talk will be a review of the experimental situation.

2. Phenomenological formalism

Omega–rho mixing is simplest described [1–6] in terms of the complex and symmetric** mass matrix

$$M = \begin{pmatrix} M_\varrho & -\delta \\ -\delta & M_\omega \end{pmatrix},$$

where $M_\varrho = m_\varrho - 1/2i\Gamma_\varrho$, $M_\omega = m_\omega - 1/2i\Gamma_\omega$. In the absence of electromagnetic interactions,

$$\delta = 0,$$

and the two eigenvectors of M

$$|\varrho\rangle, |\omega\rangle$$

* On leave of absence from the Department of Nuclear Physics, University of Helsinki, Finland.

** Due to time reversal invariance.

are G-parity eigenstates. In the presence of electromagnetic interactions

$$\delta \neq 0,$$

and the eigenvalues of M become

$$M_{\tilde{\varrho},\tilde{\omega}} = \frac{M_\varrho + M_\omega}{2} \pm 1/2 \sqrt{(M_\varrho - M_\omega)^2 + 4\delta^2}, \tag{1}$$

with the eigenstates

$$\begin{aligned} |\tilde{\varrho}\rangle &= |\varrho\rangle - \frac{\delta}{M_{\tilde{\varrho}} - M_\omega} |\omega\rangle, \\ |\tilde{\omega}\rangle &= \frac{-\delta}{M_{\tilde{\omega}} - M_\varrho} |\varrho\rangle + |\omega\rangle. \end{aligned} \tag{2}$$

From Eq. (1) it follows that

$$M_{\tilde{\varrho}} - M_\omega = M_\varrho - M_{\tilde{\omega}}.$$

Introducing a parameter

$$\varepsilon = + \delta/(M_{\tilde{\varrho}} - M_\omega) = |\varepsilon| e^{i\varphi_\varepsilon}$$

the eigenstates (2) can be rewritten

$$\begin{aligned} |\tilde{\varrho}\rangle &= |\varrho\rangle - \varepsilon|\omega\rangle, \\ |\tilde{\omega}\rangle &= + \varepsilon|\varrho\rangle + |\omega\rangle. \end{aligned} \tag{3}$$

The states $|\tilde{\varrho}\rangle$ and $|\tilde{\omega}\rangle$ are not orthogonal. To first order in ε, the system biorthogonal to (3) is

$$\begin{aligned} \langle\tilde{\varrho}'| &= \langle\varrho| - \varepsilon\langle\omega|, \\ \langle\tilde{\omega}'| &= + \varepsilon\langle\varrho| + \langle\omega|. \end{aligned} \tag{4}$$

To the same order in ε, the mixed ϱ–ω propagator can be written

$$\begin{aligned} P &= |\tilde{\varrho}\rangle (M_{\tilde{\varrho}} - m)^{-1} \langle\tilde{\varrho}'| + |\tilde{\omega}\rangle (M_{\tilde{\omega}} - m)^{-1} \langle\tilde{\omega}'| \\ &= \frac{|\varrho\rangle\langle\varrho|}{M_{\tilde{\varrho}} - m} - \varepsilon \frac{|\omega\rangle\langle\varrho| + |\varrho\rangle\langle\omega|}{M_{\tilde{\varrho}} - m} + \\ &+ \frac{|\omega\rangle\langle\omega|}{M_{\tilde{\omega}} - m} - \varepsilon \frac{|\varrho\rangle\langle\omega| + |\omega\rangle\langle\varrho|}{M_{\tilde{\omega}} - m}. \end{aligned} \tag{5}$$

The final state of interest in strong interactions is the 2π state (in principle also the 3π state, although not yet of practical importance). The matrix element $\langle 2\pi|\omega\rangle$ is of order ε. To first order in ε, therefore, the matrix element for the strong process

$$i \to (\varrho, \omega) \to 2\pi$$

can be written

$$T_{i,2\pi} = \frac{T_{i,\varrho}\, T_{\varrho,2\pi}}{M_{\tilde{\varrho}} - m} - \varepsilon \frac{T_{i,\omega}\, T_{\varrho,2\pi}}{M_{\tilde{\varrho}} - m} + \frac{T_{i,\omega}\, T_{\omega,2\pi}}{M_{\tilde{\omega}} - m} + \varepsilon \frac{T_{i,\omega}\, T_{\varrho,2\pi}}{M_{\tilde{\omega}} - m}\,. \tag{6}$$

where $T_{i,V}$ is the amplitude for V production from the initial state i. At the level of the simple phenomenological description adopted here, spins enter only into the problem of coherence. Let the spins of the initial state, the vector meson, and the remaining final state particles (same for ω and ϱ production) be λ_i, λ_V and λ_f, respectively, and let us denote the collection of spin indices by just one superscript, λ. Then the 2π mass distribution is described by

$$\frac{d\sigma_{2\pi}}{dm} = \frac{1}{N_i} \sum_{\lambda} |T^{\lambda}_{i,2\pi}|^2 \equiv \langle |T^{\lambda}_{i,2\pi}|^2 \rangle, \tag{7}$$

where N_i is the number of initial spin states. Eq. (7) says that amplitudes with the same spins λ add coherently, whereas amplitudes with different spins λ add incoherently.

In general, both vector mesons are produced from all initial spin states, and I shall consider this case first. I shall later come back to the special case of $\bar{p}n$ annihilation at rest, where states of opposite G-parity proceed from different initial spin states.

2.1. *General case*

We must now decide which of the terms in Eq. (6) to keep, for the obvious reason that strong interactions cannot determine too many parameters. The second term is obviously indistinguishable from the first one, and very small. The third term which describes the G-violating electromagnetic decay $\omega \to 2\pi$ in the absence of mixing, is known to be too small to account alone for an effect of the order of $\Gamma_{\omega\to 2\pi} > 0.1$ MeV. Besides, GOURDIN et al. [4] maintain that the third term is exactly cancelled by a part of the fourth term. The simplest approach [3, 4] is then to neglect it, but keep the fourth term. [This does not exclude that future large experiments will require the use of

these and other [6] small terms.] Eq. (7) then becomes

$$\frac{d\sigma_{2\pi}}{dm} = \left\langle \left| \frac{T^{\lambda}_{i,\varrho} T^{\lambda}_{\varrho,2\pi}}{M_{\tilde{\varrho}} - m} + \varepsilon \frac{T^{\lambda}_{i,\omega} T^{\lambda}_{\varrho,2\pi}}{M_{\tilde{\omega}} - m} \right|^2 \right\rangle . \tag{8}$$

Let us simplify Eq. (8) by writing

$$A^{\lambda}_{\varrho} \equiv T^{\lambda}_{i,\varrho} T^{\lambda}_{\varrho,2\pi}$$
$$A^{\lambda}_{\omega} \equiv T^{\lambda}_{i,\omega} T^{\lambda}_{\varrho,2\pi},$$

and introduce the relative phases φ_λ between the amplitudes A^{λ}_{ϱ} and A^{λ}_{ω}. Eq. (8) can then be written

$$\frac{d\sigma_{2\pi}}{dm} = \frac{\langle |A^{\lambda}_{\varrho}|^2 \rangle}{|M_{\tilde{\varrho}} - m|^2} + |\varepsilon|^2 \frac{\langle |A^{\lambda}_{\omega}|^2 \rangle}{|M_{\tilde{\omega}} - m|^2} + \\ + \frac{\varepsilon^* \langle e^{-i\varphi_\lambda} |A^{\lambda}_{\varrho}| \, |A^{\lambda}_{\omega}| \rangle}{(M_{\tilde{\varrho}} - m)\,(M_{\tilde{\omega}} - m)^*} + \frac{\varepsilon \langle e^{i\varphi_\lambda} |A^{\lambda}_{\varrho}| \, |A^{\lambda}_{\omega}| \rangle}{(M_{\tilde{\varrho}} - m)^*\,(M_{\tilde{\omega}} - \omega)} . \tag{9}$$

The spin-average of the phases φ_λ can now be expressed in terms of an *over-all production phase* $\bar{\varphi}$ and a real number α which measures the *degree of coherence*:

$$\langle e^{\pm i\varphi_\lambda} |A^{\lambda}_{\varrho}| \, |A^{\lambda}_{\omega}| \rangle = e^{\pm i\bar{\varphi}} \alpha \langle |A^{\lambda}_{\varrho}|^2 \rangle^{1/2} \langle |A^{\lambda}_{\omega}|^2 \rangle^{1/2}, \tag{10}$$

where obviously

$$0 \leq \alpha \leq 1. \tag{11}$$

Note that if φ_λ is the same for all spins, then $\bar{\varphi} = \varphi_\lambda$, and if in addition vector mesons are produced in only one spin state, then also $\alpha = 1$. Introducing in Eq. (10) the notation

$$\langle |A^{\lambda}_{\sigma}|^2 \rangle^{1/2} = \langle |A_{\varrho}| \rangle$$
$$\langle |A^{\lambda}_{\varrho}|^2 \rangle^{1/2} = \langle |A_{\omega}| \rangle,$$

and substituting it into Eq. (9), it follows that the 2π mass distribution can be written

$$\frac{d\sigma_{2\pi}}{dm} = \left| \frac{\langle |A_{\varrho}| \rangle}{M_{\tilde{\varrho}} - m} + \varepsilon \alpha e^{i\bar{\varphi}} \frac{\langle |A_{\omega}| \rangle}{M_{\tilde{\omega}} - m} \right|^2 + |\varepsilon|^2 (1 - \alpha^2) \frac{\langle |A_{\omega}| \rangle^2}{|M_{\tilde{\omega}} - m|^2} . \tag{12}$$

Thus the fit of Eq. (12) to an experimental distribution ideally determines the

parameters

1. $\varphi_\varepsilon + \bar{\varphi}$, over-all phase,

2. $|\varepsilon|^2 \dfrac{\Gamma_{\varrho\to 2\pi}}{\Gamma_{\omega\to 3\pi}} = \dfrac{\Gamma_{\omega\to 2\pi}}{\Gamma_{\omega\to 3\pi}} \equiv R$ branching ratio, and

3. α, degree of coherence,

provided that $\langle |A_\varrho| \rangle$ and $\langle |A_\omega| \rangle$ are known from $\varrho \to 2\pi$ and $\omega \to 3\pi$ decays, respectively. In practice it may be impossible to determine so many parameters, but then the bounds (11) on α can be used to set limits on R.

The phase φ_ε can be estimated from theoretical arguments, and it can be determined from the reaction $e^+e^- \to \pi^+\pi^-$ (ideally they should agree!). For the time being, all strong interaction analyses take $\varphi_\varepsilon = \pi/2$ to be a reasonably well established fact.

When the over-all phase

$$\varphi_t = \varphi_\varepsilon + \bar{\varphi} + \arg\left[(M_{\tilde{\varrho}} - m)/(M_{\tilde{\omega}} - m)\right] \tag{13}$$

is $n\pi$, with an n odd (even), a dip (peak) appears in the 2π mass distribution (12), due to destructive (constructive) interference. It can easily be calculated that

$$\varphi_{\omega\varrho} \equiv \arg \frac{M_{\tilde{\varrho}} - m}{M_{\tilde{\omega}} - m} = \tan^{-1}\left[\frac{1}{2} \frac{\Gamma_{\tilde{\omega}}(m_{\tilde{\varrho}} - m) - \Gamma_{\tilde{\varrho}}(m_{\tilde{\omega}} - m)}{(m_{\tilde{\varrho}} - m)(m_{\tilde{\omega}} - m) + 1/4\,\Gamma_{\tilde{\varrho}}\,\Gamma_{\tilde{\omega}}}\right]. \tag{14}$$

It follows that

1. $\varphi_{\omega\varrho} = 0$ at $m = m_0 \approx m_{\tilde{\omega}} + 2$ MeV

2. $\varphi_{\omega\varrho}$ never attains $\pm\pi/2$

3. $\varphi_{\omega\varrho}$ is $\begin{cases} \text{minimal } (\approx -75°) \text{ at } m \approx m_0 - 1/2\sqrt{\Gamma_\varrho \Gamma_\omega} \approx m_\varrho \\ \text{maximal } (\approx +40°) \text{ at } m \approx m_0 + 1/2\sqrt{\Gamma_\varrho \Gamma_\omega}\,. \end{cases}$

Note that GFQ [3] implicitly assume that

$$\frac{M_{\tilde{\varrho}} - m}{M_{\tilde{\varrho}} - M_{\tilde{\omega}}} = 1 \text{ (real)}\,. \tag{15}$$

This is true at $m_0 \approx m_\omega$, but at $m = m_{\tilde{\varrho}}$ the assumption (15) already represents a neglect of about 19°, and at about 580 MeV the argument of Eq. (15) is $+\pi/2$. At our present state of knowledge, however, this neglect is unimportant.

We reproduce in Table I below some of the GFQ predictions [3], based on a Regge pole model.

Table I

Reaction	Predicted [3] interference effect
$\pi^+ p \to \pi^+ \pi^- \Delta^{++}$	Dip
$\pi^+ n \to \pi^+ \pi^- \Delta^+$	Dip
$\pi^+ n \to \pi^+ \pi^- p$	Dip
$\pi^- p \to \pi^+ \pi^- n$	Peak
$\pi^- p \to \pi^+ \pi^- \Delta^0$	Peak
$\pi^- n \to \pi^+ \pi^- \Delta^-$	Peak
$K^- p \to \pi^+ \pi^- \Lambda$	Constructive below ω, destructive above

2.2. *Case of incoherent G-states*

In $\bar{p}n$ annihilation at rest, having predominantly $L = 0$, and always $I = 1$, it follows that $C = (-1)^{S+1}$. Thus states of opposite G proceed from initial states of opposite spin S, and therefore they are completely incoherent. In Eq. (6) the first term is therefore incoherent with respect to all the other terms. Among the last three terms we again neglect term three in comparison with term four (for reasons given above), and the 2π mass distribution (7) becomes

$$\frac{d\sigma_{2\pi}}{dm} = \frac{\langle |A_\varrho^\lambda|^2 \rangle}{|M_{\tilde{\varrho}} - m|^2} + |\varepsilon|^2 \langle |A_\omega^\lambda|^2 \rangle \left| \frac{1}{M_{\tilde{\varrho}} - m} - \frac{1}{M_{\tilde{\omega}} - m} \right|^2. \tag{16}$$

Obviously this cross-section does not have any unknown interference phases, nor does it depend on the degree of coherence. The only unknown is $|\varepsilon|^2$. In the case of absence of any ω peak in the 2π mass distribution, Eq. (16) can be used to set an upper limit on $|\varepsilon|^2$.

3. Reaction $K^- p \to \Lambda \pi^+ \pi^-$

This reaction has been studied by FLATTÉ et al. [7] at K^- momenta 1.5, 1.7, 2.1, and 2.6 GeV/c. The reaction has the advantage of permitting easy comparison with strongly decaying ω's, in

$$K^- p \to \Lambda \omega \to \Lambda \pi^+ \pi^- \pi^0.$$

In fact, FLATTÉ et al. have what is probably the world's largest individual sample of $\omega \to \pi^+ \pi^- \pi^0$ events (about 8000 events).

Fig. 1–4 show the $\pi^+ \pi^-$ mass distributions for the four different momenta. Only the sample with 1.5 GeV/c shows a signal in the ω-region, the other samples are obviously consistent with a ϱ meson signal alone.

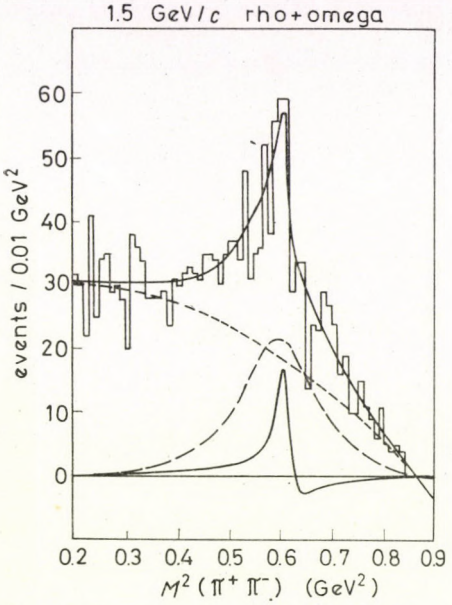

Fig. 1. The $\pi^+\pi^-$ mass-squared distribution from 1.5 GeV/c $K^-p \to \Lambda\pi^+\pi^-$ [7]

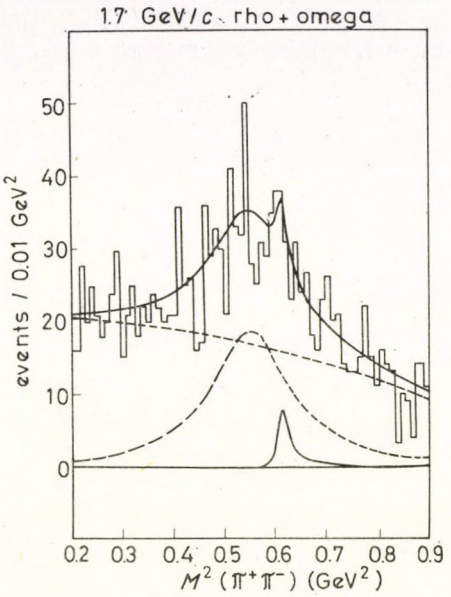

Fig. 2. The $\pi^+\pi^-$ mass-squared distribution from 1.7 GeV/c $K^-p \to \Lambda\pi^+\pi^-$ [7]

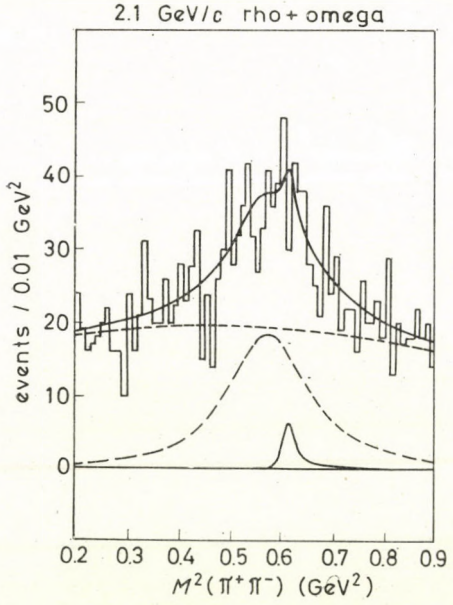

Fig. 3. The $\pi^+\pi^-$ mass-squared distribution from 2.1 GeV/c $K^-p \to \Lambda\pi^+\pi^-$ [7]

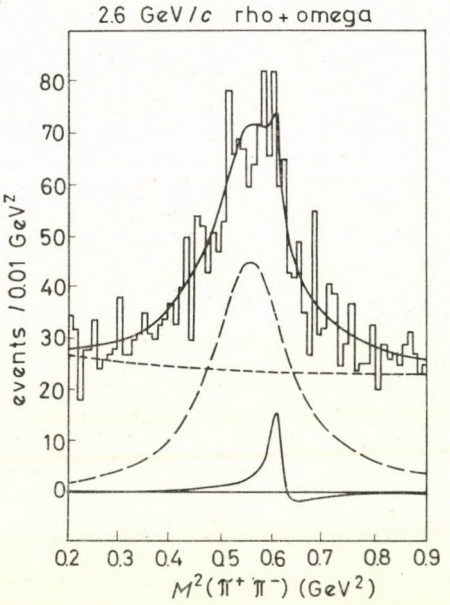

Fig. 4. The $\pi^+\pi^-$ mass-squared distribution from 2.6 GeV/c $K^-p \to \Lambda\pi^+\pi^-$ [7]

FLATTÉ tests the hypothesis that no ω signal exists in the data, by forming the difference in χ^2 between a ϱ fit and a $\varrho + \omega$ fit. The $\varrho + \omega$ fit contains the terms

$$\begin{aligned}&\text{(polynomial background)} + (\varrho\text{-Breit}-\text{Wigner}) + \\ &+ (\varrho\text{-background interference}) + (\omega\text{-Breit}-\text{Wigner}) + \\ &+ (\omega\text{-background interference}).\end{aligned}$$

The ϱ fit lacks the two last terms.

In Table II below, I quote the confidence levels given by FLATTÉ [7] for accepting the hypothesis that no ω signal exists.

Table II

Momentum (GeV/c)	Confidence level (%)
1.5	0.07
1.7	30.0
2.1	70.0
2.6	7.5

FLATTÉ uses the 1.5 GeV/c sample and condition (11) to set a limit

$$R = \frac{\Gamma(\omega \to \pi^+ \pi^-)}{\Gamma(\omega \to \pi^+ \pi^- \pi^0)} > 0.2\%$$

at the 90% confidence level. He concludes that the other samples are not in disagreement with this, since they essentially determine $R \geq 0$.

Another way of stating it is that the 1.5 GeV/c sample has a 3.4σ ω effect, whereas the other samples have none.

The possibility, advanced by FLATTÉ, that some of the kinematical variables may vary rapidly with total energy due to the nearness of the reaction threshold, may well account for the disappearance of the ω signal with increasing energy. However, nothing forces us to make that assumption. At present, unfortunately, we cannot therefore rule out the possibility of a 3.4σ fluctuation at one energy in this experiment.

4. Reaction $\pi^- p \to n\pi^+ \pi^-$

Unlike the previous reaction, this reaction has an undetected neutral particle present, and so the resolution is inferior. On the other hand, the statistics are enormous, this reaction having been studied extensively. One would therefore expect to see some interference effects, if not peaks, then shoulders.

Only in the case of exceptional resolution, and the validity of the GFQ arguments, would one expect to see a narrow spike.

Let us first turn to two recent experiments, neither one published, and therefore I do not know whether their resolutions are exceptional. SHARON HAGOPIAN reports [8] a fairly large sample (2437 events) of 2.3 GeV/c events, with momentum transfer $3\mu^2 < |t| < 12\mu^2$. The data are binned in 12 MeV wide bins, just the width of the ω, and chosen such that one bin exactly falls on the ω mass, 778–790 MeV. This bin shows a 4σ spike. Fitting Eq. (12) under the approximation (15), HAGOPIAN obtains

$$\bar{\varphi} + \varphi_\varepsilon = -107^\circ \pm 17^\circ + \frac{\pi}{2} .$$

The other recent experiment is due to RANGASWAMY, WENTZEL et al. [9], and it is a spark chamber experiment done at several momenta: 3, 4, 4.5, and 5 GeV/c. Thus, if the total interference phase or degree of coherence between ω and ϱ varies considerably with the incident energy, the ω effect should get washed out. Yet this experiment sees a 3σ spike in the bin 780–800 MeV, in a selection of $0.2 \leq |t| \leq 0.4$ (GeV/c)^2. $-0.6 \leq \cos\theta_{\pi\pi} \leq 0.3$ (1736 events).

Let me draw three conclusions from these experiments:

i) If the narrow spike is the ω, then it has survived in spite of addition of several momenta (RANGASWAMY). If you add HAGOPIAN and RANGASWAMY, that is, beam momenta ranging from 2.3 to 5 GeV/c, the spike also survives.

ii) RANGASWAMY et al. have less than half the number of events of HAGOPIAN in the ϱ region.

iii) The data agrees with the GFQ prediction [3], *cf.* Table 1.

Let me now contrast this information with my compilation [10] of earlier experiments, ranging from 1.6 to 3.2 GeV/c, and selected with momentum transfers $|t| < 10\mu^2$. Fig. 5 shows 13192 $\pi^+\pi^-$ events, kindly supplied by groups in Bari, BNL, Bologna, Colorado, LRL Berkeley, Orsay, Pennsylvania, Purdue, Saclay, and Wisconsin.

As you can see, the bins 770–790 MeV fluctuate insignificantly above the pure ϱ-meson fit. If there is any effect in the ω-region of more significance, I would like to suggest that the bins 770–820 MeV indicate a steeper slope than does the left side of the ϱ peak. Certainly, there is nothing like a cumulated HAGOPIAN–RANGASWAMY peak in this total histogram.

Let me now disturb your peace of mind by Fig. 6, which shows a compilation [11] of 12773 $\pi^-\pi^0$ events from the reaction

$$\pi^- p \to \pi^-\pi^0 p,$$

also with $|t| < 10\mu^2$ (from the same groups, except for BNL).

This system, of course, contains no ω-effect. What is interesting to note is that the ω-region looks quite similar to the ω-region in the $\pi^+\pi^-$ sample:

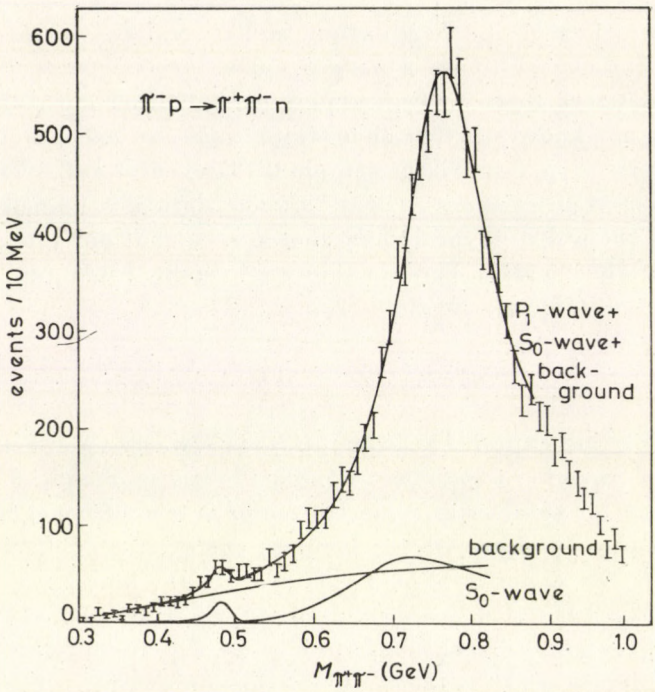

Fig. 5. The $\pi^+\pi^-$ mass distribution from a compilation [10] of 1.6–3.2 GeV/c $\pi^- p \to \pi^+\pi^- n$ with $|t| < 10\mu^2$

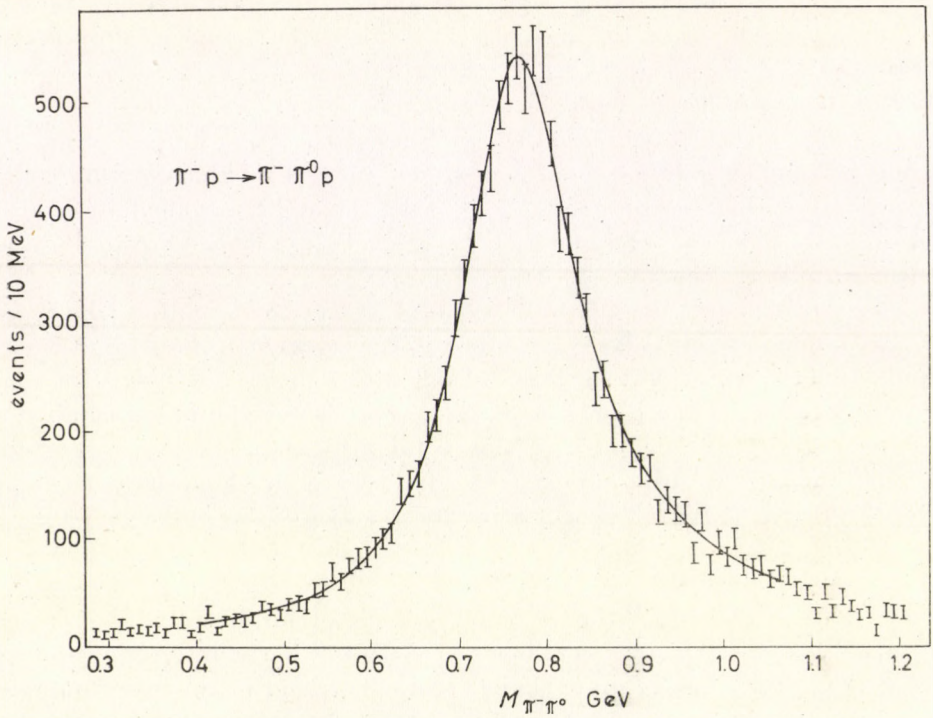

Fig. 6. The $\pi^-\pi^0$ mass distribution from a compilation [11] of 1.6–3.2 GeV/c $\pi^- p \to \pi^- \pi^0 p$ with $|t| < 10\mu^2$

the bins 780–800 MeV fluctuate insignificantly above the pure ϱ-meson fit, and the region 780–820 MeV suggests a steeper slope than does the left side of the peak.

I do not want to claim any unheard-of $I = 1$ effect, I just want to warn that the slight asymmetry in the $\pi^+\pi^-$ system in the ω-region should not be taken blindly as an evidence for ω–ϱ interference. In fact, in the hunt of $\omega \to 2\pi$ decay, one too easily forgets that the $\pi^+\pi^-$ system usually is produced in a state of mixed I-spins, and that one had better make sure that any effect to be explained by the ω indeed is an $I = 0$ effect, experimentally.

To underline my warning, please look at Fig. 7, which shows the combined $\pi^+\pi^-$ and $\pi^-\pi^0$ compilations: the steep slope on the right-hand side of the ϱ peak is quite obvious. I do not have any numbers for its significance. On the same Figure I have drawn in the HAGOPIAN [8] $\pi^+\pi^-$ data. Recall that the RANGASWAMY [9] statistics were less than half of HAGOPIAN's statistics.

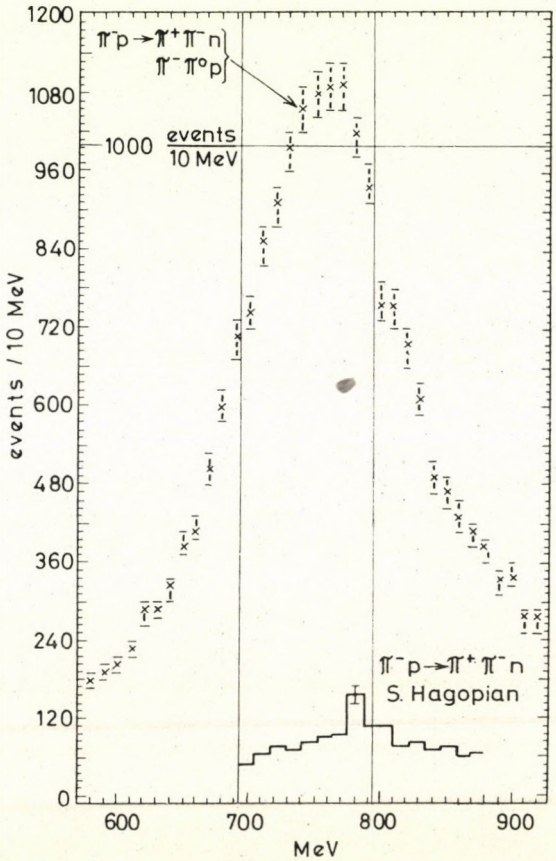

Fig. 7. The data from Figs. 5 and 6 added. The solid histogram is from 2.3 GeV/c $\pi^- p \to \pi^+ \pi^- n$ [8], $3\mu^2 < |t| < 12\mu^2$

To conclude, I do not think that the recent evidence [8, 9] for ϱ–ω interference in this reaction is very convincing, even at the level of 3 or 4 standard deviations, unless it is demonstrated that the resolution is much better than in earlier experiments.

5. Reaction $\pi^+ p \to \pi^+ \pi^- \Delta^{++}$

In 1967 I compiled [12] all then available data for this reaction, from four experiments done by groups from Aachen–Berlin–Birmingham–Bonn–Hamburg–London (I.C.)–Munich, Columbia–Rutgers, LRL Berkeley, and UC San Diego–Michigan. The beam momenta ranged from 2.35 GeV/c to 4.0 GeV/c and the sample consisted of 3236 events of $|t| < 30\mu^2$, or 1250 events of $|t| < 10\mu^2$.

There was an indication of structure which could be due to the ω, a dip in the 770–790 MeV bins, see Fig. 8. However, the effect was hardly more than 1 standard deviation, and it has almost only historical interest now.

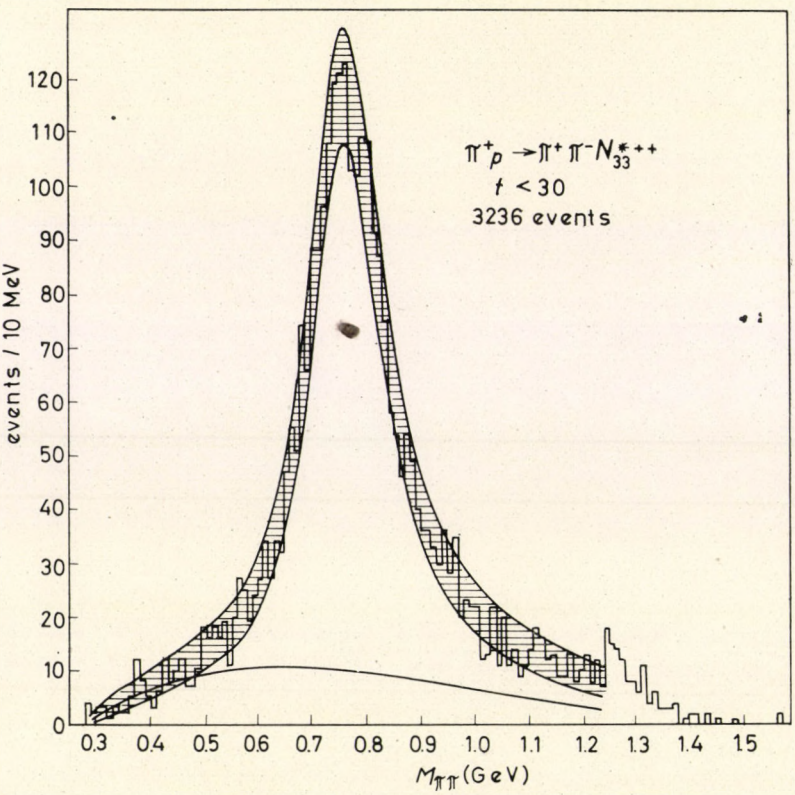

Fig. 8. The $\pi^+\pi^-$ mass distribution from a compilation [12] of 2.35–4.0 GeV/c $\pi^+ p \to \pi^+\pi^- \Delta^{++}$, with $|t| < 30\mu^2$

The next important experiment is due to GOLDHABER et al. [13], who already had contributed to the 1967 compilation, but who now have almost three times more events than the total 1967 compilation. Fig. 9 shows a significant dip in one bin, 780–790 MeV, plotting 3300 events of $|t| < 0.22$ (GeV/c)^2.

Note that the GFQ prediction [3] for this reaction is precisely a dip.

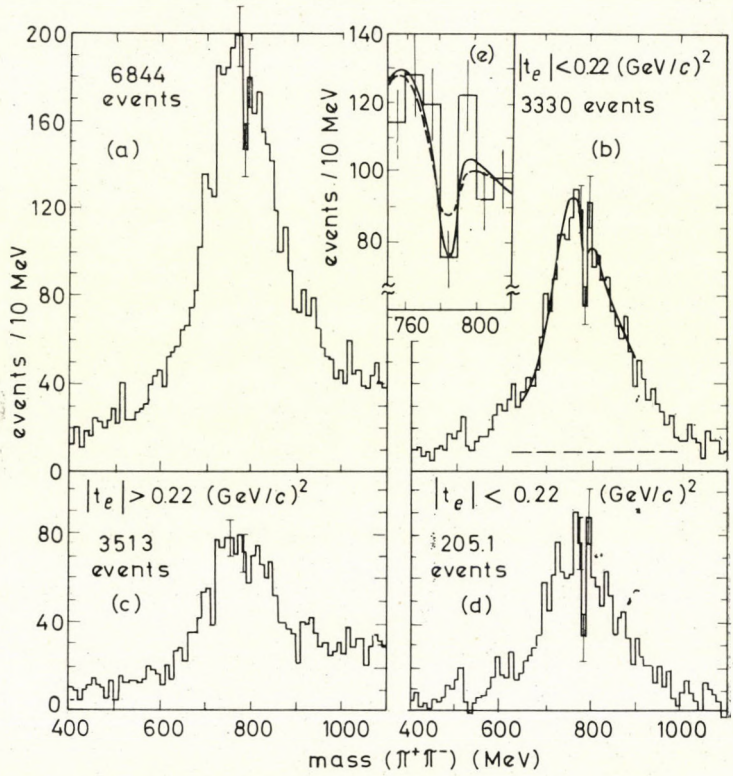

Fig. 9. The $\pi^+\pi^-$ mass distribution from 3.4–4.0 $\pi^+p \to \pi^+\pi^-\Delta^{++}$ [13]. (a) The entire data (b) selection $|t| < 0.22$ (GeV/c)^2; (c) selection $|t| > 0.22$ (GeV/c)^2; (d) selection $|t| < 0.22$ (GeV/c) with background subtraction from both sides of the Δ^{++} band; (e) enlargement of the ϱ^0–ω interference region from (b)

The validity of the GOLDHABER dip should be judged from their resolution. This reaction allows a very good resolution, since there are four particles, all charged, in the final state. GOLDHABER [13] quotes a (Gaussian) resolution function of full width 10 ± 1 MeV at half maximum (FWHM), which, if true, renders the dip credible.

Fitting the dip with Eq. (12) under the assumption (15), Goldhaber quotes a phase of

$$\bar{\varphi} + \varphi_\varepsilon = 86° \pm 17° \to \pi/2.$$

The lower limit on R from condition (11) is

$$R > 1.5\% \quad \text{with } 68\% \text{ confidence}$$
$$R > 0.25\% \quad \text{with } 95\% \text{ confidence.}$$

In the GFQ notation, the result is $\delta = 2.7$ MeV, and with 95% confidence $\delta > 1.1$ MeV.

The beam had a momentum of 3.7–4.0 GeV/c in GOLDHABER's experiment [13]. Fresh support seems to come from JACKSON et al. [14] at 5.5 GeV/c, but I have no figure. At the Washington APS meeting, only a fraction of a large exposure was presented in a preliminary way, and a dip of not too great significance seemed present.

However, this reaction is not free from serious contradiction, either. FLATTÉ et al. [15] have about three times more events than GOLDHABER [13], with the same selection, but at higher momentum, 7.0 GeV/c. In some preliminary $\pi^+\pi^-$ distributions they see no trace of any kind of ω-effect. But the experiment is not yet written up, and thus one may still hope that the absence of a dip can be explained by a relatively wide resolution function. Obviously information on the momentum spread of the beam is crucial.

6. Reaction $\pi^- p \to \pi^+ \pi^- \pi^- p$

This reaction is similar to the previous one, for instance what concerns the attainable resolution, but there is no prominent Δ^0 production, and that makes the GFQ predictions [3] worthless in this case.

At CERN, ABRAMOVITCH et al. [16] have over 4000 events at 3.9 GeV/c, and they claim a resolution (FWHM) in the ω-region of about 8 MeV*. They see a dip and a peak which, by various selections, can be increased in significance from 2.5 to 4σ, see Fig. 10.

The distribution can be well fitted with a constructive ϱ–ω interference of a size corresponding to

$$R > 1.1\% \quad \text{with } 95\% \text{ confidence.}$$

This experiment does not seem to be contradicted by any similar experiment!

7. Reaction $\bar{p}p \to \pi^+ \pi^- \pi^+ \pi$

In this reaction one also has a good resolution. Recently there have been two claims [17–18], for ω–ϱ interference in annihilation in flight. Let me discuss these experiments first.

* The ω width in the reaction $\pi^- p \to \pi^+\pi^-\pi^0\pi^- p$ comes out to be 8.8 $\pm$ 3 MeV.

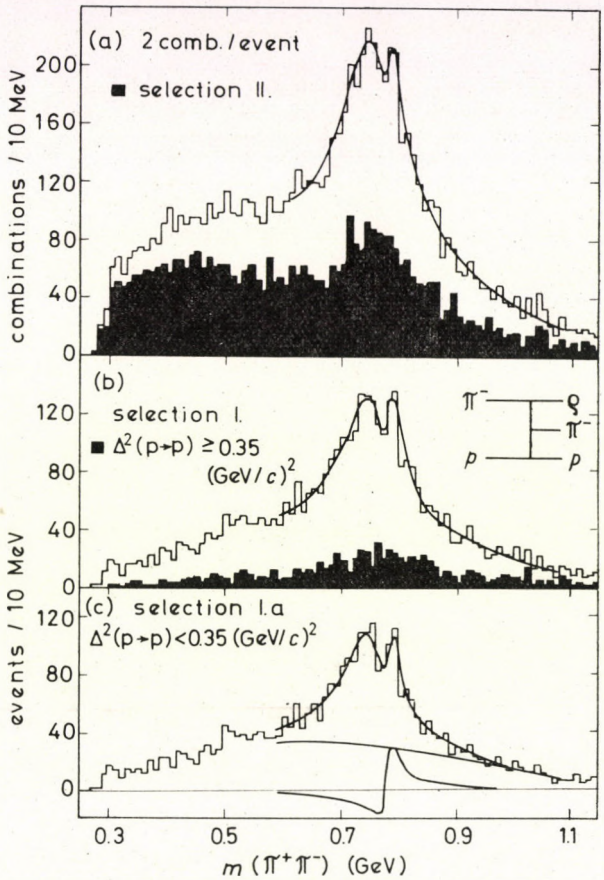

Fig. 10. The $\pi^+\pi^-$ mass distribution from 3.9 GeV/c $\pi^- p \to \pi^+\pi^-\pi^- p$ [16]. Selection I corresponds to the $\pi^+\pi_i^-$ combination for which $D_j > D_i$ ($i, j = 1$ or 2) where $D_1 = \Delta^2(\pi^-_2) - \Delta^2(\pi^+\pi^-_1)$ and $D_2 = \Delta^2(\pi^-) - \Delta^2(\pi^+\pi^-_2)$. Selection II is the complementary selection

Allison et al. [17] have published results concerning 1448 events at momenta 1.26–1.65 GeV/c, and they have communicated information about an experiment of a similar size at 2.3 GeV/c. In the ω region, the 2π mass resolution of the 1.26–1.65 GeV/c experiment is quoted as 10 ± 1 MeV (FWHM). The uncut data show peaks at the ω mass in both experiments, cf. Fig. 11. Fitting the data with Eq. (12) and the assumption

$$\varphi_\varepsilon = \pi/2.$$

Allison et al. find the parameter values shown in Figs. 12 and 13. In the Figures, Φ corresponds to our $\bar{\varphi}$. From this, one can draw the conclusions:

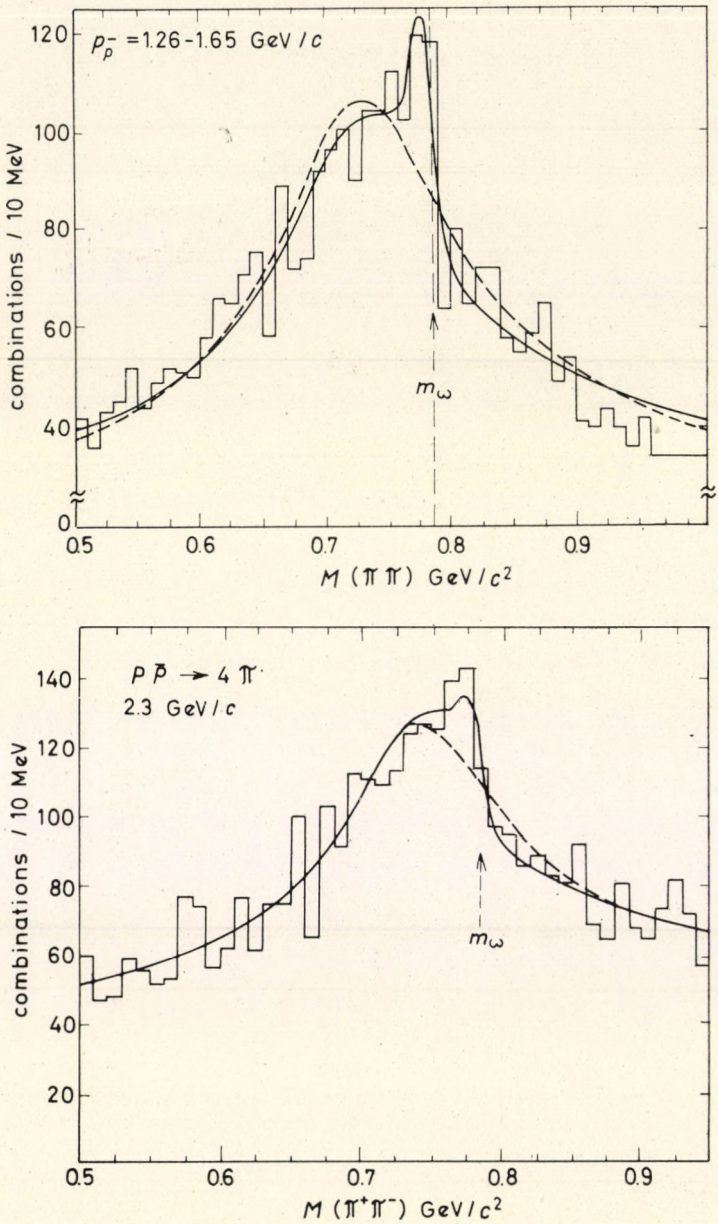

Fig. 11. The $\pi^+\pi^-$ mass distributions from 1.26–1.65 and 2.3 GeV/c $\bar{p}p \to \pi^+\pi^-\pi^+\pi^-$ [17]

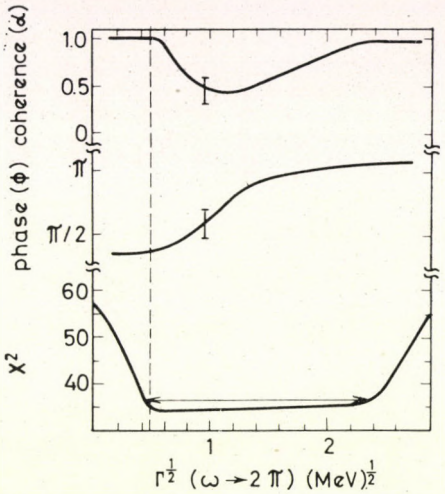

Fig. 12. The best value of χ^2, the corresponding phase $\Phi = \bar{\Phi}$, and coherence α for different values of $\Gamma^{1/2}_{\omega^+ 2\pi}$. The horizontal arrow indicates the 95% confidence limits for $\Gamma^{1/2}_{\omega^+ 2\pi}$ at $\Delta\chi^2 = 2.7$. From 1.26–1.65 GeV/c $\bar{p}p \to \pi^+\pi^-\pi^+\pi^-$ [17]

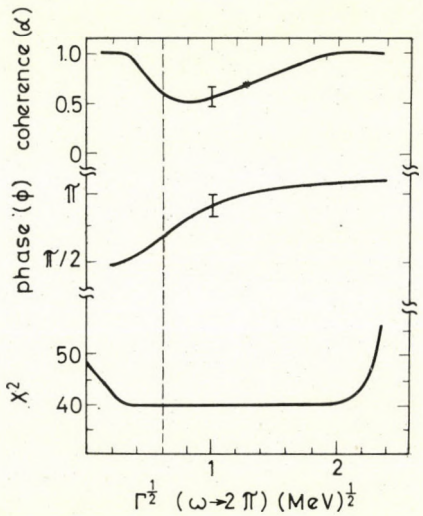

Fig. 13. Same as Fig. 12, but corresponding to the 2.3 GeV/c $\bar{p}p \to \pi^+\pi^-\pi^+\pi^-$ experiment [17]

1. the effect seen corresponds to 3.5σ in the 1.26–1.65 GeV/c experiment, but is hardly significant in the 2.3 GeV/c experiment;

2. the information on α is not very significant, $\alpha \sim 0.75 \pm 0.25$;

3. the limit (11) allows one to deduce that $R > 1.4\%$ with 95% confidence in the 1.26–1.60 GeV/c experiment (the authors give $\Gamma^{1/2}_{\omega \to 2\pi} = 0.63 \pm \pm 0.23$ MeV$^{1/2}$).

At similar energies, 1.63–2.20 GeV/c, CHAPMAN et al. [18] report over 3000 events, with a resolution of 11 ± 2 MeV (FWHM). The mass distribution for the uncut sample, and for a selection $-0.2 > t > -0.3$ is shown in Fig. 14. Although the statistics are better than either of ALLISON's samples, there is no ω peaking. However, the steep drop is there.

Making an analysis similar to ALLISON et al. [17], CHAPMAN et al. conclude that

$$R > 0.75\% \text{ with } 95\% \text{ confidence,}$$
$$\bar{\varphi} = 95°\text{–}125°.$$

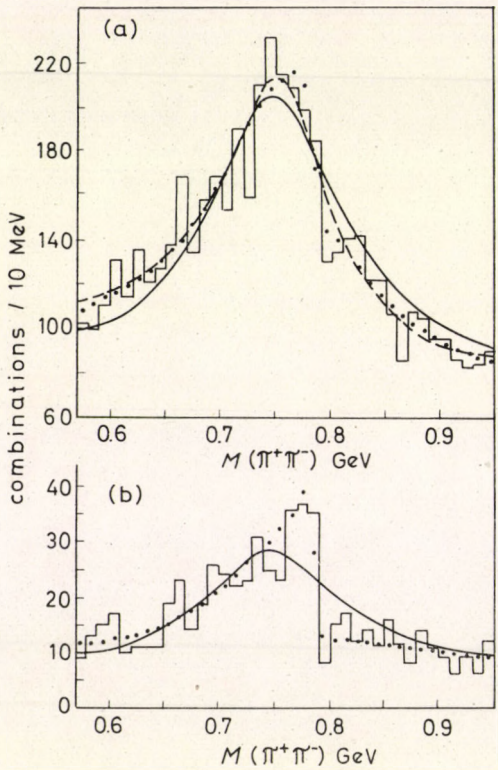

Fig. 14. The $\pi^+\pi^-$ mass distribution from 1.6–2.2 GeV/c $\bar{p}p \to \pi^+\pi^-\pi^+\pi^-$ [18]. (a) Selection $0.2\ (\text{GeV/c})^2 \leq |t| \leq 0.3\ (\text{GeV/c})^2$

The selection in Fig. 14b to improve the ω signal actually makes it less credible. It is very hard to understand a t-dependence which makes the degree of coherence very high in the sample $-0.2 > t > -0.3$, whereas in other t-selections no ω–ϱ effect appears, as noted by the authors [18]. Also, when ϱ-background interference is allowed, the ω–ϱ effect in the total data becomes quite insignificant.

Since ALLISON et al. have permitted themselves to add data from different momenta (1.26–1.65 GeV/c), and since CHAPMAN et al. have permitted themselves the same procedure (1.65–2.20 GeV/c), and since ALLISON's 2.3 GeV/c value looks not very different from CHAPMAN's, I have permitted myself to add all these experiments together. The result is shown in Fig. 15. (I have

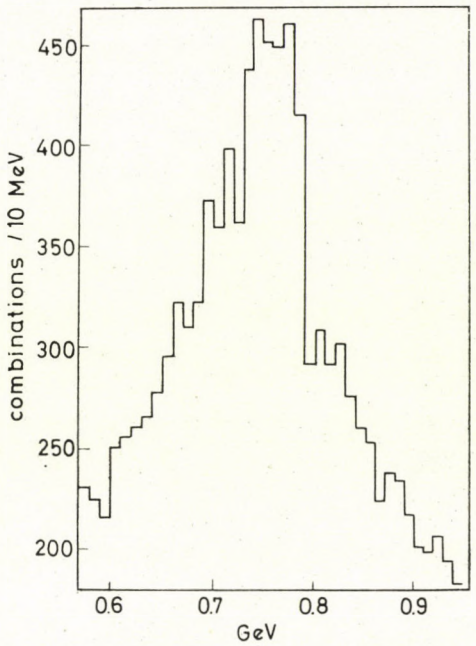

Fig. 15. The data from Figs. 11 and 14 added

not drawn any error bars, because the theory of statistics does not tell us what the errors are of binned *combinations* of events.) As you can see, no ω peak remains. However, there is a spectacular drop in the ω region, of large significance, indicating that some very important destructive interference occurs. I would hope that the groups with these data (and some more recent data at 1.5–2 GeV/c, being analyzed at Michigan State University) would get together, and analyze their total distributions.

On the other hand, this reaction may contain other types of interference, which could produce the drop in Fig. 15. For instance, ϱ–ϱ interference could do it. Note that Fig. 15 does resemble the asymmetric peak in Fig. 7, from the added $\pi^+\pi^-n$ and $\pi^-\pi^0p$ final states.

Let me now briefly show CLAYTON et al. [19] who have less data, 816 events at 2.5 GeV/c, Fig. 16. The events are in 25 MeV bins, and therefore I could not add them to the previous Figure. At this level of statistics, as you can see, there is not really anything to be learned about possible ω–ϱ interference.

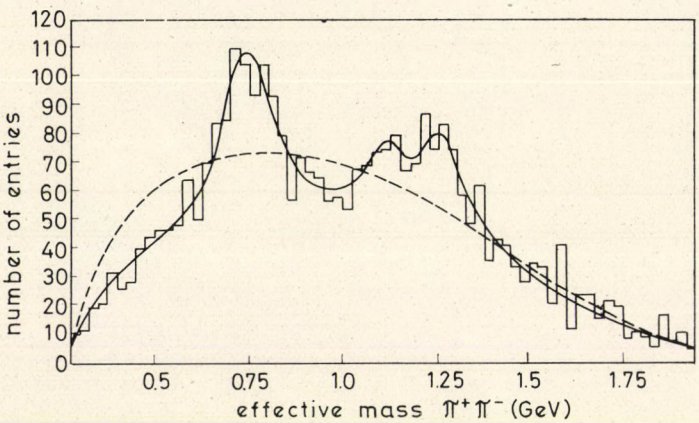

Fig. 16. The $\pi^+\pi^-$ mass distribution from 2.5 GeV/c $\bar{p}p \to \pi^+\pi^-\pi^+\pi^-$ [19]

In annihilation at rest, no claims for ω–ϱ interference have been made. However, the accumulated statistics is quite good, and the reaction is just as interesting. Let me just show the $\pi^+\pi^-$ distributions from the two largest experiments, BALTAY et al. [20] in Fig. 17 and DIAZ et al. [21] in Fig. 18. Nothing spectacular appears, and it is debatable whether there is a conspicuous drop in the 800 MeV region or not. DIAZ et al. have a resolution of 12–13 MeV (FWHM).

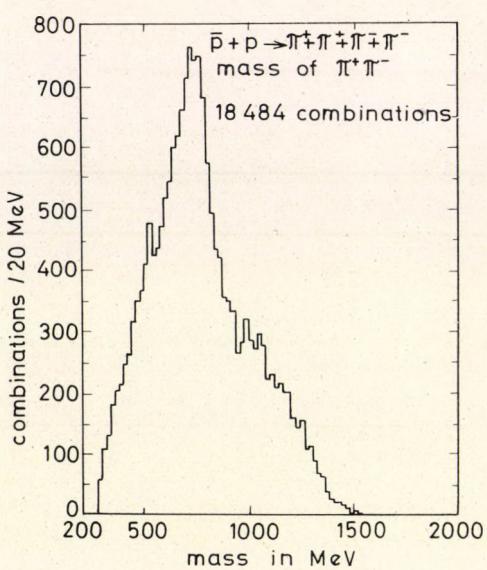

Fig. 17. The $\pi^+\pi^-$ mass distribution from $\bar{p}p \to \pi^+\pi^-\pi^+\pi^-$ at rest [20]

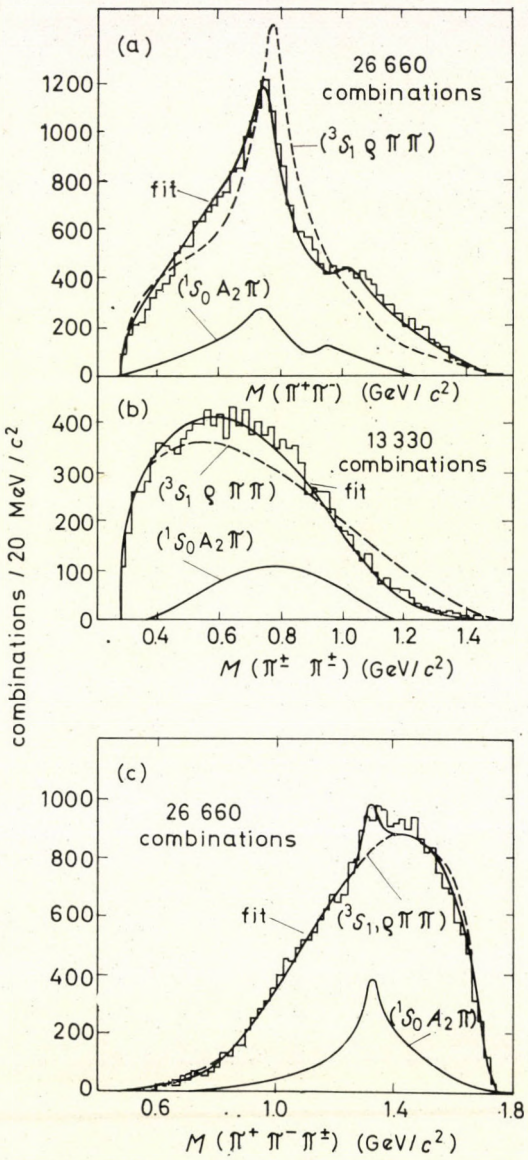

Fig. 18. The $\pi^+\pi^-$ mass distribution from $\bar{p}p \to \pi^+\pi^-\pi^+\pi^-$ at rest [21]

8. Reactions $\bar{p}n \to \pi^+\pi^-\pi^-$, $\pi^+\pi^-\pi^-\pi^\circ$, $2\pi^+3\pi^-$

As already discussed in Section 2, these reactions are particularly interesting since here the $G = +$ and $G = -$ production amplitudes of ω and ϱ add incoherently. One can then use the information for setting upper limits to R (in particular if no ω effect is seen).

BIZZARRI et al. [22] have 5156 events (at rest) of the all charged 3π final state, 6019 events of the 4π state, and 1496 events of the 5π state. Unfortunately, there seems to be very little ϱ production in these reactions, the ϱ being a small signal on a very high background.

BIZZARRI et al. [22] see no ω–ϱ interference effect. If they fit the data with ω, ϱ and an arbitrary background, they get an upper limit

$$R < 3.6\% \text{ with } 95\% \text{ confidence.}$$

9. Conclusions

The phenomenological theory for ω–ϱ mixing is essentially the same in strong interactions as in electromagnetic interactions, but the experimental information from strong reactions is very meagre and often contradictory, so only a very simple phenomenological formalism is required. The parameters one can expect to determine are very few and often highly correlated. In one simple parametrization, Eq. (12), the parameters are:

1. $\varphi_\varepsilon + \bar{\varphi}$, where φ_ε is the phase of the ϱ–ω mixing parameter ε and $\bar{\varphi}$ is the strong ω production phase relative to the ϱ,

2. $$R = \frac{\Gamma_{\omega\to 2\pi}}{\Gamma_{\omega\to 3\pi}} = |\varepsilon|^2 \frac{\Gamma_{\varrho\to 2\pi}}{\Gamma_{\omega\to 3\pi}},$$

3. α, the degree of coherence.

In all cases studied until now (except for BIZZARRI et al. [22]), α and $|\varepsilon|$ are so strongly correlated that only a lower limit for R could be deduced, using the properties that

$$0 \leq \alpha \leq 1.$$

The phase φ_ε can be determined in colliding electron beam experiments, and is usually taken to be $\pi/2$. It is possible to advance theoretical arguments [3, 4] for this value. The strong phase $\bar{\varphi}$ is approximately predicted by the Regge pole model of GFQ [3].

A particular warning applies to reactions where the possible ω–ϱ interference produces only a shoulder or a steep fall-off on the ϱ. The shape assumed for the ϱ then becomes quite important. Thus a non-relativistic, narrow-reso-

nance Breit–Wigner formula will not do for the ϱ meson, nor will an energy-independent width Γ_ϱ.

Compiled $\pi^+\pi^-$ histograms from the reactions $\pi^- p \to \pi^+\pi^- n$ [4] and $\bar{p}p \to 2\pi^+2\pi^-$ [17, 18] indeed show such structure, and are therefore open to this warning.

The asymmetry in the ϱ^0 peak in the reaction [10] $\pi^- p \to \pi^+\pi^- n$ looks very much like an asymmetry in the ϱ^- peak from $\pi^- p \to \pi^-\pi^0 p$ [10, 11], so there is some indication that $I = 1$ effects may play an unknown role in the ω–ϱ interference region.

The steep fall-off in the compiled $\pi^+\pi^-$ spectrum from $\bar{p}p \to 2\pi^+2\pi^-$ in flight [17, 18] need not necessarily be associated with ω–ϱ interference, since the $2\pi^+2\pi^-$ final state needs many amplitudes for its description, and some of them could interfere in this region (e.g. ϱ–ϱ interference).

The reaction $K^- p \to \Lambda\pi^+\pi^-$, studied [7] at four energies, shows what looks like an ω–ϱ interference effect only at one (the lowest) energy. Thus one has to introduce a fairly strong energy-dependence of $\bar{\varphi}$ or α, or perhaps one is the victim of a large statistical fluctuation.

The reaction $\pi^+ p \to \pi^+\pi^- \Delta^{++}$ shows a dip in some [12–14], but not all [15] experiments; the only quoted lower limit on R is [13] 0,25% (at 95% confidence limit).

The only experiment which is not (yet?) contradicted studies [16] $\pi^- p \to$ $\to \pi^+\pi^-\pi^- p$, and derives a lower limit

$$R > 1.1\% \text{ (95\% confidence)}.$$

Finally there is a preliminary upper limit

$$R < 3.6\% \text{ (95\% confidence)}$$

from $\bar{p}n \to 3\pi, 4\pi, 5\pi$ at rest [22], where no ω-signal is seen. In $\bar{p}n$ annihilation states of opposite G-parity are incoherently produced, and therefore they offer the only opportunity to set an upper limit to R from the absence of a signal. Adding the functions $\chi^2(R)$ from the experiments of ABRAMOVICH et al. [16] and BIZZARRI et al. [22], one obtains

$$R = 2.2 \begin{matrix} +0.9(2.1) \\ -1.0(1.75) \end{matrix} \%,$$

where the numbers in parentheses represent 2σ errors. This R value would not change noticeably if one added the $\chi^2(R)$ functions of FLATTÉ [7] and GOLDHABER et al. [13]. In Table III we collect the experiments mentioned in the previous sections.

Table III

Strong interaction experiments

	Reaction	Momentum	Group	Ref.	Effect
1	$K^- p \to \Lambda\pi^+\pi^-$	1.5	LRL/Gp. A	7	3.7 σ peak, constructive intf.
	$K^- p \to \Lambda\pi^+\pi^-$	1.7, 2.1, 2.6	LRL/Gp. A	7	No effect
2	$\pi^- p \to \pi^+\pi^- n$	2.3	FSU—PENN	8	4 σ spike
3	$\pi^- p \to \pi^+\pi^- n$	3, 4, 4.5, 5	LRL/Wentzel	9	3 σ spike
4	$\pi^- p \to \pi^+\pi^- n$	1.6–3.2	Compilation	10	No effect
5	$\pi^- p \to \pi^-\pi^0 p$	1.6–3.2	Compilation	11	$I = 1$ effect?
6	$\pi^+ p \to \pi^+\pi^- \Delta^{++}$	2.35–4.0	Compilation	12	Dip, not significant
7	$\pi^+ p \to \pi^+\pi^- \Delta^{++}$	3.4–4.0	LRL/Goldhaber	13	Dip, destructive intf.
8	$\pi^+ p \to \pi^+\pi^- \Delta^{++}$	5.5	Toronto	14	Preliminary dip
9	$\pi^+ p \to \pi^+\pi^- \Delta^{++}$	7.0	LRL/Gp. A	15	No effect
10	$\pi^- p \to \pi^+\pi^-\pi^- p$	3.9	CERN	16	4 σ peak, constructive intf.
11	$\bar{p}p \to \pi^+\pi^-\pi^+\pi^-$	1.26–1.65	ANL	17	3.5 σ peak
12	$\bar{p}p \to \pi^+\pi^-\pi^+\pi^-$	2.3	ANL	17	Small peak
13	$\bar{p}p \to \pi^+\pi^-\pi^+\pi^-$	1.6–2.2	Ann Arbor	18	Small interference
14	$\bar{p}p \to \pi^+\pi^-\pi^+\pi^-$	2.5	Liverpool—Athens	19	No effect
15	$\bar{p}p \to \pi^+\pi^-\pi^+\pi^-$	at rest	Columbia	20	No effect
16	$\bar{p}p \to \pi^+\pi^-\pi^+\pi^-$	at rest	CERN—CdF	21	No effect
17	$\bar{p}n \to 3\pi, 4\pi, 5\pi$	at rest	Rome—Syracuse	22	No effect

I enjoyed useful discussions about the material, covered in Section 2 with my friend JÁN PIŠÚT, CERN and Bratislava. I am also indebted to Professor G. GOLDHABER, Berkeley, Professor S. GLASHOW, Harvard, and Dr. V. CHALOUPKA, CERN, who have let me use material they had assembled for similar review talks. I am grateful to Drs. W. ALLISON and D. RHINES, Argonne, Drs. R. BIZZARRI, P. GUIDONI and I. LAAKSO, Rome, and Dr. S. HAGOPIAN, for communicating to me unpublished results.

REFERENCES

1. S. GLASHOW, Phys. Rev. Letters, **7,** 469, 1961.
2. G. FEINBERG, Phys. Rev. Letters, **8,** 151, 1962; J. BERNSTEIN and G. FEINBERG, Nuovo Cimento, **25,** 1343, 1962; S. COLEMAN and H. SCHNITZER, Phys. Rev., **134B,** 863, 1964; J. HARTE and R. SACHS, Phys. Rev., **135B,** 459, 1964; J. YELLIN, Phys. Rev., **147,** 1080, 1966.
3. A. GOLDHABER, G. FOX and C. QUIGG, Phys. Letters, **30B,** 249, 1969.
4. M. GOURDIN, L. STODOLSKY and F. RENARD, Phys. Letters, **30B,** 347, 1969.
5. D. HORN, Phys. Rev., **D1,** 1421, 1970.
6. R. SACHS and J. WILLEMSEN, Phys. Rev., **D2,** 133, 1970.
7. S. FLATTÉ, D. HUWE, J. MURRAY, J. SHAFER, F. SOLMITZ, M. STEVENSON and C. WOHL, Phys. Rev., **145,** 1050, 1966. S. FLATTÉ, Phys. Rev., **155,** 1517, 1967; ibid. **1D,** 1, 1970.
8. S. HAGOPIAN, Thesis, Univ. of Pennsylvania, 1969; and Phys. Rev. Letters, **25,** 1050, 1970.

9. T. RANGASWAMY, Thesis, Univ. of California, UCRL-19464, 1970.
10. L. DUBAL and M. ROOS, Nuclear Phys., **B12**,, 146, 1969.
11. J. PIŠÚT and M. ROOS, Nuclear Phys., **B6**, 325, 1968.
12. M. ROOS, Nuclear Phys., **B2**, 615, 1967.
13. G. GOLDHABER, W. BUTLER, D. COYNE, B. HALL, J. MACNAUGHTON and G. TRILLING, Phys. Rev. Letters, **23**, 1351, 1969.
14. W. JACKSON, M. BANTING, I. BLOODWORTH, J. PRENTICE and T. YOON, BAPS **15**, 513, 1970.
15. S. FLATTÉ, private communication, 1970.
16. M. ABRAMOVICH, H. BLUMENFELD, F. BRUYANT, V. CHALOUPKA, S. U. CHUNG, J. DIAZ, F. MARTIN, L. MONTANET and J. RUBIO, Nuclear Phys., **B**, **20**, 209, 1970.
17. W. ALLISON, W. COOPER, T. FIELDS and D. RHINES, Phys. Rev. Letters, **24**, 618, 1970 and private communications.
18. J. CHAPMAN, J. DAVIDSON, R. GREEN, J. LYS, B. ROE and J. VAN DER VELDE, Nuclear Phys., **B24**, 445, 1970.
19. J. CLAYTON, P. MASON, H. MUIRHEAD, D. WALDRON, R. RIGOPOULOS, P. TSILIMIGRAS and A. VAYAKI-SERAFIMIDOU, Univ. of Liverpool preprint, 1970.
20. C. BALTAY, P. FRANZINI, G. LÜTJENS, J. SEVERIENS, D. TYCKO and D. ZANELLO, Phys. Rev., **145**, 1103, 1966.
21. J. DIAZ, PH. GAVILLET, G. LABROSSE, L. MONTANET, W. SWANSON, P. VILLEMOES, M. BLOCH, P. FRENKIEL, C. GHESQUIÉRE, E. LILLESTØL, and A. VOLTE, Nuclear Phys., **B16**, 238, 1970, and private communications.
22. R. BIZZARRI, G. CIAPETTI, U. DORE, M. GASPERO, P. GUIDONI, I. LAAKSO, F. MARZANO and G. MONETI, Phys. Rev. Letters, **25**, 1385, 1970.

ОМЕГА—РО ИНТЕРФЕРЕНЦИЯ В СИЛЬНЫХ ВЗАИМОДЕЙСТВИЯХ

М. РУУС

Резюме

Построен феноменологический формализм для омега-ро смешивания, и рассмотрено его влияние на сильное взаимодействие в большом числе реакций.

Acta Physica Academiae Scientiarum Hungaricae, Tomus 31 (1–3), pp. 241–250 (1972)

POSSIBLE RELATIONS BETWEEN CURRENT ALGEBRA AND MESON POLE DOMINANCE

By

B. RENNER

INSTITUTE 2 FOR THEORETICAL PHYSICS, THE UNIVERSITY, HAMBURG
GERMAN FEDERAL REPUBLIC

The suggestion is made there is an overlap among the information obtained from current algebra and from meson pole dominance principles. In simple models it is shown that current algebra results can be rederived from meson pole dominance principles alone, up to an unknown scale of the weak axial current. A non-compact alternative to the usual $SU_2 \times SU_2$ current algebra is shown to be inconsistent with meson pole dominance.

Introduction

In this lecture I will report on work in progress. Its interpretation is still tentative, its further development is yet uncertain. For the steps taken so far in the present program, the credit is to be shared with J. ELLIS and J. DE AZCARRAGA, who have contributed many of the arguments I will present in the following.

To motivate the program, we recall some steps in the development of current algebra. When the theory was proposed by GELL-MANN, it was presented in terms of basic quantum mechanical principles: an assumption of simple commutators for simple observables. Owing to a lack of experimental data on photon and neutrino reactions it remained essentially untestable for over two years, until ADLER and WEISBERGER utilized the approximation of pion pole dominance for the divergence of the weak axial current to derive their celebrated sum rule. In the subsequent developments which include in successive stages soft-pion theorems, hard pion calculations and chiral Lagrangians, the principle of pion pole dominance gained a central role, and Nambu's original interpretation as partial conservation of the weak axial vector current was revived indicating the proximity of a chiral $SU_2 \times SU_2$ symmetry limit as the pion mass is taken to zero.

So far, pion pole dominance has been used mainly in an auxiliary capacity to test the current algebra commutators. To my knowledge, it was MANDELSTAM who first explicitly turned the argument round and demonstrated the implications of pion pole dominance on current algebra. In some generality he showed that in the zero pion-mass limit the commutator of two weak axial currents $A_\mu^i(x)$

$$[\int A_0^i(x)\,(dx)^3,\ A_\mu^j(y)] = ie^{ijk}\,V_\mu^k(y) \tag{1}$$

gives rise to a conserved vector current as a consequence of Adler zeros.

This statement becomes trivial in theories where the limit of massless pions implies conservation of the axial current, because the commutator of a conserved charge with a conserved current necessarily produces a conserved current. Later, DASHEN and DASHEN and WEINSTEIN argued that it is only in such theories with approximate chiral symmetry where the use of pion pole dominance is plausible. To illustrate their point of view, let us consider the Goldberger–Treiman relation

$$(2m_N)\,(g_A/g_V) \approx -\,(\sqrt{2}\,F_\pi)\,(\sqrt{2}\,G_{NN\pi}\,, \tag{2}$$

which connects the axial vector coupling constant (g_A/g_V) in nucleon decay with the pion decay constant $(\sqrt{2}\,F_\pi)$ and the charged pion–nucleon Yukawa coupling constant $(\sqrt{2}\,G_{NN\pi})$. The most popular, though perhaps not most considerate derivation starts by assuming an unsubtracted dispersion relation in momentum transfer for the form factor of the weak axial divergence

$$\langle p\,|\partial A^W|\,n\rangle = i(2\,m_N)\bar{U}_p\gamma_5 G(\Delta^2)U_n \tag{3}$$

with

$$G(0) = (g_A/g_V)$$

and

$$2m_N\,G(\Delta^2) = \frac{(\sqrt{2}\,F_\pi\,m_\pi^2)\,(\sqrt{2}\,G_{NN\pi})}{\Delta^2 - m_\pi^2} + \frac{1}{2\pi i}\int_{9m_\pi^2}^{\infty} \frac{\operatorname{disc} G(s)}{s-\Delta^2} \tag{4}$$

and then retains only the pion pole contribution for $\Delta^2 \approx 0$, disregarding the three-pion and higher cuts (and any anomalous thresholds) which start at $\Delta^2 = 9m_\pi^2$ and above. The 10% disagreement of the Goldberger–Treimann relation is then sometimes quoted as an illustration of the principle that the influence of singularities can be estimated by the inverse of their distance from the point of comparison. Such a principle, however, would entirely disregard the possibility of the singularities having different strengths, i.e. different sizes of pole residues and cut discontinuities. This is particularly relevant in the present case, as the pion pole residue contains the factor m_π^2 which is to be considered small to the same extent as the pole denominator is considered small. To maintain pole dominance, we require that the cut discontinuity be similarly small, i.e. of the order $0(m_\pi^2)$ like the pole residue. To see how stringent a requirement this is, we consider a model for some typical cut contributions to the Goldberger–Treiman relation.

From among the contributions to the three-pion cut

$$\operatorname{disc} G(s) \sim \sum_N \delta(m_N^2 - s) < 0\,|\partial A^W|\,N\rangle\,\langle N\,|\,n\bar{p}\rangle \tag{5}$$

we select the intermediate states $|\varrho\pi\rangle$. Just to estimate orders of magnitude, let us suppose that the strong interaction matrix element $\langle\varrho\pi\,|\,n\bar{p}\rangle$ is adequat-

ely characterized as being of the same order of magnitude as the pion–nucleon coupling constant $G_{NN\pi}$; we then have to demand that $\langle 0 \mid \delta A \mid \varrho\pi \rangle$ should be of order $0(m_\pi^2)$, to make the Goldberger–Treiman relation plausible. To illustrate that this is not obvious, we rewrite

$$\langle 0 \mid \delta A \mid \varrho\pi \rangle = (i)\ (p^\varrho + p^\pi)_\mu\ \langle 0 \mid A^\mu \mid \varrho\pi \rangle \tag{6}$$

and we make a simple model for the terms $\langle 0 \mid A^\mu \mid \varrho\pi \rangle$ of two Feynman graphs (Fig. 1):

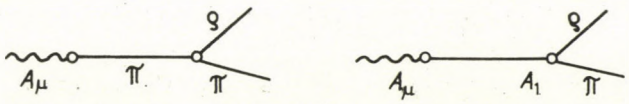

Substituting contemporary estimates for the coupling constants, we find that each one of the contributions exceeds considerably the required order $0(m_\pi^2)$, and the Goldberger–Treiman relation can only be plausibly maintained if there is a near-cancellation among them. The only understood mechanism — to our present knowledge — to provide such a cancellation is the proximity of our world to a chiral symmetry limit with all matrix elements of ∂A being proportional to m_π^2. Indeed, we find the required cancellation if we substitute the coupling constants and their signs as prescribed by the appropriate chiral Lagrangians. The details are presented in [8].

In summary we find an interesting situation: pion-pole dominance may be exactly valid only in the limit of chiral symmetry. The same effects which are responsible for the non-conservation of the axial current, also limit the application of pion-pole dominance to its divergence. Turning this argument round, we may arrive at a working hypothesis which generalizes MANDELSTAM's result (see above) to theories with finite pion mass: To the same accuracy as we accept pion-pole dominance, we are bound to find the vector current in the commutator of two axials [Eq. (1)] conserved, or alternatively: any possible non-conservation of the vector current in the commutator of two axials is associated with corrections to pion-pole dominance and cannot be seen in the tests where pion-pole dominance is used as an approximation.

This is an example of how statements on current algebra and meson-pole dominance can become interrelated. We suggest that there is a certain overlap of information. Although current algebra by itself may be formulated in a variety of theories with or without pion-pole dominance, the principle of pion-pole dominance for the axial divergence — which is not obvious by itself — implies definite information on possible current algebra structures. Our objective will be to study this information in definite models and also to extract

further constraints following from the related hypothesis of vector and axial vector meson dominance for the transversal components of the currents.

There is one piece of information, however, characteristic of current algebra, which we can never hope to extract from meson-pole dominance or related dynamical principles: the specification of the scale of the weak axial current. This is because we have always been treating weak interactions exacty. Recalling that on this level weak couplings enter the unitarity relations only in a linearized form, we see that we can never determine their scale.

The best we can, therefore, hope to deduce from meson-pole dominance orl related principles is a statement that, within the model considered, we can make the same deductions as if we had assumed the following current algebra:

$$[\int \hat{A}_0^i(x)\,(dx)^3,\ \int \hat{A}_0^j(x)\,(dx)^3] = ie^{ijk}(\alpha^2)\int \hat{V}_0^k(x)\,(dx)^3. \tag{7}$$

We have denoted the currents of the model by a caret, to distinguish them from the physical currents for which we have $\alpha = 1$, according to GELL-MANN. Obviously, once we have Eq. (7), we can always replace $\hat{A}_\mu^i$ by $\alpha \hat{A}_\mu^i = A_\mu^i$ by merely rescaling weak coupling constants. To first order, this does not cause any inconsistencies.

At present, we are unable to make any further statements on general grounds, and we turn to the study of specific models.

1. Tree-graph model for pion amplitudes

Most of the credit for this Section is due to J. ELLIS.

The prediction of pion scattering amplitudes has been a very fruitful field of application for current algebra. Using chiral Lagrangians, we obtain a tree graph model, with the one-pion irreducible parts taken to second order in the momenta. This prediction is proposed to be valid for low energies: $p^2 \ll m_\varrho$.

We want to see to what extent we can reproduce such a model without assuming current algebra. The only assumption we will make is the postulate of ADLER zeros: a pion amplitude is required to vanish wherever we extrapolate one pion to zero energy-momentum and leave to the others on mass-shell. As it is well known, ADLER zeros are a consequence of pion-pole dominance for the divergence of the axial current.

$$\langle f|\pi(P), i\rangle = \frac{(p^2 - m_\pi^2)}{F_\pi m_\pi^2}\langle f|\partial A|i\rangle = \frac{(p^2 - m_\pi^2)}{F_\pi m_\pi^2}\cdot (iP)^\mu \langle f|A_\mu|i\rangle, \tag{8}$$

$$\to 0 \text{ as } p \to 0.$$

As a preliminary, we study the four-pion amplitude. To second order in the momenta, on and off-shell, its most general form has been given by WEINBERG

$$\langle \pi_\alpha \pi_\beta | \pi_\gamma \pi_\delta \rangle = \delta_{\alpha\beta}\delta_{\gamma\delta}(A + B(p_\alpha + p_\beta)^2 + C\,((p_\alpha - p_\gamma)^2 + (p_\alpha - p_\delta^2)) + \\ + \text{(permutations in isospin indices)}. \tag{9}$$

ADLER zeros give the constraint

$$A + (B + 2C)m_\pi^2 = 0. \tag{10}$$

From the scale of the axial current [Eq. (1)], WEINBERG deduces

$$(C - B) = 1/F_\pi^2. \tag{11}$$

To fully determine the amplitude, yet another input is needed: an assumption on the mode of chiral symmetry breaking. Excluding σ terms of isospin two from the four-pion amplitude, WEINBERG derives $C = 0$. This, however, is not a deduction from current algebra alone, and any value of C can in fact be reproduced from a standard chiral Lagrangian by making a suitable assumption on the mode of chiral symmetry breaking.

We see that for the four-pion amplitude, Eq. (11) is the only deduction from current algebra, not implied in meson pole dominance [Eq. (1)]. Through the size of the pion decay constant F_π, it fixes the scale of the weak axial current in terms of strong interaction parameters, as discussed above, yet it contains a further piece of information: the fact that $(C - B)$ is positive. This is necessary for a compact $SU_2 \times SU_2$ current algebra to hold, rather than a non-compact SO (3, 1) or E_3. As J. ELLIS has shown in detail, the construction of chiral Lagrangians can be performed without difficulties with these generalized current algebras, and ADLER zeros can be guaranteed by a suitable choice of the pion interpolating field

$$\partial A^i = F_\pi^2 m_\pi^2 \varphi_\pi^i. \tag{12}$$

Nevertheless, there is a striking physical difference between theories with compact and non-compact current algebras, which cannot be removed just by rescaling pure weak-interaction quantities. Consider, for instance, the ADLER WEISBERGER relation for $(\pi\pi)$ scattering which would follow from a generalized current algebra:

$$[\int A_0^i(x)\,(dx)^3, \int A_0^j(y)\,(dy)^3] = ie^{ijk} \cdot \alpha \cdot \int V_0^k(x)\,(dx)^3. \tag{13}$$

$$\alpha = (F_\pi)^2 \int_{(2m_\pi)^2}^{\infty} \frac{ds}{(s - m_\pi^2)^2} \left(\sigma_{\pi^+\pi^-}^{\text{tot}}(s) - \sigma_{\pi^+\pi^+}^{\text{tot}}(s)\right) \frac{2P_\pi^{\text{L}} m_\pi}{\pi}. \tag{14}$$

Obviously $\alpha \leq 0$ would demand $\sigma^{\text{tot}}_{\pi^+\pi^+} s \geq \sigma^{\text{tot}}_{\pi^+\pi^-}$, at least in average, which is totally at odds with our present understanding. By assuming absence of exotic states, the non-compact current algebra can be excluded fairly trivially (since noncompact algebras cannot have finite dimensional unitary representations), but we will see in the next section that we can also exclude them through vector meson dominance — which may be less trivial.

To complete the discussion of the pion model, we ought to see whether the present balance of information continues to hold for many-pion amplitudes: given any three-graph model for pion interactions with second order polynomials in the momenta to approximate the one-pion irreducible parts and with ADLER zeros, we can always find a generalized chiral Lagrangian which reproduces the model, utilizing three sources of indeterminacy:

1. the scale of the axial current (α) in terms of Eq. (13);
2. the compactness property of the algebra (sign α in terms of Eq. (13));
3. the mode of chiral symmetry breaking.

For the four-pion amplitude, this statement follows trivially from the proceding discussion: for the $(2N)$ pion amplitude let us use an inductive argument to balance the degrees of freedom.

Assuming that we have chosen the amplitudes for $(2N-2)$ pions in accordance with ADLER zeros, we have no longer any freedom in constructing the reducible parts of the $(2N)$ pion amplitudes, and new information may come only from an irreducible "contact" contribution. Assuming that there are two possible choices, say C_1 and C_2, for this contact term, we realize that the difference $(C_1 - C_2)$ must have all the ADLER zeros by itself. As J. ELLIS has shown in detail, there is only one such form for $(2N) \geq 6$ pions:

$$(C_1 - C_2) = \gamma_N \left\{ \left(\sum_{i=1}^{2N} p_2^i \right) - (2N-1) m_\pi^2 \right\} \tag{15}$$

with an unspecified multiplicate constant γ_N. We now realize the restrictive power of the requirement of ADLER zeros: only N constants are left free in the construction of a $(2N)$-pion amplitude.

The same can be seen to be the case for (generalized) chiral Lagrangians. We concentrate here on the case of $SU_2 \times SU_2$; the cases of SO(2,2) and E_3 are similar. Let us recall some details in the construction of chiral Lagrangians.

Once the pion field has been chosen according to Eq. (11) to guarantee ADLER zeros, and the scale of the axial current has been set by identifying the pion decay constant F_π, the kinetic part of the chiral Lagrangian is uniquely determined in terms of covariant derivatives, and the only freedom left is in the construction of the chiral symmetry breaking generalized pion mass term

$$H^{(B)} = \sum_{n=1}^{\infty} a_n H_n, \tag{16}$$

where the operators H_n are the isoscalar parts of the $SU_2 \times SU_2$ operator multiplets $(n/2, n/2)$. Their construction in terms of pion fields

$$H_n = \sum_{i=0}^{\infty} b_n^i (\varphi^2)^i \tag{17}$$

is uniquely fixed, once Eq. (11) has been imposed: however, their relative weights are unconstrained.

Collecting terms of second order in the pion fields we set

$$\frac{m_\pi^2}{2} = \sum_{n=1}^{\infty} a_n b_n^1 . \tag{18}$$

Terms of N^{th} order give just one unspecified contact term

$$C_N = \sum_{n=1}^{\infty} a_n b_n^N \tag{1'}$$

which can be given any value, to match the indeterminacy of γ_N in Eq. (15) by suitably adjusting the parameters a_n. This completes the present demonstration; more detailed arguments can be found in [8] and [9].

Before leaving the subject, let us recall that despite the indeterminacies left after imposing ADLER zeros in pion amplitudes, MANDELSTAM's suggestion has been verified in the present model: the theory with meson-poles dominanc is always equivalent to one where the commutator of two axial currenaeproduces a conserved vector current.

2. The $\langle A, A, V \rangle$ vertex

As a first step to include effects of vector and axial vector meson dominance, we investigate a classic object: the vertex of one vector and two axial currents. After many attempts, its structure has been clarified by SCHNITZER and WEINBERG with the joint use of current algebra and a specific form of meson-pole dominance. As regards meson-pole dominance, we shall make the same assumptions as SCHNITZER and WEINBERG did: the only singularities we allow will be poles of A_1, ϱ and π-mesons and the irreducible vertices will be constrained to be low-order polynomials in the momenta in the problem.

As regards current algebra, we continue to assume the isospin algebra and the commutators of axial vector currents with vector currents, but we do not make any specific assumption about the commutator of two axial currents

$$[\int A_0^i(x)\,(dx)^3,\, A_\mu^j(y)]^{\text{def}} = i\tilde{X}_\mu^{ij}(y) . \tag{20}$$

$\widetilde{X}^{ij}_{\mu}(y)$ is taken to be some unspecified vector current; only its isospin-one component enters the problem.

It can easily be seen that the commutator of two axial currents contributes only in one Ward identity:

$$\begin{aligned} 0 = {} & ip^{\mu} \cdot \int\int (dx)^4 (dy)^4 \, e^{ipx} \, e^{ipy} \langle 0 | T^x \left\{ A^i_{\mu}(x), A^j_{\nu}(y), V^k_{\lambda}(0) \right\} | 0 \rangle + \\ & + \int\int (dx)^4 (dy)^4 \, e^{ipx} \, e^{ipy} \langle 0 | T^x \left\{ \partial A^i(x), A^j_{\nu}(y), V^h_{\lambda}(0) \right\} | 0 \rangle + \\ & + i \int\int (dx)^4 \, e^{i(p+q)x} \langle 0 | T^x \left\{ \widetilde{X}^{ij}_{\nu}(x), V^k_{\lambda}(0) \right\} | 0 \rangle - \\ & - i \, e^{ijk} \int\int (dy)^4 \, e^{iqy} \langle 0 | T^x \left\{ A^j_{\nu}(y), A^j_{\lambda}(0) \right\} | 0 \rangle . \end{aligned} \tag{21}$$

In the third term, only intermediate states of total spin-one can contribute, since for all others $< 0 \,|\, V^k_{\lambda} |\, s >$ would vanish. So only the transversal components of $\widetilde{X}^{y}_{\nu}$ enter the calculation; longitudinal components, if at all possible, cannot contribute. So, within the framework of the present calculation, $\widetilde{X}^{ij}_{\nu}$ acts like a conserved current of isospin one

$$\widetilde{X}^{ij}_{\mu} = e^{ijk} \, X^k_{\mu}. \tag{22}$$

Using now our specific meson pole structure, we see that the ϱ-meson is the only possible intermediate state in the third term of Eq. (21) to cause a singularity in $(p+q)^2$. This has the effect of confining all the information about X_{μ} to a single coupling constant:

$$\langle 0 \mid X^k_{\mu} \mid \varrho \rangle = \alpha \langle 0 \mid V^k_{\mu} \mid \varrho \rangle = \langle 0 \mid \alpha V^k_{\mu} \mid \varrho \rangle \tag{23}$$

with the parameter a being defined through Eq. (23). So, we find again the same predictions from meson pole dominance alone as if we had assumed in addition:

$$[\int A^i_0(x) \, (dx)^3, A^j_{\mu}(y)] = i e^{ijk} \alpha \, V^k_{\mu}(y). \tag{24}$$

The non-trivial aspect of this model is the fact that there we can demonstrate that α has to be positive for consistency. The details of the algebra are unfortunately somewhat long; they have been presented in a paper by J. DE AZCARRAGA and the present author. The important fact is that, for consistency of the solution of the Ward identity in terms of reduced vertices, the first Weinberg sum rule has to be satisfied, which reads in the present case:

$$F^2_{\pi} + \frac{f^2_A}{m^2_A} = \alpha \frac{f^2_{\varrho}}{m^2_{\varrho}} . \tag{25}$$

Positivity requires $\alpha \geq 0$; a non-compact alternative to the usual $SU_2 \times SU_2$ current algebra is not compatible with vector meson dominance.

3. Hopes and conclusions

It is fairly difficult to judge what has been achieved so far. The outcome will lie somewhere between two extremes:

1. It may turn out that the systems studied so far have reproduced the current algebra structures from meson pole dominance because of their limited degrees of freedom. As soon as we study more complicated systems, new sources of indeterminacy will open up. Even in this case we would attach some value to the recognition that the examples so far studied, which have been chosen from among the standard applications of current algebra, have not tested the theory to any greater extent than to a scale factor. We would have to call even more intensely for neutrino data to properly test its validity.

2. It may also turn out that a very considerable amount of current algebra structures may be deduced from a dynamical hypothesis like meson pole dominance. Dominance of single mesons in certain channels is not the most realistic principle, however, in our contemporary understanding of strong-interaction dynamics. Both the recent successes of duality theories with infinite recurrences and the still unexplained dipole fits to nucleon electromagnetic form factors clearly demonstrate the need for a different dynamics than based on nearby singularities. The hope remains, however, that the present model studies may lead to the formulation of new concepts which may eventually allow us to search for relations between current algebra and more realistic dynamical theories, like those based on duality.

REFERENCES

1. M. GELL-MANN, Phys. Rev., **125,** 1067, 1962.
2. S. L. ADLER, Phys. Rev. Letters, **14,** 1051, 1965.
3. W. I. WEISBERGER, Phys. Letters, **14,** 1047, 1965.
4. S. WEINBERG, Rapporteur's Review at the 14th International Conference on High Energy Physics, Vienna, 1968, p. 253.
5. R. F. DASHEN and M. WEINSTEIN, Phys. Rev., **183,** 1245, 1969; R. F. DASHEN and M. WEINSTEIN, Phys. Rev., **183,** 1261, 1969.
6. S. MANDELSTAM, Phys. Rev., **168,** 1884, 1968.
7. S. L. ADLER, Phys. Rev., **137,** B 1022, 1965.
8. B. RENNER, Schladming lectures 1970. Acta Physica Austriaca, Suppl. VII. 91, 1970.
9. J. ELLIS, Nuclear Physics, **B21,** 217, 1970.
10. S. WEINBERG, Phys. Rev. Letters, **17,** 616, 1966.
11. H. SCHNITZER and S. WEINBERG, Phys. Rev., **164,** 1828, 1967.
12. J. DE AZCARRAGA and B. RENNER, Nuclear Physics, **B23,** 236, 1970.

О ВОЗМОЖНЫХ СВЯЗЯХ МЕЖДУ АЛГЕБРОЙ ТОКОВ И АППРАКСИМАЦИЕЙ МЕЗОННЫМИ ПОЛЮСАМИ

Б. РЕННЕР

Резюме

Предложена идея, согласно которой между информациями, получаемыми из алгебры токов и принципов аппраксимации мезонными полюсами имеется частичное совпадение. На простых моделях показано, что результаты алгебры токов с точностью до неизвестной калибровки слабого аксиального тока могут быть получены для мезонов из одних принципов аппраксимации мезонными полюсами. Доказывается, что некомпактный вариант обычной $SU_2 \times SU_2$ алгебры токов является несовместимым с аппраксимацией мезонными полюсами.

Acta Physica Academiae Scientiarum Hungaricae, Tomus 31 (1—3), pp. 251—258 (1972)

CURRENT COMMUTATORS AT SMALL TIME DIFFERENCES

By

I. FARKAS and G. PÓCSIK

INSTITUTE FOR THEORETICAL PHYSICS, ROLAND EÖTVÖS UNIVERSITY, BUDAPEST

Using the equal-time current algebra and the divergence conditions, we calculate the current commutators for small time differences. It is shown that the commutators are explicitly model-dependent and the contributions of the symmetry-breaking terms do not drop out. The physical content of the current commutators of non-equal time is discussed in terms of new sum rules. We point out that the disconnected contributions are necessary for the consistency of the sum rules. The sum rules favour the field algebra.

I. Introduction

In spite of the enormous successes of the equal-time current algebra, extension of the current commutators for non-equal times is an urgent and difficult task. Up to now, the motivation for generalized current algebra is twofold.[1] In order to clarify the meaning of the infinite momentum method, attempts have been made for an extension of the current algebra near the light cone [1, 2]. 2. The light cone commutators control the high energy behaviour, therefore theories of generalized current algebras were developed on the light cone [3, 4, 5] to study inelastic processes at high energies.

These generalized current algebras are, however, postulated with a certain arbitrariness, as far as the compatibility with the divergence conditions (*PCAC*, *CVC*, etc.) and the presence of the symmetry-breaking terms are concerned. In Section II we show that the equal-time current algebra and the divergence conditions determine the extension to non-equal times, at least in a small strip along the space-axis. It is explicitly seen that the generalized commutators are model-dependent and, in general, the contributions of the symmetry-breaking terms do not drop out.

The next question concerns the physical content of the generalized current commutators (Section III). In the case of conserved vector currents we describe a simple method leading to sum rules. The new system of sum rules becomes inconsistent if one neglects the disconnected contributions. The sum rules favour the field algebra.

II. Non-equal-time current commutators

We confine ourselves to $SU_3 \times SU_3$ algebra and write [6]

$$[j_0^a(x), J_\mu^b(y)]_{x_0=y_0} = if_{abc}\,\delta(\bar{x}-\bar{y})\,[jJ]_\mu^c(x) + S(j_0, J_\mu)\,. \tag{1}$$

Here j_μ^a, J_μ^a are vector or axial vector currents, $S(j, J)$ means possible gradient terms and $[j\ J]$ is a suitable vector or axial vector current, $[VA] = [AV] = A$, $[AA] = [VV] = V$. We suppose that the current divergences are given *(CVC, PCAC)*

$$\partial_\mu j_a^\mu = d_a, \quad \partial_\mu J_a^\mu = D_a. \tag{2}$$

To calculate the current commutators at small time differences, we subject $j_0^a(x)$ to a small time translation; then our task is reduced to the calculation of

$$\left[\frac{\partial_0^n\, j_0^a(\bar{x}, y_0)}{\partial y_0^n}\,, J_\mu^b(y)\right]$$

and this can be done for the first few derivatives.

Case $n = 1$. First, let us take $\mu = 0$ and substitute (1) and (2); we get

$$\begin{aligned}[\partial_0 j_0^a(\bar{x}, y_0),\ J_0^b(y)] &= [d^a(\bar{x}, y_0),\ J_0^b(y)] + \\ &+ i\,f_{abc}\,[j\,J]_k^c(y)\,\partial_k\,\delta(\bar{x}-\bar{y}) + \partial_k\,S(j_k,\ J_0),\ \ k = 1, 2, 3.\end{aligned} \tag{3}$$

The commutator on the right-hand side can be taken from the localized version of GELL-MANN, OAKES and RENNER's charge-current divergence commutator [7], so, this term carries the symmetry breaking and it is not compensated by other terms.

The case $\mu = k$ is more difficult because of the unknown (although small) $[d^a, J_k^b]$ [8]:

$$\begin{aligned}[\partial_0 j_0^a(\bar{x}, y_0),\ J_k^b(y)] &= [d^a(\bar{x}, y_0),\ J_k^b(y)] + \\ &+ i\,\alpha f_{abc}\,[j\,J]_0^c(y)\,\partial_k\,\delta(\bar{x}-\bar{y}) + \alpha\,\partial_i\,S(j_i J_k),\end{aligned} \tag{4}$$

where $\alpha = 0$ for field algebra and $\alpha = 1$ for quark algebra. For conserved SU_3 vector currents the term $[d^a, J_k^b]$ is absent.

Case $n = 2$. The corresponding commutator remains, in general, unknown (except for special cases) due to the presence of the symmetry-breaking terms.

For $\mu = 0$ one gets [9]:

$$\begin{aligned}[\partial_0^2 j_0^a(\bar{x}, y_0), J_0^b(y)] &= [\partial_0\, d^a(\bar{x}, y_0), J_0^b(y)] - \\ &- [\partial_i j_i^a(\bar{x}, y_0), D^b(y)] + if_{abc}\,\partial_0\,[jJ]_k^c(y)\,\partial_k\,\delta(\bar{x}-\bar{y}) - \\ &- i\alpha f_{abc}\,\partial_k^y\big(\partial_k\,\delta(\bar{x}-\bar{y})\,[jJ]_0^c(y)\big] + \partial_k\,\partial_0\,S(j_k, J_0) - \alpha\,\partial_l^y\,\partial_k\,S(j_k, J_l)\,.\end{aligned} \tag{5}$$

The first two commutators on the right-hand side are absent in the case of SU_3-symmetric vector currents, $d^a = D^a = 0$, while, in general, they are determined by

$$\partial_0[d^a,\ J_0^b] - [d^a,\ D^b] - [d^a,\ \partial_k\ J_k^c] - [\partial_k J_k^a,\ D^b]. \tag{6}$$

We again take the first term from [7]; the second term vanishes in some simple cases, for example, by requiring canonical equal-time commutation relations for pion and kaon-field operators, etc.

In case of $\mu = k$

$$[\partial_0^2\, j_0^a(\bar{x},\ y_0),\ J_k^b(y)] = [\partial_0 d^a(\bar{x},\ y_0),\ J_k^b(y)] + \partial_l^x[\partial_0\, j_l^a(\bar{x},\ y_0),\ J_k^b(y)]. \tag{7}$$

When $d^a \neq 0$, the first term of the right-hand side is non-vanishing [8]; the second term is known at present only in field algebra.

Finally, let us remark that the commutator $n = 3$ is completely known in field algebra for SU_3-symmetric vector currents. At the same time, in the case $n = 4$, only the commutator $\mu = 0$ is known.

Summarizing, we see that the current commutator of non-equal time depends on the model from which the equal-time commutator of the space components is calculated, and, it depends also on the value of the divergence of the current.

III. Sum rules

For the sake of simplicity we shall deal with SU_3-symmetric vector currents, $d_a = 0$, and consider $[V_0^a(x),\ V_l^b(y)]$, $l = 1,\ 2,\ 3$ for $x_0 = y_0$ small enough. From Section II one writes

$$\begin{aligned}\left[V_0^a\left(\frac{1}{2}x\right),\ V_l^b\left(-\frac{1}{2}x\right)\right] &= i f_{abc}\,\delta(\bar{x})\,V_l^c\left(-\frac{1}{2}x\right) S(V_0, V_l) + \\ &+ \alpha x_0\,\partial_k\,\delta(\bar{x})\left[\delta_{kl} f_{abc}\ V_4^c\left(-\frac{1}{2}x\right) - i\varepsilon_{klm}\times\right. \\ &\left.\times\left(\sqrt{\frac{2}{3}}\,\delta_{ab}\ A_m^0\left(-\frac{1}{2}x\right) + d_{abc}\,A_m^c\left(-\frac{1}{2}x\right)\right)\right],\end{aligned} \tag{8}$$

provided x_0 is small.

Let us take (8) between spinless single particle states of the same mass and show how one gets sum rules if an expansion like (8) is given.

We introduce the following notation

$$P_\mu = \frac{1}{2}(p_{1\mu}+p_{2\mu}),\ Q_\mu = \frac{1}{2}(q_{1\mu}+q_{2\mu}),$$

$$\Delta_\mu = p_{2\mu}-p_{1\mu} \equiv q_{1\mu}-q_{2\mu},\ \nu = PQ,\ t = \Delta^2, \tag{9}$$

$$t^{ab}_{0t}(p_1; p_2; Q) = \int_{-\infty}^{\infty} e^{iQx}\left\langle p_2\left|\left[V^a_0\left(\frac{1}{2}x\right), V^b_l\left(-\frac{1}{2}x\right)\right]\right|p_1\right\rangle d^4x \tag{10}$$

and

$$g(z) = \frac{e^{iz\delta}-1}{iz}, \tag{11}$$

where δ is a small parameter, and we choose $p_1 \neq p_2$. Assuming $S(V_0,\ V_l)$ is a c-number, from (8) and (10) we arrive at the sum rule:

$$\frac{1}{2\pi}\int_{-\infty}^{\infty} dQ_0\, t^{ab}_{0l}(p_1; p_2; Q)\, g(k_0-Q_0) =$$
$$- if_{abc}\, P_l\, F^c(t)\, g\left(k_0 - \frac{1}{2}\Delta_0\right) - i\alpha f_{abc}\, F^c(t)\, P_0 \times \tag{12}$$
$$\times \left(Q_l - \frac{1}{2}\Delta_l\right)\frac{dg(z)}{dz}\bigg|_{z=k_0-\frac{1}{2}\Delta_0}$$

The axial vectors A^0_m, A^c_m and $S(V_0,\ V_l)$ could not give any contributions to Eq. (12).

The form factor $F^c(t)$ is defined by the equation

$$\langle p_2 \mid V^c_\mu(0) \mid p_1 \rangle = F^c(t) P_\mu. \tag{13}$$

Since in (8) we have kept only the first derivative, the sum rule (12) contains terms of order δ and δ^2, everything else has to be neglected. It is, however, important that this must be done after having calculated the integral (12), otherwise extra convergence problems could appear.

The matrix element $t^{ab}_{\mu\nu}(p_1;\ p_2;\ Q)$ can be decomposed into its invariant parts in the following way:

$$t^{ab}_{\mu\nu}(p_1; p_2; Q) = a_1 P_\mu P_\nu + a_2 P_\mu \Delta_\nu + a_3 P_\mu Q_\nu + a_4 \Delta_\mu P_\nu + a_5 \Delta_\mu \Delta_\nu + \tag{14}$$
$$+ a_6 \Delta_\mu Q_\nu + a_7 Q_\mu P_\nu + a_8 Q_\mu \Delta_\nu + a_9 Q_\mu Q_\nu + a_{10} g_{\mu\nu}$$

with invariants a_i dependent on ν, t, q_1^2, q_2^2. Substituting (14) into (12) we get:

$$\frac{1}{2\pi}\int_{-\infty}^{\infty} dQ_0(a_1 P_0 + a_4 \Delta_0 + a_7 Q_0) g(k_0 - Q_0) = \\ = i f_{abc} F(t)\left[\delta + \frac{1}{2} i\delta^2 \left(k_0 - \frac{1}{2}\Delta_0\right)\right], \tag{15}$$

$$\frac{1}{2\pi}\int_{-\infty}^{\infty} dQ_0(a_2 P_0 + a_5 \Delta_0 + a_8 Q_0) g(k_0 - Q_0) = \\ = -\frac{1}{2}\alpha f_{abc} P_0 F^c(t) \frac{1}{2}\delta^2, \tag{16}$$

$$\frac{1}{2\pi}\int_{-\infty}^{\infty} dQ_0(a_3 P_0 + a_6 \Delta_0 + a_9 Q_0) g(k_0 - Q_0) = \\ = \alpha f_{abc} F^c(t) P_0 \frac{1}{2}\delta^2. \tag{17}$$

As we have remarked, the left-hand sides of Eqs. (15)–(17) must be considered in the order δ^2 after integration. If we would expand $g(k_0 - Q_0)$ in δ, the sum rules obtained immediately from the equal-time commutators $[\partial_0^n j_0^a, J_\mu^b]$ would be exactly recovered. Keeping the terms of order x_0^2 in (8), even the terms of order δ^3 would be exact in Eqs. (15)–(17).

The advantage of the equations such as (15)–(17) is that they include information coming from the usual current algebra and the time derivatives (in the present example $n = 1$, see Eq. (4)). At the same time, they show the usual dependence on the reference system [10, 11] and also a model-dependence through α.

In what follows we derive the $P_0 \to \infty$ sum rules. First let us assume that the limit $P_0 \to \infty$ may be taken under the integrals (15)–(17); then we are led to a contradiction. To see this, we first define the $P_0 \to \infty$ system [11]

$$P^\mu = (\gamma\sqrt{P^2},\ 0,\ 0,\ -\gamma\sqrt{P^2}),\ \Delta_\mu = (0,\ \Delta_1,\ \Delta_2,\ 0), \\ Q_\mu = (Q_3,\ Q_1,\ Q_2,\ Q_3),\ dQ_0 = \frac{d\nu}{\gamma\sqrt{P^2}}, \\ \gamma \to \infty. \tag{18}$$

q_1^2, q_2^2 become independent of ν. Then, we get from Eq. (15) in the limit $P_0 \to \infty$

$$\frac{1}{2\pi} g(k_0 - Q_3)\int_{-\infty}^{\infty} d\nu\, a_1 = i f_{abc} F^c\left[\delta + \frac{1}{2} i\delta^2 k_0\right]; \tag{19}$$

since $Q_3 \neq 0$, this could be satisfied only by a vanishing form factor. In the same way, Eqs. (16) and (17) are consistent only if $\alpha F^c = 0$, that is in field algebra.

So, we conclude that, in general, the infinite mass contributions are necessary for the consistency of the $P_0 \to \infty$ sum rules [11]. That is, interchanging the limit $P_0 \to \infty$ and the integration over Q_0, the contributions of the disconnected diagrams must be separately taken into account. Let us denote by a_i^d the disconnected contributions to the invariants a_i; then the contributions of the disconnected graphs to the integrals (15)–(17) in the limit $P_0 \to \infty$ are in turn:

$$\lim_{P_0 \to \infty} \frac{1}{2\pi} \int_{-\infty}^{\infty} dQ_0 (a_1^d P_0 + a_7^d Q_0)\, g(k_0 - Q_0) = A_1 \delta + \frac{1}{2} i\delta^2 A_2 , \tag{20}$$

$$\lim_{P_0 \to \infty} \frac{1}{2\pi} \int_{-\infty}^{\infty} dQ_0 (a_2^d P_0 + a_8^d Q_0)\, g(k_0 - Q_0) = B_1 \delta + \frac{1}{2} i\delta^2 B_2 , \tag{21}$$

$$\lim_{P_0 \to \infty} \frac{1}{2\pi} \int_{-\infty}^{\infty} dQ_0 (a_3^d P_0 + a_9^d Q_0)\, g(k_0 - Q_0) = C_1 \delta + \frac{1}{2} i\delta^2 C_2 , \tag{22}$$

where

$$Q_0 = \frac{\nu}{\gamma \sqrt{P^2}} - \beta Q^3 , \quad \gamma = (1 - \beta^2)^{-\frac{1}{2}} . \tag{23}$$

The functions $A_1, \ldots, C_2$ are defined by Eqs. (20)–(22), their detailed forms depend on the dynamics. In pole approximation we know that the disconnected contributions are finite and we have seen that at least one of A_1 and A_2 (B_1 and B_2, C_1 and C_2 in the quark model) is non-vanishing.

Finally, comparing the coefficients of δ and δ^2 in (15)–(17), we get the following sum rules for $P_0 \to \infty$:

$$\frac{1}{2\pi} \int_{-\infty}^{\infty} d\nu a_1 + A_1 = i f_{abc} F^c , \tag{24}$$

$$\frac{Q_3}{2\pi} \int_{-\infty}^{\infty} d\nu a_1 + k_0 A_1 = A_2 , \tag{25}$$

$$\frac{1}{2\pi} \int_{-\infty}^{\infty} d\nu a_2 + B_1 = 0 , \tag{26}$$

$$(Q_3 - k_0)\, B_1 + B_2 = \frac{1}{2} i\alpha P_0 f_{abc} F^c , \tag{27}$$

$$\frac{1}{2\pi} \int_{-\infty}^{\infty} d\nu a_3 + C_1 = 0 , \tag{28}$$

$$(Q_3 - k_0) C_1 + C_2 = -i\alpha P_0 f_{abc} F^c . \tag{29}$$

Here (24), (26), (28) correspond to the usual current algebra sum rules [12], while the others are new ones. For $\alpha = 1$ the right-hand sides of Eqs. (27) and (29) become infinite, since B_2 and C_2 cannot compensate these infinities; only the field algebra ($\alpha = 0$) is consistent with the $P_0 \to \infty$ sum rules [13]. It is, however, important to emphasize that at this conclusion we assume the existence of the integrals of a_2 and a_3 in Eqs. (26) and (28).

IV. Discussion

In the present paper we have shown that the equal-time current algebra and the divergence conditions determine the non-equal-time current commutators in a small strip along the space-axis. The model-dependence and the symmetry-breaking terms in the generalized current commutators were shown. The purpose of Section III was to present such a method which expresses the non-equal-time commutators in terms of sum rules. These generalized sum rules contain also the information coming from the time derivatives [14] and they are significant, for instance, in connection with the theory of high-energy inelastic scattering.

In the specific example based on Eq. (8) we deal with conserved vector currents and get the sum rules (15)–(17) and (24)–(29), respectively, as restrictions for the scattering of scalar and vector particles. Although they verify our general statements above, their immediate evaluation cannot be carried out because of the lack of the experimental data concerning the scattering of spinless and spin-one octet particles. Nevertheless, it is important to establish the crucial role of the disconnected diagrams in (24)–(29) and that the sum rules are compatible with the field algebra provided (26) and (28) converge.

REFERENCES

1. H. Leutwyler, Acta Phys. Austriaca, Suppl. V., 320, 1968.
2. J. Jersak and J. Stern, Nuovo Cimento, **59A**, 315, 1969.
3. S. Okubo, Physics, **3**, 165, 1967.
4. R. A. Brandt, Phys. Rev. Letters, **23**, 1260, 1969.
5. R. L. Ingraham, Preprint, March, 1970.
6. Metric: $+ - - -$
7. M. Gell-Mann, R. J. Oakes and B. Renner, Phys. Rev., **175**, 2195, 1968.
8. From the work of F. Csikor and G. Pócsik, Nuovo Cimento, **42A**, 413, 1966, one concludes $\langle 0 \mid [d^a(\bar{x},y_0)j^a_k(y)] \mid 0\rangle = 0$. The same result follows from the work of S. Okubo Nuovo Cimento, **43A**, 1015, 1966 and D. Boulware and S. Deser, Phys. Rev., **151**, 1278, 1966.
9. $\langle 0 \mid [\partial_0 d^a(\bar{x},y_0)j^a_0(y)] \mid 0\rangle = 0$ see [8]
10. S. Fubini and G. Furlan, Physics, **1**, 229, 1965.
11. D. Amati, R. Jengo and E. Remiddi, Nuovo Cimento, **51A**, 999, 1967.
12. S. Fubini, Nuovo Cimento, **43**, 475, 1966.
13. Similar conclusion has been reached in pole approximation by I. Montvay, Acta Phys. Hung., **25**, 407, 1968.
14. An application for the second time derivative of the chirality operator is treated by I. Farkas and G. Pócsik, ITP-Budapest Report No. 279, June 1970.

КОММУТАТОРЫ ТОКА ПРИ МАЛЫХ ИНТЕРВАЛАХ ВРЕМЕНИ

И. ФАРКАШ и Г. ПОЧИК

Резюме

Используя алгебру токов при равенстве времен, и условия расходимости, рассчитаны коммутаторы тока для малых интервалов времени. Показано, что коммутаторы явно зависят от модели, и вклады от членов, нарушающих симметрию не отнадают. Рассмотрено физическое содержание коммутаторов тока в терминах новых правил сумм. Показано, что для последовательности правил сумм необходимо наличие вкладов несвязанных диаграмм. Правила сумм дают предпочтение алгебре поля.

Acta Physica Academiae Scientiarum Hungaricae, Tomus 31 (1–3), pp. 259–264 (1972)

MEASUREMENT OF THE $K_L + p \to K_S + p$ REGENERATION AMPLITUDE AT HIGH ENERGIES

DUBNA—SERPUKHOV—BUDAPEST COLLABORATION*

The measurement of the K^0 regeneration amplitude in the energy range 15—35 GeV using the Serpukhov proton synchrotron is reported.

1. Introduction

The K^0 regeneration experiment aimed at determining the difference of the complex K^0p and $\bar{K}^0p$ forward scattering amplitudes:

$$\Delta f = f - \bar{f}.$$

This can be done by measuring the $K_L p \to K_S p$ regeneration amplitude, ϱ, since they are related to each other by the following formula:

$$\varrho(p) = \frac{\pi N}{m} i \Delta f(p) \frac{1 - e^{\left(i\Delta m - \frac{\gamma_s}{2}\right)\frac{lm}{p}}}{\frac{\gamma_s}{2} - i\Delta m}.$$

Here N is the number of scattering centres per cm^3. Note that ϱ stands for the quantity known as transmission regeneration amplitude, which is characterized by the fact that all scattering centres act coherently. m and p are the mass and momentum of the incoming kaon, Δm is the K_L—K_S mass difference, γ_s is the total width (or inverse mean life $1/\tau_s$) of the K_S meson, finally, l is the length of the regenerator. We neglect the total width of the K_L, γ_L, in comparison with γ_s.

Experimentally one uses K_L beam, puts into it a regenerator (in our case a 3 m long liquid H_2 target), and counts the number of $\pi^+\pi^-$ decays of the transmission-regenerated K_S mesons downstream the regenerator. The number of this type of decays is given by the following formula:

$$N_{+-}(p,t) = S_L(p)\,\varepsilon(p,t)\cdot\gamma(K_S \to \pi^+\pi^-)\cdot\left\{|\varrho|^2 e^{-\gamma_s t} + |\eta_{+-}|^2 + \right.$$
$$\left. + 2|\varrho|\,|\eta_{+-}|\, e^{-\frac{\gamma_s}{2}t}\cos(\Delta m t + \Phi_\varrho - \Phi_{+-})\right\}, \tag{1}$$

* Presented by E. NAGY, Central Research Institute for Physics, Budapest.

where $S_L(p)$ is the number of K_L mesons just behind the regenerator, $\varepsilon(p, t)$ is the detection efficiency, a function of p and the proper time t, elapsed in the K^0 restframe. The three terms in the bracket have the well-known meaning: close to the regenerator, say at $t \leq 2\,\tau_s$, we observe the regenerated K_S mesons, the intensity of which is rapidly falling off; very far, say at $t \geq 6\,\tau_S$, the $\pi^+\pi^-$ decays occur only because of the CP violation, the intensity of the decays is roughly constant and proportional to $|\eta_{+-}|^2$, often called Fitch level, which is the ratio of rates:

$$|\eta_{+-}|^2 = \frac{\gamma(K_L \to \pi^+\pi^-)}{\gamma(K_S \to \pi^+\pi^-)} .$$

In between one observes the interference of the $K_S \to \pi^+\pi^-$ and $K_L \to \pi^+\pi^-$ decay amplitudes, which offers the possibility to measure the phase difference $\Phi_\varrho - \Phi_{+-}$, Φ_ϱ and Φ_{+-} being the phase of ϱ and of η_{+-}, respectively. In conclusion, the time dependence of N_{+-} at fixed K_L momentum, p, gives information on the complex ϱ/η_{+-}, more explicitly on the two real numbers $|\varrho/\eta_{+-}|$ and $\Phi_\varrho - \Phi_{+-}$.

2. Experimental layout

The K_L beam was extracted by the usual technique from the Serpukhov 70 GeV proton synchrotron, putting an Al target into the internal proton beam. Charged particles were removed by a swipping magnet, and γ rays were absorbed by means of a lead filter. The remaining neutral component was collimated so that the average divergence of the beam at the entrance of the 3 m long liquid hydrogen regenerator was about 0.6 mrad.

Behind the regenerator an anticounter ensured that the outgoing particles were neutral. This counter was followed by a magnetic spectrometer [1], shown in Fig. 1. The first part of the spectrometer consisted of a 6 m long decay zone where the $\pi^+\pi^-$ decay took place. The spatial coordinates of the produced two charged tracks were measured before and behind a 2 m long magnet, 10 kG in strength, by wire spark chambers that enabled us to know both the decay position and the three-momentum of the neutral kaon. Crossing geometry, also indicated in the Figure, ensured by triggering counters, strongly disfavoured the registration of $K_L \to 3\,\pi$ decays, and considerably reduced the remaining background from the leptonic three-body decays as well. We had another facility to recognize muonic decay products by letting them traverse a 2 m thick iron wall and then registering them by counters.

The signals from the wire spark chambers and counters were recorded on-line on magnetic tapes, which, in turn were further analysed using off-line geometrical reconstruction [2] and SUMEX type programs.

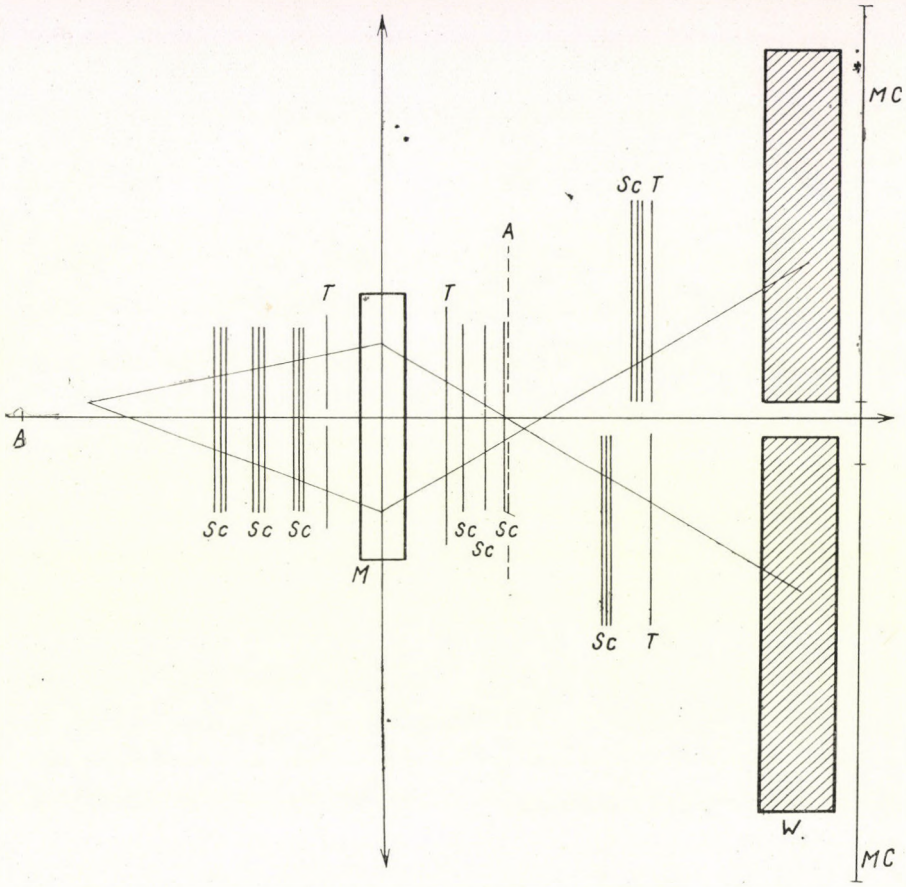

Fig. 1. The magnetic spectrometer. *A* — anticounters, *T* — triggering counters, *SC* — spark chambers, *M* — magnet, *MC* — muon counters, *W* — iron wall

3. Results

The presence of $K_L \to \pi^+\pi^-$ and regenerated $K_S \to \pi^+\pi^-$ decays could have been demonstrated by the effective mass distribution calculated for the reconstructed events assuming that both charged particles were pions. We have observed a narrow peak in this distribution around the K^0 mass with a half-width of $\pm$ 5 MeV in cases when θ^2, the square of the mean deviation of the K^0 meson from the average beam direction was less than 0.6 (mrad)^2 (Fig. 2). On the other hand, inspecting the θ^2 distribution we observed sharp peak in the forward direction (small θ^2) when the effective mass lied around the K^0 mass (Fig. 3).

In order to determine $N_{+-}(p, t)$ (cf. Eq. (1)) we chose therefore events from the mass interval 0.488–0.508 GeV, and for background subtraction we analysed the θ^2 distribution. The number of $\pi^+\pi^-$ decays, N_{+-}, was determin-

ed in each proper time interval by counting down the events having $\theta^2 \leq 0.6$ (mrad)^2 and situated beyond the background level, which latter was fixed using a linear extrapolation from the $\theta^2 > 0.6$ (mrad)^2 region.

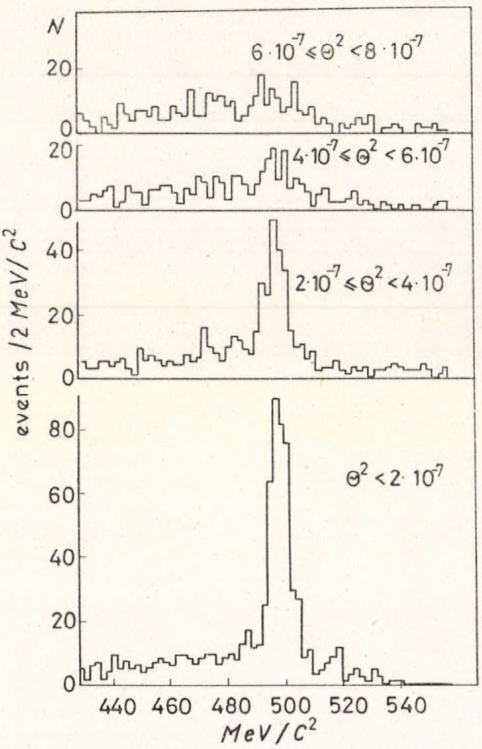

Fig. 2. The effective mass distribution of transmission-regenerated events. Gradually growing peak is observed around the K° mass when θ^2 decreases

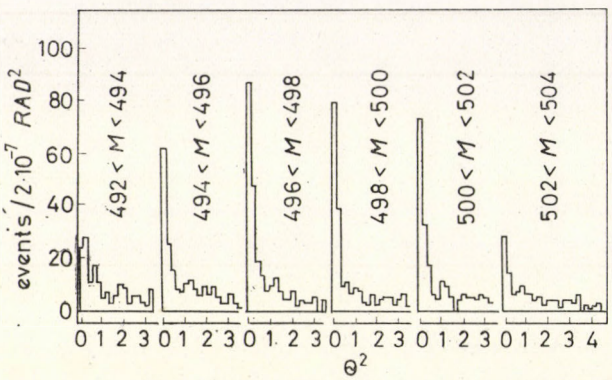

Fig. 3. The θ^2 distribution of events having an effective mass around the K° mass. The forward peak is significantly enhanced when M coincides with the kaon mass

Having calculated $\varepsilon(p, t)$ by Monte Carlo method, we had all to deduce ϱ/η_{+-}. Assuming η_{+-} to be the same as measured at lower energies, we arrived at the final result, presented also at the XVth International Conference in Kiev [3].

Fig. 4 shows $|\Delta f|$ normalised to the kaon momentum, p. The difference of the K^0p and $\overline{K}^0p$ total cross sections

$$\Delta\sigma = \sigma^{tot}_{K^0p} - \sigma^{tot}_{\overline{K}^0p} = \frac{Im\,\Delta f}{4\pi\, p}$$

is plotted in Fig. 5.

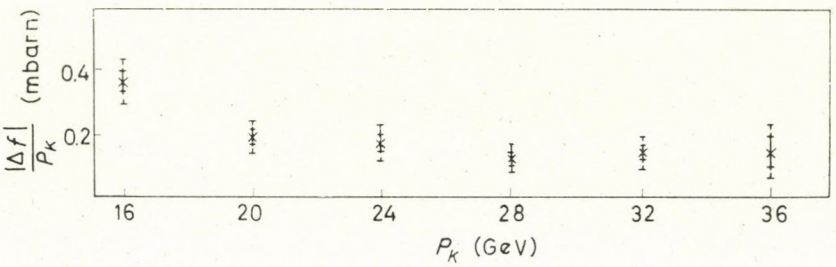

Fig. 4. The quantity $|\Delta f|/p$ as a function of p

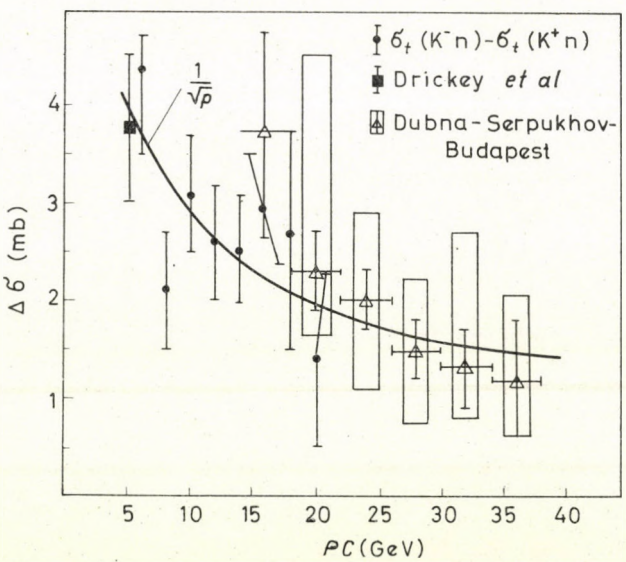

Fig. 5. The behavior of the difference of K^0p and $\overline{K}^0p$ total cross sections as a function of the kaon momentum, p

In both cases errors of two kinds are associated with the experimental points; the smaller ones indicate only statistical fluctuations, whereas the greater error bars take possible systematic errors into account as well.

Because of the rather large errors, no definite conclusion can yet be drawn. We have indication for the maintenance of the Pomeranchuk theorem, and there is some evidence against constant phase models.

REFERENCES

1. S. G. Basiladze et al., Preprint Dubna, P1-5361, 1970.
2. G. Vesztergombi, The Program VILLA 333, to be published.
3. Dubna—Serpukhov—Budapest Collaboration. Presented by I. A. Savin at the XVth International Conference on High Energy Physics, Kiev, 1970.

ИЗМЕРЕНИЕ АМПЛИТУДЫ РЕГЕНЕРАЦИИ $K_L + p \to K_S + p$ ПРИ ВЫСОКАХ ЭНЕРГИЯХ

Совместная работа Дубна—Серпухов—Будапешт

Резюме

Описано измерение амплитуды регенерации K^0 мезонов в интервале энергий 15—35 Гэв, проведенное на Серпуховском ускорителе.

Acta Physica Academiae Scientiarum Hungaricae, Tomus 31 (1–3), pp. 265–272 (1972)

CALCULATION OF COMPLEX-CONJUGATE PAIRS OF REGGE TRAJECTORIES WITH THE SCALAR BETHE–SALPETER EQUATION

By

K. LADÁNYI

RESEARCH GROUP FOR THEORETICAL PHYSICS OF THE HUNGARIAN ACADEMY OF SCIENCES, BUDAPEST

The BETHE–SALPETER equation of scalar particles is reduced to a form which is tractable numerically. This formalism is applied to the numerical calculation of Regge trajectories. Particular attention is paid to the level mixing effects of the mass difference leading to complex-conjugate pairs of trajectories. The calculations include the imaginary part of the total energy at real values of the angular momenta.

I. Introduction

Considerable interest has recently been attached to the properties of the relativistic Bethe-Salpeter (BS) equations [1, 2] in the ladder approximation. The numerical program initiated by SCHWARTZ [3] and SCHWARTZ and ZEMACH [4] demonstrated that the classic work of WICK [5] and CUTKOSKY [6] may be extended by using conventional computational techniques. Following the first calculations, many results have been obtained both in the bound [7] and scattering regions [8]. This development has been exploited in detailed numerical calculations of Regge trajectories for spinless particles [9–10]. CUTKOSKY and DEO [9] found surprising collision phenomena among the trajectories which indicate the existence of complex branches in particular unequal mass situations.

The calculations of CUTKOSKY and DEO are limited to real angular momenta at real values of s (s is the squared energy). This talk is concerned with extending the numerical calculations to complex energies. The explicit computations were done below elastic threshold at real angular momenta. A detailed report of this work will be published elsewhere [11].

II. Reduction of the BS equation

We consider the homogeneous BS equation of two scalar particles with masses m_1 and m_2 which interact via the exchange of a third scalar particle with nonzero mass $\varkappa$. The BS wave function ψ satisfies the differential equation [4]

$$(L-\lambda V)\,\psi = 0\,, \tag{1}$$

where λ is the coupling strength and V denotes the ladder approximation of the interaction. In the center-of-mass system the Wick-rotated operators L and V are

$$L = \left[-\Box + 2\mu_1 E \frac{\partial}{\partial x_4} - \mu_1^2 s + m_1^2 \right] \cdot \left[-\Box - 2\mu_2 E \frac{\partial}{\partial x_4} - \mu_2^2 s + m_2^2 \right], \tag{2}$$

$$V = \frac{4\varkappa}{R} K_1(\varkappa R), \tag{3}$$

$$\Box = \sum_{i=1}^{4} \frac{\partial^2}{\partial x_i^2}, \qquad R = \left(\sum_{i=1}^{4} x_i^2 \right)^{1/2}, \tag{4}$$

where $s = E^2$, E is the total c.m. energy, the x_i' s ($i = 1, 2, \ldots, 4$) denote the components of the relative coordinate, and the parameters μ_1 and μ_2 are constrained by the condition $\mu_1 + \mu_2 = 1$. For the K_1 function we used an approximation proposed by Vosko [12]:

$$yK_1(y) \cong \frac{(1+y)e^{-y} + a(1+2y)\, e^{-2y}}{1+a}, \; a = 0.66746 . \tag{5}$$

We can make the usual separation

$$\psi = \psi_l = \Phi_l(R, \theta)\, Y_{lm}(\vartheta, \varphi), \tag{6}$$

where the angles θ, ϑ, φ are defined by

$$x_1 = R \sin\theta \sin\vartheta \sin\varphi, \; x_2 = R \sin\theta \sin\vartheta \cos\varphi, \; x_3 = R \sin\theta \cos\vartheta,$$
$$x_4 = R \cos\theta.$$

Our starting point is the expansion of ψ_l in terms of the normalized four-dimensional spherical harmonic functions $Y_{nlm}(\theta, \vartheta, \varphi)$:

$$\psi_l = \sum_{q=0}^{\infty} \sum_{h=0}^{\infty} a_{qh} \varphi_{lqh}, \tag{7}$$

$$\varphi_{lqh} = f_{lqh}(R)\, Y_{l+q,\, lm}(\theta, \vartheta, \varphi). \tag{8}$$

Schwartz [3] suggested the following basis functions:

$$f_{lqh}(R) = R^{l+q+h} e^{-\alpha R}, \tag{9}$$

where α is a nonlinear scale parameter.

Instead of the functions φ_{lqh}, Cutkosky and Deo used basis functions

φ'_{lqh} of the form

$$\varphi'_{lqh} = \varphi_{lqh}\, e^{\gamma R \cos\theta} \tag{10}$$

where the parameter $\gamma = \gamma(E)$ was chosen to incorporate the differences in the asymptotic behaviour of the solution when $\cos\theta = \pm 1$. On the other hand, it should be noted that the redefinition

$$\mu_1 \to \mu_1 + \delta, \qquad \mu_2 \to \mu_2 - \delta \tag{11}$$

produces the transformation

$$\psi \to \psi\, e^{\delta E R \cos\theta} \tag{12}$$

in the wave function of the BS equation (1)–(2), but the eigenvalue λ is independent of δ. Thus, the use of the factor exp $[\gamma R \cos\theta]$ (see Eq. (10)) may be avoided by a transformation of the parameters μ_1 and μ_2. In the present calculations we choose the convention $\mu_1 = \mu_2 = 1/2$ and a mass scale in which the external masses are

$$m_1 = 1 + \Delta, \qquad m_2 = 1 - \Delta. \tag{13}$$

It is convenient to introduce a second set of basis-functions χ_{lpk}:

$$\chi_{lpk} = g_{lpk}(R)\, Y_{l+p,\,lm}(\theta, \vartheta, \varphi). \tag{14}$$

In particular, we may choose

$$g_{lpk}(R) = R^{l+p+k}\, e^{-\beta R}. \tag{15}$$

We now can formulate the BS problem (1)–(2) in the space of states defined by the basis functions φ_{lgh} and χ_{lgk}. One obtains the following system of inhomogeneous linear equations

$$\sum_{q=0}^{Q} \sum_{h=0}^{H} \sum_{\nu=0}^{1} \langle \chi_{lpk} | D_{\mu\nu} - \lambda V_{\mu\nu} |\, \varphi_{lqh} \rangle\, a_{qh\nu} = 0 \tag{16}$$

for

$$p = 0,\ 1, \ldots,\ Q, \quad k = 0,\ 1 \ldots,\ H, \quad \mu = 0,\ 1, \tag{17}$$

and $Q \to \infty$, $H \to \infty$. The matrix elements can be written as

$$\langle \chi_{lpk} | B | \varphi_{lqh} \rangle = \int_0^\infty dR R^3 \int_0^\pi d\theta \sin^2\theta \int_0^\pi d\vartheta \sin\vartheta \int_0^{2\pi} d\varphi \chi^*_{lpk}\, B\, \varphi_{lqh}, \tag{18}$$

$$V_{00} = -V_{11} = V, \quad V_{01} = V_{10} = 0, \tag{19}$$

$$D_{00} = -D_{11} = \left[-\Box + 1 + \Delta^2 - \frac{1}{4}(u^2 - v^2)\right]^2 - (u^2 - v^2)\frac{\partial^2}{\partial x_4^2} - 4\Delta u \frac{\partial}{\partial x_4} - \left(4\Delta^2 + \frac{1}{4}u^2 v^2\right), \tag{20}$$

$$D_{01} = D_{10} = uv\left[-\Box + 1 + \Delta^2 - \frac{1}{4}(u^2 - v^2)\right] + 2uv\frac{\partial^2}{\partial x_4^2} + 4\Delta v \frac{\partial}{\partial x_4}, \tag{21}$$

with

$$u = 1/2\,(E + E^*)\; v = \frac{1}{2_i}(E - E^*). \tag{22}$$

In addition, we have

$$a_{qh\acute{o}} = \frac{1}{2}(a_{qh} + a^*_{qh}), \quad a_{qh1} = \frac{1}{2_i}(a_{qh} - a^*_{qh}), \tag{23}$$

where the a_{qh}'s are the coefficients in decomposition (7). The explicit evaluation of the matrix elements is included in [11].

Equations (16)–(17) can be continued in the angular momentum plane, the Regge trajectories correspond to the nontrivial solutions. Approximate solutions of this problem may be calculated by setting finite values of Q and H in Eqs. (16)–(17). The corresponding secular equation is

$$\text{Det}\,|D - \lambda V| = 0, \tag{24}$$

where, of course, the matrix elements

$$\langle \chi_{lpk} | D_{\mu\nu} - \lambda V_{\mu\nu} | \varphi_{lqh} \rangle$$

depend on l, u and v. The solutions of this problem result in the Rayleigh–Ritz approximations [3] by requiring $\chi_{lpk} = \varphi_{lpk}$. On the other hand, we obtain the method of moments if $\chi_{lpk} \neq \varphi_{lpk}$ [13–14]. We emphasize that in these methods unpleasant difficulties may be encountered because the unequal-mass BS problem involves nonhermitean or nondefinite matrices. Our calculations have been carried out by using a generalized least-squares technique. Details of this method can be found in [11].

III. Results and discussion

We computed some Regge trajectories in the region $-4 \leq \text{Res} \lesssim 3.5$, $-0.5 \lesssim l \lesssim 1.5$ ($l = l^*$). All calculations were done for exchanged mass $\varkappa = 1$ and the coupling strength was adjusted as $\lambda = 16.38$ to place the

highest-lying (parent) trajectory of an equal-mass system ($\Delta = 0$) through $l = 1$ at zero energy. The trajectories were calculated by using 14 basis functions φ_{lqh}. Figs. 1–3 do not include results near the threshold and some turning points where the convergence of the results is seen to be poor.

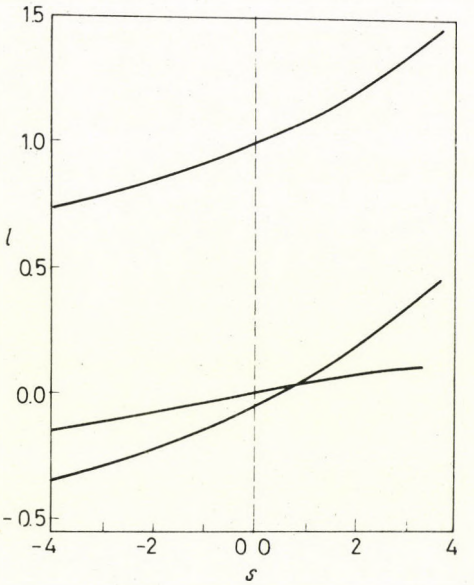

Fig. 1. Regge trajectories for equal-mass systems. The parameters are $\Delta = 0$, $\lambda = 16.38$, $\varkappa = 1$

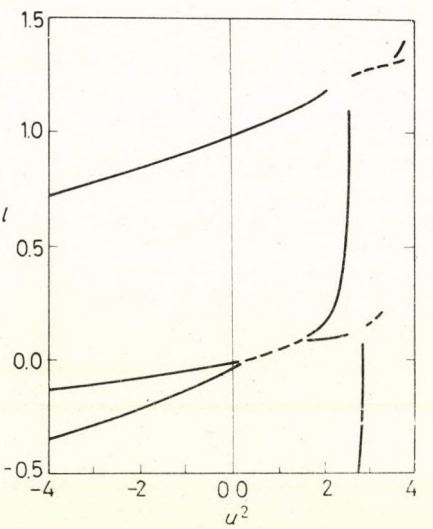

Fig. 2. Effect of the mass difference. The Regge trajectories were obtained for $\Delta = 0.3$, $\lambda = 16.38$, $\varkappa = 1$. Solid lines represent real trajectories at real squared energies. Dashed curves are the complex branches

Fig. 1 shows the equal-mass situation ($\Delta = 0$). We observe two intersecting trajectories which correspond to excited states with opposite time-parity. The effects of the mass difference are summarized in Figs. 2–3 by choosing $\Delta = 0.3$. Consider first the region where trajectories of the equal-mass system are seen to cross ($s \approx 0.75$, $l \approx 0.03$). Since the corresponding states have opposite time parity, the mixing effect of the anti-Hermitean operator $4\Delta u\partial/\partial x_4$ (see Eq. (20)) leads to a complex-conjugate pair of trajectories which connect two colliding real branches according to previous perturbation arguments. Fig. 3 shows the details of this complex branch including the imaginary part of the energy. In addition, Fig. 2 includes two other complex branches of the type already seen.

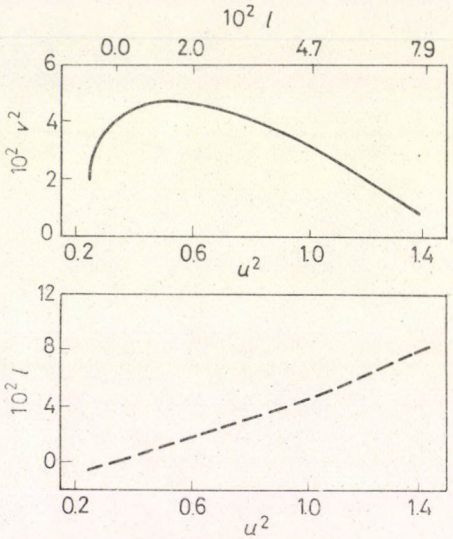

Fig. 3. Details of the first complex branch of Fig. 2 ($\Delta = 0.3$, $\lambda = 16.38$, $\varkappa = 1$)

We conclude that the slopes of Regge trajectories are very model dependent and detailed numerical calculations are necessary before any conclusion can be drawn.

REFERENCES

1. Y. NAMBU, Progr. Theor. Phys., **5**, 614, 1950; M. GELL-MANN and F. LOW, Phys. Rev., **84**, 350, 1951; J. SCHWINGER, Proc. Natl. Acad. Sci. U. S., **37**, 452, 1951; E. E. SALPETER and H. A. BETHE, Phys. Rev., **84**, 1232, 1951.
2. For a summary see, e.g., N. NAKANISHI, Suppl. Progr. Theor. Phys., **43**, 1, 1969.
3. C. SCHWARTZ, Phys. Rev., **137**, B717, 1965.
4. C. SCHWARTZ and C. ZEMACH, Phys. Rev., **141**, 1454, 1966.
5. G. C. WICK, Phys. Rev., **96**, 1127, 1954.
6. R. E. CUTKOSKY, Phys. Rev., **95**, 1135, 1954.
7. K. D. ROTHE, Phys. Rev., **170**, 1548, 1968; A. PAGNAMENTA, Nuovo Cimento, **53A**, 30, 1968; P. NARANAYASWAMY and A. PAGNAMENTA, Nuovo Cimento, **53A**, 635, 1968; K. LADÁNYI, Nuovo Cimento, **56A**, 173, 1968; E. zur LINDEN and H. MITTER, Nuovo

Cimento, **61B**, 389, 1969; D. KERSHAW, H. SNODGRASS and C. ZEMACH, SLAC preprint, 1970; D. KERSHAW and C. ZEMACH, SLAC preprint, 1970; E. zur LINDEN, MPI preprint, 1970; P. BREITENLOHNER, MPI preprint, 1970.
8. M. LEVINE, J. TJON and J. WRIGHT, Phys. Rev., **154**, 1433, 1967; R. M. SAENGER, J. Math. Phys., **8**, 2366, 1967; R. HAYMAKER, Phys. Rev. Letters, **18**, 968, 1967; Phys. Rev., **165**, 1790, 1968; K. LADÁNYI, Nuovo Cimento, **61A**, 173, 1969; B. C. MCINNIS, Phys. Rev., **183**, 1474, 1969.
9. R. E. CUTKOSKY and B. B. DEO, Phys. Rev. Letters, **19**, 1256, 1967.
10. E. zur LINDEN, Nuovo Cimento, **63A**, 181, 1969; W. B. KAUFMANN, Phys. Rev., **187**, 2051, 1969; R. N. MADAN, R. W. HAYMAKER and R. BLANKENBECLER, Phys. Rev., **172**, 1788, 1968; R. GATTO and P. MENOTTI, CERN preprint, 1970.
11. K. LADÁNYI, Nuovo Cimento, **70A**, 405, 1970.
12. S. H. VOSKO, J. Math. Phys., **1**, 505, 1960.
13. E.g., L. V. KANTOROVICH and V. I. KRYLOV, Approximation Methods in Higher Analysis (New York, 1958), p. 150.
14. For applications in the nonrelativistic quantum mechanics see, e.g., É. SZONDY and T. SZONDY, Acta Phys. Hung., **20**, 253, 1966.

РАСЧЕТ КОМПЛЕКСНО-СОПРЯЖЕННЫХ ПАР ТРАЕКТОРИЙ РЕДЖЕ С ПОМОЩЬЮ СКАЛЯРНОГО УРАВНЕНИЯ БЕТЕ—СОЛПИТЕРА

К. ЛАДАНИ

Резюме

Уравнение Бете—Солпитера для скалярных частиц приведено к упрощенному виду, допускающему численное решение. Этот формализм применен к расчету траекторий Редже. Особое внимание уделено эффектам смешивания уровней при различных массах, приводящим к комплексно сопряженным парам траекторий. Также рассчитана мнимая часть полной энергии при вещественных значениях углового момента.

Acta Physica Academiae Scientiarum Hungaricae, Tomus 31 (1–3), pp. 273–276 (1972)

LOCAL REPRESENTATIONS FOR FORWARD SCATTERING

By

F. NIEDERMAYER

INSTITUTE FOR THEORETICAL PHYSICS, ROLAND EÖTVÖS UNIVERSITY
BUDAPEST

It is shown that the JOST–LEHMANN representation may be written in a more simple form in the case of forward scattering, which is similar to the DESER–GILBERT–SUDARSHAN representation. The existence condition for the DGS representation is analyzed and some features of this representation are shown.

Introduction

Let us consider the odd, local commutator function $f(x) = \langle p \mid [J(x), J(0)] \mid p \rangle$ where p is a one-particle state, for simplicity with unit mass at rest. $p = (1, 0, 0, 0)$ $-f(x) = f(-x)$ and $f(x) = 0$ for $x^2 < 0$. The Fourier transform of $f(x)$ may be written in two forms: in the general JOST–LEHMANN representation [1] and in the more simple DESER–GILBERT–SUDARSHAN representation [2]. The DGS representation is:

$$\tilde{f}(q) = \int \varepsilon(q_0 - \beta)\, \delta(q^2 - 2q_0\beta - \sigma) h(\sigma, \beta)\, d\sigma\, d\beta, \sigma \geqslant 0, |\beta| \leqslant 1\,. \qquad (1)$$

The JL representation is:

$$\tilde{f}(q) = \int \varepsilon(q_0)\delta(q_0^2 - (q-u)^2 - \varkappa^2)\, \Phi(\varkappa^2, u)\, d\varkappa^2\, d^3u\,, \; \varkappa^2 \geqslant 0, \mid u \mid \leqslant 1\,. \qquad (2)$$

The functions h, Φ are tempered distributions.

In the case of forward scattering, the function $f(x)$ depends only on x^2 and px, therefore, the JL representation has a rotational symmetry in the 3-dimensional variable u, that is $\Phi(\varkappa^2, u)$ depends only on $\mid u \mid$. The other variables may be eliminated using the following lemma:

If $F(x)$ is rotation-invariant distribution, then a one-dimensional, even distribution $\hat{F}(u)$, $-\infty < u < +\infty$ may be defined, which for every test function $\varphi(x)$ satisfies

$$\int F(x)\, \varphi(x)\, d^3x = \int_{-\infty}^{+\infty} \hat{F}(u)\, \hat{\varphi}(u)\, du\,,$$

where

$$\hat{\varphi}(u) = \frac{1}{4\pi} \int_{|x|=u} \varphi(x)\, d\Omega \quad \text{for } u \geqslant 0 \quad \text{and} \quad \hat{\varphi}(-u) = \hat{\varphi}(u)\,.$$

It may also be shown that if $F(x)$ is restricted to $|x| \leqslant 1$, then $\hat{F}(u)$ vanishes outside the region $|u| \leqslant 1$.

Now taking $\sigma = \varkappa^2 + u^2$ and using the rotational symmetry we get the form:

$$\tilde{f}(q) = \int \varepsilon(q_0)\, \delta(q^2 - 2\,|q|\, u\cos\vartheta - \sigma)\, \Phi_1(\sigma, u)\, d\sigma\, du\, \frac{1}{2}\, d\cos\vartheta,$$

where the one-dimensional integral over u is understood. Here we have $u\cos\vartheta$ as the argument of the δ function, but Φ_1 depends only on u. Taking a test function φ instead of the δ function, we have an integral of the form:

$$\int \varphi\,(u\cos\vartheta)\, F(u) du\, \frac{1}{2}\, d\cos\vartheta = \int_{-1}^{1} du F(u)\, \frac{1}{2u} \int_{-u}^{u} \varphi(\beta)\, d\beta\,.$$

This may be rewritten in the form $\int_{1-}^{1} F_1(\beta)\varphi(\beta)d\beta$, where $F_1(\beta)$ is a distribution with the same support and symmetry properties as $F(u)$.

So we can write a representation which is equivalent to the JOST–LEHMANN representation:

$$\tilde{f}(q) = \int \varepsilon(q_0)\delta(q^2 - 2\beta\,|q| - \sigma)h_1(\sigma_1\,\beta)\, d\sigma\, d\beta,\ \sigma \geqslant 0,\ |\beta| \leqslant 1. \tag{3}$$

The Regge and the Bjorken limits of $\tilde{f}(q)$ are defined by the singularities and the asymptotic behaviour for $h\,(\sigma, \beta)$ or $h_1(\sigma, \beta)$. Since $|q| = \sqrt{\nu^2 - q^2} \sim q_0 \equiv \nu$ in the Regge and Bjorken limits, the same structure of h and h_1 results in the same asymptotic behaviour in both limits in both representations (1) and (3).

The existence condition for DGS representation

According to JOST–LEHMANN, every tempered distribution that is odd, local and has a support in the momentum space like the commutator $< p \mid [J(x),\ J(0)] \mid p >$, may be written as $f(x) = L(x;\ x)$, where $L(x;\ \eta)$ is an odd, Lorentz invariant distribution in x, and is an infinitely differentiable function in η, the Fourier transform of which

$$\tilde{L}(q\,;u) \equiv \varepsilon(q_0)\, \Phi(q^2\,;u) = \int e^{iqx + iu\eta} L(x\,;\eta)\, d^4\, x d^3\eta$$

vanishes outside the region $q^2 \geqslant 0,\ |u| \leqslant 1$.

The Fourier transform of $f(x)$ gives the well known J. L. representation:

$$\tilde{f}(q) = \int \tilde{L}(q_0,\ q - u;\ u) d^3u = \int \varepsilon(q_0)\delta(q_0 - (q-u)^2 - \varkappa^2)\, \Phi\,(\varkappa^2,\ u)\, d\varkappa^2\, d^3\, u\,,$$

As $\tilde{L}(q;\ u)$ has finite support in u, according to the Paley—Wiener theorem $L(x;\ \eta)$ is an entire analytic function in η with polynomial behaviour along the real axis and exponential behaviour along the imaginary axis. In our case $L(x;\eta)$ is rotation-invariant in η, so we can define the function $\hat{L}(x;v)$ as $L(x;\eta) = \hat{L}(x;\ \eta^2)$. This function has in the direction $v \to +\infty$ polynomial, in the direction $v \to -\infty$, roughly speaking, exponential behaviour.

If the DGS representation for $f(x)$ exists, then there exists a function $K(x;\ \eta_0)$ similar to the JL function $L(x;\ \eta)$, which is even and entire analytic in η_0 and $f(x) = K(x;\ x_0)$. It may also be defined as $K(x;\ \eta_0^2) = K(x;\ \eta_0)$. In this case, one can write the corresponding JL representation:

$$f(x) = K(x;\ x_0) = \hat{K}(x,\ x^2) = \hat{K}(x;\ x^2 + x^2) = \hat{L}(x;\ x^2),$$

that is

$$\hat{L}(x;\ \eta^2) = \hat{K}(x;\ \eta^2 + x^2),$$

and it may be shown that it is a convenient JL function or in the other form:

$$\hat{L}(x;\ \eta_0^2 - x^2) = \hat{K}(x;\ \eta_0^2) = K(x;\ \eta_0).$$

If $x^2 \to +\infty$, then the argument $\eta_0^2 - x^2 \to -\infty$. Therefore, the left-hand side may increase exponentially and in general is not a tempered distribution, but the right-hand side is always tempered. So we can formulate the existence condition as follows: For $f(x)$ there exists the DGS representation if and only if the corresponding JL function $L(x;\ \eta) = \hat{L}(x;\ \eta^2)$ has the property that $\hat{L}(x;\ c^2 - x^2)$ is a tempered distribution in x.

The DGS representation does not exist for example in the case when

$$\tilde{L}(q;\ u) = \varepsilon(q_0)\delta(q^2 - 1)\delta(u^2 - 1)$$

$$L(x;\ \eta) \simeq \Delta(x,\ 1)\cos|\eta|, \quad f(x) \simeq \Delta(x,\ 1)\cos|x|,$$

and $\hat{L}(x,\ c^2 - x^2) \simeq \Delta(x,\ 1)\cos\sqrt{c^2 - x^2}$. The last function behaves as $\Delta(x,\ 1)$ ch x_0 if $x_0 \to \infty$ and is not tempered, therefore the DGS representation does not exist in this case.

The same existence condition is also valid for even functions $f(x)$. The JL representation for this is:

$$\tilde{f}(q) = q_0 \int \varepsilon(q_0)\delta(q_0^2 - (q - u)^2 - \varkappa^2)\,\Phi(\varkappa^2;\ u)\,d\varkappa^2\,d^3u$$

and the DGS representation may also be transformed to a similar form ($\nu \equiv q_0$):

$$\tilde{f}(q) = \int \varepsilon(\nu - \beta)\delta(q^2 - 2\nu\beta - \sigma)h(\sigma,\ \beta)\,d\sigma\,d\beta =$$
$$= \nu \int \varepsilon(\nu - \beta)\delta(q^2 - 2\nu\beta - \sigma)h_1(\sigma, \beta)\,d\sigma\,d\beta,$$

where $h(\sigma, \beta)$ is even in β, and

$$h_1(\sigma,\beta) = -2\frac{\partial}{\partial\sigma}\int_{-1}^{\beta} h(\sigma,\ \beta')\,d\beta'.$$

(The distribution h_1 obeys the same support condition as h). Thus one may compare the two representations for even functions as well.

It can be shown in a similar manner that the "generalized" DGS representation may be rewritten in the usual form:

$$\sum_{n=0}^{N} \nu^n \int \varepsilon(\nu-\beta)\,\delta(q^2-2\beta\nu-\sigma)\,h_n(\sigma,\beta)\,d\sigma\,d\beta = \\ = \int \varepsilon(\nu-\beta)\,\delta(q^2-2\beta\nu-\sigma)\,h(\sigma,\beta)\,d\sigma\,d\beta.$$

Finally, it would be interesting to investigate the analytic properties of the amplitudes in forward scattering using the JL representation.

The author's thanks are due to Dr. J. KUTI for useful discussions.

REFERENCES

1. R. JOST and H. LEHMANN, Nuovo Cimento, **5**, 1598, 1957.
2. S. DESER, W. GILBERT and E. C. G. SUDARSHAN, Phys. Rev., **115**, 731, 1959.

ЛОКАЛЬНЫЕ ПРЕДСТАВЛЕНИЯ ДЛЯ РАССЕЯНИЯ ВПЕРЕД

Ф. НИДЕРМАЙЕР

Резюме

Показано, что в случае рассеяния вперед представление Йоста—Лемана может быть написано в более простом виде, подобном представлению Дезера—Гильберта—Сударшана. Проанализировано условие существования для DGS — представления, и указываются некоторые черты этого представления.

The *Acta Physica* publish papers on physics, in English, German, French and Russian.
The *Acta Physica* appear in parts of varying size, making up volumes.
Manuscripts should be addressed to:

Acta Physica, Budapest 502, P. O. B. 24.

Correspondence with the editors and publishers should be sent to the same address.
The rate of subscription is $ 16.00 a volume.
Orders may be placed with "Kultúra" Foreign Trade Company for Books and Newspapers (Budapest I., Fő u. 32. Account No. 43-790-057-181) or with representatives abroad.

Les *Acta Physica* paraissent en français, allemand, anglais et russe et publient des travaux du domaine de la physique.
Les *Acta Physica* sont publiés sous forme de fascicules qui seront réunis en volumes.
On est prié d'envoyer les manuscrits destinés à la rédaction à l'adresse suivante:

Acta Physica, Budapest 502, P. O. B. 24.

Toute correspondance doit être envoyée à cette même adresse.
Le prix de l'abonnement est de $ 16.00 par volume.
On peut s'abonner à l'Entreprise du Commerce Extérieur de Livres et Journaux «Kultúra» (Budapest I., Fő u. 32. — Compte-courant No. 43-790-057-181) ou à l'étranger chez tous les représentants ou dépositaires.

«*Acta Physica*» публикуют трактаты из области физических наук на русском, немецком, английском и французском языках.
«*Acta Physica*» выходят отдельными выпусками разного объема. Несколько выпусков составляют один том.
Предназначенные для публикации рукописи следует направлять по адресу:

Acta Physica, Budapest 502, P. O. B. 24.

По этому же адресу направлять всякую корреспонденцию для редакции и администрации. Подписная цена — $ 16.00 за том.
Заказы принимает предприятие по внешней торговле книг и газет «*Kultúra*» (Budapest I., Fő u. 32. Текущий счет: № 43-790-057-181) или его заграничные представительства и уполномоченные.

Reviews of the Hungarian Academy of Sciences are obtainable at the following addresses:

ALBANIA

Drejtorija Qändrone e Pärhapjes
dhe Propagandimit të Librit
Kruga Konferenca e Päzes
Tirana

AUSTRALIA

A. Keesing
Box 4886, GPO
Sydney

AUSTRIA

Globus
Höchstädtplatz 3
A-1200 Wien XX

BELGIUM

Office International de Librairie
30, Avenue Marnix
Bruxelles 5
Du Monde Entier
5, Place St. Jean
Bruxelles

BULGARIA

Hemus
11 pl Slaveikov
Sofia

CANADA

Pannonia Books
2, Spadina Road
Toronto 4, Ont.

CHINA

Waiwen Shudian
Peking
P. O. B. 88

CZECHOSLOVAKIA

Artia
Ve Směčkách 30
Praha 2
Poštovní Novinová Služba
Dovoz tisku
Vinohradská 46
Praha 2
Mad'arska Kultura
Václavské nám. 2
Praha 1
Slovart A. G.
Gorkého
Bratislava

DENMARK

Ejnar Munksgaard
Nörregade 6
Copenhagen

FINLAND

Akateeminen Kirjakauppa
Keskuskatu 2
Helsinki

FRANCE

Office International de Documentation
et Librairie
48, rue Gay Lussac
Paris 5

GERMAN DEMOCRATIC REPUBLIC

Deutscher Buch-Export und Import
Leninstraße 16
Leipzig 701
Zeitungsvertriebsamt
Fruchtstraße 3—4
1004 Berlin

GERMAN FEDERAL REPUBLIC

Kunst und Wissen
Erich Bieber
Postfach 46
7 Stuttgart S.

GREAT BRITAIN

Blackwell's Periodicals
Oxenford House
Magdalen Street
Oxford
Collet's Subscription Import
Department
Dennington Estate
Wellingsborough. Northants.
Robert Maxwell and Co. Ltd.
4—5 Fitzroy Square
London W. 1

HOLLAND

Swetz and Zeitlinger
Keizersgracht 471—487
Amsterdam C.
Martinus Nijhof
Lange Voorhout 9
The Hague

INDIA

Hind Book House
66 Babar Road
New Delhi 1

ITALY

Santo Vanasia
Via M. Macchi 71
Milano
Libreria Commissionaria Sansoni
Via La Marmora 45
Firenze

JAPAN

Kinokuniya Book-Store Co. Ltd.
826 Tsunohazu 1-chome
Shinjuku-ku
Tokyo
Maruzen and Co. Ltd
P. O. Box 605
Tokyo-Central

KOREA

Chulpanmul
Phenjan

NORWAY

Tanum-Cammermeyer
Karls Johansgt 41—43
Oslo 1

POLAND

RUCH
ul. Wronia 23
Warszawa

ROUMANIA

Cartimex
Str. Aristide Briand 14—18
Bucureşti

SOVIET UNION

Mezhdunarodnaya Kniga
Moscow G—200

SWEDEN

Almqvist and Wiksell
Gamla Brogatan 26
S—101 20 Stockholm

USA

F. W. Faxon Co. Inc.
15 Southwest Park
Westwood Mass. 02090
Stechert Hafner Inc.
31. East 10th Street
New York, N. Y. 10003

VIETNAM

Xunhasaba
19, Tran Quoc Toan
Hanoi

YUGOSLAVIA

Forum
Vojvode Mišića broj 1
Novi Sad
Jugoslovenska Knjiga
Terazije 27
Beograd

28. IV. 1972 Index: 26.022

ACTA PHYSICA

ACADEMIAE SCIENTIARUM HUNGARICAE

TOMUS XXXI FASCICULUS 4

AKADÉMIAI KIADÓ, BUDAPEST
1972

ACTA PHYS. HUNG. APAHAQ 31 (4) 277–403 (1972)

ACTA PHYSICA

ACADEMIAE SCIENTIARUM HUNGARICAE

SZERKESZTI

KOVÁCS ISTVÁN

Az *Acta Physica* angol, német, francia vagy orosz nyelven közöl értekezéseket. Évente két kötetben, kötetenként 4—4 füzetben jelenik meg. Kéziratok a szerkesztőség címére (Budapest XI., Budafoki út 8.) küldendők.

Megrendelhető a belföld számára az Akadémiai Kiadónál (Budapest V., Alkotmány utca 21. Bankszámla 05-915-111-46), a külföld számára pedig a „Kultúra" Könyv- és Hírlap Külkereskedelmi Vállalatnál (Budapest I., Fő utca 32. Bankszámla 43-790-057-181 sz.), vagy annak külföldi képviseleteinél és bizományosainál.

The *Acta Physica* publish papers on physics in English, German, French or Russian, in issues making up two volumes per year. Subscription price: $16.00 per volume. Distributor: KULTURA Hungarian Trading Co. for Books and Newspapers (Budapest 62, P.O. Box 149) or its representatives abroad.

Die *Acta Physica* veröffentlichen Abhandlungen aus dem Bereich der Physik in deutscher, englischer, französischer oder russischer Sprache, in Heften die jährlich zwei Bände bilden.

Abonnementspreis pro Band: $16.00. Bestellbar bei: KULTURA Buch- und Zeitungs-Außenhandelsunternehmen (Budapest 62, Postfach 149) oder bei seinen Auslandsvertretungen.

Les *Acta Physica* publient des travaux du domaine de la physique, en français, anglais, allemand ou russe, en fascicules qui forment deux volumes par an.

Prix de l'abonnement: $16.00 par volume. On peut s'abonner à l'Entreprise du Commerce Extérieur de Livres et Journaux KULTURA (Budapest 62, P.O.B. 149) ou chez ses représentants à l'étranger.

«*Acta Physica*» публикуют трактаты из области физических наук на русском, немецком, английском и французском языках.

«*Acta Physica*» выходят отдельными выпусками, составляющими два тома в год.

Подписная цена = $16.00 за том. Заказы принимает предприятие по внешней торговле книг и газет KULTURA (Budapest 62, P.O.B. 149.) или его заграничные представительства и уполномоченные.

Acta Physica Academiae Scientiarum Hungaricae, Tomus 31 (4), pp. 277—283 (1972)

IMPEDANCE, EQUIVALENT CIRCUIT AND STABILITY BEHAVIOUR OF MEDIUM-PRESSURE DISCHARGES

By

H. DEUTSCH

SEKTION PHYSIK/ELEKTRONIK DER E.M.A.-UNIVERSITÄT GREIFSWALD, DDR

(Received 18. VI. 1970)

An equivalent circuit of a medium pressure column is derived at low current and stability behaviour is considered on this basis.

Studies of the dynamic behaviour of discharges [1], [2] have shown that it is possible to derive quantitative information about the efficiency of various elementary processes (direct ionization, stepwise ionization) in the discharge mechanism. This possibility is of particular importance in instances when single elementary processes (e.g. triple collisions) have but a small effect on the static characteristics of a discharge, but a significant influence on the dynamic behaviour. From investigations of the dynamic behaviour it was found that tentative suggestions about the stability of the discharge [3], [4] could be made, although in order to get easily surveyable stability criteria it was necessary to derive an equivalent circuit of the discharge [5]. The positive low-pressure columns at weak currents have already been investigated in this direction. The object of this paper is first to derive an equivalent circuit of a positive medium-pressure column at low current and then to consider stability on this basis.

1. Equivalent circuit of a medium-pressure column at low current

The differential equation for the impedance behaviour of the positive column of a medium-pressure column, which is necessary to build up a suitable equivalent circuit, may be derived satisfactorily from the following system of initial equations [2]:

$$\begin{aligned} &\partial Ne/\partial t + Ne/\tau_e - P_e = 0, \\ &\partial M/\partial t + M/\tau_m - P_m = 0, \\ &\partial R/\partial t + R/\tau_r - P_r = 0, \\ &J - \pi e_0 r_\sigma^2 N_e b_e E = 0, \end{aligned} \tag{1}$$

where P_e/N^2, P_m/N^2 etc. are used as defined in [2].

Since plasma parameters E, Ne, M and R are to be subjected to variations whenever a disturbance δI_0 is impressed on the discharge current I_0 and only minor disturbances will be permitted

$$\left(\frac{\delta I_0}{I_0} \ll 1,\ \frac{\delta E}{E_0} \ll 1\right),$$

taking the above expressions with

$$\begin{aligned} E &= E_0(1 + x_1) = E_0 + u, \\ N_e &= N_{e_0}(1 + x_2), \\ M &= M_0(1 + x_3), \\ R &= R_0(1 + x_4), \\ I &= I_0(1 + x_5) = I_0 + i, \end{aligned} \tag{2}$$

we get the following system of equations:

$$\begin{aligned} \frac{\partial x_2}{\partial t} &= b_{11}x_1 + b_{12}x_2 + b_{13}x_3 + b_{14}x_4, \\ \frac{\partial x_3}{\partial t} &= b_{21}x_1 + b_{22}x_2 + b_{23}x_3 + b_{24}x_4, \\ \frac{\partial x_4}{\partial t} &= b_{31}x_1 + b_{32}x_2 + b_{33}x_3 + b_{34}x_4, \\ x_5 &= b_{41}x_1 + x_4. \end{aligned} \tag{3}$$

The b_{ik} and a_{ik} defined in [2] or b_i, respectively, show the correlations

$$\begin{aligned} b_{11} &= -Na_{11}, & b_{31} &= -N\left(\frac{Ne/N}{R/N}\right)a_{41}, \\ b_{12} &= -Nb_1, & & \\ b_{13} &= -Na_{13}, & b_{32} &= -N\left(\frac{Ne/N}{R/N}\right)a_{42}, \\ b_{14} &= -Na_{14}, & & \\ b_{21} &= -N\left(\frac{Ne/N}{M/N}\right)a_{21}, & b_{33} &= -N\left(\frac{Ne/N}{R/N}\right)a_{43}, \\ b_{22} &= -N\left(\frac{Ne/N}{M/N}\right)a_{22}, & b_{34} &= -N\left(\frac{Ne/N}{R/N}\right)b_3, \\ b_{23} &= -N\left(\frac{Ne/N}{M/N}\right)b_2, & b_{41} &= a_{31}, \\ b_{24} &= -N\left(\frac{Ne/N}{M/N}\right)a_{24}. & & \end{aligned} \tag{4}$$

The wanted differential equation for the dynamic behaviour of a positive column which has been subjected to a minor disturbance is obtained by stepwise elimination of x_2, x_3 and x_4 through repeated differentiation of Eqs. (3):

$$\frac{c_0}{a_0}\frac{d^3 i}{dt^3} + \frac{c_1}{a_0}\frac{d^2 i}{dt^2} + \frac{c_2}{a_0}\frac{di}{dt} + \frac{c_3}{a_0} i = \\ = \frac{d^3 u}{dt^3} + \frac{a_1}{a_0}\frac{d^2 u}{dt^2} + \frac{a_2}{a_0}\frac{du}{dt} + \frac{a_3}{a_0} u. \tag{5}$$

The state of the plasma is characterized by the coefficients c_0, $c_1 \ldots a_0$, a_1, where combinations of the b_{ik} occur. With reference to the three inertial factors which show as a time derivation in the balance equation we get a linear homogeneous equation of third order.

In earlier experimental and theoretical investigations (Fig. 1) it was discovered that a marked resonance effect among others could be formed for the impedance condition, which suggests that a corresponding equivalent circuit (Fig. 2) is possible for weak-current discharges at medium pressures. With reference to the three inertial factors which are reflected as time derivations in the balance equations three reactances were taken into consideration in the equivalent circuit.

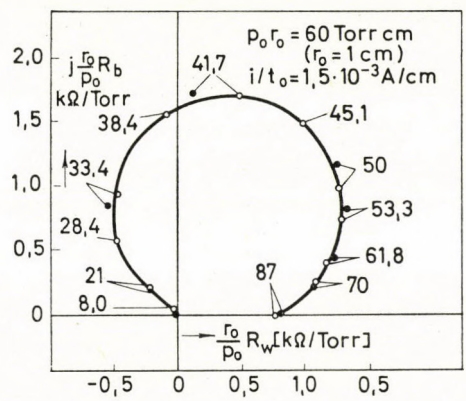

Fig. 1. Calculated and measured impedance characteristics of a neon discharge [2]. [$p_0 r_0$ = 60 torr cm; r_0 = 1 cm; $i/r_0 = 1.5 \cdot 10^{-3}$ A/cm]. ○ theory; ● experiment. Numerical values refer to the corresponding reduced frequencies in cps/torr

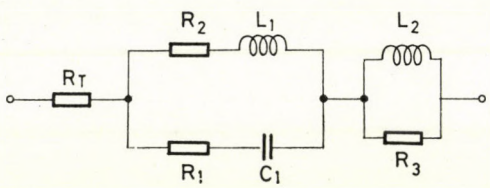

Fig. 2. Equivalent circuit of the positive column of a low-current medium-pressure glow-discharge (. . . taking the three intertial factors into consideration)

The differential equation for this at first empirically introduced equivalent circuit is:

$$\alpha \frac{d^3 i}{dt^3} + \beta \frac{d^2 i}{dt^2} + \gamma \frac{di}{dt} + \delta i = \frac{d^3 u}{dt^3} + A \frac{d^2 u}{dt^2} + B \frac{du}{dt} + Cu, \tag{6}$$

where coefficients α, β, ... are combinations of the quantities R_T, R_1, R_2, R_3, L_1, L_2 and C_1.

Eqs. (5) and (6) are isomorphic; so that with due regard to the plasma parameters reflected in the b_{ik} it is immediately possible to calculate the resistances, inductances and capacities by comparing coefficients. In the calculations presentation of the quantities of the equivalent circuit in a similarity scheme was abandoned from the first both because a higher pressure had to be expected with greater triple collision destruction in the medium-pressure discharge and because this process does not conform with the B-invariant similarity law [6].

From the comparison of coefficients a system of seven equations with seven unknown quantities is obtained. The solution of the equation system is here restricted to real — and hence physically suggestive — values for reactances: the solution was carried out graphically and numerically.

The quantities of the equivalent circuit were calculated by using the characteristic quantities of the homogeneous medium-pressure neon column for a given case of discharge [2] ($p_0 = 60$ torr; $I_0 = 1{,}5 \cdot 10^{-3}$ A; $r_0 = 1$ cm). The detailed calculation yielded the following results:

$L_1 = 1.55$ Henry
$L_2 = 1 \cdot 10^{-3}$ Henry
$C_1 = 2.67 \cdot 10^{-9}$ Farad
$R_3 = 1.30 \cdot 10^2$ Ohm
$R_2 = -1.74 \cdot 10^4$ Ohm
$R_T = +1.60 \cdot 10^4$ Ohm
$R_1 = +2.90 \cdot 10^4$ Ohm

The calculated values were tested by substituting them into the following relation for the impedance of the equivalent circuit:

$$Z = R_T + \frac{R_1 R_2 + \frac{L_1}{C_1} + j\left(R_1 \omega L_1 - R_2 \frac{1}{\omega C_1}\right)}{R_1 + R_2 + j\left(\omega L_1 - \frac{1}{\omega C_1}\right)} + \frac{R_3 j \omega L_2}{R_3 + j \omega L_2}. \tag{7}$$

The check demonstrated that the last term on the r.h.s. of the relation (7) contributes only very little to Z, hence the impedance behaviour of the positive

column of a medium-pressure discharge is essentially determined by the first two terms, i.e. by the equivalent circuit of Fig. 3.

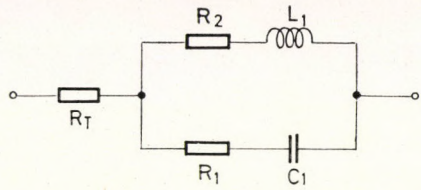

Fig. 3. "Reduced" equivalent circuit

2. Stability considerations

The following considerations refer only to discharges with a long positive column, the dynamic behaviour of which is essentially characterized by that of the positive column and are based on a procedure for establishing stability criteria outlined by GRANOWSKI [3], except that the differential characteristic of a discharge in an equivalent circuit representation is used as the starting point instead of a differential characteristic derived immediately from the balance equation.

In the case investigated here the differential characteristic of the gaseous space in the equivalent circuit scheme is:

$$A^* \frac{d^2 i}{dt^2} + B^* \frac{di}{dt} + D^* i = A'' \frac{d^2 u}{dt^2} + B'' \frac{du}{dt} + u\,, \tag{8}$$

where

$$\begin{aligned} A^* &= R_T C_1 L_1 + R_1 C_1 L_1, \\ B^* &= R_1 R_T C_1 + R_2 R_T C_1 + R_2 R_1 C_1 + L_1, \\ D^* &= R_T + R_2, \\ A'' &= C_1 L_1, \\ B'' &= R_1 C_1 + R_2 C_1. \end{aligned}$$

For the further derivation of stability criteria we need a differential characteristic of the outer circuit in a general form (Fig. 4) which is taken over from an earlier work [4] (cf. also [3]):

$$CRL \frac{d^2 i}{dt^2} + L \frac{di}{dt} + Ri = - CR \frac{du}{dt} - u\,. \tag{9}$$

The general approach in investigating stationarity problems is to permit a small disturbance of a given state and to find out the time changes. If the

disturbance recedes after a certain lapse of time the discharge is a stationary one, if not, it is non-stationary. As the differential equations (8) and (9) are linear in i and u, the following form is used for the disturbances of current and voltage:

$$\begin{aligned} i &= i_0 e^{\omega t}, \\ u &= u_0 e^{\omega t}, \end{aligned} \tag{10}$$

where i_0 refers to the initial deviation of the current from the stationary value I_0, and u_0 refers to the initial voltage deviation (i_0 and ω are generally complex quantities).

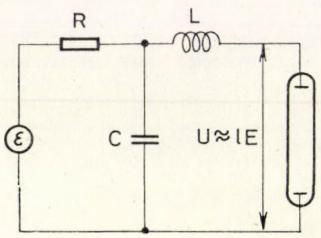

Fig. 4. Electrical circuit for the general case: U = voltage across the tube, E = voltage gradient, l = length of the positive column

With (10), by evaluating the differential characteristics of the gaseous space (8) and of the outer circuit (9), the following equation for calculating ω is obtained:

$$g_4\omega^4 + g_3\omega^3 + g_2\omega^2 + g_1\omega + g_0 = 0 \tag{11}$$

with

$$\begin{aligned} g_0 &= R + R_A, \\ g_1 &= L + L_1 + CRR_A + RR_1C_1 + RR_2C_1 + R_1R_TC_1 + R_2R_TC_1 + R_2R_1C_1, \\ g_2 &= LCR + LC_1\{R_1 + R_2\} + L_1C_1\{R_T + R_1 + R\} + \\ &\quad + CC_1R\{R_1R_T + R_2R_T + R_2R_1 + L_1C_1\}, \\ g_3 &= CC_1LR\{R_1 + R_2\} + C_1LL_1 + CC_1L_1R\{R_1 + R_T\}, \\ g_4 &= RCC_1LL_1. \end{aligned}$$

$R_A = R_T + R_2$ is the differential resistance at zero frequency. The behaviour is evidently stationary when the real parts of all roots of Eq. (11) are negative. According to the theorem of HURWITZ [7], the necessary and sufficient condition for this is:

$$D_1 = g_1 > 0\,; \qquad D_2 = \begin{vmatrix} g_1 & g_0 \\ g_3 & g_2 \end{vmatrix} > 0$$

$$D_3 = \begin{vmatrix} g_1 & g_0 & 0 \\ g_3 & g_2 & g_1 \\ 0 & g_4 & g_3 \end{vmatrix} > 0; \qquad D_4 = \begin{vmatrix} g_1 & g_0 & 0 & 0 \\ g_3 & g_2 & g_1 & g_0 \\ 0 & 0 & 0 & g_4 \end{vmatrix} > 0 \tag{12}$$

where $g_0 > 0$. This stationarity condition requires that all coefficients g_μ $(\nu = 0 \ldots 4)$ of the characteristic equation should be positive in sign. In the following we shall restrict ourselves to a discussion of the necessary conditions g_ν $(\nu = 0 \ldots 4) > 0$, because it is rather difficult to deal in a complex discussion with stationarity conditions in the general form (12).

From the above necessary conditions one immediately obtains the well-known Kaufmann criteria

$$R + R_A > 0, \tag{13}$$

$$L + CRR_A > 0, \tag{14}$$

when there is a restriction to the static characteristics, i.e. when L_1, C_1 and R_1 are made identical with zero. In the general case, however, one has to make full use of all the criteria for stability tests.

As presumed by Kaufmann one cannot change the first stability criterion (13) just by taking into account the dynamic behaviour, while in the second criterion it is necessary to add the inductance L_1 of the discharge once to the inductance L of the outer space (cf. [4]); furthermore, additional terms, which are supplied by the self-capacity of the discharge C_1 with the resistances R_T, R_1, R_2 or R, respectively, will occur for the second condition. Apart from these "extended" Kaufmann conditions three more conditions will occur which are accounted for only by the consideration of the dynamic behaviour of the discharge. Consequently, these conditions become effective when the dynamic behaviour of the circuit is co-determined by the discharge.

REFERENCES

1. H. Deutsch und A. Rutscher, Beitr. Plasmaphys., **8,** 205, 1968.
2. H. Deutsch und S. Pfau, Beitr. Plasmaphys., **9,** 129, 1969.
3. W. L. Granowski, "Der elektrische Strom im Gas" 2. Auflage, Akademie Verlag 437, Berlin, 1955.
4. H. Deutsch, Wiss. Z. der Elektrotechnik, **13,** 99, 1969; **14,** 64, 1969.
5. F. A. Benson und M. W. Bradshaw, Proc. VII ICPIG Beograd, **1,** 372, 1966; Proc. I.E.E. **113,** 62, 1966.
6. S. Pfau, A. Rutscher und K. Wojaczek, Beitr. Plasmaphys., **9,** 333, 1969.
7. R. Zurmühl, "Praktische Mathematik für Ingenieure und Physiker", Springer-Verlag, Berlin—Göttingen—Heidelberg 79, 1963.

ИМПЕДАНС, ЭКВИВАЛЕНТНАЯ СХЕМА И СТАБИЛЬНОСТЬ РАЗРЯДА СРЕДНЕГО ДАВЛЕНИЯ

Г. ДОЙЧ

Резюме

Определена эквивалентная схема столба маломощного разряда среднего давления и рассмотрены условия стабильности.

Acta Physica Academiae Scientiarum Hungaricae, Tomus 31 (4), pp. 285—291 (1972)

AN ISOLATED CHARGED DISTRIBUTION IN UNIFIED FIELD THEORY

By

D. N. PANT

DEPARTMENT OF MATHEMATICS, BANARAS HINDU UNIVERSITY, VARANASI, INDIA

(Received 19. I. 1971)

Einstein's Unified Field Theory equations (1953) have been considered in order to find the external field of an isolated charged distribution for a special axially symmetric case. The field equations have been solved in two cases. In one case the space-time becomes flat and the electrostatic field is found to be constant in the direction of the axis of symmetry. The solution for the other case is non-existent.

1. Introduction

It has recently been found [1] that in EINSTEIN's Unified Field Theory the spherically symmetric solution representing the external field of a localized charge does not exist. In this paper the possibility of an axially symmetric izolated charged distribution has been explored in order to obtain its external field. The total field of such a charged distribution is given by

$$g_{ij} = \underset{\text{v}}{g_{ij}} + g_{ij},$$

where

$$g_{11} = \frac{g_{22}}{\varrho^2} = g_{33} = -e^{-2\mu},\ g_{44} = e^{2\mu},\ g_{ij} = 0\ (i \neq j), \tag{1.1}$$

$$\underset{\text{v}}{g_{12}} = \nu,\ \underset{\text{v}}{g_{23}} = \sigma,\ \underset{\text{v}}{g_{13}} = \underset{\text{v}}{g_{14}} = \underset{\text{v}}{g_{24}} = \underset{\text{v}}{g_{34}} = 0. \tag{1.2}$$

Here μ, ν and σ are functions of ϱ and ζ. (We shall use x^1 and x^3 for ϱ and ζ, respectively.) In the absence of ν and σ the total field reduces to the axially symmetric conformastat metric [2]

$$ds^2 = -e^{-2\mu}(d\varrho^2 + \varrho^2 d\varphi^2 + d\zeta^2) + e^{2\mu}dt^2. \tag{1.3}$$

The field equations considered here are those of EINSTEIN (1953) [3]:

$$g_{ij,k} - g_{sj}\Gamma^s_{ik} - g_{is}\Gamma^s_{kj} = 0\,, \tag{1.4a}$$

$$\Gamma^s_{\underset{\text{v}}{is}} = 0\,, \tag{1.4b}$$

$$\underset{\text{v}}{R_{ij}} = 0\,, \tag{1.4c}$$

$$\underset{\text{v}}{R_{ij,k}} + \underset{\text{v}}{R_{jk,i}} + \underset{\text{v}}{R_{ki,j}} = 0\,, \tag{1.4d}$$

where

$$R_{\underline{ik}} = \Gamma^{a}_{\underline{ik},a} - \frac{1}{2}(\Gamma^{a}_{\underline{ia},k} + \Gamma^{a}_{\underline{ka},i}) - \Gamma^{a}_{\underline{ib}}\Gamma^{b}_{\underline{ak}} + \Gamma^{a}_{\underline{ik}}\Gamma^{b}_{\underline{ab}} - \Gamma^{a}_{\underset{\vee}{ib}}\Gamma^{b}_{\underset{\vee}{ak}}, \tag{1.5a}$$

$$R_{\underline{ik}} = \Gamma^{a}_{\underline{ik},a} - \Gamma^{a}_{\underline{ib}}\Gamma^{b}_{\underset{\vee}{ak}} - \Gamma^{a}_{\underset{\vee}{ib}}\Gamma^{b}_{\underline{ak}} + \Gamma^{a}_{\underset{\vee}{ik}}\Gamma^{b}_{\underline{ab}}. \tag{1.5b}$$

The external field of the isolated charge is the vacuum electrostatic field characterized by

$$\mathfrak{I}^{4} = (\sqrt{-g}\, F^{4\beta}), \beta = 0 \tag{1.6}$$

where $\mathfrak{I}^{4}$ denotes the charge density of the external field.

The investigation has been carried out for the two cases $\nu \neq 0$, $\sigma = 0$ and $\nu = 0$, $\sigma \neq 0$. In the first case it is observed that the presence of the electrostatic field represented by (1.2) does not affect the gravitational field represented by (1.1). In the second case it is found that there does not exist any non-trivial solution representing the external field of the isolated charge.

The field considered here is static. Comma and semicolon preceding a suffix denote respectively partial differentiation and covariant differentiation with respect to the affine connection Γ^{k}_{ij}.

2. Preliminary calculations

The non-vanishing components of g^{ij} in (1.1), (1.2) are given by

$$\begin{aligned} g^{\underline{11}} &= \frac{e^{2\mu}}{g}(\sigma^2 + \varrho^2 e^{-4\mu}), \; g^{\underline{13}} = \frac{e^{2\mu}}{g}\sigma\nu, \\ g^{\underline{22}} &= \frac{e^{-2\mu}}{g}, \; g^{\underline{33}} = \frac{e^{2\mu}}{g}(\nu^2 + \varrho^2 e^{-4\mu}), \; g^{\underline{44}} = e^{-2\mu}, \\ g^{\underline{12}}_{\vee} &= -\frac{\nu}{g}, \; g^{\underline{23}}_{\vee} = -\frac{\sigma}{g}. \end{aligned} \tag{2.1}$$

Also

$$g = -(\nu^2 + \sigma^2 + \varrho^2 e^{-4\mu}). \tag{2.2}$$

The electromagnetic field tensor F_{ij} is defined by

$$F_{ij} = \frac{1}{2}\epsilon_{ijkl}(\sqrt{-g}\, g^{kl}_{\vee}).$$

The non-vanishing components of F_{ij} are

$$F_{14} = \frac{\sigma}{\sqrt{-g}}, \qquad F_{34} = \frac{\nu}{\sqrt{-g}}. \tag{2.3}$$

Also

$$F^{14} = -\frac{\sigma}{\sqrt{-g}}, \quad F^{34} = -\frac{\nu}{\sqrt{-g}}. \tag{2.4}$$

Eq. (1.6) thus turns out to be

$$\nu_{,3} + \sigma_{,1} = 0. \tag{2.5}$$

Eqs (1.4a) determine 64 affine connections. In the present case only 20 affine connections are found to be non-vanishing.

3. Field equations and their solution

Case (i). If $\nu \neq 0$ and $\sigma = 0$, Eq. (2.5) becomes

$$\nu_{,3} = 0, \tag{3.1}$$

which implies that ν is a function of ϱ alone. Further, Eqs (1.4b) reduce to the single equation

$$\left(\frac{\nu}{\varrho} - \nu_{,1} - 2\nu\mu_{,1}\right) e^{-2\mu} = 0 \tag{3.2}$$

which integrates to

$$\mu = -\frac{1}{2}\log\left(\frac{\nu b}{\varrho}\right) \tag{3.3}$$

where b is an arbitrary function of ζ.

Eqs. (1.5a) and (1.5b) determine R_{ij} and R_{ij}. Substituting these in the field equations (1.4c), (1.4d) and simplifying them with the help of (3.1)—(3.3) we obtain

$$\begin{aligned}
R_{11} &\equiv \left\{\frac{b_{,3}(1-b^2)}{b(1+b^2)}\right\}_{,3} + \frac{2b_{,3}^2}{(1+b^2)^2} - \left(\frac{\nu_{,11}}{\nu} - \frac{\nu_{,1}}{\nu\varrho} + \frac{1}{\varrho^2}\right) = 0, \\
R_{13} &\equiv \frac{b_{,3}}{4b}\left(\frac{\nu_{,1}}{\nu} - \frac{1}{\varrho}\right) = 0, \\
R_{22} &\equiv \frac{\varrho^2}{2}\left\{\frac{\dot{b}_{,3}(1-b^2)}{b(1+b^2)}\right\}_{,3} + \frac{\varrho^2 b_{,3}^2}{(1+b^2)^2} - \frac{1}{2}\left(\varrho + \frac{\nu_{,1}\varrho^2}{\nu}\right)_{,1} + \\
&\quad + \frac{1}{2b^2}\left(1 - \frac{\nu_{,1}\varrho}{\nu}\right)^2 + \frac{1}{2\varrho}\left(\varrho + \frac{\nu_{,1}\varrho^2}{\nu}\right) = 0, \\
R_{33} &\equiv \left\{\frac{b_{,3}(1-b^2)}{b(1+b^2)}\right\}_{,3} - \frac{b_{,3}^2}{b^2} - \left(\frac{\nu_{,11}}{\nu} - \frac{\nu_{,1}^2}{\nu^2} + \frac{\nu_{,1}}{\nu\varrho}\right) = 0, \\
R_{44} &\equiv -\frac{\varrho^2}{2\nu^2}\left\{\left(\frac{b_{,3}}{b^3}\right)_{,3} + \frac{b_{,3}^2(1+2b^2)}{b^4(1+b^2)}\right\} + \frac{1}{2b^2}\left\{\frac{\varrho^2}{\nu^2}\left(\frac{1}{\varrho} - \frac{\nu_{,1}}{\nu}\right)\right\}_{,1} \\
&\quad - \left(\frac{\varrho}{\nu b}\right)^2\left(\frac{\nu_{,1}}{\nu} - \frac{1}{\varrho}\right)\left(\frac{\nu_{,1}}{\nu} - \frac{1}{2\varrho}\right) = 0
\end{aligned} \tag{3.4}$$

and

$$R_{\underset{\vee}{12},3}+R_{\underset{\vee}{23},1}\equiv \varrho\left\{\left(\frac{b_{,3}}{1+b^2}\right)_{,3}-\frac{b_{,3}^2(1-b^2)}{2b(1+b^2)^2}+\right.$$
$$\left.+\frac{1}{2b}\left(\frac{\nu_{,1}}{\nu}-\frac{1}{\varrho}\right)^2\right\}_{,3}+\frac{b_{,3}}{b^2}\left(1-\frac{\nu_{,1}\varrho}{\nu}\right)_{,1}=0.$$

It can be easily seen that the above equations will be satisfied if, and only if,

$$b_{,3}=0 \tag{3.5}$$

and

$$\frac{\nu_{,1}}{\nu}-\frac{1}{\varrho}=0\,. \tag{3.6}$$

The corresponding solution is

$$\nu=c\varrho, \tag{3.7}$$

$$e^{-2\mu}=bc=\text{const.} \tag{3.8}$$

where c is a constant of integration. From Eqs. (2.2), (2.3), (3.7) and (3.8)

$$F_{14}=0\,,\quad F_{34}=\frac{1}{\sqrt{1+b^2}}=\text{const.}$$

It follows that the electrostatic field is distributed in the direction of the z-axis only and is constant. Also, it is obvious from (3.8) that the space-time is flat.

It is worth mentioning here that TIWARI and MISRA [3] have shown that the empty space-time field equations for the metric (1.3) demand that μ be a constant. This implies that the presence of ν does not affect μ.

Case (ii). If $\sigma\neq 0$ but $\nu=0$, Eq. (2.5) reduces to

$$\sigma_{,1}=0. \tag{3.9}$$

Thus σ is no longer a function of ϱ. Eq. (1.4b) reduce to the single equation

$$\sigma_{,3}+2\sigma\mu_{,3}=0 \tag{3.10}$$

which on integration gives

$$\mu=-\frac{1}{2}\log a\sigma\,, \tag{3.11}$$

where a is an arbitrary function of ϱ.

Using (3.9)—(3.11), we find that field equations (1.4c) and (1.4d) simplify

to

$$R_{\underline{11}} \equiv -\frac{1}{2}\left(\frac{\sigma_{,3}}{\sigma}\right)_{,3} + \frac{1}{2a^2(1+a^2\varrho^2)}\left\{(1-a^2\varrho^2)aa_{,11}\right.$$
$$\left. - \frac{2(1+3a^2\varrho^2)}{(1+a^2\varrho^2)}a_{,1}^2 - \varrho a^3\frac{(9+a^2\varrho^2)}{(1+a^2\varrho^2)}a_{,1} - \frac{2a^4(1-3a^2\varrho^2)}{(1-a^4\varrho^4)}\right\} = 0, \tag{3.12a}$$

$$R_{\underline{22}} \equiv -\frac{\varrho^2}{2\sigma}\sigma_{,33} + \frac{(1+a^2\varrho^2)}{2a^2\sigma^2}\sigma_{,3}^2 + \frac{\varrho^2(1-a^2\varrho^2)}{2a(1+a^2\varrho^2)}a_{,11} - \frac{\varrho^2(1+2a^2\varrho^2-a^4\varrho^4)}{2a^2(1+a^2\varrho^2)^2}a_{,1}^2$$
$$+ \frac{1}{(1-a^4\varrho^4)^2}\left\{\frac{\varrho}{2a}(2-a^2\varrho^2+15a^4\varrho^4+a^6\varrho^6-a^8\varrho^8)a_{,1}\right. \tag{3.12b}$$
$$\left. + 1+3a^2\varrho^2+7a^4\varrho^4+a^6\varrho^6\right\} = 0,$$

$$R_{\underline{33}} \equiv -\frac{\sigma_{,33}}{2\sigma} + \frac{(1-a^2\varrho^2)}{2a(1+a^2\varrho^2)}a_{,11} - \frac{(1+2a^2\varrho^2-a^4\varrho^4)}{2a^2(1+a^2\varrho^2)^2}a_{,1}^2$$
$$- \frac{1}{2(1-a^4\varrho^4)^2}\{a\varrho(11-a^2\varrho^2+5a^4\varrho^4+a^6\varrho^6)a_{,1} \tag{3.12c}$$
$$+4a^2(1+a^4\varrho^4)\} = 0,$$

$$R_{\underline{44}} \equiv -\frac{1}{2a^2\sigma^2}\left(\frac{\sigma_{,3}}{\sigma}\right)_{,3} + \frac{1}{2a^4\sigma^2(1+a^2\varrho^2)}\{-(1+a^2\varrho^2)aa_{,11} \tag{3.12d}$$
$$+(2+a^2\varrho^2)a_{,1}^2 - \varrho a^3 a_{,1}\} = 0,$$

$$R_{13} \equiv -\frac{a_{,1}\sigma_{,3}}{2a\sigma} = 0 \tag{3.12e}$$

and

$$R_{\underset{\vee}{12},3} + R_{\underset{\vee}{23},1} \equiv -\frac{a_{,1}}{a^2}\left(\frac{\sigma_{,3}}{\sigma}\right)_{,3} + \left\{\frac{\sigma_{,3}^2}{2a\sigma^2} + \frac{\varrho^2 a_{,11}}{1+a^2\varrho^2} - \frac{\varrho^2(1+3a^2\varrho^2)}{2a(1+a^2\varrho^2)}a_{,1}^2\right.$$
$$\left. + \frac{2\varrho a_{,1}}{(1+a^2\varrho^2)^2} + \frac{a(1+3a^4\varrho^4)}{(1-a^4\varrho^4)^2}\right\}_{,1} = 0. \tag{3.12f}$$

Eq. (3.12e) gives either

$$\sigma_{,3} = 0, \tag{3.13}$$

or

$$a_{,1} = 0. \tag{3.14}$$

Firstly we will consider (3.13). Using this, (3.12d) integrates to

$$a_{,1} = \frac{Ba^2}{\sqrt{1+a^2\varrho^2}}, \tag{3.15}$$

where B is an arbitrary constant. Using (3.13) and (3.15) we find that (3.12a) simplifies to

$$\frac{a^2}{2(1+a^2\varrho^2)^3(1-a^2\varrho^2)}\{B^2a^6\varrho^6+6(B^2+1)a^4\varrho^4+(4-7B^2)a^2\varrho^2- \\ -10Ba\varrho\sqrt{1+a^2\varrho^2}\ (1-a^2\varrho^2)-2\}=0. \tag{3.16}$$

which will be satisfied if either

$$a = 0 \tag{3.17}$$

or

$$B^2a^6\varrho^6 + 6(1+B^2)a^4\varrho^4 + (4-7B^2)a^2\varrho^2 - 10Ba\varrho(1-a^2\varrho^2)\sqrt{1+a^2\varrho^2} - 2 = 0. \tag{3.18}$$

The latter is an algebraic equation in $a\varrho$ which on solving will give $a\varrho$ in terms of B, i.e. a constant. Therefore Eq. (3.15), on integration, gives

$$a\varrho = -\frac{1}{\sqrt{B^2-1}}. \tag{3.19}$$

From (3.19) and (3.18) it is found that $B = 0$, which makes (3.15) and (3.19) inconsistent.

On the other hand, the possibility (3.17) is inadmissible as a is appearing in the denominator in the field equations (3.12). Thus we conclude that the field equations (3.12) become inconsistent if (3.13) is considered. We arrive at the similar conclusion after considering the possibility (3.14). Hence it follows that in this particular case, (1.1) and (1.2) are incompatible.

Acknowledgements

The author is grateful to Dr. R. TIWARI for his guidance in the investigation. His thanks are also due to Dr. S. R. ROY for useful discussions.

REFERENCES

1. R. Tiwari and D. N. Pant, Phys. Letters, A, London **33**, 505, 1970.
2. J. L. Synge, Relativity — The General Theory, North Holland Pub. Comp., Amsterdam (1960), p. 341.
3. A. Einstein, The Meaning of Relativity (4th ed.), Princeton University Press, Princeton, Appendix II, 130—165.
4. R. Tiwari and M. Misra, Proc. Nat. Inst. Sci. India, A, **28** (6), 857, 1962.

ВНЕШНЕЕ ПОЛЕ ЛОКАЛИЗОВАННОГО ЗАРЯДА В ЕДИНОЙ ТЕОРИИ ПОЛЯ

Д. Н. ПЭНТ

Резюме

Изучены уравнения Эйнштейна (1Ж53) для единой теории поля с целью нахождени внешнего поля локализованного распределения заряда в случае специальнай односной симметрии. Уравнения поля решены для двух случаев. В одном из них четырехмерное пространство будет плоским и в направлении, оси симметрии, электростатическое поле сохраняет постоянное значениес Для другого случая решения не существует.

Acta Physica Academiae Scientiarum Hungaricae, Tomus 31 (4), pp. 293—325 (1972)

DIE WECHSELSTROMELEKTROOSMOSE

Von

Z. LÁSZLÓ[1]

VEREINIGTE GLÜHLAMPEN UND ELEKTRIZITÄTS-A.G. BUDAPEST

(Eingegangen: 4. II. 1971)

Jene Flüssigkeitstransporterscheinung, die durch ein elektrisches Wechselspannungsfeld in den Poren eines Diaphragmas, in einem Kapillarensystem oder in einer Kapillare hervorgerufen wird, wurde von uns als Wechselstromelektroosmose benannt. Diese elektrokinetische Erscheinung tritt in zwei Grundfällen ein:

a) Die Kapillaren des Diaphragmas sind von zylindrischer Form und an beiden Seiten des Diaphragmas befinden sich verschiedene Flüssigkeiten, z. B. Lösungsmittel—Elektrolytlösung.

b) Die Kapillaren des Diaphragmas sind konusförmig und an beiden Seiten des Diaphragmas befindet sich die gleiche Flüssigkeit.

Es werden die Regeln angegeben, nach welchen die Elektroosmose abläuft. So wurde u. a. festgestellt, dass der elektroosmotische Druck eine quadratische Funktion der Feldstärke ist. Das Zustandekommen der Erscheinung wurde auf jene ponderomotorischen Kräfte zurückgeführt, die in der Doppelschicht an der Kapillarenwand infolge des Wechselspannungsfeldes auftreten.

1. Einleitung

Aus der Fachliteratur sind folgende vier elektrokinetische Erscheinungen bekannt:

Elektroosmose;
Strömungspotential;
Elektrophorese;
Setzungspotential.

Auf Grund unserer Untersuchungen beschrieben wir eine neue elektrokinetische Erscheinung [1], und benannten diese als Wechselstromelektroosmose. Folgende Betrachtungen führten uns zur Untersuchung dieser Erscheinung:

Das elektrische Feld übt seine Wirkung auf eine Substanz nach den Gesetzen der Elektrodynamik auf zweierlei Art aus:

1. Es wirkt auf die geladenen Teilchen in der Substanz,
2. es wirkt auf die Substanz als Dielektrikum.

[1] Dr. Zoltán László, Budapest XIII. (Ungarn), Pozsonyi út 24.

Bei der Elektroosmose, oder genauer gesagt bei der Gleichstromelektroosmose übt das elektrische Feld seine Wirkung auf die geladenen Teilchen der Doppelschicht an der Kapillarenwand aus, und ruft die Strömung der Flüssigkeit in dieser Weise hervor. Es muss aber in Betracht genommen werden, dass die DK der Flüssigkeit in der Doppelschicht an der Kapillarenwand anders ist, als im Inneren der Kapillare, da die Ionen in der Doppelschicht die DK der Flüssigkeit verändern. Dies bedeutet, dass an der Kapillarenwand infolge des elektrischen Feldes auch eine ponderomotorische Kraft auftritt. Bei den üblichen Bedingungen der Gleichstromelektroosmose ist aber diese ponderomotorische Kraft vertikal zur Kapillarenwand und ruft so keinen Flüssigkeitstransport hervor. Wollen wir die ponderomotorische Kraft zur Geltung kommen lassen, so müssen die Versuchsbedingungen so verändert werden, dass die ponderomotorische Kraft eine Komponente in Richtung der Kapillarenachse bekomme. Es bieten sich zwei Möglichkeiten dazu. Die eine ist, dass die Kapillaren zylinderförmig sind, aber es sind an beiden Seiten des Diaphragmas verschiedene Flüssigkeiten, z. B. Lösungsmittel—Elektrolytlösung. Die andere Möglichkeit ist, dass die Kapillaren des Diaphragmas nicht zylindrisch, sondern konusförmig sind, an beiden Seiten des Diaphragmas befindet sich aber die gleiche Flüssigkeit. Damit die Gleichstromelektroosmose die durch die ponderomotorischen Kräfte hervorgerufene Erscheinung nicht verwäscht, schien es angebracht, die Versuche mit Wechselstrom durchzuführen.

Die Versuche beweisen die Richtigkeit der Betrachtungen, die erwartete Erscheinung tritt auf. Da die Wechselstromelektroosmose von einer anderen Kraft hervorgerufen wird, als die Gleichstromelektroosmose und auch ihre Gesetze andere sind, muss sie als eine neue elektrokinetische Erscheinung betrachtet werden.

In der vorliegenden Arbeit, in der auch die Ergebnisse früherer Versuche berücksichtigt wurden, werden neue Versuchsergebnisse angeführt, die mit den Grundlagen der Erscheinung verbunden sind. Ferner wird eine einheitliche Deutung der Erscheinung angegeben.

2. Beschreibung der Versuchseinrichtung

Als Messgefäss diente ein U-förmiges Glasrohr (Abb. 1), in dessen untersten Teil ein Diaphragma eingeschmolzen wurde. In beide Schenkel des Gefässes ragten Platinblechelektroden. Der Abstand zwischen den Elektroden betrug 20 mm. Die Wechselspannung lieferte ein Hochspannungstransformator. Falls die Versuche mit einer Wechselspannung von 50 Hz durchgeführt wurden, schalteten wir die Netzspannung auf die Primärspule des Transformators, bei anderen Frequenzen war die Spannungsquelle ein Tonfrequenzgenerator. Die Sinusförmigkeit der Spannung wurde mittels eines Oszillographen geprüft.

Das Gefäss wurde mit Leitungswasser (+18 °C), oder mit einer CO_2-Alkohol-Mischung (—78 °C) gekühlt, oder im Wasserbad erwärmt. Bei der Beschreibung der Versuche wird die Frequenz der Wechselspannung und die Temperatur der Flüssigkeiten nur dann erwähnt, wenn die Versuche mit einer anderen Frequenz als 50 Hz, und nicht mit Leitungswasser gekühlt durchgeführt wurden.

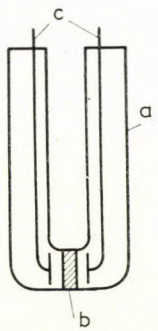

Abb. 1. Messgefäss zur Wechselstromelektroosmose.
a) Glasrohr, b) Diaphragma, c) Platinelektroden

Als Diaphragmen mit zylindrischen Kapillaren wurden Jenaer Sinterglasfilterplatten G2, G3, G4 bzw. G5 verwendet. Ein Diaphragma aus einer einzigen zylindrischen Kapillare wurde dadurch hergestellt, dass in eine 2,5 mm starke Scheidewand aus Glas, die die beiden Schenkel des U-förmigen Gefässes trennte, eine Bohrung von 0,2 mm gebohrt wurde.

Zur Herstellung eines porösen Diaphragmas, bei welchem die Durchmesser der Poren von der einen Seite zur anderen sich erweitern, wurden durch Mahlen und Sieben zweierlei Glaspulver von verschiedener Feinheit hergestellt. Diese wurden dann entsprechend aufeinander gepresst, und gesintert. Die Durchlässigkeit eines auf dieser Weise gewonnenen Diaphragmas war kleiner als die einer Jenaer Glasfilterplatte G4, aber grösser als einer Filterplatte G5. Ein Diaphragma mit einer konusförmigen Kapillare wurde durch einbohren in Konusform in die Glasplatte zwischen den beiden Schenkeln des U-förmigen Glasrohres hergestellt. Die Bohrung hatte einen Durchmesser von 0,3 bzw. 1,2 mm, die Dicke der Glasplatte betrug 2,5 mm.

Die Wechselstromelektroosmose offenbart sich dadurch, dass die Wechselspannung in den beiden Schenkeln des Messgefässes eine Niveaudifferenz der Flüssigkeiten hervorruft. In jenen Fällen, wenn sich zu beiden Seiten des Diaphragmas verschiedene Flüssigkeiten befinden, verschwindet die Niveaudifferenz mit der Zeit, da sich die Flüssigkeiten mischen. Sind die Flüssigkeiten zu beiden Seiten des Diaphragmas die gleichen, so ist die Niveaudifferenz in der Zeit konstant.

3. Versuche mit porösen Glasdiaphragmen

(Die Porendurchmesser sind an beiden Flächen des Diaphragmas gleich.)

3.1. *Der Einfluss der Beschaffenheit des verwendeten Elektrolyts*

Es wurde der zeitliche Ablauf der Wechselstromelektroosmose bei Verwendung verschiedener Elektrolyte untersucht, wobei als Diaphragmen Jenaer Glasfilterplatten, als Lösungsmittel Wasser verwendet wurde. Die Messungen wurden mit Lösungen von $1 \cdot 10^{-3}$ und $1 \cdot 10^{-4}$ normaler Konzentration durchgeführt. Bei diesen Konzentrationen läuft die Erscheinung noch mit genügender Merkbarkeit, aber ohne Störeffekte infolge von Wärmeentwicklung durch den Wechselstrom, ab. Die bei den Untersuchungen verwendeten Elektrolyte konnten, auf Grund ihres Einflusses auf die Erscheinung, in drei Gruppen eingeteilt werden. Innerhalb einer Gruppe ist der Einfluss der Elektrolyte praktisch der gleiche.

I. Gruppe: HCl, HNO_3, H_2SO_4, NaOH, KOH

II. Gruppe: LiCl, NaCl, KCl, CsCl, LiJ, NaJ, KJ

III. Gruppe: $AlCl_3$, $Al(NO_3)_3$, $ThCl_4$, $Th(NO_3)_4$

Die Messergebnisse wurden in den Abbildungen 2, 3, und 4 dargestellt, indem aus jeder Gruppe je ein Elektrolyt herausgehoben und die mit diesem Elektrolyt gewonnenen Ergebnisse aufgetragen wurden. In den Abbildungen stellen die Abszissen die Zeit, die Ordinaten die Niveaudifferenz der Flüssigkeiten in den beiden Schenkeln des Gefässes dar. Wenn im Rohr die Lösung stieg, dann ist die Niveaudifferenz auf die positive Ordinatenachse aufgetragen, wenn aber das Lösungsmittel, dann ist die Niveaudifferenz auf die negative Achse aufgetragen.

Wie es aus den Abbildungen ersichtlich ist, steigt bei einem Diaphragma G2 in jedem Fall, d. h. unabhängig vom Elektrolyt, von der Konzentration und von der Spannung, immer das Lösungsmittel.

Bei einem Diaphragma G4, bei Verwendung eines Elektrolyts aus Gruppe I steigt die Lösung, unabhängig von Konzentration und Spannung. Bei den Messungen mit den Elektrolyten der Gruppe III stieg das Lösungsmittel bei beiden verwendeten Lösungskonzentrationen, wurden aber höhere Spannungen angelegt, stieg zwar in manchen Fällen das Lösungsmittel, dann aber die Lösung. Die Elektrolyte der II. Gruppe üben eine Wirkung aus, die einen Übergang zwischen der Gruppe I und III bildet. Ist die Konzentration der Lösung klein, so steigt immer die Lösung, bei höheren Konzentrationen kann im Anfangsstadium der Messung auch das Lösungsmittel steigen, falls kleinere

Spannungen angewendet wurden. Im Falle eines Diaphragmas G4 kommt also die spezifische Wirkung der Elektrolyte zur Geltung. Diese spezifische Wirkung besteht darin, dass der Elektrolyt das Steigen der Lösung mehr oder weniger fördert.

Im Falle eines Diaphragmas G3 bildet der Ablauf der Erscheinung einen Übergang zwischen der Erscheinung in Verbindung mit den Diaphragmen G2 bzw. G4. Bei kleinen Konzentrationen ist die Strömungsrichtung der Elektroosmose unabhängig von der Beschaffenheit des Elektrolyts (es steigt immer

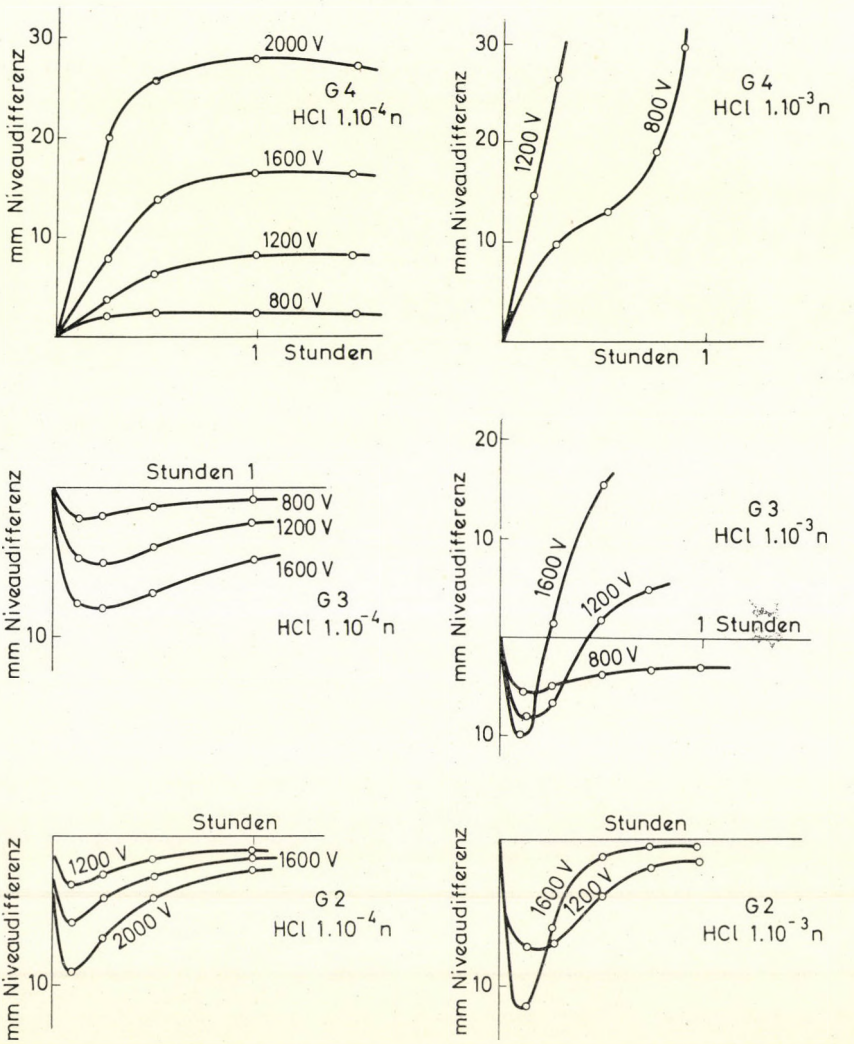

Abb. 2. Die Niveaudifferenz als Funktion der Zeit im Falle von $1 \cdot 10^{-4}$ bzw. $1 \cdot 10^{-3}$ n wässerigen HCl-Lösungen—Wasser, Diaphragmen G4, G3, G2 und verschiedenen Spannungen

das Lösungsmittel), bei höheren Konzentrationen ist die Strömungsrichtung elektrolytabhängig.

Es soll bemerkt werden, dass bei den Messungen grösste Sorgfalt angewendet wurde, wenn die Messungen mit einem anderen Elektrolyt fortge-

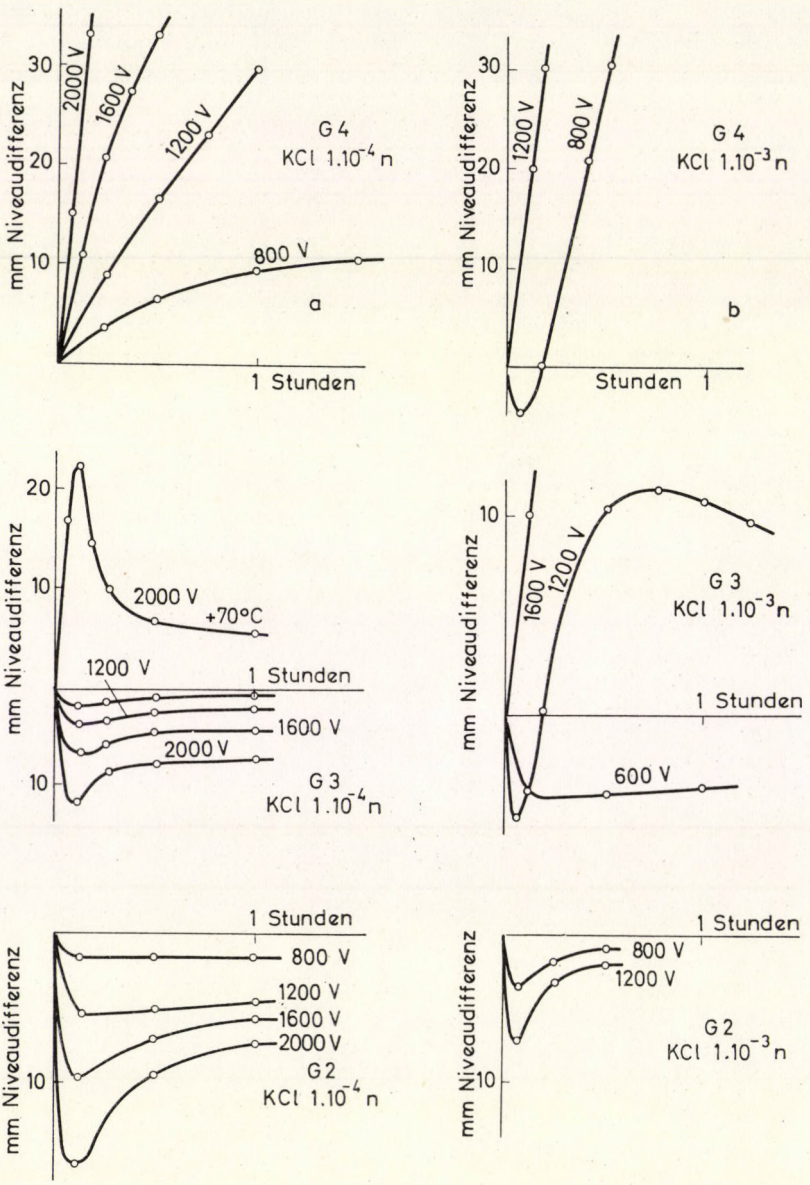

Abb. 3. Die Niveaudifferenz als Funktion der Zeit im Falle von $1 \cdot 10^{-4}$ bzw. $1 \cdot 10^{-3}$ n KCl-Lösung in Wasser—Wasser, Diaphragmen G4, G3, G2 und verschiedenen Spannungen

setzt werden sollten. In diesem Falle wurde das Diaphragma immer gründlich gewaschen, die Lösung und das Lösungsmittel in das Gefäss eingefüllt, und einige Stunden lang im Gefäss gelassen, damit die Adsorptionserscheinungen ablaufen können. Erst dann wurden die neuen Flüssigkeiten eingefüllt, und mit der Messung begonnen.

Aus den Versuchen konnten folgende Regeln herausgelesen werden:

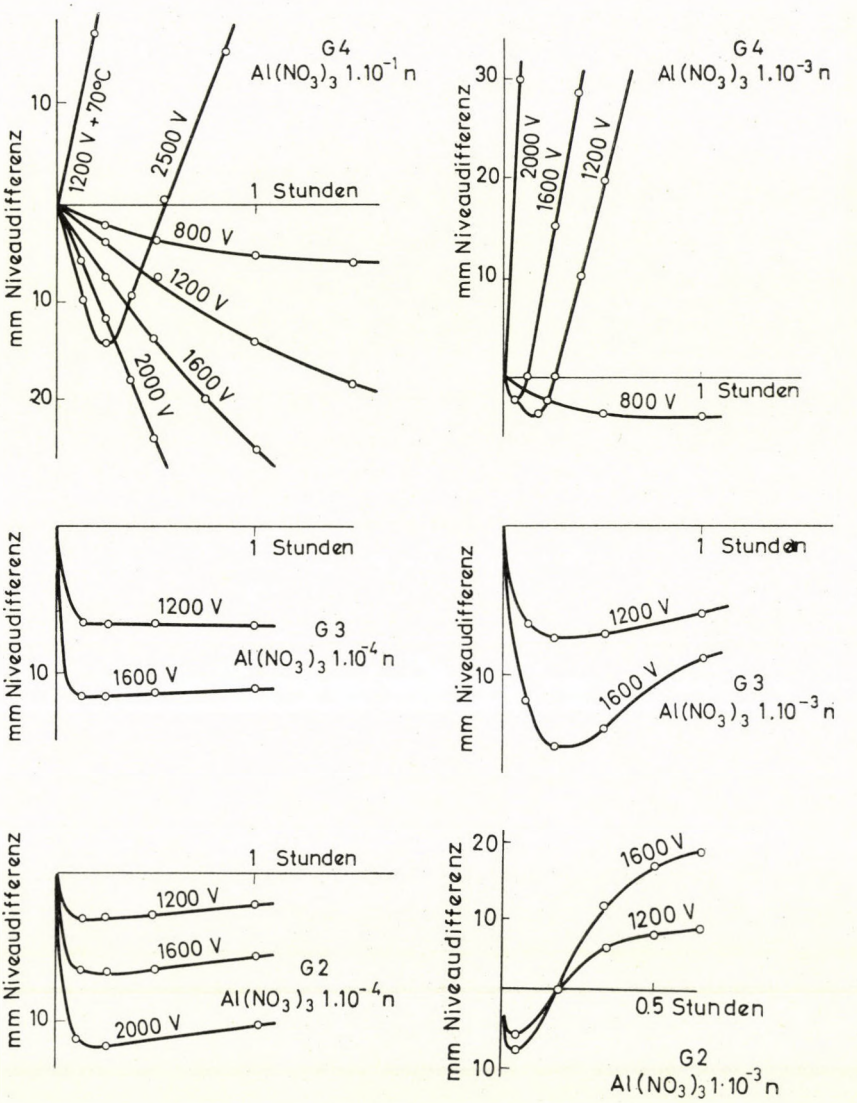

Abb. 4. Die Niveaudifferenz als Funktion der Zeit im Falle von $1 \cdot 10^{-4}$ bzw. $1 \cdot 10^{-3}$ n wässerigen $Al(NO_3)_3$-Lösungen—Wasser, Diaphragmen G4, G3, G2 und verschiedenen Spannungen

Regel 1. Bei Diaphragmen mit grösseren Kapillarendurchmessern ($>40\,\mu$) steigt bei Anwendung von Wechselspannung das Lösungsmittel, unabhängig von der Beschaffenheit des Elektrolyts, seiner Konzentration und der Grösse der Spannung.

Regel 2. Mit Verringerung des Kapillarendurchmessers wächst die Wahrscheinlichkeit, dass die Lösung steigt.

Regel 3. Mit Verringerung des Kapillarendurchmessers kommt die spezifische Wirkung des Elektrolyts immer mehr zur Geltung, indem die verschiedenen Elektrolyte das Steigen der Lösung in folgender Reihenfolge fördern: Säuren > Basen > einwertige Elektrolyte > mehrwertige Elektrolyte.

Regel 4. Eine niedrigere Wechselspannung fördert das Steigen des Lösungsmittels, eine höhere das Steigen der Lösung.

3.2. *Die Wirkung niedriger Spannungen*

Um die Wirkung von niedrigen Spannungen zu untersuchen, wurden als Elektroden kreisförmige Siebe aus Platindraht verwendet, welche unmittelbar auf die Diaphragmen gelegt wurden. Mit einem Diaphragma G4, $5 \cdot 10^{-4}$-n HCl als wässerige Lösung und Wasser als Lösungsmittel stieg bei einer Wechselspannung von 300 V das Lösungsmittel, bei einer Spannung von 600 V die Lösung. Auf Grund des Versuches können wir feststellen:

Regel 5. Mit Anwendung genügend niedriger Spannung kann erreicht werden, dass das Lösungsmittel steige, was immer der Elektrolyt und die Elektrolytkonzentration seie.

3.3. *Die Wirkung der Beschaffenheit des Lösungsmittels*

Es wurde der Ablauf der Wechselstromelektroosmose bei Verwendung von verschiedenen Lösungsmitteln untersucht. Die Lösungsmittel waren: Azeton, Methyl-, Äthyl- und Isobutylalkohol, die Lösungen aber 10^{-4}-n KJ-Lösungen mit diesen Lösungsmitteln, ausgenommen die Lösung in Isobutylalkohol, bei welcher eine solche Konzentration wegen der schlechten Löslichkeit nicht erreicht werden konnte, hier wurde eine gesättigte Lösung verwendet. Wurde ein Diaphragma G2 angewendet, so stieg bei jedem Lösungsmittel und bei jeder Spannung das Lösungsmittel. Die Messergebnisse mit den Diaphragmen G3 und G4 sind in Abb. 5 dargestellt. Es kann aus der Abbildung herausgelesen werden, dass eine höhere Spannung das Steigen der Lösung fördert, wie das Regel 4 fordert. Wie diese Regel zur Geltung kommt, das hängt aber auch von der stofflichen Beschaffenheit des Lösungsmittels ab. Am meisten ausgeprägt ist seine Gültigkeit beim Azeton, dessen Molekeln am wenigsten zur Ordnung neigen, am wenigsten ausgeprägt beim Isobutylalkohol, in welchem die molekulare Ordnung am grössten ist, bei diesem steigt

auch noch dann das Lösungsmittel, wenn eine Spannung von 4000 V angewendet wurde. Aus den Messungen kann festgestellt werden:

Regel 6. Je mehr das Lösungsmittel eine molekulare Ordnung aufweist, um so kleiner ist die Tendenz, dass die Lösung bei der Anlegung einer Wechselspannung steigt.

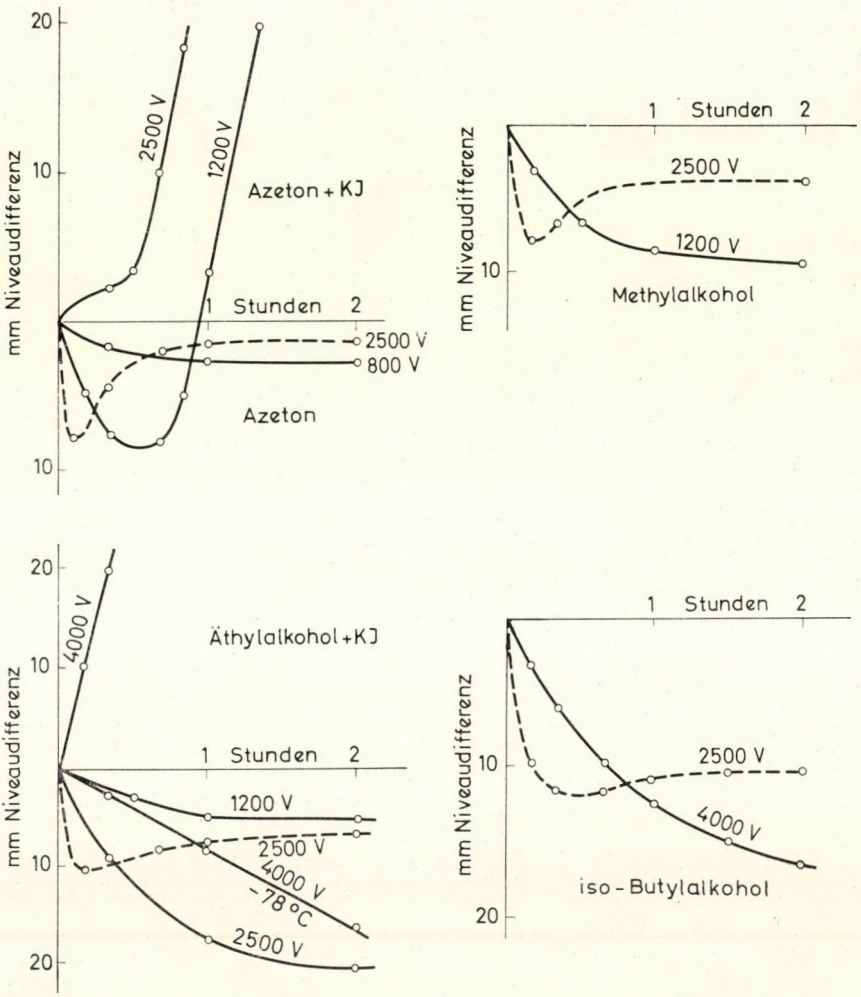

Abb. 5. Die Niveaudifferenz als Funktion der Zeit zwischen $1 \cdot 10^{-4}$ normaler KJ-Lösung—Lösungsmittel, wenn als Lösungsmittel Azeton, Methyl- bzw. Äthylalkohol verwendet wurde. Beim Versuch mit Isobutylalkohol als Lösungsmittel wurde eine gesättigte Lösung von KJ in Isobutylalkohol verwendet. ——— als Diaphragma diente eine Glasfilterplatte G4; ---------- als Diaphragma diente eine Glasfilterplatte G3

3.4. *Die Wirkung der Temperatur*

Die Wirkung der Temperatur wurde dadurch untersucht, dass bei der Temperatur des Leitungswassers, bzw. bei +70 °C parallele Messungen durchgeführt wurden. Die Diaphragmen und die Flüssigkeitspaare waren: G3, $1 \cdot 10^{-4}$-n wässerige KCl-Lösung — Wasser bzw. G4, $1 \cdot 10^{-4}$-n wässerige $Al(NO_3)_3$ Lösung — Wasser. Ausserdem wurde noch eine Messung bei der Temperatur von Kohlensäureschnee und $\approx$ 18 °C mit einem Diaphragma G4, $1 \cdot 10^{-4}$-n KJ äthylalkoholige KJ Lösung — Äthylalkohol angesetzt. Die Messergebnisse sind in den Abbildungen 3, 4, und 6 dargestellt. Aus diesen kann festgestellt werden:

Regel 7. Eine niedrigere Temperatur begünstigt das Steigen des Lösungsmittels, eine höhere die der Lösung.

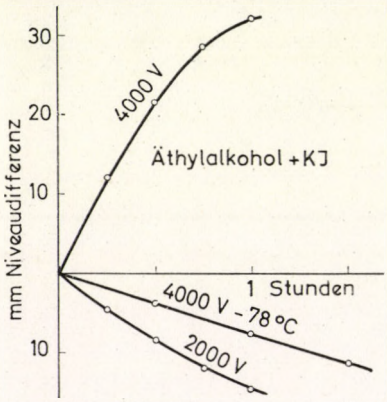

Abb. 6. Die Niveaudifferenz als Funktion der Zeit im Falle von $1 \cdot 10^{-4}$ n Lösung von KJ in Äthylalkohol—Äthylalkohol, Diaphragma G4, Wechselspannung von 4000 V bei einer Temperatur von +18 bzw. —78 °C

3.5. *Die Wirkung der Elektrolytkonzentration*

Die in Abb. 3b angeführten Messergebnisse zeigen — im Vergleich mit Abb. 3a — dass eine Erhöhung der Elektrolytkonzentration das Steigen des Lösungsmittels begünstigt. Da aber eine erhöhte Elektrolytkonzentration — bei gleichbleibender Spannung — eine grössere Wärmemenge in der Kapillare erzeugt, begünstigt dies gemäss Regel 7 das Steigen der Lösung. Die beiden Wirkungen arbeiten gegeneinander, und demzufolge kann eine Regel von allgemeiner Geltung mit Sicherheit nicht festgelegt werden.

3.6. *Die Wirkung der Wechselspannungsfrequenz*

Der Ablauf der Wechselstromelektroosmose wurde auch bei einer Wechselspannungsfrequenz, die höher als 50 Hz ist, untersucht. Ist die Formel der Wechselspannung nicht sinusartig, sondern so verzerrt, dass die Spannung in der einen Halbperiode grösser ist — das kann mittels eines Oszilloskops kontrolliert werden — so tritt als Resultat eine Gleichstromelektroosmose auf. Besteht dieser Fehler, so dreht sich die Strömungsrichtung der Elektroosmose um, wenn bei den Elektroden die Stromzuführungen aufgetauscht werden. Dieser Fehler trat bei unseren Versuchen nicht auf.

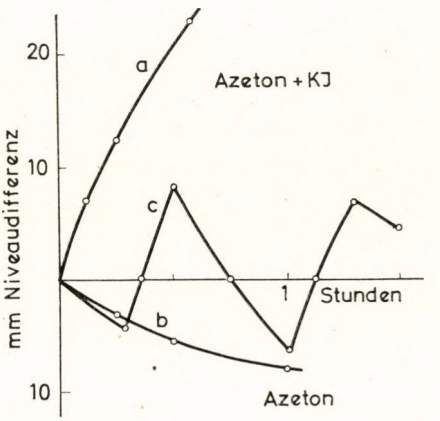

Abb. 7. Die Niveaudifferenz als Funktion der Zeit im Falle von $1 \cdot 10^{-5}$ n Lösung von KJ in Azeton—Azeton, Diaphragma G4, Wechselspannung von 4000 V.
a) Frequenz der Spannung 50 Hz. Es steigt die Lösung. b) Frequenz der Spannung 1000 Hz. Es steigt das Lösungsmittel. c) Frequenz abwechselnd 50 bzw. 1000 Hz

Der Ablauf der Elektroosmose wurde u. a. mit einem Diaphragma G4, $1 \cdot 10^{-5}$-n Lösung von KJ in Azeton—Azeton bei den Frequenzen von 50 und 1000 Hz, bei einer Spannung von 4000 V untersucht. Die Messresultate sind in Abb. 7 angegeben. Während bei einer Frequenz von 50 Hz die Lösung steigt, kehrt sich die Strömungsrichtung bei einer Frequenz von 1000 Hz um. Die Messung wurde auch so durchgeführt, dass abwechselnd 50 bzw. 1000 Hz angelegt wurde. Bei einem Diaphragma G2 und den angegebenen Flüssigkeitspaaren hatte die Erhöhung der Wechselspannungsfrequenz keinen Richtungswechsel der elektroosmotischen Strömung zur Folge. Aus den Messungen folgt:

Regel 8. Eine Wechselspannung niedrigerer Frequenz (50 Hz) begünstigt das Steigen der Lösung, eine von höherer Frequenz (1000 Hz) das Steigen des Lösungsmittels.

Es wurde auch die Abhängigkeit des osmotischen Druckes von der Frequenz der Wechselspannung untersucht. Die Messungen wurden bei den Flüs-

sigkeiten: $1 \cdot 10^{-5}$-n Lösung von KJ in Azeton—Azeton durchgeführt, mit einer Spannung von 4000 V, wobei die Frequenz von 50 Hz bis 1000 Hz geändert wurde. Der osmotische Druck wurde aus den maximalen Niveaudifferenzen ermittelt. Dass die Flüssigkeiten sich während der Messung mischen, beeinflusst die Messwerte nicht. Davon konnten wir uns überzeugen, wir bekamen nämlich die gleichen Druckwerte, wenn die Frequenz in umgekehrter Reihenfolge geändert wurde. Die Messergebnisse sind in Abb. 8 dargestellt.

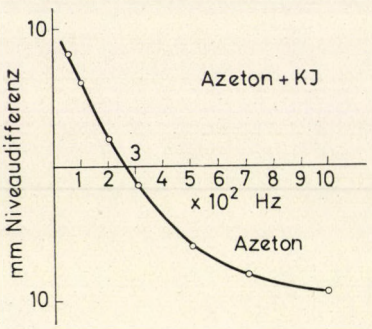

Abb. 8. Der elektroosmotische Druck als Funktion der Wechselspannungsfrequenz im Falle von $1 \cdot 10^{-4}$ n Lösung von KJ in Azeton—Azeton, Diaphragma G3, 4000 V

Die Frequenzabhängigkeit des osmotischen Druckes war auch in jenen Fällen Gegenstand unserer Untersuchung, als die Änderung der Wechselspannungsfrequenz ein Umkehren der elektroosmotischen Strömungsrichtung nicht zur Folge hatte. Diese Messungen wurden mit einem Diaphragma G3 durchgeführt, wobei die Wechselspannung 1500 V betrug, und $1 \cdot 10^{-4}$-n Lösung von KJ in Methylalkohol bzw. Methylalkohol verwendet wurde. Die Messergebnisse sind in Abb. 9 dargestelit.

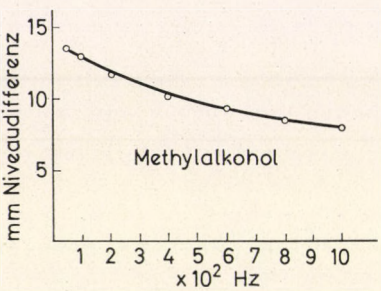

Abb. 9. Der elektroosmotische Druck als Funktion der Wechselspannungsfrequenz im Falle von $1 \cdot 10^{-4}$ n Lösung von KJ in Methylalkohol—Methylalkohol, Diaphragma G3, 1500 V

Mittels eines Hochfrequenzgenerators wurde eine Spannung von 2500 V und eine Frequenz von 380 kHz erzeugt. Mit dieser Hochfrequenzspannung konnte keine elektroosmotische Erscheinung beobachtet werden. Es kann festgestellt werden:

Regel 9. Erhöht man die Frequenz der Wechselspannung, so vermindert sich der elektroosmotische Druck und wird endlich gleich Null.

In Tabelle I sind die Messergebnisse der verschiedenen Messungen zusammengefasst, bei welchen als Lösungsmittel Azeton bzw. Äthylalkohol, als Lösung $1 \cdot 10^{-4}$-n Lösung von KJ in den genannten Lösungsmitteln verwendet wurde. Verschiedene Jenaer Glasfilter dienten als Diaphragmen, und die Wechselspannung hatte einen Wert von 4000 V, bei Frequenzen von 50 bzw. 1000 Hz. In der Tabelle bedeutet Ziffer 1 die Lösung, Ziffer 2 das Lösungsmittel. Die erste Ziffer in den Kolonnen der Tabelle bezieht sich auf Messungen mit 50 Hz, die zweite auf solche mit 1000 Hz. Infolge der Wechselspannung steigt die der Ziffer entsprechende Flüssigkeit. Die in dieser Tabelle zusammengefassten Messergebnisse sind mit den oben angegebenen Regeln im Einklang, und bestätigen hiedurch deren Gültigkeit.

3.7. *Die Wirkung der an der Diaphragmenoberfläche adsorbierten Luftschicht*

Bei den bisher erörterten Untersuchungen befand sich keine Luftschicht an der Oberfläche des Diaphragmas. Das konnte so erreicht werden, dass im Messgefäss das entsprechende Lösungsmittel zuerst zum Kochen gebracht wurde, und im Weiteren das Gefäss nie getrocknet wurde, das zu untersuchende Lösungsmittel und die Lösung berührte beim Einfüllen eine vorher bereits benetzte Oberfläche.

Wurde das Messgefäss an der Luft bei 300 °C ausgetrocknet, und die zu untersuchenden Flüssigkeiten dann eingefüllt, so konnte in der Strömungsrichtung der Wechselstromelektroosmose eine Änderung auftreten, im Vergleich zu der Erscheinung, welche sich mit einem Diaphragma ohne adsorbierte Luft abspielt. In Abb. 10 ist der Ablauf der Wechselstromelektroosmose mit Diaphragmen G3 und G4 mit einer adsorbierten Luftschicht bzw. ohne die dargestellt. Hierbei diente als Lösungsmittel Wasser, die Lösung war eine $1 \cdot 10^{-4}$-n wässerige KJ Lösung. Es ist zu sehen, dass im gegebenen Fall die an der Oberfläche der Diaphragmenkapillaren adsorbierte Luftschicht die osmotische Strömungsrichtung verändert hat.

Die Untersuchungen wurden an verschiedenen Flüssigkeitspaaren (Lösung—Lösungsmittel) durchgeführt. Die daraus gewonnenen Messergebnisse sind in Tabelle II angegeben, die Ziffern in den Kolonnen der Tabelle geben die Kennummer der steigenden Flüssigkeiten an. Zum Vergleich sind auch die Messdaten der Versuche mit luftlosen Diaphragmen angegeben. Die Elektrolytkonzentrationen und Spannungswerte sind so gewählt worden, dass mit einem luftfreien Diaphragma — wenigstens zu Beginn der Messung — das Lösungsmittel steigen soll. Wie man sieht, kann die adsorbierte Luft die Strömungsrichtung umkehren. Diese Wirkung kommt am stärksten bei dem Diaphragma G4 zum Vorschein, bei dem Diaphragma G2 gar nicht. Ferner

Acta Physica Academiae Scientiarum Hungaricae 31, 1972

Tabelle I

Flüssigkeitspaar		Diaphragma G2		Diaphragma G3						Diaphragma G4					
		$t = -78$ °C $t = +15$ °C $t = +45$ °C		$t = -78$ °C		$t = +15$ °C		$t = +45$ °C		$t = -78$ °C		$t = +15$°C		$t = +45$ °C	
Nr. 1	Nr. 2	50 und 1000 Hz		50 und 1000 Hz						50 und 1000 Hz					
Azeton + KJ	— Azeton	2	2	2	2	1	2	1	2	1	2	1	2	1	2
Äthylalkohol + KJ	— Äthylalkohol	2	2	2	2	2	2	2	2	2	2	1	2	1	2

Tabelle II

Flüssigkeitspaar		Konzentration 10^{-5} n	Diaphragma G2		Diaphragma G3			Diaphragma G4		
			Spannung kV	Ohne und mit adsorbierter Luft	Spannung kV	Ohne adsorbierte Luft	Mit adsorbierter Luft	Spannung kV	Ohne adsorbierte Luft	Mit adsorbierter Luft
Nr. 2	Nr. 1									
Wasser + KJ	— Wasser	6	2,0	2	2,0	2	1	1,2	2	1
Azeton + KJ	— Azeton	6	2,5	2	2,5	2	1	1,2	2	1
Methylalkohol + KJ	— Methylalkohol	6	2,5	2	2,5	2	2	1,2	2	1
Äthylalkohol + KJ	— Äthylalkohol	6	2,5	2	2,5	2	2	1,2	2	1
Isobutylalkohol + KJ	— Isobutylalkohol	gesättigt	2,5	2	2,5	2	2	3,7	2	2

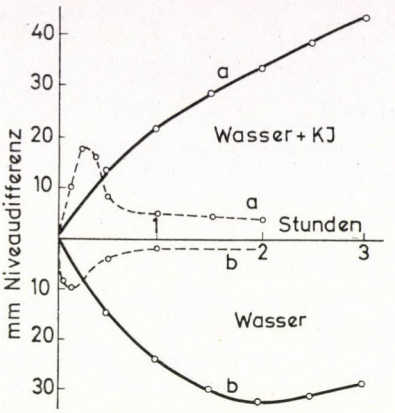

Abb. 10. Die Niveaudifferenz als Funktion der Zeit im Falle von $1 \cdot 10^{-4}$ n wässeriger KJ-Lösung—Wasser. a) Diaphragma mit adsorbierter Luftschicht; b) Diaphragma ohne Luftschicht. ——— Diaphragma G4 und Spannung von 1200 V; ---------- Diaphragma G3 und Spannung von 1900 V

kann beobachtet werden, dass die Strömungsrichtung beim Isobutylalkohol, der zur Assoziation seiner Molekeln am meisten neigt, durch die adsorbierte Luftschicht nicht geändert werden konnte.

Falls die an der Diaphragmenoberfläche adsorbierte Luft die elektroosmotische Strömungsrichtung nicht ändert, so wird die Niveaudifferenz kleiner, wie dies aus Abb. 11 ersichtlich ist. Wir können daher feststellen:

Regel 10. Die an der Wand der Kapillaren adsorbierte Luft begünstigt das Steigen der Lösung und verursacht dadurch entweder eine Richtungs-

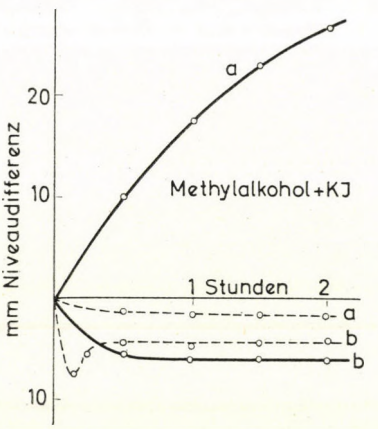

Abb. 11. Die Niveaudifferenz als Funktion der Zeit im Falle von $1 \cdot 10^{-4}$ n Lösung von KJ in Methylalkohol—Methylalkohol. a) Diaphragma mit adsorbierter Luftschicht; b) Diaphragma ohne Luftschicht. ——— Diaphragma G4 und Spannung von 1200 V; ---------- Diaphragma G3 und Spannung von 1900 V

wechsel der elektroosmotischen Strömung oder verringert wenigstens das Steigen des Lösungsmittels. Diese Regel ist für Kapillaren mit kleinen Durchmessern gültig. Bei grösseren Durchmessern ($> 40\ \mu$) beeinflusst die adsorbierte Luftschicht die Elektroosmose nicht. Die Grösse der Wirkung hängt auch von der Beschaffenheit des Lösungsmittels ab, indem bei Flüssigkeiten, die zur inneren Ordnung ihrer Molekel sehr geneigt sind, die Wirkung kleiner ist.

Es sei bemerkt, dass im Falle, wenn an der Wand eines porösen Diaphragmas (z. B. G4) sich eine adsorbierte Luftschicht befindet, und das Diaphragma zwei Flüssigkeiten von verschiedener Oberflächenspannung voneinander trennt, auch ohne ein elektrisches Feld eine sehr beträchtliche Niveaudifferenz entsteht. Bei unseren elektroosmotischen Untersuchungen waren die gelösten Substanze kapillarinaktiv, und so kam ohne ein elektrisches Feld keine Niveaudifferenz zustande, auch dann nicht, wenn das Diaphragma mit Luft beschaffen war.

Auf Grund der letztgenannten Versuche kann Regel 1 ergänzt werden:

Regel 1. Bei Diaphragmen mit grösseren Kapillarendurchmessern ($> 40\ \mu$) lässt eine Wechselspannung das Lösungsmittel steigen, unabhängig von der Qualität des Lösungsmittels und des Elektrolyts von der Konzentration des Letzteren, von der Temperatur, von der Höhe und der Frequenz der Spannung und unabhängig davon, ob an der Oberfläche des Diaphragmas sich eine adsorbierte Luftschicht befand oder nicht.

3.8. *Versuche mit Diaphragma G5*

War das Diaphragma eine Jenaer Glasfilterplatte G5, so konnte erst nach mehrstündiger Beobachtung eine Niveaudifferenz von einigen Millimetern festgestellt werden, und zwar nur bei niedrigen Spannungen (< 1200 V), wenn Elektrolytlösung—Lösungsmittel als Flüssigkeitspaar verwendet wurde. In diesen Fällen stieg die Lösung. Bei einer höheren Spannung (4000 V) kam kein Flüssigkeitstransport zustande. Es kann festgestellt werden:

Regel 11. Bei Diaphragmen mit sehr kleinen Kapillarendurchmessern ($< 1{,}7\ \mu$) kann nur bei niedrigen Spannungen (< 1200 V) eine Wechselstromelektroosmose beobachtet werden.

3.9. *An beiden Seiten des Diaphragmas befinden sich verschiedene Flüssigkeiten*

Befanden sich im Messgefäss zwei verschiedene Alkohole u. zwar Methyl-, Äthyl-, n-Propyl oder n-Amylalkohol, und wurde eine Wechselspannung angelegt, so strömte bei luftfreien Diaphragmen G2, G3 und G4 immer der Alkohol mit kleinerem Molekulargewicht zum anderen Alkohol mit dem grösseren Molekulargewicht hinüber.

Wenn die verwendeten Flüssigkeiten nicht Mitglieder einer homologen

Reihe sind, so hängt die elektroosmotische Strömungsrichtung von den Porendurchmessern des Diaphragmas ab, und es konnte keine Regel festgestellt werden, welche die Strömungsrichtung bestimmt.

Es ist merkwürdig, dass bei Verwendung von Äthylalkohol—Wasser als Flüssigkeitspaar und einem Diaphragma G2, eine Wechselspannung von 4000 V Äthylalkohol in solchem Masse zum Wasser durchströmen lässt, dass das Wasserniveau höher wird als das Niveau des Äthylalkohols. In unserem Falle war der spezifische Widerstand des Äthylalkohols der fünffache des spezifischen Widerstandes des Wassers. Dieser Versuch beweist, dass bei grösseren Kapillarendurchmessern nicht immer jene Flüssigkeit zur anderen durchströmt, welche das grössere Leitvermögen besitzt. Dies hätte nämlich aus unseren Versuchen mit Elektrolytlösung—Lösungsmittel eventuell als Regel herausgelesen werden.

3.10. *Die Abhängigkeit des elektroosmotischen Druckes von der Feldstärke*

Zur Untersuchung der Abhängigkeit des elektroosmotischen Druckes von der Feldstärke müssen Elektrolyt, Diaphragma und Spannung so gewählt werden, dass die elektroosmotische Strömungsrichtung bei sämtlichen Versuchen die gleiche bleibe. Wir verwendeten als Flüssigkeitspaar $1 \cdot 10^{-4}$-n wässerige HCl-Lösung und Wasser, und als Diaphragma eine Filterplatte G4. Die Spannungswerte wurden so niedrig gewählt, dass die sich einstellenden maximalen Niveaudifferenzen mit unserem Messgefäss noch zu bestimmen seien. Diese Spannungswerte waren 500, 1000 und 1500 V, die sich einstellenden Niveaudifferenzen 4, 15 und 34 mm. Um Konzentrationsänderungen infolge von Niveauänderungen zu vermeiden verfuhren wir so, dass wir Vorversuche gemacht haben und dann die Flüssigkeiten in die Schenkel des Messgefässes so hoch eingefüllt haben, dass die zu erwartenden Niveaudifferenzen annähernd schon bei Beginn ausgebildet seien. Auf Grund der Messungen kann festgestellt werden:

Regel 12. Der elektroosmotische Druck ist eine quadratische Funktion der Feldstärke.

3.11. *Die Abhängigkeit der elektroosmotischen Strömungsgeschwindigkeit von der Feldstärke*

Die Gesichtspunkte nach welchen Elektrolyt, Spannungswerte und Diaphragma hier ausgewählt wurden, waren die gleichen wie im Punkt 3.10. So wurde auch hier $1 \cdot 10^{-4}$-n wässerige HCl Lösung und Wasser, bzw. Diaphragma G4 verwendet und bei verschiedenen Spannungen die in der Zeiteinheit sich einstellenden Niveaudifferenzen gemessen. Bei der Wahl der Zeiteinheit und der Spannungswerte wurde darauf geachtet, dass die Niveaudifferenzen im Vergleich zum elektroosmotischen Druck niedrig seien. Die

Spannungswerte waren 1500, 2500, 3000 V, das Verhältnis der Niveaudifferenzen in der Zeiteinheit 1 : 2,3 : 4,1, woraus folgt:

Regel 13. Die elektroosmotische Strömungsgeschwindigkeit ist eine quadratische Funktion der Feldstärke.

3.12. *Die Abhängigkeit des elektroosmotischen Druckes vom Kapillarenradius*

Zur Bestimmung des Zusammenhanges zwischen dem Kapillarenradius des Diaphragmas und dem elektroosmotischen Druck, benötigen wir wenigstens die Kenntnis des Verhältnisses der Kapillarenradii. Dieses Verhältnis wurde mit Hilfe der Gleichstromelektroosmose bestimmt, da dort der Zusammenhang zwischen dem osmotischen Druck und dem Kapillarenradius bekannt ist. Das Verhältnis der durchschnittlichen Kapillarenradii der Diaphragmen G3 bzw. G4 ergab sich auf Grund unserer Messungen zu 2,1 : 1. Die mit einer Wechselspannung von 3500 V durchgeführten Messungen wurden an einem Flüssigkeitspaar: $6 \cdot 10^{-5}$-n Lösung von KJ in Azeton—Azeton durchgeführt. Für den osmotischen Druck ergaben sich die Werte von 43 bzw. 180 mm Alkoholsäulendruck [1]. Das Verhältnis der Kapillarenradii ist also 4,41, das Verhältnis der osmotischen Drücke 4,18 das mit ausreichender Genauigkeit das folgende Ergebnis bietet:

Regel 14. Der elektroosmotische Druck ist dem Quadrat des Radius der Diaphragmenkapillaren umgekehrt proportional.

Wir müssen darauf aufmerksam machen, dass die Porendurchmesser der Jenaer Glasfilterplatten, die die gleiche Kennummer tragen, gewisse Streuungen zeigen. Diese Streuung der Porendurchmesser lässt sich im Ablauf der Wechselstromelektroosmose — in der Strömungsrichtung — spüren. Die Abweichungen, die bei Filtern von gleichen Kennummern auftreten, liegen aber stets in der Richtung, wie das aus den festgestellten Regeln zu erwarten ist, wenn die wirklichen Kapillarendurchmesser in Rechnung genommen werden.

4. Versuche bei welchen als Diaphragma eine Glasplatte mit einer zylindrischen Bohrung angewendet wurde

Wird bei unserem U-förmigen Gefäss als Diaphragma ein in eine Glasplatte gebohrtes zylindrisches Loch gewählt, (Durchmesser der Bohrung betrug 0,2 mm, ihre Länge 2,5 mm) und füllt man in den einen Schenkel ein Lösungsmittel, in den anderen eine Elektrolytlösung, so erfolgt bei Anlegen einer Wechselspannung auch in diesem Falle ein Flüssigkeitstransport. In allen Fällen strömt die Lösung zum Lösungsmittel hinüber, unabhängig von den Parametern, die im Abschnitt 3 erörtert waren, also ähnlich wie das bei einem Diaphragma G2 der Fall ist.

In Abb. 12 ist diejenige Niveaudifferenz als Funktion der Zeit dargestellt, die sich beim Flüssigkeitspaar: $1 \cdot 10^{-4}$-n wässerige KJ-Lösung—Wasser bei Anlegen einer Wechselspannung von 1000 V einstellt (Kurve *a*). Bei der gleichen Zusammenstellung wurde auch der Ablauf der Gleichstromelektroosmose bei einer Gleichspannung von 500 V untersucht, wobei die negative Elektrode sich im Lösungsmittel (Kurve *b*) bzw. in der Lösung (Kurve *c*) befand. Im letzteren Fall lief die Elektroosmose nicht so ab, wie bei einem Dia-

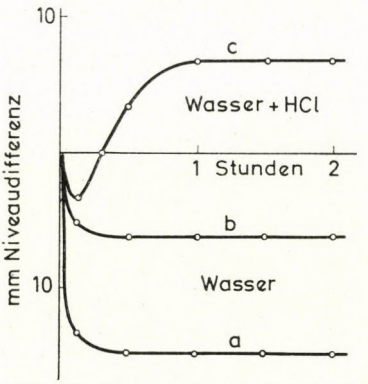

Abb. 12. Die Niveaudifferenz als Funktion der Zeit im Falle eines zylindrischen Lochdiaphragmas, $1 \cdot 10^{-4}$ n wässeriger HCl-Lösung—Wasser. a) Wechselspannung von 1000 V; b) Gleichspannung von 500 V, die negative Elektrode im Lösungsmittel; c) Gleichspannung von 500 V, die negative Elektrode in der Lösung

phragma G2, indem zu Beginn des Versuches die Lösung zum Lösungsmittel hinüberströmte und erst später die Regel, die die Strömungsrichtung bei der Gleichstromelektroosmose bestimmt, zur Geltung kam.

Ähnlich wie bei der Wechselstromelektroosmose mit einem Diaphragma G2, konnten auch hier die Beobachtungen, die sich auf die Strömungsrichtung bei Lösung—Lösungsmittel beziehen, nicht einfach so zusammengefasst werden, dass bei Anlegen einer Wechselspannung immer die Flüssigkeit mit grösserem elektrischen Leitvermögen zur anderen hinüberströmt. Um das zu beweisen sei in Abb. 13 der Ablauf der Wechselstromelektroosmose mit Äthylalkohol—Wasser dargestellt, wo der fünfmal schlechter leitende Alkohol zum Wasser hinüberströmt.

Auf Grund von ausführlichen Untersuchungen sind folgende Regeln bei diesem Diaphragma und bei Verwendung von Elektrolytlösung—Lösungsmittel gültig:

Regel 1. Bei Anlegen einer Wechselspannung fliesst die Lösung zum Lösungsmittel hinüber, unabhängig von der Beschaffenheit des Lösungsmittels und der Lösung, unabhängig von der Konzentration der Lösung, von der Temperatur der Flüssigkeiten, von der Grösse der Spannung, von deren Fre-

quenz und davon ob sich an der Oberfläche der Kapillarenwand eine adsorbierte Gasschicht befindet oder nicht.

Regel 2. Der elektroosmotische Druck ist dem Quadrat der Feldstärke proportional.

Regel 3. Der elektroosmostische Druck ist dem Radius der Diaphragmenkapillare umgekehrt proportional.

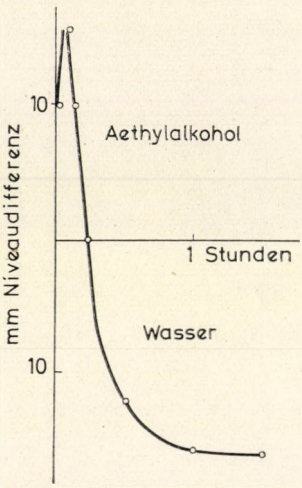

Abb. 13. Die Niveaudifferenz als Funktion der Zeit im Falle von Äthylalkohol—Wasser, eines zylindrischen Lochdiaphragmas und einer Wechselspannung von 3500 V

5. Versuche mit porösen Glasdiaphragmen, bei welchen die Porendurchmesser gegen die eine Seite des Diaphragmas hin zunehmen

5.1. *Versuche mit destillierten Flüssigkeiten*

Waren beide Flüssigkeiten im Messgefäss mit dem oben genannten Diaphragma reine, destillierte Lösungsmittel (Wasser, Azeton, Methyl-, Äthylalkohol), so strömt bei Anlegung von Wechselspannung (2—4 kV) die Flüssigkeit in der Kapillare bei allen Temperaturen in jene Richtung, in welcher die Poren sich verjüngen.

5.2. *Versuche mit $1 \cdot 10^{-4}$-normalen Elektrolytlösungen*

Mit $1 \cdot 10^{-4}$-normaler wässeriger KCl oder $Al(NO_3)_3$ Lösung und einer Wechselspannung von 0,5—1,5 kV strömt die Flüssigkeit in der Kapillare ebenfalls bei allen Temperaturen in die Richtung der kleineren Porenöffnungen.

5.3. *Versuche mit 5 · 10 $^{-4}$-normalen Elektrolytlösungen*

Mit 5 · 10 $^{-4}$-normalen wässerigen KCl oder $Al(NO_3)_3$ Lösungen ist die Strömungsrichtung bei Anlegung von 1000 V je nach der Badtemperatur verschieden. Bei Leitungswassertemperatur steigt die Flüssigkeit an der Feinporenseite, bei einem Warmbad (+75 °C) an der anderen, an der grobporigen Seite des Diaphragmas. Wird wechselweise kaltes, bzw. warmes Wasser durch das Bad geleitet, so ändert sich die Strömungsrichtung dementsprechend. Die Messergebnisse bei einer KCl Lösung sind in Abb. 14 angegeben. Die Abszissen-

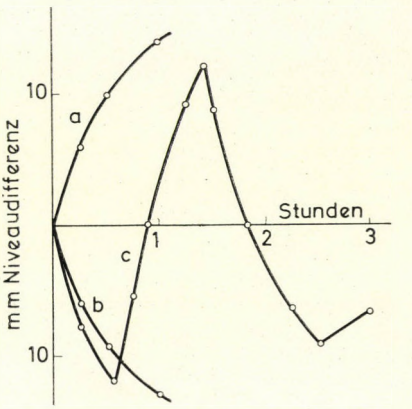

Abb. 14. Die Niveaudifferenz als Funktion der Zeit im Falle von 5 · 10^{-4} n wässeriger KCl-Lösung, einer Wechselspannung von 1000 V und eines Diaphragmas bei welchem die Porendurchmesser in eine Richtung zunehmen. a) Bei einem Wasserbad von +18 °C. Es steigt die Flüssigkeit an der Feinporenseite. b) Bei einem Wasserbad von +75 °C. Es steigt die Flüssigkeit an der Grobporenseite. c) Im Falle einer Wasserbadtemperatur von abwechselnd +18 bzw. +75 °C

werte geben die Zeit an, die positiven Ordinatenwerte die Niveaudifferenz zwischen Feinporenseite und Grobporenseite. Negative Ordinatenwerte bedeuten also, dass die Flüssigkeit an der Grobporenseite stieg.

5.4. *Versuche mit 1 · 10 $^{-3}$-normalen Elektrolytlösungen*

Mit 1 · 10 $^{-3}$-normalen wässerigen KCl oder $Al(NO_3)_3$ Lösungen stieg bei Anlegung einer Wechselspannung von 500 V die Flüssigkeitssäule an der Feinporenseite, bei 1000 V aber die an der Grobporenseite, unabhängig von der Badtemperatur. Die Messergebnisse für eine KCl Lösung und Leitungswassertemperatur sind in Abb. 15 angegeben.

5.5. *Versuche mit* $1 \cdot 10^{-2}$*-normaler Elektrolytlösung*

Mit einer $1 \cdot 10^{-2}$-normalen wässerigen KCl Lösung stieg bei Anlegung einer Wechselspannung von 250 V stets die Flüssigkeit an der Feinporenseite, unabhängig von der Badtemperatur.

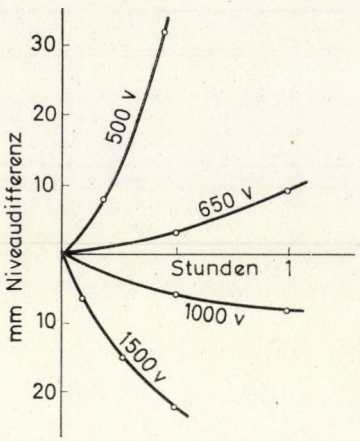

Abb. 15. Die Niveaudifferenz als Funktion der Zeit im Falle von $1 \cdot 10^{-3}$ n wässeriger KCl-Lösung, einer Wechselspannung von verschiedenen Werten und eines Diaphragmas, bei welchem die Porendurchmesser in eine Richtung zunehmen

5.6. *Die Wirkung der an der Diaphragmenoberfläche adsorbierten Luft*

Bei den bisherigen Versuchen mit konusförmigen Poren war die Diaphragmenoberfläche frei von einer adsorbierten Luftschicht. Eine adsorbierte Luftschicht kann in der Strömungsrichtung der Wechselstromelektroosmose eine Änderung herführen. Eine solche Änderung tritt auf Grund unserer Messungen nur dann ein, wenn ohne eine Luftschicht die Flüssigkeit an der Feinporenseite stieg. Abb. 16 zeigt einen typischen Fall mit destilliertem Wasser bei Anlegung einer Wechselspannung von 300 V. Der verschiedene Ablauf der Elektroosmose mit bzw. ohne eine adsorbierte Luftschicht ist klar sichtbar.

5.7. *Die Abhängigkeit der elektroosmotischen Strömungsgeschwindigkeit von der Feldstärke*

Es wurden die Flüssigkeitsmengen bestimmt, welche bei Verwendung von Wasser und bei Anlegung von 50, 100 bzw. 200 V in vier Stunden durchströmen. Das Verhältnis dieser Mengen betrug: 1 : 4,2 : 15,7.

Aus den Versuchsergebnissen kann herausgelesen werden, dass mit reinen, destillierten Lösungsmitteln, und mit sehr verdünnten Elektrolytlösungen

($1 \cdot 10^{-4}$-n) stets die Flüssigkeit an der Feinporenseite steigt, unabhängig von der Badtemperatur und dem Wert der Wechselspannung. Diese Strömungsrichtung bleibt bestehen, wenn die Elektrolytkonzentration höher ist, aber die Spannungswerte niedriger sind. Eine erhöhte Elektrolytkonzentration allein hat also noch keinen entscheidenden Einfluss auf die Strömungsrichtung.

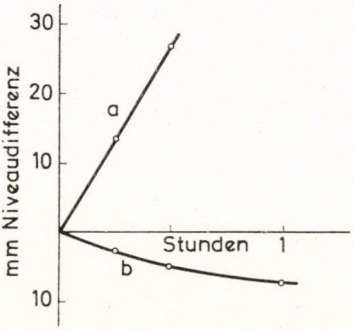

Abb. 16. Die Niveaudifferenz als Funktion der Zeit im Falle von destilliertem Wasser, einer Wechselspannung von 3000 V und eines Diaphragmas, bei welchem die Porendurchmesser in eine Richtung zunehmen. a) Diaphragma ohne Luftschicht. Es steigt die Flüssigkeit an der Feinporenseite. b) Diaphragma mit adsorbierter Luftschicht. Es steigt die Flüssigkeit an der Grobporenseite

Erst bei höheren Spannungswerten oder bei höheren Badtemperaturen dreht sich die Strömungsrichtung um. Es können folgende Regeln festgestellt werden:

Regel 1. Die Strömungsrichtung im Inneren der Diaphragmenkapillare richtet sich gegen das Ende mit dem kleineren Durchmesser, falls reine Lösungsmittel oder sehr verdünnte Elektrolytlösungen ($1 \cdot 10^{-4}$-n) verwendet werden. Die Strömungsrichtung ist hierbei unabhängig vom Elektrolyt, von der Spannung und der Temperatur.

Regel 2. Eine Erhöhung der Elektrolytkonzentration ermöglicht das Steigen der Flüssigkeit an der Grobporenseite.

Regel 3. Durch die Wahl einer genügend niedriger Spannung kann immer erreicht werden, bei was immer für einem Elektrolyt und Elektrolytkonzentration, dass die Strömung der Flüssigkeit im Inneren der Diaphragmenkapillare gegen das Ende mit dem kleineren Durchmesser sich richte.

Regel 4. Eine Erhöhung der Temperatur der Elektrolytlösung fördert das Steigen der Flüssigkeit an der Grobporenseite.

Regel 5. Eine Verwendung von höherer Wechselspannung fördert das Steigen der Flüssigkeit an der Grobporenseite.

Regel 6. Eine adsorbierte Luftschicht an der Diaphragmenoberfläche fördert das Steigen der Flüssigkeit an der Grobporenseite.

Regel 7. Die elektroosmotische Strömungsgeschwindigkeit ist eine quadratische Funktion der Feldstärke.

Eine Messung des osmotischen Druckes war bei diesem Diaphragma nicht möglich, infolge des hohen osmotischen Druckes und der kleinen Strömungsgeschwindigkeit bei diesem kleinen Porendurchmesser. Da beim Versuch 5.7 kleine Spannungen angelegt wurden und Wasserkühlung angewendet wurde, sowie die Messung eine lange Zeit in Anspruch nahm, kann die Temperatur und so auch die Viskosität des destillierten Wassers bei den Messungen mit den drei Spannungswerten als praktisch gleich angenommen werden. Die Hagen-Poiseuille'sche Gleichung, auf unser System angewendet, gibt uns die Möglichkeit den Zusammenhang zwischen dem osmotischen Druck und der Spannung auf Grund der Durchströmungsgeschwindigkeit abzuschätzen. Es kann festgestellt werden:

Regel 8. Der wechselstromelektroosmotische Druck ist eine quadratische Funktion der Feldstärke.

6. Versuche bei welchen als Diaphragma eine Glasplatte mit einer konusförmigen Bohrung verwendet wurde

6.1. *Versuche mit reinen, destillierten Flüssigkeiten*

Wird in beide Teile des Messgefässes die gleiche destillierte Flüssigkeit (Wasser, Azeton, Methyl-, Äthylalkohol) gleich hoch eingefüllt, und eine Wechselspannung (2—4 kV) angelegt, so kommt eine Niveaudifferenz zustande,so dass die Flüssigkeit in der Bohrung in jene Richtung strömt, in welcher sich das Lochdiaphragma verjüngt. Die Niveaudifferenz stellt sich in einigen Minuten nach Anlegung der Spannung ein.

6.2. *Versuche mit* $1 \cdot 10^{-4}$*-normalen Elektrolytlösungen*

Mit einer $1 \cdot 10^{-4}$-normalen wässerigen Lösung von KCl oder $Al(NO_3)_3$ und einer Wechselspannung von 2—4 kV steigt die Flüssigkeit wie bei den Versuchen 6.1 an der schmalen Lochseite. Die dabei gemessenen Niveaudifferenzen bei KCl und verschiedenen Spannungswerten waren folgende:

Spannung kV	Niveaudifferenz mm
2	7
3	15
4	28

Mit $1 \cdot 10^{-3}$-normalen Elektrolytlösungen kann die Messung wegen elektrischer Durchschläge nicht mehr durchgeführt werden.

Bei derartigen Diaphragmen hat eine adsorbierte Luftschicht, die Temperatur, die Grösse und die Frequenz der Wechselspannung auf die elektroosmotische Strömungsrichtung keinen Einfluss.

Auf Grund der Versuche kann festgestellt werden:

Regel 1. Die Flüssigkeit strömt auf die Wirkung der Wechselspannung im Inneren der Bohrung gegen die kleinere Öffnung.

Regel 2. Der elektroosmotische Druck ist eine quadratische Funktion der Feldstärke.

7. Deutung der Wechselstromelektroosmose

Es liegt nahe, die Wechselstromelektroosmose auf die Gleichstromelektroosmose zurückzuführen, da sich während der einzelnen Halbperioden der Wechselspannung eine Gleichstromelektroosmose abspielt. Falls die Wechselspannung nicht symmetrisch sinusförmig ist, sondern in der einen Halbperiode die Amplitude grösser ist, kann auch eine Erscheinung, die von Gleichstromelektroosmose herrührt, beobachtet werden. Bei unseren Messungen kam dieser Fall nicht vor, wie das in 3.6 behandelt wurde.

Bei einem Teil unserer Versuche war die Elektrolytkonzentration an beiden Seiten des Diaphragmas verschieden, deshalb kann es angenommen werden, dass die Strömungsgeschwindigkeit in den nacheinanderfolgenden Halbperioden verschieden ist, auch bei regelmässig sinusförmiger Wechselspannung. Diese verschiedene Strömungsgeschwindigkeit könnte dann den Wechselspannungseffekt hervorrufen. Da aber bei der Gleichstromelektroosmose der Druck eine lineare Funktion der Feldstärke ist, wäre auch dieser Differenzialeffekt eine lineare Funktion der Feldstärke, was mit den Versuchsergebnissen im Widerspruch steht.

Da eine Wechselstromelektroosmose auch dann eintritt, wenn sich an beiden Seiten des Diaphragmas die gleiche Flüssigkeit befindet (Fall *b*), kann die Erscheinung auf die Gleichstromelektroosmose nicht zurückgeführt werden, in diesem Fall herrscht ja vollständige Symmetrie was die Gleichstromelektroosmose betrifft.

Bei der Gleichstromelektroosmose ist die Strömungsrichtung mit den Diaphragmen G2, G3 und G4 gleich. Deshalb kann man aus der Gleichstromelektroosmose keine Erscheinung ableiten, bei welcher die elektroosmotische Strömungsrichtung die Funktion der Kapillarenradii ist.

Da sich im Kapillarensystem durch den Strom Wärme entwickelt, wurde das Auftreten von Thermodiffusion in Betracht gezogen, aber weder im Ganzen, noch im Einzelnen konnte das Versuchsmaterial dadurch gedeutet werden. So kann z. B. die verschiedene Strömungsrichtung bei Anwendung von Diaphragmen mit verschiedenen Kapillarenradien mittels Thermodiffusion

nicht gedeutet werden. Das Auftreten von Niveaudifferenzen kann mit Thermodiffusionserscheinungen deswegen auch nicht erklärt werden, weil die Thermodiffusion bei Lösungen und porösen Glasdiaphragmen zu einem unbeachtlichen Effekt führt [2].

Da sich bei einer Gruppe der Erscheinungen an beiden Seiten des Diaphragmas Lösungen von verschiedenen Elektrolytkonzentrationen befinden, besteht hier die Möglichkeit eines bipolaren Membrans. Ohne einen elektrischen Strom bildet sich aber keine Niveaudifferenz, und so kann ein bipolares Membran nicht angenommen werden. Das Bild des Stromes am Oszilloskop zeigte keinen Gleichrichtereffekt.

Es könnte noch der Gedanke auftauchen, dass die Erscheinung bei Diaphragmen mit grösseren Porendurchmessern ($> 40\ \mu$) und bei Lochdiaphragmen, wenn als Flüssigkeitspaare Lösungsmittel—Elektrolytlösung verwendet wird, auf die Strömung der hydratierten Ionen zurückgeführt werden kann, da in diesen Fällen immer die Lösung zum Lösungsmittel hinüberströmt. Die Versuche aber, bei denen die Flüssigkeitspaare reine Lösungsmittel waren, haben bewiesen (Punkt 3.9 und Abschnitt 4) dass nicht unbedingt die Flüssigkeit mit grösserer Leitfähigkeit zur anderen hinüberströmt. Dadurch fällt die obige Annahme zur Deutung der Erscheinung weg.

Wollen wir zur Deutung der Wechselstromelektroosmose gelangen, so müssen wir jene Kraft eingehend untersuchen, welche in einem elektrischen Feld auf ein Dielektrikum wirkt. Laut den Gesetzen der Elektrodynamik ist die auf die Volumeneinheit wirkende Kraft gleich

$$\mathfrak{K} = \varrho\mathfrak{E} - \frac{1}{8\pi}(\mathfrak{E}^2 \cdot \operatorname{grad} \varepsilon), \tag{1}$$

wo ϱ die Ladungsdichte, ε die DK des Stoffes und $\mathfrak{E}$ die Feldstärke bezeichnet.

Legen wir auf die Elektroden eine Gleichspannung an, so ruft das erste Glied in (1) die bekannte Gleichstromelektroosmose hervor, da sich an der Diaphragmenwand eine Doppelschicht ausbildet.

Im Falle einer Wechselspannung verursacht, wie bereits gezeigt wurde, das erste Glied der Gl. (1) keine merkbare elektroosmotische Erscheinung. Das zweite Glied lässt aber mehr hoffen, da es dem Quadrat der Feldstärke proportional ist. Dabei muss beachtet werden, dass sich die DK der Flüssigkeiten durch die Einwirkung von Ionen verringert, und zwar dadurch, dass Molekeln in einer Hydrat- bzw. Solvathülle von einem äusseren elektrischen Feld weniger geordnet werden können. Diese Wirkung der Ionen hat man im Falle von Wasser und Methylalkohol mittels Messungen bewiesen [3].

In unseren Versuchen, in welchen je zwei Elektrolytlösungen verschiedener Konzentration sich an beiden Seiten des Diaphragmas befanden, tritt in der Diaphragmenkapillare ein Konzentrationsfall in Achsenrichtung auf.

Infolge dessen erscheint im elektrischen Feld eine ponderomotorische Kraft. Mit dieser Kraft kann aber die Erscheinung nicht erklärt werden, da diese Kraft immer das Lösungsmittel zur Lösung hinüberströmen liesse. Darum muss anstatt dieser Kraft eine grössere gesucht werden. Die mit dem Ionenkonzentrationsfall verbundene ponderomotorische Kraft muss auch deswegen verworfen werden, da — wie bereits darauf hingewiesen wurde, — eine Wechselstromelektroosmose auch bei gleichen Flüssigkeiten an beiden Seiten des Diaphragmas auftritt.

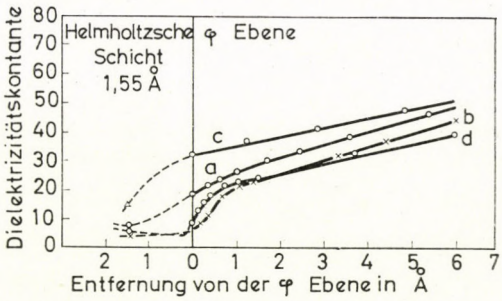

Abb. 17. Die Dielektrizitätskonstante des Wassers in der Nähe der Kapillarenwand nach CONWAY und Mitarbeitern

a) $\zeta = 0{,}1$ V
b) $\zeta = 0{,}2$ V
} Konzentration = 0,1 g Ionen/l;

c) $\zeta = 0{,}1$ V
d) $\zeta = 0{,}2$ V
} Konzentration = 0,2 g Ionen/l.

In den Kapillaren des Diaphragmas verursachen die Ionen der an der Diaphragmenwand sich bildenden Doppelschicht eine Änderung der DK. CONWAY, BOCKRIS und AMMAR [4] berechneten — eine Stern'sche Doppelschicht angenommen — den Verlauf der DK an der Kapillarenwand, wenn an beiden Seiten des Diaphragmas die Ionenkonzentration in Wasser gleich ist. Ihre Ergebnisse sind in Abb. 17 angeführt. Die ponderomotorischen Kräfte, die in einem elektrischen Feld infolge von dieser Doppelschicht auftreten, verursachen nur dann einen Flüssigkeitstransport, wenn die Kräfte eine Komponente in der Richtung der Kapillarenachse haben. Wenn die Kapillaren zylinderförmig sind und an beiden Seiten des Diaphragmas die Ionenkonzentration der Elektrolytlösung gleich ist, dann haben die ponderomotorischen Kräfte keine Komponente in der Achsenrichtung und das Wechselspannungsfeld verursacht — im Einklang mit der Erfahrung — keinen Flüssigkeitstransport. Die ponderomotorischen Kräfte besitzen in jenem Falle eine Komponente in der Richtung der Kapillarenachse, wenn entweder die Konzentration der Elektrolytlösung oder die Kapillarendurchmesser an beiden Seiten des Diaphragmas verschieden sind.

Bevor wir uns mit der Gestaltung der DK in der Doppelschicht eingehender beschäftigen, wollen wir auf die Versuchsergebnisse gestützt suchen,

was für Kräfte an der Kapillarenwand anzunehmen sind um die Erscheinung deuten zu können. Die Versuche beweisen, dass bei Wahl von einer entsprechend niedriger Spannung es immer erreicht werden kann, dass bei einem Fall des Typs *a* das Lösungsmittel (3.2) bei einem Fall vom Typ *b* die Flüssigkeit an der Feinporenseite (5.4; 5.5) steige. Da bei Diaphragmen mit grossen Porendurchmessern nur die obenerwähnte Strömungsrichtung möglich ist, bei Diaphragmen mit kleinen Porendurchmessern aber diese Richtung mit niedriger Spannung immer erreichbar ist, kann diese für die Grunderscheinung charakteristisch aufgefasst werden. Die elektroosmotischen Strömungen mit umgekehrter Strömungsrichtung wären dann eine Folge von sekundären

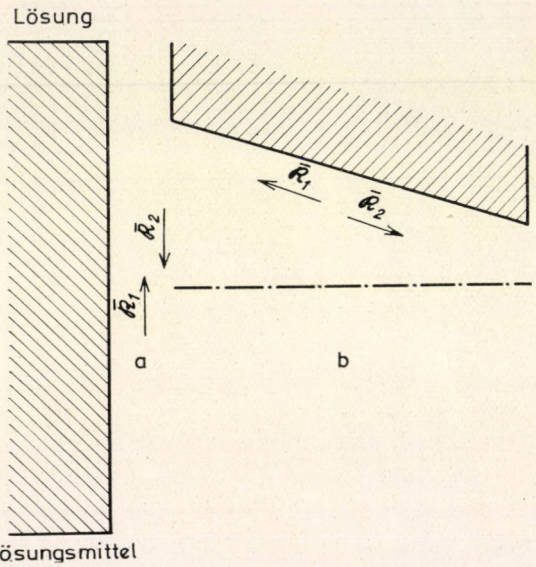

Abb. 18. Ponderomotorische Kräfte, welche im elektrischen Wechselspannungsfeld an der Kapillarenwand wirken a) im Falle einer zylindrischen Kapillare, Lösung—Lösungsmittel, b) im Falle einer konusförmigen Kapillare, homogener Flüssigkeit

Effekten (z. B. Wärmeeffekt des Stromes). Ein Beweis dafür ist, dass die umgekehrte Strömungsrichtung, die sich bei höheren Spannungen einstellt, durch intensive Kühlung wieder zurückgekehrt werden kann (3.4). Demgemäss scheint es zweckmässig zu sein zwei, zur Kapillarenwand parallele Kräfte anzunehmen, von denen die eine sich bei steigender Temperatur verringert. Wenn wir diese letztere Kraft mit der äusseren, locker gebundenen und auch durch die Temperatur beeinflussbaren Ionenschicht in Verbindung bringen, entfernen wir uns von der Wirklichkeit nicht. Im Falle von zylindrischen Kapillaren zeigt die Temperaturabhängige Kraft ($\Re_2$) in die Richtung zum Lösungsmittel, im Falle von konusförmigen Kapillaren in die Richtung zur Verjüngung (Abb. 18). Mit der Annahme der beiden Kräfte kann die Erscheinung folgendermassen gedeutet werden:

Die Regeln 3/7 und 5/4, die sich auf die Temperaturabhängigkeit der osmotischen Strömungsrichtung beziehen, folgen von selbst, da gemäss Spezifikation der Kräfte eine Erhöhung der Temperatur die Kraft $\Re_2$ verringert, eine Herabsenkung der Temperatur aber diese Kraft erhöht, dadurch dass die Temperaturänderung auf die locker gebundene Ionenschicht einwirkt.

Auch die Regeln 3/4 und 5/5, die sich auf den Zusammenhang zwischen elektroosmotischer Strömungsrichtung und Spannungsgrösse beziehen, werden verständlich, da die Temperatur der in den Diaphragmenkapillaren befindlichen Flüssigkeit auch von der Spannungsgrösse abhängt.

Auf unsere Annahme der beiden Kräfte gestützt können wir aber noch nicht erklären, warum wir bei übrigens gleichbleibenden Versuchsbedingungen eine verschiedene Strömungsrichtung bekommen, wenn die Porendurchmesser der Diaphragmen verschieden sind. Diese verschiedene Strömungsrichtung allein durch einen Wärmeeffekt des Stromes zu erklären ist nämlich unangemessen, da auf Grund von Berechnungen die in der Volumeneinheit der Kapillaren frei werdende Wärme gleich ist und vom Kapillarendurchmesser nicht abhängt. Die verschiedene Strömungsrichtung kann nur so gedeutet werden, wenn wir annehmen, dass die Kraft $\Re_2$ in den Diaphragmen mit kleineren Porendurchmessern kleiner ist, als in solchen mit grösseren Porendurchmessern, oder wenigstens, dass auf Einwirkung der übrigens gleichen Wärmemengen sich diese Kraft bei kleineren Porendurchmessern stärker verringert als bei grösseren Porendurchmessern. Da wir die Kraft $\Re_2$ mit der äusseren Ionenschicht der elektrischen Doppelschicht in Beziehung gebracht haben, bedeutet unsere Annahme, dass sich die genannte Ionenschicht bei kleineren Porendurchmessern nicht so ungehindert ausbilden kann als bei grösseren Porendurchmessern. Auf diese Weise ist Regel 3/2 zu deuten.

Nach Gl. (1) ist die Wechselspannungselektroosmose eine quadratische Funktion der Feldstärke, im Einklang mit den Regeln 3/12, 4/2, 5/8 und 6/2. In Annäherung kann auf unsere Kapillarensysteme die Hagen-Poiseuille'sche Gleichung angewendet werden, daraus ergeben sich die Regeln 3/13, 3/14, 4/3 und 5/7.

Die in der Kapillare sich befindliche Flüssigkeit übt nach dem ersten Glied in Gl. (1) im Wechselspannungsfeld eine oszillierende Bewegung aus. Die Amplitude dieser oszillierenden Bewegung wird infolge der grossen Masse der Flüssigkeit bei höheren Frequenzen (1000 Hz) kleiner. Die Folge ist, dass die Ausbildung der locker gebundenen Ionenschicht von einer Wechselspannung höherer Frequenz weniger gestört wird, als von einer Wechselspannung niedriger Frequenz. So wird Regel 4/8, der sich auf die Frequenzabhängigkeit der elektroosmotischen Strömungsrichtung bezieht, verständlich.

Wird angenommen, dass bei Anlegung einer Wechselspannung von sehr hoher Frequenz (380 kHz) die Halbperiodenzeit der Wechselspannung bereits zu klein im Vergleich zu jener Zeit wird, die zur Ausbildung und Ordnung

der Doppelschicht nötig ist, so muss damit gerechnet werden, dass sich in einem solchen Hochfrequenzfeld eine Doppelschicht eigentlich nicht gänzlich entfalten kann. Dadurch fällt die Wechselstromelektroosmose aus, wie das Regel 3/9 aussagt.

Eine adsorbierte Luftschicht an der Diaphragmenoberfläche stört die Ausbildung der locker gebundenen diffusen Ionenschicht in Diaphragmen mit kleineren Porendurchmessern, und dadurch wird Regel 3/10 und 5/6 verständlich.

Gemäss Spezifikation der Kräfte ist die Struktur der äusseren Ionenschicht bei grossen Porendurchmessern ($> 40\ \mu$) bereits so stark, dass sie von höherer Temperatur, Spannung oder deren Frequenz und einer adsorbierten Luftschicht nicht wesentlich beeinflusst werden kann. So werden die Regeln 3/1, 4/1 und 6/1 verständlich.

Bei kleineren Porendurchmessern ist die Struktur der äusseren, diffusen Ionenschicht schwächer, die Ausbildung der Ionenschicht wird von den spezifischen Eigenschaften der Ionen stark beeinflusst, und die Regel 3/3 wird verständlich.

Im Falle von Flüssigkeiten, die zur molekularen Ordnung mehr geneigt sind, kann die Ionenschicht von äusseren Einwirkungen weniger gestört werden, als dies bei Flüssigkeiten mit kleinerer Neigung zur molekularen Ordnung der Fall ist. Dadurch wird Regel 3/6 erklärlich.

Wegen der kleinen Porendurchmesser und wegen des Wärmeeffekts des Stromes bildet sich bei einem Diaphragma G5 und einer hohen Spannung keine solche Doppelschicht, die eine Wechselstromelektroosmose zur Folge hätte, wie das auch in Regel 3/11 enthalten ist.

In jenen Fällen, in welchen sich an beiden Seiten des Diaphragmas verschiedene Flüssigkeiten befinden, die sich voneinander in mehreren Parametern unterscheiden (DK, Eigenschaften und Konzentration der Ionen, molekulare Ordnung usw.) konnten keine eindeutig gültige Regeln für den Ablauf der Wechselstromelektroosmose festgestellt werden (3.9). Dies ist verständlich, wenn wir in Betracht ziehen, dass die oben genannten Parameter den Ablauf der Wechselstromelektroosmose wesentlich beeinflussen, und dass sich in den Kapillaren noch dazu eine Mischung dieser Flüssigkeiten befindet.

Eine Erklärung für die anomale Gleichstromelektroosmose die in Abb. 12 dargestellt ist, ergibt sich aus dem 2. Glied der Gl. (1) welches Glied wegen dem spezialen Diaphragma auch im Falle von Gleichspannung neben dem 1. Glied zur Geltung kommt (solange die Ionenkonzentrationsdifferenz gross ist). Dies beweist die Gültigkeit von Gl. (1).

Die Wechselstromelektroosmose wurde also mittels zwei, zur Kapillarenwand parallelen, willkürlich angenommenen Kräften erklärt. Das Dasein dieser Kräfte wurde dadurch bestätigt, dass die Folgerungen mit der Erfahrung im Einklang waren. Wir wollen jetzt nachweisen, dass eine Annahme sol-

cher Kräfte auch theoretisch begründet ist, da unsere Anschauungen hinsichtlich der Struktur der Doppelschicht das Auftreten dieser Kräfte ermöglichen.

Wenn die Flüssigkeit keine Elektrolytzusätze enthält, und das Diaphragma jenem in Abs. 5 und 6 entspricht, genügt zur Deutung der Wechselstromelektroosmose die Annahme der Stern'schen Doppelschicht, welche aus einer monoionigen und einer diffusen Ionenschicht besteht (Abb. 19a). Grad ε und dementsprechend die ponderomotorische Kraft, ($\mathfrak{K}_2$) ist senkrecht zur Diaphragmenwand. Die in der Achsenrichtung liegende Komponente ($\mathfrak{R}_2$) dieser Kraft verursacht den Flüssigkeitstransport. Die Temperatur hat auf die Stern'sche Doppelschicht praktisch keinen Einfluss, und so ist es verständlich, dass die Erscheinung in diesem Falle von der Temperatur und dem Spannungswert unabhängig ist.

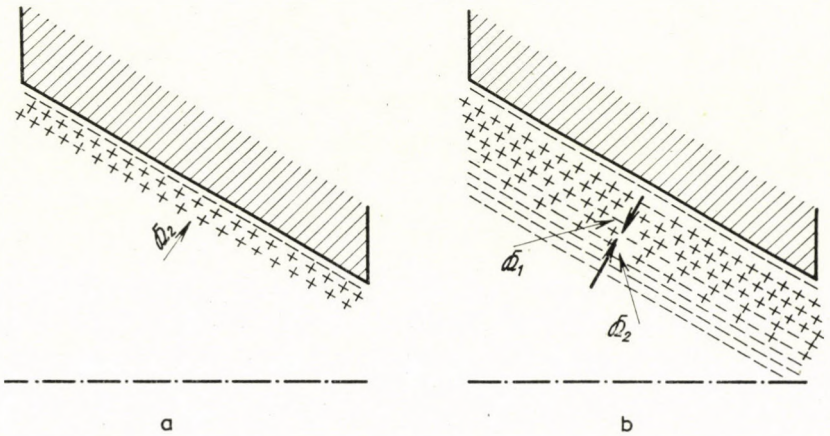

Abb. 19. Die Struktur der elektrischen Doppelschicht in einer konusförmigen Kapillare und die ponderomotorischen Kräfte, welche in einem Wechselspannungsfeld auftreten. a) Im Falle einer kleinen Elektrolytkonzentration. b) Im Falle von grösserer Elektrolytkonzentration ($1 \cdot 10^{-3}$ n)

Enthält die Flüssigkeit bei gleichbleibendem Diaphragma Elektrolyt, so wird dadurch die Doppelschicht modifiziert, indem wegen der grösseren Ionenkonzentration zur positiven Ionenschicht nach Abb. 19a eine locker gebundene negative Ionenschicht hinzukommt (Abb. 19b). Zwischen den beiden Ionenschichten befindet sich eine Übergangsschicht mit gemischter Ladung. Eine Betrachtung der Ladungsverteilung in den einzelnen Schichten lehrt uns, dass die Ladungsdichte in der gemischten Schicht grösser ist, als in den Schichten mit gleichartigen Ionen, welche Ionen sich abstossen. Demzufolge richten sich von den Schichten mit einheitlicher Ladung ponderomotorische Kräfte ($\mathfrak{K}_1$, $\mathfrak{K}_2$) gegen die Schicht mit gemischter Ladung. Neben der Kraft $\mathfrak{K}_2$ tritt auch eine Kraft $\mathfrak{K}_1$ auf, welche senkrecht zur Kapillarenwand nach innen zeigt.

Bei niedriger Temperatur und Spannung ist die Kraft $\mathfrak{K}_2$ im Übergewicht. Erhöht man die Temperatur oder die Spannung, so mischen sich die locker gebundene Ionenschicht und die Schicht mit gemischter Ladung. Da hiedurch grad ε klein wird, verschwindet die Kraft $\mathfrak{K}_2$ praktisch, und die Kraft $\mathfrak{K}_1$ kommt zur Geltung. Diese Betrachtungen liefern eine Erklärung für die Temperatur-, Spannung- und Elektrolytkonzentrationsabhängigkeit der Elektroosmose im Falle der genannten Diaphragmen.

Bei zylinderförmigen Diaphragmenkapillaren nehmen wir jene allgemeinere Form der Doppelschicht an, in welcher auch die innere Ionenschicht von diffuser Struktur ist, und tragen wir der Elektrolytkonzentrationsdifferenz an beiden Seiten des Diaphragmas Rechnung. Die Ladungsverteilung ist in diesem Falle in Abb. 20 dargestellt. Nach der äusseren Schicht mit gemischter

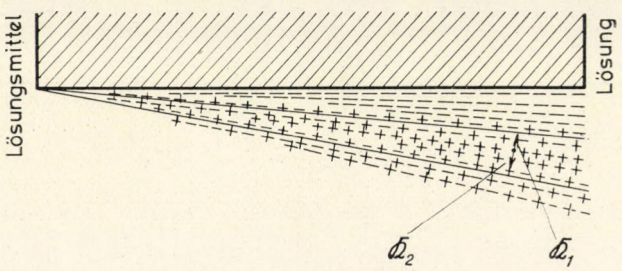

Abb. 20. Die Struktur der elektrischen Doppelschicht an der Kapillarenwand und die ponderomotorischen Kräfte, welche in einem Wechselspannungsfeld auftreten, wenn sich an dem einen Ende der Kapillare ein Lösungsmittel, an dem anderen eine Lösung befindet

Ladung bildet sich keine weitere Schicht mit gleichartigen Ionen aus, da an der einen Seite des Diaphragmas sich Lösungsmittel befindet, sondern es bildet sich eine diffuse Schicht gemischter Ladung aus. Dies hat bei niedriger Temperatur und Spannung zur Folge, dass die Kraft $\mathfrak{K}_2$ Lösung zum Lösungsmittel hinüberströmen lässt.

Bei hoher Temperatur oder Spannung verschwindet die Übergangsschicht infolge von Vermischung der Flüssigkeiten miteinander praktisch beinahe vollständig, und so strömt durch die Kraft $\mathfrak{K}_1$ das Lösungsmittel zur Lösung.

Nehmen wir an, dass auch im Falle von Diaphragmen mit konusförmigen Kapillaren alle Ionenschichten diffus sind, so hat das auf die oben beschriebene Ausbildung der ponderomotorischen Kräfte keine Auswirkung.

Es sei bemerkt, als eine merkwürdige Eigenschaft der Wechselstromelektroosmose, dass bei Verwendung von Diaphragmen mit grösseren Porendurchmessern ($> 40\ \mu$) mittels einer Wechselspannung (ohne Gleichrichtung) in jedem Falle (unabhängig von den Parametern) dauerhaft ein Flüssigkeitstransport in eine Richtung hervorgerufen werden kann.

SCHRIFTTUM

1. Z. László, J. Chem. Phys., **17,** 508, 1949; **18,** 133, 1950; **18,** 568, 1950; **19,** 800, 1951; **20,** 1807, 1952; Kolloid-Z., **114,** 161, 1949; **121,** 157, 1951; **128,** 100, 1952; **131,** 18, 1953; **137,** 34, 1954; **141,** 4, 1955; **145,** 3, 1956; **151,** 52, 1957; **156,** 76, 1958; Z. Phys. Chem., **224,** 1, 1963; **248,** 210, 1971; im Druck (1972).
2. Z. B., H. P. Hutchison, I. S. Nixon und K. G. Denbigh, Disc. Faraday Soc., No 3, 48, 1948.
3. H. Sack, Physik. Z., **27,** 206, 1926; **28,** 199, 1927; G. Fischer und W. D. Schaffeld, Ann. Phys., **25,** 450, 1936; J. B. Hasted, D. M. Ritson und C. H. Collie, J. Chem. Phys., **16,** 1, 1948; G. H. Haggis, J. B. Hasted und T. J. Buchanan, J. Chem. Phys., **20,** 1452, 1952; J. A. Lane und J. A. Saxon, Proc. Roy. Soc., London **214A,** 531, 1952.
4. B. E. Conway, J. M. Brockris und I. A. Ammar, Trans. Faraday Soc., **47,** 456, 1951.

ЭЛЕКТРООСМОС ПЕРЕМЕННОГО НАПРЯЖЕНИЯ

З. ЛАСЛО

Резюме

Мы назвали электроосмосом переменного напряжения явление переноса в жидкостях, которое происходит под действием электрического поля переменного напряжения через порыстую диафрагму, капиллярную систему, или капилляр. Это электрокинетическое явление возникает в двух основных случаях.

а) Капилляры диафрагмы имеют циллиндрическую форму, на двух сторонах диафрагмы находятся разные жидкости, напр. растворитель — раствор электролита.

б) Капилляры диафрагмы имеют коническую форму и на двух сторонах диафрагмы находятся одинаковые жидкости.

Даны правила, по которым протекает процесс электроосмоса. Так, среди прочего, установлено, что электроосмотическое давление является квадратичной функцией напряженности поля. Возникновение явления связано с пондеромоторными силами, возникающими в двойном слое у стенки капилляра под действием поля переменного напряжения.

Acta Physica Academiae Scientiarum Hungaricae, Tomus 31 (4), pp. 327—333 (1972)

SPIN CUT-OFF FACTORS FROM (n,2n) REACTIONS OF NUCLEI WITH $N < 50$

By

D. HORVÁTH* and A. KISS

DEPARTMENT OF ATOMIC PHYSICS, ROLAND EÖTVÖS UNIVERSITY, BUDAPEST

(Received 19. IV. 1971)

The available experimental data on isomeric ratios measured in (n,2n) reactions are re-evaluated using a method based on the HUIZENGA—VANDENBOSCH assumptions. So far only the experimental values of isomeric (n,2n) cross section ratios reported for nuclei with $N < 50$ at 14 MeV have been re-analysed. The dependence of the extracted spin cut-off factors on the parameters used is discussed, and the latter are compared with the values predicted by the Fermi gas model; their ratios are found to be about 0.5.

Introduction

In recent years many isomeric ratios measured in (n,2n) reactions at 14 MeV have been evaluated by means of the HUIZENGA—VANDENBOSCH method [1]. However, the spin cut-off factors obtained by different authors are not comparable, as different adaptations of the method, employing various approximations and data for nuclear temperature, transmission coefficients, level density parameters, pairing energies and gamma multiplicities have been applied. Re-analysis of the available experimental data utilizing the same sources for the parameters might make it possible to investigate the dependence of the spin cut-off factors on the choice of models. It is the aim of the authors to perform this task along the lines of a recent study of (n,gamma) reactions [2]. As a first step, data for the $N < 50$ "island of isomerism" were re-evaluated.

The main features of the calculation for extracting the spin cut-off factors from (n, 2n) isomeric cross-section ratios are essentially the same as described elsewhere [10].

The nuclear level density adopted is

$$\varrho(U, J) \alpha \ (2J + 1) \exp\left\{2\sqrt{aU} - \left(J + \frac{1}{2}\right)^2 \Big/ 2\sigma^2\right\},$$

where a is the zero spin level density parameter, σ the spin cut-off factor, and J the angular momentum. The effective excitation energy is $U = E - \varepsilon\delta$,

* Present address: Central Research Institute for Physics, Budapest.

where E is the incident neutron energy in CM system, $\delta = 16/a$ is the pairing energy of one nucleon, and ε is the parity factor:

$$\varepsilon = \left\{ \begin{matrix} 2 & \text{for even} \\ 1 & \text{for odd-mass} \\ 0 & \text{for odd} \end{matrix} \right\} \text{ nuclei}$$

The mean energy of the emitted neutrons is assumed to be twice the nuclear temperature, T, given by $U = T^2 - 4T$. For the zero-spin level density parameter a we have applied Newton's formula $a = 0.095 \cdot (j_N + j_Z + 1) \cdot A^{2/3}$. The values for the averaged shell spins j_N and j_Z were taken from [2].

Assuming there are dipole radiations only, the mean number of emitted photons is $1/2 \sqrt{aU'}$, where U' is the average excitation energy after the second neutron emission.

The calculated zero-spin level density parameters, pairing corrections, mean neutron energies and average numbers of emitted photons are shown in Table I. The isomeric ratios examined and the spin cut-off factors calculated from them are displayed in Table II. In some cases only a lower limit for

Table I

Actual values of reaction parameters

E is the bombarding energy in CM system, a the zero-spin level density parameter, δ the pairing energy correction, E_1 and E_2 the energies of the evaporating neutrons, n the average γ multiplicity

Target	E	Target		Residual		E_1	E_2	n
		a	δ	a	δ			
^{70}Zn	14.5	12.38	2.6	11.19	1.4	2.1	1.2	2
^{74}Se	13.9	12.29	2.6	11.07	1.4	2.1	0	0
^{76}Ge	13.8	13.06	2.4	12.95	1.2	2.0	0.7	1
^{78}Se	14.5	12.72	2.6	12.60	1.3	2.1	0.6	0
^{80}Se	14.5	12.93	2.4	12.82	1.3	2.1	0.8	2
^{81}Br	14.8	13.62	1.17	13.52	0	2.24	1.00	2
	14.3					2.20	0.91	2
	13.8					2.17	0.81	1
	13.3					2.13	0.70	1
^{82}Se	14.2	10.76	3.0	13.04	1.2	2.2	0.8	2
^{85}Rb	13.9	11.62	1.4	13.97	0	2.3	0.8	1
^{86}Sr	14.5	12.95	2.4	15.30	1.1	2.1	0	0
^{87}Rb	14.5	12.43	1.3	11.41	0	2.2	1.1	2
^{88}Sr	14.5	13.77	2.4	12.75	1.3	2.0	0	0
^{90}Zr	14.0	17.17	1.8	16.09	1.0	1.8	0	0
^{92}Mo	14.5	17.43	1.8	16.34	1.0	1.9	0	0

Table II

Cross-section ratios and spin cut-off factors

The reactions are considered at the bombarding energies reported in Table I. The numbers in parentheses after the data refer to the literature. Isomeric ratios marked "*" were obtained by dividing the experimental isomeric cross-section with a computed ground-state one. "*" means that the measured isomeric ratio cannot be compared with the calculated one

Residual nucleus	Isomeric ratio measurement				Calculated spin cut-off factors		
	E	R	σ	Ref.	our	other's	Ref.
^{69}Zn	14.7	0.56(11)	2.8(3)	[10]	$2.6^{+1.7}_{-0.6}$	—	
^{73}Se	14.1	0.86(8)	—	[5]	$3.8^{+\infty}_{-1.6}$	2.9	[6]
	14.4	0.82(5)	—	[17]	3.3 ± 1.2	2.7	[6]
						4.2 ± 0.5	[10]
^{75}Ge	14.8	0.62(8)	3(1)	[12]	2.1 ± 0.2	$4.8^{+1.8}_{-0.8}$	[6]
	14.5	0.42(8)	1.80(15)	[9]	1.7 ± 0.2	—	
	15.0	0.74(5)	—	[15]	2.5 ± 0.3	6.0	[6]
^{77}Se	14.7	0.51*	2.7	[13]	1.6	—	
^{79}Se	14.7	0.83*	3.3	[13]	3	—	
^{80}Br	13.5	0.623(36)	—	[15]	3.9 ± 0.5	—	
	13.9	0.635(51)	—	[15]	$3.9^{+0.9}_{-0.4}$	—	
	14.0	0.52(4)	4.4(3)	[8]	$3\ \pm0.3$	—	
	14.6	0.637(34)	—	[15]	$4\ \pm0.4$	—	
		0.58(7)	—	[18]	3.5 ± 0.5	$6\ \pm1$	[12]
						$4.9^{+1.2}_{-0.6}$	[6]
	14.7	0.72(8)	$6\ \pm1$	[14]	$5.6^{+\infty}_{-1.5}$	—	
	14.9	0.635(30)	—	[15]	3.9 ± 0.3	5.6 ± 0.8	[6]
		0.62(2)	5.4(3)	[6]	3.7 ± 0.3	—	
^{81}Se	14.4	0.80(5)	—	[17]	3.1 ± 0.4	$4.6^{+0.9}_{-0.5}$	[6]
						2.9 ± 0.2	[10]
	14.7	0.74(2)	3.0(5)	[13]	3.6 ± 0.1	4.0 ± 0.2	[6]
^{84}Rb	14.1	0.52(5)	3.96(6)	[11]	4.2 ± 0.6	—	
	14.7	0.55(20)	4.9(5)	[14]	$4.6^{+\infty}_{-1.6}$	—	
^{85}Sr	14.6	0.47(5)	—	[18]	4.6 ± 1.5	2.3 ± 0.1	[6]
						2.5 ± 0.5	[12]
	14.7	0.80(15)	3.0(5)	[14]	?	—	
^{86}Rb	14.7	0.37(12)	2.9(5)	[14]	$3\ \pm0.5$	—	
^{87}Sr	14.7	0.74*		[14]	3.5	—	
^{89}Zr	14.7	0.80(17)	3.5 ± 0.5	[14]	$3.4^{+\infty}_{-1.5}$	—	
	14.8	0.72(8)	5.5 ± 1	[12]	$2.4^{+1.0}_{-0.5}$	$2.2^{+0.9}_{-0.4}$	[6]
		0.82(16)	4.2(3)	[10]	$4.2^{+\infty}_{-2.3}$	—	
^{91}Mo	14.7	0.96(38)	6(1)	[14]	?	—	
	14.8	0.91(18)	6	[10]	?	—	
		0.80(10)	8.5(15)	[16]	3.4 ± 1.2	2.0	[6]
	14.9	0.82(1)	3.5(4)	[6]	3.8 ± 0.4	—	

the σ-value could be determined (an example is presented in Fig. 3). The transmission coefficients were taken from [3], the neutron binding energies and nuclear level spins from [4].

Discussion

Because expressions for the level densities of both the target and residual nuclei are used in the calculations, it must first be decided which of the two nuclei involved in the (n,2n) reaction is characterized by the extracted spin cut-off parameter. The case of the ^{86}Sr (n,2n) ^{85}Sr^{m,g} reaction, illustrated in Fig. 1, provides a typical example. The Figure clearly shows that the first

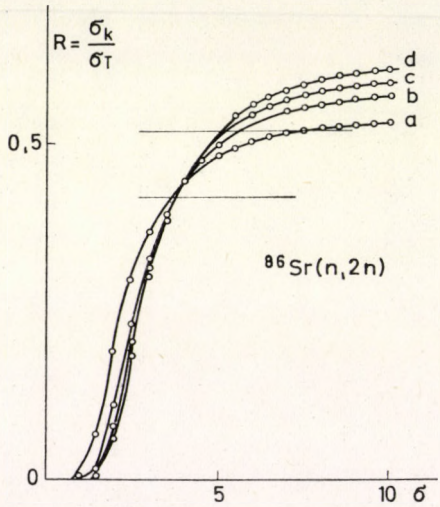

Fig. 1. Calculated isomeric ratio curves for the ^{86}Sr (n, 2n) reaction after the emission of (a) 1 neutron; (b) 2 neutrons; (c) 2 neutrons and 1 photon; (d) 2 neutrons and 2 photons. The shaded area corresponds to isomeric ratio measured by STROHAL et al. [18]

neutron evaporation process plays the most important role in determining the isomeric ratio. This reflects the fact that the second neutron to be emitted does not carry away much orbital momentum and thus does not considerably alter the spin distribution. The gamma multiplicity is low for the same reason. This conclusion is generally valid in (n, 2n) reactions at about 14 MeV, which means that the σ-values obtained belong primarily to the target nucleus.

The energy dependence of the calculated isomeric ratios is shown in Fig. 2. The ratios seem to be insensitive to small changes of the energy of the incident neutron beam around 14 MeV (the investigated region is 13—15 MeV).

Although the transmission coefficients are strongly dependent on mass number, orbital momentum and the form and parameters selected for the

optical potential, the calculated isomeric ratios are not sensitive to them. The differences of about 1% between the isomeric ratio curves for the Se isotopes, which have the same data except for mass number and neutron binding energy, corresponds to the differences in the transmission coefficients of the isotopes.

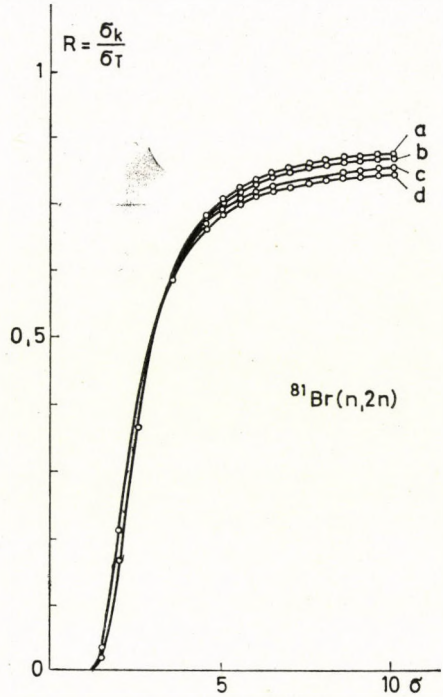

Fig. 2. Calculated isomeric ratio curves for the ^{81}Br(n, 2n) reaction at (a) 14.8; (b) 14.3; (c) 13.8; (d) 13.3 MeV incident neutron energy (in CM system)

The spin cut-off factor and the inertia momentum of nuclei are related by the expression $\sigma^2 = \Theta \cdot T/\hbar^2$. In the energy region examined the Fermi gas model predicts a rigid-body momentum of Θ_R, whereas pairing models predict values $\Theta_P < \Theta_R$. The Θ/Θ_R ratios are plotted against mass numbers in Fig. 4.

All the ratios are far below unity, as predicted by the pairing models.

Table III

Spin cut-off factors for the reaction ^{86}Sr(n,2n) with the measured isomeric ratio of [18] after emitting (a) 1 neutron; (b) 2 neutrons; (c) 2 neutrons and 1 photon; (d) 2 neutrons and 2 photons

a	*b*	*c*	*d*
4.6	4.5	4.4±0.6	4.3±0.5

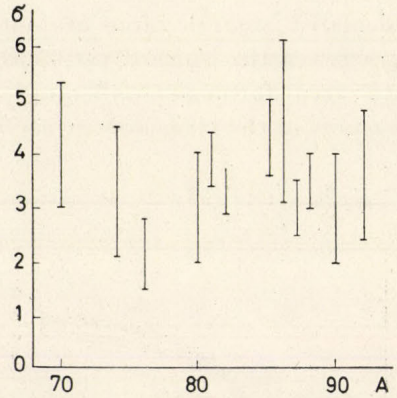

Fig. 3. Plot of spin cut-off factors against mass numbers

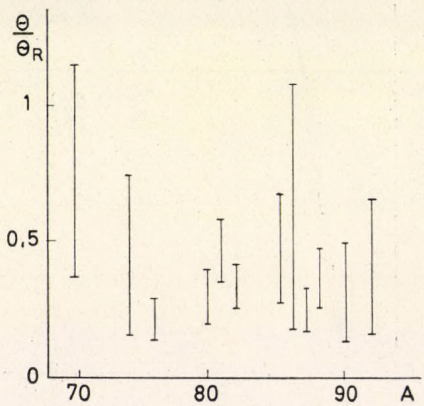

Fig. 4. Ratio of "measured" and rigid-body moments of inertia of nuclei vs mass number

Acknowledgement

The authors are indebted to A. ÁDÁM and P. HRASKÓ for their helpful discussions.

REFERENCES

1. J. R. HUIZENGA and R. VANDENBOSCH, Phys. Rev., **120,** 1305, 1960. R. VANDENBOSCH and J. R. HUIZENGA, Phys. Rev., **120,** 1313, 1960.
2. А. В. Мальшев: Плотности уровней и структура атомных ядер, Атомиздат, Москва, 1969.
3. A. LINDNER, Report IKF-17 EANDC (E) 73 "U" 1966.
4. B. S. DZELEPOW and L. K. PEKER, Decay Schemes of Radioactive Nuclei $A < 100$, "Nauka" Moscow—Leningrad, 1966.
5. M. BORMANN et al., Zeits. Naturforsch., **21A,** 988, 1966.
6. G. CURZIO and P. SONA, Nuovo Cim., **B54,** 319, 1968.
7. P. DECOWSKY et al., Report IBD "P" 1041/I/Pl 1968.
8. F. FUKUZAWA, J. Phys. Soc. Japan **16,** 237, 1961.

9. M. Guidetti and C. Oldano, Lett. Nuovo Cim., **1**, 95, 1969.
10. J. Károlyi et al., Nucl. Phys., **A122**, 234, 1968.
11. N. Kneissl et al., Nucl. Phys. **A135**, 395, 1969.
12. S. K. Mangal and P. S. Gill, Nucl. Phys., **49**, 510, 1963.
13. B. Minetti and A. Pasquarelli, Nucl. Phys., **A100**, 186, 1967.
14. B. Minetti and A. Pasquarelli, Nucl. Phys., **A118**, 449, 1968.
15. S. Okumura, Nucl. Phys., **A93**, 74, 1967.
16. R. Prasad and D. C. Sarkar, Nucl. Phys., **A94**, 476, 1967.
17. P. V. Rao and R. W. Fink, Phys. Rev., **154**, 1023, 1967.
18. P. Strohal et al., Nucl. Phys., **30**, 49, 1962.
19. G. S. Mani et al., Rapport CEA 2380, 1963.

СПИНОВЫЕ КОЭФФИЦИЕНТЫ ОБРЕЗАНИЯ ДЛЯ ЯДЕР $N < 50$ ПО РЕАКЦИЯМ (n, 2n)

Д. ХОРВАТ и А. КИШ

Резюме

Проведен пересмотр экспериментальных данных по изомерным отношениям, полученных из измерений реакций типа (n, 2n). Для этого используется метод, основанный на предположениях Гюйзенги-Ванденбоша.

До сих пор такой пересмотр был проведен только в случае экспериментальных значений отношений изомерных сечений (n, 2n), относящихся к ядрам $N < 50$ при энергии 14 MeV. Рассматривается зависимость извлеченных спиновых коэффициентов обрезания от использованных параметров и параметры спинового обрезания сравниваются со значениями, предсказанными моделю Ферми—газа; оказывается, что их отношения приблизительно равны 0,5.

Acta Physica Academiae Scientiarum Hungaricae, Tomus 31 (4), pp. 335—344 (1972)

THERMODYNAMICS OF STRONGLY ANHARMONIC CRYSTALS I

By

T. SIKLÓS and V. L. AKSIENOV

JOINT INSTITUTE FOR NUCLEAR RESEARCH, LABORATORY OF THEORETICAL PHYSICS, DUBNA, USSR

(Received 1. VI. 1971)

The properties under arbitrary external pressure of the face-centred cubic lattice displaying nearest-neighbour central force interaction are investigated. The instability temperature, critical temperature, phonon frequencies, phonon widths and thermodynamical properties of the lattice are calculated in the high-temperature limit.

Introduction

A self-consistent (S.C.) theory of strongly anharmonic crystals has been recently developed [1]—[3] which allows all higher-order terms of lower-order perturbation theory to be taken into account in a S.C. manner. Properties of the three-dimensional face-centred cubic (f.c.c.) lattice with nearest-neighbour central force interaction were earlier investigated for small pressures [4] and, in a pseudoharmonic approximation for arbitrary external pressure [5].

In the present paper the properties of the same lattice under an arbitrary external pressure are considered with allowance for damping of the S.C. phonons.

In Section 1 a S.C. system of equations is obtained for determination of the physical properties of the crystal at a fixed (arbitrary) pressure. In Section 2 the instability temperature, critical temperature, phonon frequencies, phonon widths and thermodynamical properties of the lattice are calculated in the high-temperature limit.

1. S.C. system of equations for strongly anharmonic crystals at fixed pressure

We consider a f.c.c. lattice consisting of N identical atoms of mass M, using a previously developed S.C. system of equations for investigating f.c.c. lattices with nearest-neighbour central force interaction [4].

The one-phonon Green's function is obtained in the following form:

$$G_k(\omega) = \ll A_k | A_k^+ \gg_\omega = \frac{2\omega_k}{\omega^2 - \omega_k^2 - 2\omega_k \pi_k(\omega)} . \tag{1.1}$$

The frequencies $\omega_k\,(k = \{\vec{k}, j\})$ in Eqs. (1.1.) are described in the pseudoharmonic approximation [3] by

$$\omega_k^2 = \frac{f(\Theta, l)}{f}\,\omega_{0k}^2\,, \tag{1.2}$$

where ω_{0k} is the harmonic frequency corresponding to the strength constant f at $P = 0$. The external pressure is denoted by P.

The renormalized phonon frequencies ϵ_k and phonon widths Γ_k are determined approximately by

$$\epsilon_k \approx \omega_k + \operatorname{Re} \Pi_k(\epsilon_k);\ \Gamma_k = -Im\ \Pi_k(\omega + i\delta). \tag{1.3}$$

The self-energy operator in the effective cubic approximation takes the form:

$$\Pi_k(\omega) = \sum_{p,p'} |\tilde{V}_3(-k, p, p')|^2 \left\{(n_p + n_{p'} + 1)\,\frac{\omega_p + \omega_{p'}}{\omega^2 - (\omega_p + \omega_{p'})^2} - \right.$$
$$\left. - (n_p - n_{p'})\,\frac{\omega_p - \omega_{p'}}{\omega^2 - (\omega_p - \omega_{p'})^2}\right\}, \tag{1.4}$$

where $n_p = [\exp(\omega_p/\Theta) - 1]^{-1}$.

In the central-pair force model the function $|\tilde{V}_3|^2$ reads

$$|\tilde{V}_3(-k, p, p')|^2 = \frac{\Delta(\vec{p} + \vec{p}' - \vec{k})}{4M^3 N \omega_k\,\omega_p\,\omega_{p'}}\,g^2(\Theta, l)\,F^2(-k, p, p')\,, \tag{1.5}$$

where $F(k_1, k_2, k_3)$ is a dimensionless sum over the lattice points [4].

The pseudoharmonic $f(\Theta, l)$ and the effective cubic $g(\Theta, l)$ strength constants in Eqs. (1.2) and (1.5) are determined in the S.C. manner:

$$f(\Theta, l) = \tilde{\varphi}''(l);\quad g(\Theta, l) = \tilde{\varphi}'''(l)\,, \tag{1.6}$$

where $\tilde{\varphi}(l)$ is the S.C. potential, which in certain approximation [4] is given by

$$\tilde{\varphi}(l) = \sum_{n=0}^{\infty} \frac{1}{n!}\left[\frac{1}{2}\,\overline{u^2(l)}\right]^n \varphi^{(2n)}(l)\,. \tag{1.7}$$

Here $\overline{u^2(l)}$ is the mean square relative displacement of neighbouring atoms and can be written, using the Green's function (1.1), in the form

$$\overline{u^2(l)} = \frac{1}{z f(\Theta, l) N} \sum_k \omega_k \frac{1}{\pi} \int_0^{\infty} d\omega \coth \frac{\omega}{2\Theta}\,[-Im\,G_k(\omega + i\delta)]\,, \tag{1.8}$$

where z is the number of the nearest neighbours (for the f.c.c. lattice $z = 12$).

The properties of the lattice are determined both by the temperature $\Theta = kT$ and by the volume V of the crystal or the external pressure P. These parameters satisfy the following equation [3], [4]:

$$P = -\frac{zl}{6v}\tilde{\varphi}'(l) = -\frac{2\sqrt{2}}{l^2}\tilde{\varphi}'(l), \tag{1.9}$$

where $v = (V/N) = l^3/\sqrt{2}$, and l is the equilibrium separation of neighbouring atoms.

The thermal properties of an anharmonic crystal are determined by the internal energy E and free energy F and can be written in the following forms [1], [3], [4]:

$$E = \langle H \rangle = \frac{Nz}{2}\left\{\tilde{\varphi}(l) + \frac{1}{2}f(\Theta, l)\overline{u^2(l)}\right\} + 5\tilde{F}_3(\Theta)\,, \tag{1.10}$$

$$F = F_0 + \frac{Nz}{2}\left\{\tilde{\varphi}(l) - \frac{1}{2}f(\Theta, l)\,\overline{u^2(l)}\right\} + \tilde{F}_3(\Theta)\,, \tag{1.11}$$

where

$$F_0 = \Theta \sum_k \ln\left\{2\sinh \omega_k/2\Theta\right\} \tag{1.12}$$

and the effective cubic anharmonic contribution to the free energy reads

$$\tilde{F}_3(\Theta) = -\frac{1}{6}\sum_{k,p,p'} |\tilde{V}_3(-k, p, p')|^2 \left\{\frac{(1+n_p)\,(1+n_{p'})\,(1+n_k) - n_p\, n_{p'}\, n_k}{\omega_p + \omega_{p'} + \omega_k} + \right.$$
$$\left. + \frac{n_k(1+n_p+n_{p'}) - n_p\, n'_{p,}}{\omega_p + \omega_{p'} - \omega_k}\right\}. \tag{1.13}$$

Therefore both the dynamic (1.3) and thermodynamical (1.10, 1.11) properties of the anharmonic crystal are determined by the S.C. system of equations (1.1)—(1.9). To solve them we must introduce the interatomic pair potential $\varphi(R)$ into Eq. (1.7), which as before [4] is taken as the model Morse potential. For Eq. (1.7) we get

$$\tilde{\varphi}(l) = \epsilon\left\{e^{-2a(l-r_0)}\, e^{2y} - 2e^{-a(l-r_0)}\, e^{y/2}\right\}, \tag{1.14}$$

where ϵ is the depth of the Morse potential and r_0 is the average distance between neighbouring atoms in the harmonic approximation. The strength constant in the harmonic approximation is given by $f = \varphi''(r_0) = 2\epsilon a^2$, while $y = (f/2\epsilon)\overline{u^2(l)} = (ar_0)^2[\overline{u^2(l)}/r_0^2]$ is the dimensionless mean square relative displacement of the neighbouring atoms. In the following we take $ar_0 = 6$ since with this value the deviation of a LENNARD-JONES (12-6) interatomic potential from the Morse potential is rather small in the domain of the thermal expansion of the lattice [1].

Let us consider the case in which the external pressure $P=$ const. but in contrast to [4] is not necessarily small. If P is fixed the equilibrium lattice constant depends on the temperature of the crystal and the equilibrium separation of neighbouring atoms can then be written

$$l(\Theta) = l_0 + \delta l = r_0 \left\{ 1 + \frac{1}{4} y + \frac{\delta l}{r_0} \right\}, \tag{1.15}$$

where l_0 is the equilibrium separation at $P = 0$, which can be found from Eq. (1.9) and (1.14). It is convenient to introduce the reduced pressure $P^* = P(\sigma^3/\epsilon)$, where $\sigma^6 = r_0^6/2$ is the parameter of the Lennard-Jones (12-6) interatomic potential. Eq. (1.9), taken with (1.14) and (1.15), thus reads

$$P^* = \frac{24}{(l/r_0)^2} e^{-y} e^{-6\frac{\delta l}{r_0}} \left\{ e^{-6\frac{\delta l}{r_0}} - 1 \right\}. \tag{1.16}$$

Using Eqs. (1.14), (1.15) and (1.16), the dimensionless pseudoharmonic strength constant α can be written according to (1.6) as follows

$$\alpha^2 = \frac{f(\Theta, l)}{f} = \frac{P^*}{12} \left(\frac{l}{r_0} \right)^2 + \frac{e^{-y}}{2} (1+\gamma) \tag{1.17}$$

where

$$\gamma = \left\{ 1 + \frac{P^*}{6} \left(\frac{l}{r_0} \right)^2 e^y \right\}^{1/2}. \tag{1.18}$$

Solving the last equation for y, we get

$$y = \ln \frac{\alpha^2 - \frac{P^*}{24} \left(\frac{l}{r_0} \right)^2}{\left[\alpha^2 - \frac{P^*}{12} \left(\frac{l}{r_0} \right)^2 \right]^2}. \tag{1.19}$$

Consequently, the expressions for the S.C. potential (1.14), the equilibrium separation of neighbouring atoms (1.15), and the effective cubic strength constant (1.6) can be written

$$\tilde{\varphi}(l) = -\epsilon \left\{ \alpha^2 - \frac{P^*}{8} \left(\frac{l}{r_0} \right)^2 \right\} = -\epsilon \left\{ \frac{e^{-y}}{2} (1+\gamma) - \frac{P^*}{24} \left(\frac{l}{r_0} \right)^2 \right\}, \tag{1.20}$$

$$\frac{l}{r_0} = 1 + \frac{1}{12} \ln \frac{\alpha^2 - \frac{P^*}{24} \left(\frac{l}{r_0} \right)^2}{\left[\alpha^2 - \frac{P^*}{12} \left(\frac{l}{r_0} \right)^2 \right]^4} = 1 + \frac{1}{4} y - \frac{1}{6} \ln \frac{1+\gamma}{2}, \tag{1.21}$$

$$\frac{g(\Theta, l)}{g} = \left\{ \alpha^2 - \frac{P^*}{36} \left(\frac{l}{r_0} \right)^2 \right\} = \frac{P^*}{18} \left(\frac{l}{r_0} \right)^2 + \frac{e^{-y}}{2} \{1+\gamma\}, \tag{1.22}$$

where $g = \varphi'''(r_0) = -6\epsilon a^3$.

Evaluation of the ω-integral in (1.8) is not so easy in the case of finite phonon widths as it was in the pseudoharmonic approximation [5] and has to be done numerically, but we can obtain an approximate expression for (1.8) by using the explicit form of the self-energy operator (1.4) in the high- and low-temperature limits.

2. High-temperature limit

An expression for the self-energy operator (1.4) in the high-temperature limit was earlier obtained [4] in the form

$$\Pi_k(\omega) = -\Theta \frac{g^2(\Theta, l)}{f^3(\Theta, l)} \omega_k S_k\left(\frac{2\omega}{\omega_L}\right), \tag{2.1}$$

where $S_k(2\omega/\omega_L)$ in a dimensionless sum previously calculated [6] for some values of $\{\vec{k}, j\}$, $\omega_L = \sqrt{8f(\Theta, l)/M}$ is the maximum frequency of the lattice in the pseudoharmonic approximation, and $\omega_D \approx 1.05\omega_L$.

Taken with the explicit form (2.1) of the self-energy operator Eq. (1.8) can be written in the high-temperature limit approximately as [4]

$$\frac{z}{2} f(\Theta, l)\overline{u^2(l)} = 3\Theta \left\{\left[1 - 0.11\Theta \frac{g^2(\Theta, l)}{f^3(\Theta, l)}\right]^{-1} + \frac{1}{24}\frac{\omega_L^2}{\Theta^2}\right\}. \tag{2.2}$$

Using (1.17), (1.18) and (1.22) this can be written approximately as

$$F(y) = \frac{4y}{T^*}\left\{1 - \left[\frac{P^*\left(\frac{l}{r_0}\right)^2}{6T^*} - B\right] y\right\} - \left\{1 - \left[\frac{P^*\left(\frac{l}{r_0}\right)^2}{3T^*} - B\right] y\right\}^2 e^y, \tag{2.3}$$

where $T^* = \Theta/\epsilon$ is the reduced temperature, and $B = 0.22\{2 + 1/\gamma\}^2$. It is also convenient to introduce the dimensionless temperature $\tau = \Theta/\omega_{0L} = \lambda T^*/11.76$, where $\lambda = z\epsilon/\varepsilon_0^{(0)}$ is the dimensionless coupling constant of atoms, $\varepsilon_0^{(0)} \approx 1.02\omega_{0L}$ is the zero-point energy per atom in the harmonic approximation, and $\omega_{0L} = \sqrt{8f/M}$ is the maximum value of the harmonic vibrational frequency.

The S.C. equation (2.3) has a different number of real solutions, depending on the values of T^* and P^*. The physical solution is the one which coin-

cides with the harmonic solution as anharmonic terms tend to zero. The harmonic solution is given by

$$y_h = \frac{T^*}{4\alpha_h^2} = \frac{T^*}{2\left\{1 + \frac{P^*}{6}\left(\frac{l}{r_0}\right)_h^2 + \sqrt{1 + \frac{P^*}{6}\left(\frac{l}{r_0}\right)_h^2}\right\}}. \tag{2.4}$$

The dependence of the real solutions of Eq. (2.3) on the reduced temperature T^* and the reduced pressure P^* is shown in Fig. 1. If the pressure ($P^* < P_c^*$) and temperature [$T^* \leq T_s^*(P^*)$] are sufficiently low, Eq. (2.3) has real solu-

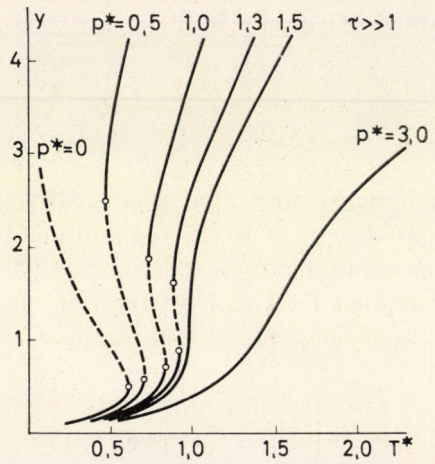

Fig. 1. Real solutions of the S.C. equation

tions. The smallest of these is the physical one and corresponds to a stable crystal state S_1. The instability temperature $T_s^*(P^*)$ is determined by the coincidence of the two real solutions: $y_1(T_s^*) = y_2(T_s^*)$ and can therefore be obtained by solving the equation system $F(y) = 0$, $F'(y) = 0$. Solution y_2 corresponds to an unstable state, which in all figures is denoted by a dotted line. For $T^* > T_s^*(P^*)$ solutions y_1 and y_2 and hence the phonon frequencies also become complex conjugates, which shows the vibrational instability of the lattice in the state S_1 corresponding to the solution y_1. It should be noted that if $P^* > 0$ in the region $T^* \geq T_s^*$, then Eq. (2.3) has another real solution, y_3 corresponding to a stable state S_3.

In the region of sufficiently high pressure or temperature $P^* \geq P_c^*$ or $T^* \geq T_c^*$ therefore, Eq. (2.3) always has two real solutions, the smallest of which, the physical solution, is a smooth function of temperature and pressure. In this case the phonon frequencies are always real. The critical temperature T_*^c and critical pressure P_c^* characterizing the disappearance of the lattice's vibrational instability are determined by the coincidence of three real solutions of Eq. (2.3): $(y_1(T_c^*, P_c^*) = y_2(T_c^*, P_c^*) = y_3(T_c^*, P_c^*)$ and thus can

be found by solution of the following system of equations: $F(y) = 0$, $F'(y) = 0$, $F''(y) = 0$. The dependence of the reduced instability temperature T_s^* on the reduced pressure P^* is presented in Fig. 2. In the high-temperature limit we get $P_c^* \approx 1.35$ for the critical pressure and $T_c^* \approx 0.98$ for the critical temperature.

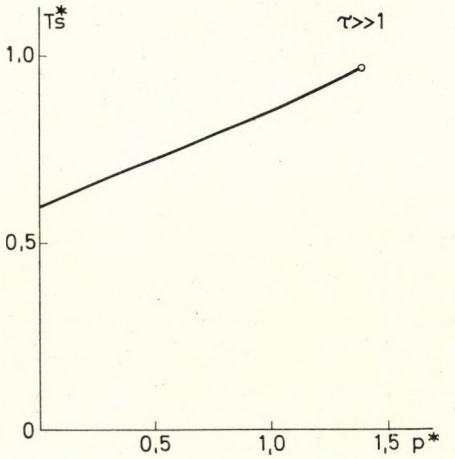

Fig. 2. Dependence of the instability temperature T_s^* on the reduced pressure P^*

Taking Eqs. (1.17), (1.18), (1.22) and (2.1), the frequencies of the renormalized phonons and their widths (1.3) can be written in the following forms:

$$\frac{\epsilon_k}{\omega_{0k}} \approx \alpha - \frac{3}{2} \cdot 10^{-2} \frac{T^*}{\alpha} (2+1/\gamma)^2, \tag{2.5}$$

$$\frac{\Gamma_k}{\omega_{0k}} = \frac{1}{2} \cdot 10^{-2} T^* \frac{1}{\alpha} (2+1/\gamma)^2. \tag{2.6}$$

In the calcu lations the approximate values $ReS_k \approx 3 \times 10^{-2}$ and $ImS_k \approx 1 \times 10^{-2}$ were taken.) The dependence of the renormalized phonon frequencies ϵ_k/ω_{0k} on the reduced temperature T^* for some values of P^* is presented in Fig. 3; Γ_k/ϵ_k is given as a function of T^* in Fig. 4. The results obtained here for $P^* \ll 1$ coincide with those found earlier [4].

In the high-temperature limit expressions (1.12) and (1.13) can be written [4], [6]

$$F_0 = 3N\Theta \ln\left(0.65 \frac{\omega_L}{\Theta}\right),$$
$$\tilde{F}_3(\Theta) = -N\Theta^2 A \frac{g^2(\Theta, l)}{f^3(\Theta, l)}, \tag{2.7}$$

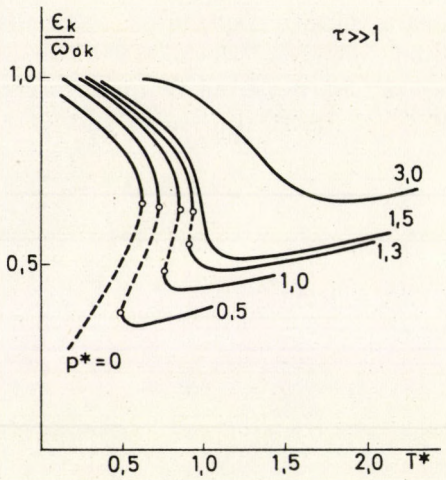

Fig. 3. Dependence of the renormalized phonon frequencies E_k/ω_{0k} on the reduced temperature T^*

where the numerical coefficient $A \approx 5.6 \times 10^{-2}$. From (1.20), (2.2) and (2.7) the internal energy (1.10) and free energy (1.11) are found to be

$$e = \frac{1}{3N\epsilon} E \approx 0.85\, T^* - 2\alpha^2 (1+0{,}7\, y) + \frac{P^*}{4}\left(\frac{l}{r_0}\right)^2, \tag{2.8}$$

$$f = \frac{1}{3N\epsilon} F \approx T^* \ln \frac{7.8\,\alpha}{\lambda T^*} - \frac{T^*}{3} - 2\alpha^2 \left(1 + \frac{y}{3}\right) + \frac{P^*}{4}\left(\frac{l}{r_0}\right)^2. \tag{2.9}$$

(In calculating free energy the value $\lambda = 20$ was used. The reduced thermodynamical potential $g = f + P^* v^*$ is plotted against the reduced tempera-

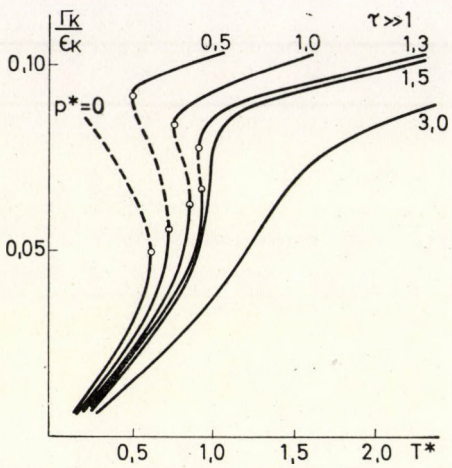

Fig. 4. Dependence of the phonon widths Γ_k/E_k on temperature T^*

ture T^* in Fig. 5. It will be noted that the function $g(T^*)$ displays a minimum at a temperature slightly lower than T_s^*. The dependence of the reduced internal energy e on the reduced temperature T^* is presented in Fig. 6. The

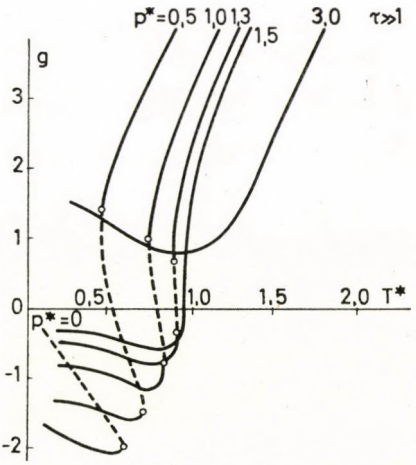

Fig. 5. The thermodynamical potential $g = f + P_v^{**}$ as a function of temperature T^*

reduction of the internal energy with increasing temperature does not appear in the pseudoharmonic approximation or in the low-temperature limit; in both cases it is an increasing function of temperature and its curves have a van der Waals character.

The dependence of the reduced volume $v^* = V\sqrt{2}/Nr_0^3 = (l/r_0)^3$ on the reduced pressure P^* is shown in Fig. 7. It should be noted that the curves

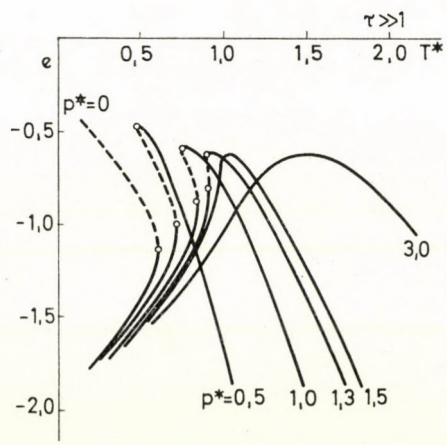

Fig. 6. The internal energy $e = (1/3\ NE)E$ as a function of temperature T^*

have a van der Waals character. An analogous result was obtained by VON HEIMENDAHL [7].

The calculation of f.c.c. lattice properties in the low-temperature limit and a detailed discussion of the results will be given in the following paper.

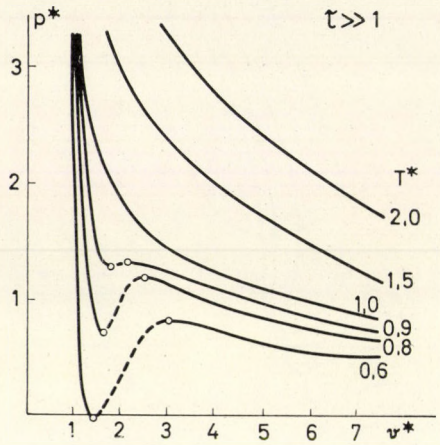

Fig. 7. Dependence of the reduced volume $v^* = (l/r_0)^3$ on the reduced pressure P^*

REFERENCES

1. PH. F. CHOQUARD, The Anharmonic Crystals, W. A. Benjamin Inc., New York/Amsterdam, 1967.
2. N. M. PLAKIDA and T. SIKLÓS, Acta Phys. Hung., **25**, 17, 1968.
3. N. M. PLAKIDA and T. SIKLÓS, Phys. Stat. Sol., **33**, 103, 1969.
4. N. M. PLAKIDA and T. SIKLÓS, Phys. Stat. Sol., **39**, 171, 1970.
5. T. SIKLÓS, Acta Phys. Hung. **30**, 193, 1971, Report JINR E4-5390, Dubna, 1970.
6. A. A. MARADUDIN, A. E. FEIN and G. H. VINEYARD, Phys. Stat. Sol., **2**, 1479, 1962. A. A. MARADUDIN, Phys. Stat. Sol., **2**, 1493, 1962.
7. L. VON HEIMENDAHL, Diplomarbeit, Technische Hochschule, München, 1970.

ТЕРМОДИНАМИКА СИЛЬНО АНГАРМОНИЧЕСКИХ КРИСТАЛЛОВ, I

Т. ШИКЛОШ и В. Л. АКСЕНОВ

Резюме

Исследуются свойства Г. Ц. К. решетки с парным центральным взаимодействием ближайших соседей в случае произвольного внешнего давления. Вычислены температура неустойчивости, критическая температура, частота фононов и их затухание, а также термодинамические величины Г. Ц. К. решетки в пределе высоких температур.

Acta Physica Academiae Scientiarum Hungaricae, Tomus 31 (4), pp. 345—351 (1972)

THERMODYNAMICS OF STRONGLY ANHARMONIC CRYSTALS II

By

T. SIKLÓS and V. L. AKSIENOV

JOINT INSTITUTE FOR NUCLEAR RESEARCH, LABORATORY OF THEORETICAL PHYSICS, DUBNA, USSR

(Received 1. VI. 1971)

The properties under arbitrary external pressure of the face-centred cubic lattice displaying nearest-neighbour central forces interaction are investigated. The instability temperature, critical temperature, phonon frequencies, phonon widths and thermodynamical properties of the lattice are calculated in the low-temperature limit.

In the preceding paper [1] properties of the f.c.c. lattice showing nearest-neighbour central force interaction were considered in the case of an arbitrary external pressure and the instability temperature, critical temperature, phonon frequencies, phonon widths and thermodynamical properties of the lattice were calculated in the high-temperature limit.

In the present paper these quantities are calculated in the low-temperature limit and the results obtained in both parts of the work are discussed.

1. The low-temperature limit ($\Theta \ll \omega_D$)

An expression for the self-energy operator (I.1.4)* in the low-temperature limit was earlier obtained [2] in the form

$$\Pi_k(\omega) = -\omega_k \frac{g^2(\Theta, l)}{f^3(\Theta, l)} \left\{ \varepsilon_0 \; S_{0k}\left(\frac{2\omega}{\omega_L}\right) + \frac{3\pi^4}{5} \frac{\Theta^4}{\omega_D^3} S_{1k}\left(\frac{2\omega}{\omega_L}\right) \right\}, \qquad (1.1)$$

where the dimensionless sums S_{0k} and S_{1k} are given in [2], [3] and $\varepsilon_0 \approx 1.02\omega_L$ is the zero-point energy per atom in the pseudoharmonic approximation. The notations are the same as in the preceding paper [1].

In the low-temperature limit (I.1.8), taken with the explicit form (1.1) of the self-energy operator, approximates to [2]

$$\frac{z}{2} f(\Theta, l)\overline{u^2(l)} = \varepsilon_0 \left[1 - \nu_0 \varepsilon_0 \frac{g^2(\Theta, l)}{f^3(\Theta, l)}\right]^{-1} + \frac{3\pi^4}{5} \frac{\Theta^4}{\omega_D^3} \left[1 + \nu_1 \varepsilon_0 \frac{g^2(\Theta, l)}{f^3(\Theta, l)}\right] \qquad (1.2)$$

with the numerical coefficients $\nu_0 \approx 7.3 \times 10^{-3}$, $\nu_1 \approx 0.10$ [2].

* The formulae of our previous paper [1] are quoted as (I.1.4) and (I.2.4) respectively.

On introducing Eqs. (I.1.17), (I.1.18) and (I.1.22), this takes the approximate form

$$\lambda\alpha y(\alpha) = \left\{1 - \frac{0{,}4}{\lambda}\,\frac{\left[\alpha^2 - \frac{P^*}{36}\left(\frac{l}{r_0}\right)^2\right]^2}{\alpha^5}\right\}^{-1} + \tag{1.3}$$

$$+ 49{,}6\left(\frac{\tau}{\alpha}\right)^4\left\{1 + \frac{5{,}4}{\lambda}\,\frac{\left[\alpha^2 - \frac{P^*}{36}\left(\frac{l}{r_0}\right)^2\right]^2}{\alpha^5}\right\},$$

where the function $y(\alpha)$ is given by (I.1.19) and (I.1.21).

In the low-temperature limit it is interesting to investigate crystals with weak coupling. The dependence of the real solutions of the S.C. equation (1.3) on the reduced temperature T^* and reduced pressure P^* for $\lambda = 3$ is given in Fig. 1a, and for $\lambda = 2$ in Fig. 1b. If $\lambda \geq \lambda_s = 2.24$ the solutions of (1.3)

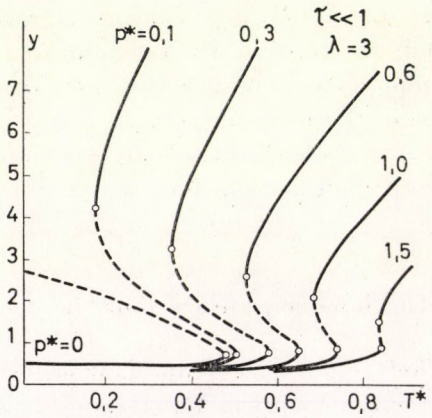

Fig. 1a. Real solutions of the S.C. equation for $\lambda = 3$

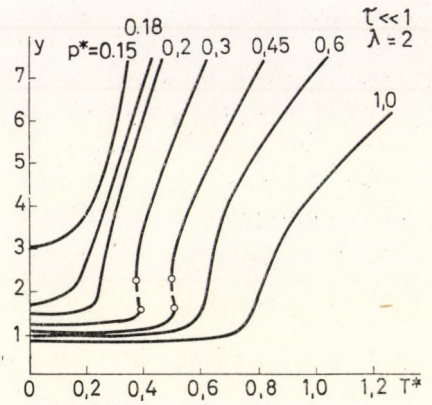

Fig. 1b. Real solutions of the S.C. equation for $\lambda = 2$

(see Fig. 1a) behave similarly to those of Eq. (I.2.3) in the high-temperature limit. The dependence of the instability temperature T_s^* on the reduced pressure P^* is likewise similar to that found in the high-temperature limit (compare Fig. 2 with Fig. 2 in [1]). For $\lambda = 3$ we get $P^* \approx 1.5$ for the critical pressure and $T^* \approx 0.82$ critical temperature.

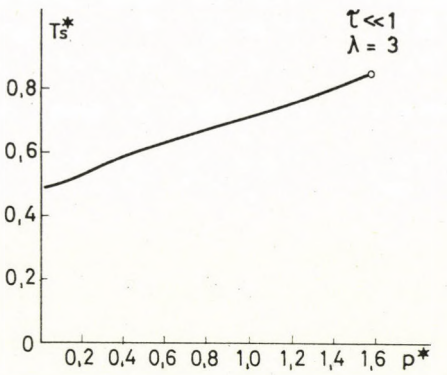

Fig. 2. Dependence of the instability temperature T_s^* on the reduced pressure P^* ($\lambda = 3$

If the coupling constant is sufficiently small ($\lambda < \lambda_s = 2.24$) the crystal becomes unstable even at $\tau = 0$, because in this case the zero-point energy is sufficiently large. But when an external pressure is applied a stable crystal state appears which behaves analogously the state where $\lambda \geq \lambda_s$ (see Fig. 1b).

The frequencies of the renormalized phonons and their widths (I.1.3), can be written according to (I.1.17), (I.1.18), (I.1.22) and (1.1) in the forms

$$\frac{\epsilon_k}{\omega_{0k}} \approx \alpha - \frac{6}{\lambda}\{2+1/\gamma\}^2 \left\{ Re\, S_{0k} + \frac{3\pi^4}{5}\left(\frac{\tau}{\alpha}\right)^4 ReS_{1k} \right\}, \tag{1.4}$$

$$\frac{\Gamma_k}{\omega_{0k}} \approx \frac{6}{\lambda}\{2+1/\gamma\}^2 \left\{ Im\, S_{0k} + \frac{3\pi^4}{5}\left(\frac{\tau}{\alpha}\right)^4 Im\, S_{1k} \right\}, \tag{1.5}$$

where γ is given by (1.18). (In the calculations the approximate values [2] $ReS_{0k} \approx Im \cdot S_{0k} \approx 1.85 \times 10^{-3}$ and $ReS_{1k} \approx Im\, S_{1k} \approx 1.25 \times 10^{-2}$ were taken.) The dependence of the renormalized phonon frequencies e_k/ω_{0k} and phonon widths Γ_k/ϵ_k on the reduced temperature for $\lambda = 3$ are presented in Figs. 3 and 4, respectively. It can be seen that both properties depend slightly on temperature in the region $T^* \leq T_s^*$. In the region $T^* > T_s^*$ the phonon widths expand rapidly, although still remaining sufficiently small. The results for $P^* \ll 1$ coincide with earlier findings [2].

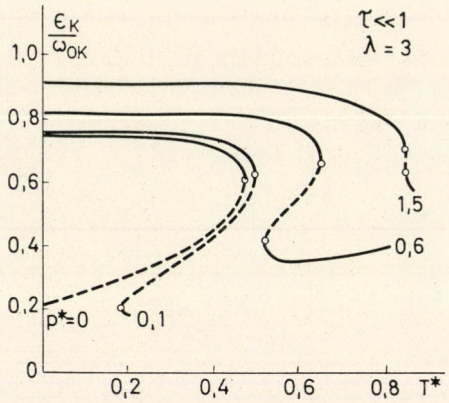

Fig. 3. Dependence of the renormalized phonon frequencies ϵ_k/ω_{0k} on the reduced temperature T^* ($\lambda = 3$)

In the low-temperature limit expressions (I.1.12) and (I.1.13) for the free energy can be written [2], [3]

$$F_0 = N\omega_L \left\{1 - \frac{\pi^4}{5}\left(\frac{\tau}{\alpha}\right)^4\right\},$$
$$\tilde{F}_3(\Theta) = -N\varepsilon_0 \frac{g^2(\Theta, l)}{f^3(\Theta, l)} \left\{\varepsilon_0 B + \frac{3\pi^4}{5}\frac{\Theta^4}{\omega_D^3} C\right\} \tag{1.6}$$

with the numerical coefficients $B \approx 1.85 \times 10^{-3}$, $C \approx 1.25 \times 10^{-2}$.

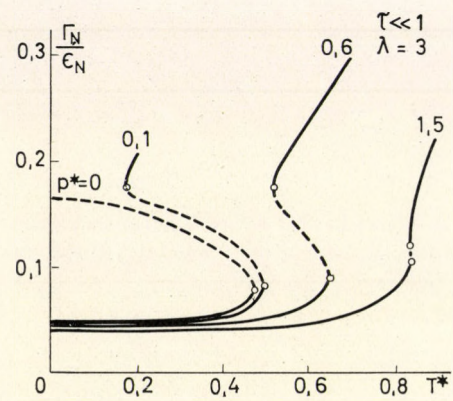

Fig. 4. Dependence of the phonon widths Γ_k/ϵ_k on temperature T^* ($\lambda = 3$)

Using (I.1.17), (I.1.18), (I.1.22) and (1.6), the expressions for the internal energy (I.1.10) and free energy (I.1.11) take the forms

$$e = \frac{1}{N\omega_{0L}} E = \frac{\lambda}{2}\left\{\alpha^2(\gamma-1) + \frac{P^*}{8}\left(\frac{l}{r_0}\right)^2\right\} + 5\tilde{f}_3\,, \tag{1.7}$$

$$f = \frac{1}{N\omega_{0L}} F = \alpha\left\{1 - \frac{\pi^4}{5}\left(\frac{\tau}{\alpha}\right)^4\right\} - \\ - \frac{\lambda}{2}\left\{\alpha^2(1+\gamma) - \frac{P^*}{8}\left(\frac{l}{r_0}\right)^2\right\} + f_3\,. \tag{1.8}$$

The reduced thermodynamical potential $g = f + IP^*v^*$, the reduced internal energy e, and the reduced entropy $s = 1/N \cdot S/K$ are presented in Figs. 5, 6 and 7, respectively, as functions of the reduced temperature T^* for $\lambda = 3$.

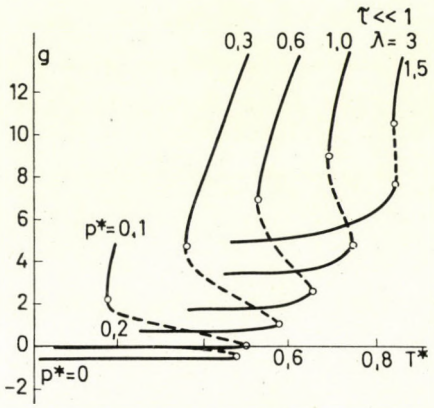

Fig. 5. The thermodynamical potential $g = f + 3P^*v^*$ as a function of temperature T^* ($\lambda = 3$)

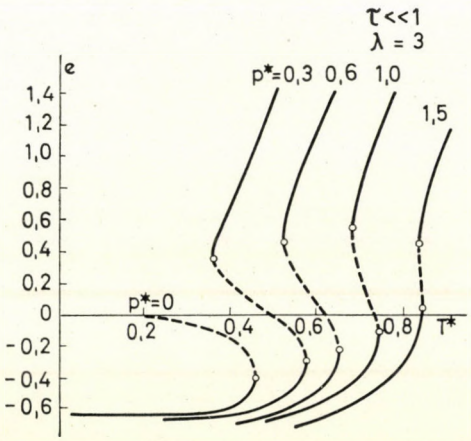

Fig. 6. The internal energy $e = 1/N\omega_{0L}\, E$ as a function of temperature T^* ($\lambda = 3$)

Curves for the function $v^*(P^*)$ in the low-temperature limit have similar van der Waals character to that found in the high-temperature limit (see Fig. 7 in [1]) and thus are not given here.

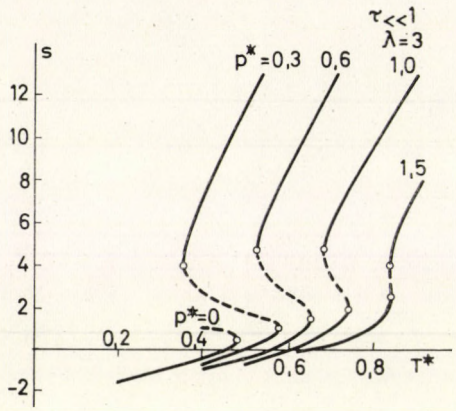

Fig. 7. The entropy $S = 1/N\ S/k$ as a function of temperature T^* ($\lambda = 3$)

2. Discussion

In both this and the preceding paper [1] the properties of strongly anharmonic crystals under fixed arbitrary external pressure have been investigated in the S.C. phonon field approximation by allowing for damping (correlations) of S.C. phonons. The results agree quite well with those obtained earlier for small pressure [2] and those calculated in the pseudoharmonic approximation for arbitrary pressure [4].

As shown by Fig. 2 in [1] ($\tau \gg 1$) and Fig. 2 in the present paper ($\tau \ll 1$) an anharmonic crystal becomes unstable at some temperature T_s if the external pressure is smaller than a critical value ($P < P_c$). This means that at T_s the crystal lattice, which is a bound state of atoms due to the attractive part of the interatomic potential, becomes unstable with respect to the propagation of the collective excitations, i.e. the S.C. phonons. Near T_s damping of phonons is sufficiently small [see Fig. 4 in [1] ($\tau \gg 1$) and Fig. 4 in the present paper ($\tau \ll 1$)], and moreover at $T \lesssim T_s$ the mean square relative displacement of neighbouring atoms is much smaller than the distance between them:

$$\sqrt{\overline{u_s^2(l)}}/l_s \approx 0.10(\tau \gg 1); \quad \sqrt{\overline{u_s^2(l)}}/l_s \approx 0.14(\tau \ll 1).$$

Therefore the long-range correlations which lead to the collective excitations play an essential role in this case and the instability at T_s indicates the breakdown of this collective excitations picture.

It should be remarked that the instability curve in Fig. 2 in [1] lies close to the reduced melting curves of inert-gas solids: $T_m^* \approx 0.5 \{1 + 0.2P^*\}$ [5]. It seems likely, therefore, that vibrational instability of anharmonic lattices plays an essential role in melting phenomenon in the low pressure region ($P < P_c$). It is interesting to note that the van der Waals behaviour of the physical properties of such crystals (see Figs. 5, and 7 in [1] and Figs. 5—7 in the present paper) shows first-order transition along the curve $T_s(P) \cdot (P < P_c)$. This is typical of the whole S.C. theoretical approach. It should be stressed, however, that in our one-phase model the second stable state, described by the upper part of the curves in Fig. 1 [1] and Fig. 1 in the present paper, is also a crystal state, but one in which the mean square relative displacement of the atoms is much larger than in the first stable state. To obtain a more realistic picture of the phase transition the possibility of a transition to the liquid state should be taken into account.

The critical temperature T_c and critical pressure P_c mark the vibrational instability of the lattice: above the critical point lattice vibrations do not destroy the bound state of atoms, which is now stabilized by the external pressure. It therefore seems natural that at higher pressures ($P \geq P_c$) we should be able to attribute the melting phenomenon to an order-disorder transition in which hard core correlations play an essential role. The investigate this problem, the hard core part of the interatomic potential and the appearance of vacancies should be considered.

Acknowledgement

It is a great pleasure to express our gratitude to Dr. N. M. PLAKIDA for helpful discussions and advice.

REFERENCES

1. T. SIKLÓS and V. L. AKSIENOV, Acta Phys. Hung. **31,** 345, 1972.
2. N. M. PLAKIDA and T. SIKLÓS, Phys. Stat. Sol., **39,** 171, 1970.
3. A. A. MARADUDIN, P. A. FLINN and R. A. COLDWELL-HORSFALL, Ann. Phys. (U.S.A.), **15,** 337, 1961.
   P. A. FLINN and A. A. MARADUDIN, Ann. Phys. (U.S.A.), **22,** 223 & 360, 1963.
4. T. SIKLÓS, Acta Phys. Hung. **30,** 193, 1971; Report JINR E4-5390, Dubna, 1970.
5. A. MICHELS and C. PRINS, Physica (Utrecht), **28,** 101, 1962.

ТЕРМОДИНАМИКА СИЛЬНО АНГАРМОНИЧЕСКИХ КРИСТАЛЛОВ, II

Т. ШИКЛОШ и В. Л. АКСЕНОВ

Резюме

Исследуются свойства Г. Ц. К. решетки с парным центральным взаимодействием ближайших соседей в случае произвольного внешнего давления. Вычислены температура неустойчивости, критическая температура, частота фононов и их затухания, а также термодинамические величины Г. Ц. К. решетки в пределе низких температур.

Acta Physica Academiae Scientiarum Hungaricae, Tomus 31 (4), pp. 353—359 (1972)

THE ABERRATION OF COMPONENTS OF DOUBLE STARS

By

L. JÁNOSSY

CENTRAL RESEARCH INSTITUTE OF PHYSICS, BUDAPEST

(Received 8. VI. 1971)

So as to clear a primitive misconception about the nature of aberration of light a short derivation of the facts is given. In particular the effects are discussed which appear when the observer or alternatively the source are set to move.

I

There exist misunderstandings about the interpretation of the effect of aberration. There are even physicists who claimed that the effect of aberration contradicts the theory of relativity.* Although the problem is quite trivial it appears worth-while to discuss the problem in a little detail and to show why the aberration depends indeed on the relative velocity of source and observer and not on the absolute velocity of the observer as it was claimed erroneously.

Suppose a luminous object A to move along a straight line with a constant velocity v. At a time t the object is in a point P and thus it is situated in a direction $\overrightarrow{OP}$ from the observer O (Fig. 2). The observer in O sees the object at the time t not in the point P but in a retarded position P' where A had been at the time t' so that the distance

$$OP' = (t - t')c.$$

The angle of aberration is the angle between the directions OP and OP' thus as can be seen from Fig. 2

$$\sin \vartheta = \frac{v}{c} \sin \alpha \,, \tag{1}$$

* See e.g. GRIMSEHL, Lehrb. d. Phys., 12. Aufl. 1952, 3. Bd., S. 286 (Teubner, Leipzig), where we find the following statement:

"Die Aberration ist unabhängig von den Bewegungen der Sterne und daher auch nicht abhängig von der Relativbewegung Stern-Erde. Dies beweisen die Beobachtungen an Doppelsternen, wie Lenard gezeigt hat. Sie geben normale Aberration. Wäre aber die Aberration abhängig von der Relativgeschwindigkeit, so müssten Doppelsternsysteme in den Stellungen C und D der Abb. 419 [reproduced here as Fig. 1] starke seitliche Trennungen aufweisen, wovon nichts beobachtet ist."

where

$$\alpha = \sphericalangle(OP, PP').$$

If the object A is at rest (relative to our system of reference) and the observer is moving with a velocity $-v$ then the angle of aberration is found to remain

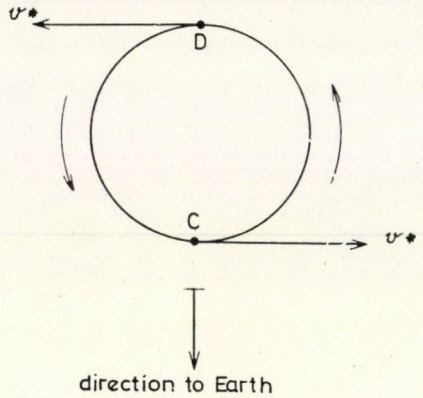

Fig. 1. "The aberration is not relative" according to GRIMSEHL

the same. The latter result can be seen readily applying a Lorentz transformation. Thus we may consider A and O in a system K' relative to which O moves and A is at rest. The transformation shows that the light registered by the moving observer at the time t does not appear to come from P but from a point P' as shown in Fig. 3. However, as the effect of aberration was erroneously used as an argument against the theory of relativity — it is useful to analyze

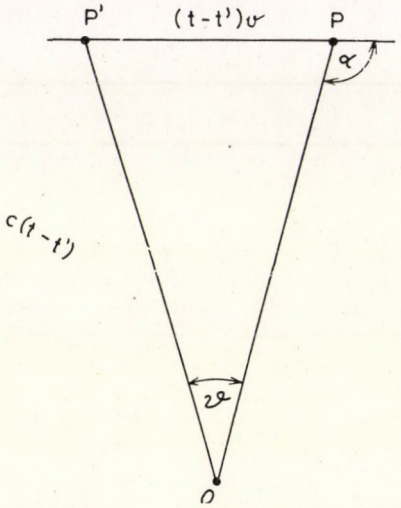

Fig. 2. Aberration of the light from a source moving with constant velocity

the process producing the effect. As the effect is of the first order in the velocity the above analysis can be carried out without the use of relativistic concepts. We come back to this question at the end of this article.

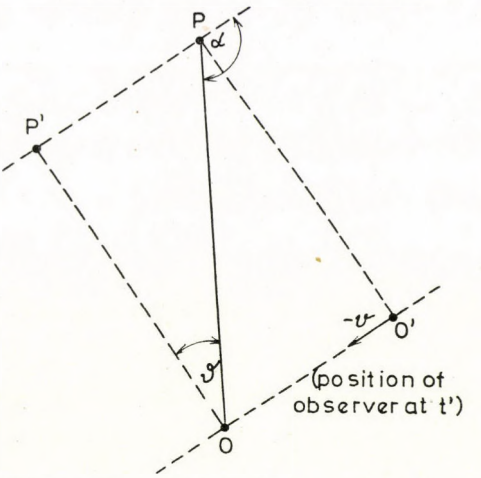

Fig. 3. Effect of aberration in the case of moving observer

We come to an apparent paradox if we apply Eq. (1) to an object which is not moving along a straight line but e.g. along a closed orbit. Consider e.g. one component of a double star moving along a circular path. If we were to apply Eq. (1) then we might suppose that the light arriving from the body moving along the closed orbit suffers considerable aberration. Indeed, the apparent positions of the object P_1', P_2', ... while the object itself is situated in points P_1, P_2, ... lie on a circle the radius of which may be considerably larger than the radius of the orbit (see Fig. 4).

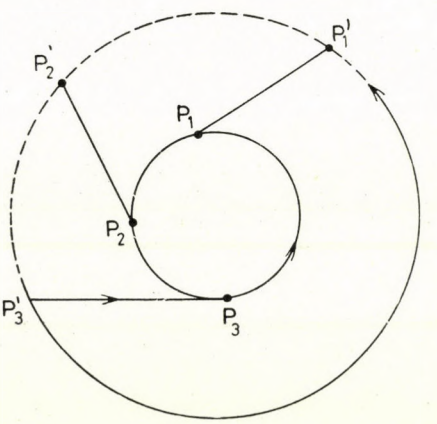

Fig. 4

If we were to apply Eq. (1) for the aberration of light emitted by the body moving along the small circle of Fig. 4 we would expect its image to move along the outer circle and therefore the aberration might be thought to increase the apparent radius of the orbit considerably. The above argument although quite incorrect, nevertheless it was brought as a serious argument against the theory of relativity and it has, to my knowledge, not been answered explicitly.

The light emitted by the star can be ascribed to oscillating atoms sharing the motion of the star. The field of the emitting atoms can be expressed in terms of retarded potentials, e.g. the vector potential produced by one individual atom can be written

$$\mathbf{A}(\mathbf{R}, t) = \int \frac{\mathbf{i}(\mathbf{r}', t')}{|\mathbf{r}' - \mathbf{R}|} d^3 r' , \tag{2}$$

$$t' = t - |\mathbf{R} - \mathbf{r}'|/c, \tag{3}$$

where $\mathbf{i}$ is the current density inside the oscillating atom. Supposing that the centre of the atom moves together with the star along an orbit $\mathbf{r}_A(t')$ then the current density $\mathbf{i}$ differs from zero only in a small vicinity of its centre, thus

$$\mathbf{i}(\mathbf{r}, t') \neq 0 \quad \text{if} \quad |\mathbf{r}_A(t') - \mathbf{r}'| < a, \tag{4}$$

where $\mathbf{r}_A$ is the coordinate vector of the centre of the atom and a is something like the radius of the atom. From (3) and (4) we see that the sources of the field which is found by the observer O at a time t are placed in a close vicinity of the orbit of P. Thus instead of Fig. 4 we have to draw a Figure 5. Thus at the time $t_1, t_2, t_3, \ldots$ when the observer registers the radiation, the source is situated in points $P_1, P_2, P_3, \ldots$ but the observer registers the radiation which was previously emitted from points $P_1', P_2', P_3', \ldots$ of the orbit. The time during which the particle moves from P_1 to P_1' is the retardation time; this time is of the order of $|\mathbf{r}_s - \mathbf{R}|/c$ where $\mathbf{r}_s$ is the centre of the orbit — the time $t - t'$ may be so large as to allow the star to complete several revolutions.

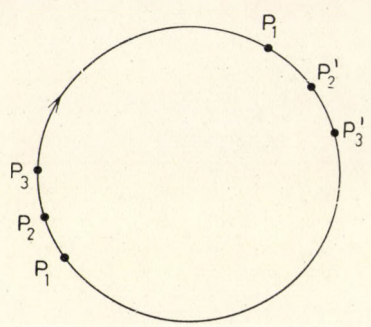

Fig. 5. Aberration of the light of a source moving along a closed orbit

The source of the radiation received at a time t in O is thus always confined to points of the orbit of P. It remains to show, that the radiation arrives in O in directions OP'_1, OP'_2, . . ., i.e. that it is coming from the direction of the retarded source. This is, however, the case as can be seen most easily from the relations given e.g. by W. HEITLER.* There we find the explicit expressions for the field of a source moving with arbitrary velocity and acceleration. Eq. (10a) on page 20 gives the electric component of the field in two terms. The first term is proportional to the inverse square of the distance, the second terms giving the radiation field, can be written

$$\mathbf{E}_{\text{rad}} = \frac{1}{s^3 c^2}\left(\mathbf{r}\times\left(\left(\mathbf{r}+\frac{\mathbf{v}}{c}r\right)\times\dot{\mathbf{v}}\right)\right). \tag{5}$$

The magnetic component of the radiation field is obtained from (10b) as

$$\mathbf{H}_{\text{rad}} = (\mathbf{E}_{\text{rad}} \times \mathbf{r})/r\,. \tag{6}$$

s is a scalar defined by

$$s = r + \frac{\mathbf{vr}}{c}$$

and $\mathbf{r}$ is the retarded distance OP' and $\mathbf{v}$, $\dot{\mathbf{v}}$ are velocity and acceleration at the retarded time t'. Thus in our notation

$$\mathbf{r} = \mathbf{r}(t'), \quad \mathbf{v} = \mathbf{v}(t'), \quad \dot{\mathbf{v}} = \dot{\mathbf{v}}(t'),$$

so that

$$(\mathbf{r}(t'))^2 - c^2(t - t')^2 = 0.$$

Thus in the case of the source moving along a close orbit $\mathbf{r} = \mathbf{r}(t')$ points always into the direction of a point of the orbit.

From (5) and (6) we find

$$(\mathbf{E}_{\text{rad}}\,\mathbf{r}) = 0,$$

and

$$\mathbf{P} = \frac{c}{4\pi}(\mathbf{E}_{\text{rad}}\times\mathbf{H}_{\text{rad}}) = \frac{c}{4\pi}E^2_{\text{rad}}\,\mathbf{r}/r\,,$$

we see thus that the radiation field is transversal to the retarded distance $\mathbf{r}(t')$ and the Poynting vector $\mathbf{P}$ is parallel to $\mathbf{r}(t')$. These relations give the explicit expressions for the retarded potentials of an arbitrary moving source.

From these results it follows that the aberration of the moving source must be taken in accord with Fig. 5. Thus at a time t the radiation appears

* W. HEITLER: The Quantum Theory of Radiation. University Press, Oxford, 1954. 3rd ed., see p. 18—21.

to come from a point of the orbit of the star, i.e. from that point of the orbit in which the star was situated at the retarded time. Thus no apparent increase of the orbit, as shown in Fig. 1 and Fig. 3, is to be expected.

II

The effect of aberration depends only on the relative velocity between source and observer. This can be seen to be the case when considering the process in two different systems of references; one where the source is at rest and in another where the observer is at rest.

Nevertheless the fact that the aberration depends on the relative velocity only involves a physical problem which we want to clarify briefly.

Consider a system of reference K in which to begin with both, source and observer, are at rest. We shall carry out our further considerations using this system of reference only.

The following two possibilities have to be considered:

1. the source S — which at $t = 0$ is at rest relative to the observer — might be subjected to acceleration so that at the time $t > T$ it moves with a constant velocity v. The observer does not notice immediately that the source has been set to move. The picture S' of S starts to move at a time $t_1 = R/c$ where R is the original distance OS. S' is seen to accelerate and to move eventually with a velocity v for times $t > T_1 = T + R_1/c$ where R_1 is the distance between O and S at the time T, the time when the acceleration has been concluded. The picture S' at a time $t > t_1$ thus points into a direction different from the direction in which it is situated and this gives the effect of aberration.

2. If the source S remains at rest relative to K but the instrument of the observer is accelerated until it moves with a velocity —v, then the radiation field in the vicinity of S remains the same, but the effect of this field on the moving instrument of observation differs from that on the instrument at rest.

The instrument of observation may be a telescope, but it might also be simply a longish metal tube. We discuss the case of a tube although the argument below is valid for any optical instrument of observation. The radiation from S can pass through the tube if its axis is directed in a direction parallel to the Poynting vector

$$\mathbf{P} = \frac{c}{4\pi} (\mathbf{E} \times \mathbf{B}), \tag{7}$$

where $\mathbf{E}$ and $\mathbf{B}$ are the electric and magnetic field strengths of the radiation field. If the tube is at an angle to $\mathbf{P}$ then the energy of the field entering the tube is absorbed by the walls. The absorption takes place through the conduction electrons in the metal. The tangential component of $\mathbf{E}$ accelerates

the electrons and those transfer energy to the metal lattice. The electrons thus set in motion extinguish by interference some of the incident radiation.

If the metal tube is set to move with a velocity $-\mathbf{v}$ then the conduction electrons obtain also such a velocity (in addition to whatever velocities they already had). The radiation field acts on the moving electrons as an effective field $\mathbf{E}_{\text{eff}}$, $\mathbf{B}_{\text{eff}}$ would act on electrons without the extra velocity, where

$$\begin{aligned} \mathbf{E}_{\text{eff}} &= \mathbf{E} - (\mathbf{v} \times \mathbf{B})/c\,, \\ \mathbf{B}_{\text{eff}} &= \mathbf{B} + (\mathbf{v} \times \mathbf{E})/c\,, \end{aligned} \tag{8}$$

where we have neglected terms of higher order in v/c. The system behaves as if a radiation with an effective Poynting vector

$$\mathbf{P}_{\text{eff}} = \frac{c}{4\pi}(\mathbf{E}_{\text{eff}} \times \mathbf{B}_{\text{eff}})\,, \tag{9}$$

was falling upon it. If we take the example of the metal tube then we see, that the moving tube has to be placed parallel to P_{eff} if we want to avoid absorption by the electrons in the walls.

From (7), (8) and (9) (neglecting further terms of the second order) we find

$$\mathbf{P}_{\text{eff}} = \mathbf{P} + \frac{1}{4\pi}[\mathbf{E} \times (\mathbf{v} \times \mathbf{E}) + \mathbf{B} \times (\mathbf{v} \times \mathbf{B})]\,.$$

The result of a simple calculation shows that

$$\sphericalangle(\mathbf{P}_{\text{eff}}\,\mathbf{P}) = \frac{v}{c}\,\sin\alpha + \text{terms of higher order},$$

where α is the angle between $\mathbf{P}$ and $\mathbf{v}$.

We see thus that the moving instrument has to be turned round by an angle $v/c \sin\alpha$ so as to allow to pass the radiation field in the same manner as the instrument at rest does it. This analysis is valid for any type of instrument, we have discussed the case of the metal tube for the sake of simplicity.

АБЕРРАЦИЯ КОМПОНЕНТ ДВОЙНЫХ ЗВЕЗД

Л. ЯНОШИ

Резюме

Для выяснения ошибочного представления в связи с аберрацией света приводится краткий обзор фактов, уделяя особое внимание эффектам, возникающим при движении источника света или наблюдателя.

Acta Physica Academiae Scientiarum Hungaricae, Tomus 31 (4), pp. 361—368 (1972)

PHOTOELECTRIC EMISSION FROM Ge_xSi_{1-x} MIXED CRYSTALS*

By

G. GERGELY, J. PEISNER, and E. KAPITÁNY

RESEARCH INSTITUTE FOR TECHNICAL PHYSICS
OF THE HUNGARIAN ACADEMY OF SCIENCES, BUDAPEST

(Received 9. VII. 1971)

Photoemission of mixed crystalline Ge_xSi_{1-x} samples was studied. Thin epitaxial layers on Si substrates were prepared by gaseous transport process. Measurements were made in 10^{-9} torr UHV on atomic clean surfaces prepared by chemical etching and heat treatment in vacuum. The quantum efficiency, threshold of photoemission, work function, electron affinity and energy distribution of photoelectrons excited by 4—6.2 eV photons were determined. A gradual shift of characteristics with composition was observed. The work function (surface Fermi level) of the samples, determined by the retarding field method of Hughes, corresponded to the bulk Fermi level.

Introduction

The crystallographic, electrical and optical properties and the band structure of Ge_xSi_{1-x} mixed crystals have been described by several authors [1—5], but only a few preliminary data on photoemission have been published [6].

Photoelectric emission studies of semiconductors are of special interest, since they can supply information about surface properties, the Fermi level, and, from a knowledge of the energy distribution of the photoelectrons [7—9], the band structure. The band structure of Ge_xSi_{1-x} systems has been analysed from the reflection spectra of polycrystalline samples by SCHMIDT [1] and TAUC and ABRAHAM [4] but apart from some preliminary results [6] no data are available on the photoelectron energy spectra or the semiconductor work functions (i.e. the Fermi level). In the work reported in this paper a method of determining work functions from purely photoelectric data by analysing the photoemission yield in a retarding field [10] was applied.

Samples

Mixed crystalline Ge_xSi_{1-x} epitaxial layers of various composition and 1—50 μ thickness were prepared in our laboratory on Si 111 substrates by a method developed by SZÉKELY and coworkers [11]. As shown by X-ray diffraction, these heteroepitaxial layers are single crystals.

* Dedicated to the memory of Prof. P. GOMBÁS.

The composition of the layers was determined by X-ray spectroscopy [11] and from their optical reflection spectra [1, 4]. The atomic clean surfaces required for determining the band structure and Fermi level were prepared by chemical etching [1, 6] and by heating the samples in UHV at 10^{-9} torr. The samples were mounted between molybdenum strips and heating was achieved by passing current through the crystals. The cleaning process was checked by LEED studies as in the earlier photoemission studies [6].

Experimental techniques

The photoelectric measurements were carried out at 10^{-9} torr in an oil-free UHV system constructed by the Tungsram Research Laboratory. Samples were mounted in a chamber with a quartz window and excited by a Spectromom 202 monochromator using a 30 W deuterium or a 150 W xenon lamp.

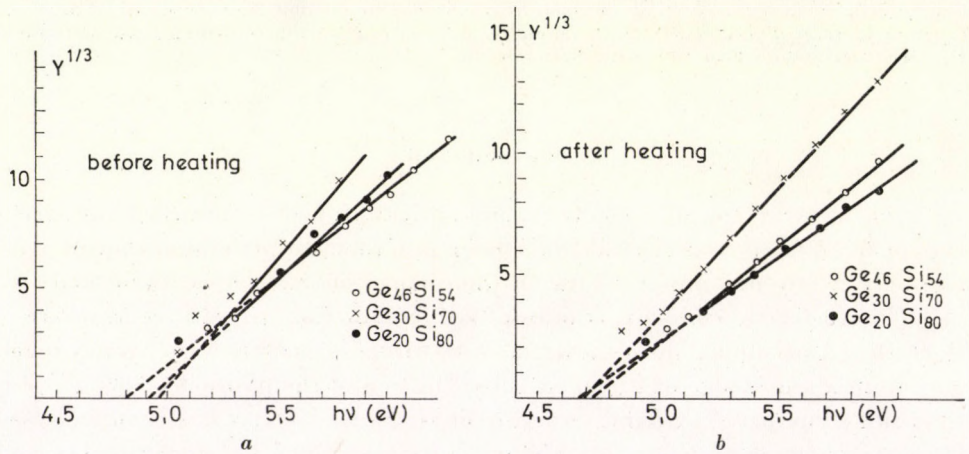

Fig. 1. Quantum efficiency of photoemission. a) Etched samples. b) Sample after vacuum heat treatment

All quartz optics were of Spectrosil quality. A D.C. retarding field method using cylindrical geometry was applied for the photoelectric measurements [12]. The collector was a glass tube coated with SnO_2 to reduce reverse current effects [10]. The photocurrent was detected with a Keithley model 610B electrometer.

The quantum efficiency $Y(E)$ was determined in absolute units as the number of photoelectrons / absorbed photon, taking into account the reflection losses.

In the surface Fermi level (work function) measurements [9] a SnO_2 collector was used. Its work function was determined by employing a high-purity silver reference sample polished, etched and heated in UHV.

Experimental results

The photoelectric threshold was determined from the intercept of $Y^{1/3}$ plots of the quantum efficiency. As can be seen from Figs. 1a and 1b, representing the quantum efficiency of etched samples and of the same samples after the vacuum heat treatment, respectively, Ge_xSi_{1-x} samples follow the $Y^{1/3}$ relationship, exhibiting quite well a gradual shift with composition. The energy distributions of photoelectrons determined for four wavelengths

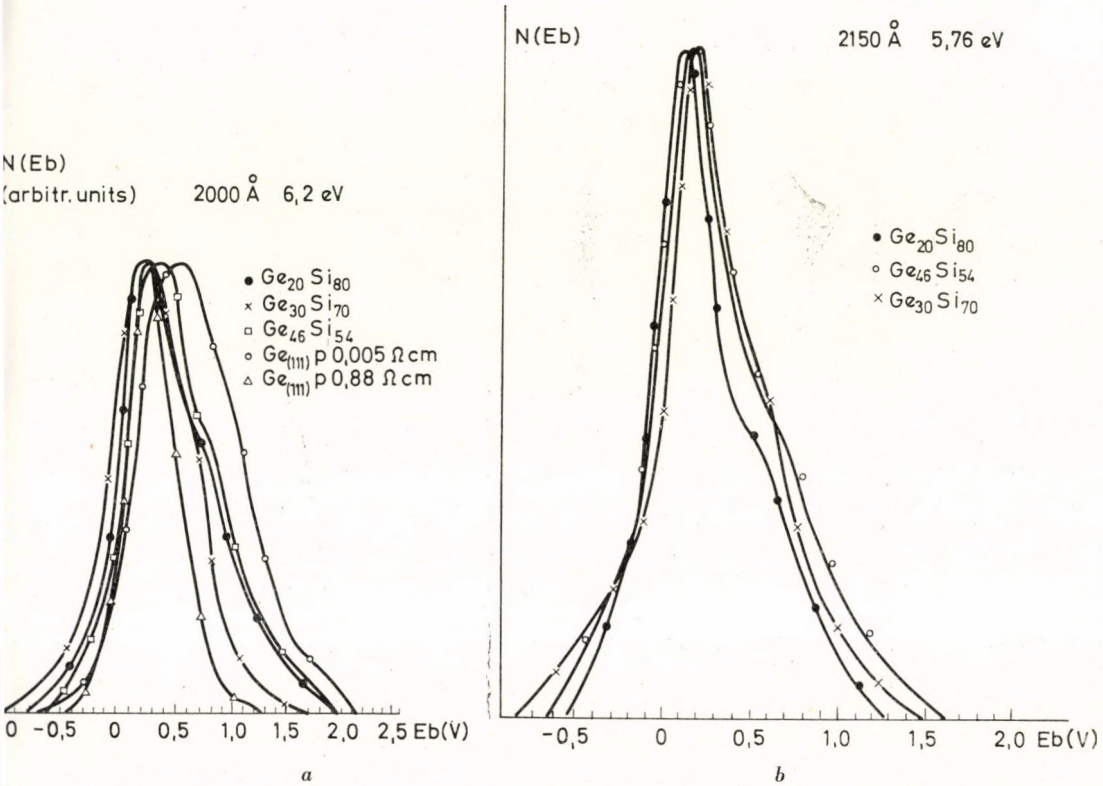

Figs. 2.a and *b*. Energy distribution of photoelectrons. E_b is the collector bias voltage

on atomic clean surfaces in UHV are presented in Figs. 2a, 2b, 2c and 2d. The surface Fermi level of Ge_xSi_{1-x} crystals was determined by the method of HUGHES.

Fig. 3 contains some typical $Y(E)$ curves exhibiting a constant displacement $\Delta h\nu$.

The photoelectric threshold, electron affinity and work function data are summarized in Table I.

The electron affinity E_A was determined from our photoemission thre-

Table I

Sample Ge_xSi_{1-x}	p/cm^3	E_p	E_w	E_A	E_F
$x = 0.20$	$3 \cdot 10^{17}$	4.66	4.45	3.65	0.21
$x = 0.30$	—	4.67	4.42	3.67	0.25
$x = 0.46$	$3 \cdot 10^{15}$	4.74	4.47	3.74	0.27
Si (111)p	10^{18}	4.70	4.58	3.6	0.12
Ge (111)p	$2 \cdot 10^{15}$	4.78	4.58	4.06	0.20

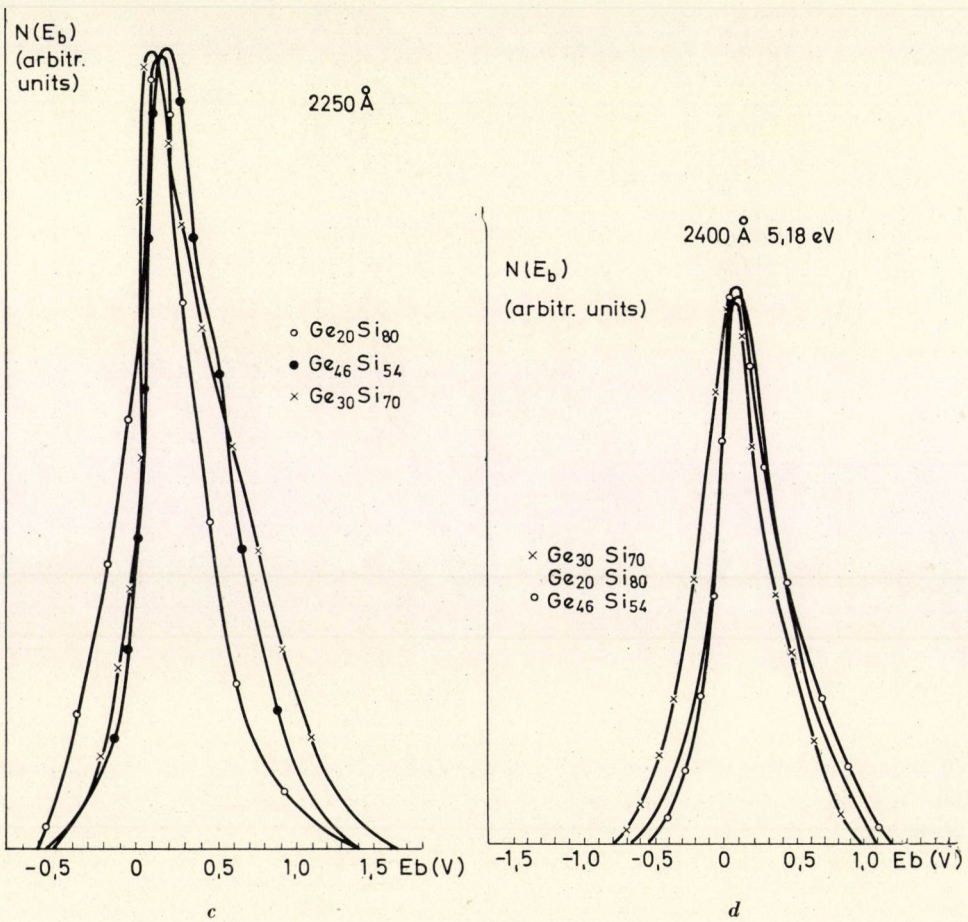

Figs. 2. c and *d*. Energy distribution of photoelectrons. E_b is the collector bias voltage

shold E_P values using the band-gap data of BRAUNSTEIN et al. [2]. Work function data (E_W) were deduced from retarding field measurements,

$$E_W = E_{W\,\mathrm{coll}} + eE_b - \Delta h\nu,$$

where E_b denotes the collector bias voltage, $E_{W\,\mathrm{coll}}$ the collector work function and $\Delta h\nu$ the shift of Y curves. All samples were of p-type, as established by thermoelectric power measurements. The carrier concentrations of the samples were determined by three-point probe measurements.

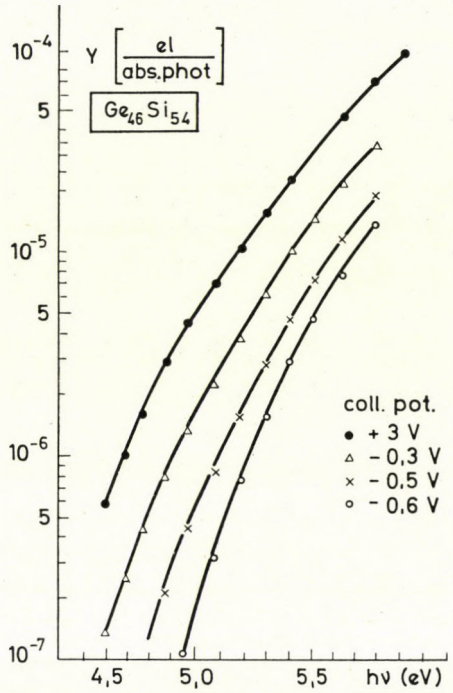

Fig. 3. Quantum efficiency spectral response determined in retarding field mode

Discussion

A number of properties of Ge_xSi_{1-x} mixed crystals can be determined from the experimental results. The shifts of the photoelectric threshold in Figs. 1a and 1b correspond to cleaning of the crystal surfaces. From the photoelectric threshold and band-gap data [2, 3] the electron affinity of the samples was calculated.

Since the energy range was limited by using quartz optics, the photoelectron energy spectrum covered only about 2 eV. These low-energy photoelectrons can be attributed to transitions from the upper levels near the top of the valence band to the conduction band [7].

As all the samples were of p-type, the Fermi level E_F (with respect to the top of the valence band) is in all cases located close to the valence band. The slight variation with carrier concentration is in agreement with the data published by SZE [14].

Photoelectric emission processes take place in a 30—70 Å deep surface layer [13, 15]. The agreement of E_F values determined by photoemission and from the carrier concentration is remarkable. Thus, the Fermi level in the 30—70 Å thick surface layer presumably corresponds to the bulk Fermi level of the samples. The thickness of the surface layer is much less than the Debye length.

Acknowledgements

Authors are indebted to Mrs. C. SZÉKELY and G. STUBNYA for preparing the samples and to B. SZENTPÁLI for the electrical measurements.

REFERENCES

1. E. SCHMIDT, Phys. Stat. Sol., **27**, 57, 1968.
2. R. BRAUNSTEIN, A. MOORE and F. HERMAN, Phys. Rev., **109**, 695, 1958.
3. F. BASSANI and D. BRUST, Phys. Rev., **131**, 1524, 1963.
4. J. TAUC and A. ABRAHÁM, J. Phys. Chem. Solids, **20**, 190, 1961.
5. F. HERMAN, R. L. KORTUM, C. D. KUGLIN and R. A. SHORT: Quantum Theory of Atoms Molecules, Solid State, Academic Press, New York
6. G. GERGELY, I. JÁNOSSY, M. MENYHÁRD, J. PEISNER, C. SZÉKELY and G. STUBNYA, Proc. Int. Conf. Phys. Chem. Semiconductor Heterojunctions Budapest, 1970. VI. p. 147.
7. N. B. KINDIG and W. E. SPICER, Phys. Rev., **138**, A561, 1965.
8. R. C. EDEN, Ph. D. Dissertation, Stanford University, 1967.
9. F. G. ALLEN and G. W. GOBELI, Phys. Rev., **144**, 558, 1966.
10. O. H. HUGHES and M. DALRYMPLE, Brit. J. Appl. Phys. (J. Phys. D.), 2 ser. **3**, L92, 1970.
11. C. SZÉKELY, I. BERTÓTI, G. STUBNYA, L. VARGA and L. GUTAI, Proc. Int. Conf. Phys. Chem. Semiconductor Heterojunctions, Budapest, 1970. VI. p. 341.
12. L. APKER, E. TAFT and J. DICKEY, Opt. Soc. Am., **43**, 78, 1953.
13. C. CHABRIER, J. CORNAZ, J. P. GOUDONNET and P. VERNIER, Optics Commun. **1**, 391, 1970.
14. S. M. SZE, Phys. of Semiconductor Devices, Wiley-Interscience, New York 1969. p. 37.
15. J. PEISNER, P. ROBOZ and P. B. BARNA, Phys. Stat. Sol. (a) **4**, 187, 1971.

ВНЕШНИЙ ФОТОЭФФЕКТ СМЕШАННЫХ КРИСТАЛЛОВ Ge_xSi_{1-x}

Г. ГЕРГЕЙ, Я. ПЕЙЗНЕР и Е. КАПИТАНЬ

Резюме

Исследован внешний фотоэффект на образцах смешанных кристаллов типа Ge_xSi_{1-x}. Тонкие эпитаксиальные слои на кремниевой подложке были получены осаждением из газовой фазы. Измерения проводились в сверхвысоком вакууме с давлением 10^{-9} торр на атомарно-чистых поверхностях, полученных при помощи химического травления и термической обработки в вакууме. Определены квантовый выход, порог внешнего фотоэффекта, работа выхода, электронное сродство, и распределение по энергии фотоэлектронов, возбуждённых фотонами с энергией 4—6,2 эв. Обнаружено, что при изменении состава происходит постепенное изменение характеристических данных. Работа выхода была измерена методом задерживающего поля, предложенным Хайсом. Работа выхода (уровень Ферми на поверхности) образцов совпадает с уровнем Ферми в объёме

Acta Physica Academiae Scientiarum Hungaricae, Tomus 31 (4), pp. 367—374 (1972)

ON SOME EFFECTS CONNECTED WITH EINSTEIN'S PRINCIPLE OF EQUIVALENCE

By

L. JÁNOSSY

CENTRAL RESEARCH INSTITUTE FOR PHYSICS, BUDAPEST

and

H-J. TREDER

DEUTSCHE AKADEMIE DER WISSENSCHAFTEN ZU BERLIN, POTSDAM-BABELSBERG, DDR

(Received 22. XI. 1971)

The article discusses the role of the $1/2\, g_{ik}\, R$ term appearing in Einstein's gravitational equations. This term did not appear in EINSTEIN's original formulation as given in 1915; however, as EINSTEIN already noticed without this term the gravitational equations lead to a hydrostatic pressure inside matter. Later he introduced this term arguing on considerations on symmetry connected with the principle of equivalence. We show in this article that this type of hydrostatic pressure would appreciably modify the configuration of atoms. Therefore it follows from the observation of atoms that the gravitational equations either obey exactly the principle of equivalence, or if there is a deviation from this principle, the deviation must be very small.

I

The dynamical equation

$$T^k_{i;\,k} = \frac{1}{\sqrt{-g}}\,(\sqrt{-g}\,T^k_i)_k - \frac{1}{2}\,g_{mn,i}\,T^{mn} = 0 \tag{1}$$

(which involves as consequence that the tensor of matter is free of divergence) can be derived either from Einstein's gravitational equations

$$R_{ik} - \frac{1}{2}\,g_{ik}\,R + \lambda g_{ik} = -\,\varkappa\,T_{ik} \tag{2}$$

(with $\varkappa = 8\pi f/c^2$, f constant of gravitation and λ the cosmological constant), or alternately from the (weak) principle of equivalence. Einstein's principle as expressed by (2) is a consequence of the Bianchi identity

$$\left(R^k_i - \frac{1}{2}\,\delta^k_i\,R + \lambda\delta^k_i\right)_{;k} = 0\,. \tag{2a}$$

It follows, however, from the principle of equivalence that the covariant formulation of the field equations of matter — in their covariant form — con-

tain already the action of gravitation upon fields of matter. It follows from this covariant formulation that the differential law of the conservation of energy and momentum of the special theory of relativity

$$T^k_{i,k} = 0 \tag{3}$$

has to be replaced in the general theory by relation (1) (see TREDER [9]).

From the dynamical equations one obtains thus as a first approximation the equations of motion of Newton.

The dynamical equation (1) remains valid if we add a tensor M_{ik} to the left hand expression of EINSTEIN's equation (2), where M_{ik} has to be a concommittant of the Riemann—Christoffel tensor and its derivatives, thus

$$M_{ik} = M_{ik}[R_{iklm}; g_{ik}]$$

and one has to suppose that M_{ik} can be represented in accord with EINSTEIN [2] and also HILBERT [4] as a variational derivative

$$M_{ik} = \frac{1}{\sqrt{-g}} \frac{\delta \mathfrak{M}}{\delta g^{ik}} . \tag{4}$$

Indeed, from (4) it follows as consequence of the covariance of the relation, making also use of the Bianchi identity that

$$M^k_{i;k} = 0. \tag{5}$$

If, however, we were to add to the left hand expression of (2) a tensorial concommittant

$$\overline{M}_{ik} = \overline{M}_{ik}[R_{iklm}; g_{ik}]$$

which cannot be expressed as a derivative of the form (4) then we have in general

$$M^k_{i;k} \neq 0. \tag{6a}$$

As a consequence of this one finds that such a tensor included into EINSTEIN's equation leads to equations of motion

$$T^k_{i;k} = -\frac{1}{\varkappa} \overline{M}^k_{i;k} \tag{6}$$

which equations of motion contradict the (weak) principle of equivalence (see TREDER [8]).

We see thus that in such a case the coupling between gravitation and matter cannot be described fully by formulating the (canonical) equations of the special theory of relativity in a covariant form. Because of (6) there appear in the equations of motion additional vectorial terms which represent additional non-Newtonian forces and the latter do not disappear identically not even in inertial systems of reference.

The correction terms thus obtained are very small if the $\overline{M}_{ik}$ consist of bilinear (or of higher order) terms of the Riemann tensor. Suppose for the moment the field equation to be of the second order; in this case we obtain additional terms $1/\varkappa\, M^{k}_{i;k}$ to the energy moment tensor of the order of the small quantity $\varkappa$.

On the other hand a linear correction term added to the left hand expression (2) can be excluded analysing the dynamics of matter.

The only linear concommittant of the R_{iklm} which might be added to the left hand of (2) is

$$\overline{M}_{ik} = \frac{\varepsilon}{2} g_{ik} R, \tag{7a}$$

where ε is a numerical constant. Using such a term the gravitation equation can be written

$$R_{kl} - \frac{1}{2} g_{kl}(1-\varepsilon) R + \lambda g_{kl} = -\varkappa T_{kl} . \tag{7}$$

If $\varepsilon \neq 1/2$ and $\lambda = 0$ one finds for the curvature

$$R = \frac{\varkappa T}{1-2\varepsilon} \quad (T = T^{i}_{i}) . \tag{7b}$$

Thus we can write with (7) also in form of EINSTEIN's field equation with a new tensor of matter

$$R_{ik} - \frac{1}{2} g_{ik} R = -\varkappa \left(T_{ik} - \frac{1}{2} \frac{\varepsilon}{2\varepsilon - 1} g_{ik} T \right), \tag{8}$$

or

$$R_{ik} = -\varkappa \left(T_{ik} - \frac{1}{2} \frac{\varepsilon - 1}{2\varepsilon - 1} T g_{ik} \right) \tag{8a}$$

with a constant

$$\varkappa = \frac{4\pi f}{c^2} \left[1 - \frac{1}{2} \frac{\varepsilon - 1}{2\varepsilon - 1} \right]^{-1}$$

which results from the comparison with the Poisson equation.

The Bianchi identity gives thus the equation of motion as

$$T^k_{i;k} = \frac{\varepsilon}{4\varepsilon - 2} T_i . \tag{9}$$

We find thus in the first approximation a correction independent of the gravitational field. (The gravitational field equation gives only an indirect argument for the introduction of such non-Newtonian extra force).

Supposing the tensor of matter to be that of an ideal fluid, i.e.

$$T^k_i = \left(\varrho + \frac{p}{c^2}\right) u_i u^k - p\delta^k_i = G u_i u^k - p\delta^k_i , \tag{10}$$

where

$$u^k = \mathrm{d}x^k/\mathrm{d}\tau, \qquad u^k u_k = c^2.$$

We have then

$$T = \varrho c^2 - 3p. \tag{10a}$$

The equation of motion is thus

$$(Gu^k)_{;k} u_i + G \frac{D}{D\tau} u_i - p_{,i} = \frac{\varepsilon}{4\varepsilon - 2} (\varrho_{,i} c^2 - 3p_{,i}). \tag{11}$$

From this we find

$$(Gu^k)_{;k} = \frac{\varepsilon}{4\varepsilon - 2} \frac{d\varrho}{d\tau} + \frac{1}{c^2} \frac{dp}{d\tau} \left(1 - \frac{3\varepsilon}{4\varepsilon - 2}\right), \tag{11a}$$

$$\left[\frac{\varepsilon}{4\varepsilon - 2} \frac{d\varrho}{d\tau} + \frac{1}{c^2} \frac{dp}{d\tau} \left(1 - \frac{3\varepsilon}{4\varepsilon - 2}\right)\right] u_i + \left(\varrho + \frac{p}{c^2}\right) \frac{D}{D\tau} u_i = \\ = \frac{\varepsilon}{4\varepsilon - 2} \varrho_{,i} c^2 + p_{,i} \left(1 - \frac{3\varepsilon}{4\varepsilon - 2}\right). \tag{11b}$$

From (11b) we see that a pressure appears as $\approx \frac{3\varepsilon}{4\varepsilon - 2} p_{,i}$ and then appears also the grad of the rest energy $\sim \varrho_{,i} c^2$ therefore the dynamic thus described is very different from the Newtonian dynamic.

The deviations thus obtained from the Newtonian dynamic are compatible with experience if we suppose either ε to be very small, or alternately if we were to suppose the equation of state of matter to be given by

$$\varrho c^2 = 3p.$$

(Thus the extra terms vanish e.g. in the particular case of the electromagnetic radiation field.)

An example of historical interest is the particular case of such field equations in the form which EINSTEIN suggested originally [1] i.e.*

$$R_{ik} = -\varkappa T_{ik} \,. \tag{12}$$

The latter corresponds to the case $\varepsilon = 1$. The relation (12) was later considered by SCHRÖDINGER [7] and was discussed recently by JÁNOSSY [5].

The degenerated case $\varepsilon = 1/2$ is contained in EINSTEIN's field equation as formulated in 1919 [3]:

$$R_{ik} - \frac{1}{4} g_{ik} R = -\varkappa T_{ik} .$$

In the latter case we have necessarily

$$T = 0. \tag{13}$$

In this case the scalar of curvature R is not defined by the state of matter but it is determined by the gravitational field.

If the dynamical equations are thus modified one has

$$T^{k}_{i\,;k} = \frac{1}{4\varkappa} R_{,i}$$

and the right hand expression gives a field of force which can be given more or less arbitrarily. According to Einstein this is the field which keeps the electron together against the repulsion of its own electromagnetic field.

The above picture which was originally thought of by Abraham and by Mie can be given also using wave mechanical concepts as we show in the second part of this article.

II

If the term $1/2\, g_{ik} R$ is left out of the EINSTEIN gravitational equation, a pressure

$$\mathbf{p} = \frac{c^2}{2} \operatorname{grad} \varrho_m \tag{14}$$

* Then, in his next paper [1] EINSTEIN remarks that the relation (12) is only possible for $T = 0$.

is obtained where ϱ_m is the density of matter. It is interesting to evaluate the deformations such a pressure were to cause on an atom. The effect of such a pressure can be most easily calculated using the wave equation in form of the hydrodynamical equations discussed in detail by one of us [6]. The latter equation may be written

$$\varrho_m \frac{d\mathbf{v}}{dt} = -\varrho \operatorname{grad}(Q+V), \tag{15}$$

$$Q = -\frac{\hbar^2}{2m}\frac{\nabla^2\varrho^{1/2}}{\varrho^{1/2}}, \quad V = \text{potential of outside forces},$$

$$\int \varrho_m d^3r = m. \tag{16}$$

Considering an electron under the influence of the outside pressure (14) only, we may put

$$V = -\frac{m}{2}c^2 \ln \varrho^{1/2}. \tag{17}$$

Therefore equilibrium configuration is obtained if $Q + V = \text{const.}$, i.e. if

$$\ln \varrho^{1/2} + \lambda_0^2 \frac{\nabla^2 \varrho^{1/2}}{\varrho^{1/2}} = \text{const.}$$

where

$$\lambda_0 = \frac{\hbar}{mc}$$

is the Compton wave length.

Introducing $\ln \varrho^{1/2} = A$ the equation can also be written

$$\lambda_0^2\left(A'' + A'^2 + \frac{2}{r}A'\right) + A = \text{const}. \tag{18}$$

provided we suppose A to have spherical symmetry. Regular solutions of (18) seem to exist only of the form

$$A = a + br^2.$$

Introducing the above expression into (5) we find $b = -1/4\,\lambda_0^2$ and thus

$$\varrho = \varrho_0\, e^{-r^2/2\lambda_0^2},$$

where ϱ_0 has to be chosen so as to satisfy the normalization (16).

We see thus that a free electron would be pressed together into a packet of radius λ_0 — this is a packet considerably smaller than the hydrogen atom.

The effect of the hypothetical pressure on a hydrogen atom can be obtained if we add to the potential (17) the Coulomb potential e^2/r of the nucleus. As the latter alone produces a packet of radius $r_H = 137\lambda_0$ it is obvious that the effect of the potential V would be much stronger than that of the Coulomb attraction and therefore the hydrogen atom would be pressed together to a packet which, apart from its inside region, would be very similar to the packet calculated for the free electron.

We see thus that a potential of the form (17) would strongly deform atoms and therefore the field equations (12) can be excluded considering the observations, e.g. of hydrogen atoms.

It remains the question what fraction of a pressure of the type (17) might be so small that it would have escaped attention? We note that from gravitational equations of the form

$$R_{ik} - \frac{1-\varepsilon}{2} g_{ik} R = -\varkappa T_{ik}$$

we expect a pressure

$$V_\varepsilon = \varepsilon V$$

if $\varepsilon = 1/137$ thus the packet to which the free electron was compressed would have a radius about equal to r_H; this pressure would still give a strong deformation of the hydrogen atom. Without estimating precisely the observations it is clear therefore that if $\varepsilon > 0$ at any rate it must be supposed $137 \mid \varepsilon \mid \ll 1$. Thus only very small deviations from the dynamical equations (1) may be compatible with observation.

REFERENCES

1. A. EINSTEIN, Berliner Berichte, 778, 779, 1915.
2. A. EINSTEIN, Berliner Berichte, 111, 1916.
3. A. EINSTEIN, Berliner Berichte, 349, 1919.
4. D. HILBERT, Göttinger Nachrichten, 395, 1915.
5. L. JÁNOSSY, Theory of Relativity Based on Physical Reality, Budapest, 1971.
6. L. JÁNOSSY and M. ZIEGLER, Acta Phys. Hung., **16**, 37, 1963.
7. E. SCHRÖDINGER, Space-Time Structure, Cambridge, 1950.
8. H-J. TREDER, Ann. d. Phys., **27**, 47, 1971.
9. H-J. TREDER, Gravitationstheorie und Equivalenzprinzip, Berlin, 1971.

О НЕКОТОРЫХ ЭФФЕКТАХ СВЯЗАННЫХ С ПРИНЦИПОМ ЭКВИВАЛЕНТНОСТИ ЭЙНШТЕЙНА

Л. ЯНОШИ и Х. Й. ТРЕДЕР

Резюме

В данной статье рассматривается роль члена $1/2\, g_{ik} R$ в гравитационных уравнениях Эйнштейна. Этот член не присутствовал в первом изложении разработанном Эйнштейном в 1915 году, и был введен позднее на основании общих соображений, связанных с принципом эквивалентности. Как это было замечено Эйнштейном в своей оригинальной работе, отсутствие этого члена приводит к гидростатическому давлению в данной среде.

Показано, что это гидростатическое давление привело бы к значительному изменению атомных конфигураций и поэтому из наблюдаемых свойств атомов следует, что уравнения гравитации действительны в форме, согласующейся с принципом эквивалентности или отличаются от этой формы только в незначительной мере.

Acta Physica Academiae Scientiarum Hungaricae, Tomus 31 (4), pp. 375—383 (1972)

COMMUNICATIONES BREVES

A SOLUTION TO THE RADIATIVE BLAST WAVE IN STELLAR INTERIORS

By

S. N. OJHA

DEPARTMENT OF MATHEMATICS, UNIVERSITY OF GORAKHPUR, GORAKHPUR (U.P.), INDIA

(Received 29. VI. 1970)

1. Introduction

OJHA and VERMA [1] studied the propagation of a spherical shock produced by a sudden point explosion in an inhomogeneous non-gravitating system by considering radiation effects and assuming the density of the gas to vary as the inverse power of the distance from the point of explosion. TAYLOR [2] discussed the solutions of the equations of a spherical shock wave produced by a strong point explosion. LIN [3] obtained solutions in the case of a cylindrical shock wave produced on account of instantaneous energy release along an infinite straight line. VERMA [4] obtained equations for the solution of the problem of cylindrical blast wave in a conducting gas. The problems referred to in [2], [3] and [4] have been discussed without any radiation effects in a non-gravitating system while in [1] radiation effects have also been considered. Following VERMA [4], this paper discusses the equations for the propagation of a symmetrically expanding spherical blast wave produced by a sudden explosion in a self-gravitating body, such as a star, with radiation effects taken into account. The medium is assumed to be a perfectly conducting plasma with radiative parameters independent of the magnetic field.

2. Equations governing the flow and field in self-gravitating bodies

The field equation and the equation for the motion, continuity and energy of a radiative spherical shock are

$$\frac{\partial u}{\partial t} + u\frac{\partial u}{\partial r} + \frac{1}{\varrho}\frac{\partial p}{\partial r} + \frac{H}{\varrho}\frac{\partial H}{\partial r} + \frac{Gm}{r^2} = 0\,, \tag{2.1}$$

$$\frac{\partial \varrho}{\partial t} + u\frac{\partial \varrho}{\partial r} + \varrho\left(\frac{\partial u}{\partial r} + \frac{2u}{r}\right) = 0\,, \tag{2.2}$$

$$\frac{\partial H}{\partial t} + u\frac{\partial H}{\partial r} + H\left(\frac{\partial u}{\partial r} + \frac{2u}{r}\right) = 0\,, \tag{2.3}$$

$$\left(\frac{\partial}{\partial t} + u\frac{\partial}{\partial r}\right)^{(E+E_H)} + (p+p_H)\left\{\frac{\partial}{\partial t}\left(\frac{1}{\varrho}\right) + u\frac{\partial}{\partial r}\left(\frac{1}{\varrho}\right)\right\} + \frac{1}{\varrho r^2}\frac{\partial}{\partial r}(Fr^2) = 0\,, \tag{2.4}$$

where

$$E = E_M + E_R\,, \qquad p = p_M + p_R\,,$$
$$E_M = \frac{H^2}{2}\,, \qquad p_M = \frac{H^2}{2}\,. \tag{2.5}$$

The suffixes M, R and H attached to a symbol denote expressions for material, radiation and magnetic terms, respectively. The quantities u, p and ϱ are the radial velocity, pressure and density at distance r from the point of explosion at any time t; the magnetic field has components $(0, 0, H)$. F is the radiation flux, G is the gravitational constant and m is the mass within the shock front at any time t such that

$$\frac{\partial m}{\partial r} = 4\pi\varrho\, r^2\,. \tag{2.6}$$

We have

$$E_M = \frac{p_M}{\varrho(r-1)}\,, \qquad E_R = \frac{3p_R}{\varrho} \tag{2.7}$$

and

$$F = -\frac{c}{\epsilon\varrho}\frac{dp_R}{dr}\,, \tag{2.8}$$

where ϵ is the coefficient of opacity and C is the velocity of light.

We assume [5] that

$$p_M = zp,$$
$$p_R = (1-z)p \qquad (0 < z < 1)$$

hence

$$E = \frac{p}{\varrho(K-1)}\,, \tag{2.9}$$

where

$$K = \frac{4(\gamma-1)+z(4-3\gamma)}{3(\gamma-1)+z(4-3\gamma)}\,, \tag{2.10}$$

γ being the usual ratio of specific heats. With the help of Eqs. (2.9), (2.2)

and (2.3), Eq. (2.4) can be written as

$$\frac{\partial p}{\partial t}+u\frac{\partial p}{\partial r}+Kp\left(\frac{\partial u}{\partial r}+\frac{2u}{r}\right)+\frac{(K-1)}{r^2}\frac{\partial}{\partial r}^{(Fr^2)}=0. \tag{2.11}$$

Let the motion be assumed to be confined within the shock front at $r = R(t)$, then the velocity of the outward moving shock is given by

$$V=\frac{dR}{dt}. \tag{2.12}$$

3. Similarity considerations

We assume the following similarity forms for the flow and field variables:

$$p = p_0 R^m f_1(\eta), \tag{3.1}$$

$$\varrho = \varrho_0 \varphi_1(\eta), \tag{3.2}$$

$$u = R^n \Phi_1(\eta), \tag{3.3}$$

$$H = H_0 R^k g_1(\eta), \tag{3.4}$$

$$F = F_0 R^l n_1(\eta), \tag{3.5}$$

$$m = m_0 R^b m_1(\eta), \tag{3.6}$$

where $\eta=r/R$ is a non-dimensional radial variable, f_1, φ_1, Φ_1, g_1, n_1 and m_1 are functions of η only, and suffix zero denotes quantities in the undisturbed state. Putting Eqs. (2.1)—(2.4) and (2.6) into their similarity form, we get

$$\frac{\dot R}{R^n}(n\Phi_1-\eta\Phi_1')+\Phi_1\Phi_1'=- \tag{3.7}$$

$$-\frac{1}{\varrho_0\varphi_1}\{p_0 R^{m-2n}f_1'+H_0 R^{2k-2n} g_1'+m_0 R^{b-2n-1} m_1 \varrho_0 \varphi_1\},$$

$$\frac{\varphi_1}{\eta}(\eta\Phi_1'+2\Phi_1)=\varphi_1'\left(\eta\frac{\dot R}{R^n}-\Phi_1\right), \tag{3.8}$$

$$\frac{\dot R}{R^n}k\eta-\left(\frac{g_1'\eta^2}{g_1}\right)+\eta\Phi_1\frac{g_1'}{g_1}+\eta\Phi_1'+2\Phi_1=0, \tag{3.9}$$

$$\frac{\dot R}{R^n}(mf_1-\eta f_1')=K\left(f_1\Phi_1'+\frac{2\Phi_1 f_1}{\eta}\right)+\frac{(k-1)}{p_0}F_0 R^{l-m-n}\left(n_1'\eta+\frac{2n_1}{\eta}\right), \tag{3.10}$$

$$m_1'=\frac{4\pi p_0}{m_0}R^{-b+3}\varphi_1\eta^2. \tag{3.11}$$

In order that all the unknowns may be expressible as functions of η alone, the following relations must be fulfilled.

$$m = 2n, \qquad k = n, \qquad 1 = 3n, \qquad b = 2n + 1 \tag{3.12}$$

and

$$\frac{\dot{R}}{R^n} = \text{constant} = C. \tag{3.13}$$

Integrating (3.13) we get

$$Ct = \frac{R^{1-n}}{1-n} + A,$$

where n is an arbitrary parameter and C an absolute constant. As $t \to 0$, $R \to 0$ and so we must have $n < 1$ and $A = 0$. Then

$$R = \{(1-n)\, Ct\}^{\frac{1}{(1-n)}} \qquad n < 1. \tag{3.14}$$

With the help of Eqs. (3.12), (3.13) and (3.14) Eqs. (3.7)—(3.11) become

$$C(n\Phi_1 - \eta\Phi_1') + \Phi_1\Phi_1' = -\frac{1}{\varrho_0\varphi_1}\{p_0 f_1' + H_0 g_1' + m_0 m_1 \varrho_0 \varphi_1\}, \tag{3.15}$$

$$\frac{\varphi_1}{\eta}(\eta\Phi_1' + 2\Phi_1) = \varphi_1'(\eta c - \Phi_1). \tag{3.16}$$

$$C\left(n\eta - \frac{g_1'\eta^2}{g_1}\right) + \eta\Phi_1\frac{g_1'}{g_1} + \eta\Phi_1' + 2\Phi_1 = 0, \tag{3.17}$$

$$C(nf_1 - \eta f_1') = K\left(f_1\Phi_1' + \frac{2\Phi_1 f_1}{\eta}\right) + \frac{(K-1)F_0}{p_0}\left(n_1' n + \frac{2n_1}{\eta}\right) \tag{3.18}$$

and the similarity transformations (3.1)—(3.6) become

$$\begin{aligned} p &= p_0 R^{2n} f_1(\eta), & \varrho &= \varrho_0 \varphi_1(\eta), \\ u &= R^n \Phi_1(\eta), & H &= H_0 R^n g_1(\eta), \\ F &= F_0 R^{3n} n_1(\eta), & m &= m_0 R^{2n+1} m_1(\eta). \end{aligned} \tag{3.19}$$

4. Initial conditions and solutions

Let the explosion take place at a point at time $t = 0$. Then $U \to 0$ as $r \to 0$, $U = 0$ for $r \neq 0$ and also $R \to 0$. In any admissible solution H and u must both be finite for $t > 0$ everywhere in $r \leq R$. Below, the case for

$n = -3/2$, an arbitrary choice, is considered. Putting this value of n in (3.14) we get,

$$R = \beta t^{2/5}, \tag{4.1}$$

where R is the radius of the shock at any time t and β is an absolute constant. From (4.1) the shock velocity is then given by

$$V = \frac{dR}{dt} = \frac{2}{5}\left(\frac{R}{t}\right). \tag{4.2}$$

Again using (4.1), the similarity transformations can be written

$$\begin{aligned} \varrho &= f_1(\xi), & u &= t^{-3/5} f_2(\xi), \\ p &= t^{-6/5} f_3(\xi), & H &= t^{-3/5} f u(\xi), \\ F &= t^{-9/5} f_5(\xi), & m &= t^{-4/5} f_6(\xi), \end{aligned} \tag{4.3}$$

where

$$\xi = r t^{-2/5}. \tag{4.4}$$

The energy equation can be put in the form

$$\frac{\partial E_T}{\partial t} + \frac{1}{r^2}\frac{\partial}{\partial r} r^{2(uI_T+F)} = 0, \tag{4.5}$$

$$E_T = \frac{1}{2}\varrho u^2 + \frac{p}{(k-1)} + \frac{H^2}{2} - \frac{Gm\varrho}{r}, \tag{4.6}$$

and

$$I_T = \frac{1}{2}\varrho u^2 + \frac{kp}{(k-1)} + H^2 - \frac{Gm\varrho}{r}. \tag{4.7}$$

Putting (4.6) into their similarity form we get

$$E_T = \frac{1}{2} f_1(\xi) t^{-6/5} f_2^2(\xi) + \frac{1}{(k-1)} t^{-6/5} f_3(\xi) + \frac{1}{2} t^{-6/5} f_4^2(\xi) - t^{-6/5} \frac{f_5(\xi)}{\xi} \tag{4.8}$$

or

$$E_T = t^{-6/5} f(\xi),$$

where

$$f(\xi) = \frac{1}{2} f_1(\xi) f_2^2(\xi) + \frac{1}{(k-1)} f_3(\xi) + \frac{1}{2} f_4^2(\xi) - \frac{f_5(\xi)}{\xi}. \tag{4.9}$$

From (4.8) we have

$$\frac{\partial E_T}{\partial r} = f'(\xi) t^{-8/5} \tag{4.10}$$

and

$$\frac{\partial E_T}{\partial t} = -6/5\, t^{-11/5} f(\xi) - t^{-6/5} f'(\xi) \frac{2}{5} r t^{-7/5}. \tag{4.11}$$

From Eqs. (4.8), (4.10) and (4.11) we find

$$\frac{\partial E_T}{\partial t} + \frac{6}{5t} E_T + \frac{2r}{5t} \frac{\partial E_T}{\partial r} = 0 \tag{4.12}$$

or

$$\frac{\partial E_T}{\partial t} + \frac{2}{5tr^2} \frac{\partial}{\partial r} (r^3 E_T) = 0. \tag{4.13}$$

From Eqs. (4.5) and (4.13) we have

$$\frac{\partial}{\partial r} \{r^2(uI_T + F)\} = \frac{\partial}{\partial r} \left(\frac{2r^2 E_T}{5t} \right) \tag{4.14}$$

or

$$(uI_T + F) = \frac{VrE_T}{R}.$$

Here the constant of integration has been taken to be zero and the value of V is substituted from (4.2).

Eq. (4.14) can also be written as

$$u' = \frac{\varkappa \left\{ \frac{1}{2} v^2 \varrho u'^2 + \frac{p}{(k-1)} + \frac{H^2}{2} - \frac{Gm\varrho}{R\varkappa} \right\}}{\left\{ \frac{1}{2} v^2 \varrho u'^2 + \frac{kp}{(k-1)} + H^2 - \frac{Gm\varrho}{R\varkappa} \right\}} - \frac{F}{vI_T}, \tag{4.15}$$

where

$$u = vu' \quad \text{and} \quad r = R\varkappa. \tag{4.16}$$

From (4.15)

$$\frac{p}{\varrho} = \frac{(k-1)}{(ku' - \varkappa)} \left\{ C_1 u'^2(\varkappa - u') + C_2 \varrho(\varkappa - 2u') + \frac{C_3 m}{\varkappa} (u' - \varkappa) - C_4 F \right\}' \tag{4.17}$$

where C_1, C_2, C_3 and C_4 are functions of time, and $H = c\varrho$ as a consequence of Eqs. (2.2) and (2.3). From (2.2) and (2.11) we obtain

$$\begin{aligned} \frac{1}{p} \frac{\partial p}{\partial r} - \frac{(k-1)}{p} \frac{\partial p}{\partial r} = -\frac{1}{pu} \frac{\partial p}{\partial t} - \frac{(k-1)}{r^2} \frac{\partial}{\partial r} (Fr^2) + \\ + \frac{(k-1)}{\varrho u} \frac{\partial \varrho}{\partial t} - \frac{1}{u} \frac{\partial u}{\partial r} - \frac{2}{r}. \end{aligned} \tag{4.18}$$

Putting the values of ξ and V in Eq. (4.3), we get the relations

$$\frac{\partial \varrho}{\partial t} = -\frac{rv}{R}\frac{\partial \varrho}{\partial r}, \tag{4.19}$$

$$\frac{\partial p}{\partial t} = -\frac{3pv}{R} - \frac{rv}{R}\frac{\partial p}{\partial r}. \tag{4.20}$$

Using these we can write Eq. (4.18) as

$$\frac{1}{p}\frac{\partial p}{\partial r} - \frac{(k-1)}{p}\frac{\partial p}{\partial r} = -\frac{2}{r} - \frac{\left(\frac{1}{v}\frac{\partial u}{\partial r} - \frac{1}{R}\right)}{\left(\frac{u}{v} - \frac{r}{R}\right)} - \frac{(k-1)\,u}{v\left(\frac{u}{v} - \frac{r}{R}\right)r^2}\frac{\partial}{\partial r}(Fr^2) \tag{4.21}$$

which on integration yields

$$\frac{p}{p^{(k-1)}} = \frac{c_5}{r^2\left(\frac{u}{v} - \frac{r}{R}\right)} \exp\int \frac{(k-1)\,u}{v\left(\frac{u}{v} - \frac{r}{R}\right)}\frac{\partial}{\partial r}(Fr^2)\,dr. \tag{4.22}$$

Substituting (4.16) in (4.22) we have

$$\frac{p}{p^{(k-1)}} = \frac{C_s'}{\varkappa^2(u'-\varkappa)} \exp\int \frac{(k-1)\,u'}{(u'-\varkappa)\varkappa^2}\frac{\partial}{\partial \varkappa}(F\varkappa^2)\,d\varkappa. \tag{4.23}$$

Eliminating p between (4.23) and (4.18) and dropping the primes, we obtain the equation

$$\varrho^{(3-k)}(r-2u) + \varrho^{(2-k)}\left\{D_1 u^2(r-u) + D_2\frac{m}{r}(u-r) - D_3 F\right\} = \frac{Du(ku-r)}{r^2(u-r)} - D_5(ku-r) \exp\int \frac{(k-1)\,u}{(u-r)\,r^2}\frac{d}{dr}(Fr^2)dr, \tag{4.24}$$

which determines ϱ. For simplicity total derivatives can be written in place of partial ones. D_1, D_2, D_3, D_4 and D_5 are constants depending upon time.

Similarly, eliminating ϱ between (4.23) and (4.18) we get

$$p^{k-2/(k-1)} - \frac{A_1(r-2u)\,p^{1/(k-1)}}{(ku-r)\left\{\frac{A_2}{r^2(u-r)} - \exp\int\frac{(k-1)u}{(u-r)r^2}\frac{d}{dr}(Fr^2)\,dr\right\}^{2/(k-1)}} =$$

$$= \frac{\left\{A_3u^2(r-u) - A_4\frac{m}{r}(r-u) - A_5F\right\}\left\{\frac{A_6}{r^2(u-r)} - \exp\int\frac{(k-1)u}{(u-r)r^2}\frac{d}{dr}Fr^2dr\right\}^{\frac{-1}{k-1}}}{(ku-r)}, \tag{4.25}$$

which determines p. A_1, A_2, A_3, A_4, A_5 and A_6 are constants depending on time.

As a consequence of (2.2), (2.3) and (4.24), we write

$$H^{(3-k)}(r-2u) + H^{(2-k)}\left\{B_1u^2(r-u) + B_2\frac{m}{r}(u-r) - B_3F\right\} = \tag{4.26}$$

$$= B_4\frac{(ku-r)}{r^2(u-r)} - B_5(ku-r)\exp\int\frac{(k-1)u}{(u-r)r^2}\frac{d}{dr}(Fr^2)\,dr,$$

where B_1, B_2, B_3, B_4 and B_5 are constants depending on time.

From Eq. (2.2), on using (4.16) and (4.17), we get

$$\frac{1}{\varrho}\left(\frac{d\varrho}{dr}\right) = \frac{1}{(r-u)}\left(\frac{du}{dr} + \frac{2u}{r}\right). \tag{4.27}$$

Differentiating (4.24) with respect to r and then using (4.27), we get

$$\varrho^{(3-k)}\left\{\frac{(3-k)(r-2u)\left(\frac{du}{dr} + \frac{2u}{r}\right)}{(r-u)} + \left(1 - \frac{2du}{dr}\right)\right\} +$$

$$+ \varrho^{(2-k)}\left[\frac{(2-k)\left(\frac{du}{dr} + \frac{2u}{r}\right)}{(r-u)}\left\{D_1u^2(r-u) + \frac{D_2m}{r}(u-r) - D_3F\right\} +\right.$$

$$\left. + \frac{d}{dr}\left\{D_1u^2(r-u) + \frac{D_2m}{r}(u-r) - D_3F\right\}\right] =$$

$$= \frac{d}{dr}\left[\frac{D_4(ku-r)}{r^2(u-r)} - D_5(ku-r)\exp\int\frac{(k-1)u}{(u-r)}\frac{d}{dr}(Fr^2)\,dr\right].$$

Eqs. (4.28) and (4.24) express the relationship between u and r, while Eqs. (4.24), (4.25), and (4.26) express ϱ, p and H in terms of r and therefore give the required solution.

Acknowledgement

The author is grateful to Dr. B. G. VERMA for his helpful suggestions and guidance in the preparation of this paper.

REFERENCES

1. S. N. OJHA and B. G. VERMA, On a radiative spherical shock in non-gravitating system (submitted for publication) 1970.
2. J. L. TAYLOR, Phil. Mag., **46,** 317, 1955.
3. S. C. LIN, J. Appl. Phys., **25,** 54, 1954.
4. B. G. VERMA, ZAMP, **21,** 119, 1970.
5. S. CHANDRA SHEKHAR, An Introduction to the Study of Stellar Structure, 1939.

Acta Physica Academiae Scientiarum Hungaricae, Tomus 31 (4), pp. 385—387 (1972)

FRIEDMANN AND HELMHOLTZ EQUATIONS FOR AN IDEAL RELATIVISTIC FLUID

By

I. ABONYI

INSTITUTE OF THEORETICAL PHYSICS, ROLAND EÖTVÖS UNIVERSITY, BUDAPEST

(Received 2. III. 1971)

The equations of motion of an ideal (i.e. inviscid, nondissipative) fluid in special relativistic hydrodynamics have the form [1]

$$\mu^{\circ} u_k \partial_k \left[\left(1 + \frac{w}{c^2} \right) u_i \right] + \partial_i p = - \partial_k E_{ik}, \tag{1}$$

$$u_k u_k = -c^2, \tag{2}$$

$$\partial_k (\mu^0 u_k) = 0, \tag{3}$$

where u_k stands for the velocity four-vector, μ^0 is the mass density of the fluid in the rest frame, the specific enthalpy

$$w = \varepsilon^0 + \frac{p}{\mu^0}, \tag{4}$$

ε^0 being the specific internal energy in the rest frame, and p is the pressure. The notation $\partial_i = \partial/\partial x_i, x_4 = ict$ is used. The fluid is supposed to be subject to the action of an external field the energy momentum tensor of which is given by E_{ik}. Use will be made of either an equation of state (e.g. barotropic) or, for the sake of generality, of the combined first and second law of thermodynamics:

$$d\varepsilon^0 + p d\left(\frac{1}{\mu^0} \right) = \Theta \, ds, \tag{5}$$

where s is the specific entropy and Θ is the temperature.

The Euler equation can be transformed to exhibit the so-called Crocco—Vázsonyi equation form

$$u_k \Omega_{ik} = \Theta \partial_i s - \frac{1}{\mu^0} \partial_k E_{ik}, \tag{6}$$

or

$$u_k \Omega_{ik} = \partial_i w - \frac{1}{\mu^0} \partial_i p - \frac{1}{\mu^0} \partial_k E_{ik}, \tag{7}$$

where

$$\Omega_{ik} = \partial_k \left[\left(1 + \frac{w}{c^2} \right) u_i \right] - \partial_i \left[\left(1 + \frac{w}{c^2} \right) u_k \right] = - \Omega_{ki} \tag{8}$$

is the vorticity tensor.

In order to obtain the relativistic form of the Friedmann equation, we may now proceed as follows. It can easily be shown that the vorticity tensor satisfies the relation

$$\partial_l \Omega_{kl} + \partial_k \Omega_{il} + \partial_l \Omega_{ik} = 0. \tag{9}$$

Applying ∂_l to Eq. (7), we obtain

$$\partial_l (u_k \Omega_{ik}) = \partial_l \partial_i w - \partial_l \left(\frac{1}{\mu^0} \partial_i p \right) - \partial_l \left(\frac{1}{\mu^0} \partial_k E_{ik} \right).$$

Antisymmetrization with respect to the indices i and l gives

$$\partial_l (u_k \Omega_{ik}) - \partial_i (u_k \Omega_{lk}) = (\mu^0)^{-2} [\partial_l \mu^0 \partial_i p - \partial_i \mu^0 \partial_l p] +$$
$$+ (\mu^0)^{-2} [\partial_l \mu^0 \partial_k E_{ik} - \partial_i \mu^0 \partial_k E_{lk}] - (\mu^0)^{-1} [\partial_l \partial_k E_{ik} - \partial_i \partial_k E_{lk}].$$

Making use of (9), we get

$$u_k \partial_k \Omega_{li} - \Omega_{ik} \partial_l u_k + \Omega_{lk} \partial_i u_k = (\mu^0)^{-2} [\partial_i \mu^0 \partial_l p - \partial_l \mu^0 \partial_i p] +$$
$$+ (\mu^0)^{-2} [\partial_i \mu^0 \partial_k E_{lk} - \partial_l \mu^0 \partial_k E_{ik}] + (\mu^0)^{-1} [\partial_l \partial_k E_{ik} - \partial_i \partial_k E_{lk}]. \tag{10}$$

It can be seen that in the nonrelativistic limit Eq. (10) takes the form

$$\frac{\partial \vec{\omega}}{\partial t} - \nabla \times (\vec{v} \times \vec{\omega}) = \nabla \times \left(\frac{1}{\varrho} \vec{F} \right) + \frac{1}{\varrho^2} [\nabla \varrho \times \nabla p],$$

where $\varrho^{-1} \vec{F}$ is the volume-force-density vector and $\vec{\omega}$ is the vorticity vector, so that Eq. (10) can be considered as the relativistic Friedmann equation.

If the fluid can be considered to be barotropic, i.e. if its equation of state is

$$\mu^0 = \varphi(p),$$

and if the external field is such that

$$\partial_l F_i - \partial_i F_l = \partial_l \partial_k E_{ik} - \partial_i \partial_k E_{lk} = 0,$$

then it is not in general enough to ensure

$$F_l \partial_i \mu^0 - F_i \partial_l \mu^0 = G_{il} = 0. \tag{11}$$

Let us assume, however, that Eq. (11) holds. Then we have from (10)

$$u_k \partial_k \Omega_{li} + \Omega_{lk} \partial_i u_k - \Omega_{ik} \partial_l u_k = 0 , \tag{12}$$

which can be envisaged as the relativistic Helmholtz equation.

REFERENCES

1. I. Abonyi, Acta Phys. Hung., **23,** 185, 1967.

Acta Physica Academiae Scientiarum Hungaricae, Tomus 31 (4), pp. 389—393 (1972)

CONTRIBUTIONS À UN MODÈLE DE DYNAMIQUE PONCTUELLE POUR LA MÉCANIQUE ONDULATOIRE

Par

Zs. Csoma

INSTITUT DE PHYSIQUE DE L'UNIVERSITÉ TECHNIQUE DE BUDAPEST, BUDAPEST

(Reçu 22. IV. 1971)

T. Mátrai a publié une interprétation de l'équation d'état de la mécanique ondulatoire [1], dans laquelle il avait l'intention d'accorder la notion du point matériel avec la description appliquée par la mécanique ondulatoire. Il est arrivé à ce »modèle de dynamique ponctuelle« comme suit:

L'équation de Schrödinger dépendante du temps de la particule de masse μ se partage par la substitution $\psi = A \exp iS/\hbar$ où A et S sont les fonctions réelles des coordonnées spatiales et du temps, en deux équations différentielles réelles:

$$\frac{1}{2\mu} \operatorname{grad}^2 S - \frac{\hbar^2}{2\mu} \frac{\Delta A}{A} + V + \frac{\partial S}{\partial t} = 0 , \tag{1}$$

$$\operatorname{div} (A^2 \operatorname{grad} S/\mu) + \frac{\partial A^2}{\partial t} = 0 . \tag{2}$$

Mátrai y employant la formule

$$\overline{p} = \mu \dot{\overline{r}} = \operatorname{grad} S \tag{3}$$

dûe à de Broglie, a déduit la relation

$$\Delta S + 2\mu \frac{d \ln A}{dt} = 0 .$$

Par cela il élimina A et reçut pour S une équation integro différentielle laquelle on peut considérer comme généralisation de mécanique ondulatoire de l'équation classique d'Hamilton—Jacobi.

Examinons donc le cas stationnaire c'est-à-dire celui, lorsque $dS/dt = -E$ est constant, alors $S = \sigma - Et$ et $\partial A/\partial t = 0$. Les équations précédentes deviennent:

$$\frac{1}{2\mu} \operatorname{grad}^2 \sigma - \frac{\hbar^2}{2\mu} \frac{\Delta A}{A} + V = E , \tag{1*}$$

$$\operatorname{div} (A^2 \operatorname{grad} \sigma) = 0. \tag{2*}$$

Pour le présent bornons nous aux forces centrales, c'est-à-dire V ne soit dépendant que du rayon vecteur. Dans ce cas la solution usuelle de l'équation de Schrödinger indépendante du temps en coordonnés polaires [2] est:

$$\psi(r, \vartheta, \varphi) = R(r), T(\vartheta), e^{im\cdot\varphi} .$$

Alors maintenant $A \equiv R.T$ et $\sigma/\hbar = m_l \varphi = m_l \operatorname{arctg} y/x$.

La formule (3) décrite en détail est en ce cas:

$$\left.\begin{aligned} \frac{\partial\sigma}{\partial x} &= \hbar m \frac{-y}{x^2+y^2} = \mu\cdot\dot{x}\,, \\ \frac{\partial\sigma}{\partial y} &= \hbar m \frac{x}{x^2+y^2} = \mu\cdot\dot{y}\,, \end{aligned}\right\} \quad \frac{\dot{x}}{\dot{y}} = \frac{dx}{dy} = -\frac{y}{x} \tag{4}$$

$$\frac{\partial\sigma}{\partial z} = 0 = \mu.\dot{z} \qquad\qquad x\dot{x}+y\dot{y} = 0. \tag{5}$$

De ceux-là z est constant, ensuite $x^2 + y^2 = R^2 = r^2 \sin^2\vartheta$ est aussi constant. A est constant au long de l'orbite circulaire, ce qui suit aussi de la stabilité de ϑ et de r. Le système d'équation du cercle

$$x = R\cos\varphi, \qquad y = R\sin\varphi.$$

Nous apprenons la dépendance de l'angle du temps, si nous dérivons les équations (4) et (5) suivant le temps:

$$\ddot{x} = -\frac{\hbar m}{\mu R^2}\dot{y} = -\left(\frac{\hbar m}{\mu R^2}\right)^2 x\,, \quad x = R\cos(\omega t+\alpha),$$

$$\ddot{x} = -\frac{\hbar m}{\mu R^2}\dot{x} = -\left(\frac{\hbar m}{\mu R^2}\right)^2 y\,, \quad y = R\cdot\sin(\omega t+\alpha),$$

où $\omega = \hbar m/\mu R^2$, indépendamment du potentiel V de la force centrale. La grandeur de l'impulsion est $p = \mu\omega R = \hbar m/R$ et sa direction est perpendiculaire sur le rayon vecteur. La longeur d'onde selon de Broglie appartenant à p est: $\lambda = h/p = 2R\pi/m$ une partie du nombre entier de la circonférence du cercle, comme cela était à attendre.

La valeur absolue du moment d'impulsion qui se rapporte au centre de force, comme à l'origine est $L = \hbar m/R \cdot r = \hbar m/\sin\vartheta$. Identifions cela avec la valeur-propre $\hbar\sqrt{l(l+1)}$ de l'opérateur du moment d'impulsion; en réduisant l'égalité, nous recevons, que $m/\sin\vartheta = \sqrt{l(l+1)}$, ce qui signifie, que l'angle ϑ est quantifié. En même temps $\Delta A/A = m^2/r^2\sin^2\vartheta - l(l+1)/r^2$ est à

cause de l'égalité précédente zéro. Alors, dans le cas du champ central l'équation de Schrödinger du modèle soumis à l'examen passe en équation d'énergie classique. Cependant les solutions ne sont que des orbites circulaires lesquels ne se trouvent pas dans le plan xy: c'est que $\vartheta = \pi/2$ s'impose seulement comme cas de limite, si p. ex. $l = m$ tend à l'infini. La direction du vecteur du moment d'impulsion n'est pas fixet n'est pas perpendiculaire sur le plan de l'orbite. Cette constatation est en harmonie avec cela, que $-\hbar^2/2\mu \cdot \Delta A/A$ nommé »potentiel quantique«, chez MÁTRAI le membre complémentaire de l'énergie cinétique, bien qu'il soit zéro le long des orbites circulaires reçus, mais dépend en outre non seulement de r mais aussi de l'angle ϑ. Ainsi à cause de cela »la force quantique« n'est pas centrale.

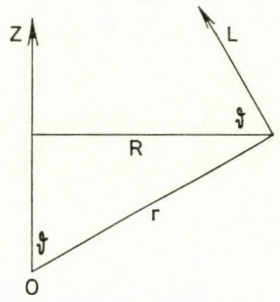

Fig. 1

Si nous employons les susdits spécialement à l'atome H, alors μ est la masse et $-e$ est la charge de l'électron et $V = -e^2/r$. D'après les précedents les valeurs possibles de l'énergie an long des orbites circulaires permises sont:

$$\frac{\hbar^2}{2\mu}\,\frac{l(l+1)}{r^2} - \frac{e^2}{r}\,.$$

Identifions cela avec les valeurs-propres de l'opérateur hamiltonien $E_n = -e^2/2a_0n^2$ où a_0 signifie le rayon de Bohr le plus petit. Ainsi de l'équation de second degré reçue pour la valeur absolue du rayon vecteur on obtient:

$$r = a_0\, n^2\left(1 \pm \sqrt{1 - \frac{l(l+1)}{n^2}}\right).$$

Si $l = n - 1$ et n tend à l'infini, alors r se rapproche asymptotiquement au rayon de l'orbite n-ième de Bohr.

Les trajectoires discrètes reçues ne ressemblent que formellement à la notion de l'orbite circulaire dans le sens de Bohr, car selon [1] et [3] le point

matériel est accompagné par un champ de vitesse étendu dans le cas stationnaire aussi. Par cela nous avons alors quitté le cadre conceptionnel de la physique classique.

Examinons comme deuxième exemple le cas de l'oscillateur spatial [2]. Maintenant $V = 2\pi^2\mu\nu^2r^2$ et les valeurs-propres de l'énergie: $(n + 3/2)h\nu$. Alors maintenant $h^2l(l+1)/8\pi^2\mu r^2 + 2\pi^2\mu\nu^2r^2 = (n + 3/2)h\nu$. De cela nous recevons pour r^2 une équation du second degré, d'où:

$$r^2 = h\,\frac{2n+3 \pm \sqrt{(2n+3)^2 - 4l(l+1)}}{8\pi^2\mu\nu}\,.$$

Comme on voit, la fréquence de l'oscillateur ne figure que dans le dénominateur. C'est pourquoi la vitesse angulaire du mouvement circulaire est proportionnelle à la fréquence, en effet

$$\omega = \frac{hm_l}{2\pi\mu r^2 \sin^2\vartheta} = \frac{hl(l+1)}{2\pi\mu r^2 m_l} = \frac{l(l+1)\cdot 4\pi\cdot\nu}{m_l\left[2n+3 \pm \sqrt{(2n+3)^2 - 4l(l+1)}\right]}$$

Si maintenant $m = l = n - 1$, alors

$$\omega = \frac{4\pi\nu n}{2n+3+\sqrt{16n+9}}\,.$$

Si encore n tend à l'infini, alors la limite de ω est $2\pi\nu$.

Puisque la vitesse angulaire est indépendante du potentiel, c'est pourquoi dans le cas d'un assez grand $n = l + 1$ il reste valable, non seulement pour l'oscillateur spatial mais aussi pour l'atome H, que $\nu = (E_n - E_{n-1})/h$, la fréquence »émittée« s'accorde asymptotiquement avec la fréquence du mouvement circulaire. (Le principe de correspondance.)

Le modèle examiné, en cas stationnaire présenté sur deux exemples des forces centrales ne peut pas être dit déterministique dans le sens classique d'accord avec les constatations publiées dans [1] à la page 328. C'est que, si $\mu \cdot \dot{\bar{r}}$ signifie l'impulsion de la particule, alors la position et la vitesse initiale ne peuvent être données arbitrairement, car le rayon vecteur et les valeurs absolues de l'impulse ne peuvent prendre des grandeurs quelconques. La direction du rayon vecteur est quantifiée, la direction de l'impulse ne peut être que perpendiculaire sur la direction du rayon vecteur et sa grandeur dépend de r et de ϑ.

Les resultats reçus pour le champ central peuvent être généralisés. L'équation de Schrödinger indépendante du temps a une solution différente des fonctions propres écrites en forme $\psi_n = A_n(x, y, z) \cdot \exp(i\,\sigma_n/\hbar)$, qu'on peut nommé trivial: $\psi = K \cdot \exp(is/\hbar)$ où K est constant et $\mathrm{grad}^2\, s = 2\mu(E - V)$.

Cette fonction d'onde ne peut pas être normée ainsi que l'onde plane avec amplitude constante. Cette solution coïncide avec les fonctions propres ψ_n le long des trajectoires, lesquelles se donnent comme lignes de section des troupes de surface $A_n(x, y, z) = K$ avec la surface $\text{grad}^2 \sigma_n = 2\mu(E_n - V)$ qui est équivalente à $\Delta A_n = 0$. Dans le cas des champs centraux aussi un nombre infini des trajectoires est possible car la symétrie autour de Z se rapporte à une axe de direction quelconque. Les lignes de section des surfaces de la sphère du rayon r_n tracées du centre attractif par les plans quelconques seront ces orbites.

Dans le cas du spectre d'énergie continu les surfaces $\Delta A_E = 0$ ne constituent pas un multiple discret. Parmi les trajectoires obtenues on peut trouver à chaque E de telles, lesquelles appartiennent à la valeur $K = 0$. C'est la même chose dans le cas du spectre discret. On peut nommé ces trajectoires, qui se donnent comme les lignes de section des surfaces $A_E(x, y, z) = 0$ et $\Delta A_E = 0$: »orbites interdites«. On trouve telles lignes chez la diffraction de l'onde d'électron ou rayon catodique par une fente étroite.

LITTÉRATURE

1. T. Mátrai, Acta Phys. Hung., **28,** 323, 1970.
2. P. Gombás et D. Kisdi: Bevezetés a hullámmechanikába és alkalmazásaiba. Akadémiai Kiadó, 1967.
3. G. Marx, Acta Acad. Paedag. Sopianae. Ser. 6. p. 54. 1966.

Acta Physica Academiae Scientiarum Hungaricae, Tomus 31 (4), pp. 395—399 (1972)

PHOTO-PRODUCTION OF THE A_1^0 AXIAL VECTOR MESON

By

M. EL-KISHEN

PHYSICS DEPARTMENT, FACULTY OF SCIENCE, CAIRO UNIVERSITY, CAIRO, UAR

(Received 25. V. 1971)

1. Introduction

There has been little theoretical or experimental study of the photo-production of the A_1^0 axial vector meson. Our aim is to obtain the total cross-section of A_1^0 on proton via one virtual photon exchange by using the partially conserved vector current hypothesis [1]. At very small momentum transfer and for transverse polarization, the photon should act like a neutral meson ϱ^0.

It is well known that spin-one particle cannot decay into a system containing two identical spin-one particles [2], but a gauge-invariant amplitude for the A_1^0 vertex can still be written down, since one of the particles is off the mass shell.

2. Total cross-section

The Feynman's diagram corresponding to photo-production of A_1^0 on a proton using the photon propagator is shown in Fig. 1.

The nucleon vertex of the left-hand side is connected to the boson vertex $A_1^0\gamma\gamma$ by means of a virtual photon. The interaction at the nucleon vertex is

$$ie\bar{u}(p_2)\left[F_1\gamma_\mu+\frac{K}{2M}(p_{2\nu}-p_{1\nu})\,\sigma_{\nu\mu}F_2\right]u(p_1), \tag{1}$$

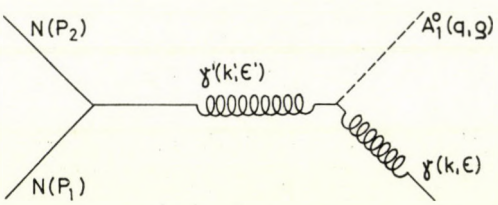

Fig. 1

while at the boson vertex the amplitude of the $A^0_{1\gamma\gamma}$ coupling is [3]

$$\begin{aligned}\epsilon_{\lambda\mu\sigma\alpha}\varrho_\sigma[\epsilon'_\lambda\epsilon_\eta(k\cdot k')-k'_\lambda\epsilon_\eta(\epsilon'\cdot k)-\epsilon'_\lambda k_\eta(\epsilon\cdot k')](k_\alpha-k'_\alpha)+\\+\epsilon_{\lambda\eta\sigma\alpha}\varrho_\sigma[\epsilon_\lambda\epsilon_\eta k'^2-k'_\lambda\epsilon_\eta(\epsilon'\cdot k')]k_\alpha,\end{aligned}\tag{2}$$

where F_1 and F_2 are the isovector parts of the electric and magnetic form factors for a physical single nucleon, respectively; K is the proton anomalous magnetic moment in units of $e/2M$; M is the proton mass; p_1 and p_2 are the 4-momentum vectors of the incident and outgoing proton; k and k' are the four momentum vectors of the incident and virtual photon; ϵ, ϵ' and ϱ are the polarization vectors of the incident photon, virtual photon and outgoing A^0_1 meson.

The whole amplitude for the photo-production of A^0_1 is

$$\begin{aligned}A_{fi}=Ye\bar{u}(p_2)\left[\gamma_\lambda F_1+\frac{K}{2M}(p_{2\nu}-p_{1\nu})\sigma_{\nu\lambda}F_2\right]u(p_1)\cdot\\\cdot\frac{1}{k'^2}\epsilon_{\lambda\eta\sigma\alpha}\varrho_\sigma[\{\epsilon_\eta(k\cdot k')-k_\eta(\epsilon\cdot k')\}(k_\alpha-k'_\alpha)+\epsilon_\eta k_\alpha k'^2]-\\-Ye\bar{u}(p_2)\left[(\gamma\cdot k)F_1+\frac{K}{2M}(p_{2\nu}-p_{1\nu})\sigma_{\nu\beta}k_\beta F_2\right]u(p_1)\cdot\\\cdot\frac{1}{k'^2}\epsilon_{\lambda\eta\sigma\alpha}\varrho_\sigma k'_\lambda\epsilon_\eta(k_\alpha-k'_\alpha),\end{aligned}\tag{3}$$

where Y is the $A^0_1\gamma\gamma$ coupling constant. The normalization conditions for the vector particles are

$$\sum\epsilon_\mu\epsilon_\nu=\delta_{\mu\nu},\tag{4}$$

$$\sum\varrho_\mu\varrho_\nu=\delta_{\mu\nu}+\frac{q_\mu q_\nu}{m^2},\tag{5}$$

where m is the mass of the axial vector meson A^0_1. The unpolarized differential cross-section is given by

$$d\sigma=\left(\frac{eY}{2\pi}\right)^2\frac{E_2}{2E}\sum_{\text{spin}}|A_{fi}|^2d\Theta,\tag{6}$$

where $d\Theta$ is

$$d\Theta=\delta^4(p_1+k-p_2-q)\frac{d^3p_2}{2E_2}\frac{d^3q_1}{2E_{A^0_1}}.\tag{7}$$

The phase space of the volume element $d\Theta$ may be written [4] as

$$d\Theta=\frac{\pi}{y}dx.\tag{8}$$

The variables x and y are given by

$$x = \frac{(q \cdot k)}{M^2} \; ; \quad y = 2\frac{(p_1 \cdot k)}{M^2} \, . \tag{9}$$

Taking [5]

$$F_1 = F_2 = \frac{1}{\left(1 + \dfrac{5(p_1 - p_2)^2}{4M^2}\right)^2} \tag{10}$$

the total cross-section σ is

$$\sigma = -\frac{e^2 Y^2 M^2}{16\,\pi y^2} \int_{x_1}^{x_2} \frac{F(x, y)\, dx}{4\left(\dfrac{m^2}{2M^2} + x\right)^2 \left(\dfrac{5}{2}\right)^4 \left[\dfrac{4M^2 - 5m^2}{10M^2} - x\right]^4} \, . \tag{11}$$

The function $F(x, y)$ has the form

$$\begin{aligned} F(x, y) = {} & 6bx^5 + \left[8a + 6c + b\left(\frac{3m^2}{M^2} - 16 + 4y\right)\right] x^4 + \\ & + \left[4ay\left(y - \frac{m^2}{M^2}\right) + 2cy\left(\frac{m^2}{M^2} - y\right) - by^2 \frac{m^2}{M^2}\right] x^2 + \\ & + \left[4a\left(\frac{m^2}{M^2} + 2 - 2y\right) + c\left(\frac{3m^2}{M^2} - 16 + 4y\right) + 2b\left(\frac{m^2}{M^2}\, y - y^2\right)\right] x^3 + \\ & + \left[y^2 \frac{m^2}{M^2}\,(2a - c)\right] x, \end{aligned} \tag{12}$$

where

$$a = (1+K)^2, \; b = K^2, \; c = 4K(1+K) + \frac{m^2 - 4M^2}{2M^2} K^2 \tag{13}$$

and [6]

$$Y = \frac{8.8 \times 10^{-2}}{M^2} \, . \tag{14}$$

The function under the integral of Eq. (11) has the algebraic form

$$\frac{F(x, y)}{(c_1 + x)^2 (c_2 - x)^4} \quad \text{with } c_1 = \frac{m^2}{2M^2} \, , c_2 = \frac{4M^2 - 5m^2}{10M^2} \, . \tag{15}$$

This can be written

$$\begin{aligned} \frac{F(x, y)}{(c_1 + x)^2 (x - c_2)^4} = {} & \frac{A_1}{(x_2 - c_2)^4} + \frac{A_2}{(x - c_2)^3} + \frac{A_3}{(x - c_2)^2} + \frac{A_4}{(x - c_2)} + \\ & + \frac{B_1}{(c_1 + x)^2} + \frac{B_2}{(c_1 + x)} \end{aligned} \tag{16}$$

with

$$\left.\begin{aligned} A_1 &= \left[\frac{F(x,y)}{(c_1+x)^2}\right]_{x=c_2}, \\ A_2 &= \left[\frac{\partial}{\partial x}\frac{F(x,y)}{(c_1+x)^2}\right]_{x=c_2}, \\ A_3 &= \left[\frac{\partial^2}{\partial x^2}\frac{F(x,y)}{(c_1+x)^2}\right]_{x=c_2}, \\ A_4 &= \left[\frac{\partial^3}{\partial x^3}\frac{F(x,y)}{(c_1+x)^2}\right]_{x=c_2} \end{aligned}\right\} \tag{17}$$

and

$$\left.\begin{aligned} B_1 &= \left[\frac{F(x,y)}{(x-c_2)^4}\right]_{x=-c_1}, \\ B_2 &= \left[\frac{\partial}{\partial x}\frac{F(x,y)}{(x-c_2)^4}\right]_{x=-c_1}. \end{aligned}\right\}$$

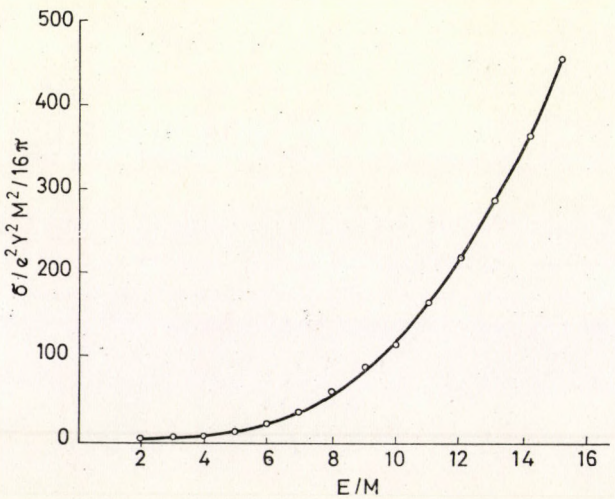

Fig. 2

Substituting from Eqs. (15), (16) and (17) into Eq. (11) and performing the integration, we obtain

$$\sigma = \frac{e^2 Y^2 M^2}{(5)^4 4\pi y^2}\left[\frac{A_1}{3(x-c_2)^3} + \frac{A_2}{2(x-c_2)^2} + \frac{A_3}{(x-c_2)} - A_4 \ln(x-c_2) + \right. \\ \left. + \frac{B_1}{x+c_1} - B_2 \ln(x+c_1)\right]_{x_1}^{x_2}, \tag{18}$$

The limits of integration x_1 and x_2 have the following values:

$$x_2 = \frac{y\left(\frac{m^2}{M^2} - y\right) - y\sqrt{\left(\frac{m^2}{M^2} + y\right)^2 - 4\frac{m^2}{M^2}}}{4(1-y)}, \tag{19}$$

$$x_1 = \frac{y\left(\frac{m^2}{M^2} - y\right) + y\sqrt{\left(\frac{m^2}{M^2} + y\right)^2 - 4\frac{m^2}{M^2}}}{4(1-y)}. \tag{20}$$

Fig. 2 shows the total cross-section for photo-production of the axial vector meson A_1^0. The calculations were made in the laboratory system for different photon energies up to 15 nucleon mass units. It can be seen from the curve that the cross-section increases with the photon energy. As the incident photon energy tends to infinity, the momentum transfer goes to zero at one of the limits of the integration. This shows that the use of a photon propagator is not appropriate for extremely high energies.

REFERENCES

1. R. H. DALITZ, Proc. Phys. Soc., **A 64,** 667, 1951.
2. C. N. YANG, Phys. Rev., **77,** 242, 1950.
3. L. ROSENBERG, Phys. Rev., **129,** 2786, 1963.
   S. L. ADLER, Phys. Rev., **177,** 2426, 1969.
4. W. WILLIAMSON, Jr., Am. J. Phys., **33,** 987, 1965.
5. Proceedings of the International Conference on Nuclear Structure (Phys. Soc. of Japan), Tokyo, 1967.
   N. CABIBO and R. CATTO, Nuovo Cim., **15,** 304, 1960.
   T. D. LEE and C. N. YANG, Phys. Rev. Letters, **4,** 307, 1960.
6. T. H. CHANG, Nuovo Cim., LXIX, A, N, 2, 239, 1970.

RECENSIO

A. G. PACHOLCZYK:

Radio Astrophysics: Nonthermal Processes in Galactic and Extragalactic Sources

XXI + 269, W. H. Freeman and Co., San Francisco, 1970. Price 15 US Dollars

The book evolved from the course in radio astronomy the author taught for three years as Associate Professor of Astronomy at the University of Arizona. It may be found of general interest to physicists, because the author emphasizes the fundamental physics of radio astronomy instead of observational results and descriptive data, which are presented only by references to the literature. After an introductory chapter on receivers and antennae a summary of the physics of plasmas in a magnetic field follows. Chapters 3 and 4 deal with synchrotron radiation in vacuo and in a plasma, and Chapter 5 with Compton scattering. The interpretation of the spectra of discrete radio sources and physical conditions in radio sources is briefly discussed in Chapters 6 and 7. The final chapter is concerned with radio spectral lines.

L. DETRE

CORRIGENDA

ON THE DERIVATION OF THE HARTREE–FOCK EQUATIONS

By

I. MAYER

CENTRAL RESEARCH INSTITUTE FOR CHEMISTRY OF THE
HUNGARIAN ACADEMY OF SCIENCES, BUDAPEST

(Acta Phys. Hung. **30**, 373, 1971)

A misprint (incorrect sign) which distorts the meaning has been found in Eq. (5). Eq. (5) should read

$$E_2 = H_{00} + \frac{1}{2}(H_{00} - H_{11})\left[\sqrt{1 + \frac{4|H_{01}|^2}{(H_{00} - H_{11})^2}} - 1\right]. \qquad (5)$$

TIRED LIGHT AND THE "MISSING MASS" PROBLEM

By

W. YOURGRAU and J. F. WOODWARD

FOUNDATION OF PHYSICS, UNIVERSITY OF DENVER
DENVER, COLORADO 80210, USA

(Acta Phys. Hung. **30**, 325, 1971)

Lines 10–13 of Section IV (page 327) should be replaced by:"finite rest mass. In order to obtain equation (2) one may modify the electromagnetic equations by taking a potential (Φ) of the form

$$\Phi \sim e^{-\mu r}/r$$

for the electrostatic and monopole magnetostatic fields. Such a substitution yields immediately a Poynting vector of the form" ...

Printed in Hungary

A kiadásért felel az Akadémiai Kiadó igazgatója — Műszaki szerkesztő: Várhelyi Tamás

A kézirat nyomdába érkezett: 1972. I. 18. — Terjedelem: 11,5 (A/5) ív, 58 ábra

72.72987 Akadémiai Nyomda, Budapest — Felelős vezető: Bernát György

NOTES TO CONTRIBUTORS

I. PAPERS will be considered for publication in Acta Physica Hungarica only if they have not previously been published or submitted for publication elsewhere. They may be written in English, French, German or Russian.

Papers should be submitted to

Prof. I. Kovács, Editor
Department of Atomic Physics, Polytechnical University
Budapest 112, Budafoki út 8, Hungary

Papers may be either articles with abstracts or short communications. Both should be as concise as possible, articles in general not exceeding 25 typed pages, short communications 8 typed pages.

II. MANUSCRIPTS

1. Papers should be submitted in two copies. Articles should be accompanied by abstracts in the language of the paper together with a copy of the title, name of author(s) and abstract in Russian if the paper is in English, French or German, and in one of the latter three languages if the paper is in Russian. If a translation of the abstract cannot be provided, this will be arranged by the Editor.

2. The text of papers must be of high stylistic standard, requiring minor corrections only.

3. Manuscripts should be typed in double spacing on good quality paper, with generous margins.

4. The name of the author(s) and of the institutes where the work was carried out should appear on the first page of the manuscript.

5. Particular care should be taken with mathematical expressions. The following should be clearly distinguished, e.g. by underlining in different colours: special founts (italics, script, bold type, Greek, Gothic, etc.); capital and small letters; subscripts and superscripts, e.g. x^2, x_2; small *l* and 1; zero and capital O; in expressions written by hand: e and l, n and u, *v* and v, etc.

6. References should be numbered serially and listed at the end of the paper in the following form: J. Ise and W. D. Fretter, Phys. Rev., *76*, 933, 1949.

For books, please give the initials and family name of the author(s), title, name of publisher, place and year of publication, e.g.: J. C. Slater, Quantum Theory of Atomic Structures, I, McGraw-Hill Book Company Inc., New York, 1960.

References should be given in the text in the following forms: Heisenberg [5] or [5].

7. Captions to illustrations should be listed on a separate sheet, not inserted in the text.

III. ILLUSTRATIONS AND TABLES

1. Each paper should be accompanied by two sets of illustrations, one of which must be ready for the blockmaker. The other set attached to the copy of the manuscript may be rough drawings in pencil or photocopies.

2. Illustrations must not be inserted in the text.

3. All illustrations should be identified in blue pencil by the author's name, abbreviated title of the paper and figure number.

4. Tables should be typed on separate pages and have captions describing their content. Clear wording of column heads is advisable. Tables should be numbered in Roman numerals (I, II, III, etc.).

IV. MANUSCRIPTS not in conformity with the above Notes will immediately be returned to authors for revision. The date of receipt to be shown on the paper will in such cases be that of the receipt of the revised manuscript.

INDEX

COMMUNICATIONES BREVES

Acta Phys. Hung. Tom. 31. No. 4, Budapest, 10. VIII. 1972 Index: 26.022